Drug Bioavailability
Estimation of Solubility, Permeability, Absorption and Bioavailability
Edited by H. van de Waterbeemd, H. Lennernäs and P. Artursson

Drug Bioavailability: Estimation of Solubility, Permeability, Absorption and Bioavailability.
Edited by Han van de Waterbeemd, Hans Lennernäs and Per Artursson

ISBN: 3-527-30438-X

Methods and Principles in Medicinal Chemistry

Drug Bioavailability

Estimation of Solubility, Permeability, Absorption and Bioavailability

Edited by Han van de Waterbeemd, Hans Lennernäs and Per Artursson

WILEY-VCH

Series Editors

Prof. Dr. Raimund Mannhold
Biomedical Research Center
Molecular Drug Research Group
Heinrich-Heine-Universität
Universitätsstraße 1
40225 Düsseldorf
Germany
raimund.mannhold@uni-duesseldorf.de

Prof. Dr. Hugo Kubinyi
BASF AG Ludwigshafen
c/o Donnersbergstraße 9
67256 Weisenheim am Sand
Germany
kubinyi@t-online.de

Prof. Dr. Gerd Folkers
Department of Applied Biosciences
ETH Zürich
Winterthurerstr. 190
8057 Zürich
Switzerland
folkers@pharma.anbi.ethz.ch

Volume Editors

Dr. Han van de Waterbeemd
Pfizer Global Research and Development
Department of Drug Metabolism, IPC 351
Sandwich, Kent CT13 9NJ
UK
han_waterbeemd@sandwich.pfizer.com

Prof. Dr. Hans Lennernäs
Biopharmaceutics Group
Department of Pharmacy
Uppsala University
S-751 23 Uppsala
Sweden
hans.lennernaes@biof.uu.se

Prof. Dr. Per Artursson
Division of Pharmaceutics
Department of Pharmacy
Uppsala University
S-751 23 Uppsala
Sweden
per.artursson@galenik.uu.se

Library of Congress Card No.: applied for
British Library Cataloguing-in-Publication Data: A catalogue record for this book is available from the British Library
Bibliographic information published by Die Deutsche Bibliothek
Die Deutsche Bibliothek lists this publication in the Deutsche Nationalbibliografie; detailed bibliographic data is available in the Internet at http://dnb.ddb.de

Printed in the Federal Republic of Germany.
Printed on acid-free paper.

Composition Asco Typesetters, Hong Kong
Printing betz-druck gmbh, Darmstadt
Bookbinding Litges & Dopf Buchbinderei GmbH, Heppenheim

ISBN 3-527-30438-X

Contents

Preface

The processes involved in drug discovery have changed considerably in the past decade. Today we have access to the full human as well as several bacterial genomes offering a rich source of molecular targets to treat diseases. Methods in biology have moved to ultra-high-throughput screening (uHTS) of such precedented and unprecedented targets. Chemistry adapted to this progress by developing methods such as combinatorial and parallel synthesis allowing the rapid synthesis of hundreds to hundreds of thousands molecules in reasonable quantities, purities and timelines.

Historical data on the fate of potential drugs in development indicate that major reasons for attrition include toxicity, efficacy and pharmacokinetics/drug metabolism. Therefore, in today's drug discovery the evaluation of absorption, distribution, metabolism and elimination (ADME) of drug candidates is performed early in the process. In the last 10 years drug metabolism and physicochemical *in vitro* screening methods have increasingly been introduced. In recent years these methods more and more became medium to high throughput in order to cope with increasing numbers of compounds to evaluate after HTS.

Although HTS seems to be a very efficient approach, it must be stressed that there is also a high cost associated with it. Interest is thus shifting to prediction and simulation of molecular properties, which might hopefully lead to overall more efficient processes.

The next vague of tools will be around computational or *in silico* ADME approaches. These will allow to include ADME into the design of combinatorial libraries, the evaluation of virtual libraries, as well as in selecting the most promising compounds to go through a battery of *in vitro* screens, possibly even replacing some of these experimental screens. Several of these computational tools are currently under development as will be discussed in this volume.

For reasons of convenience for the patient and compliance to the therapy, most drugs are administered orally. To keep the dose at the lowest possible level, high oral absorption and high bioavailability are prime properties to optimise in a new drug. Drug bioavailability is the outcome of a complex chain of events, and is among others influenced by the drug's solubility, permeability through the gastrointestinal wall, and its first pass gut wall and liver metabolism. Excluding liver metabolism, all other factors are characterized by the term oral absorption. Per-

meability through the gut wall can be favoured or hindered through the effect of various transporter proteins such as P-glycoprotein. Our increased knowledge and understanding of all of these processes involved in permeability, oral absorption and bioavailability will make predictive tools more robust.

This volume gives an overview of the current status and an outlook to future more reliable predictive approaches. It is subdivided in five sections dealing with studies of membrane permeability and oral absorption, drug dissolution and solubility, the role of transporters and metabolism in oral absorption, computational approaches to drug absorption and bioavailability, and finally with certain drug development issues.

The series editors would like to thank Han van de Waterbeemd, Hans Lennernäs, and Per Artursson for their enthusiasm to put together this book and to work with such a fine selection of authors. We also express our gratitude to Frank Weinreich and Gudrun Walter of Wiley-VCH for their valuable contributions to this project.

March 2003

Raimund Mannhold, Düsseldorf
Hugo Kubinyi, Weisenheim am Sand
Gerd Folkers, Zürich

Foreword

This book aims at bringing together the strategies and tools currently available to investigate and make predictions about oral absorption and bioavailability of drugs in humans. Ideally, such predictive models can be used in drug discovery from the design of compounds and libraries throughout lead optimisation to clinical candidate selection. This book also aims to discuss more complex *in vivo* aspects of oral drug delivery.

The volume is divided into five sections. Part one looks at the experimental study of membrane permeability and oral absorption. In Part two, problems of measuring and prediction solubility, as one of the key determinants in the absorption process, will be discussed in detail. In the next part, progress in the science around transporter proteins and gut wall metabolism and their effect on the overall absorption process is presented. Part four looks at the *in silico* approaches and models to predict permeability, absorption and bioavailability. In the last part of the book, a number of drug development issues will be highlighted, which could have an important impact of the overall delivery strategies for oral pharmaceutical products.

In summary, progress in predicting oral absorption is based on a much better understanding of the transport processes across the intestinal epithelium along the gastrointestinal tract. The identification of the key physicochemical properties, and in addition the identification of key transporter proteins and metabolising enzymes in the gut wall has led to the development of new *in vitro* and *in vivo* screens that allow reasonably accurate estimates of oral absorption in man to be made. Predicting bioavailability is more challenging, but very promising progress has been made in recent years, both via the combination of several *in vitro* measures, as well as the development of predictive *in silico* tools. In many cases, the validity and the accuracy of the applied methods have been investigated to some extent, but more mechanistic research is needed in order to improve the performance of the various methods used in this field of drug development.

We are very grateful to the many contributors to this book. Their insightful chapters are the body of this book. Some were prepared to stand in at the last minute, and still delivered within the deadline, which is always a relief to the editors. Finally we thank Frank Weinreich for his continuous encouragement and light pressure to get the chapters in press on time.

December 2002,

Sandwich — Han van de Waterbeemd
Uppsala — Hans Lennernäs
Uppsala — Per Artursson

List of Authors

Dr. Bertil Abrahamsson
AstraZeneca R&D
Department of Preformulation and Biopharmaceutics
431 83 Mölndal
Sweden

Dr. Balaji Agoram
USC School of Pharmacy
Department of Pharmaceutical Sciences
1985 Zonal Ave. PSC 700
Los Angeles, CA 90089-9121
USA

Prof. Dr. Gordon Amidon
University of Michigan
College of Pharmacy
Ann Arbor, MI 48109
USA
glamidon@umich.edu

Prof. Dr. Per Artursson
Department of Pharmacy
Biomedical Centre
Uppsala University
751 23 Uppsala
Sweden
per.artursson@galenik.uu.se

Dr. Alex Avdeef
PION Inc
5 Constitution Way
Woburn, MA 01801
USA
aavdeef@pion-inc.com

Kevin Beaumont
Pfizer Global Research and Development
Department of Drug Metabolism
IPC 331
Sandwich, Kent CT13 9NJ
UK
kevin_beaumont@sandwich.pfizer.com

Dr. Christel A. S. Bergström
Division of Pharmaceutics
Department of Pharmacy
Biomedical Centre, Box 580
Uppsala University
751 23 Uppsala
Sweden
christel.bergstrom@farmaci.uu.se

Prof. Dr. Michael B. Bolger
USC School of Pharmacy
Department of Pharmaceutical Sciences
1985 Zonal Ave. PSC 700
Los Angeles, CA 90089-9121
USA
bolger@usc.edu

Dr. Emanuele Carosati
Laboratory for Chemometrics and Chemoinformatics
Chemistry Department
University of Perugia
Via Elce di Sotto 10
06123 Perugia
Italy

Dr. John Comer
Sirius Analytical Instruments Ltd.
Riverside
Forest Row Business Park
Forest Row, East Sussex RH18 5HE
UK
john.comer@sirius-analytical.com

Dr. Charles L. Crespi
Gentest™ a BD Biosciences Company
6 Henshaw Street
Woburn, MA 01801
USA
charles_crespi@BD.com

Prof. Dr. Gabriele Cruciani
Laboratory for Chemometrics

University of Perugia
Via Elce di Sotto 10
06123 Perugia
Italy
gabri@chemiome.chm.unipg.it

Dr. Chau M. Du
Pion Inc.
5 Constitution Way
Woburn, MA 01801
USA

Dr. Anne Engelbrecht Thomsen
Royal Danish School of Pharmacy
Department of Pharmaceutics
2 Universitetsparken
2100 Copenhagen
Denmark
antt@dfh.dk

Dr. Holger Fischer
University of Basel, Biocenter
Klingelbergstrasse 70
CH-4056 Basel
Switzerland

Dr. Robert Fraczkiewicz
USC School of Pharmacy
Department of Pharmaceutical Sciences
1985 Zonal Ave. PSC 700
Los Angeles, CA 90089-9121
USA

Prof. Dr. Sven Frøkjær
Royal Danish School of Pharmacy
Department of Pharmaceutics
2 Universitetsparken
2100 Copenhagen
Denmark
sf@dfh.dk

Dr. Gladys E. Granero
University of Michigan
College of Pharmacy
Ann Arbor, MI 48109
USA

Dr. Markus Haeberlein
AstraZeneca R&D Södertälje
151 85 Södertälje
Sweden

Dr. Barry Jones
Pfizer Global Research and Development
Department of Drug Metabolism
IPC 664
Sandwich, Kent CT13 9NJ
UK
barry_jones@sandwich.pfizer.com

Dr. Johan Karlsson
AstraZeneca R&D
DMPK and Bioanalytical Chemistry
431 83 Mölndal
Sweden

Dr. Christopher P. Landowski
University of Michigan
College of Pharmacy
Ann Arbor, MI 48109
USA

Dr. Ewa Landwojtowicz
University of Basel, Biocenter
Klingelbergstrasse 70
CH-4056 Basel
Switzerland

Prof. Dr. Hans Lennernäs
Biopharmaceutics Group
Department of Pharmacy
Uppsala University
751 23 Uppsala
Sweden
hans.lennernas@biof.uu.se

Dr. Xiaochun Li Blatter
University of Basel, Biocenter
Klingelbergstrasse 70
CH-4056 Basel
Switzerland

Dr. Chris Lipinski
Pfizer Global Research and Development
Eastern Point Road
Groton, CT 06340
USA
christopher_a_lipinski@groton.pfizer.com

Dr. Chris Logan
AstraZeneca R&D Charnwood
Physical & Metabolic Science
Bakewell Road
Loughborough, Leics LE11 5RH
UK
chris.logan@astrazeneca.com

Dr. Arun Mandagere
Pfizer Global Research and Development
Ann Arbor Laboratories
Strategic Resources/Lead Discovery
2800 Plymouth Road
Ann Arbor, MI 48106
USA
arun.mandagere@pfizer.com

Prof. Dr. Raimund Mannhold
Department of Laser Medicine
Molecular Drug Research Group
Heinrich-Heine-Universität
Universitätsstr. 1
40225 Düsseldorf
Germany

Dr. James W. McFarland
Reckon.dat Consulting
217 Blood Street
Lyme, CT 06371-3509
USA
reckon.dat@attglobal.net

Dr. M. Meniconi
Laboratory for Chemometrics and Chemoinformatics
Chemistry Department
University of Perugia
Via Elce di Sotto 10
06123 Perugia
Italy

Dr. Ulf Norinder
AstraZeneca R&D
Discovery – Medicinal Chemistry
S-151 85 Södertälje
Sweden
ulf.norinder@astrazeneca.com

Dr. Niclas Petri
Biopharmaceutics Group
Department of Pharmacy
Uppsala University
S-751 23 Uppsala
Sweden

Dr. Chandrasekharan Ramachandran
University of Michigan
College of Pharmacy
Ann Arbor, MI 48109
USA

PD Dr. Anna Seelig
University of Basel, Biocenter
Department of Biophysical Chemistry
Klingelbergstrasse 70
CH-4056 Basel
Switzerland
anna.seelig@unibas.ch

Dr. Ho-Chul Shin
University of Michigan
College of Pharmacy
Ann Arbor, MI 48109
USA

Dr. Boyd Steere
USC School of Pharmacy
Department of Pharmaceutical Sciences
1985 Zonal Ave. PSC 700
Los Angeles, CA 90089-9121
USA

Prof. Dr. Bente Steffansen
Royal Danish School of Pharmacy
Department of Pharmaceutics
2 Universitetsparken
2100 Copenhagen
Denmark
bds@dfh.dk

Prof. Dr. Yuichi Sugiyama
University of Tokyo
Graduate School of Pharmaceutical Sciences
7-3-1 Hongo, Bunkyo-ku
Tokyo 113-0033
Japan
sugiyama@mol.f.u-tokyo.ac.jp

Dr. Duxin Sun
University of Michigan
College of Pharmacy
Ann Arbor, MI 48109
USA

Prof. Dr. Hiroshi Suzuki
University of Tokyo
Graduate School of Pharmaceutical Sciences
7-3-1 Hongo, Bunkyo-ku
Tokyo 113-0033
Japan
hsuzuki@mol.f.u-tokyo.ac.jp

Dr. Staffan Tavelin
Division of Pharmaceutics
Department of Pharmacy
Biomedical Centre, Box 580
Uppsala University
S-751 23 Uppsala
Sweden
staffan.tavelin@farmaci.uu.se

Dr. Anna-Lena Ungell
AstraZeneca R&D
DMPK and Bioanalytical Chemistry
S-431 83 Moelndal
Sweden
anna-lena.ungell@astrazeneca.com

Dr. Han van de Waterbeemd
Pfizer Global Research and Development
PDM, Department of Drug Metabolism
IPC 351

Sandwich, Kent, CT13 9NJ
UK
han_waterbeemd@sandwich.pfizer.com

Prof. Dr. Clive G. Wilson
University of Strathclyde
Department of Pharmaceutical Sciences
27 Taylor Street
Glasgow, G4 0NR
UK
c.g.wilson@strath.ac.uk

Dr. Ismael Zamora
Lead Molecular Discovery
Fransecs Cananes 1-3, 2-1
08190 Sant Cugat del Valles
Spain
ismael.zamora@telefonica.net

I
Studies of Membrane Permeability and Oral Absorption

Drug Bioavailability: Estimation of Solubility, Permeability, Absorption and Bioavailability.
Edited by Han van de Waterbeemd, Hans Lennernäs and Per Artursson

ISBN: 3-527-30438-X

1
Physico-chemical Approaches to Drug Absorption

Han van de Waterbeemd

Abbreviations

ADME	Absorption, distribution, metabolism, elimination (excretion)
BBB	Blood–brain barrier
BMC	Biopartitioning micellar chromatography
Caco-2	Adenocarcinoma cell line derived from human colon
CNS	Central nervous system
DMSO	Dimethyl sulfoxide
EVA	Ethylenevinyl acetate copolymer
IAM	Immobilized artificial membrane
ILC	Immobilized liposome chromatography
MAD	Maximum absorbable dose
MEKC	Micellar electrokinetic chromatography
MLR	Multiple linear regression
NMR	Nuclear magnetic resonance
PAMPA	Parallel artificial membrane permeation assay
PASS	Prediction of activity spectra for substances
PK	Pharmacokinetics
QSAR	Quantitative structure–activity relationship
QSPR	Quantitative structure–property relationship
SPR	Surface plasmon resonance
WDI	World Drug Index

Symbols

AP_{SUV}	Absorption potential measured in small unilamellar vesicles (SUV)
Brij35	Polyoxyethylene(23)lauryl ether
CLOGP	Logarithm of the calculated octanol/water partition coefficient (for neutral species)
diff$(\log P^{N-I})$	Difference between $\log P^N$ and $\log P^I$
$\Delta \log P$	Difference between log P in octanol/water and alkane/water

Drug Bioavailability: Estimation of Solubility, Permeability, Absorption and Bioavailability.
Edited by Han van de Waterbeemd, Hans Lennernäs and Per Artursson

ISBN: 3-527-30438-X

log D	Logarithm of the distribution coefficient, usually in octanol/water at pH 7.4
log P	Logarithm of the partition coefficient, usually in octanol/water (for neutral species)
log P^I	Logarithm of the partition coefficient of a given compound in its fully ionized form, usually in octanol/water
log P^N	Logarithm of the partition coefficient of a given compound in its neutral form, usually in octanol/water
MW	Molecular weight
pK_a	Ionization constant in water
S	Solubility
SITT	Small intestinal transit time (4.5 h = 270 min)
SIWV	Small intestinal water volume (250 mL)
V	Volume

1.1 Introduction

An important part of the optimization process of potential leads to candidates suitable for clinical trials is the detailed study of the absorption, distribution, metabolism and excretion (ADME) characteristics of the most promising compounds. Experience has learned that physico-chemical properties play a key role in drug metabolism and pharmacokinetics (DMPK) [1–3]. As an example, physico-chemical properties relevant to oral absorption are described in Fig. 1.1. It is important to note that these properties are not independent, but closely related to each other.

The change in work practice towards higher-throughput screening (HTS) in

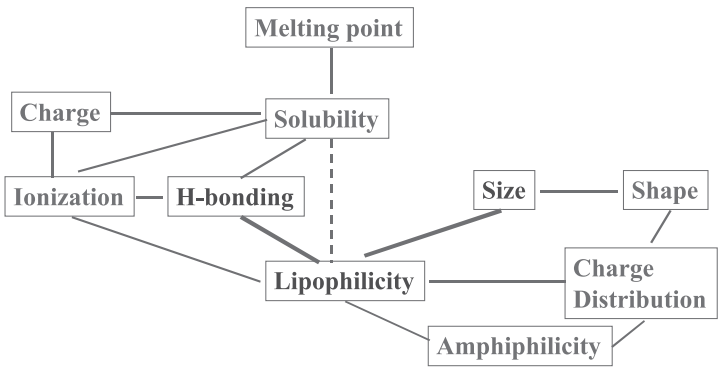

Fig. 1.1. Relationships between various physico-chemical properties believed to influence oral drug absorption.

biology using combinatorial libraries has also increased the demands on more physico-chemical and ADME data. This chapter will review the key physico-chemical properties – both how they can be measured as well as how they can be calculated in some cases.

In addition, the calculation of many different 1D, 2D and 3D descriptors is possible using a range of commercially available software packages, such as Sybyl, Cerius2, Tsar, Molconn-Z and Hybot. Several new descriptor sets are based on quantification of 3D molecular surface properties, and these have been explored for the prediction of, e.g., Caco-2 permeability and oral absorption. It is pointed out here that a number of these "new" descriptors are strongly correlated to the more traditional physico-chemical properties.

1.2 Drug-like Properties

Several papers have discussed the thesis that drugs have distinct properties that differentiate them from other chemicals. Using neural networks [4, 5] or a decision tree approach [6], a compound can be predicted as being "drug-like" with an error rate of c. 20%. Similarly, in a study on drugs active as central nervous system (CNS) agents and using neural networks based on Bayesian methods, CNS-active drugs could be distinguished from CNS-inactive ones [7]. A further approach consists of training of the program PASS [8], which originally was intended to predict activity profiles and thus is suitable for predicting potential side effects.

Based on an analysis of the key properties of compounds in the World Drug Index (WDI), the now well-accepted rule-of-5 has been derived [9, 10]. It was concluded that compounds are most likely to have poor absorption when the molecular weight (MW) is >500, the calculated octanol/water partition coefficient (CLOGP) is >5, number of H-bond donors is >5, and the number of H-bond acceptors >10. Computation of these properties is now available as an ADME (absorption, distribution, metabolism, excretion) screen in commercial software such as Tsar (from Accelrys). The rule-of-5 should be seen as a qualitative absorption/permeability predictor [11], rather than as a quantitative predictor [12]. The property-distribution in drug-related chemical databases has been studied as another approach to understand "drug-likeness" [13, 14]. These aforementioned analyses all point to a critical combination of physico-chemical and structural properties [15] which, to a large extent, can be manipulated by the medicinal chemist. This approach in medicinal chemistry has been called property-based design [2]. Under properties in this context we intend physico-chemical as well as pharmaco- and toxicokinetic properties. For a long-time, these have been neglected by most medicinal chemists who, in many cases, only sought the strongest receptor binding as an ultimate goal. However, this has changed dramatically, and the principles of drug-like compounds are now being used in computational approaches towards the rational design of combinatorial libraries [16].

1.3 Dissolution and Solubility

Each cellular membrane can be considered as a combination of a physico-chemical and biological barrier to drug transport. On occasion, poor physico-chemical properties may be overcome by an active transport mechanism. However, before any absorption can take place at all, the first important properties to consider are dissolution and solubility. Many cases of solubility-limited absorption have been reported, and therefore solubility is now seen as a property to be addressed during the early stages of drug discovery. Only compound that is in solution is available to permeate across the gastrointestinal membrane; hence, solubility has long been recognized as a limiting factor in the absorption process, and this has led to the implementation of solubility screens in the early stages of drug design [9, 10]. Excessive lipophilicity is a common cause of poor solubility and can lead to erratic and incomplete absorption following oral administration. Estimates of desired solubility for good oral absorption depend on the permeability of the compound and the required dose, as illustrated in Table 1.1 [10].

The incorporation of an ionizable center, such as an amine or similar function, into a template can bring a number of benefits, including water solubility. A key step in the discovery of the protease inhibitor, indinavir was the incorporation of a basic amine (and a pyridine) into the backbone of hydroxyethylene transition state mimic compounds L-685,434 to enhance solubility (and potency) (Fig. 1.2) [17].

Tab. 1.1. Desired solubility correlated to expected doses [10].

Dose [mg/kg]	*Permeability High*	*Medium*	*Low*
0.1	1*	5	21
1	10	52	207
10	100	520	2100

*$\mu g\ mL^{-1}$

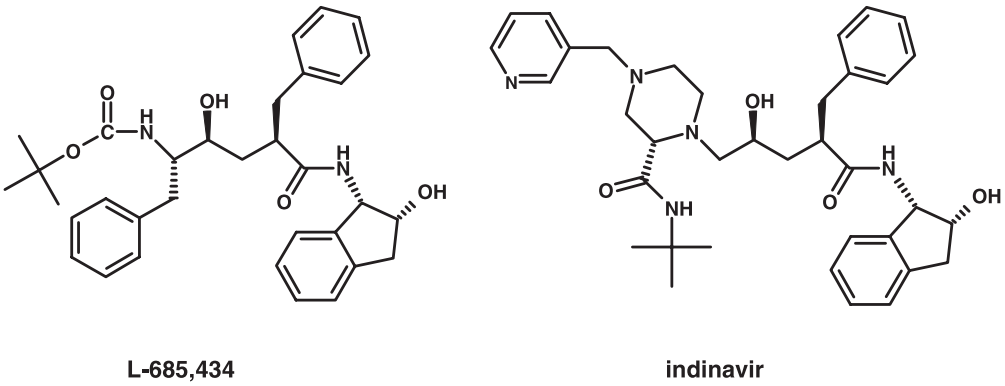

L-685,434 **indinavir**

Fig. 1.2. Structures of indinavir and analogue L-685,434.

The concept of maximum absorbable dose (MAD) was introduced [18, 19] and relates drug absorption to solubility via Eq. (1):

$$MAD = S \times ka \times SIWV \times SITT \quad (1)$$

where

S = solubility (mg mL^{-1}) at pH 6.5
Ka = transintestinal absorption rate constant (min^{-1})
SIWV = small intestinal water volume (mL), assumed to be c. 250 mL
SITT = small intestinal transit time (min), assumed to be 4.5 h = 270 min.

High-throughput solubility measurements have been developed which can be used in early discovery [9, 20–22].

Dissolution testing has been used as a prognostic tool for oral drug absorption [23]. A Biopharmaceutics Classification Scheme (BCS) has been proposed under which drugs can be categorized into four groups according to their solubility and permeability properties [24]. Because both permeability as well as solubility can be further dissected into more fundamental properties, it has been argued that the principal properties are not solubility and permeability, but rather molecular size and hydrogen bonding [25]. The BCS has been adopted as a regulatory guidance for bioequivalence studies.

1.3.1 Calculated Solubility

As a key first step towards oral absorption, considerable effort has been directed towards the development of computational solubility prediction [26–30]. However, partly due to a lack of large experimental datasets measured under identical conditions, today's methods are not sufficiently robust for reliable predictions [31]. Nonetheless, further fine-tuning of these models can be expected since high-throughput data have become available for their construction.

1.4 Ionization (pK_a)

The dogma based on the pH-partition theory that only neutral species cross a membrane has been challenged [11]. Using cyclic voltammetry, it was shown that compounds in their ionized form pass into organic phases and might well cross membranes in this ionized form [32]. Various ways that an ion may cross a membrane have been described [33], including transport as an ion (trans- and/or para-

cellular), as an ion pair, or protein-assisted (using the outer surface of a protein which spans the membrane).

The importance of drug ionization in the *in vitro* prediction of *in vivo* absorption has been discussed [34]. When the apical pH used in Caco-2 studies was lowered from 7.4 to 6.0, a better correlation was obtained with *in vivo* data, demonstrating that careful selection of experimental conditions *in vitro* is crucial to have a reliable model. Studies with Caco-2 monolayers also suggested that the ionic species may contribute considerably to overall drug transport [35].

Therefore, a continued interest exists in the role of pK_a in absorption, which often is related to its effect on lipophilicity and solubility. New methods to measure pK_a values are being explored [36], e.g., using electrophoresis [37], and an instrument for high-throughput pK_a measurement has recently been announced [38].

The difference between the log P of a given compound in its neutral form ($\log P^N$) and its fully ionized form ($\log P^I$) has been termed *diff*($\log P^{N-I}$). This term contains series-specific information, and expresses the influence of ionization on the intermolecular forces and intramolecular interactions of a solute [32, 39]. It is unclear at present how these latter concepts can be used in drug design.

1.5 Lipophilicity

Octanol/water partition (log P) and distribution (log D) coefficients are widely used to make estimates for membrane penetration and permeability, including gastrointestinal absorption [40, 41], blood–brain barrier (BBB) crossing [42, 43], and correlations to pharmacokinetic properties [1]. In 1995 and 2000, specialized but very well attended meetings were held to discuss the role of log P in drug research [44, 45].

Several approaches for higher-throughput lipophilicity measurements have been developed in the pharmaceutical industry [38], including automated shake-plate methods [46], and some of these are now available commercially [47]. A convenient method to measure octanol/water partitioning is based on potentiometric titration; this is called the pH-method [48].

Although traditional octanol/water distribution coefficients are still widely used in quantitative structure–activity relationships (QSAR) and in ADME/pharmacokinetic (PK) studies, alternatives have been proposed. To cover the variability in biophysical characteristics of different membrane types, a set of four solvents has been suggested – sometimes called the "critical quartet" [49–51]. The 1,2-dichloroethane (DCE)/water system has been promoted as a good alternative to alkane/water due to its far better dissolution properties [50, 51], but it may be used only rarely due to its carcinogenic properties.

The two major components of lipophilicity are molecular size and hydrogen bonding [52], each of which will be discussed below.

1.5.1 Calculated log P

A number of comprehensive reviews on lipophilicity estimation have been published and are recommended for further reading [53–55]. Due to its key importance, a continued interest is seen in the development of good log P estimation programs [56, 58]. Most log P approaches are limited due to a lack of parameterization of certain fragments, but for the widely used CLOGP program a new version has recently become available which avoids missing fragments [59]. Although most log P programs refer to the octanol/water system, there is one exception: this is based on Rekker's fragmental constant approach, and a log P calculating for aliphatic hydrocarbon/water partitioning has been reported [60]. These values may offer a better predictor for uptake in the brain.

1.6 Molecular Size and Shape

Molecular size can be further limiting factor in oral absorption [61]. The Lipinski rule-of-5 proposes an upper MW limit of 500 as being acceptable for orally absorbed compounds [9]. Size and shape parameters are generally not measured, but rather calculated. One measured property is the so-called cross-sectional area, which is obtained from surface activity measurements [62].

1.6.1 Calculated Size Descriptors

Molecular weight is often taken as the size descriptor of choice, mainly because it is easy to calculate and is generally in the chemist's mind. However, other size and shape properties are equally very simple to calculate and may offer a better guide to estimate potential for permeability. As yet, no systematic studies have been reported which investigate this in detail. Cross-sectional area (A_D, obtained from surface activity measurements) has been reported as being a useful size descriptor to discriminate compounds which can access the brain ($A_D < 80\,Å^2$) from those that are too large to cross the BBB [62]. Similar studies have been performed to define a cut-off for oral absorption [63].

1.7 Hydrogen Bonding

Molecular size and hydrogen bonding have been unraveled as the two major components of log P or log D [52, 64, 65]. In recent years it has been found that the

hydrogen bonding capacity of a drug solute correlates reasonably well with passive diffusion. Initially Δ log P, the difference between octanol/water and alkane/water partitioning, was suggested as a good measure for solute H-bonding [42, 64, 66], but this involves tedious experimental work and it seems that calculated descriptors for hydrogen bonding can now be assessed very conveniently.

1.7.1 Calculated Hydrogen-Bonding Descriptors

Considerable interest is focused on the calculation of hydrogen-bonding capability for use in QSAR studies, for the design of combinatorial libraries, and for the correlation of absorption and permeability data [67–70]. A number of different descriptors for hydrogen bonding have been discussed [71], one of the simplest being the count of the number of hydrogen bond-forming atoms [72].

A simple measure of hydrogen-bonding capacity is polar surface area, summing the fractional contributions to surface area of all nitrogen and oxygen atoms [73]. This was used to predict passage through the BBB [43, 74, 75], flux across a Caco-2 monolayer [76] (Eq. 2), and human intestinal absorption [77, 78]. The physical explanation is that polar groups are involved in desolvation when they move from an aqueous extracellular environment to the more lipophilic interior of membranes. The polar surface area (PSA) thus represents at least part of the energy involved in membrane transport. PSA is dependent on the conformation, and the original method [73] is based on a single minimum energy conformation. Others [77] have taken into account conformational flexibility and coined a dynamic PSA, in which a Boltzmann-weighted average PSA is computed. However, it has been shown that PSA calculated for a single minimum energy conformation is in most cases sufficient to produce a sigmoidal relationship to intestinal absorption, differing very little from the dynamic PSA described above (see Fig. 1.1) [78]. Recently, a rapid calculation of PSA as a sum of fragment-based contributions has been published [79], allowing these calculations to be used for large datasets such as combinatorial or virtual libraries. The sigmoidal relationship can be described by $A\% = 100/[1 + (PSA/PSA_{50})^{\gamma}]$, where A% is percentage of orally absorbed drug, PSA_{50} is the PSA at 50% absorption level, and γ is a regression coefficient [80]. Others have used a Boltzmann sigmoidal curve given by $y = \text{bottom} + (\text{top} - \text{bottom})/(1 + \exp((x_{50} - x)/\text{slope}))$ [78].

Poorly absorbed compounds have been identified as those with a PSA $> 140\,\text{Å}^2$, but considerably more scatter was found around the sigmoidal curve observed for a smaller set of compounds [78]. This is partly due to the fact that many compounds do not show only simple passive diffusion, but are also affected by active carriers, efflux mechanisms involving P-glycoprotein (P-gp) and other transporter proteins, as well as gut wall metabolism. A further refinement in the PSA approach is expected to come from taking into account the strength of the hydrogen bonds, which in principle already is the basis of the HYBOT approach described below.

Tab. 1.2. *In-vitro* models for membrane permeability.

Permeability model	*Reference*
Octanol/water distribution	
Phospholipid veshicles	109
Liposome binding	102, 103
IAM – immobilized artificial membranes	90, 91
ILC – immobilized liposome chromatography	96
Impregnated (or artificial) membranes	76
PAMPA	82
Filter IAM	84–86
Micellar electrokinetic chromatography (MEKC)	98
Transil particles	105, 106
SPR biosensor	107
Hexadecane-coated polycarbonate filters	87, 88
Biopartitioning micellar chromatography (BMC)	99

1.8 Amphiphilicity

A combination of the hydrophilic and hydrophobic parts of a molecule defines that molecule's amphiphilicity. A program has been described to calculate this property and calibrated against experimental values obtained from surface activity measurements [81]. It is possible that these values may be used to predict the effect on membranes leading to cytotoxicity or phospholipidosis, but they may also contain information (yet to be unraveled) on permeability.

1.9 Permeability

1.9.1 Artificial Membranes

When screening for absorption by passive membrane permeability (Table 1.2) artificial membranes have the advantage of offering a highly reproducible and high-throughput system. Artificial membranes have been compared with Caco-2 cells [76], and in passive diffusion studies they behave very similarly. This has formed the focus of a parallel artificial membrane permeation assay (PAMPA) for rapid prediction of transcellular absorption potential [82, 83]. In this system, the permeability of a molecule through a membrane formed by a mixture of lecithin and an inert organic solvent on a hydrophobic filter support was assessed. Although not completely predictive, the PAMPA identifies definite trends in the ability of a molecule to permeate membranes by passive diffusion, and this may be valuable in screening large compound libraries. This system is now commercially available

[84], and further optimization of the experimental conditions have been investigated [85, 86]. Predictability increases when a pH of 6.5 or 5.5 is used on the donor side [86]. It was also shown that a co-solvent such as dimethyl sulfoxide (DMSO) can have a marked effect depending on the nature – whether basic or acidic – of the compound [86].

A similar system has been reported based on polycarbonate filters coated with hexadecane [87, 88]. This system consists of a 9–10 μm hexadecane liquid layer immobilized between two aqueous compartments. In this set up, the rate at which lipophilic compounds were seen to diffuse through the unstirred water layer became rate-limiting. In order to mimic the *in vivo* environment permeability, measurements were repeated at different pH values in the range 4–8, and the highest transport value was used for correlation with the percentage absorbed in humans. This provides a sigmoidal dependence – which is better than measuring values at a single pH such as 6.8.

Hydrogen-bonding ability assessed as the difference in partition coefficients of drugs at pH 6.0 between polar (diethyl ether and chloroform) and nonpolar (isooctane) solvents has been measured [89]. Adsorption of drugs to a cation-exchange resin was used as an index for electricity (polarity). Permeation rates across a silicon or ethylenevinyl acetate copolymer (EVA) artificial membrane was combined with the above descriptors using multiple linear regression (MLR) and gives reasonable correlations ($r = 0.88$) with in-situ single-pass perfusion data in rats. However, this approach should be explored more fully in humans.

1.9.2 IAM, ILC, MEKC, and BMC

Immobilized artificial membranes (IAM) are another means of measuring lipophilic characteristics of drug candidates and other chemicals [90–94]. IAM columns may better mimic membrane interactions than the isotropic octanol/water or other solvent/solvent partitioning system. These chromatographic indices appear to be a significant predictor of passive absorption through the rat intestine [95].

Immobilized liposome chromatography (ILC) is an (albeit related) alternative to IAM [96, 97]. Compounds with the same log P were shown to have very different degrees of membrane partitioning on ILC, depending on the charge of the compound [97].

Another relatively new lipophilicity scale proposed for use in ADME studies is based on micellar electrokinetic chromatography (MEKC) [98], while a further variant known as biopartitioning micellar chromatography (BMC) uses mobile phases of Brij35 [polyoxyethylene(23)lauryl ether] [99]. The retention factors of 16 beta-blockers obtained with BMC using sodium dodecyl sulfate as the micelle-forming agent correlated well with the permeability coefficients in Caco-2 monolayers and apparent permeability coefficients in rat intestinal segments [100].

Each of these scales produced a lipophilicity index that was related to – but not identical to – that obtained with octanol/water partitioning.

1.9.3 Liposome Partitioning

Liposomes, which are lipid bilayer vesicles prepared from mixtures of lipids, also provide a useful tool for studying passive permeability of molecules through lipid. For example, this system has been used to demonstrate the passive nature of the absorption mechanism of monocarboxylic acids [101].

Liposome partitioning of ionizable drugs can be determined by titration, and has been correlated with human absorption [102–104]. A new absorption potential parameter has been suggested, as calculated from liposome distribution data and the solubility–dose ratio, which shows an excellent sigmoidal relationship with human passive intestinal absorption (Eq. 2) [102, 103].

$$AP_{SUV} = \log(\text{distribution} \times \text{solubility} \times V/\text{dose}) \quad (2)$$

Here, AP_{SUV} is the absorption potential measured from the distribution in small unilamellar vesicles (SUV) at pH 6.8, the solubility was measured at pH 6.8 in simulated intestinal fluid, V is the volume of intestinal fluid, and dose is a mean single oral dose. Liposome partitioning is only partly correlated with octanol/water distribution.

A further partition system based on the use of liposomes, and marketed as Transil®, has also been investigated [105, 106].

1.9.4 Biosensors

Following the attachment of liposomes to a biosensor surface, the interactions between a drugs and the liposomes can be monitored directly using surface plasmon resonance (SPR) technology. SPR measures changes in the refractive index at the sensor surface caused by changes in mass, and in this way drug–liposome interactions have been measured for 27 drugs and compared with the fraction absorbed in humans [107]. A reasonable correlation was obtained, but it most likely that the SPR method represents simply another way of measuring ''lipophilicity''. The throughput was 100 substances in 24 h, but this may be improved as the system undergoes further development.

1.9.5 Ghost Erythrocytes and Diffusion Constants

Several mechanisms are involved in the permeability through Caco-2 cells. In order to obtain a more pure measure of membrane permeability, an experimental method based on ghost erythrocytes (red blood cells which have been emptied of their intracellular content) and diffusion constant measurements using nuclear magnetic resonance (NMR) has been proposed [108].

References

1 Smith, D. A., Jones, B. C., Walker, D. K., Design of drugs involving the concepts and theories of drug metabolism and pharmacokinetics, *Med. Res. Rev.* **1996**, *16*, 243–266.

2 Van de Waterbeemd, H., Smith, D. A., Beaumont, K., Walker, D. K., Property-based design: optimisation of drug absorption and pharmacokinetics, *J. Med. Chem.* **2001**, *44*, 1313–1333.

3 Smith, D. A., Van de Waterbeemd, H., Walker, D. A., *Pharmacokinetics and Metabolism in Drug Design*, Wiley-VCH, Weinheim, 2001.

4 Ajay, Walters, W. P., Murcko, M. A., Can we learn to distinguish between drug-like and nondrug-like molecules? *J. Med. Chem.* **1998**, *41*, 3314–3324.

5 Sadowski, J., Kubinyi, H., A scoring scheme for discriminating between drugs and nondrugs, *J. Med. Chem.* **1998**, *41*, 3325–3329.

6 Wagener, M., Van Geerestein, V. J., Potential drugs and nondrugs: prediction and identification of important structural features, *J. Chem. Inf. Comput. Sci.* **2000**, *40*, 280–292.

7 Ajay, Bemis, G. W., Murcko, M. A., Designing libraries with CNS activity, *J. Med. Chem.* **1999**, *42*, 4942–4951.

8 Anzali, S., Barnickel, G., Cezanne, B., Krug, M., Filimonov, D., Poroikov, V., Discriminating between drugs and nondrugs by prediction of activity spectra for substances (PASS), *J. Med. Chem.* **2001**, *44*, 2432–2437.

9 Lipinski, C. A., Lombardo, F., Dominy, B. W., Feeney, P. J., Experimental and computational approaches to estimate solubility and permeability in drug discovery and development settings, *Adv. Drug Del. Rev.* **1997**, *23*, 3–25.

10 Lipinski, C., Drug-like properties and the causes of poor solubility and poor permeability, *J. Pharmacol. Toxicol. Methods* **2000**, *44*, 235–249.

11 Pagliara, A., Resist, M., Geinoz, S., Carrupt, P.-A., Testa, B., Evaluation and prediction of drug permeation, *J. Pharm. Pharmacol.* **1999**, *51*, 1339–1357.

12 Stenberg, P., Luthman, K., Ellens, H., Lee, C. P., Smith, Ph. L., Lago, A., Elliott, J. D., Artursson, P., Prediction of the intestinal absorption of endothelin receptor antagonists using three theoretical methods of increasing complexity, *Pharm. Res.* **1999**, *16*, 1520–1526.

13 Ghose, A. K., Viswanadhan, V. N., Wendoloski, J. J., A knowledge-based approach in designing combinatorial or medicinal chemistry libraries for drug discovery. 1. A qualitative and quantitative characterization of known drug databases, *J. Comb. Chem.* **1999**, *1*, 55–68.

14 Oprea, T. L., Property distribution of drug-related chemical databases, *J. Comput.-Aided Mol. Des.* **2000**, *14*, 251–264.

15 Blake, J. F., Chemoinformatics – predicting the physicochemical properties of drug-like molecules, *Curr. Opin. Biotechnol.* **2000**, *11*, 104–107.

16 Matter, H., Baringhaus, K. H., Naumann, T., Klabunde, T., Pirard, B., Computational approaches towards the rational design of drug-like compound libraries, *Combinat. Chem. High Throughput Scr.* **2001**, *4*, 453–475.

17 Vacca, J. P., Dorsey, B. D., Schleif, W. A., Levin, R. B., McDaniel, S. L., Darke, P. L., Zugay, J., Quintero, J. C., Blahy, O. M., Roth, E., Sardana, V. V., Schlabach, A. J., Graham, P. L., Condra, J. H., Gotlib, L., Holloway, M. K., Lin, J., Chen, I. W., Vastag, K., Ostovic, D., Anderson, P. S., Emini, E. A., Huff, J. R., L-735,524: an orally bioavailable human immunodeficiency virus type 1 protease inhibitor, *Proc. Natl. Acad. Sci. USA* **1994**, *91*, 4096–4100.

18 Johnson, K., Swindell, A., Guidance in the setting of drug particle size specifications to minimize variability in absorption, *Pharm. Res.* **1996**, *13*, 1795–1798.

19 Curatolo, W., Physical chemical properties of oral drug candidates in the discovery and exploratory development settings, *Pharm. Sci. Technol. Today* **1998**, *1*, 387–393.

20 Bevan, C. D., Lloyd, R. S., A high-throughput screening method for the determination of aqueous drug solubility using laser nephelometry in microtiter plates, *Anal. Chem.* **2000**, *72*, 1781–1787.

21 Avdeef, A., High-throughput measurements of solubility profiles, in: *Pharmacokinetic Optimization in Drug Research; Biological, Physicochemical and Computational Strategies.* Testa, B., Van de Waterbeemd, H., Folkers, G., Guy, R. (eds), Wiley-VCH, Weinheim & Verlag HCA, Zurich, **2001**, pp. 305–325.

22 Avdeef, A., Berger, C. M., pH-metric solubility. 3. Dissolution titration template method for solubility determination, *Eur. J. Pharm. Sci.* **2001**, *14*, 281–291.

23 Dressman, J. B., Amidon, G. L., Reppas, C., Shah, V. P., Dissolution testing as a prognostic tool for oral drug absorption: immediate release dosage forms, *Pharm. Res.* **1998**, *15*, 11–22.

24 Amidon, G. L., Lennernäs, H., Shah, V. P., Crison, J. R. A., A theoretical basis for a biopharmaceutic drug classification: the correlation of in vitro drug product dissolution and in vivo bioavailability, *Pharm. Res.* **1995**, *12*, 413–420.

25 Van de Waterbeemd, H., The fundamental variables of the biopharmaceutics classification system (BCS): a commentary, *Eur. J. Pharm. Sci.* **1998**, *7*, 1–3.

26 Huuskonen, J., Estimation of aqueous solubility in drug design, *Comb. Chem. High Throughput Scr.* **2001**, *4*, 311–316.

27 McFarland, J. W., Avdeef, A., Berger, C. M., Raevsky, O. A., Estimating the water solubilities of crystalline compounds from their chemical structures alone, *J. Chem. Inf. Comput. Sci.* **2001**, *41*, 1355–1359.

28 Livingstone, D. J., Ford, M. G., Huuskonen, J. J., Salt, D. W., Simultaneous prediction of aqueous solubility and octanol/water partition coefficient based on descriptors derived from molecular structure, *J. Comput.-Aided Mol. Des.* **2001**, *15*, 741–752.

29 Bruneau, P., Search for predictive generic model of aqueous solubility using Bayesian neural nets, *J. Chem. Inf. Comput. Sci.* **2001**, *41*, 1605–1616.

30 Liu, R., So, S.-S., Development of quantitative structure–property relationship models for early ADME evaluation in drug discovery. 1. Aqueous solubility, *J. Chem. Inf. Comput. Sci.* **2001**, *4*, 1633–1639.

31 Van de Waterbeemd, H., High-throughput and in silico techniques in drug metabolism and pharmacokinetics, *Curr. Opin. Drug Dis. Dev.* **2002**, *5*, 33–43.

32 Caron, G., Gaillard, P., Carrupt, P. A., Testa, B., Lipophilicity behavior of model and medicinal compounds containing a sulfide, sulfoxide, or sulfone moiety, *Helv. Chim. Acta* **1997**, *80*, 449–461.

33 Camenisch, G., Van de Waterbeemd, H., Folkers, G., Review of theoretical passive drug absorption models: historical background, recent development and limitations, *Pharm. Acta. Helv.* **1996**, *71*, 309–327.

34 Boisset, M., Botham, R. P., Haegele, K. D., Lenfant, B., Pachot, J. L., Absorption of angiotensin II antagonists in Ussing chambers, Caco-2, perfused jejunum loop and in vivo: importance of drug ionization in the in vitro prediction of in vivo absorption, *Eur. J. Pharm. Sci.* **2000**, *10*, 215–224.

35 Palm, K., Luthman, K., Ros, J., Grasjo, J., Artursson, P., Effect of molecular charge on intestinal epithelial drug transport: pH-dependent transport of cationic drugs, *J. Pharmacol. Exp. Ther.* **1999**, *291*, 435–443.

36 Saurina, J., Hernandez-Cassou, S.,

Tauler, R., Izquierdo-Ridorsa, A., Spectrophotometric determination of pK_a values based on a pH gradient flow-injection system, *Anal. Chim. Acta* **2000**, *408*, 135–143.

37 Jia, Z., Ramstad, T., Zhong, M., Medium-throughput pK_a screening of pharmaceuticals by pressure-assisted capillary electrophoresis, *Electrophoresis* **2001**, *22*, 1112–1118.

38 Comer, J., Tam, K., Lipophilicity profiles: theory and measurement, in: *Pharmacokinetic Optimization in Drug Research; Biological, Physicochemical and Computational Strategies*. Testa, B., Van de Waterbeemd, H., Folkers, G., Guy, R. (eds), Wiley-VCH, Weinheim & Verlag HCA, Zurich, **2001**, pp. 275–304.

39 Caron, G., Reymond, F., Carrupt, P. A., Girault, H. H., Testa, B., Combined molecular lipophilicity descriptors and their role in understanding intramolecular effects, *Pharm. Sci. Technol. Today* **1999**, *2*, 327–335.

40 Winiwarter, S., Bonham, N. M., Ax, F., Hallberg, A., Lennernäs, H., Karlen, A., Correlation of human jejunal permeability (in vivo) of drugs with experimentally and theoretically derived parameters. A multivariate data analysis approach, *J. Med. Chem.* **1998**, *41*, 4939–4949.

41 Artursson, P., Karlsson, J., Correlation between oral drug absorption in humans and apparent drug permeability coefficients in human intestinal epithelial (Caco-2) cells, *Biochem. Biophys. Res. Commun.* **1991**, *175*, 880–885.

42 Young, R. C., Mitchell, R. C., Brown, Th. H., Ganellin, C. R., Griffiths, R., Jones, M., Rana, K. K., Saunders, D., Smith, I. R., Sore, N. E., Wilks, T. J., Development of a new physicochemical model for brain penetration and its application to the design of centrally acting H2 receptor histamine antagonists, *J. Med. Chem.* **1988**, *31*, 656–671.

43 Van de Waterbeemd, H., Camenisch, G., Folkers, G., Chrétien, J. R., Raevsky, O. A., Estimation of blood–brain barrier crossing of drugs using molecular size and shape, and H-bonding descriptors, *J. Drug Target.* **1998**, *2*, 151–165.

44 Pliska, V., Testa, B., Van de Waterbeemd, H. (eds), *Lipophilicity in Drug Action and Toxicology*. VCH, Weinheim, **1996**.

45 Testa, B., Van de Waterbeemd, H., Folkers, G., Guy, R. (eds), *Pharmacokinetic Optimization in Drug Research*. Wiley-VCH, Weinheim and VHCA, Zurich, **2001**.

46 Hitzel, L., Watt, A. P., Locker, K. L., An increased throughput method for the determination of partition coefficients, *Pharm. Res.* **2000**, *17*, 1389–1395.

47 Chait, A., Zaslavsky, B., ALOGP – A new automated log P direct partitioning workstation, *LogP2000*, Lausanne, **2000**, Switzerland. Abstracts book, p. O-C5.

48 Avdeef, A., pH-Metric log P. II: Refinement of partition coefficients and ionization constants of multiprotic substances, *J. Pharm. Sci.* **1993**, *82*, 183–190.

49 Leahy, D. E., Morris, J. J., Taylor, P. J., Wait, A. R., Membranes and their models: towards a rational choice of partitioning system, in: *QSAR: Rational Approaches to the Design of Bioactive Compounds*. Silipo, C., Vittoria, A. (eds), Elsevier, Amsterdam, **1991**, pp. 75–82.

50 Steyeart, G., Lisa, G., Gaillard, P., Boss, G., Reymond, F., Girault, H. H., Carrupt, P. A., Testa, B., Intermolecular forces expressed in 1,2-dichloroethane-water partition coefficients. A solvatochromic analysis, *J. Chem. Soc. Faraday Trans.* **1997**, *93*, 401–406.

51 Caron, G., Steyaert, G., Pagliara, A., Reymond, F., Crivori, P., Gaillard, P., Carrupt, P. A., Avdeef, A., Comer, J., Box, K. J., Girault, H. H., Testa, B., Structure–lipophilicity relationships of neutral and protonated β-blockers. Part 1. Intra- and intermolecular effects in

isotropic solvent systems, *Helv. Chim. Acta* **1999**, *82*, 1211–1222.

52 Van de Waterbeemd, H., Testa, B., The parametrization of lipophilicity and other structural properties in drug design, *Adv. Drug Res.* **1987**, *16*, 85–225.

53 Buchwald, P., Bodor, N., Octanol-water partition: searching for predictive models, *Curr. Med. Chem.* **1998**, *5*, 353–380.

54 Carrupt, P. A., Testa, B., Gaillard, P., Computational approaches to lipophilicity: methods and applications, *Rev. Comp. Chem.* **1997**, *11*, 241–315.

55 Mannhold, R., Van de Waterbeemd, H., Substructure and whole molecule approaches for calculating log P, *J. Comput.-Aided Mol. Des.* **2001**, *15*, 337–354.

56 Wildman, S. A., Crippen, G. M., Prediction of physicochemical parameters by atomic contributions, *J. Chem. Inf. Comput. Sci.* **1999**, *39*, 868–873.

57 Nicklin, P. L., Irwin, W. J., Timmins, P., Morrison, R. A., Uptake and transport of the ACE-inhibitor ceronapril (SQ 29852) by monolayers of human intestinal absorptive (Caco-2) cells in vitro, *Int. J. Pharmaceut.* **1996**, *140*, 175–183.

58 Spessard, G. O., ACD Labs/log P dB 3.5 and ChemSketch 3.5, *J. Chem. Inf. Comput. Sci.* **1998**, *38*, 1250–1253.

59 Leo, A. J., Hoekman, D., Calculating log P(oct) with no missing fragments: the problem of estimating new interaction parameters, *Perspect. Drug Discov. Des.* **2000**, *18*, 19–38.

60 Mannhold, R., Rekker, R. F., The hydrophobic fragmental constant approach for calculating log P in octanol/water and aliphatic hydrocarbon/water systems, *Perspect. Drug Disc. Des.* **2000**, *18*, 1–18.

61 Chan, O. H., Stewart, B. H., Physicochemical and drug-delivery considerations for oral drug bioavailability, *Drug Discov. Today* **1996**, *1*, 461–473.

62 Fischer, H., Gottschlich, R., Seelig, A., Blood–brain barrier permeation: molecular parameters governing passive diffusion, *J. Membr. Biol.* **1998**, *165*, 201–211.

63 Fischer, H., *Passive diffusion and active transport through biological membranes – Binding of drugs to transmembrane receptors*, PhD Thesis, **1998**, University of Basel, Switzerland.

64 El Tayar, N., Testa, B., Carrupt, P. A., Polar intermolecular interactions encoded in partition coefficients: an indirect estimation of hydrogen-bond parameters of polyfunctional solutes, *J. Phys. Chem.* **1992**, *96*, 1455–1459.

65 Abraham, M. H., Chadha, H. S., Applications of a solvation equation to drug transport properties, in: *Lipophilicity in Drug Action and Toxicology*. Pliska, V., Testa, B., Van de Waterbeemd, H. (eds), VCH, Weinheim, Germany, **1996**, pp. 311–337.

66 Von Geldern, T. W., Hoffmann, D. J., Kester, J. A., Nellans, H. N., Dayton, B. D., Calzadilla, S. V., Marsch, K. C., Hernandez, L., Chiou, W., Dixon, D. B., Wu-Wong, J. R., Opgenorth, T. J., Azole endothelin antagonists. 3. Using Δ log P as a tool to improve absorption, *J. Med. Chem.* **1996**, *39*, 982–991.

67 Dearden, J. C., Ghafourian, T., Hydrogen bonding parameters for QSAR: comparison of indicator variables, hydrogen bond counts, molecular orbital and other parameters, *J. Chem. Inf. Comput. Sci.* **1999**, *39*, 231–235.

68 Raevsky, O. A., Schaper, K.-J., Quantitative estimation of hydrogen bond contribution to permeability and absorption processes of some chemicals and drugs, *Eur. J. Med. Chem.* **1998**, *33*, 799–807.

69 Raevsky, O. A., Fetisov, V. I., Trepalina, E. P., McFarland, J. W., Schaper, K.-J., Quantitative estimation of drug absorption in humans for passively transported

compounds on the basis of their physico-chemical parameters, *Quant. Struct.-Act. Relat.* **2000**, *19*, 366–374.

70 Van de Waterbeemd, H., Camenisch, G., Folkers, G., Raevsky, O. A., Estimation of Caco-2 cell permeability using calculated molecular descriptors, *Quant. Struct.-Act. Relat.* **1996**, *15*, 480–490.

71 Van de Waterbeemd, H., Intestinal permeability: prediction from theory, in: *Oral Drug Absorption*. Dressman, J. B., Lennernäs, H. (eds), Dekker, New York, **2000**, pp. 31–49.

72 Österberg, Th., Norinder, U., Prediction of polar surface area and drug transport processes using simple parameters and PLS statistics, *J. Chem. Inf. Comput. Sci.* **2000**, *40*, 1408–1411.

73 Van de Waterbeemd, H., Kansy, M., Hydrogen-bonding capacity and brain penetration, *Chimia* **1992**, *46*, 299–303.

74 Kelder, J., Grootenhuis, P. D. J., Bayada, D. M., Delbressine, L. P. C., Ploemen, J.-P., Polar molecular surface as a dominating determinant for oral absorption and brain penetration of drugs, *Pharm. Res.* **1999**, *16*, 1514–1519.

75 Clark, D. E., Rapid calculation of polar molecular surface area and its application to the prediction of transport phenomena. 2. Prediction of blood–brain barrier penetration, *J. Pharm. Sci.* **1999**, *88*, 815–821.

76 Camenisch, G., Folkers, G., Van de Waterbeemd, H., Comparison of passive drug transport through Caco-2 cells and artificial membranes, *Int. J. Pharmaceut.* **1997**, *147*, 61–70.

77 Palm, K., Luthman, K., Ungell, A.-L., Strandlund, G., Beigi, F., Lundahl, P., Artursson, P., Evaluation of dynamic polar molecular surface area as predictor of drug absorption: comparison with other computational and experimental predictors, *J. Med. Chem.* **1998**, *41*, 5382–5392.

78 Clark, D. E., Rapid calculation of polar molecular surface area and its application to the prediction of transport phenomena. 1. Prediction of intestinal absorption, *J. Pharm. Sci.* **1999**, *88*, 807–814.

79 Ertl, P., Rohde, B., Selzer, P., Fast calculation of molecular polar surface area as a sum of fragment-based contributions and its application to the prediction of drug transport properties, *J. Med. Chem.* **2000**, *43*, 3714–3717.

80 Stenberg, P., Norinder, U., Luthman, K., Artursson, P., Experimental and computational screening models for the prediction of intestinal drug absorption, *J. Med. Chem.* **2001**, *44*, 1927–1937.

81 Fischer, H., Kansy, M., Bur, D., CAFCA: a novel tool for the calculation of amphiphilic properties of charged drug molecules, *Chimia* **2000**, *54*, 640–645.

82 Kansy, M., Senner, F., Gubernator, K., Physicochemical high throughput screening: parallel artificial membrane permeation assay in the description of passive absorption processes, *J. Med. Chem.* **1998**, *41*, 1007–1010.

83 Kansy, M., Fischer, H., Kratzat, K., Senner, F., Wagner, B., Parrilla, I., High-throughput artificial membrane permeability studies in early lead discovery and development, in: *Pharmacokinetic Optimization in Drug Research; Biological, Physicochemical and Computational Strategies*. Testa, B., Van de Waterbeemd, H., Folkers, G., Guy, R. (eds), Wiley-VCH, Weinheim and Verlag HCA, Zurich, **2001**, pp. 447–464.

84 Avdeef, A., Strafford, M., Block, E., Balogh, M. P., Chambliss, W., Khan, I., Drug absorption in vitro model: filter-immobilized artificial membranes 2. Studies of the permeability properties of lactones in *Piper methysticum* Forst, *Eur. J. Pharm. Sci.* **2001**, *14*, 271–280.

85 Sugano, K., Hamada, H., Machida, M., Ushio, H., High throughput prediction of oral absorption: improvement of the composition of the lipid solution used in parallel

artificial membrane permeation assay, *J. Biomol. Screen.* **2001**, *6*, 189–196.

86 Sugano, K., Hamada, H., Machida, M., Ushio, H., Saitoh, K., Terada, K., Optimised conditions of bio-mimetic artificial membrane permeation assay, *Int. J. Pharm.* **2001**, *228*, 181–188.

87 Faller, B., Wohnsland, F., Physicochemical parameters as tools in drug discovery and lead optimization, in: *Pharmacokinetic Optimization in Drug Research; Biological, Physicochemical and Computational Strategies*. Testa, B., Van de Waterbeemd, H., Folkers, G., Guy, R. (eds), Wiley-VCH, Weinheim and Verlag HCA, Zurich, **2001**, pp. 251–274.

88 Wohnsland, F., Faller, B., High-throughput permeability pH profile and high-throughput alkane/water log P with artificial membranes, *J. Med. Chem.* **2001**, *44*, 923–930.

89 Sugawara, M., Takekuma, Y., Yamada, H., Kobayashi, M., Iseki, K., Miyazaki, K., A general approach for the prediction of the intestinal absorption of drugs: regression analysis using the physicochemical properties and drug-membrane electrostatic interaction, *J. Pharm. Sci.* **1998**, *87*, 960–966.

90 Yang, C. Y., Cai, S. J., Liu, H., Pidgeon, C., Immobilized artificial membranes – screens for drug–membrane interactions, *Adv. Drug Del. Rev.* **1996**, *23*, 229–256.

91 Ong, S., Liu, H., Pidgeon, C., Immobilized-artificial-membrane chromatography: measurements of membrane partition coefficient and predicting drug membrane permeability, *J. Chromatogr. A.* **1996**, *728*, 113–128.

92 Stewart, B. H., Chan, O. H., Use of immobilized artificial membrane chromatography for drug transport applications, *J. Pharm. Sci.* **1998**, *87*, 1471–1478.

93 Ducarne, A., Neuweis, M., Goldstein, S., Massingham, R., IAM retention and blood brain barrier penetration, *Eur. J. Med. Chem.* **1998**, *33*, 215–223.

94 Reichel, A., Begley, D. J., Potential of immobilized artificial membranes for predicting drug penetration across the blood–brain barrier, *Pharm. Res.* **1998**, *15*, 1270–1274.

95 Genty, M., Gonzalez, G., Clere, C., Desangle-Gouty, V., Legendre, J.-Y., Determination of the passive absorption through the rat intestine using chromatographic indices and molar volume, *Eur. J. Pharm. Sci.* **2001**, *12*, 223–229.

96 Lundahl, P., Beigi, F., Immobilized liposome chromatography of drugs for model analysis of drug–membrane interactions, *Adv. Drug Deliv. Rev.* **1997**, *23*, 221–227.

97 Norinder, U., Österberg, Th., The applicability of computational chemistry in the evaluation and prediction of drug transport properties, *Perspect. Drug Disc. Des.* **2000**, *19*, 1–18.

98 Trone, M. D., Leonard, M. S., Khaledi, M. G., Congeneric behavior in estimations of octanol-water partition coefficients by micellar electrokinetic chromatography, *Anal. Chem.* **2000**, *72*, 1228–1235.

99 Molero-Monfort, M., Escuder-Gilabert, L., Villanueva-Camanoas, Sagrado, S., Medina-Hernandez, M. J., Biopartitioning micellar chromatography: an in vitro technique for predicting human drug absorption, *J. Chromatogr. B* **2001**, *753*, 225–236.

100 Detroyer, A., VanderHeyden, Y., Cardo-Broch, S., Garcia-Alvarez-Coque, M. C., Massart, D. L., Quantitative structure–retention and retention–activity relationships of β-blocking agents by micellar liquid chromatography, *J. Chromatogr. A.* **2001**, *912*, 211–221.

101 Takagi, M., Taki, Y., Sakane, T., Nadai, T., Sezaki, H., Oku, N., Yamashita, S., A new interpretation of salicylic acid transport across the lipid bilayer: implications of pH-dependent but not carrier-mediated absorption from the gastrointestinal

tract, *J. Pharmacol. Exp. Ther.* **1998**, *285*, 1175–1180.

102 Balon, K., Riebesehl, B. U., Muller, B. W., Drug liposome partitioning as a tool for the prediction of human passive intestinal absorption, *Pharm. Res.* **1999**, *16*, 882–888.

103 Balon, K., Riebesehl, B. U., Muller, B. W., Determination of liposome partitioning of ionizable drugs by titration, *J. Pharm. Sci.* **1999**, *88*, 802–806.

104 Avdeef, A., Box, K. J., Comer, J. E. A., Hibbert, C., Tam, K. Y., pH-Metric log P 10. Determination of liposomal membrane-water partition coefficients of ionizable drugs, *Pharm. Res.* **1998**, *15*, 209–215.

105 Escher, B. I., Schwarzenbach, R. P., Westall, J. C., Evaluation of liposome-water partitioning of organic acids and bases. 2. Comparison of experimental determination methods, *Environ. Sci. Technol.* **2000**, *34*, 3962–3968.

106 Loidl-Stahlhofen, A., Eckrt, A., Hartmann, T., Schottner, M., Solid-supported lipid membranes as a tool for determination of membrane affinity: high-throughput screening pf a physicochemical parameter, *J. Pharm. Sci.* **2001**, *90*, 599–606.

107 Danelian, E., Karlén, A., Karlsson, R., Winiwarter, S., Hansson, A., Löfås, S. Lennernäs, H., Hämäläinen, D., SPR biosensor studies of the direct interaction between 27 drugs and a liposome surface: correlations with fraction absorbed in humans, *J. Med. Chem.* **2000**, *43*, 2083–2086.

108 Zamora, I., Oprea, T. I., Ungell, A.-L., Prediction of oral drug permeability, in *Rational Approaches to Drug Design.* Höltje, H.-D., Sippl, W. (eds) *Prous Science, Barcelona*, **2001**, pp. 271–280.

109 Austin, R. P., Davis, A. M., Manners, C. N., Partitioning of ionising molecules between aqueous buffers and phospholipid vesicles, *J. Pharm. Sci.*, **1995**, *84*, 1180–1183.

2
High-throughput Measurement of log D and pK_a

John E. A. Comer

Abbreviations

ADME	Absorption, distribution, metabolism, elimination (excretion)
CHI	Chromatographic hydrophobicity index
DMSO	Dimethyl sulfoxide
MEEKC	Microemulsion electrokinetic chromatography
TFA	Target factor analysis

Symbols

β	Cumulative ionization constant (stability constant)
CLOGP	Logarithm of the calculated octanol/water partition coefficient (for neutral species)
log k	Chromatographic capacity factor
Δ log P	Difference between log P in octanol/water and alkane/water
log D	Logarithm of the distribution coefficient in octanol/water at pH 7.4
log P	Logarithm of the partition coefficient in octanol/water (for neutral species)
log P^1	Logarithm of the partition coefficient of a given compound in octanol/water in its monoprotonated form
log P^0	Logarithm of the partition coefficient of a given compound in octanol/water in its unprotonated form (It will be stated when log P or log D refers to other pH conditions or solvent systems)
MW	Molecular weight
pK_a	Ionization constant in water
p_oK_a	Apparent ionization constant in water/octanol system
S	Solubility
V	Volume

Drug Bioavailability: Estimation of Solubility, Permeability, Absorption and Bioavailability.
Edited by Han van de Waterbeemd, Hans Lennernäs and Per Artursson

ISBN: 3-527-30438-X

2.1 Introduction

During the discovery and development of new drugs, it is typical to start with a large number of newly discovered molecules and to test them against biochemical targets. Those which show activity may be considered as candidates for further development. It is now widely thought that the next stage in compound selection is to identify those which are more likely to be absorbed and distributed in the body. While a number of routes exist for absorption of drugs through membranes and tissues, transport by passive diffusion is the most common. To be absorbed by this route, drugs must be sufficiently lipophilic to penetrate the lipid cores of membranes, but not so lipophilic that they get stuck there. Lipophilicity is usually expressed by the octanol/water partition coefficient (log P) or distribution coefficient (log D). Although octanol/water partitioning is a surrogate for interaction of drugs with true membranes, it has proved a remarkably enduring concept – probably because it is relatively easy and quick to measure – and because the information encoded is "good enough" to make useful approximations about a drug's behavior.

Most drugs are ionized in aqueous solution (Table 2.1), and can therefore exist in a neutral or a charged state, depending on the pH of the local environment. Molecules are more lipophilic when neutral than when charged. Ionization is expressed by the aqueous ionization constant, pK_a. As pointed out below, log D is a pK_a-dependent term for ionizable drugs. Permeability and aqueous solubility are also pK_a-dependent. Lipophilicity, pK_a, permeability through artificial membranes and

Tab. 2.1. Number of ionizable drugs in World Drug Index 1999.

Total number of drugs in study (ionizable and non-ionizable)	51,596
Percentage which are ionizable	62.9% of total
Percentage of acids with …	
1 acid group, no base	11.6
2+ acid, no base	2.9
Percentage of bases with …	
1 base, no acid	42.9
2+ base, no acid	24.6
Percentage of ampholytes with …	
1 acid and 1 base	7.5
1 acid and 2+ bases	3.9
1 base and 2+ acids	3.2
Others	3.4

Numbers established via 2D search using Chem-X software of compounds listed in World Drug Index, 1999. With thanks to Tim Mitchell and Ryszard Koblecki, Millennium Pharmaceuticals Ltd., Cambridge, UK.

aqueous solubility are the four principal physico-chemical parameters measured during high-throughput physico-chemical profiling [1], and the underlying philosophy of pharmaceutical profiling has been further explored [2]. A review of physico-chemical profiling showing the relationships between the four parameters has been published [3]. Readers are referred to these reviews for a wider understanding of the importance of log D and pK_a and their inter-dependence.

The difficulty of designing active molecules, coupled with commercial pressures to introduce new products, sometimes oblige medicinal chemists to develop drugs that have properties which are not ideal. This can lead to difficulties in development and manufacture, and may result in a costly product failure. It is therefore prudent to discover problematic molecules at an early stage and discontinue them from development. Molecules with appropriate physico-chemical properties may be considered suitable candidates for further development, and most pharmaceutical development groups have in-house rules for assessing these properties. It has been suggested that drugs which fail to meet the "rule-of-5" criteria [4] are unlikely to be absorbed, and should be discontinued from development. One of these rules states that log P should be below 5. Log D values and some suggested implications for drug development are listed in Table 2.2. To obtain high-quality values for physico-chemical properties, it is necessary for them first to be measured, and several methods for the rapid measurement of pK_a and log D have been developed. These methods are reviewed in this chapter.

Tab. 2.2. Log D values and their implications for drug development.

Log D at pH 7.4	*Implications for drug development*
Below 0	Intestinal and CNS permeability problems. Susceptible to renal clearance. If MW $<$ 300, may be absorbed by the slower paracellular route.
0 to 1	May show a good balance between permeability and solubility. At lower values, CNS permeability may suffer.
1 to 3	Probably an optimum range for CNS and non-CNS orally active drugs. Low metabolic liabilities. Generally good CNS penetration.
3 to 5	Solubility tends to become lower. Metabolic liabilities tend to increase.
Above 5	Low solubility and poor oral bioavailability. Erratic absorption. High metabolic liability, although potency may still be high. Basic amines tend to show high to very high V_D (Volume of distribution = ratio of overall tissue binding to plasma protein binding)

Adapted from a slide presented by M. Shalaeva at "New Technologies to Increase Drug Candidate Survivability" Conference, Philadelphia, March 2002.

2.2
Relationship between Ionization and Lipophilicity

Partitioning in a two-phase system such as octanol/water may be depicted in a lipophilicity profile. Figure 2.1 shows lipophilicity profiles for three common classes of ionizable drug, namely a monoprotic base (propranolol), a monoprotic acid (diclofenac), and an ordinary ampholyte (morphine). The curves depicted are shown as solid lines at pH values within 2 pH units of the maximum log D value. At more remote pH values, the molecule may partition in its ionized form, for example as an ion-pair with an inorganic counter-ion. The magnitude of ion-pair partitioning will depend on the ionic strength of the aqueous phase and the lipophilicity of the available counter-ions. As these factors can vary according to the choice of buffer or background electrolyte, the relevant parts of the lipophilicity profiles are shown as dashed lines.

The general form of the equation for lipophilicity profiles is shown below:

$$D_{p[H]} = \frac{P^0 + [H]\beta_1 P^1 + [H]^2\beta_2 P^2 + \cdots}{1 + [H]\beta_1 + [H]^2\beta_2 + \cdots} \quad (1)$$

In this equation, $D_{p[H]}$ represents the distribution coefficient at a particular pH, and may also be expressed as

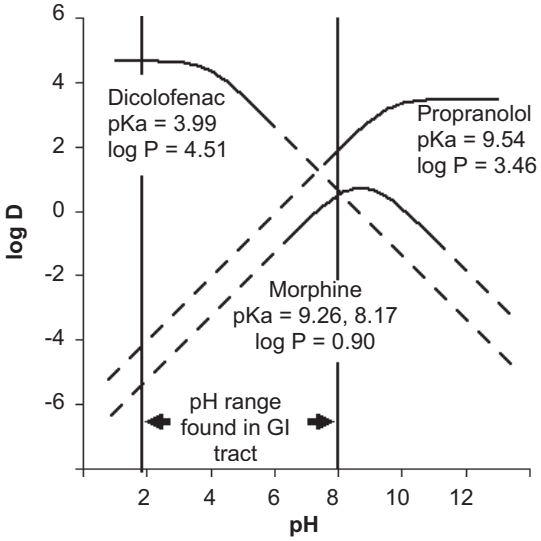

Fig. 2.1. Lipophilicity profiles for diclofenac (acid), propranolol (base) and morphine (ampholyte). Dashed lines indicate the pH range where molecule may partition in its ionized form. Log D for the ionized form will depend on conditions of solution.

$$D_{p[H]} = \frac{[\text{unionized} + \text{ionized species}]_{\text{octanol}}}{[\text{unionized} + \text{ionized species}]_{\text{water}}} \quad (2)$$

The term p[H] represents the pH value of the solution expressed on a concentration scale [5], where [H] represents the concentration of hydrogen ions H^+. P^0 represents the partition coefficient of the unprotonated species, P^1 is the monoprotonated species, and so on. P may also be expressed as

$$P = \frac{[\text{a single species}]_{\text{octanol}}}{[\text{the same species}]_{\text{water}}} \quad (3)$$

The widely used term "log P" refers to the logarithm of the partition coefficient P of the unionized species, which is P^0 for a base with no acidic functions, and P^1 for a monoprotic acid or an ordinary ampholyte. Log P is equal to log D at any pH remote from the pK_a where the molecule exists entirely in its unionized form. Log D at any pH is equal to log P for a non-ionizable molecule.

The terms β_1, β_2 are stability constants, defined as follows for bases:

$$X^0 + H^+ = XH^+ \qquad K_{a1} \qquad K_{a1} = \beta_1$$

$$XH^+ + H^+ = XH_2^{++} \qquad K_{a2} \qquad K_{a1}K_{a2} = \beta_2$$

$$XH_2^{++} + H^+ = XH_3^{+++} \qquad K_{a3} \qquad K_{a1}K_{a2}K_{a3} = \beta_3, \text{ etc}$$

where K_{a1}, K_{a2}, K_{a3}, etc. are ionization constants (similar equations exist for acids and ampholytes). The term "pK_a" is thus

$$pK_a = -\log K_a$$

In view of the relationship between P, D and K_a, it is possible to calculate log D at any pH using Eq. (1) if log P and pK_a values are known. To do so, it is necessary also to know whether the sample is an acid, base or ampholyte, how many pK_as it has, and which ones are acidic and which are basic. The calculation of log D is relatively straightforward for reference samples with only one pK_a, but becomes complicated for development samples which are poorly characterized. Commercial software exists for predicting log P and pK_a values. In this author's experience, the pK_a prediction feature of ACD software (Advanced Chemistry Development Inc. Toronto, Canada) has proved to be a reliable technique of predicting *how many* pK_as a molecule has, and which are acids or bases. While it is possible using software to predict both log P and pK_a *values*, errors are likely in each prediction, which are compounded in the prediction of log D. Although the *in silico* prediction of log D is error-prone, the predicted results are useful in the design of log D assays in order to choose appropriate experimental conditions for measuring different ranges of log D.

2.3 Measuring log D

2.3.1 Shake-flask Method

The classical measurement of log D is by shake-flask experiment. In this method, the sample is dissolved in a flask containing both aqueous buffer solution and partition solvent. The flask is shaken to equilibrate the sample between the two phases, and the phases are then allowed to separate. The pH of the aqueous phase is measured, and the concentration of sample is measured in each phase, generally using high-performance liquid chromatography (HPLC) with ultraviolet (UV) detection. There must be no undissolved substance present in the solutions sampled from either phase. From these values the log D at the experimental pH can be calculated. A lipophilicity profile can be obtained by measuring shake-flask log D at several different pH values without knowing the pK_a value(s). Because of its simplicity and clear relationship to the partitioning phenomenon, the shake-flask method is regarded as a benchmark method against which other methods are validated.

When performed manually, the shake-flask method is rather slow, though it can be automated using robotics to achieve a higher throughput. An automated shake-flask method has been described [6] in which solutions in water/octanol are prepared in capped chromatography vials. After shaking and settling, the robot removes samples from each phase by piercing a septum in the vial cap and lowering a needle into the vial. The needle may be pushed through the octanol phase into the aqueous phase without any apparent contamination of the aqueous sample, and a photograph showing this is displayed in the reference. This micro-shake-flask method for determining log D pH 7.4 values allowed the analysis of typically 24 samples per day per instrument person. The authors have since further developed and automated the sample preparation using a robotic sample processor to increase the throughput. A similar method with a throughput of about 96 samples per day has been described [7] in which the traditional shake-flask method has been transferred on to 96-well shake-plate technology and a robotic liquid handler has been used for sample preparation. An autosampler samples the organic and aqueous phases directly from the plate. Analyses are performed by reverse-phase (RP) HPLC. A validation of the automated method is presented for a range of compounds with log D values between -2 and 4. An instrument based on a similar procedure has been marketed by Analyza Inc.

The shake-flask method has some drawbacks, however. One problem that occurs occasionally is the formation of micro-emulsions which remain stable for hours or days, and prevent the two solvent layers from separating. In this case it is not possible to measure the concentration of analyte in each phase. More generally, the upper and lower range of log D values is limited by problems of solution handling. For very high log D values the sample is much more soluble in octanol than in water. For example, if log D is 4 the sample is 10,000 times more soluble in octa-

nol. Unless very small volumes of octanol are used, virtually all the sample will dissolve in the octanol, and the concentration in the aqueous phase will be too low to measure. However, if a very small volume of octanol is used (e.g., 0.1 mL of octanol + 2.0 mL aqueous buffer), it is difficult to sample automatically from the octanol phase. These problems do no occur in pH-metric or direct chromatographic methods.

2.3.2 pH-metric Method

Another source of high-quality measurement of log D values, though only for ionizable drugs, is the pH-metric method. In this method, log P is calculated from the difference between the apparent pK_a (p_oK_a) measured in a dual-phase system, the volume ratio of the phases and the aqueous pK_a. First described 50 years ago [8], this method was overlooked until the early 1990s, when it was developed at Sirius as the basis for log P measurement in the GLpKa instrument. The pH-metric method has been extensively described [9–13].

To use this method, the sample is dissolved in a system containing two phases (e.g., water and octanol) such that the solution is at least about 5×10^{-4} M. The solution is acidified (or basified) and titrated with base (or acid) under controlled conditions. The shape of the ensuing titration curve is compared with the shape of a simulated curve, which is created *in silico*. The estimated p_oK_a values (together with other variables used to construct the simulated curve such as substance concentration factor, CO_2 content of the solution and acidity error) are allowed to vary systematically until the simulated curve fits as closely as possible to the experimental curve. The p_oK_a values required to achieve the best fit are assumed to be the correct measured p_oK_a values. This computerized calculation technique is called ''refinement'', and is described elsewhere [14, 15].

Equations have been published [16] which relate pK_a and p_oK_a values to partition coefficient (P) values for monoprotic acids and bases, and diprotic acids, bases and ampholytes. For example, P^1 for a monoprotic acid is calculated from

$$P^1 = \frac{10^{p_oK_a - pK_a} - 1}{r} \tag{4}$$

and P_0 for a monoprotic base is calculated from

$$P^0 = \frac{10^{-(p_oK_a - pK_a)} - 1}{r} \tag{5}$$

where

$$r = \frac{\text{volume of partition solvent}}{\text{volume of aqueous phase}} \tag{6}$$

Lipophilicity profiles are readily calculated from pH-metric data, as pH, P and K_a are known and can be used in Eq. (1).

In the pH-metric method, sample concentration is not measured at any stage. Hence, the method can be used for measurement of all ionizable samples, with or without a UV chromophore. However, it cannot be used for lipophilic weak bases with low pK_a or lipophilic weak acids with high pK_a if values shift to p_oK_as outside the measurable range (2–12) [17]. The method can be used over a wide range of octanol/water volume ratios as the pH is measured in the dual-phase system, without any need for complete separation of phases. The measurement range is ultimately defined by the volume ratio [18], and extends between about log P −2 and 6.0 in 0.15 M KCl media. Higher values may be measured if deionized water is used instead of a high ionic-strength aqueous phase. The pH-metric method can be automated so that a dual-phase titration is completed in 35–40 min. In principle, up to 40 samples could be titrated in a 24-h period, but more realistically samples may require repeated analysis under different conditions and so a lower throughout will be achieved.

2.3.3 Direct Chromatographic Methods

The use of chromatography has some important advantages that make it suitable for higher-throughput measurement of log D in a drug discovery setting. Samples do not have to be accurately weighed before analysis. The methods are compatible with the use of a dimethyl sulfoxide (DMSO)-solvated samples in 96-well plate format, and they require very small amounts of sample for each assay. On the other hand, most methods described in the literature use detectors based on UV spectroscopy, and are not suitable for samples without UV absorbance. A number of chromatographic methods for measuring lipophilicity have been described.

2.3.3.1 Chromatographic Hydrophobicity Index (CHI)

In the CHI method [19], a gradient created from aqueous buffer and solvent is used as the eluent. A solution of the sample in a solvent is injected into a column while the gradient has a low solvent content. Under these conditions the sample binds to the column and is retained there. The solvent content of the gradient is gradually increased, and when it is sufficiently high the sample will dissolve and elute from the column, where it may be detected. The system is calibrated using retention times of a set of standards with known CHI values. Analysis times of 5 min per sample have been reported for the CHI method using 50 mM ammonium acetate buffer at pH 7.4 and acetonitrile together with a Luna C-18 column, and it is probably the fastest method in routine use. A correlation with log D octanol/water has been reported, though results are normally quoted on a CHI scale. A potential problem with CHI is the uncertainty of the pH of the buffer solution as the solvent content varies, though methods have been developed for correcting pH in CHI experiments to aqueous pH values [20].

The retention depends on the nature of both the stationary phase and the organic modifier in the mobile phase. Therefore CHI values obtained using different systems show different sensitivities towards solute characteristics. This has been studied systematically and used for the quantitative calculation of solute molecular descriptors (H-bond donor capacity, H-bond acceptor capacity and dipolarity/polarizability) for application in a general solvation equation [21].

2.3.3.2 Microemulsion Electrokinetic Chromatography (MEEKC)

The method of MEEKC has been used to measure lipophilicity [22, 23]. In this method, a microemulsion made from aqueous buffer solution, *n*-butanol, heptane and a surfactant is placed inside a fused silica capillary. DMSO-solvated samples are prepared in the buffer with dodecaphenone, a highly lipophilic marker (M), and injected at the anode end of the capillary. A UV detector is placed near the cathode. Under the influence of applied electric field, negatively charged droplets of organic solvent migrate towards the anode in a direction opposite to the electroosmotic flow (EOF). A neutral solute that resides wholly in the aqueous phase will migrate with the EOF with a migration time of T_{EOF}, while a solute that resides wholly in the organic phase will migrate at the velocity of the organic droplets T_M. The migration time (T_R) of most solutes will be between T_{EOF} and T_M, and a capacity factor log k may be calculated from

$$\log k = \log\left[\frac{T_R - T_{EOF}}{(1 - T_R/T_M)T_{EOF}}\right] \tag{7}$$

Log k appears to correlate with log P for standards between log P −0.5 to 5.0. One limitation of this method is that solutes must be electrically neutral at the pH of the buffer solution because electrophoretic mobility of the charged solute leads to migration times outside the range of T_M and T_{EOF}. Basic samples are therefore run at pH 10, and acidic samples at pH 3, thus ensuring that most weak acids and bases will be in their neutral form. This method has been used in a preclinical discovery environment with a throughput of 100 samples per week [24].

2.3.3.3 Chromatography in the Presence of Octanol

Both CHI and MEEKC must be regarded as surrogate chromatographic models for octanol/water partitioning, since no octanol is used in the measurements. Octanol/water was initially adopted for measurement of partition coefficients because of the difficulties in standardizing earlier methods using olive oil/water. Its value in the prediction of drug–membrane interaction is related to the tendency of water-saturated *n*-octanol to form into near-spherical clusters in which the hydroxyl groups of 16 or so octanol molecules are coordinated around a core of water molecules with the hydrocarbon chains pointing outwards [25]. This creates a phase which shares some of the characteristics of a phospholipid membrane bilayer such as those that exist in the human body, namely regions where lipophilic character

predominates as in the core of a lipid membrane, adjacent to regions where a polar character is in evidence, as is the case at a membrane surface. This tendency for aggregation may be shared to some extent with other aliphatic *n*-alcohols, though octanol is a good choice for use in chemical analysis because it is neither very volatile nor very viscous.

Octanol/water cannot fully model the combination of charge and polarity that occurs in phospholipid head groups, and it is not sensitive to the hydrogen-bond donor character of solutes [26]. Partitioning into other partition solvents, liposomes and immobilized artificial membranes have all been used to extend the partition model. However, Log P octanol/water is by far the most widely used descriptor for lipophilicity. Log P octanol/water values have been measured for large numbers of compounds, and measured values for many developed drugs have been published. This database of measured values has been used to train software for the calculation of log P from structure alone, and several commercial programs are available for this purpose. In view of these factors, it seems desirable for high-throughput screening to explore the use of chromatographic methods for log D measurement that as far as possible are made in the octanol/water system.

2.3.3.4 **Reversed-Phase Chromatography**

An experimental log P method (ElogP) based on reversed-phase chromatography using C18 columns and peak detection by multiwavelength UV has been described for measurement of neutral molecules [27], and adapted for measurement of log D of basic molecules (ElogD) [28]. The eluent consists of an aqueous buffer solution at pH 7.4, which may be mixed with varying proportions of methanol. Samples are analyzed at three different ratios of methanol to buffer. Capacity factors (log k′) are calculated from the retention times at each ratio (T_R), and extrapolated to 0% methanol to obtain a value for log k'_w (w = water). Published correlations between log k'_w and literature values for log D show significant improvement in linearity and fit when a small amount of *n*-octanol is added to the mobile phase. To attain a higher throughput, a calculation of the expected log P or log D values is carried out, and appropriate percentages of methanol are calculated such that the time required to elute the sample will fall into an acceptable range. A throughput of 270 compounds per week with log D values ranging between −1.0 and 5.5 has been reported.

2.3.3.5 **Liquid–Liquid Partition Chromatography**

At Sirius, a dedicated instrument (Profiler LDA) has been developed for the rapid measurement of log D by liquid–liquid partition chromatography. In this instrument the column is coated with a layer of octanol, and the retention times are therefore truly related to octanol/water partitioning. Although the method used was first described 25 years ago [29], it has been difficult to apply in an automated system because of the tendency of octanol to be flushed from the column by the eluent, thus requiring frequent renewals of the octanol coating. In our method, the octanol coating is kept in place by reversing the direction of the eluent after each

sample has run through the column. The mobile phase is saturated with octanol, which also helps to preserve the column life. More than 1000 chromatograms are typically run before re-coating of the column is required. When it becomes necessary, the column is re-coated by pumping octanol through it, followed by two blank runs for reconditioning.

Samples are taken directly from 10 mM DMSO-solvated stocks in 96-well plates. Typically, 2 μL of sample is aspirated, and injected on to the column – this represents about 8 μg of sample with MW = 400. The retention time (R_t) of peaks eluting from the column is related to the capacity factor log k by Eq. (8):

$$\log k = \log\left[\frac{R_t - T_0}{T_0}\right] \tag{8}$$

where T_0 is the time required to clear the volume of the system (this is a constant value of a few seconds).

Peaks are detected by multi-wavelength UV spectroscopy. To enhance peak heights for weakly-absorbing species, the absorbances at 75 wavelengths are added together and plotted against log (time). To achieve acceptable experiment times over a wide range of log D values, two columns are used, together with two mobile phases. Suitable choices of column and eluent are shown in Table 2.3. Each Run Type is calibrated by injecting a mixture of five standards with known log D values, and determining the corresponding log k values. Samples are then assayed by Run Type 1, which will measure the more lipophilic samples. The chromatogram is run for up to 15 min, which is sufficient for peaks of solutes with log D values up to 5.5 to be eluted. In principle, higher log D values could be measured if the assay time was longer. Samples for which no peak was observed may be re-assayed using Run Types 2 and 3, which are used to measure lower values down to −1.0. The total assay time can be minimized if software is used to predict the expected log D values of each sample. Experiments to validate this instrument have been performed (Table 2.4), and Fig. 2.2 shows correlations with measured log D values that are published here for the first time. A measurement throughput of over 100 samples per day can be realistically achieved using this instrument.

Tab. 2.3. Liquid–liquid chromatographic methods for the measurement of log D. Selection of column and mobile phase.

Run type	***1***	***2***	***3***
Log D range	5.5 to 2.0	3.5 to 1.0	2.0 to −1.0
Column	1-cm column, octanol-coated	1-cm column, octanol-coated	15-cm column, octanol-coated
Eluent	Phosphate buffer (10 mM) at pH 7.4, containing 30% methanol	Phosphate buffer (10 mM) at pH 7.4	Phosphate buffer (10 mM) at pH 7.4

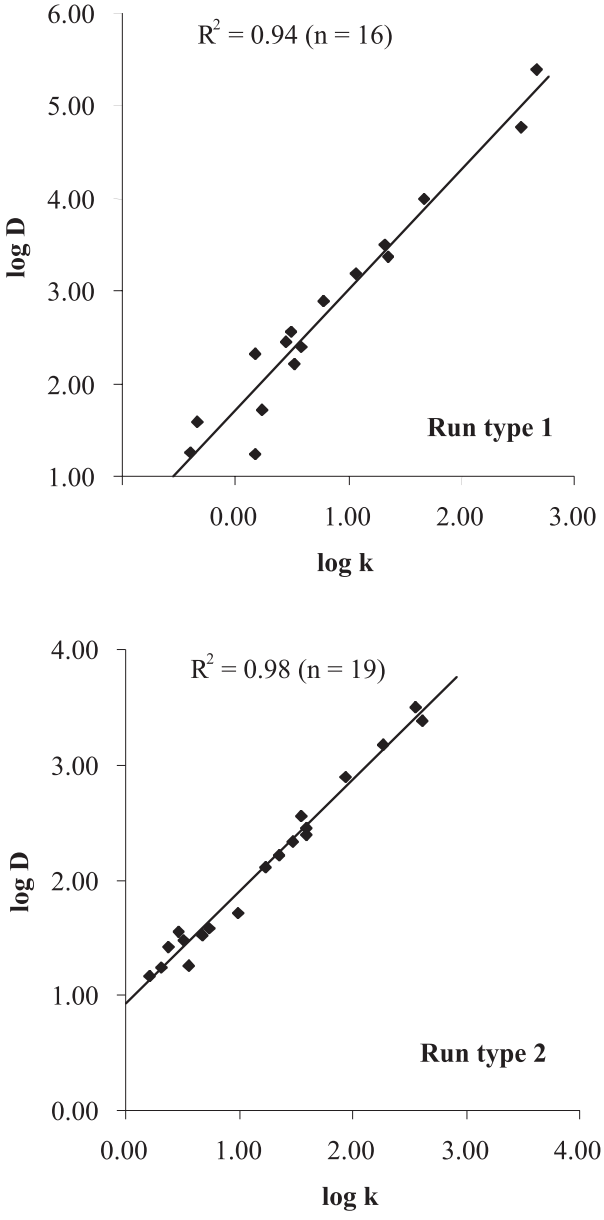

Fig. 2.2. Log D measurement by liquid–liquid chromatography of compounds listed in Tab. 2.4. Note the scatter in measurement of compounds with low log D using Run type 1, caused because retention times are too short. These compounds are more reliably measured using Run type 2.

Tab. 2.4. Liquid–liquid chromatographic methods for measurement of log D at pH 7.4. Results for a series of validation compounds.

Run type	*1 log k*	*2 log k*	*log D*	*Reference*
Acetanilide		0.21	1.16	47
Diclofenac	0.18	0.32	1.24	48
4-Methoxyphenol		0.38	1.41	9
Propranolol	−0.39	0.56	1.26	49
Phenol		0.51	1.48	9
1-Benzlyimidazole		0.67	1.52	50
4-Nitrophenol		0.47	1.55	51
Acetophenone	−0.34	0.74	1.58	62
Lidocaine	0.23	0.99	1.71	49
Anisole		1.23	2.11	64
Diltiazam	0.53	1.35	2.22	52
Quinine	0.18	1.48	2.33	49
Tetracaine	0.59	1.59	2.39	48
4-Chlorophenol	0.45	1.60	2.45	9
3-Chlorophenol	0.50	1.55	2.56	9
4-Iodophenol	0.78	1.95	2.90	9
Benzophenone	1.07	2.27	3.18	64
Diphenylamine	1.32	2.56	3.50	53
Chlorpromazine	1.36	2.61	3.38	49
Diphenyl ether	1.67		4.21	64
Bifonazole	2.53		4.77	63
Tolnaftate	2.67		5.40	27

2.4 Measuring pK_a

2.4.1 Review of Methods

It is difficult to devise a rigorous definition of pK_a that rolls easily off the tongue. For an aqueous solution of a compound with a single ionizable group, the ionization constant (or acid dissociation constant) pK_a is defined as the pH at which 50% of the compound is in its ionized form and 50% in its neutral form [30]. This definition must be extended through the use of properly derived equilibrium equations to cover molecules with more than one ionizable group. The degree of ionization at a given pH can be calculated for any molecule once the pK_a(s) are known.

To measure pK_a values it is necessary to expose the compound to an environment of changing pH, and to monitor a particular property that changes as a function of the ionization state of the molecule. Traditional pK_a methods have included solubility and conductivity methods [31]. These are slow, and require both large quantities of material and skilled operators. Some more rapid methods

Tab. 2.5. Shift in pK_a values with increasing methanol content in water/methanol mixtures (all solutions 0.15 M in KCl).

Diclofenac	% methanol	0%	29.1	39.0	47.8
	pK_a/apparent pK_a	3.99	4.57	4.67	4.97
Chlorpromazine	% methanol	0%	20.1	30.1	40.0
	pK_a/apparent pK_a	9.24	9.08	8.83	8.68

include pH-metric titration, hybrid pH/UV titration, hybrid capillary electrophoresis (CE)/UV and pH gradient titration.

2.4.2 The Effect of Co-solvents on pK_a

Most methods of pK_a measurement were developed using water-soluble samples. However, many drugs are poorly soluble in water alone, and require the presence of a water-miscible co-solvent to keep them in aqueous solution. The solvent affects the pK_a in two ways: (i) it causes the pH scale to shift; and (ii) it causes the pK_a to shift. The consequence is that apparent pK_a values measured in the presence of solvent are different from aqueous values.

For the sake of improving throughput, it is tempting to ignore this effect, and to work always in water/solvent mixtures and report the apparent pK_a values, which may be considered "good enough" for use during early-stage development. As shown in Table 2.5 however, the shifts can be quite high. An error in pK_a of 0.5 units, when applied in a calculation of log D from a log P would cause an error in log D estimation of about 0.5 log D units. It would also cause a significant error in pH-metric measurement of solubility. When pK_as are close to the physiological pH in the region where the drug is absorbed, errors in pK_a could have a significant effect on predictions of drug behavior.

The semi-empirical Yasuda–Shedlovsky technique of extrapolating a series of apparent pK_a values obtained in several ratios of water/solvent to obtain an aqueous value is well established [32, 33], but three or more experiments are required and this adds significantly to assay times. A method of calculating aqueous pK_as for various classes of organic acids and bases from single apparent pK_a values obtained in water/solvent mixtures has been reported [34], and shows promise as a means of further speeding pK_a measurement.

2.4.3 pH-Metric Titration

The pH-metric method is an important reference method because it can be used to measure all pK_as between 2 and 12, with or without a UV chromophore, provided that the sample can be dissolved in water or water/co-solvent over the pH range of interest. In this method, the sample solution is titrated with acid or base, the titration is monitored with a glass pH electrode, and the pK_a is calculated from the

change in shape of the titration curve compared with that of a blank titration without sample present [16]. A sample concentration of at least $\sim 5 \times 10^{-4}$ M is required in order for any significant change in shape to be detectable between pH 3 and 11, and a larger concentration is required outside this range [17]. Although pH-metric pK_a titration in volumes as low as 100 μL has been reported using pH micro-electrodes [35], the physical size of glass pH electrodes and stirrers generally dictate that the smallest practical volume of sample solution is about 5 mL. This requires more than 1 mg of sample for a compound with a MW of 400 to achieve a concentration of 5×10^{-4} M. A typical titration between pH 3 and 11 requires about 45 measured pH values. The need to wait for equilibrium after each pH measurement means that titrations typically take 20–40 min to perform. With experiments designed for optimum speed, perhaps 30–40 titrations could be performed during one 24-h day using an automated instrument (Sirius GLpKa), though up to 5 min per titration data set must be allowed for calculating results from the data. Sample throughput will be lower if the Yasuda–Shedlovsky technique is used for poorly soluble samples, and some samples may be too insoluble to measure even at high levels of co-solvent. While the pH-metric method is not fast enough for rapid screening, it provides a valuable back-up for the measurement of samples without UV absorbance.

2.4.4
Hybrid pH-Metric/UV Method

Significantly smaller sample concentrations (10^{-5} M or below) are required for pK_a measurement by the hybrid pH-metric/UV method, in which multi-wavelength UV absorbance of the sample solution is monitored throughout the titration. Samples must have a chromophore, and the absorbance must change as a function of ionization. Recent advances in this method have enabled pK_a measurement in volumes less than 8 mL by use of a fiber optics dip probe in a titration cell, and this has been automated on the Sirius GLpKa with D-PAS attachment. During measurement, samples are acid–base titrated across a pH range that includes the pK_a(s), and multiwavelength UV spectra are measured at each pH. The pK_as are calculated using a technique based on target factor analysis (TFA) [36]. The apparatus has been used for determination of pK_as of samples with multiple ionization centers [37], and determination of protonation microconstants of zwitterionic molecules [38, 39]. Titrations take up to 30 min because of the need to wait for electrode stability. The ability to work at lower concentrations increases the scope for measuring pK_as of poorly soluble samples by the Yasuda–Shedlovsky technique, but throughput will be lower if this technique is used.

2.4.5
Other Methods

Recently, a flow-injection method has been reported in which pK_a values are measured by UV absorbance after injection into a flowing phosphoric acid buffer [40].

No mention of throughput was made. Measurement of pK_a by UV after separation by CE has been described for acids [41] and bases [42], and while this method only requires small sample quantities, the rate of throughput is currently about 20 samples per day [23, 43]. A rate-limiting step in the CE method is the need to make separate experimental runs at different buffered pH values in order to determine the relative concentration of ionized species at each pH.

2.4.6 pH Gradient Titration

At Sirius, a dedicated instrument (Profiler SGA) has been developed for the rapid measurement of pK_a by a patented technique that we have called pH gradient titration [44]. In this technique, samples are injected into a flowing pH gradient, which is created by mixing an acidified and a basified linear buffer together using syringe pumps running at inversely varying speeds. During the gradient the pH varies linearly, and may be predicted from the time elapsed since the start of gradient generation. This eliminates the need for pH measurement, which is the rate-limiting step in conventional titration. The gradient and sample pass through a diode array UV spectrophotometer, and pK_as are determined from changes in absorption as a function of pH. Typical assay cycle is 4 min per sample (including a gradient time of 90 s), leading to throughput of over 200 samples per day.

The linear buffer is created by mixing several weak acids and bases in varying concentrations such that the titration curve is linear in terms of pH, and the ionic

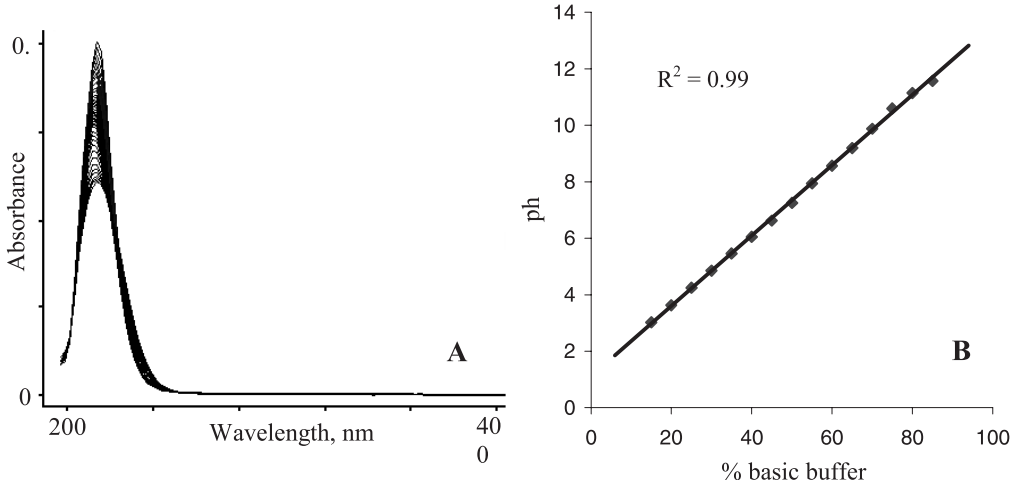

Fig. 2.3. (A) UV absorbance of linear buffer solution. The solution was acidified and titrated with 0.5 M KOH. Each line represents UV absorbance at a single pH. The graph comprises 46 spectra between pH 2.5 and 12.2. Absorbance of buffer is negligible above 240 nm. (B) Experiments to demonstrate the linearity of the pH gradient. Aliquots of acidic and basic buffers were mixed and the pH measured. pH results are the mean of two readings. Average SD of pH measurements between pH 3.0 and 11.6 was $\pm$0.004 pH.

strength approximates to 0.15 M at any pH. The buffer components were chosen because of their low UV absorbance, and have a total of nine pK_as spaced approximately equally over the pH range 2 to 12. The absorbance and linearity of the buffer are shown in Fig. 2.3.

Experimental data consist of measured absorbance, wavelength, and pH (which is calculated from the time elapsed from the start of gradient generation). pK_a values are obtained by differentiation, or by TFA. Differentiation is used for standards, and for samples with single or well-separated pK_as associated with adequate UV absorbance change (Fig. 2.4). Results are obtained by differentiating the absorbance at each wavelength with respect to pH, and taking the pH of the peak maxima to indicate the pK_a value.

TFA is used for samples with weak absorbance changes or overlapping pK_as. In TFA, absorbance (A) with respect to wavelength and pH is expressed as a matrix *A*. Two other matrices are set up. The *C* matrix shows the concentration (C) of each

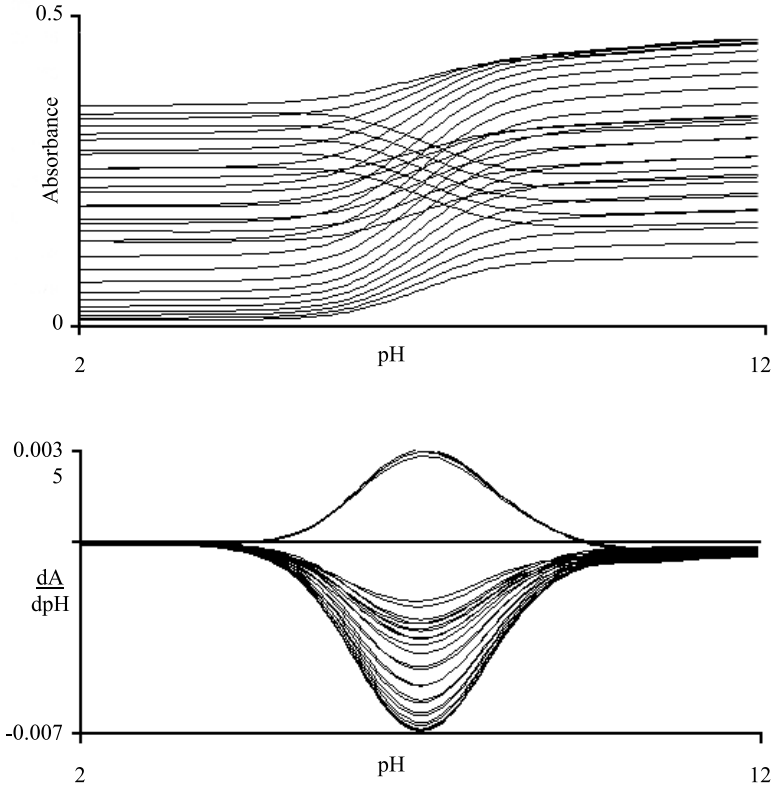

Fig. 2.4. UV spectra for nitrofurantoin, showing calculation of results by First Derivative (FD). Top graph shows UV absorbance (A) versus pH. Lower graph shows dA/dpH versus pH. The pK_a result (6.91) is indicated by the position of the peak maxima on the pH axis.

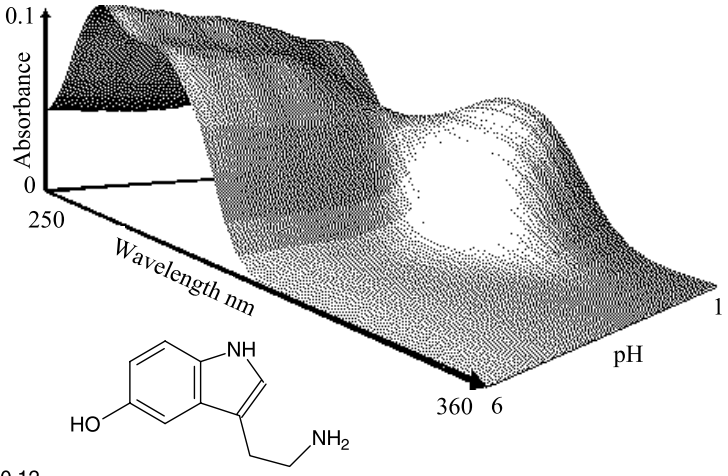
0.1
Absorbance
0
250
Wavelength nm
360
6
pH
1
NH
HO
NH2

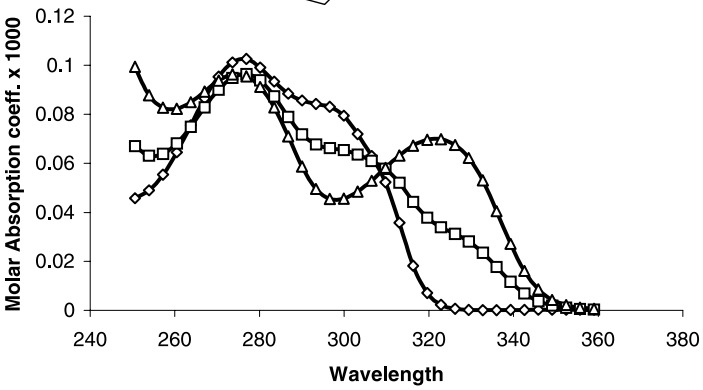
Molar Absorption coeff. x 1000
0.12
0.1
0.08
0.06
0.04
0.02
0
240
260
280
300
320
340
360
380
Wavelength

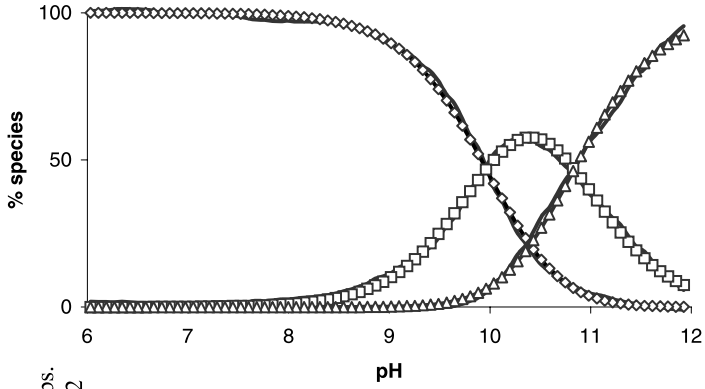
% species
100
50
0
6
7
8
9
10
11
12
pH

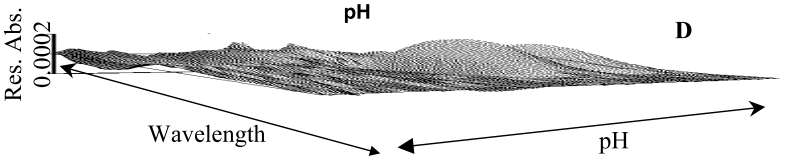
Res. Abs.
0.0002
Wavelength
pH
D

species as a function of pH, and the *E* matrix shows molar absorptivity (extinction coefficient, E) of each species as a function of wavelength. By invoking Beer's law, which states that A = CE (over a practical concentration range), the matrices are related by a similar equation, $A = CE$. Initially, the elements of the *C* and *E* matrices are estimated. During TFA, values for these elements are systematically optimized until $A - CE$ tends to a minimum value. The concentration (C) of each species as a function of pH is a function of the pK_a(s) of the sample, so pK_a(s) are derived from the *C* matrix (visualized as the graph of % species versus pH) after the equation has been minimized. Molar absorptivities may be derived from the *E* matrix (visualized as the graph of absorptivity versus wavelength) [45]. Unless the data are ''perfect'', there will be some unassigned absorbance, which is expressed in a plot of residual absorbance. TFA is summarized in Fig. 2.5.

A validation study has been published showing good correlation between pK_a values measured by this method and previously measured values for a series of pharmaceutical drug candidates with unpublished structures [46]. In this study, all results were calculated by differentiation. More recently, we have carried out a validation study based on 85 reference compounds, with most results calculated by TFA. The results of this study show an excellent correlation with published values [65]. Table 2.6 shows a selection of these results for a number of ampholytic and zwitterionic molecules with a total of 42 pK_as, plotted against literature values with $r^2 = 0.99$ (Fig. 2.6). In our laboratories we are currently seeking to automate the TFA calculation so that very little user intervention is required, and we are investigating water/solvent media of different compositions to find an optimal solvent system for dissolving the greatest number of poorly water-soluble analytes.

2.5 Some Thoughts about High-throughput Analytical Chemistry

Analysts like to make chemical measurements to the highest quality they can, and this is possible with modern instrumentation and good analytical practice. Chemical parameters are generally measured more accurately and reproducibly than parameters measured in biological systems, and the results are more reliable than values calculated by software from structure alone (e.g., calculated log P, pK_a). Of all the information available to medicinal chemists, measured chemical parameters are probably the most reliable. With these thoughts in mind, it makes sense not to

← **Fig. 2.5.** Measurement of pK_as of serotonin by target factor analysis (TFA). (A) 3-D spectrum produced by serotonin in pH gradient experiment (equivalent to *A* matrix). (B) Molar absorptivity of three serotonin species (equivalent to *E* matrix). (C) Distribution of species (equivalent to *C* matrix). In this graph the three sets of data points denote the three ionized species of serotonin. The solid lines behind the points indicate the best fit of the data to these points. (D) Residual absorbance. This graph denotes the unaccounted absorbance after the best fit has been obtained. For a good result, the absorbance range should be less than 0.01 × total absorbance range shown in (A).

Tab. 2.6. Measured versus literature values for pK_as of ampholytic and zwitterionic compounds.

Sample	*Method*	*SGA result (SD)*	*Lit pK_a*	*Reference*
5-Hydroxyquinoline	FD	8.32 (01), 4.93 (01)	8.54, 5.22	55, 56
Acyclovir	FD	9.32 (03), 2.25 (04)	9.25, 2.27	54
Albendazole	FD	9.77 (01), 3.13 (03)	9.93, 3.28	33
Enrofloxacin	TFA	7.83 (16), 6.04 (11)	7.75, 6.16	A*
Famotidine	FD	11.32 (01), 6.84 (02)	11.19, 6.74	57
Labetalol	TFA	9.38 (04), 7.42 (06)	9.36, 7.41	37
Nicotinic acid	TFA	4.62 (01), 2.43 (01)	4.63, 2.10	37
Niflumic acid	TFA	4.87 (11), 2.00 (01)	4.44, 2.24	9
Nitrazepam	FD	10.37 (04), 2.86 (09)	10.37, 3.02	9
Norfloxacin	TFA	8.61 (01), 6.29 (02)	8.70, 6.40	58
Ofloxacin	TFA	8.30 (01), 6.01 (02)	8.31, 6.09	9
Oxytetracycline	TFA	9.19 (01), 6.87 (07), 3.19 (02)	9.11, 7.32, 3.27	59
Pefloxacin	TFA	7.37 (16), 6.11 (05)	7.80, 6.02	60
Physostigmine	FD	8.13 (08), 2.61 (06)	8.17, 2.00	31, 37
Piroxicam	TFA	5.32 (01), 2.53 (18)	5.07, 2.33	48
Serotonin	TFA	10.91 (14), 9.89 (08)	10.90, 9.92	B[+]
Sotalol	TFA	9.75 (02), 8.25 (08)	9.72, 8.28	48
Sulfanilamide	FD	10.42 (05), 2.17 (13)	10.43, 2.00	9
Sulpiride	TFA	9.79 (00), 8.95 (01)	10.19, 9.00	61
Tetracycline	TFA	9.43 (02), 7.16 (10), 3.33 (06)	9.30, 7.68, 3.30	59

All measurements in duplicate except acyclovir (×3) and labetalol (×5).
Results obtained by First Derivative (FD) or Target Factor Analysis (TFA).
* A: Sirius, unpublished pH-metric result.
[+] B: K. Takács-Novák, Semmelweis University, Budapest, pH-metric result, personal communication, January 2002.

sacrifice measurement quality for speed during the design of instrumentation. High-throughput methods should only be introduced if they meet satisfactory standards for accuracy and reproducibility.

Note that it is highly desirable that the identity of every sample is confirmed before analysis, and that samples are adequately pure for the measurement in question. In the pH-metric methods, the sensor is a pH electrode and cannot distinguish between analyte and impurity. In the methods that depend on UV absorbance, if a sample contains an impurity with stronger absorbance than the sample, then the calculation of results from experimental data is complicated. Combinatorial samples are by nature poorly characterized, and even in the chromatographic methods in which analyte and impurity will be separated, it may be difficult to assign the peaks unambiguously. It is therefore advisable to purify samples before they are submitted for analysis of log D and pK_a.

All of the methods described and referenced here are capable of producing high-quality, accurate results, but only if the raw data are correctly interpreted and analyzed to detect (and correct) for issues arising from issues such as low solubility, ion pair partition or multiple ionizable groups with overlapping pK_as. It is not

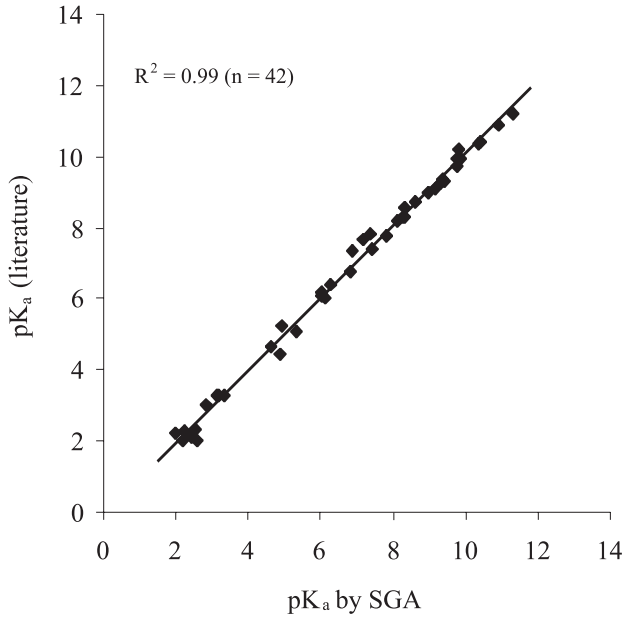

Fig. 2.6. pK_a measurement by pH gradient titration of compounds listed in Tab. 2.6.

sufficient simply to invest in the equipment for performing high-throughput measurements. There also must be an infrastructure in place that deals with the quality assurance (QA) and quality control (QC) of samples to ensure that issues do not arise such as incorrect compound dispensing, or decomposition in storage of DMSO solutions. In this regard, there is a clear need for skilled physical chemists to be involved in data analysis and interpretation.

An important consideration is that instruments and software should be as easy to use as possible. If scientists have to measure hundreds of samples per day, they do not have much time to devote to each result. Some of the techniques required to obtain results from experimental data are complex, and involve significant amounts of calculation – pH-metric refinement and TFA are good examples. It is worth striving to make such techniques as automated as possible, so that users have little to do except look at the results. Somehow, instrument and software designers must provide visualization tools to help users judge the quality of each result quickly and correctly, and the use of these instruments must become more or less instinctive if we are to implement high-throughput analytical techniques successfully. Scientists must be able to devote their intellectual resources to interpreting the data – not to measuring it.

Acknowledgments

I could not have completed this chapter without the help of colleagues and collaborators. Among my colleagues at Sirius I particularly thank Steve Elliott for his

work on liquid–liquid chromatography, Karl Box for his knowledge about pK_a measurement; and Roger Allen and Keith Foster for creating much of our software. I am also grateful to Alex Avdeef of *p*ION and Kin Tam of AstraZeneca who derived many of the equations used to calculate log D and pK_a results from experimental data, as well as Derek Reynolds of Reytek, Li Di of Wyeth and Marina Shalaeva of Pfizer, who gave me valuable suggestions.

References

1 Kerns, E. H., High throughput physicochemical profiling for drug discovery, *J. Pharm. Sci.* **2001**, *90*, 1838–1858.
2 Kerns, E. H., Di, L., Multivariate pharmaceutical profiling for drug discovery, *Curr. Top. Med. Chem.* **2002**, *2*, 87–98.
3 Avdeef, A., Physicochemical profiling (solubility, permeability and charge state), *Curr. Top. Med. Chem.* **2001**, *1*, 277–351.
4 Lipinski, C. A., Lombardo, F., Dominy, B. W., Feeney, P. J., Experimental and computational approaches to estimate solubility and permeability in drug discovery and development settings, *Adv. Drug Del. Rev.* **2001**, *46*, 3–26.
5 Avdeef, A., Bucher, J. J., Measurements of the concentration of hydrogen ions with a glass electrode: calibrations using the Prideaux and other universal buffer solutions and a computer-controlled automatic titrator, *Anal. Chem.* **1978**, *50*, 2137–2142.
6 Valkó, K., Measurements of physical properties for drug design in industry, in: *Separation Methods in Drug Synthesis and Purification*, *Handbook of Analytical Separations*, Volume 1. Smith, R. M. (ed.), Elsevier, Amsterdam, **2000**, pp. 539–542.
7 Hitzel, L., Watt, A. P., Locker, K. L., An increased throughput method for the determination of partition coefficients, *Pharm. Res.* **2000**, *17*, 1389–1395.
8 Dyrssen, D., Studies on the extraction of metal complexes IV. The dissociation constants and partition coefficients of 8-quinolinol (oxine) and *N*-nitroso-*N*-phenylhydroxylamine (cupferron), *Sven. Kem. Tidskr.* **1952**, *64*, 213–224.
9 Slater, B., McCormack, A., Avdeef, A., Comer, J. E. A., pH-Metric log P. 4. Comparison of partition coefficients determined by shake-flask, HPLC and potentiometric methods, *J. Pharm. Sci.* **1994**, *83*, 1280–1283.
10 Hersey, A., Hill, A. P., Hyde, R. M., Livingstone, D., Principles of method selection in partition studies, *Quant. Struct.-Act. Relat.* **1989**, *8*, 288–296.
11 Caron, G., Gaillard, P., Carrupt, P.-A., Testa, B., Lipophilicity behavior of model and medicinal compounds containing a sulfide, sulfoxide, or sulfone moiety, *Helv. Chim. Acta* **1997**, *80*, 449–462.
12 Seiler, P., The simultaneous determination of partition coefficients and acidity constant of a substance, *Eur. J. Med. Chem.* **1974**, *9*, 665–666.
13 Takács-Novák, K., Avdeef, A., Interlaboratory study of log P determination by shake-flask and potentiometric methods, *J. Pharm. Biomed. Anal.* **1996**, *14*, 1405–1413.
14 Avdeef, A., pH-Metric log P. 2. Refinement of partition coefficients and ionization constants of multiprotic substances, *J. Pharm. Sci.* **1993**, *82*, 183–190.
15 Applications and Theory Guide to pH-Metric pK_a and log P Determination, Sirius Analytical Instruments Ltd, Forest Row, UK, **1993**.
16 Avdeef, A., pH-Metric log P. 1. Difference plots for determining ion-pair octanol-water partition coefficients of multiprotic substances, *Quant. Struct.-Act. Relat.* **1992**, *11*, 510–517.
17 Comer, J., Avdeef, A., Box, K. J.,

Limits for successful measurement of pK_a and log P by pH-metric titration, *Amer. Lab.* **1995**, *4*, 36C–36I.

18 Kramer, S. D., Begu, S., Marrier, J. M., Forster, C., Gautier, J. C., Saudemon, P., Devoiselle, J. M., Wunderli-Allenspach, H., Potentiometric log P determination in the liposome/water system: advantages and limitations, *Pharm. Res.* **1998**, *15*, 1310–1313.

19 Valko, K., Bevan, C., Reynolds, D., Chromatographic hydrophobicity index by fast-gradient RP HPLC: a high-throughput alternative to log P log D, *Anal. Chem.* **1997**, *69*, 2022–2029.

20 Canals, I., Valko, K., Bosch, E., Hill, A. P., Roses, M., Retention of ionisable compounds on HPLC. 8. Influence of mobile phase pH change on the chromatographic retention of acids and bases during gradient elution, *Anal. Chem.* **2001**, *73*, 4937–4945.

21 Plass, M., Valko, K., Abraham, M. H., Determination of solute descriptors of tripeptide derivatives based on high-throughput gradient high-performance liquid chromatography retention data, *J. Chromatogr. A.* **1998**, *803(1–2)*, 51–60.

22 Gluck, S. J., Benko, M. H., Hallberg, R. K., Steele, K. P., Indirect determination of octanol-water partition coefficients by microemulsion electrokinetic chromatography, *J. Chromatogr. A.* **1996**, *744(1–2)*, 141–146.

23 Poole, S. K., Durham, D., Kibbey, C., Rapid method for estimating the octanol-water partition coefficient (log P-ow) by microemulsion electrokinetic chromatography, *J. Chromatogr. B. Biomed. Appl.* **2000**, *745*, 117–126.

24 Kibbey, C. E., Poole, S. K., Robinson, B., Jackson, J. D., Durham, D., An integrated process for measuring the physicochemical properties of drug candidates in a preclinical discovery environment, *J. Pharm. Sci.* **2001**, *90*, 1164–1175.

25 Franks, N. P., Abraham, M. H., Lieb, W. R., Molecular-organization of liquid n-octanol – an x-ray-diffraction analysis, *J. Pharm. Sci.* **1993**, *82*, 466–470.

26 van de Waterbeemd, H., Kansy, M., Hydrogen-bonding capacity and brain penetration, *Chimia* **1992**, *46*, 299–303.

27 Lombardo, F., Shalaeva, M. Y., Tupper, K. A., Gao, F., Abraham, M. H., ElogP(oct): a tool for lipophilicity determination in drug discovery, *J. Med. Chem.* **2000**, *43*, 2922–2928.

28 Lombardo, F., Shalaeva, M. Y., Tupper, K. A., Gao, F., ElogD(oct): a tool for lipophilicity determination in drug discovery. 2. Basic and neutral compounds, *J. Med. Chem.* **2001**, *44*, 2490–2497.

29 Mirrlees, M. S., Moulton, S. J., Murphy, C. T., Taylor, P. J., Direct measurement of octanol-water partition coefficients by high-pressure liquid chromatography, *J. Med. Chem.* **1976**, *19*, 615–619.

30 Benet, L. Z., Goyan, J. E., Potentiometric determination of dissociation constants, *J. Pharm. Sci.* **1967**, *56*, 665–680.

31 Albert, A., Serjeant, E. P., *The Determination of Ionization Constants*, 3rd edition. Chapman & Hall, London, **1984**.

32 Avdeef, A., Comer, J. E. A., Thomson, S. J., pH-Metric log P. 3. Glass electrode calibration in methanol-water, applied to pK_a determination of water-insoluble substances, *Anal. Chem.* **1993**, *65*, 42–49.

33 Takács-Novák, K., Box, K. J., Avdeef, A., Potentiometric pK_a determination of water-insoluble compounds: validation study in methanol/water mixtures, *Int. J. Pharm.* **1997**, *151*, 235–248.

34 Rived, F., Canals, I., Bosch, E., Roses, M., Acidity in methanol-water, *Anal. Chim. Acta* **2001**, *439*, 315–333.

35 Morgan, M. E., Liu, K., Anderson, B. D., Microscale titrimetric and spectrophotometric methods for

determination of ionization constants and partition coefficients of new drug candidates, *J. Pharm. Sci.* **1998**, *87*, 238–245.

36 Allen, R. I., Box, K. J., Comer, J., Peake, C., Tam, K. Y., Multi-wavelength spectrophotometric determination of acid dissociation constants of ionizable drugs, *J. Pharm. Biomed. Anal.* **1998**, *17*, 699–712.

37 Tam, K. Y., Takács-Novák, K., Multiwavelength spectrophotometric determination of acid dissociation constants: a validation study, *Anal. Chim. Acta* **2001**, *434*, 157–167.

38 Takács-Novák, K., Tam, K. Y., Multi-wavelength spectrophotometric determination of acid dissociation constants – Part V: microconstants and tautomeric ratios of diprotic amphoteric drugs, *J. Pharm. Biomed. Anal.* **2000**, *21*, 1171–1182.

39 Tam, K. Y., Quéré, L., Multiwavelength spectrophotometric resolution of the micro-equilibria of cetirizine, *Anal. Sci.* **2001**, *17*, 1203–1208.

40 Saurina, J., Hernandez-Cassou, S., Tauler, R., Izquierdo-Ridorsa, A. A., Spectrophotometric determination of pK_a values based on a pH gradient flow-injection system, *Anal. Chim. Acta* **2000**, *408*, 135–143.

41 Gluck, S. J., Steele, K. P., Benko, M. H., Determination of acidity constants of monoprotic and diprotic acids by capillary electrophoresis, *J. Chromatogr. A* **1996**, *745*, 117–125.

42 Caliaro, G. A., Herbots, A. A., Determination of pK_a values of basic new drug substances by CE, *J. Pharm. Biomed. Anal.* **2001**, *26*, 427–434.

43 Jia, Z. J., Ramstad, T., Zhong, M., Medium-throughput pK_a screening of pharmaceuticals by pressure-assisted capillary electrophoresis, *Electrophoresis* **2001**, *22*, 1112–1118.

44 Hill, A., Bevan, C., Reynolds, D., Analytical method and apparatus therefore, **1999**, UK Patent WO99/13328.

45 Hendriksen, B. A., Sanchez-Felix, M. V., Tam, K. Y., A new multi-wavelength spectrophotometric method for the determination of the molar absorption coefficients of ionisable drugs, *Spectrosc. Lett.* **2002**, *35*, 9–19.

46 Box, K. J., Comer, J. E. A., Hosking, P., Tam, K. Y., Trowbridge, L., Hill, A., Rapid physicochemical profiling as an aid to drug candidate selection, in: *High Throughput Screening: The Next Generation*. Dixon, G. K., Major, J. S., Rice, M. J. (eds), BIOS Scientific Publishers Ltd., Oxford, **2000**, pp. 67–74.

47 Nakagawa, Y., Izumi, K., Oikawa, N., Sotomatsu, T., Shigemura, M., Fujita, T., Analysis and prediction of hydrophobicity parameters of substituted acetanilides, benzamides and related aromatic-compounds, *Environ. Toxicol. Chem.* **1992**, *11*, 901–916.

48 Sirius Technical Application Notes, 2.; Sirius Analytical Instruments Ltd., Forest Row, RH18 5DW, UK, **1995**.

49 Sirius Technical Application Notes, 1.; Sirius Analytical Instruments Ltd., Forest Row, RH18 5DW, UK, **1994**.

50 Box, K. J., Comer, J., Peake, C., A new instrument for measuring pK_a values and partition coefficients (log P), Poster at Brighton Crop Protection Conference, **1993**.

51 Escher, B. I., Schwarzenbach, R. P., Partitioning of substituted phenols in liposome-water, biomembrane-water, and octanol-water systems, *Environ. Sci. Technol.* **1996**, *30*, 260–270.

52 Pade, V., Stavchansky, S., Estimation of the relative contribution of the transcellular and paracellular pathway to the transport of passively absorbed drugs in the Caco-2 cell culture model, *Pharm. Res.* **1997**, *14*, 1210–1215.

53 Rogers, K. S., Cammarata, A., Superdelocalizability and charge density. A correlation with partition coefficients, *J. Med. Chem.* **1969**, *12*, 692–693.

54 Sammes, P. G., Drayton, C. J., Hansch, C., Taylor, J. B., *Comprehensive Medicinal Chemistry*, Volume 6. Pergamon Press, Oxford, **1990**.

55 Palm, V. A., *Table of Rate and*

Equilibrium Constants of Heterocyclic Organic Reactions, Moscow, **1975**.

56 Mason, S. F., The tautomerism of N-heteroaromatic hydroxy-compounds. Part III. Ionisation constants, *J. Chem. Soc.* **1958**, 674–685.

57 Avdeef, A., Berger, C. M., Brownell, C., pH-metric solubility. 2: Correlation between the acid-base titration and the saturation shake-flask solubility-pH methods, *Pharm. Res.* **2000**, *17*, 85–89.

58 Buckingham, D. A., Clark, C. R., Nangia, A., The acidity of norfloxacin, *Aust. J. Chem.* **1990**, *43*, 301–309.

59 Stephens, C. R., Murai, K., Brunings, K. J., Woodward, R. B., Acidity constants of the tetracycline antibiotics, *J. Am. Chem. Soc.* **1956**, *78*, 4155–4157.

60 Takács-Novák, K., Noszal, B., Hermecz, I., Kereszturi, G., Podanyi, B., Szasz, G., Protonation equilibria of quinolone antibacterials, *J. Pharm. Sci.* **1990**, *79*, 1023–1028.

61 Van Damme, M., Hanocq, M., Molle, L., Étude critique de méthodes de détermination potentiométrique en mileux aqueux et hydroalcooliques des constantes d'acidité de certains benzamides substitutes, *Analusis* **1979**, *7*, 499–504.

62 Fujita, T., Iwasa, J., Hansch, C., A new substituent, π, derived from partition coefficients, *J. Am. Chem. Soc.* **1965**, *86*, 5175–5180.

63 Hansch, C., Leo, A., Hoekman, D., *Exploring QSAR. Hydrophobic, Electronic and Steric Coefficients.* American Chemical Society, Washington, DC, **1995**, pp. 3–216.

64 Leo, A., Hansch, C., Elkins, D., Partition coefficients and their uses, *Chem. Rev.* **1971**, *71*, 525–616.

65 Box, K., Bevan, C., Comer, J., Hill, A., Allen, R., Reynolds, D., High throughput measurement of pKa values in a mixed-buffer linear pH gradient system. *Anal. Chem. In press.*

3
High-throughput Measurement of Permeability Profiles

Alex Avdeef

Abbreviations

Caco-2	Human colon adenocarcinoma cell line used as an absorption model
cmc	Critical micelle concentration
DOPC	Dioleoylphosphatidylcholine
PAMPA	Parallel artificial membrane permeability
MDCK	Madin–Darby canine kidney cell line
SLS	Sodium lauryl (dodecyl) sulfate
UWL	Unstirred water layer (2.4 mm thickness in PAMPA, when plates are not shaken or stirred)

Symbols

K_p, $K_{d(pH)}$	Partition coefficient (a.k.a., log P) and apparent, pH-dependent, partition coefficient (a.k.a., log D), respectively
P_e	Effective permeability (not corrected for the UWL) (units cm s^{-1})
P_m	Membrane permeability ($1/P_m = 1/P_e - 1/P_u$) (units cm s^{-1})
P_u	UWL permeability (units cm s^{-1})
P_o	Intrinsic permeability (of the uncharged species) (units cm s^{-1})
R	Moles of drug dissolved in the artificial membrane divided by total moles of drug (usually expressed as a percentage)
R_a	Asymmetry ratio, defined as $(V_D/V_A)(P_e^{(A\rightarrow D)}/P_e^{(D\rightarrow A)})$, where V_D and V_A are donor and acceptor solution volumes, respectively, and the superscripts refer to the two possible directions of transport

3.1
Introduction

This review describes recent improvements in the measurement of the passive transport of molecules across artificial phospholipid membranes anchored inside

Drug Bioavailability: Estimation of Solubility, Permeability, Absorption and Bioavailability.
Edited by Han van de Waterbeemd, Hans Lennernäs and Per Artursson

ISBN: 3-527-30438-X

microfilters, using a technique called parallel artificial membrane permeability assay (PAMPA). The focus is on a new method variant that allows the determination of the permeability of compounds across (and their retention by) *concentrated* and *negatively* charged phospholipid bilayer membrane barriers (up to 74% wt/vol lecithin in dodecane), in a permeation cell containing an ionic surfactant in the acceptor compartment. The surfactant strongly binds transported lipophilic drugs to create a sink state that models *in vivo* conditions. It also may be involved in the direct desorption of membrane-retained molecules. The sample concentrations in both the donor and the acceptor compartments of the permeation cell are measured rapidly by 96-well microtiter plate UV spectrophotometry. The primary application of this technique is in high-throughput physico-chemical properties screening, which is important in the selection of the most promising drug candidate molecules in pharmaceutical research.

Using combinatorial chemistry to generate new molecules, in the course of a year a large company may screen a staggering number of molecules for biological activity. These tests are performed with high-throughput screening robotic systems, which assess a candidate molecule's potency against a specific target. In the post-human genome era, as disease-related genes are discovered with accelerating frequency, thousands of additional opportunities arise to test new drug targets. A successful "hit" at the early stage is just the beginning in a long journey before a molecule can become a drug. Ultimately, a minuscule number of molecules are successful, with many failing due to problems related to absorption in the intestine. The molecules may function in a microtiter plate, but in the body they are unable to reach their therapeutic target sites.

To reach such a site, a molecule must permeate through many road blocks formed by cell membranes. These are composed of phospholipid bilayers – "oily" barriers that greatly attenuate the passage of charged or highly polar molecules. Often, cultured cells, such as Caco-2 or Madin–Darby canine kidney (MDCK) cells [1–4], are used for this purpose, but the tests are costly. Other types of permeability measurements based on artificial membranes have been considered, the aim being to improve efficiency and lowering costs. One such approach, PAMPA, has been described by Kansy *et al.* [5].

3.2
Key Historical Developments in Artificial-Membrane Permeability Measurement

Mueller *et al.* [6] discovered in 1962 that when a small quantity of a phospholipid (2% wt/vol alkane solution) was carefully placed over a small hole (0.5 mm) in a thin sheet of Teflon or polyethylene (10–25 μm thick), a thin film gradually forms at the center of the hole, with excess lipid flowing towards the perimeter (forming a "Plateau–Gibbs border"). Eventually, the central film turns optically black as a single (5 nm-thick) bilayer lipid membrane (BLM) forms over the hole. Suitable lipids for the formation of a BLM are mostly isolated from natural sources, e.g.,

lipids such as phosphatidylcholine (PC), phosphatidylethanolamine (PE), phosphatidylserine (PS), phosphatidylinositol (PI), sphingomyelin (Sph), and others. Such membranes have been viewed as useful models of the more complex natural membranes.

However, a serious drawback in using BLMs as a model system is that they are extremely fragile (requiring a vibration-damping platform and a Faraday cage), and tedious to prepare. That notwithstanding, Walter and Gutknecht [7] studied the permeation of a series of simple carboxylic acids across egg PC/decane BLMs. Intrinsic permeability coefficients, P_o, were determined from tracer fluxes, and a straight-line relationship was observed between $\log P_o$ and hexadecane/water partition coefficients, $\log K_p$, for all but the smallest carboxylic acid (formic): $\log P_o = 0.90 \log K_p + 0.87$. Using a similar BLM system, Xiang and Anderson [8] studied the pH-dependent transport of a series of α-methylene-substituted homologs of *p*-toluic acid. These authors compared the permeabilities to partition coefficients determined in octanol/, hexadecane/, hexadecene/, and 1,9-decadiene/water systems. The lowest correlation was found with octanol, whilst with the hexadecane/water system, $\log P_o = 0.85 \log K_p - 0.64$ ($r^2 = 0.998$), and with the decadiene/water system, $\log P_o = 0.99 \log K_p - 0.17$ ($r^2 = 0.996$). Corrections for the unstirred water layer were key to these analyses.

Efforts to overcome the limitations of the fragile membranes (thought to be as delicate as soap bubbles) have evolved with the use of membrane supports, e.g., polycarbonate filters or other more porous microfilters [9].

Cools and Janssen [10] studied the effect of background salt on the permeability of warfarin through octanol-impregnated membranes (Millipore ultrafiltration filters, VSWP, 0.025 μm pores). At a pH where warfarin was in its ionized form, it was found that increasing background salt increased permeability. This observation was thought to support an ion pair mechanism of transport of charged drugs across real biological membranes. However, current understanding of the structure of wet octanol [11] suggests that this isotropic solvent system may not be a suitable model for passive diffusion of charged drugs across phospholipid bilayers.

Camenisch *et al.* [12] measured the pH 7.4 permeabilities of a diverse group of drugs across octanol- and isopropylmyristate-impregnated artificial membranes (Millipore GVHP mixed cellulose ester filters, 0.22 μm pores), and compared them to permeabilities of the Caco-2 system, and octanol/water apparent partition coefficients, $\log K_{d(7.4)}$. It is reasonably clear that the *uncharged* drug species were the passive-diffusion permeants. (When the GVHP membrane was not impregnated with a lipid, the permeabilities of all the tested drugs were high and largely undifferentiated, indicating only the unstirred water layer resistance.) Over the range of lipophilicities, the curve relating the effective permeability, $\log P_e$, to $\log K_{d(7.4)}$ was seen as sigmoidal in shape, and only linear in the mid range. Between $\log K_{d(7.4)}$ −2 and 0, $\log P_e$ values correlated with the apparent partition coefficients. However, outside that range, there was no correlation between permeabilities and the octanol/water partition coefficients. At the high end, the permeabilities of very lipophilic molecules are limited by the unstirred water layer and

not the membrane *per se*. At the other extreme, very hydrophilic molecules were observed to be more permeant than predicted by octanol, due to an unidentified mechanism.

Kansy *et al*. [5, 13], at Hoffman-La Roche, published a widely read study of the permeation of drugs across phospholipid-coated filters. The report by these authors could not have come at a better time – just when the paradigm was shifting into screening for biopharmaceutic properties at high speeds, alongside the biological screening. Their PAMPA method has attracted much favorable attention, and has spurred the development of a commercial instrument [14, 15]. The Roche investigators were able to relate their measured fluxes to human absorption values with a hyperbolic curve, much like that indicated in Caco-2 screening. The outliers in their assays were molecules known to be actively transported. Since the artificial membranes have no active transport systems and no metabolizing enzymes, the assay would not be expected to model actively transported molecules. What one sees with PAMPA is pure passive diffusion, principally of the uncharged species. During the period between 2000 and 2001, several publications have emerged which describe PAMPA-like systems [14–23].

The system reported by Avdeef and coworkers [14, 15, 23] is an extension of the Roche approach, with several novel features described, including a way to assess membrane retention. In the PAMPA assay, a ''sandwich'' is formed from a 96-well microtiter plate and a 96-well microfilter plate, such that each composite well is divided into two chambers: donor at the bottom and acceptor at the top, separated by a 125 μm-thick microfilter disc (0.45 μm pores), coated with a 2% wt/vol dodecane solution of dioleoylphosphatidylcholine (DOPC), under conditions that multilamellar bilayers form inside the filter channels when the system contacts an aqueous buffer solution [9]. The Roche group used an artificial membrane formulation consisting of egg lecithin (mixed lipid containing mainly cholesterol, PC, PE, and PI) in dodecane [13]. Thin (6–10 μm), low porosity (20%), polycarbonate filters [18, 19], used in Caco-2 assays, appear too fragile for high-throughput PAMPA applications; better reproducibility has been achieved with the thicker (125 μm), higher-porosity (70%) filters reported by the Roche group.

Avdeef [23] derived the iso-pH (same pH in donor and acceptor wells) permeability equation which directly takes into account the membrane retention of a drug:

$$P_e = -\frac{2.303\ V_D}{A(t-\tau_{SS})}\left(\frac{1}{1+V_D/V_A}\right)\log_{10}\left[1-\left(\frac{1+V_A/V_D}{(1-R)}\right)\left(\frac{C_A(t)}{C_D(t=0)}\right)\right] \qquad (1)$$

where A = area of filter (cm^2), t = time (s), τ_{SS} = steady-state time (s), V_A and V_D are the acceptor and donor volumes (cm^3), respectively, and $C_A(t)$ and $C_D(t)$ are the measured acceptor and donor sample concentrations (mol cm^{-3}) at time t, respectively. An equivalent expression to that of Eq. (1) is obtained by the substitution of the argument of the log term with $[-V_D/V_A + (1 + V_D/V_A)/(1 - R)\ (C_D(t)/C_D(0))]$. The retention factor, R, is defined as $1 - [C_D(t) + C_A(t)\cdot V_A/V_D]/C_D(0)$.

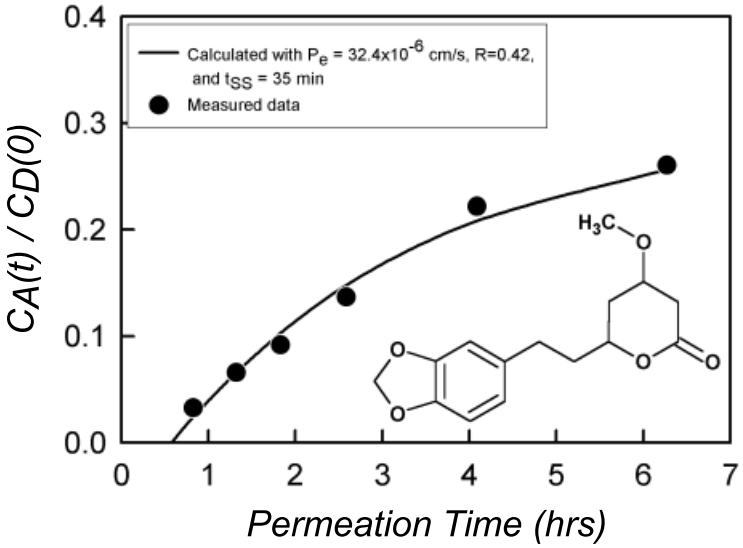

Fig. 3.1. Appearance of dihydromethysticin in the acceptor compartment as a function of time.

Figure 3.1 shows the appearance of dihydromethysticin in the acceptor well as a function of time [15]. The solid curve is a least-squares fit of the data points to Eq. (1), with the parameters: $P_e = 32 \times 10^{-6}$ cm s^{-1}, R = 0.42, and t_{SS} = 35 min. The membrane retention, R, is often stated as a mole percentage (%R) of the sample (rather than a fraction). Its value can at times be very high – up to 90% for chlorpromazine and 70% for phenazopyridine, when 2% wt/vol DOPC in dodecane is used. Figure 3.2 shows a plot of log %R versus log $K_{d(7.4)}$, the octanol/water apparent partition coefficient. It appears that retention is due to the lipophilicity of molecules; this may be a good predictor of the pharmacokinetic volume of distribution or of protein binding.

Cultured-cell assays also are subject to sample retention by the monolayer. Wils *et al.* [24] reported retentions as high as 44%, whereas Sawada *et al.* [25–27] cited values as high as 89%. This is undoubtedly a common phenomenon with research compounds, which are often highly lipophilic, yet the effect seems to be ignored in most reported studies.

Faller and Wohnsland [18, 19] developed the PAMPA assay using phospholipid-free hexadecane, supported on 10 μm-thick polycarbonate filters, and were able to demonstrate interesting predictions. Their PAMPA method appeared to be a satisfactory substitute for obtaining alkane/water partition coefficients, which are usually very difficult to measure directly, due to the poor solubility of drug molecules in alkanes. Apparently, membrane retention was not measured.

Sugano and coworkers [21, 22] explored the lipid model containing several different phospholipids, resembling the mixture found in reconstituted brush-border membrane (BBM) lipids [30, 31], and demonstrated improved property predictions. The best-performing lipid composition consisted of a 3% wt/vol lipid solu-

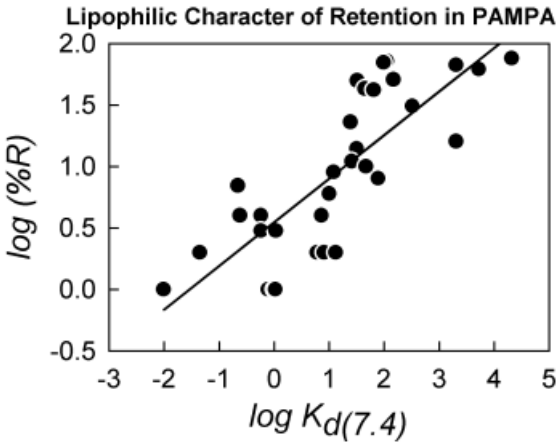

Fig. 3.2. Log of %mole fraction membrane retention versus log of apparent octanol/water partition coefficient at pH 7.4. Microfilters were impregnated with 2% wt/vol DOPC in dodecane.

tion in 1,7-octadiene (lipid consisting of 33% wt/wt cholesterol, 27% PC, 27% PE, 7% PS, 7% PI). The donor and acceptor compartments were adjusted in the pH interval between 5.0 and 7.4 [21]. With such a mixture, membrane retention is expected to be extensive when lipophilic drugs are assayed.

The structure of the filter-immobilized artificial membranes is generally unknown. Thompson *et al.* [9] hypothesized that polycarbonate filters had a single bilayer per pore, and presented interesting evidence for this concept. Hennesthal and Steinem [28], using scanning force microscopy, estimated that a single bilayer spans exterior pores of porous alumina. These observations may be incomplete, as there is considerable complexity to the spontaneous process of the formation of BLMs. When a 2% PC-dodecane solution is suspended in water, with water content >40 wt%, the lipid solution can take on the inverted hexagonal structure, where the polar head groups of the PC face water channels in a cylindrical structure [29]. Such structures can alter transport properties, compared to those of normal lamellar phases. (It may be possible to model the paracellular transport mechanism, should the presence of aqueous pores be established.) Suspensions of 2% PC-dodecane have been titrated potentiometrically from pH 10 down to pH 3. Along the way, at about pH 4, the pH electrode stopped functioning and appeared to be choked by a clear gelatinous coating, suggesting that some sort of phase transition had taken place at that point (A. Avdeef, unpublished results). It is particularly important in the PAMPA method that all depositions of the phospholipid be done under highly standardized procedures. Comparing the observed PAMPA permeability of salicylic acid to that observed in a BLM experiment [7], given the additivity of inverse permeabilities, it has been estimated that a permeant traverses many bilayers in passing through the 125 μm phospholipid-impregnated sponge-

like filters (data not shown). So far, the case for a single bilayer has not been definitively made.

3.3 The Ideal *in vitro* Artificial Membrane Permeability Model

3.3.1 Lipid Compositions in Biological Membranes

Proulx [30] summarized the published lipid compositions of BBM isolated from epithelial cells from pig, rabbit, mouse and rat small intestines. Table 3.1 shows the lipid make-up for the rat, averaged from five reported studies [30]. On a molar basis, cholesterol accounts for about 50% of the total lipid content (37% on a weight basis). Thus, the cholesterol content in BBM is higher than that found in kidney epithelial (MDCK) and brain endothelial cells (Table 3.1). Slightly different BBM lipid distribution was reported by Alcorn *et al.* [31]; here, the outer (luminal) leaflet of the BBM was seen to be rich in sphingomyelin content, while the inner leaflet (cytosol) was rich in PE and PC. Apical (brush border) and basolateral lipids are different in epithelia. The basolateral membrane content (not reported by

Tab. 3.1. Lipid compositions (%w/w) of biological membranes.[a]

Lipid[b]	*BBM*[c]	*BBB*[d]	*MDCK*[e]
PC	20	19	22
PE	18	23	29
PS	6	16	15
PI	7	7	10
Sph	7	9	10
FA		4	1
CHO+CE	37	22	10
TG		1	1

[a] The %w/w values in this table for BBB and MDCK are conversions from the originally reported %mol/mol units.
[b] PC = phosphatidylcholine; PE = phosphatidylethanolamine; PS = phosphatidylserine; PI = phosphatidylinositol; Sph = sphingomyelin; FA = fatty acid; CHO = cholesterol; CE = cholesterol ester; TG = triglycerides.
[c] BBM = brush border membrane, rat (average of four studies); from Ref. [30].
[d] BBB = blood–brain barrier lipid, RBE4 = rat endothelial immortalized cell line; from Ref. [37].
[e] MDCK = Madin–Darby canine kidney cultured epithelial cells; from Ref. [38].

Proulx) is high in PC, whereas the BBM has nearly the same PC as PE content. Krämer *et al.* [37, 38] reported MDCK and BBM lipid composition profiles, listed in Table 3.1, for comparative purposes.

3.3.2
Permeability–pH Considerations

The effective permeability of ionizable molecules depends on pH, and the shapes of the permeability–pH profiles can be theoretically predicted when the pK_a of the molecule is known [7]. The pH dependency of ionizable molecules is illustrated in Fig. 3.3 for a series of weak acids (A. Avdeef, not published). It is clear that if the "wrong" pH is used in screening the permeabilities of molecules, then highly promising molecules (e.g., probenecid; Fig. 3.3) may be characterized as false negatives. The ideal pH to use for *in vitro* screening ought to reflect the *in vivo* pH conditions.

Said *et al.* [32] directly measured the "acid microclimate" on the surface of gas-

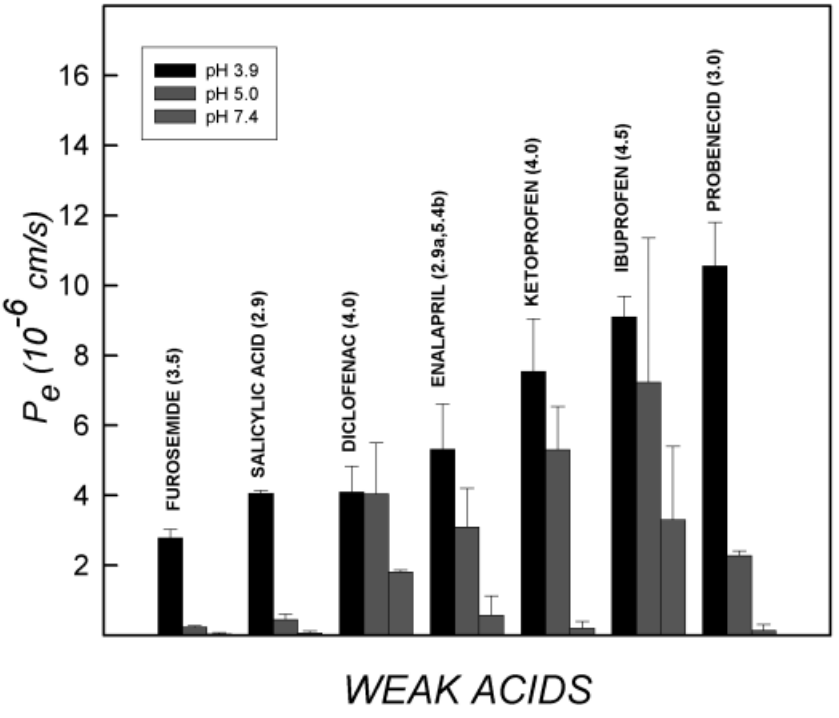

Fig. 3.3. Effective permeabilities measured at three pH values for a series of weak acids. Iso-pH conditions were used, i.e., the pH was the same in the donor and acceptor compartments. In general, the molecules with low pK_as show the highest permeabilities at low pH. At high pH, the species are predominantly negatively charged and are not very permeable. The pK_as of the molecules are indicated in parentheses after the name.

Tab. 3.2. Microclimate pH on the apical side of epithelial cells in the gastrointestinal (GI) tract in rats [32].

Position in the GI tract	*Microclimate pH*
Stomach	8.0
Proximal duodenum	6.4
Distal duodenum	6.3
Proximal jejunum	6.0
Mid jejunum	6.2
Distal jejunum	6.4
Proximal ileum	6.6
Mid ileum	6.7
Distal ileum	6.9
Proximal colon	6.9
Distal colon	6.9

trointestinal tract epithelial cells (intact with mucous layer) in rats. The pH on the apical (donor) side of the cells varied from 6.0 to 8.0, while the pH on the basolateral (acceptor) side was 7.4. Furthermore, the pH gradient between the donor and acceptor sides varied with position in the gastrointestinal tract, as indicated in Table 3.2. Others have measured microclimate pH as low as 5.2 [35].

Yamashita *et al.* [33] determined drug permeabilities by performing Caco-2 assays under two pH conditions: pH 6.0_{donor}–$7.4_{acceptor}$ and pH 7.4_{donor}–$7.4_{acceptor}$. These choices adequately span the microclimate range in the gastrointestinal tract. Weak acids were more permeable under the gradient-pH condition, compared to the iso-pH condition, whereas weak bases behaved in the opposite manner and uncharged molecules showed the same permeabilities under the two conditions. The gradient-pH set of permeability measurements provided a better prediction of human absorption than the iso-pH set ($r^2 = 0.85$ and 0.50, respectively).

In designing the ideal screening strategy, it appears important to consider using pH-gradients. If the *in vivo* conditions are to be mimicked, at least two effective permeability measurements should be attempted, as suggested by the above researchers: pH 6.0_{donor}–$7.4_{acceptor}$ (“gradient-pH”) and pH 7.4_{donor}–$7.4_{acceptor}$ (“iso-pH”), the microclimate pH range spanned in the gastrointestinal tract.

3.3.3 Role of Serum Proteins

Sawada and coworkers [25–27] studied the iso-pH 7.4 MDCK permeabilities of very lipophilic molecules, including chlorpromazine (CPZ) [25]. These authors included 3% wt/vol bovine serum albumin (BSA) on the apical (donor) side, and 0.1–3% BSA on the basolateral (acceptor) side, and found that plasma protein binding greatly affected the ability of molecules to permeate cellular barriers. They observed cell tissue retention of CPZ ranging from 65 to 85%, depending on the

amount of BSA present in the receiving compartment. They concluded that the rapid rate of disappearance of lipophilic compounds from the donor compartment was controlled by the unstirred water layer (UWL) (thus about the same for most lipophilic compounds); however, the very slow appearance of the compounds in the receiving compartment depended on the rate of desorption from the basolateral side of the membranes, which strongly depended on the presence of serum proteins in the receiving compartment. They recommended the use of serum proteins in the receiving compartment, so as to better mimic the *in vivo* conditions when using cultured cells, as *in vitro* assays.

Yamashita *et al.* [33] also studied the effect of BSA on transport properties in Caco-2 assays. These authors observed that the permeability of highly lipophilic molecules could be rate-limited by the process of desorption from the cell surface into the receiving solution, due to high membrane retention and very low water solubility. They recommended using serum proteins in the acceptor compartment when lipophilic molecules were being assayed – a common circumstance in discovery settings.

3.3.4
Effects of Cosolvents, Bile Acids, and other Surfactants

Yamashita *et al.* [33] added up to 10 mM taurocholic acid (cmc 2.9 mM), cholic acid (cmc 2.5 mM), or sodium lauryl sulfate (SLS, low ionic strength cmc 8.2 mM) to the donating solutions in Caco-2 assays. Although the two bile acids did not interfere in the transport of dexamethasone, SLS caused the Caco-2 cell junctions to become leakier, even at the sub-cmc 1 mM level. The permeability of dexamethasone was also decreased at 10 mM SLS.

These general observations have been confirmed in PAMPA measurements in our laboratory, using the 2% DOPC-dodecane lipid. With highly lipophilic molecules, glycocholic acid added to the donor solution slightly reduced permeabilities, taurocholic acid significantly increased permeabilities, but SLS arrested membrane transport altogether in several cases (especially cationic, surface active drugs such as CPZ) (data not shown).

Yamashita *et al.* [33] tested the effect of PEG400, DMSO, and ethanol, with up to 10% added to solutions in Caco-2 assays. PEG400 caused a dramatic decrease (75%) in the permeability of dexamethasone at 10% co-solvent concentration; DMSO caused a 50% decrease, but ethanol had only a slight decreasing effect. Sugano *et al.* [22] also studied the effect of PEG400, DMSO, and ethanol (up to 30%) in their PAMPA assays. In general, water-miscible co-solvents are expected to decrease the membrane/water partition coefficients. In addition, the decreased dielectric constants of the co-solvent/water solutions should give rise to a higher proportion of the ionizable molecule in the *uncharged* state [23]. These two effects oppose each other, and in general the increasing levels of co-solvents were observed to lead to decreasing permeabilities. However, ethanol made the weak acid ketoprofen (pK_a 4.12) more permeable with increasing co-solvent levels – an effect which was consistent with the increasing pK_a and the decreasing dielectric con-

stant of the co-solvent mixtures (leading to a higher proportion of uncharged species at a given pH). However, the same reasoning cannot be used to explain why the weak base propranolol (pK_a 9.5) decreased in permeability with increasing amounts of ethanol. This effect may be due to the increased solubility of propranolol in water with the added ethanol in relation to the solubility in the membrane phase. This leads to a lowered membrane/water (co-solvent) partition coefficient, hence lowering flux due to a diminished sample concentration gradient in the membrane (Fick's law) [23]. DMSO and PEG400 each dramatically reduced permeabilities for several of the molecules studied.

3.3.5
Components of the Ideal

The literature survey in this section suggests that the ideal *in vitro* permeability assay would have pH 6.0 and 7.4 in the donor wells, with pH 7.4 in the acceptor wells. (Such a two-pH combination could differentiate acids from bases and non-ionizables by the differences between the two P_e values.) Furthermore, the acceptor side would have 3% wt/vol BSA to maintain a sink condition (or some sink-forming equivalent). The donor side may benefit from having a bile acid (i.e., taurocholic or glycocholic, 5–15 mM), to solubilize the most lipophilic sample molecules. The ideal lipid barrier would have a composition similar to those in Table 3.1, with the membrane possessing a substantial negative charge (mainly from PI). Excessive DMSO/other co-solvents would be best avoided, due to their unpredictable effects.

3.4
New Directions in PAMPA

3.4.1
Concentrated and Charged Phospholipid Membranes

Hydrogen bonding and electrostatic interactions between the sample molecules and the phospholipid bilayer membranes are thought to play a key role in the transport of such molecules. When dilute 2% wt/vol phospholipid in alkane is used in the artificial membrane [15, 23], the effect of hydrogen bonding and electrostatic effects may be underestimated.

Recently in our group, model membrane permeation barriers have been constructed with concentrated phospholipid solutions, 10–74% wt/vol soy lecithin (approximate %w/w lipid composition 24% PC, 18% PE, 12% PI; cf. Table 3.1) in dodecane, supported on high-porosity, hydrophobic microfilters. This newly formulated lipid has a net negative charge at pH 7.4, which further increases above pH 8, as the ethanolamine groups deionize. Also tested were 10% wt/vol egg lecithin lipid solutions in dodecane (approximate composition 73% PC, 11% PE,

1% PI, 2% LysoPI). The inositol content was four times higher in soy than in egg lecithin.

However, when up to 74% phospholipid fractions are used, severe experimental problems arise. With lipophilic sample molecules, the use of concentrated phospholipid artificial membranes leads to two unwanted effects: (1) near-complete membrane retention (90–100%); and (2) highly diminished permeability (extinguished in some cases). Both of these effects are presumably due to excessive drug–membrane binding.

These adverse effects are almost eliminated by using an ionic surfactant to create a very strong sink condition in the *acceptor* compartment of the permeation cell, and this is the principal focus of our latest research. The charge on the micelles formed from the surfactant also appears to play a role in this respect.

3.4.2
Gradient-pH Permeability Equation

For ionizable molecules, sink conditions can also be created by pH gradients. Thus, additional PAMPA improvements can be achieved using such gradients between the donor and acceptor compartments of the permeation cell. A new three-chamber diffusion differential equation has been derived, that takes into account gradient-pH conditions and membrane retention of the drug molecule (which clearly still exists – albeit lessened – in spite of the sink condition created). The flux at time t, J(t), in units of mol cm^{-2} s^{-1}, can be defined by two equivalent expressions [34]: $J(t) = P_e^{(D\rightarrow A)}C_D(t) - P_e^{(A\rightarrow D)}C_A(t)$; and $J(t) = -(V_D/A)dC_D(t)/dt$, where the effective permeability coefficient is denoted by P_e (units of cm s^{-1}). Two different coefficients need to be considered, one denoted by the superscript (D→A), corresponding to donor pH_D (e.g., 5.0, 6.5 or 7.4) to acceptor pH_A (7.4) transport, and the other denoted by the superscript (A→D), corresponding to the reverse-direction transport. The two equivalent flux relationships can be reduced to an ordinary differential equation in $C_D(t)$, which may be solved by standard techniques [Ruell, Chau, Tsinman, Avdeef, in preparation], using integration limits from τ_{ss} to t (not 0 to t),

$$P_e^{(D\rightarrow A)} = -\frac{2.303\ V_D}{A(t-\tau_{ss})}\left(\frac{1}{1+R_a}\right)\log_{10}\left[-R_a + \left(\frac{1+R_a}{1-R}\right)\left(\frac{C_D(t)}{C_D(t=0)}\right)\right] \qquad (2)$$

where $R_a = (V_D/V_A)(P_e^{(A\rightarrow D)}/P_e^{(D\rightarrow A)})$, the "sink" asymmetry ratio. When the aqueous solution conditions (exclusive of the sample) are identical in the two chambers of the permeation cell, $R_a = V_D/V_A$, and Eq. (2) becomes equivalent to Eq. (1). This presumes that the system is free of surfactant.

In general, Eq. (2) has two unknowns: $P_e^{(A\rightarrow D)}$ and $P_e^{(D\rightarrow A)}$. In surfactant-free assays, the following method is used to solve Eq. (2). At least two assays are done: one as gradient-pH (e.g., pH 5.0_{donor}–$7.4_{acceptor}$) and the other as iso-pH (e.g., pH 7.4_{donor}–$7.4_{acceptor}$), with a pH in common to the two assays. For iso-pH,

$P_e^{(A\rightarrow D)} = P_e^{(D\rightarrow A)}$. This case can be solved directly with Eq. (1). Then, iteratively, Eq. (2) is solved for $P_e^{(D\rightarrow A)}$. Initially, R_a is assumed to be V_D/V_A, but with each iteration, the R_a estimate is improved by using the calculated $P_e^{(D\rightarrow A)}$ and the $P_e^{(A\rightarrow D)}$ taken from the iso-pH case. The process continues until self-consistency is reached.

If surfactant is added to the acceptor wells, then in general, $P_e^{(A\rightarrow D)}$ and $P_e^{(D\rightarrow A)}$ are not the same under iso-pH conditions. The acceptor-to-donor permeability needs to be solved by performing a separate iso-pH assay, where the surfactant is added to the *donor* side, instead of the acceptor side. The value of P_e is determined, using Eq. (1), and used in gradient-pH cases in place of $P_e^{(A\rightarrow D)}$, as described in the preceding paragraph. The gradient-pH calculation procedure is also iterative.

In iso-pH surfactant-free solutions, the concentration of the sample in the acceptor wells cannot exceed that in the donor wells. With gradient-pH conditions, this limitation is lifted. At very long times, the concentrations in the donor and acceptor chambers reach equilibrium values, depending on the pH gradient:

$$C_D(\infty)/C_A(\infty) = P_e^{(A\rightarrow D)}/P_e^{(D\rightarrow A)} \tag{3}$$

This limiting ratio can be predicted for any gradient-pH combination, provided that the pK_as of the molecule, the unstirred water layer (UWL), P_u, and the intrinsic, P_o, permeabilities are known [23]. In some of the gradient-pH assays, it is not uncommon to have nearly all of the sample move to the *acceptor* side, due to the sink conditions created, sometimes limiting the determination of concentrations. Shorter permeation times solve the problem, a welcome prospect in a high-throughput application. A 2- to 4-h period suffices, this being a considerable reduction over the original 15-h permeation time [5].

3.4.3
Permeability Measurements: High-phospholipid in Surfactant-free Solutions

Table 3.3 lists the pH 7.4 permeability and retention values of a series of well-known drug substances, grouped as bases, acids, and neutral molecules. The 2% DOPC-dodecane represents a high-purity charge-neutral phospholipid solution, whereas all the other phospholipid mixtures in the table contain progressively increasing (up to 68%) lecithin in dodecane, with substantial negatively charged PI content. Egg lecithin, having lower PI content, was also studied. All cases in Table 3.3 are without added surfactant.

Most of the permeabilities of the bases decrease steadily as the phospholipid fraction increases, though there are some significant exceptions. Metoprolol, which is moderately permeable in the DOPC lipid, becomes a top performer in 10% egg lecithin, though at the 68% soy level this molecule also shows reduced transport.

The permeabilities of the acid examples rise with increasing phospholipid content, up to 20% lipid, with rank ordering preserved (data not shown). Naproxen and ketoprofen show the most dramatic increases in going from 2% to 10% lipid membranes – somewhat higher in soy than in egg. Piroxicam shows less

Tab. 3.3. Permeability and retention in lipids of different compositions, at pH 7.4 in surfactant-free solutions (P_e in 10^{-6} cm/s units).

Sample	*2% DOPC*		*10% Egg*		*10% Soy*		*68% Soy*	
	P_e	%R	P_e	%R	P_e	%R	P_e	%R
Diltiazem.HCl	17.4	21	11.1	50	4.6	87	2.0	90
Phenazopyridine	15.2	70	6.1	91	5.8	95	5.3	99
Desipramine	12.3	40	5.5	89	1.2	97	3.2	91
Alprenolol	11.9	16	12.5	65	2.5	92	4.8	95
Imipramine	11.2	57	7.0	83	0.0	98	1.8	96
Propranolol	10.2	19	5.7	73	2.4	93	2.5	95
Verapamil	9.7	40	10.7	73	1.4	94	0.2	94
Promethazine	7.3	70	2.5	85	0.9	94	0.1	97
Metoprolol	0.7	12	17.8	71	6.0	44	3.2	73
Ranitidine	0.01	1	0.21	8	0.41	8	0.13	16
Sulpiride	0.01	1	0.22	5	0.19	12	0.10	16
Amiloride	0.003	0	0.006	15	0.004	14	0.000	0
Ibuprofen	2.7	38	7.8	58	4.0	63	1.6	30
Piroxicam	2.2	3	2.6	15	2.6	8	1.6	8
Naproxen	0.2	5	1.4	12	2.0	6	0.5	2
Ketoprofen	0.06	5	0.48	12	0.96	4	0.17	10
Theophylline	0.05	0	0.31	6	0.65	6	0.10	7
Salicyclic acid	0.03	1	0.04	15	0.13	2	0.03	9
Furosemide	0.02	1	0.01	19	0.02	4	0.01	17
Hydrochlorothiazide	0.01	1	0.01	24	0.02	6	0.02	3
Acetaminophen	0.01	3	0.86	0	0.68	4	0.00	0
Sulphasalazine	0.007	1	0.002	2	0.001	1	0.002	3
Griseofulvin	11.7	18	10.5	42	7.2	44	5.4	73
Progesterone	7.3	83	2.8	93	5.8	91	2.6	93
Carbamazepine	7.1	10	8.6	19	6.1	29	5.3	55
Caffeine	1.6	11	1.9	6	1.8	6	1.6	13
Antipyrine	0.8	14	1.3	27	1.2	7	0.5	8

sensitivity to lipid changes. For higher phospholipid concentrations, all the acid permeabilities decrease.

The nonionizable molecules respond to the changes in the phospholipid content, with griseofulvin having the highest permeability in the lowest phospholipid-containing membranes.

3.4.4
Membrane Retention Measurements: High-phospholipid in Surfactant-free Solutions

The most remarkable change of properties in going from 2% to 10% phospholipid occurs with the membrane retention of the bases. Most of the bases are retained above 90% in all of the soy lecithin cases (up to 68%). This is largely due to the

added electrostatic attractions between positively charged sample molecules and the negatively charged membrane constituents.

Acids show small, steady increases in membrane retention with increasing phospholipid content. Even though the acids are negatively charged at pH 7.4, as are a portion of the membrane constituents, the increasing phospholipid content draws the sample molecules in, due to increased hydrogen-bonding and any other lipophilic forces arising from the phospholipids (increased membrane/water partition coefficient).

Neutral molecules show a range of retention properties between those of acids and bases. Progesterone membrane retention is very high in all cases, while griseofulvin and carbamazepine retentions steeply increase with phospholipid content.

The patterns of retention follow the lipophilicity properties of the molecules, as indicated by octanol/water apparent partition coefficients.

3.4.5
Egg Lecithin and the Degree of Negative Charge

The negative charge content in the egg lecithin is about four times *less* than in the soy lecithin used. This is clearly evident in the membrane retention parameters for the bases at the 10% lecithin levels (Table 3.3), being about 20–30% lower for the lipophilic bases in egg, compared with soy.

With acids, the membrane retention actually *increases* in the case of egg lecithin, compared with soy. This may be due to decreased repulsions between the negatively charged sample and negatively charged phospholipid, allowing H-bonding and other lipophilic forces to more fully realize in the less negatively charged egg lecithin membranes.

The neutral molecules display about the same transport properties in soy and egg lecithin, in line with the absence of direct electrostatic effects.

3.4.6
Summary: Increasing Phospholipid Content in the Absence of Sink Conditions

As the amount of phospholipid increases in the dodecane solution injected into the filters, the effects of H-bonding and electrostatics increase in the transport process. Generally, the membrane retention of the lipophilic molecules increases with increasing lecithin content, most dramatically in the case of lipophilic bases (due to the added electrostatic attractions). Such losses of compound to the membrane pose a challenge to the analysis of concentrations, which can be significantly diminished (to undetectable levels at times) in the aqueous compartments. At the same time, the permeability decreases to near vanishing values in 68% soy lecithin-dodecane membranes. Under these conditions, the permeabilities of the lipophilic bases and acids converge to similar values, significantly departing from the expected values based on lipophilic properties (see Table 3.6) and the pH-partition hypothesis. This is mainly affected by excessive drug–membrane binding,

which would not be expected under *in vivo* conditions in the presence of naturally occurring sink conditions. Thus, the raising of the phospholipid content *alone* does not generally benefit the PAMPA method.

3.4.7 Effects of Surfactant on High-phospholipid Membrane Permeability and Retention

The transport properties of the molecules in concentrated soy lecithin (see Table 3.3) do not adequately model the *in vivo* permeabilities reported by Winiwarter *et al.* [36] (see Table 3.6). The strategy to overcome this shortcoming involves creating a significant sink condition in the acceptor wells. However, the

Tab. 3.4. Permeability and retention in various lipids, at pH 7.4 with 35 mM SLS in acceptor wells (P_e in 10^{-6} cm s^{-1} units).

Sample	*2% DOPC*		*10% Egg*		*10% Soy*		*74% Soy*	
	P_e	*%R*	P_e	*%R*	P_e	*%R*	P_e	*%R*
Diltiazem	33.9	13	27.6	12	35.8	22	3.5	61
Phenazopyridine	31.4	26	20.3	44	15.8	47	3.9	75
Desipramine	25.1	22	21.8	30	33.2	33	1.7	59
Alprenolol			23.1	27	30.6	30	2.6	71
Imipramine	22.2	21	31.8	23	30.1	38	5.0	63
Propranolol	14.3	16	16.1	24	27.1	39	0.0	62
Verapamil	37.4	17	23.4	20	25.6	31	1.8	71
Promethazine	31.5	12	31.2	17	26.7	25	3.7	61
Quinine	2.7	13	9.9	31	24.6	44	2.6	67
Metoprolol	0.4	3	23.4	19	26.4	27	4.0	52
Prazosin			3.8	20	28.6	16	0.4	49
Ranitidine	0.01	0	0.16	7	0.34	8	0.00	3
Sulpiride	0.14	1	0.04	5	0.22	6	0.10	3
Amiloride	0.00	1	0.00	7	0.01	9	0.00	5
Terbutaline	0.06	0	0.13	6	0.17	14	0.00	1
Ibuprofen	2.4	7	10.3	16	3.6	32	2.0	33
Piroxicam	2.0	3	2.7	6	2.3	6	1.0	6
Naproxen	0.3	1	0.9	4	1.8	10	0.2	1
Ketoprofen	0.17	2	0.61	1	0.83	9	0.00	4
Theophylline			0.44	5	0.51	7	0.02	6
Salicyclic acid			0.90	3	0.24	13	0.17	0
Furosemide	0.04	1	0.06	4	0.04	14	0.00	10
Hydrochlorothiazide	0.00	1	0.11	4	0.00	11	0.01	5
Acetaminophen			0.00	3	1.2	8	0.00	0
Sulphasalazine	0.03	3	0.01	3	0.00	2	0.00	2
Griseofulvin	18.2	10	19.0	15	31.8	25	13.4	44
Progesterone	22.7	34	29.4	22	37.6	40	31.8	39
Carbamazepine	6.4	13	10.7	19	16.5	23	2.1	38
Caffeine	1.2	4	2.2	5	1.5	8	1.2	8
Antipyrine	0.6	4	1.9	3	1.6	6	1.0	1

use of BSA or other serum proteins, although easily effected, is not practical in high-throughput screening, since the UV absorption due to the proteins would make determination of the compound concentrations in the acceptor compartments by direct UV spectrophotometry nearly impossible in most cases. Without knowledge of the concentration of sample in the acceptor compartment, the determination of membrane retention would not be possible. Some PAMPA practitioners, using BSA to create sink conditions, assume that membrane retention is zero. It is neither reasonable nor warranted to expect that membrane retention is eliminated in the presence of serum proteins or other practical substitutes in the acceptor compartment. Since lipophilic molecules have affinity for *both* the membrane lipid and the serum proteins, retention should be diminished, by the extent of the relative lipophilicities of the drug molecules in membrane lipid versus serum proteins, and by the relative volumes of the two competitive-binding phases. Generally, the serum proteins cannot extract all of the sample molecules from the phospholipid membrane phase at equilibrium. Thus, to measure permeability under sink conditions, it is still necessary to characterize the extent of membrane retention. This had not been done generally.

We have found that the negatively charged surfactant SLS can be successfully substituted for the serum proteins used by several other investigators. In low ionic strength solutions, the cmc of SLS is 8.1 mM [39]. We explored the use of both sub-cmc (data not shown) and micelle-level concentrations. Saturated micelle solutions (35 mM, approximately the solubility of SLS at room temperature) are most often used in our group.

The effect of the surfactant is most dramatic for the bases and neutral molecules studied, as shown in Table 3.4. Permeabilities increased by about four-fold for the lipophilic bases and neutral molecules, and membrane retentions were decreased by 50% in most cases of bases and neutral compounds.

Tab. 3.5. Permeability (10^{-6} cm s^{-1}) and retention in 20% wt./vol. soy lecithin, at iso-pH 5.0, 6.5, 7.4 with 35 mM SLS in acceptor wells.

Sample	***pH 5.0***	***%R***	***pH 6.5***	***%R***	***pH 7.4***	***%R***
Desipramine	10.4	35	19.4	35	29.7	39
Propranolol	37.4	31	26.0	37	25.8	40
Verapamil	9.1	30	20.7	20	31.6	31
Metoprolol	2.9	17	16.1	25	28.6	26
Ranitidine	0.00	4	0.03	2	0.31	14
Piroxicam	10.2	24	8.9	12	3.2	17
Naproxen	11.8	50	6.6	12	2.3	13
Ketoprofen	9.5	37	6.5	12	1.2	12
Furosemide	0.8	25	0.0	2	0.0	11
Carbamazepine	19.5	27	17.9	18	15.3	26
Antipyrine	0.9	17	3.0	11	1.7	14

The transport properties of the acids did not respond significantly to the presence of surfactant. This may be because at pH 7.4 the acids are negatively charged, as are the phospholipid membranes and also the surfactant micelles; electrostatic repulsions balanced out the attractive forces due to increased membrane lipophilicity.

3.4.8 Quality and Usefulness of the UV Spectra

The use of direct UV spectrophotometry to measure sample concentrations in pharmaceutical research is uncommon, presumably due to the prevalence and attractiveness of high-performance liquid chromatography (HPLC) and liquid chromatography/mass spectrometry (LC/MS) methods. Consequently, most researchers are unfamiliar with the value of UV detection, mainly that it is generally much faster than other methods – a very important asset in high-throughput screening.

If samples are highly impure or decompose readily, then use of the UV method is inappropriate, and LC/MS has been shown to be the most suitable detection system under such conditions [15]. When used carefully, LC/MS produces excellent results; however, when LC/MS data-taking is driven very rapidly (e.g., 20 min/plate), disappointing results have been noted in collaborative studies (data not shown).

Figure 3.4a shows the acceptor, donor, and reference spectra of 48 μM propranolol after a 15 h PAMPA assay using 20% wt/vol soy lecithin in dodecane. The sum of the donor (3 μM) and the acceptor (<1 μM) well concentrations indicates that 45 μM is lost to the membrane. In the absence of a sink-creating surfactant, only a trace of propranolol reached the acceptor wells after 15 h, with 94% of the compound trapped in the membrane, compared with 19% in the 2% wt/vol DOPC case (see Table 3.3). The effective permeability in 20% soy fell to 1.8×10^{-6} cm s^{-1}, compared with the DOPC value of 10.2×10^{-6} cm s^{-1}.

With 35 mM SLS in the acceptor compartment (Fig. 3.4b), the amount of propranolol reaching the acceptor wells is dramatically increased, with the concomitant decrease in membrane retention from 94% to 41%. Furthermore, the effective permeability rises to 25.1×10^{-6} cm s^{-1} (a more than ten-fold increase), presumably due to the desorption effect of the SLS creating an effective sink condition. Only 3 h permeation time was used in this case (Fig. 3.4b). With such a sink at work, one can lower the permeation time to less than 2 h and still obtain very useful UV spectra, and this represents a major benefit for high-throughput requirements.

The weighted residuals plots in Fig. 3.4 are the results of the analyses, where the shape of the reference spectra are matched to those of acceptor and donor spectra by least-squares refinement. Poor shape-analysis leads to high weighted residuals, which can reveal impurities, decomposition, or other artifacts. In the present cases, no difficulties were encountered.

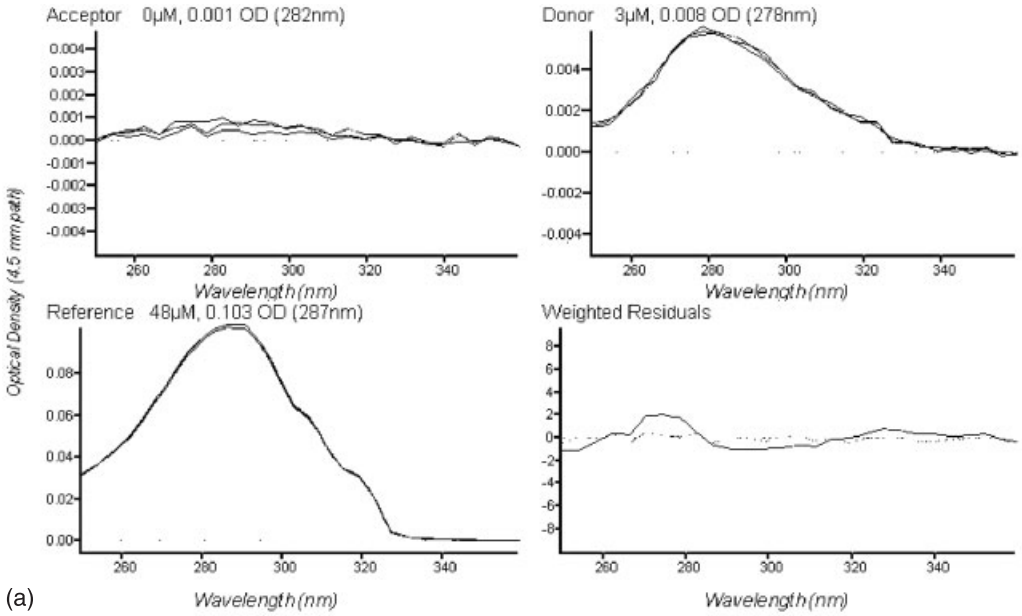

(a)

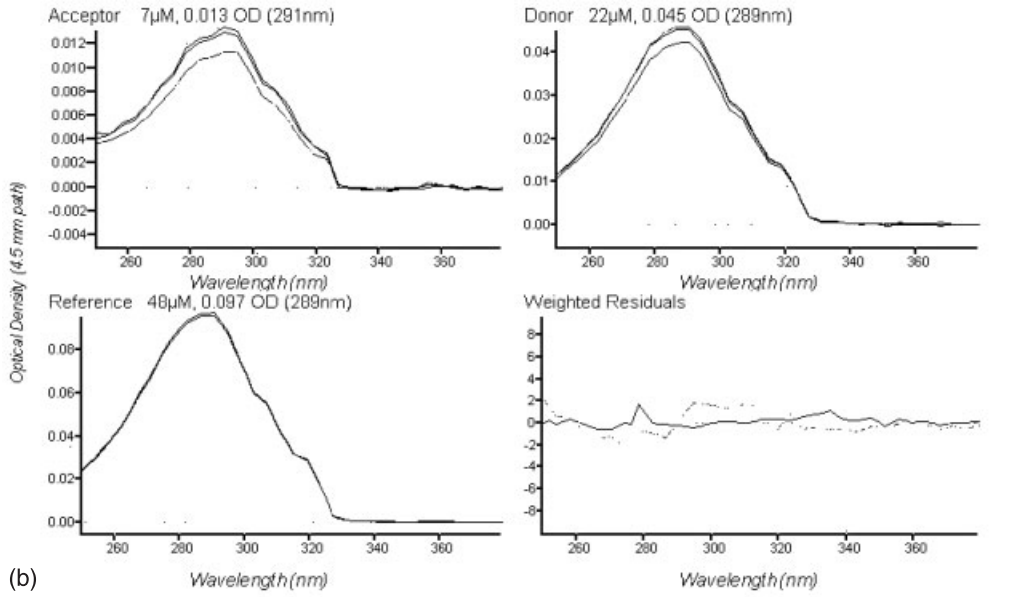

(b)

Fig. 3.4. Microtiter plate UV spectra taken in triplicate of propranolol reference, donor, and acceptor solutions, at iso-pH 7.4 in 20% wt/vol soy lecithin in dodecane. (a) After 15 h permeation time, surfactant-free; (b) 3 h, 35 mM in acceptor wells. The weighted residuals plots indicate that the shapes of spectra in donor and acceptor wells are in agreement with those in the reference wells, confirming that neither decomposition nor impurities were detectable.

3.4.9

Iso-pH and Gradient-pH Mapping in 2% DOPC-Dodecane

To illustrate the subtle differences between the iso-pH and gradient-pH methods, ketoprofen was used in a series of simulation calculations. Figure 3.5a shows the concentration–time profiles for ketoprofen under an iso-pH condition. Consider the case of iso-pH 3, where the molecule is essentially uncharged in solution (pK_a

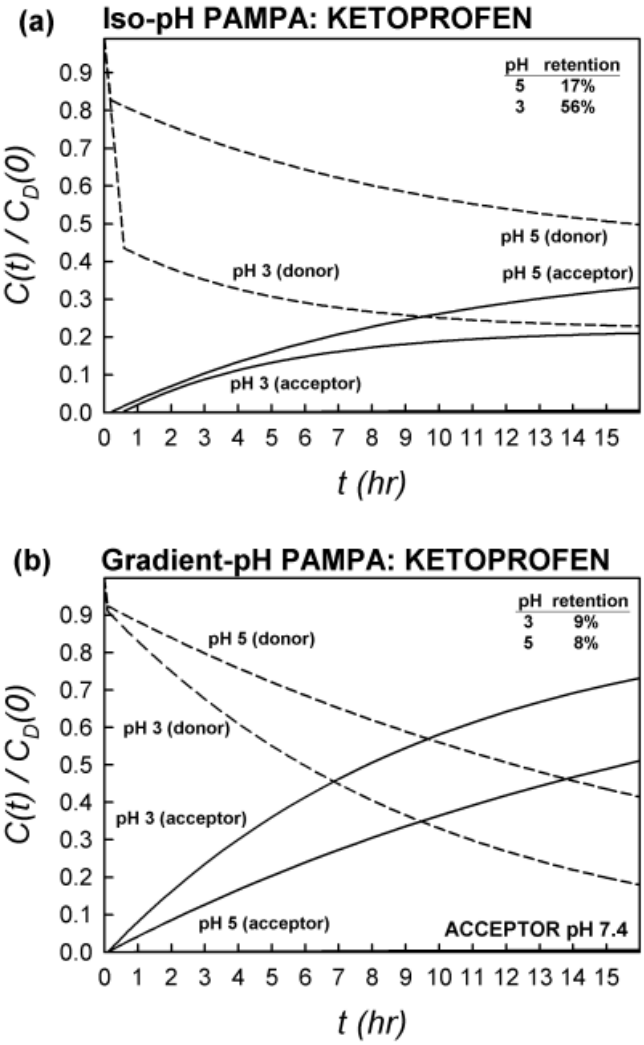

Fig. 3.5. Comparison of concentration–time profiles of ketoprofen under (a) iso-pH, and (b) gradient-pH conditions. The sink condition caused by pH gradients lowers the membrane retention from 56% to 9%, and hastens the transport of the weak acid.

4.12 at I = 0.01 M; see Table 3.6). The dashed curve in Fig. 3.5a (donor concentration) corresponding to pH 3 indicates a steep descent during the first 30 min of the permeation. This is the phase where the membrane is loaded with the sample – the ''build-up'' phase in membrane retention; in this case, 56% of the ketoprofen is retained by the membrane. The solid curve (acceptor concentration) in Fig. 3.5a

Tab. 3.6. Pharmacokinetic and physico-chemical properties.[a]

Sample	*%f_A*	*Human jejunal P_e (10^{-4} cm s^{-1})*[b]	*I = 0.01 M*				*Charge*	
			log $K_{d(7.4)}$	*pK_{a1}*	*pK_{a2}*	*pK_{a3}*	*Profile*	*Type*
Phenazopyridine			3.31	5.15			+ > o	Base
Verapamil	95	6.7	2.51	9.07			+ > o	Base
Promethazine	80		2.44	9.00			+ > o	Base
Quinine	80		2.19	4.09	8.55		++ > + > o	Base
Imipramine	99		2.17	9.51			+ > o	Base
Diltiazem	99		2.16	8.02			+ > o	Base
Prazosin	50		2.00	7.11			+ > o	Base
Propranolol	99	2.9	1.41	9.53			+ > o	Base
Desipramine	95	4.4	1.38	10.16			+ > o	Base
Alprenolol	93		0.86	9.51			+ > o	Base
Metoprolol	95	1.3	−0.24	9.56			+ > o	Base
Ranitidine	50	0.43	−0.53	1.96	8.31		++ > + > o	Base
Amiloride	50		−0.60	8.65			+ > +-	Base
Ibuprofen	80		1.44	4.59			o > -	Acid
Acetaminophen	100		0.34	9.78			o > -	Acid
Naproxen	99	8.8	0.09	4.32			o > -	Acid
Sulphasalazine	13		0.08	2.80	8.25	10.96	o > - > = > =-	Acid
Theophylline	98		0.00	8.70			o > -	Acid
Ketoprofen	100	8.4	−0.11	4.12			o > -	Acid
Hydrochlorothiazide	67	0.04	−0.18	8.91	10.25		o > - > =	Acid
Furosemide	61	0.05	−0.24	3.67	10.93		o > - > =	Acid
Salicyclic acid	100		−1.68	3.02			o > -	Acid
Piroxicam	100	7.8	0.00	2.33	5.22		+ > o > -	Ampholyte
Sulpiride	35		−1.15	9.12	10.14		+ > o > -	Ampholyte
Terbutaline	60	0.3	−1.35	8.67	10.12	11.32	+ > +- > - > =	Zwitterion
Progesterone	91		3.89				o	Neutral
Griseofulvin	28		2.47				o	Neutral
Carbamazepine	100	4.3	2.45				o	Neutral
Antipyrine	100	4.5	0.56				o	Neutral
Caffeine	100		−0.07				o	Neutral

[a] $\%f_A$ is the fraction absorbed following an oral dose taking; log $K_{d(7.4)}$ is the apparent octanol/water partition coefficient; pK_a are ionization constants, values corrected to 0.01 M ionic strength used in the PAMPA assay; charge profile refers to the order in which charges on the molecules change as pH is raised from 2 to 10.
[b] From Ref. [36].

corresponding to pH 3 begins to grow, but not until the membrane retention is fully achieved (30 min). After 16 h, the descending donor curve and the ascending acceptor curve nearly meet at $C(t)/C_D(0)$ of about 0.2. (In the absence of membrane retention, the convergence concentration ratio would have been 0.5, instead of 0.2.) The lower value indicates that the measurement of sample concentrations might not be as sensitive, as more than half of the sample is "lost" to the membrane.

Now consider the gradient-pH case, with pH_D 3 and pH_A 7.4. In Fig. 3.5b, the dashed curve (donor concentration) corresponding to pH 3 decreases more steeply after the retention period than that of the previous iso-pH example. Furthermore, there is not the large initial drop due to the disappearance of the sample into the membrane; in the gradient-pH case, retention drops from 56% to 9%. Thus, more of the compound is available for sample concentration determination. The solid curve (acceptor concentration) corresponding to pH 3 also grows more rapidly than in the iso-pH example. The dashed and solid curves cross at 7 h, with $C(t)/C_D(0)$ close to the 0.5 value. Note also, that about 70% of the compound ends up in the acceptor well at the end of 16 h – much higher than is possible with the iso-pH method.

We are currently exploring the experimental applications of the gradient-pH PAMPA method with surfactant-induced sink condition. Some of our preliminary

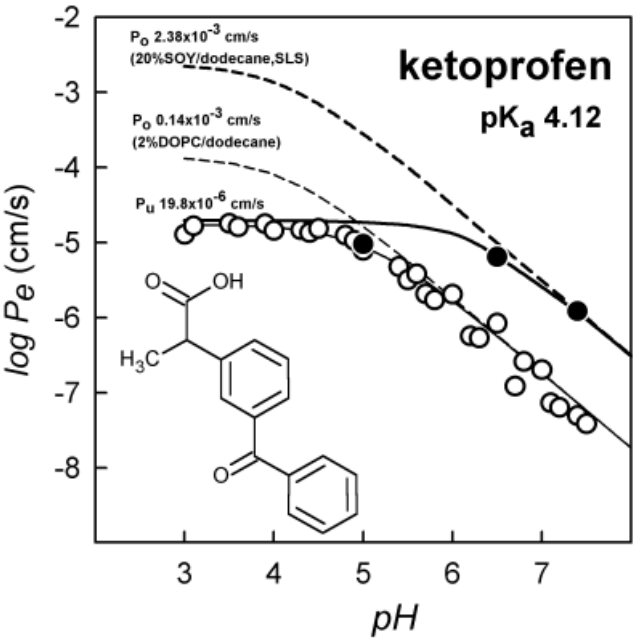

Fig. 3.6. Log permeability–pH profiles of ketoprofen in 2% wt/vol DOPC in dodecane (open circles) and 20% wt/vol soy lecithin in dodecane (filled circles). The weak acid is about 17 times more permeable in soy than in DOPC, as indicated by the calculated intrinsic permeabilities, P_o. The UWL limits the actual transport in both systems, to permeability values P_u 19.8 $\times$ 10^{-6} cm s^{-1}. The dashed curves are calculated from the differences between the true pK_a and the apparent pK_a^{flux} values (see text).

results are intriguing, and suggest that charged drug molecules, such as propranolol and quinine, can permeate the soy lecithin membranes substantially at pH 5, an abandonment to the pH-partition hypothesis. More will be reported on this point in the near future.

3.4.10
Iso-pH Mapping in 20% Soy Lecithin-Dodecane, with Surfactant

Figure 3.6 compares iso-pH permeabilities of ketoprofen at various pH values in a 2% DOPC-dodecane model (open circles) and the 20% soy lecithin with SLS in the acceptor compartment (filled circles, data in Table 3.5). In the presence of the latter negatively charged lipids (with the make-up similar to that of BBM in Table 3.1), ketoprofen is intrinsically more permeable, by a factor of 17. The UWL limit, indicated by the solid curves in low-pH solutions, and consistent with the permeability P_u 19.8×10^{-6} cm s^{-1} (log P_u -4.7), masks the true intrinsic permeability of the membranes, P_o. However, it is possible to deduce the membrane permeability if the pK_a is known. In Fig. 3.6, the bending in the dashed (calculated) curves at pH 4 corresponds to the pK_a of the molecule. Due to the UWL, the point of bending is shifted to higher pH values in the solid (measured) curves. The difference between the apparent pK_a (pK_a^{flux} 5.3 for DOPC and 6.3 for soy) and the true pK_a (4.12) is the same as the difference between log P_o and log P_u [23].

3.4.11
Predictions of *in vivo* Human Jejunal Permeabilities using the Improved 20% Soy Lecithin with Surfactant *in vitro* PAMPA Technique

The studies of various compositions revealed that the 20% soy lecithin-dodecane membrane with 35 mM in the acceptor wells has substantially improved predictive value compared with the 2% DOPC model. Fine-tuning of the model components may be guided by the *in vitro–in vivo* (IV–IV) correlations, comparing the improved PAMPA model permeabilities to the human jejunal permeabilities measured by Winiwarter *et al.* [36] (Table 3.6). Table 3.7 lists the results of comparisons of various models. The best correlations were realized with the 20% soy lecithin-dodecane system, employing 35 mM SLS in the acceptor compartment, but a better

Tab. 3.7. *in vitro–in vivo* correlations, PAMPA versus human jejunal permeabilities.

PAMPA lipid model	*Equation: log P_e (human jejunal) = a + b log P_e (PAMPA)*			
	pH	*a*	*b*	r^2
2% DOPC	7.4	−0.946	0.453	0.417
10% egg, no surfactant	7.4	−0.410	0.588	0.490
10% egg, 35 mM SLS	7.4	0.012	0.634	0.669
20% soy, 35 mM SLS	6.5	−1.140	0.453	0.715

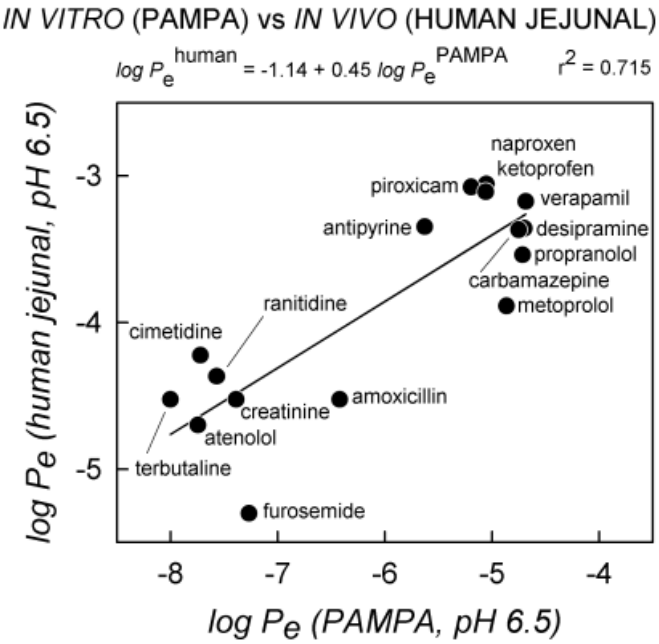

Fig. 3.7. Correlation between human jejunal and PAMPA permeabilities (see Tab. 3.7 and text).

correlation was realized with iso-pH 6.5 than with iso-pH 7.4. Figure 3.7 shows the best correlation plot, based on the pH 6.5 model mentioned above. Other combinations have become evident to us, which may further improve the IV-IV correlations.

Acknowledgments

I wish to thank my colleagues at pION, Chau Du, Jeffrey Ruell, Konstantin Tsinman, and Dmytro Voloboy for expertly collecting and analyzing PAMPA data. I am indebted to Per Nielsen, Cynthia Berger (pION), Li Di, Hanlan Liu, Edward Kerns (Wyeth-Ayerst), Manfred Kansy (Roche), and other PAMPA practitioners for many stimulating discussions.

References

1 Hidalgo, I. J., Kato, A., Borchardt, R. T., Binding of epidermal growth factor by human colon carcinoma cell (Caco-2) monolayers, *Biochem. Biophys. Res. Commun.* **1989**, *160*, 317–324.

2 Hilgers, A. R., Conradi, R. A., Burton, P. S., Caco-2 cell monolayers as a model for drug transport across the intestinal mucosa, *Pharm. Res.* **1990**, *7*, 902–910.

3 Artursson, P. J., Epithelial transport of drugs in cell culture. I: a model for studying the passive diffusion of drugs over intestinal absorptive (Caco-2) cells, *Pharm. Sci.* **1990**, *79*, 476–482.

4 Amidon, G. L., Lennernäs, H., Shah, V. P., Crison, J. R., A theoretical basis for a biopharmaceutic drug classification: the correlation of in vitro drug product dissolution and

in vivo bioavailability, *Pharm. Res.* **1995**, *12*, 413–420.

5 Kansy, M., Senner, F., Gubernator, K., Physicochemical high throughput screening: parallel artificial membrane permeability assay in the description of passive absorption processes, *J. Med. Chem.* **1998**, *41*, 1007–1010.

6 Mueller, P., Rudin, D. O., Tien, H. T., Westcott, W. C., Reconstitution of cell membrane structure in vitro and its transformation into an excitable system, *Nature* **1962**, *194*, 979–980.

7 Walter, A., Gutknecht, J., Monocarboxylic acid permeation through lipid bilayer membranes, *J. Membr. Biol.* **1984**, *77*, 255–264.

8 Xiang, T.-X., Anderson, B. D., Substituent contributions to the transport of substituted p-toluic acids across lipid bilayer membranes, *J. Pharm. Sci.* **1994**, *83*, 1511–1518.

9 Thompson, M., Lennox, R. B., McClelland, R. A., Structure and electrochemical properties of microfiltration filter-lipid membrane systems, *Anal. Chem.* **1982**, *54*, 76–81.

10 Cools, A. C., Janssen, L. H. M., Influence of sodium ion-pair formation on transport kinetics of warfarin through octanol-impregnated membranes, *J. Pharm. Pharmacol.* **1983**, *35*, 689–691.

11 Franks, N. P., Abraham, M. H., Lieb, W. R., Molecular organization of liquid n-octanol: an X-ray diffraction analysis, *J. Pharm. Sci.* **1993**, *82*, 466–470.

12 Camenisch, G., Alsenz, J., van de Waterbeemd, H., Folkers, G., Estimation of permeability by passive diffusion through Caco-2 cell monolayers using the drugs' lipophilicity and molecular weight, *Eur. J. Pharm. Sci.* **1998**, *6*, 313–319.

13 Kansy, M., Fischer, H., Kratzat, K., Senner, F., Wagner, B., Parrilla, I., High-throughput artificial membrane permeability studies in early lead discovery and development, in: *Pharmacokinetic Optimization in Drug Research.* Testa, B., van de Waterbeemd, H., Folkers, G., Guy, R. (eds), Verlag Helvetica Chimica Acta, Zürich and Wiley-VCH, Weinheim, **2001**, pp. 447–464.

14 Avdeef, A., High-throughput measurement of solubility profiles, in: *Pharmacokinetic Optimization in Drug Research.* Testa, B., van de Waterbeemd, H., Folkers, G., Guy, R. (eds), Wiley-VCH, Weinheim, **2001**, pp. 305–326.

15 Avdeef, A., Strafford, M., Block, E., Balogh, M. P., Chambliss, W., Khan, I., Drug absorption in vitro model: filter-immobilized artificial membranes. 2. Studies of the permeability properties of lactones in *Piper methysticum* Forst, *Eur. J. Pharm. Sci.* **2001**, *14*, 271–280.

16 Johnson, S., Lin, F., Cheng, H. Y., Hung, S., Saunders, J., Zheng, W., Seibel, G., Using molecular structure to assess permeability in a discovery setting, in: 220th ACS National Meeting, Washington, DC, August **2000**.

17 Zhu, C., Chen, T.-M., Hwang, K., A comparative study of parallel artificial membrane permeability assay for passive absorption screening, in: CPSA2000: The Symposium on Chemical and Pharmaceutical Structure Analysis. Milestone Development Services. Princeton, NJ, 26–28 September **2000**.

18 Faller, B., Wohnsland, F., Physicochemical parameters as tools in drug discovery and lead optimization, in: *Pharmacokinetic Optimization in Drug Research.* Testa, B., van de Waterbeemd, H., Folkers, G., Guy, R. (eds), Verlag Helvetica Chimica Acta, Zürich and Wiley-VCH, Weinheim, **2001**, pp. 257–274.

19 Wohnsland, F., Faller, B., High-throughput permeability pH profile and high-throughput alkane/water log P with artificial membranes, *J. Med. Chem.* **2001**, *44*, 923–930.

20 Hwang, K., Predictive artificial membrane technology for high throughput screening, in: *New Technologies to Increase Drug Candidate*

Survivability Conference. SR Institute. 17–18 May **2001**, Somerset, NJ.

21 Sugano, K., Hamada, H., Machida, M., Ushio, H., High throughput prediction of oral absorption: improvement of the composition of the lipid solution used in parallel artificial membrane permeability assay, *J. Biomolec. Screen.* **2001**, *6*, 189–196.

22 Sugano, K., Hamada, H., Machida, M., Ushio, H., Saitoh, K., Terada, K., Optimized conditions of bio-mimetic artificial membrane permeability assay, *Int. J. Pharm.* **2001**, *228*, 181–188.

23 Avdeef, A., Physicochemical Profiling (Solubility, Permeability, and Charge State), *Curr. Topics Med. Chem.* **2001**, *1*, 277–351.

24 Wils, P., Warnery, A., Phung-Ba, V., Legrain, S., Scherman, D., High lipophilicity decreases drug transport across intestinal epithelial cells, *J. Pharmacol. Exp. Ther.* **1994**, *269*, 654–658.

25 Sawada, G. A., Ho, N. F. H., Williams, L. R., Barsuhn, C. L., Raub, T. J., Transcellular permeability of chlorpromazine demonstrating the roles of protein binding and membrane partitioning, *Pharm. Res.* **1994**, *11*, 665–673.

26 Sawada, G. A., Barsuhn, C. L., Lutzke, B. S., Houghton, M. E., Padbury, G. E., Ho, N. F. H., Raub, T. J., Increased lipophilicity and subsequent cell partitioning decrease passive transcellular diffusion of novel, highly lipophilic antioxidants, *J. Pharmacol. Exp. Ther.* **1999**, *288*, 1317–1326.

27 Sawada, G. A., Williams, L. R., Lutzke, B. S., Raub, T. J., Novel, highly lipophilic antioxidants readily diffuse across the blood-brain barrier and access intracellular sites, *J. Pharmacol. Exp. Ther.* **1999**, *288*, 1327–1333.

28 Hennesthal, C., Steinem, C., Pore-spanning lipid bilayers visualized by scanning force microscopy, *J. Am. Chem. Soc.* **2000**, *122*, 8085–8086.

29 Lichtenberg, D., Micelles and liposomes, in: *Biomembranes: Physical Aspects.* Shinitzky, M. (ed.), VCH, Weinheim, **1993**, pp. 63–96.

30 Proulx, P., Structure-function relationships in intestinal brush border membranes, *Biochim. Biophys. Acta* **1991**, *1071*, 255–271.

31 Alcorn, C. J., Simpson, R. J., Leahy, D. E., Peters, T. J., Partition and distribution coefficients of solutes and drugs in brush border membrane vesicles, *Biochem. Pharmacol.* **1993**, *45*, 1775–1782.

32 Said, H. M., Blair, J. A., Lucas, M. L., Hilburn, M. E., Intestinal surface acid microclimate in vitro and in vivo in the rat, *J. Lab. Clin. Med.* **1986**, *107*, 420–424.

33 Yamashita, S., Furubayashi, T., Kataoka, M., Sakane, T., Sezaki, H., Tokuda, H., Optimized conditions for prediction of intestinal drug permeability using Caco-2 cells, *Eur. J. Pharm. Sci.* **2000**, *10*, 195–204.

34 Weiss, T. F., *Cellular Biophysics.* Volume I: Transport. The MIT Press, Cambridge, MA, **1996**.

35 Shiau, Y.-F., Fernandez, P., Jackson, M. J., McMonagle, S., Mechanisms maintaining a low-pH microclimate in the intestine, *Am. J. Physiol.* **1985**, *248*, G608–G617.

36 Winiwarter, S., Bonham, N. M., Ax, F., Hallberg, A., Lennernäs, H., Karlen, A., Correlation of human jejunal permeability (in vivo) of drugs with experimentally and theoretically-derived parameters. A multivariate data analysis approach, *J. Med. Chem.* **1998**, *41*, 4939–4949.

37 Krämer, S. D., Begley, D. J., Abbott, N. J., American Association of Pharmacological Science, Annual Meeting, **1999**.

38 Krämer, S. D., Hurley, J. A., Abbott, N. J., Begley, D. J., Lipids in blood-brain barrier models in vitro I: TLC and HPLC for the analysis of lipid classes and long polyunsaturated fatty acids, submitted.

39 Helenius, A., Simons, K., Solubilization of membranes by detergents, *Biochim. Biophys. Acta* **1975**, *413*, 29–79.

4
Caco-2 and Emerging Alternatives for Prediction of Intestinal Drug Transport: A General Overview

Per Artursson and Staffan Tavelin

Abbreviations

2/4/A1	Conditionally immortalised cell line derived from foetal rat intestine
ABC	ATP-binding Cassette
ATCC	American Type Culture Collection
Caco-2	Adenocarcinoma cell line derived from human colonic epithelia
cDNA	complementary DNA
ECACC	European Collection of Cell Cultures
LC/MS/MS	liquid chromatography-mass spectrometry system
LLC-PK1	Cell line derived from pig kidney epithelia
MDCK	Madin-Darby canine kidney cell line derived from dog kidney epithelia
MDR1	Multidrug resistance protein 1 (ABCB1)
MRP2	Multidrug resistance-associated protein 2 (ABCC2)
OATP2	Organic anion-transporting polypeptide 2 (SLC21A6)
PEPT1	Oligopeptide transporter (Solute carrier family 15, member 1 (SLC15A1))

Symbols

Å	Ångstrom ($1 \cdot 10^{-10}$ m)
K_m	Substrate concentration at half the velocity of V_{max}
V_{max}	Maximum velocity of transport

4.1 Introduction

More than a decade ago, Caco-2 cells grown on permeable supports were introduced as an experimental tool for mechanistic studies of intestinal drug transport [1–4]. At the same time it was suggested that the Caco-2 model was suitable for screening intestinal drug permeability and predicting the oral absorption potential

Drug Bioavailability: Estimation of Solubility, Permeability, Absorption and Bioavailability.
Edited by Han van de Waterbeemd, Hans Lennernäs and Per Artursson

ISBN: 3-527-30438-X

of new drug substances [5]. After some initial scepticism Caco-2 cells were gradually accepted as a versatile *in vitro* tool for predictive and mechanistic studies of intestinal drug absorption.

Several factors spurred the development of Caco-2 and similar cell models. These included 1. the awareness that inferior pharmacokinetic properties, including insufficient drug absorption, remained the major reason for the failure of new drug candidates in the clinical phase [6], 2. the insight that drug absorption across biological barriers is a fairly complex process involving several pathways and that it can therefore not easily be delineated in experimental animals [7], and 3. the introduction of combinatorial chemistry in drug discovery [8]. Since the large number of compounds obtained by combinatorial chemistry could not be accommodated by the conventional absorption models based on experimental animals, this factor was probably the most important for the implementation of the Caco-2 model in many drug discovery settings.

As with all new techniques that are rapidly embraced by the scientific community, the initial enthusiasm and in some cases uncritical use of Caco-2 cells unravelled the limitations of this *in vitro* model [7] and other, similar models e.g. [9]. A period of critical evaluation followed and today the majority of researchers using these models are aware not only of their advantages, but also of their limitations. In the following, we will briefly discuss the research opportunities that Caco-2 cells offer and also give a few examples of the successful application of these cell cultures in drug discovery. We will also discuss the limitations of Caco-2 cells and discuss new research that addresses these limitations.

4.2
Research Opportunities with the Caco-2 Cell Model

4.2.1
Transport Mechanisms

The enthusiasm for using Caco-2 cells and other epithelial cell cultures in studies of drug transport processes has been explained by the ease with which new information can be derived from these fairly simple *in vitro* models [7]. For instance, drug transport studies in Caco-2 cells grown on permeable supports are easy to perform under controlled conditions. This makes it possible to extract information about specific transport processes that would be difficult to obtain in more complex models such as those based on whole tissues from experimental animals. Much of our knowledge about active and passive transport mechanisms in epithelia has therefore been obtained from Caco-2 cells and other epithelial cell cultures [10–15]. This has been possible since Caco-2 cells are unusually well differentiated. In many respects they are therefore functionally similar to the human small intestinal enterocyte, despite the fact that they originate from a human colorectal carcinoma [16, 17].

A variety of transport systems are extensively expressed in Caco-2 cells and this

may obscure the study of a specific transporter, especially if the transporter lacks a specific substrate, as in the case of most efflux transporters of the ABC-transporter family [18]. However, the expression of multiple transport systems in Caco-2 may be an advantage in studies of 1. the interplay between several transporters [19–21], 2. the interplay between drug metabolism and drug transport [22–26], and 3. the relative contribution of passive and active transport mechanisms to the overall transport of a drug e.g. [27]. Another potential advantage is the fact that the human origin of Caco-2 cells provides information on human transporters in the well-differentiated enterocyte. Important differences in transport parameters for the human ABC transporters MDR1 and MRP2 were recently observed between Caco-2 cells and what is probably the most popular epithelial expression system with regard to transporters, the MDCK cell line [28, 29]. Differences between the Caco-2 and MDCK cell lines have also been reported with regard to the activity of peptide transporters [30]. Since MDCK cells originate from the canine kidney epithelium, it may be speculated that the difference is a result of either the species difference or the different "organ origin" of the cell line.

The abundant expression of a variety of transporters in Caco-2 cells also makes it attractive to apply functional genomics tools, such as cDNA arrays in order to map the expression [31] and relative abundance of these transporters [32]. Also, genomic mapping of surface receptors on Caco-2 cells can be performed to study receptor-mediated endocytosis and other endocytotic pathways for larger molecules in enterocytes [33–36].

Caco-2 cells can also be used for studies of passive transport mechanisms that are not easily studied in more complex models, such as whole tissue models, or *in vivo*. For instance, the relative contribution of passive transcellular and paracellular transport [13], the effect of charge on paracellular transport [37] and the effect of solvent drag [38]. Further, studies of pH-dependent permeability of basic drugs showed that these drugs are transported across the cell monolayers not only in their uncharged but also in their charged form, thus challenging the validity of the pH-partitioning theory for epithelial tissues [39]. Furthermore, Caco-2 cells have been used to investigate the effects of pharmaceutical excipients that may enhance passive drug transport either by enhancing the solubility of the compound e.g. [40–43] or by affecting the epithelial integrity [44–48]. More recently protocols to optimise drug transport have been suggested by inclusion of solubility-enhancing agents (co-solvents, detergents, albumin) [49–52]. A complicating factor in using solubility-enhancing agents is that they may affect the passive transport rate [52, 53], as well as the function of active transport proteins [54]. More work remains to be done in this area, however, to improve the study conditions, especially for low-solubility drugs.

4.2.2
Prediction of Drug Permeability *In Vivo*

Initially the good relationship between the passive drug transport across Caco-2 cells and the absorbed fraction after oral administration to humans [5] may be

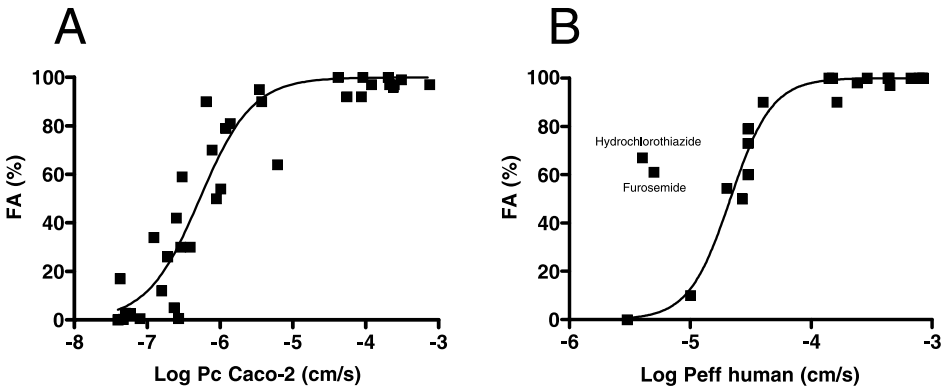

Fig. 4.1. Relationship between the absorbed fraction (FA) of structurally diverse sets of orally administered drugs and permeability coefficients obtained in Caco-2 cell monolayers (A) (data compiled from publications by Artursson's laboratory [105, 114]) and after *in vivo* perfusion of the human jejunum (B) (data compiled from publications by Lennernäs' laboratory [63, 115]). Sigmoidal relationships were obtained between FA and the permeability coefficients in both models.

surprising, given that oral drug absorption is influenced by many factors besides drug permeability, such as drug solubility, dissolution, active transport and, in some cases, pre-systemic metabolism [55]. The first study with Caco-2 cells was performed under highly controlled conditions on registered drugs that did not have solubility problems and that were largely passively transported. Also, their metabolism could be accounted for [5]. Similar good results are obtained when the same parameters are strictly controlled in expanded data sets (Fig. 4.1A). However, many drug discovery scientists initially became disappointed when the experimental in-house compounds gave relationships with a much larger scatter than reported in the original publication e.g. [56]. These results are not surprising considering the fact that the majority of discovery compounds had been neither characterised nor optimised with regard to chemical stability, metabolism, solubility or (if available in crystalline form) dissolution rate. Another contributing factor to this difference is related to the experimental design. Caco-2 predictions of oral drug absorption using small data sets are generally carried out manually by multiple samples at different time-points, and full attention is also given to e.g. mass balance issues and the contribution from active transport. In contrast, relationships using large data sets are normally established in automated systems using a few or single samples only, and little consideration is given to e.g. mass balance issues. Unfortunately, studies of large data sets are often performed using propriety compounds and the structures of the compounds are generally not disclosed, which makes it impossible for the independent researcher to investigate the results in detail. Nevertheless there are several reports that have indicated the usefulness of Caco-2 permeability data obtained in automated systems, in predictions of oral absorption e.g. [57–59] and bioavailability [60].

The complex relationship between the absorbed fraction and intestinal perme-

ability is underscored by the fact that not even human intestinal permeability studies on registered drugs using the Loc-I-Gut perfusion technique [61, 62] (see Chapter 78) provide a perfect relationship between with the absorbed fraction after oral administration (Fig. 4.1B). For instance, hydrochlorothiazide and furosemide are under-predicted in this technique [63].

It is noteworthy that the relationships in Fig. 4.1A were established using structurally diverse data sets and that analogous series of compounds often give better relationships. Consequently, Caco-2 cells have often been used to rank compounds in analogous compound series and libraries. When such data sets are used, Caco-2 cell permeability measurements provide the opportunity to establish structure-permeability relationships for quite different analogous series of drugs. Several examples of the latter case have been published recently. For example, these include series of conventional drugs [64–68], peptides and peptide mimetics [69–73] as well as compounds generated in high throughput drug discovery [74, 75]. Although most of these structure-permeability relationships have been established for passive membrane permeability, there are also examples of structure-permeability relationships for series of drugs that are absorbed via an active transport mechanism [76–78].

4.3 Limitations of Caco-2 Cells in Predicting Intestinal Drug Transport

4.3.1 Technical Issues

The collective experience of Caco-2 cells indicates that their performance varies from one laboratory to another [79, 80]. In this regard Caco-2 cells are not different from other cell culture models based on polyclonal transformed cell lines. The reasons for the variable performance of Caco-2 cells, can be minimised by education and training in good cell culture practice [17, 81, 82]. Here, we only note that a major reason for the different results obtained with Caco-2 cells is related to the interval of passage number at which the cells are studied. It is therefore important to define a limited number of passages that can be used for the experiments. Caco-2 cells obtained from the American Type Culture Collection (ATCC; www.atcc.org) or from the European Collection of Cell Cultures (ECACC; www.ecacc.org) are normally at passage 20–40, while in our laboratory we consistently use Caco-2 cells with the passage numbers 90–105. Our experience is that within this interval of passages the cells perform very consistently, provided that identical cell culture conditions are used. For instance, in our laboratory the passive permeability of the integrity marker mannitol across these cell monolayers has not varied by more than twofold since 1987 (unpublished observations). This is remarkable, since a large variation in the mannitol permeability of Caco-2 cells ($0.18 - 22.1 \times 10^{-6}$ cm/s) has been reported elsewhere in the literature [80]. We conclude that in con-

trast to what is generally believed it is possible to maintain the permeability characteristics of Caco-2 cells over long time periods, at least in the same laboratory.

Another technical limitation of work with Caco-2 cells is the long culture time that is required to obtain full differentiation of the cells. It takes three weeks to obtain differentiated cell monolayers of Caco-2 cells on filter inserts [1, 3, 4]. In some screening laboratories this is considered too long and too demanding to be practicable and culture protocols have been developed to speed up the differentiation process, usually to less than one week [83–85]. Today at least one three-day system based on proprietary media supplements and collagen-coated filter inserts, is available (www.bd.com/labware). Although limited, the published information about the performance of Caco-2 monolayers cultivated under these accelerated protocols suggests that the cells are not fully differentiated and therefore have to be used at a certain time point, for example on day three, to obtain reproducible results, since the degree of differentiation may vary from one day to another. By contrast, fully differentiated Caco-2 cells cultivated using the standard 21-day procedure maintain most properties for at least 1 week and can therefore be used at 21–28 days, which partly compensates for the long cultivation time.

Some laboratories have found an alternative to the short-term cultures by using cell lines other than Caco-2 cells. The most popular of these is Madin-Darby canine kidney (MDCK) cells, an epithelial cell line from the dog kidney. MDCK cells have been suggested to perform as well as Caco-2 cells in studies of passive drug permeability [56]. These cells have also been used to optimise the conditions for studies of low-solubility drugs [53]. However, as noted previously, the active transport processes of this cell line can be quite different to those of Caco-2 cells [28–30]. Another cell line that only requires short-term culture is 2/4/A1, which is a conditionally immortalised rat intestinal epithelial cell line [86]. The 2/4/A1 cell line is discussed in Section 4.3.2.2 below.

4.3.2 Limitations Related to Transport Studies and Their Solutions

4.3.2.1 Active Transport

The functional expression of many relevant drug transport systems in Caco-2 cells, which may complicate the interpretation of the results, is a further weakness. For instance, when drug-like compounds are screened in Caco-2 cells, they are usually used at low concentrations (the μM-range seems to be common). At such low concentrations many active drug transport processes may not be saturated. The results may suggest that, say, an efflux system dramatically limits the permeability of the drug(s) when simple calculations may show that the same drug administered to humans will be presented to the intestinal epithelium of the upper small intestine at a much higher concentration (mM) than used in the screening [87, 88]. Since the transport mechanism may be saturated at higher concentrations, the drug efflux may sometimes be considered as an *in vitro* artefact that will not be relevant in the *in vivo* situation, at least for compounds that are given at higher doses.

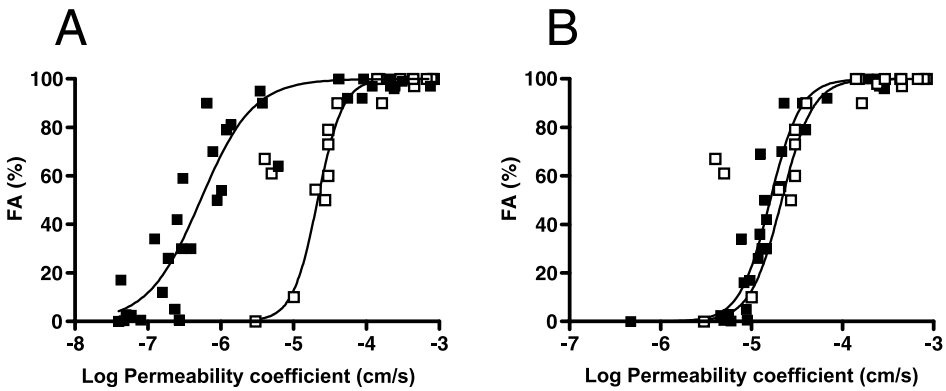

Fig. 4.2. Comparison between the permeability coefficients obtained after *in vivo* perfusion of the human jejunum (open symbols) (data compiled from publications by Lennernäs' laboratory [63, 115]) and Caco-2 (filled symbols) (data compiled from publications by Artursson's laboratory [105, 114]) (A) and 2/4/A1 (filled symbols) [105] (B). There is a quantitative overlap in permeability between completely absorbed drugs in Caco-2 and in human jejunum, while the permeability for the incompletely absorbed drugs are approximately 2 orders of magnitude lower in Caco-2 than in the human jejunum. In contrast, the relationship in 2/4/A1 is almost completely overlapping that in the human jejunum for both the completely and the incompletely absorbed drugs.

A potential problem is "false efflux" in that many laboratories prefer to study drug transport in cell culture at an apical pH of around 6.0–6.5 (in order to mimic the acid microclimate of the upper small intestine) and a basolateral pH of 7.4 [89]. This results in basic drugs becoming more charged at the apical side than at the basolateral side. The reverse will be true of acidic drugs. Therefore, the passive permeability of a basic drug will be lower in the apical to basolateral (absorptive) direction than in the opposite direction, since a smaller amount of uncharged drug is available to drive the passive transport across the cell membrane from the apical side of the cells. Thus, an apical pH of 6.0–6.5 may reflect the situation in the part of small intestine where the acid microclimate exists [90, 91], it may give a false impression of an active efflux mechanism. A solution to this problem is to perform the transport studies at equal pH, preferably 7.4, on both the apical and the basolateral side [89]. The drawback with this approach is that proton-driven transporters such as PEPT1 will be at least partly inactivated under these conditions.

Another limitation is that there is no quantitative relationship between active drug transport in the cell culture models and *in vivo* e.g. [92, 93]. The reason may be that the expression level of the transporter in Caco-2 cells is not comparable to that *in vivo* or that there is a difference in effective surface area (see Section 4.3.2.2 below). One solution to this problem is to determine the apparent transport constants, K_m and V_{max}, for each transporter and subsequently, to determine a scaling factor. However, this is not readily done. In addition these studies are further complicated by the lack of specific substrates. For example, there are almost no specific substrates for the drug efflux transporters [18]. Therefore, other epithelial

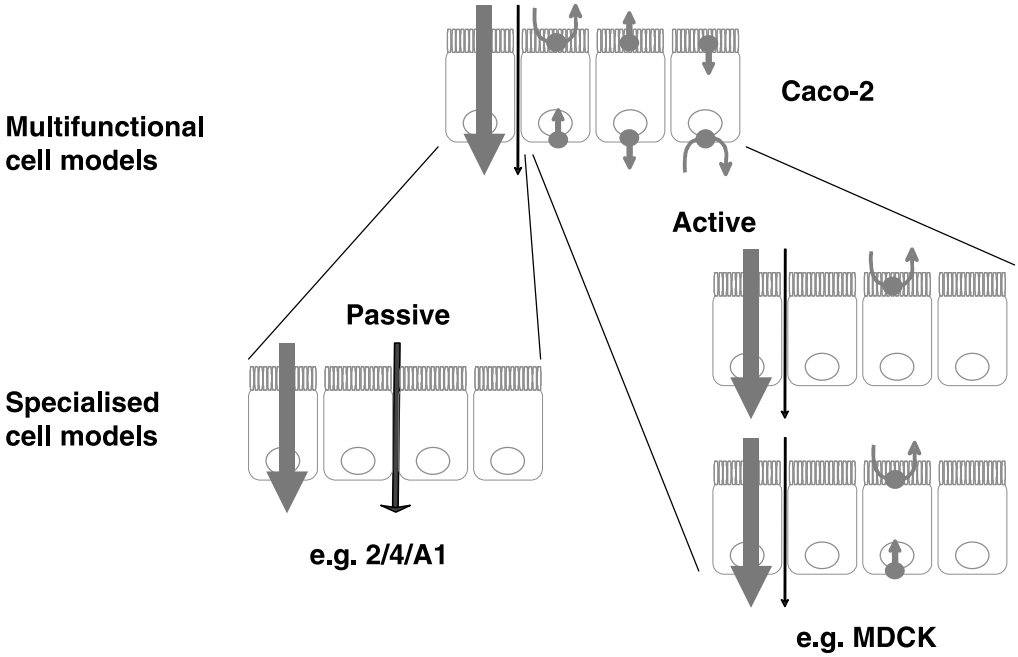

Fig. 4.3. Studies of specific drug transport routes in multifunctional cell models such as Caco-2 may be complicated, since there is a lack of specific substrates for many drug transporters. Therefore, specialised cell models, that accommodate mainly passive (2/4/A1) or selected active (e.g. MDCK-MDR1) transport pathways are preferred in some cases.

cell culture models, such as LLC-PK1 and MDCK, which have a low background expression of the various transporters, have been stably transfected to express high levels of a specific transporter e.g. [94–97] (Fig. 4.3). These models have become increasingly popular for the characterisation of specific transporters since, in theory, the requirement for specific substrates should be lower in these models. Unfortunately they are not perfect since they also express several transporters that may complicate interpretation of the results [28, 96, 98] (Fig. 4.3).

Another emerging problem with the transgenic expression systems is that the active drug transport of some drugs may be mediated by two (or more) transporters simultaneously or in series [99]. In this context it was recently reported that the transport of pravastatin, a substrate for both the basally located OATP2 and the apically located drug efflux transporter MRP2, was better described in MDCK cells double-transfected with these two transporters than in cell lines transfected with only one of the transporters [100]. For this reason, transgenic cell lines over-expressing a single transporter may be insufficient when more complex drug transport mechanisms are to be elucidated. Unfortunately it is difficult to generate double-transfected cell lines that retain the required differentiated properties. Caco-

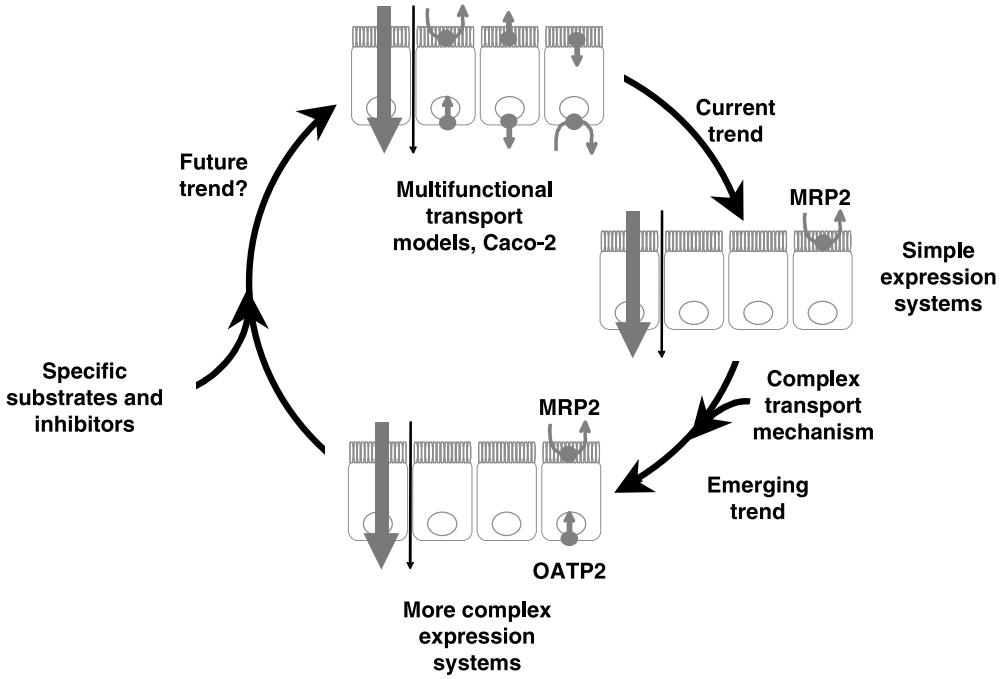

Fig. 4.4. A current trend in drug transport studies is to use simplified cell models that facilitate the characterisation of selected drug transport mechanisms. However, recent research suggests that such simplified systems are not useful in cases where two or more drug transporters act in synergy. Development of cell models for such complex transport mechanisms will require the technically demanding overexpression of various combinations of drug transport proteins. If more specific markers (substrates and inhibitors) for the various drug transporters are discovered, a detailed characterisation of drug transport mechanisms may be possible in multifunctional cell models such as the Caco-2 model in the future.

2 cells may therefore remain a viable future alternative also in the future in some of these situations, provided that sufficiently specific substrates or inhibitors can be identified (Fig. 4.4).

In conclusion, there are several drawbacks to the use of Caco-2 cells in studies of active drug transport. Despite these drawbacks, we note that a recent comprehensive study comparing various P-glycoprotein drug efflux assays in drug discovery came to the conclusion that the Caco-2 transport assay is the method of choice, since it displays a biased responsiveness towards compounds with low or moderate permeability – in other words, towards compounds whose intestinal permeability is most likely to be significantly affected by drug efflux mechanisms [101].

4.3.2.2 **Passive Transport**

As for active drug transport, there is no quantitative relationship between passive drug permeability in Caco-2 cells *in vitro* and drug transport in the human small

intestine *in vivo* [93, 102]. Apart from high-permeability drugs which partition into the cell membranes at comparable, rapid, speeds *in vitro* and *in vivo*, compounds of intermediate or low permeability have a lower permeability in the Caco-2 model than *in vivo*. As can be seen in Fig. 4.2A, this difference increases with a decrease in compound permeability. There are two major reasons for this difference.

First, the paracellular route is tighter in Caco-2 cells than that in the small intestine *in vivo*. While the average pore radius of the tight junctions in the human small intestine is around 8–13 Å [103], the corresponding radius in Caco-2 cells is about 4 Å. Since low-permeability drugs are generally more polar than high-permeability drugs, they tend to distribute more slowly into the cell membranes. However, at least a fraction of the drugs are transported through the water pores of the tight junctions, via the paracellular pathway. If this pathway is narrower, as in Caco-2 cells, the permeability will become lower than in the *in vivo* situation. We recently proposed a solution to this problem by exploiting a more leaky cell culture model established from the rat foetal intestine, 2/4/A1 [86, 102]. This cell line, which has a paracellular permeability comparable to that of the human small intestinal epithelium *in vivo*, gives a better quantitative relationship with human permeability data generated in the Loc-I-Gut perfusion technique [102] (Fig. 4.2B). Interestingly, the 2/4/A1 cell line seems not to express functional (drug) transporters [104], which makes it an interesting alternative in studies of passive permeability. Indeed, recent data from our laboratory suggest that 2/4/A1 cells better predict the human absorption of intermediate- to low-permeability drugs than do Caco-2 cells [105]. Another advantage of the 2/4/A1 cell line is that relatively large amounts of low-permeability drugs are transported, thus eliminating the need for expensive analysis equipment such as a LC/MS/MS system.

Although the 2/4/A1 cell culture model gives a quantitative relationship with human intestinal permeability, a second factor not accommodated in this model, the absorptive surface area, may also be responsible for the discrepancy in drug permeability between Caco-2 cells and the human intestine *in vivo*. The anatomical surface area of the small intestine is enlarged by villi and crypts and this surface enlargement is normally not accounted for in drug permeability studies *in vivo* or *in vitro*. The reason for this shortcoming is that the absorptive surface area is a variable that is dependent on the membrane permeability of the drug [79] and therefore difficult to calculate. A high-permeability drug will be absorbed across a limited surface area (the area covered by the enterocytes at the tips of the villi) since the drug will partition very rapidly to the nearest available cell membrane or bind rapidly to the nearest available transporter. Thus, it has been calculated that the most rapidly absorbed compound known to date, glucose, has an absorptive surface area that covers only a small part of the total anatomical surface area of the small intestine [106]. By contrast, a low-permeability drug does not distribute rapidly into the cell membrane and therefore has a longer residence time in the intestinal fluids. During this time the drug will diffuse along the crypt-villus axis, to eventually be absorbed over a larger absorptive surface area. To our knowledge, no attempts have been made to derive an expression for the variability in absorptive surface area. To complicate things even further, the paracellular permeability

increases from the villus tips towards the crypts [107]. It is therefore impossible to speculate upon the relative contribution of the paracellular pathway and the increased absorptive surface area to the passive transport of low-permeability drugs. Here we can only conclude that it is possible to mimic human small intestinal permeability to drugs by using a more leaky cell culture model (such as 2/4/A1) than the Caco-2 model. As an alternative, correction factors for the low paracellular permeability in Caco-2 cells and other membrane models have been introduced [108, 109].

4.4 Conclusion

We conclude that Caco-2 cell cultures remain a versatile and general model for studies of drug transport mechanisms and screening of drug permeability. However, new, alternative models that express fewer drug transport pathways may be preferable in situations where specific drug transport mechanisms are to be studied. Thus, a current trend is to develop alternative models to Caco-2 cells by the reductionist approach, either by isolating the study of specific transporters to various transgenic cell lines or by isolating the study of passive transport to cell lines in which transporters are functionally redundant (Fig. 4.3). An even more reductionist approach is to use models that only consist of a membrane barrier e.g. [110–113] (see also Chapter 3).

Acknowledgements

This work was supported by grants from The Swedish National Board for Laboratory Animals (97-46), The Swedish Foundation for Research without Animal Experiments, The Swedish Research Council (9478), The Wallenberg Foundation, AstraZeneca, Bristol-Myers Squibb and GlaxoSmithKline.

References

1 Hidalgo, I. J., T. J. Raub, and R. T. Borchardt. Characterization of the human colon carcinoma cell line (Caco-2) as a model system for intestinal epithelial permeability, *Gastroenterology* **1989**, *96*, 736–749

2 Artursson, P. Epithelial transport of drugs in cell culture. I: A model for studying the passive diffusion of drugs over intestinal absorptive (Caco-2) cells, *J. Pharm. Sci.* **1990**, *79*, 476–482

3 Hilgers, A. R., R. A. Conradi, and P. S. Burton. Caco-2 cell monolayers as a model for drug transport across the intestinal mucosa, *Pharm. Res.* **1990**, *7*, 902–910

4 Wilson, G., I. F. Hassan, C. J. Dix, I. Williamson, R. Shah, M. MacKay, and P. Artursson. Transport and permeability properties of human Caco-2 cells: an in vitro model of the intestinal epithelial barrier, *J. Control. Release* **1990**, *11*, 25–40

5 Artursson, P. and J. Karlsson. Correlation between oral drug absorption in humans and apparent drug permeability coefficients in human intestinal epithelial (Caco-2)

cells, *Biochem. Biophys. Res. Commun.* **1991**, *175*, 880–885

6 Prentis, R. A., Y. Lis, and S. R. Walker. Pharmaceutical innovation by the seven UK-owned pharmaceutical companies (1964–1985), *Br. J. Clin. Pharmacol.* **1988**, *25*, 387–396

7 Artursson, P. and R. T. Borchardt. Intestinal drug absorption and metabolism in cell cultures: Caco-2 and beyond, *Pharm. Res.* **1997**, *14*, 1655–1658

8 Floyd, C., C. Leblanc, and M. Whittaker. Combinatorial chemistry as a tool for drug discovery, *Prog. Med. Chem.* **1999**, *36*, 91–168

9 Gumbleton, M. and K. L. Audus. Progress and limitations in the use of in vitro cell cultures to serve as a permeability screen for the blood-brain barrier, *J. Pharm. Sci.* **2001**, *90*, 1681–1698

10 Hu, M. and R. Borchardt. Mechanism of L-alpha-methyldopa transport through a monolayer of polarized human intestinal epithelial cells (Caco-2)., *Pharm. Res.* **1990**, *7*, 1313–1319

11 Hunter, J., M. A. Jepson, T. Tsuruo, N. L. Simmons, and B. H. Hirst. Functional expression of P-glycoprotein in apical membranes of human intestinal Caco-2 cells. Kinetics of vinblastine secretion and interaction with modulators, *J. Biol. Chem.* **1993**, *268*, 14991–14997

12 Dantzig, A. H., J. A. Hoskins, L. B. Tabas, S. Bright, R. L. Shepard, I. L. Jenkins, D. C. Duckworth, J. R. Sportsman et al. Association of intestinal peptide transport with a protein related to the cadherin superfamily, *Science* **1994**, *264*, 430–433

13 Adson, A., P. S. Burton, T. J. Raub, C. L. Barsuhn, K. L. Audus, and N. F. Ho. Passive diffusion of weak organic electrolytes across Caco-2 cell monolayers: uncoupling the contributions of hydrodynamic, transcellular, and paracellular barriers, *J. Pharm. Sci.* **1995**, *84*, 1197–1204

14 de Vrueh, R., P. Smith, and C. Lee. Transport of L-valine-acyclovir via the oligopeptide transporter in the human intestinal cell line, Caco-2., *J. Pharmacol. Exp. Ther.* **1998**, *286*, 1166–1170

15 Lee, K. and D. R. Thakker. Saturable transport of H2-antagonists ranitidine and famotidine across Caco-2 cell monolayers, *J. Pharm. Sci.* **1999**, *88*, 680–687

16 Fogh, J., J. M. Fogh, and T. Orfeo. One hundred and twenty-seven cultured human tumor cell lines producing tumors in nude mice, *J. Natl. Cancer Inst.* **1977**, *59*, 221–226

17 Zweibaum, A., M. Laburthe, E. Grasset, and D. Louvard, *Use of cultured cell lines in studies of intestinal cell differentiation and function*, in *Handbook of Physiology, Section 6: The Gastrointestinal System*, S. Schultz, Editor. 1991, American Physiological Society: Bethesda. p. 223–255

18 Litman, T., T. E. Druley, W. D. Stein, and S. E. Bates. From MDR to MXR: new understanding of multidrug resistance systems, their properties and clinical significance, *Cell Mol. Life Sci.* **2001**, *58*, 931–959

19 Hu, M. and R. Borchardt. Transport of a large neutral amino acid in a human intestinal epithelial cell line (Caco-2): uptake and efflux of phenylalanine., *Biochim. Biophys. Acta* **1992**, *1135*, 233–244

20 Wenzel, U., B. Meissner, F. Doring, and H. Daniel. PEPT1-mediated uptake of dipeptides enhances the intestinal absorption of amino acids via transport system b(0, +), *J. Cell. Physiol.* **2001**, *186*, 251–259

21 Luo, F., P. Paranjpe, A. Guo, E. Rubin, and P. Sinko. Intestinal transport of irinotecan in Caco-2 cells and MDCK II cells overexpressing efflux transporters Pgp, cMOAT, and MRP1., *Drug Metab. Dispos.* **2002**, *30*, 763–770

22 Raeissi, S. D., I. J. Hidalgo, J. Segura-Aguilar, and P. Artursson. Interplay between CYP3A-mediated metabolism and polarized efflux of terfenadine and its metabolites in intestinal epithelial Caco-2 (TC7) cell

monolayers, *Pharm. Res.* **1999**, *16*, 625–632

23 Hochman, J., M. Chiba, M. Yamazaki, C. Tang, and J. Lin. P-glycoprotein-mediated efflux of indinavir metabolites in Caco-2 cells expressing cytochrome P450 3A4., *J. Pharmacol. Exp. Ther.* **2001**, *298*, 323–330

24 Engman, H. A., H. Lennernäs, J. Taipalensuu, C. Otter, B. Leidvik, and P. Artursson. CYP3A4, CYP3A5, and MDR1 in human small and large intestinal cell lines suitable for drug transport studies, *J. Pharm. Sci.* **2001**, *90*, 1736–1751

25 Cummins, C. L., W. Jacobsen, and L. Z. Benet. Unmasking the dynamic interplay between intestinal P-glycoprotein and CYP3A4, *J. Pharmacol. Exp. Ther.* **2002**, *300*, 1036–1045

26 Paine, M. F., L. Y. Leung, H. K. Lim, K. Liao, A. Oganesian, M. Y. Zhang, K. E. Thummel, and P. B. Watkins. Identification of a novel route of extraction of sirolimus in human small intestine: roles of metabolism and secretion, *J. Pharmacol. Exp. Ther.* **2002**, *301*, 174–186

27 Flanagan, S. D., L. H. Takahashi, X. Liu, and L. Z. Benet. Contributions of saturable active secretion, passive transcellular, and paracellular diffusion to the overall transport of furosemide across adenocarcinoma (Caco-2) cells, *J. Pharm. Sci.* **2002**, *91*, 1169–1177

28 Tang, F., K. Horie, and R. T. Borchardt. Are MDCK cells transfected with the human MRP2 gene a good model of the human intestinal mucosa?, *Pharm. Res.* **2002**, *19*, 773–779

29 Tang, F., K. Horie, and R. T. Borchardt. Are MDCK cells transfected with the human MDR1 gene a good model of the human intestinal mucosa?, *Pharm. Res.* **2002**, *19*, 765–772

30 Putnam, W. S., L. Pan, K. Tsutsui, L. Takahashi, and L. Z. Benet. Comparison of bidirectional cephalexin transport across MDCK and caco-2 cell monolayers: interactions with peptide transporters, *Pharm. Res.* **2002**, *19*, 27–33

31 Sun, D., H. Lennernäs, L. S. Welage, L. Barnett, C. P. Landowski, D. Foster, D. Fleisher, K.-D. Lee et al. Comparison of Human Duodenum and Caco-2 Gene Expression Profiles for 12,000 Gene Sequences Tags and Correlation with Permeability of 26 Drugs., *Pharm. Res.* **2002**, *19*, 1400–1416

32 Taipalensuu, J., H. Törnblom, G. Lindberg, C. Einarsson, F. Sjöqvist, H. Melhus, P. Garberg, B. Sjöström et al. Correlation of gene expression of ten drug efflux proteins of the atp-binding cassette transporter family in normal human jejunum and in human intestinal epithelial caco-2 cell monolayers, *J. Pharmacol. Exp. Ther.* **2001**, *299*, 164–170

33 Kerneis, S., A. Bogdanova, J. Kraehenbuhl, and E. Pringault. Conversion by Peyer's patch lymphocytes of human enterocytes into M cells that transport bacteria., *Science* **1997**, *277*, 949–952

34 Gullberg, E., M. Leonard, J. Karlsson, A. M. Hopkins, D. Brayden, A. W. Baird, and P. Artursson. Expression of specific markers and particle transport in a new human intestinal M-cell model, *Biochem. Biophys. Res. Commun.* **2000**, *279*, 808–813

35 Ghosh, S. Human M cells delivered in a box, *Gastroenterology* **2001**, *121*, 1520–1521

36 Fotopoulos, G., A. Harari, P. Michetti, D. Trono, G. Pantaleo, and J. Kraehenbuhl. Transepithelial transport of HIV-1 by M cells is receptor-mediated., *Proc. Natl. Acad. Sci. U S A* **2002**, *99*, 9410–9414

37 Adson, A., T. J. Raub, P. S. Burton, C. L. Barsuhn, A. R. Hilgers, K. L. Audus, and N. F. Ho. Quantitative approaches to delineate paracellular diffusion in cultured epithelial cell monolayers, *J. Pharm. Sci.* **1994**, *83*, 1529–1536

38 Karlsson, J., U. A., J. Gråsjö, and P. Artursson. Paracellular drug transport across intestinal epithelia: influence of charge and induced water flux., *Eur. J. Pharm. Sci.* **1999**, *9*, 47–56

39 Palm, K., K. Luthman, J. Ros, J. Gråsjö, and P. Artursson. Effect of molecular charge on intestinal epithelial drug transport: pH-dependent transport of cationic drugs, *J. Pharmacol. Exp. Ther.* **1999**, *291*, 435–443

40 Tötterman, A. M., N. G. Schipper, D. O. Thompson, and J. P. Mannermaa. Intestinal safety of water-soluble beta-cyclodextrins in paediatric oral solutions of spironolactone: effects on human intestinal epithelial Caco-2 cells, *J. Pharm. Pharmacol.* **1997**, *49*, 43–48

41 Aungst, B., N. Nguyen, J. Bulgarelli, and K. Oates-Lenz. The influence of donor and reservoir additives on Caco-2 permeability and secretory transport of HIV protease inhibitors and other lipophilic compounds., *Pharm. Res.* **2000**, *17*, 1175–1180

42 Saha, P. and J. Kou. Effect of solubilizing excipients on permeation of poorly water-soluble compounds across Caco-2 cell monolayers., *Eur. J. Pharm. Biopharm.* **2000**, *50*, 403–411

43 Takahashi, Y., H. Kondo, T. Yasuda, T. Watanabe, S. Kobayashi, and S. Yokohama. Common solubilizers to estimate the Caco-2 transport of poorly water-soluble drugs., *Int. J. Pharm.* **2002**, *246*, 85

44 Anderberg, E. K., C. Nyström, and P. Artursson. Epithelial transport of drugs in cell culture. VII: Effects of pharmaceutical surfactant excipients and bile acids on transepithelial permeability in monolayers of human intestinal epithelial (Caco-2) cells, *J. Pharm. Sci.* **1992**, *81*, 879–887

45 Hochman, J., J. Fix, and E. LeCluyse. In vitro and in vivo analysis of the mechanism of absorption enhancement by palmitoylcarnitine., *J. Pharmacol. Exp. Ther.* **1994**, *269*, 813–822

46 Tomita, M., I. M. Hayash, and S. Awazu. Absorption-enhancing mechanism of EDTA, caprate, and decanoylcarnitine in Caco-2 cells., *J. Pharm. Sci.* **1996**, *85*, 608–611

47 Lindmark, T., Y. Kimura, and P. Artursson. Absorption enhancement through intracellular regulation of tight junction permeability by medium chain fatty acids in Caco-2 cells, *J. Pharmacol. Exp. Ther.* **1998**, *284*, 362–369

48 Ouyang, H., S. L. Morris-Natschke, K. S. Ishaq, P. Ward, D. Liu, S. Leonard, and D. R. Thakker. Structure-activity relationship for enhancement of paracellular permeability across Caco-2 cell monolayers by 3-alkylamido-2-alkoxypropylphosphocholines, *J. Med. Chem.* **2002**, *45*, 2857–2866

49 Yamashita, S., T. Furubayashi, M. Kataoka, T. Sakane, H. Sezaki, and H. Tokuda. Optimized conditions for prediction of intestinal drug permeability using Caco-2 cells, *Eur. J. Pharm. Sci.* **2000**, *10*, 195–204

50 Pal, D., C. Udata, and A. K. Mitra. Transport of cosalane-a highly lipophilic novel anti-HIV agent-across caco-2 cell monolayers, *J. Pharm. Sci.* **2000**, *89*, 826–833

51 Krishna, G., K. Chen, C. Lin, and A. A. Nomeir. Permeability of lipophilic compounds in drug discovery using in-vitro human absorption model, Caco-2, *Int. J. Pharm.* **2001**, *222*, 77–89

52 Rege, B. D., L. X. Yu, A. S. Hussain, and J. E. Polli. Effect of common excipients on Caco-2 transport of low-permeability drugs, *J. Pharm. Sci.* **2001**, *90*, 1776–1786

53 Taub, M. E., L. Kristensen, and S. Frokjaer. Optimized conditions for MDCK permeability and turbidimetric solubility studies using compounds representative of BCS classes I–IV, *Eur. J. Pharm. Sci.* **2002**, *15*, 331–340

54 Hugger, E. D., K. L. Audus, and

R. T. Borchardt. Effects of poly(ethylene glycol) on efflux transporter activity in Caco-2 cell monolayers, *J. Pharm. Sci.* **2002**, *91*, 1980–1990

55 Rowland, M. and T. Tozer, *Clinical Pharmacokinetics*, Lea and Febinger, Malvern 1989

56 Irvine, J. D., L. Takahashi, K. Lockhart, J. Cheong, J. W. Tolan, H. E. Selick, and J. R. Grove. MDCK (Madin-Darby canine kidney) cells: A tool for membrane permeability screening, *J. Pharm. Sci.* **1999**, *88*, 28–33

57 Pickett, S. D., I. M. McLay, and D. E. Clark. Enhancing the hit-to-lead properties of lead optimization libraries, *J. Chem. Inf. Comput. Sci.* **2000**, *40*, 263–272

58 Stevenson, C., P. Augustijns, and R. Hendren. Use of Caco-2 cells and LC/MS/MS to screen a peptide combinatorial library for permeable structures., *Int. J. Pharm.* **1999**, *15*, 103–115

59 McKenna, J. M., F. Halley, J. E. Souness, I. M. McLay, S. D. Pickett, A. J. Collis, K. Page, and I. Ahmed. An algorithm-directed two-component library synthesized via solid-phase methodology yielding potent and orally bioavailable p38 MAP kinase inhibitors, *J. Med. Chem.* **2002**, *45*, 2173–2184

60 Mandagere, A. K., T. N. Thompson, and K. K. Hwang. Graphical model for estimating oral bioavailability of drugs in humans and other species from their Caco-2 permeability and in vitro liver enzyme metabolic stability rates, *J. Med. Chem.* **2002**, *45*, 304–311

61 Knutson, L., B. Odlind, and R. Hällgren. A new technique for segmental jejunal perfusion in man, *Am. J. Gastroenterol.* **1989**, *84*, 1278–1284

62 Lennernäs, H. Human jejunal effective permeability and its correlation with preclinical drug absorption models, *J. Pharm. Pharmacol.* **1997**, *49*, 627–638

63 Winiwarter, S., N. M. Bonham, F. Ax, A. Hallberg, H. Lennernäs, and A. Karlen. Correlation of human jejunal permeability (in vivo) of drugs with experimentally and theoretically derived parameters. A multivariate data analysis approach, *J. Med. Chem.* **1998**, *41*, 4939–4949

64 Palm, K., K. Luthman, A. L. Ungell, G. Strandlund, and P. Artursson. Correlation of drug absorption with molecular surface properties, *J. Pharm. Sci.* **1996**, *85*, 32–39

65 Liang, E., J. Proudfoot, and M. Yazdanian. Mechanisms of transport and structure-permeability relationship of sulfasalazine and its analogs in Caco-2 cell monolayers, *Pharm. Res.* **2000**, *17*, 1168–1174

66 Ekins, S., G. L. Durst, R. E. Stratford, D. A. Thorner, R. Lewis, R. J. Loncharich, and J. H. Wikel. Three-dimensional quantitative structure-permeability relationship analysis for a series of inhibitors of rhinovirus replication, *J. Chem. Inf. Comput. Sci.* **2001**, *41*, 1578–1586

67 Palanki, M. S., P. E. Erdman, L. M. Gayo-Fung, G. I. Shevlin, R. W. Sullivan, M. E. Goldman, L. J. Ransone, B. L. Bennett et al. Inhibitors of NF-kappaB and AP-1 gene expression: SAR studies on the pyrimidine portion of 2-chloro-4-trifluoromethylpyrimidine-5-[N-(3′,5′-bis(trifluoromethyl)phenyl)carboxamide], *J. Med. Chem.* **2000**, *43*, 3995–4004

68 Proudfoot, J. R., R. Betageri, M. Cardozo, T. A. Gilmore, S. Glynn, E. R. Hickey, S. Jakes, A. Kabcenell et al. Nonpeptidic, monocharged, cell permeable ligands for the p56lck SH2 domain, *J. Med. Chem.* **2001**, *44*, 2421–2431

69 Conradi, R. A., A. R. Hilgers, N. F. Ho, and P. S. Burton. The influence of peptide structure on transport across Caco-2 cells, *Pharm. Res.* **1991**, *8*, 1453–1460

70 Conradi, R. A., A. R. Hilgers, P. S. Burton, and J. B. Hester. Epithelial cell permeability of a series of peptidic HIV protease inhibitors: amino-

terminal substituent effects, *J. Drug Target.* **1994**, *2*, 167–171

71 Burton, P. S., R. A. Conradi, N. F. Ho, A. R. Hilgers, and R. T. Borchardt. How structural features influence the biomembrane permeability of peptides, *J. Pharm. Sci.* **1996**, *85*, 1336–1340

72 Werner, U., T. Kissel, and W. Stuber. Effects of peptide structure on transport properties of seven thyrotropin releasing hormone (TRH) analogues in a human intestinal cell line (Caco-2), *Pharm. Res.* **1997**, *14*, 246–250

73 Goodwin, J. T., R. A. Conradi, N. F. Ho, and P. S. Burton. Physicochemical determinants of passive membrane permeability: role of solute hydrogen-bonding potential and volume, *J. Med. Chem.* **2001**, *44*, 3721–3729

74 Stenberg, P., K. Luthman, H. Ellens, C. P. Lee, P. L. Smith, A. Lago, J. D. Elliott, and P. Artursson. Prediction of the intestinal absorption of endothelin receptor antagonists using three theoretical methods of increasing complexity, *Pharm. Res.* **1999**, *16*, 1520–1526

75 Schipper, N. G., T. Österberg, U. Wrange, C. Westberg, A. Sokolowski, R. Rai, W. Young, and B. Sjöström. In vitro intestinal permeability of factor Xa inhibitors: influence of chemical structure on passive transport and susceptibility to efflux, *Pharm. Res.* **2001**, *18*, 1735–1741

76 Brandsch, M., I. I. Knutter, F. Thunecke, B. Hartrodt, I. I. Born, V. Borner, F. Hirche, G. Fischer et al. Decisive structural determinants for the interaction of proline derivatives with the intestinal H+/peptide symporter., *Eur. J. Biochem.* **1999**, *266*, 502–508

77 Friedrichsen, G., P. Jakobsen, M. Taub, and M. Begtrup. Application of enzymatically stable dipeptides for enhancement of intestinal permeability. Synthesis and in vitro evaluation of dipeptide-coupled compounds, *Bioorg. Med. Chem.* **2001**, *9*, 2625–2632

78 Nielsen, C., R. Andersen, B. Brodin, S. Frokjaer, M. Taub, and B. Steffansen. Dipeptide model prodrugs for the intestinal oligopeptide transporter. Affinity for and transport via hPepT1 in the human intestinal Caco-2 cell line., *J. Control. Release* **2001**, *11*, 129–138

79 Artursson, P., K. Palm, and K. Luthman. Caco-2 monolayers in experimental and theoretical predictions of drug transport, *Adv. Drug Deliv. Rev.* **2001**, *46*, 27–43

80 Delie, F. and W. Rubas. A human colonic cell line sharing similarities with enterocytes as a model to examine oral absorption: advantages and limitations of the Caco-2 model, *Crit. Rev. Ther. Drug Carrier Syst.* **1997**, *14*, 221–286

81 Artursson, P., J. Karlsson, G. Ocklind, and N. Schipper, *Studying transport processes in absorptive epithelia.*, in *Epithelial cell culture-A Practical Approach*, A. J. Shaw, Editor. 1996, Oxford Press: New York. p. 111–133

82 Tavelin, S., J. Gråsjö, J. Taipalensuu, G. Ocklind, and P. Artursson, eds. *Applications of epithelial cell culture in studies of drug transport.* Methods in Molecular Biology, ed. C. Wise. Vol. 188. 2002

83 Chong, S., S. A. Dando, and R. A. Morrison. Evaluation of Biocoat intestinal epithelium differentiation environment (3-day cultured Caco-2 cells) as an absorption screening model with improved productivity, *Pharm. Res.* **1997**, *14*, 1835–1837

84 Liang, E., K. Chessic, and M. Yazdanian. Evaluation of an accelerated Caco-2 cell permeability model, *J. Pharm. Sci.* **2000**, *89*, 336–345

85 Yamashita, S., K. Konishi, Y. Yamazaki, Y. Taki, T. Sakane, H. Sezaki, and Y. Furuyama. New and better protocols for a short-term Caco-2 cell culture system, *J. Pharm. Sci.* **2002**, *91*, 669–679

86 Paul, E. C. A., J. Hochman, and A. Quaroni. Conditionally immortalized intestinal epithelial cells. novel approach for study of differentiated enterocytes., *Am. J. Physiol.* **1993**, *265*, C266–C278

87 Curatolo, W. Physical chemical properties of oral drug candidates in the discovery and exploratory development settings, *Pharm. Sci. Technol. Today* **1998**, *1*, 387–393

88 Stenberg, P., C. A. Bergström, K. Luthman, and P. Artursson. Theoretical predictions of drug absorption in drug discovery and development, *Clin. Pharmacokinet.* **2002**, *41*, 877–899

89 Neuhoff, S., I. Zamora, A. L. Ungell, and P. Artursson. pH-dependent bi-directional transport of weak basic drugs across Caco-2 monolayers, submitted.

90 Fallingborg, J., L. Christensen, M. Ingeman-Nielsen, B. Jacobsen, K. Abildgaard, and H. Rasmussen. pH-profile and regional transit times of the normal gut measured by a radiotelemetry device., *Aliment. Pharmacol. Ther.* **1989**, *3*, 605–613

91 McEwan, G. and M. Lucas. The effect of E. coli STa enterotoxin on the absorption of weakly dissociable drugs from rat proximal jejunum in vivo, *Br. J. Pharmacol.* **1990**, *101*, 937–943

92 Chong, S., S. A. Dando, K. M. Soucek, and R. A. Morrison. In vitro permeability through caco-2 cells is not quantitatively predictive of in vivo absorption for peptide-like drugs absorbed via the dipeptide transporter system, *Pharm. Res.* **1996**, *13*, 120–123

93 Lennernäs, H., K. Palm, U. Fagerholm, and P. Artursson. Comparison between active and passive drug transport in human intestinal epithelial (Caco-2) cells in vitro and human jejunum in vivo., *Int. J. Pharm.* **1996**, *127*, 103–107

94 Pastan, I., M. M. Gottesman, K. Ueda, E. Lovelace, A. V. Rutherford, and M. C. Willingham. A retrovirus carrying an MDR1 cDNA confers multidrug resistance and polarized expression of P-glycoprotein in MDCK cells, *Proc. Natl. Acad. Sci. U S A* **1988**, *85*, 4486–4490

95 Evers, R., G. J. Zaman, L. van Deemter, H. Jansen, J. Calafat, L. C. Oomen, R. P. Oude Elferink, P. Borst et al. Basolateral localization and export activity of the human multidrug resistance-associated protein in polarized pig kidney cells, *J. Clin. Invest.* **1996**, *97*, 1211–1218

96 Evers, R., M. Kool, L. van Deemter, H. Janssen, J. Calafat, L. C. Oomen, C. C. Paulusma, R. P. Oude Elferink et al. Drug export activity of the human canalicular multispecific organic anion transporter in polarized kidney MDCK cells expressing cMOAT (MRP2) cDNA, *J. Clin. Invest.* **1998**, *101*, 1310–1319

97 Kinoshita, S., H. Suzuki, K. Ito, K. Kume, T. Shimizu, and Y. Sugiyama. Transfected rat cMOAT is functionally expressed on the apical membrane in Madin-Darby canine kidney (MDCK) cells., *Pharm. Res.* **1998**, *15*, 1851–1856

98 van der Sandt, I. C., M. C. Blom-Roosemalen, A. G. de Boer, and D. D. Breimer. Specificity of doxorubicin versus rhodamine-123 in assessing P- glycoprotein functionality in the LLC-PK1, LLC-PK1:MDR1 and Caco-2 cell lines, *Eur. J. Pharm. Sci.* **2000**, *11*, 207–214

99 Cui, Y., J. Konig, and D. Keppler. Vectorial transport by double-transfected cells expressing the human uptake transporter SLC21A8 and the apical export pump ABCC2, *Mol. Pharmacol.* **2001**, *60*, 934–943

100 Sasaki, M., H. Suzuki, K. Ito, T. Abe, and Y. Sugiyama. Transcellular transport of organic anions across a double-transfected Madin-Darby canine kidney II cell monolayer expressing both human organic anion-transporting polypeptide (OATP2/SLC21A6) and Multidrug resistance-associated protein 2 (MRP2/ABCC2), *J. Biol. Chem.* **2002**, *277*, 6497–6503

101 Polli, J. W., S. A. Wring, J. E. Humphreys, L. Huang, J. B.

Morgan, L. O. Webster, and C. S. Serabjit-Singh. Rational use of in vitro P-glycoprotein assays in drug discovery, *J. Pharmacol. Exp. Ther.* **2001**, *299*, 620–628

102 Tavelin, S., V. Milovic, G. Ocklind, S. Olsson, and P. Artursson. A conditionally immortalized epithelial cell line for studies of intestinal drug transport, *J. Pharmacol. Exp. Ther.* **1999**, *290*, 1212–1221

103 Fine, K. D., C. A. Santa Ana, J. L. Porter, and J. S. Fordtran. Effect of changing intestinal flow rate on a measurement of intestinal permeability, *Gastroenterology* **1995**, *108*, 983–989

104 Tavelin, S., J. Taipalensuu, F. Hallböök, K. Vellonen, V. Moore, and P. Artursson. An Improved Cell Culture Model Based on 2/4/A1 Cell Monolayers for Studies of Intestinal Drug Transport. Characterization of Transport Routes., *Pharm. Res.* **2003**, *20*, 373–381.

105 Tavelin, S., J. Taipalensuu, L. Söderberg, R. Morrison, S. Chong, and P. Artursson. Prediction of the oral absorption of low permeability drugs using small intestinal-like 2/4/A1 cell monolayers, *Pharm. Res.* **2003**, *20*, 397–405.

106 Levitt, M., C. Fine, J. Furne, and D. Levitt. Use of maltose hydrolysis measurements to characterize the interaction between the aqueous diffusion barrier and the epithelium in the rat jejunum., *J. Clin. Invest.* **1996**, *97*, 2308–2315

107 Fihn, B. M., A. Sjöqvist, and M. Jodal. Permeability of the rat small intestinal epithelium along the villus-crypt axis: effects of glucose transport, *Gastroenterology* **2000**, *119*, 1029–1036

108 Tanaka, Y., Y. Taki, T. Sakane, T. Nadai, H. Sezaki, and S. Yamashita. Characterization of drug transport through tight-junctional pathway in Caco-2 monolayer: comparison with isolated rat jejunum and colon., *Pharm. Res.* **1995**, *12*, 523–528

109 Sugano, K., N. Takata, M. Machida, K. Saitoh, and K. Terada. Prediction of passive intestinal absorption using bio-mimetic artificial membrane permeation assay and the paracellular pathway model, *Int. J. Pharm.* **2002**, *241*, 241–251

110 Camensih, G., G. Folkers, and H. van de Waterbeemd. Comparision of passive drug transport through Caco-2 cells and artificial membranes, *Int. J. Pharm.* **1997**, *147*, 61–70

111 Kansy, M., F. Senner, and K. Gubernator. Physicochemical high throughput screening: parallel artificial membrane permeation assay in the description of passive absorption processes, *J. Med. Chem.* **1998**, *41*, 1007–1010

112 Wohnsland, F. and B. Faller. High-throughput permeability pH profile and high-throughput alkane/water log P with artificial membranes, *J. Med. Chem.* **2001**, *44*, 923–930

113 Avdeef, A., M. Strafford, E. Block, M. Balogh, W. Chambliss, and I. Khan. Drug absorption in vitro model: filter-immobilized artificial membranes. 2. Studies of the permeability properties of lactones in Piper methysticum Forst, *Eur. J. Pharm. Sci.* **2001**, *14*, 271–280

114 Stenberg, P., U. Norinder, K. Luthman, and P. Artursson. Experimental and computational screening models for the prediction of intestinal drug absorption, *J. Med. Chem.* **2001**, *44*, 1927–1937

115 Lennernäs, H., L. Knutson, T. Knutson, A. Hussain, L. Lesko, T. Salmonson, and G. Amidon. The effect of amiloride on the in vivo effective permeability of amoxicillin in human jejunum: experience from a regional perfusion technique., *Eur. J. Pharm. Sci.* **2002**, *15*, 271–277

5
Cell Cultures in Drug Discovery: An Industrial Perspective

Anna-Lena Ungell and Johan Karlsson

Abbreviations

ADMET	Absorption, distribution, metabolism, elimination, toxicity
ATCC	American Type Culture Collection
BCRP	Breast cancer-resistance protein
BSA	Bovine serum albumin
CD	Candidate drug
CFTR	Cystic fibrosis transmembrane conductance exporter family
CNS	Central nervous system
CYP	Cytochrome P450 system
DMSO	Dimethyl sulfoxide
ECACC	European collection of cell cultures
ER	Efflux ratio (transport basolateral to apical divided by transport apical to basolateral)
HEPES	*N*-2-hydroxyethyl-piperazine-*N*′-2-ethanesulfonic acid
HTS	High-throughput screening
LC/MS	Liquid chromatography combined with mass spectrometry detection
MDCK	Madin–Darby canine kidney cells
MES	4-Morpholineethane ethanesulfonic acid
MDR	Multidrug resistance
MRP	Multidrug resistance-associated protein
MTT	3-[4,5-Dimethylthiazol-2yl]2,5-diphenyltetrazolium bromide
NCE	New chemical entity
NPSA	Nonpolar surface area
LDH	Lactate dehydrogenase
LI	Lead identification (phase)
LLC-PK1	Pig kidney cell line
LNAA	Large neutral amino acid transporter
LO	Lead optimization (phase)
PEG	Polyethylene glycol
PePT	Dipeptide carrier

Drug Bioavailability: Estimation of Solubility, Permeability, Absorption and Bioavailability.
Edited by Han van de Waterbeemd, Hans Lennernäs and Per Artursson

ISBN: 3-527-30438-X

PG	Propylene glycol
PSA	Polar surface area
QSPR	Quantitative structure–property relationship
SDS	Sodium dodecyl sulfate
SPR	Structure–property relationship
TER	Transepithelial electrical resistance
TEM	Transmission electron microscopy

Symbols

Fa (or Fabs%)	Fraction of the oral dose absorbed *in vivo*/in humans
log D	Logarithm of the distribution coefficient in octanol/water at a certain pH
log P	Logarithm of the partition coefficient in octanol/water (for neutral species)
MW	Molecular weight
P_{app}	Apparent permeability coefficient

5.1 Introduction

The development of molecular drug discovery technologies has dramatically accelerated the process of discovering new pharmacophores in the pharmaceutical industry. Methods that expedite the development of lead drug candidates to bind to the vast number of different targets are now more generally derived from combinatorial synthesis and will enhance the drug discovery process substantially. Although different "quick and easy" methods can provide a substantial amount of data for many different biological parameters (e.g. potency, and ADMET properties) simultaneously, there are still some questions remaining which concern the quality of data obtained and how to interpret, combine and use the data for further early *de-novo* design. Since several of the biological parameters needed for design of new chemical entities (NCEs) do not follow the same rules of quantitative structure–property relationship (QSPR), parts of the molecule may be changed to serve optimization of the different parameters separately (Fig. 5.1). However, if changes in a structural fragment are connected to several valuable biological parameters, optimization should not be performed on one biological function at a time but instead be combined, e.g., combine optimization of potency with ADMET properties [1] as well as permeability and solubility [2–4].

One of the limiting factors for the successful therapeutic application of new drugs is their transport into the system, e.g., over the intestinal membrane, into the cell interior to the target receptor, or into the central nervous system (CNS). In order to obtain high-quality and useful predictive values for these transport processes there is a need for highly standardized *in vitro* models, permitting easy screening of a large number of molecules. This means that both the requirements

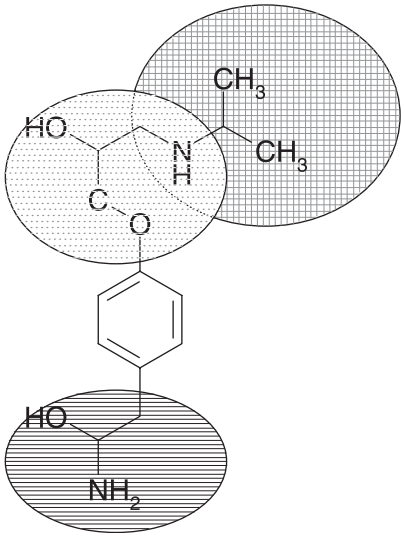

Fig. 5.1. Schematic drawing of a structure of a molecule showing an optimization approach for evaluation of structural parts governing metabolic stability (⊖), potency (⊙) and permeability (▨). If structural elements have overlapping properties for DMPK and/or potency, optimization needs to be performed on several parameters simultaneously. Note that this molecule is only used to exemplify the strategy.

of quality and quantity should be fulfilled in the assessment. The absorption process can be influenced by a number of factors such as, solubility, membrane partitioning, metabolism, and transporters [5–7]. The rationale of evaluating oral availability for compounds can be divided into a "two-step" process (Fig. 5.2), since evaluation of the complex *in vivo* situation is difficult to perform using *in vivo* animal methods for a large quantity of drug molecules. The first step of this two-step process represents the prediction of the intrinsic permeability by the use of *in silico* methods or physico-chemical approaches and/or the direct determination of a biological permeation value. The second step is the most important one, and involves the actual prediction of the fraction absorbed (f_{abs}%) in humans from the permeability values. It can also include other important factors such as solubility, dissolution from dosage forms, regional differences in permeability, transit times in different regions, and blood flow in different regions.

All techniques available for experimental studies of oral drug absorption have different complexities and provide different possibilities for rapid and accurate screening. The high quality of the data obtained from *in vitro* techniques should be emphasized, since many compounds in today's screening methods can produce false indications due to low solubility, adsorption onto plastics and within cellular compartments, metabolism during transport, etc. All of these points require optimization in order for the different aims of each method to be used in the various phases of screening. In contrast to experimentally based screening techniques are the *in silico* predictions of intestinal permeability. These provide a large number of

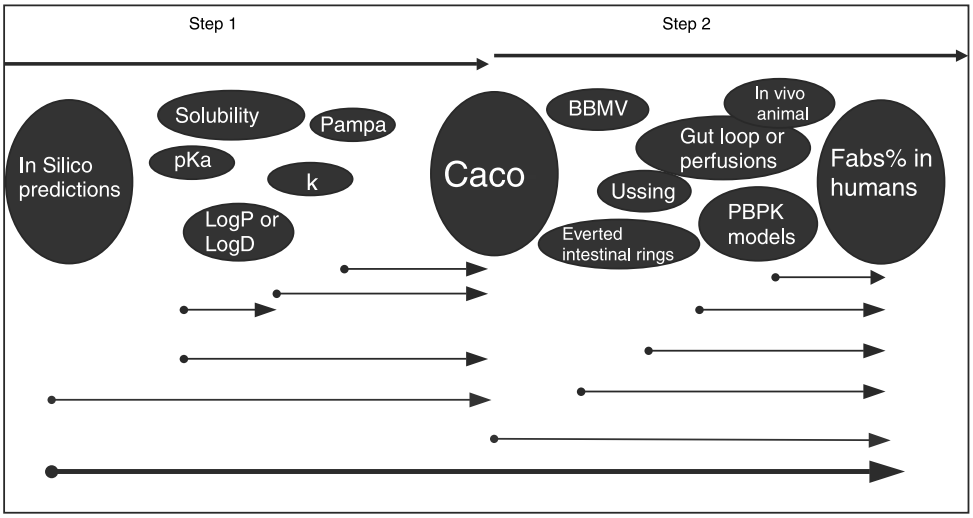

Fig. 5.2. Two-step process for evaluation of intestinal drug absorption. The first step represents the prediction of intestinal permeability (e.g., over Caco-2 monolayers) from in-silico models or from physico-chemical properties. The second step involves the prediction of human fraction absorbed from the intestinal permeability value obtained using different *in vitro* or *in vivo* techniques.

compounds that are predicted only by their molecular structure, with the behavior of the molecule within a biological test system perhaps being overlooked.

5.2 Permeability Screening in Different Phases of Discovery

In the early phases of drug discovery, there are specific needs for evaluating the permeability for a drug over the intestinal membrane. Early screening of permeability in the lead discovery phase (LI), when the result from HTS has revealed a number of different structural groups of compounds showing activity towards the target, usually provides the base for further modifications of the structure of the molecule. In this part of the screening the problems of obtaining high-quality data is usually the highest, since many compounds at this stage are highly lipophilic, difficult to analyze, and may also be toxic to the cells. Although it is desirable to obtain a larger number of molecules through this stage in order to acquire as much structural information as possible into the lead optimization (LO) phase, the risk of losing potentially good compounds due to experimental problems may be high. Low permeability coefficients, and at the same time uncontrolled mass balance (recovery) or nondetectable (nonanalyzable) compounds, usually result in false-negative results. The evaluation of a true low permeability for a compound is even more important than high permeability, as it is more economical to exclude at

this stage as many compounds as possible with no potential for development as drugs.

The screening of permeability coefficients for orally available drugs in the LI phase can be made with the intention to:

- build a structure–property relationship (SPR) for each of the selected groups suggested from the HTS screening library, or to build a general permeability model;
- evaluate structural elements of molecules that can be optimized in a later phase (i.e., identify the potential permeability problems);
- exclude potentially poorly absorbed compounds; and
- support effect data for intracellular targets.

In the LO phase the optimization of the compounds starts, and eventually ends in the selection of the candidate drug (CD). The strategy with respect to oral drug permeability in this phase of drug discovery is aimed at:

- building a specific SPR for each of the structurally related groups of compounds and permeabilities;
- optimization of required permeability in relation to metabolism/dose/potency/solubility requirements;
- establish an *in vitro*/*in vivo* correlation using animals and prediction of human *in vivo* fabs%;
- evaluate the mechanism and route of absorption (active or passive, trans- or paracellular);
- evaluate potential involvement of transporters (will require a specific strategy for screening towards or away from a carrier, and building of SPR);
- evaluate potential drug–drug interactions (will require knowledge of dose requirements of both the NCE and of the drug of interaction);
- evaluate dose linearity; and
- evaluate regional differences in permeability for potential ER (extended release) development.

For the different purposes presented here, cell culture models can provide the basis of screening, biopharmaceutical assessments, and evaluations for mechanistic purposes and some considerations for optimal and rational design are discussed below.

5.3 Cell Cultures for Assessment of Intestinal Permeability

The most commonly used methods for studies of partitioning into a membrane, mechanisms of drug absorption, and interactions with epithelial proteins, such as transporters and enzymes, are the cell culture-based models. These are both sim-

ple and quick to use, and still reflect most of the different mechanisms involved in the absorption process. The most commonly used cell monolayer systems for evaluation of the intestinal barrier have been the Caco-2 (human colon carcinoma) cells, and MDCK (Madin–Darby canine kidney) cells. For the screening of a large number of compounds, these two cell cultures provide extremely useful tools for both preclinical screening and for mechanistic purposes, and have been used in several industries even for cassette dosing and for analyzing large combinatorial libraries [8, 9].

5.3.1 Caco-2

The main reasons for the popularity of the Caco-2 cell line are that the cells are easy to maintain in culture, and they develop unusually high degree of differentiation spontaneously under standard culture conditions. In fact, Caco-2 is the only human intestinal cell line that has been found so far spontaneously to undergo functional enterocytic differentiation. The cells exhibit a good reproducibility, robustness and functional properties of human intestinal epithelial cells. The model has proved capable of predicting the oral absorption of a variety of drug compounds [see references in 10].

The Caco-2 cell line originates from a human colon adenocarcinoma [11], and can be obtained from American Type Culture Collection (ATCC) or the European Collection of Cell Cultures (ECACC). It is a polyclonal cell line, i.e., it consists of a heterogeneous population of cells [12], which means that the properties of the cells may change with time in culture. The cells should therefore be used within a limited number of passages, especially for screening purposes over a long period of time. The heterogeneous properties of the cells may be one explanation for the differences in morphology, paracellular permeability and expression of enzymes and transporters that have been reported from different research groups [13–17]. The cell culture protocol therefore must be standardized and validated by time during screening.

Caco-2 cells form tight junctions and express many of the brush-border enzymes (hydrolases) that are found in the normal small intestine, e.g., alkaline phosphatase, sucrase and amino peptidases [18–21]; moreover, the development of enzyme activity is time-dependent. Cytochrome P450 (CYP450) isoenzymes and some phase II enzymes (e.g., glutathione-S-transferases, sulfotransferase and glucuronidase) have been identified [21–24] in these cells; however, the level of CYP expression (e.g., CYP3A4) is low in the original cells under standard cell culture conditions [25]. CYP1A1 is found to be expressed in dividing Caco-2 cells, but only minimally in confluent differentiated cells [23]. CYP3A5 activity has been demonstrated in a clone named TC7 [26, 27]. CYP3A4 is the dominating drug-metabolizing enzyme of the human small intestine, and hence a variety of approaches have been described to enhance its functional activity in Caco-2 cells. For example, Caco-2 cells have been transfected with cDNA encoding for CYP3A4 [28]. Another approach is to treat the Caco-2 cells with dihydroxy vitamin D3,

which induces an increased activity of the enzyme [29, 30]. Significant induction of CYP3A4 activity and expression has also been reported in CYP3A4-transfected cells by incubation with 12-*O*-tetradecanoylphorbol-13-acetate and sodium butyrate [31].

Several active transport systems that are normally found in the small intestinal enterocytes have been characterized in the Caco-2 cell model [13]. These include transport systems for glucose [32, 33], amino acids [34–37], dipeptides [38–40], vitamins [41], and bile acids [42, 43].

In recent years a multiplicity of other uptake and so-called efflux transporters have been identified. Among the efflux transporters, the MDR-1 gene product P-glycoprotein (P-gp) is the most extensively studied and discussed efflux transporter affecting the absorption and disposition of drugs [44–46]. Nine different efflux transporters have been identified in the Caco-2 cell line [47], both on mRNA level [47] and three of these nine efflux proteins have also been verified on protein and functional levels [48]. Interestingly, investigations by Taipalensuu showed that the normal Caco-2 cells do not overexpress the efflux transporter P-gp in comparison with human jejunum biopsies. A genetically related protein, BCRP, has also been discussed recently, but this protein seems to be less expressed in cell lines such as Caco-2 than in human jejunum [47]. The multidrug resistance-related (associated) protein family, MRPs, belonging to the family of CFTR proteins, has also been identified in Caco-2 cells [47–49], and its importance in transporting metabolites from Phase II enzymatic reactions (conjugations) has recently been proposed [50, 51]. Of the eight to ten different MRPs that have been proposed to exist, only six have been identified in Caco-2 cells, referred to as MRP1 to 6 [47, 49, 52].

The expression of the active transport systems is time-dependent and may vary with nutritional conditions [53, 54]. The culturing conditions, e.g., the passaging process, can dramatically alter the biological characteristics and transport properties of Caco-2 cell monolayers [55–58].

Paracellular (tight junction) permeability can be determined with hydrophilic marker molecules that do not partition into the cell membranes (e.g., polyethylene glycols or mannitol). The permeability of hydrophilic marker molecules in Caco-2 monolayers is relatively low, indicating the presence of well-developed tight junctions and a tight epithelium [12, 59]. The most commonly used paracellular marker molecule is mannitol, and in our laboratory, 14- to 21-day-old Caco-2 monolayers (at passage numbers 25–45) have a permeability for mannitol of $\sim$0.3–0.5×10^{-6} cm s^{-1}. The paracellular permeability in Caco-2 cells has been shown to be comparable with that in rat and human colon with respect to the molecular weight-dependent sieving in the tight junctions [60, 61]. Another way to assess the (paracellular) monolayer integrity is to measure the transepithelial electrical resistance (TER). The Caco-2 monolayers display TER properties which are closer to those of the colonic epithelium than to the small intestinal epithelium [12, 14, 43, 62, 63]. In our laboratory, the average TER value of the Caco-2 monolayers is 300 Ω cm^{-2} at passages 25 to 45. A wide span of TER values has been reported from different laboratories, ranging from 70 up several thousand Ω cm^2 [15–17]. These differences are most likely due to measurements being made at different

temperatures and with different equipment, as well as the changing properties of different clones or passage numbers of Caco-2 cells.

5.3.2 MDCK Cells

The MDCK cell line is also frequently used by pharmaceutical companies to monitor intestinal drug transport, despite its origin from dog kidney [64, 65]. An advantage with this cell line is that the monolayers reach their full differentiation already after 3–7 days in culture. There are two distinct sub clones with different TER values: high-resistance MDCK Strain I ($\sim$4000 Ω cm^2), and low-resistance MDCK Strain II ($\sim$200–300 Ω cm^2). The permeability for mannitol across MDCK monolayers is low (generally $<0.5 \times 10^{-6}$ cm s^{-1}). Irvine and co-workers reported that the correlation to oral fraction absorbed based on 55 different compounds was comparable in the Caco-2 and MDCK model systems [64], though it should be pointed out that the expression of transporters in the MDCK monolayers (from the epithelium of the dog kidney) might be very different from that of the human intestine. Thus, while MDCK monolayers may be sufficient to estimate passive epithelial transport, they are not valid for mechanistic studies or for predicting active uptake or efflux across the intestinal epithelium. In the normal MDCK cell line, a low level of P-gp has been identified [66], and uptake transporters such as OCT and its regulation by steroid hormones have also been studied [67]. However, due to the relatively low inherent expression of transporters in these cells they are popular to use for transfection. MDCK cells transfected with different transporters are available, e.g., MDR1-MDCK. This model is being used as a tool for investigating the contribution of P-gp to transepithelial transport [68–70]. An alternative cell model for assessing P-gp involvement is MDR1-transfected LLC-PK1 cells [71]. However, it appears that the MDR1-MDCK cells, like other transfected cell lines, tend to form multilayers and are not well polarized [68, 72]. The expression of CYP 3A is low and unstable in transfected Caco-2 cells [53, 73] (see section above), and in this respect better stability and higher enzymatic activity have been demonstrated in MDCK and LLC-PK1 cells transfected with CYP3A4.

5.3.3 2/4/A1 Cells

Many attempts have been made to develop cultures of normal intestinal epithelial cells by using immortalizing viruses or oncogenes. Recently, the conditionally immortalized intestinal cell line 2/4/A1 was characterized for studies of intestinal drug transport [74]. The cell line originates from fetal rat intestine and is conditionally immortalized with a temperature-sensitive mutant for the growth-promoting oncogene simian virus 40 (SV40) large T. Cells are maintained in culture at 33°C, when the oncogene is fully active and the cells proliferate rapidly. When cells are cultured at 37°C the function of the oncogene ceases and the cells stop growing and are able to produce a partly differentiated phenotype. The TER of

the 2/4/A1 monolayers has been reported to be ~25 Ω cm^2, and the apparent permeability coefficient of mannitol 15.5 × 10^{-6} cm s^{-1} – 65-fold higher than that measured in Caco-2 monolayers. Thus, the 2/4/A1 cells form much leakier monolayers than the Caco-2 cells. A steep sigmoidal relationship between the permeability coefficients of model drugs in the 2/4/A1 monolayers and oral fraction absorbed in humans has been obtained [74]. According to their relationship, drugs with Papp values >55 × 10^{-6} cm s^{-1} had a Fa >90%, while drugs with Papp values <10 × 10^{-6} cm s^{-1} had Fa <10%. This relationship was comparable with that seen for human jejunal permeability coefficients, but differed from the more shallow relationship observed for Caco-2 cells. It was concluded that the 2/4/A1 monolayers offer a valuable alternative to the tighter Caco-2 monolayers which better mimics the paracellular barrier to drug transport in the human intestine. However, it must be pointed out that the 2/4/A1 cells are poorly differentiated morphologically and lack many of the enzyme systems and transporters that are present in Caco-2 cells and in normal human small intestinal epithelia. Thus, this transport system seems only to be applicable for investigating passive transport properties of drugs without the influence/contribution of active transport mechanisms. Moreover, the culture conditions are very specific and more demanding than the relatively straightforward procedures used for Caco-2 and MDCK cells, and their use in the pharmaceutical industry has hitherto been limited.

5.3.4 HT29

HT29 is another well-studied human colon carcinoma cell line [12, 20]. When grown under standard culture conditions, and in the presence of glucose, the cells form a multilayer of undifferentiated cells, lacking tight junctions and functional polarity. However, under various culture conditions HT29 cells can undergo differentiation into polarized monolayers of mucus-secreting and/or absorptive cells. The degree of differentiation can be modulated by culturing in glucose-free medium, or by the addition of differentiation-inducing agents such sodium butyrate. In this way several permanently differentiated clonal cell lines have been established. One of these is the HT29-18-C1 subclone, which develops TER more slowly than Caco-2 cells and has been proposed as an alternative model for studying paracellular drug transport [75, 76]. The permeability of drugs supposed to be transported by the paracellular route, e.g., atenolol was significantly higher across 100 Ω cm^2 HT29-18-C1 monolayers than across 300 Ω cm^2 Caco-2 monolayers. The Caco-2 cell model is composed of only one cell type, namely absorptive enterocytes. Thus, it lacks several other cell types that are normally present in the intestinal epithelium, for example mucus-secreting goblet cells, which is better represented by the HT29 cell lines. Hence, the Caco-2 model does not contain a mucus layer, and this represents one barrier to drug absorption. Mucus-producing clones of the HT29 cell line such as HT29-H and HT29-MTX (methotrexate-induced cells) have been utilized for the development of mucus layer-containing cell culture models [77–80]. Co-cultures of Caco-2 cells and HT29-H and HT29-

MTX have also been evaluated as models with modified paracellular permeability and the additional presence of a mucus layer [77, 79, 81].

5.3.5 Other Cell Lines

Another human colonic cancer cell line is T84; this develops monolayers of high TER (~1000 Ω cm^2) when grown on permeable supports, but cells are not well differentiated and have been described as resembling a colonic crypt cell phenotype. Hence, these cells have been used mainly in studies of epithelial ion transport and are generally not considered to be adequate for drug transport studies, particularly with respect to carrier-mediated processes [10, 79, 82–84].

The rat intestinal cell line IEC-18 has been evaluated as a model to study small intestinal epithelial permeability. This cell line forms very leaky monolayers with TER of ~50 Ω cm^2 and permeability to mannitol of 8×10^{-6} cm s^{-1}. The IEC-18 model was proposed to be a better model than the Caco-2 monolayers for evaluating the small intestinal paracellular permeation of hydrophilic molecules. However, the leakier paracellular pathway is related to the poor differentiation level of the cells and an undeveloped paracellular barrier lacking peri-junctional actin-belt. In addition, due to the poor differentiation the cells have minute expression of transporters and are therefore not useful for studies of carrier-mediated transport [82, 84]

5.4 Screening for Intestinal Permeability

5.4.1 Caco-2 Culture and Transport Experiments

Cell culture models used for screening need a precultivation period, and in the following text we present the experience of our culturing and experimental set-up for the Caco-2 cell model. The cells are maintained in culture at 37°C in Dulbecco's Modified Eagle's Medium supplemented with 1% nonessential amino acid, 1.5% L-glutamine solution (200 mM), 9% fetal bovine serum, and antibiotics (penicillin and streptomycin) under an atmosphere of 5% CO_2 [12, 85, 86]. Antibiotics are added only to cells grown on the filter inserts, and are excluded from the medium used for cells grown in culture flasks. The maintenance cultures are routinely checked for mycoplasma contamination. For passaging and seeding on filters the cells are harvested from the cell culture flasks by trypsinization with a trypsin-EDTA solution (0.25% trypsin + 0.2% EDTA). It is important that a defined trypsinization procedure is continuously followed, because it will otherwise affect the character of the cell monolayers [58]. For transport studies, the Caco-2 cells are seeded onto specially designed cell culture inserts. Several filter inserts of different membrane materials and pore diameters are commercially available, e.g., Trans-

well inserts (polycarbonate; from Corning Life Sciences) and BD Falcon inserts (polyethylene terephthalate, PET; from BD Bioscience). The Caco-2 cells can be cultured directly on the polycarbonate filters without a coating of extracellular matrix such as collagen. Other cell lines may require a matrix-coated support, e.g., collagen or matrigel, for proper cell attachment and differentiation. Multilayer formation has been reported for Caco-2 cells cultured on the PET membrane inserts [87], so full testing of the filter inserts to be used is required.

We prefer to use noncoated polycarbonate membrane inserts with a pore diameter of 0.4 μm rather than membranes with larger pore diameter, e.g., 3 μm, to avoid problems with cells growing through the pores of the membrane. Large pores may result in monolayers growing on both sides of the membrane, and this may result in depolarized cells and cause misleading drug transport results. The seeding density is reported in the literature as between 0.5 and 5×10^5 cells cm^{-2}, and we use a value of 2.5×10^5 cells cm^{-2}. The optimal density is when confluence is reached rapidly, without the formation of multilayers. The cells are attached to the filters and grown for 2–3 weeks, after which they have formed confluent monolayers of well-differentiated intestinal epithelial cells [10, 12, 14, 43]. At this time the cells have morphological and biochemical properties that resemble those of normal intestinal (absorptive) enterocytes. Further, when confluency is achieved the permeability of the monolayer is constant and remains so for an additional 2 weeks [12]. This means that the same batch of monolayers can be used to study passive drug transport during this period without significant variability in the results [12, 14, 43, 59, 88]. Studies on active transport must be performed within a more defined interval, since the expression of the carriers is often dependent on culture time [42, 53]. It is also important to feed the cells on pre-scheduled weekdays, e.g., trypsinization/passaging on Mondays, change media on the following Wednesday, Friday and Monday, etc.

Drug absorption experiments are easy to perform in the cell culture model. The drug is added to the apical (mucosal) side, and the appearance of the drug on the basolateral side (serosal) is followed by time. The model also permits experiments to be carried out in the reverse direction, i.e., from the basolateral side to the apical side.

The experiments are generally performed at 37°C, with the TER being measured prior to and after the experiment to verify the monolayer integrity. The monolayers should be agitated during the experiments, not only to produce more reproducible results but also to reduce the effects of aqueous boundary layers adjacent to the epithelial membrane [89]. Without correct stirring conditions being maintained during the experiments, the measured permeability values for rapidly transported compounds will be significantly underestimated. Accurate determinations of permeability values are important in order to be able to make correct rankings and to build good prediction and SPR models.

The experiments should preferably be performed under 'sink' conditions (e.g., the drug concentration on the receiver side should be less than 10% of the concentration on the donor side during an experiment) in order to avoid bias by back-diffusion of significant amount of compound from the receiver chamber and to

maintain a "constant" applied drug concentration gradient during the course of the experiment. The following equation is generally used for calculation of the apparent permeability coefficient (P_{app}):

$$P_{app} = (dQ/dt)/(A \times C_{d0}) \quad (1)$$

where dQ/dt is the rate of appearance of drug on the receiver side, C_{d0} is the initial drug concentration on the donor side, and A is the surface area of the filter membrane.

This equation for calculation of P_{app} is easily improved by taking into account the change of donor concentration (C_d) during the experiment, which affects the concentration gradient and the driving force for passive diffusion [74]:

$$P_{app} = k \times V_r/A \quad (2)$$

where k is the change in drug concentration in the receiver chamber ($C_{r\text{-}ti}/C_{d\text{-}ti}$) per unit time, $C_{r\text{-}ti}$ is the concentration on the receiver side at the end of each time interval, $C_{d\text{-}ti}$ is the average of the donor concentration determined at the beginning and at the end of each time interval, V_r is the volume of the receiver chamber, and A is the surface area of the filter membrane. By using this method of calculation a more accurate determination of the P_{app} value is obtained, particularly for rapidly transported drugs where P_{app} values exceed 10×10^{-6} cm s^{-1}.

Culture protocols have been published which describes an accelerated differentiation process where monolayers are ready to be used after 3–7 days of culture [90–92]. One of these systems, the so-called BD BioCoat Intestinal Epithelium Differentiation Environment, is commercially available through BD Bioscience. This system is described to produce monolayers of a quality that are comparable with the typical Caco-2 cells with respect to permeability for drugs transported transcellularly. The paracellular barrier function is however low, as indicated by high mannitol permeability and low TER. The functional capacity for active uptake and efflux is not as thoroughly characterized as for the standard Caco-2 monolayers.

5.4.2 Automated Caco-2 Assay

The trend in the industry has been to automate the Caco-2 permeability assay using semi- or fully automated procedures. With such a system it is possible to obtain a throughput in order of approximately 400–500 compounds per week. Automated Caco-2 assay systems are commercially available through Tecan/BD Bioscience and Bohdan Mettler Toledo. In addition, automated systems for maintenance of cell cultures are commercially available, while totally automated systems for both maintenance and culturing of cells grown on permeable filter supports are under development, e.g., by companies such as The Automation Partnership.

Here, we briefly describe the automated Caco-2 assay used at the research site in AstraZeneca R&D Mölndal. The solubility of the test compounds is measured (or theoretically predicted) before they are run in the Caco-2 assay. In order to be able to make correct determinations of the permeability coefficient, the substance must be dissolved when added to cell monolayer in the transport experiment. Compounds with insufficient solubility are therefore not tested. We generally apply a test concentration of 10 μM, but in specific projects or under certain circumstances a concentration of only 1 μM is applied. The test compounds are first prepared in DMSO solution (1 mM) on a parent plate and are then diluted in transport buffer to give a final drug concentration of 10 μM (solution containing 1% DMSO) when added to the cell monolayers.

In this automated assay, the incubation, shaking and pipetting are performed by a Plato 7 (Rosys) robotic microplate processor. Preparations of drug donor solutions (and standards) are carried out on a MultiPROBE. The assay is developed to handle four 24-well plates with monolayers. Duplicate transport measurements are performed for each substance, and a mixture of three reference compounds is included on each plate to capture variability between assays by time/passage. The internal reference drugs we have chosen are metoprolol, zomig and melagatran, which have P_{app} values of approximately 15×10^{-6} cm s^{-1} (Fa = 100%), 1×10^{-6} cm s^{-1} (Fa = 60%), and 0.1×10^{-6} cm s^{-1} (Fa = 5%), respectively.

In the automated assay we use 14- to 18-day-old Caco-2 monolayers grown on 0.33 cm^2 polycarbonate filters. The TER of the cell monolayers are measured before they are introduced into the robot's workbench, and re-measured after completion of the transport experiments (at the same temperature as the experimental, i.e., 37°C). An automated system for TER measurements can be used, for instance the system for 24-well filter plates from World Precision Instruments. In the robot system, the basolateral chamber of the Transwell is first filled with new transport buffer, after which the experiment is started by the addition of donor drug solution to the apical side of the Caco-2 monolayers. Samples are taken immediately from the donor side to determine the initial donor concentration, and the appearance of compound on the receiver is measured by taking samples from the receiver side at 45 and 120 min. At the end of the experiment, samples are also taken from the donor side in order to obtain a measure of the change in donor concentration and to calculate mass balance (recovery) in the transport experiment. In general, the samples are collected in deep well, 96-well plates, diluted in acetonitrile and then analyzed for content by LC/MS. This assay allows accurate determinations of both low- and high-permeability compounds (P_{app} values may be in the range 0.05 to 200×10^{-6} cm s^{-1}). The overall screening capacity, with one experiment performed each day, is 220 substances per week. The recovery should be kept within limited ranges in order to assure that high-quality and accurate P_{app} values are obtained and reported. Our current limits for recovery are 80–120%. Recovery can be calculated using the following equation:

$$\text{Recovery } (\%) = [(M_{r\text{-}120} + M_{d\text{-}120})/M_{d\text{-}0}] \times 100 \quad (3)$$

where $M_{r\text{-}120}$ is the cumulative amount of drug transported to the receiver side at the end of the experiment (including amount removed in sampling), $M_{d\text{-}120}$ is the amount of drug remaining on the donor side at the end of the experiment, and $M_{d\text{-}0}$ is the amount of drug on the donor side at the start of the experiment (determined from the initial donor concentration sample). In the case that recoveries are clearly outside the set limits, P_{app} values cannot be calculated or reported with high confidence, and further investigations as to the underlying causes may be necessary. However, if recovery is low and the measured P_{app} value is high, the P_{app} value is likely to be underestimated and the interpretation of high permeability is still valid. Different approaches to handle problems with low recovery due to binding of drug to the filter and/or the plastic surfaces of the assay system are further discussed in Section 5.4.6, Optimizing experimental conditions – solubility and bovine serum albumin (BSA).

From an industrial perspective, it is important to have good data systems for downloading results into local and global databases. It is also important to have appropriate criteria for judging the quality of the data produced and whether or not these should be downloaded into the databases. There are different strategies on how to handle this issue. One strategy is to download everything in the database, i.e., the primary assay results in combination with experimental settings including important parameters for judgment of the data quality (e.g., TER and mass balance). The other strategy is to download only those data which fulfill specific quality criteria. There are, of course, pros and cons with both procedures.

Very few published data exist on the evaluation of automated systems, though one report has been made of an automated absorption assay using Caco-2 cells cultured on both sides of polycarbonate membranes [93]. The concept of culturing cells on the lower sides of the membranes was investigated as a means of improving the opportunity to study transport in the secretory basolateral to apical direction. However, this approach resulted in increased variability and impaired active transport properties of the cell monolayers, and was therefore not recommended.

5.4.3
Quality Control and Standardization of Caco-2 Assay

In order to obtain reproducible and high-quality results, a routine characterization should be performed on each new batch of cell monolayers by measuring TER and permeability to a paracellular marker such as ^{14}C-mannitol. The morphology and integrity of the monolayers should also be examined using microscopy [e.g., transmission electron microscopy (TEM) and fluorescence microscopy and staining of tight junction proteins]. Carelessness in passaging cells during the cultivation may lead to the selection of a population of cells and phenotypic drift in the biochemical and transport properties of the Caco-2 cells [55, 94]; hence, this should be checked routinely.

By standardizing the following parameters, it is possible to improve the quality of data, as well as to increase the opportunities to compare data produced by different laboratories:

- Cell cultures of controlled origin used within a restricted number of passages.
- Defined use of filter supports, growth media.
- Defined culturing protocols, seeding density, trypsinization procedures.
- Microscopic verification of monolayer morphology.
- Regularly reproduce the relationship between Fa (%) and P_{app} for a defined set of reference drugs.
- Internal standards/markers and acceptance criteria
- Specified experimental conditions (e.g., pH, stirring, drug concentration, P_{app} calculation).
- Characterization of expression and function of important enzyme and transport systems.

These suggested factors for standardization of the Caco-2 model might also be reasons for the variability in published permeability values obtained from different laboratories [86]. Clearly, data from different publications or laboratories should not be mixed without prior harmonization of the experimental protocols.

The Caco-2 cells are used at various passage numbers between 20 and 110. Caco-2 cells obtained from ATCC and ECACC are usually at passage number 20–40, and though several laboratories use Caco-2 cells at high passage, e.g., 90–105 [86] we normally use lower-passage (25–45) cells. Cells of different passage number can have very different properties with respect to paracellular permeability and functional expression of transporters. For instance, paracellular permeability to mannitol may range from 0.1 to 2.0×10^{-6} cm s^{-1}. Efflux ratios of various P-gp substrates may also vary significantly [57, 95]. Although it is a greater risk that cells with undifferentiated properties are established at high passage number, there are several examples of high-passage Caco-2 cells that show both good morphological and transport properties. Irrespective of whether low- or high-passage Caco-2 cells are used, it is recommended that the cells are used within a relatively limited range of passages for which the cells' properties have been well characterized.

5.4.4 Correlation to Fraction of Oral Dose Absorbed

Many academic and industrial laboratories have shown that the drug permeability measured in Caco-2 cell monolayers can be used to predict the oral absorption of drugs in humans. Various datasets have therefore been used to establish correlations between Caco-2 permeability and the fraction absorbed orally in humans [85, 86, 96]. Taken together, these studies show good predictability, though with a relatively wide variation in the appearance of correlation profiles between different laboratories [86]. These studies emphasize the need to establish correlations and standardization procedures in each laboratory.

As the Caco-2 cell model contains most of the important transporters, it can be used for the study not only of passive transport mechanisms but also of mechanisms involving transporters. This is a major advantage of the Caco-2 model when

compared with other simplified artificial systems in which only passive diffusion is accounted for.

Another limitation of the Caco-2 monolayers is their colonic origin and tight paracellular pathway, which tend to lead to underestimations in permeability to paracellularly transported compounds [97]. This is likely to be correct for small compounds (MW < 150) – i.e., compounds smaller than normal drugs – but it remains to be seen to what extent the Caco-2 model gives false-negative predictions of the fraction absorbed for polar drugs of normal size in humans where para-

Tab. 5.1. List of marker compounds used to establish relationship between oral dose absorbed in humans (F_a) and apparent permeability coefficient in Caco-2 monolayers.

Compound	*F_a [%]*	*F_a class*	*Reference*	*Note*
Ganciclovir	3	Low	1	
Melagatran	5	Low	In-house	
Enalaprilat	10	Low	2	
Sulphasalazine	12	Low	3	Efflux substrate
Acyclovir	17	Low	4, 5	
Chlorothiazide	25	Moderate	4, 6	Dose-dependent F, saturable abs.
Mannitol	26	Moderate	3, 7	
Atenolol	56	Moderate	3, 8	
Zomig	60	Moderate	In-house	
Ranitidine	61	Moderate	9	F_a calculated from $F_a = F/(1 - CL_H/Q_H)$. Interaction with transporters
Digoxin	81	High	10	F_a calculated from urinary exretion data of p.o. and i.v. administered P-gp substrate
Methotrexate	82	High	11	F_a calculated from urinary exretion data of p.o. and i.v. adminisitration. Reduced absorption at high doses
Quinidine	90	High	12	F_a calculated from $F_a = F/(1 - CL_H/Q_H)$. P-gp/MRP inhibitor/substrate
Antipyrine	100	High	13	
Caffeine	100	High	14	
Metoprolol	100	High	3, 15	
Probenecid	100	High	16	MRP inhibitor/substrate
Propranolol	100	High	17	
Testosterone	100	High	18	
Theophylline	100	High	19	
Verapamil	100	High	20	P-gp/MRP substrate inhibitor
D-Glucose	100	High		Glucose transporter
Glycine-proline	100	High		Dipeptide transporter
L-Leucine	100	High		Amino acid transporter
L-Phenylalanine	100	High		Amino acid transporter

F_a classification: low (<20%); moderate (20–80%); high (>80%).
F_a = fraction absorbed; F = bioavailability; CL_H = hepatic clearance;
Q_H = hepatic blood flow (21 mL min^{-1} kg^{-1} in man).
For reference numbers, see note in Ref. [170].

cellular transport might contribute to the absorption. To the best of our knowledge, no clear examples have been published indicating false-negative predictions of the fraction absorbed in humans due to underestimated paracellular Caco-2 permeability. However, in our own experience Caco-2 permeability can fail to predict rat *in vivo* fractions absorbed if the drug is restricted to the paracellular pathway.

In our own studies to establish an in-house correlation between Caco-2 permeability and extent of drug absorption in humans, a set of 25 model drugs was used (Table 5.1). The importance of concentration and pH conditions were investigated and transport was studied both in apical to basolateral (absorptive) and basolateral to apical (secretory) directions. The apparent permeability coefficients were determined at concentrations of 10, 50, and 500 μM, and at two different settings of apical/basolateral pH values: 6.5/7.4 and 7.4/7.4. The marker compounds represented a good diversity in molecular structure and transport properties and covered a range of low (<20%), moderate (20–80%) and high (>80%) extent of absorption in humans (Tab. 5.1).

Compounds absorbed by active uptake mechanisms (e.g., glucose and Gly-Pro) and compounds known to be substrates for efflux transport (e.g., digoxin, verapamil) were also included in the list. The applied concentration (10–500 μM) only had minor effects on the permeability values. Thus, the choice of concentration was not critical for this set of compounds with respect to the relationship between permeability and fraction absorbed in humans. Changing the pH on the apical donor side had significant effects on the P_{app} values of several compounds, the effects being in agreement with the acid–base properties of the compounds. The

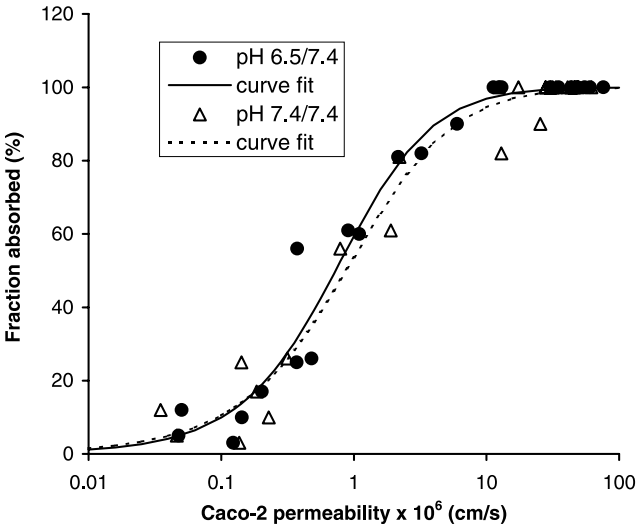

Fig. 5.3. Relationship between the oral fraction absorbed in humans and apparent permeability coefficients obtained in Caco-2 cell monoalyers at two different pH conditions. Mean apical to basolateral P_{app} values were determined at drug concentrations of 10–500 μM at pH 6.5/7.4 or 7.4/7.4 on the apical/basolateral sides of the cell monolayers.

P_{app} values for basic compounds were higher at pH 7.4 than those measured at pH 6.5, and the opposite effect was seen for acidic compounds. As expected, compounds utilizing proton-coupled transporters showed higher permeability values when the apical pH was 6.5. However, even though permeability values were altered by pH, the classification of the compounds into low, moderate or high fraction absorbed was the same at both pH conditions. Measurements of bi-directional transport at pH 7.4/7.4 and 50 μM drug concentration showed significant efflux (efflux ratios > 2) for the following compounds: acyclovir, gancyclovir, digoxin, chlorothiazide, and sulfasalazine.

A sigmoidal equation was fitted to the experimental Caco-2 permeability data [74, 86]. The profiles of the relationship between Caco-2 permeability and fraction absorbed (F_a) obtained at the two different pH settings were comparable, and predictability was equally good (Fig. 5.3). The overall profile was shifted towards slightly higher P_{app} values at pH 7.4, due to the base properties of several of the well-absorbed model drugs included in this dataset. A linear regression plot of the observed F_a values versus predicted F_a values from Caco-2 permeability at pH 6.5/7.4 gave a r^2 value of 0.97, indicating an excellent fit for the sigmoidal relationship. From the sigmoidal relationship obtained at 6.5/7.4 (Fig. 5.4), the following P_{app} banding with respect to predicted fraction absorbed (F_a) was determined (units $\times 10^{-6}$ cm s^{-1}): $P_{app} < 0.3$ predicting $F_a < 20\%$, P_{app} 0.3–2.5 predicting F_a 20–80% and $P_{app} > 2.5$ predicting Fa > 80%.

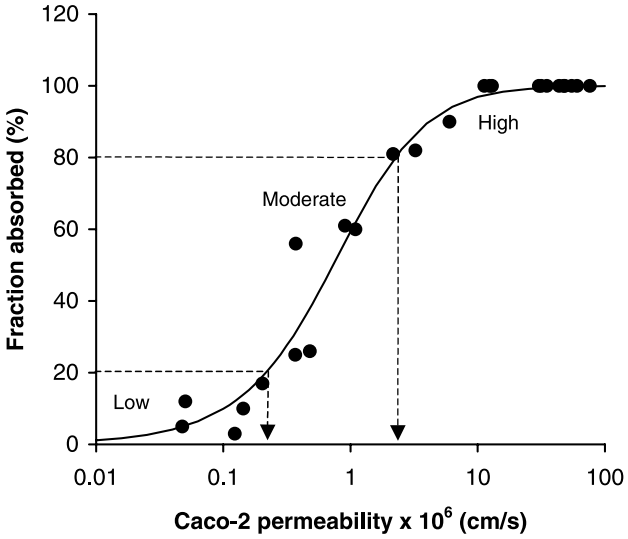

Fig. 5.4. Relationship between the oral fraction absorbed in humans and apparent permeability coefficients obtained in Caco-2 cell monolayers. P_{app} bands for predicted fraction absorbed of <20% (low), 20–80% (moderate) and >80% (high) are indicated.

5.4.5 Optimization of Experimental Conditions: pH

Two main factors have guided the need for optimization of the early screening techniques; on one hand the use of simple, quick and high-capacity cell monolayer methods, e.g., Caco-2 cell and MDCK; and on the other hand the increased synthesis of more lipophilic, insoluble compounds from combinatorial libraries. This has created a vast number of different variants of cell-based assays and has resulted in variability among the data obtained. A need for optimization of as many as possible of the different parameters in order to increase the predictivity and throughput of the model has been suggested in the literature [98–100].

The pH in the GI tract is a very important factor affecting drug absorption for ionizable drugs. pH has two main effects on drugs: one is to determine the degree of ionization (dissociation) of weak electrolytes and thereby affect the passive diffusion of the compound; and the other is to establish a proton gradient as a driving force for some transporters. The pH in the lumen of the GI tract *in vivo* in humans is variable; typically it is pH 1–2 in the stomach, 5–6.5 in the duodenum and proximal jejunum, 6.5–7.5 in the mid jejunum, and almost up to 8 in the terminal ileum [7, 101]. In the large bowel the pH varies between 6.5 and 8 from the colon ascendens to the sigmoideum. This bulk pH will affect mainly the solubility of the compound and is also thought to effect the ionization that provides a driving force for the regional difference in uptake of mainly the uncharged form [102]. However, actual transport across the epithelial membrane is affected by another pH, the so-called microclimate or surface pH, which is one pH unit lower (5.5) than the bulk pH adjacent to the epithelial cell surface in the upper small intestine created by H^+ excretion from the cell and the mucus layer [103]. A surface pH of 7.1–7.4 that is more alkaline than the lumenal pH has been reported in the human colon *in vivo* using radiotelemetry devices [104]. The pH of the apical solution has a direct impact on the transport experiments using monolayers, since the solution is in direct contact with the membrane and should therefore mimic the microclimate pH [98]. The pH on the basolateral side should in all cases reflect the pH of the extracellular fluid within the submucosa, which is under direct influence of the pH in the blood.

If the cell-based screening model should reflect the gradient under physiological conditions and also reflect the absorption across the jejunum (the main part of absorption of most drugs), then a gradient of 6.0–6.5/7.4 should be applied to the apical side [98]. Indeed, the present authors found a better correlation for several compounds ($n = 14$) to F_a% using the pH apically of 6.0 compared with a non-gradient system (pH 7.4). A similar correlation could also be established within AstraZeneca although the effect of pH on the overall correlation was limited for the compounds used (see Fig. 5.3). This indicates that for the general screening, the pH in the apical solution is of less importance, but when asymmetric transport or regional differences in transport are to be evaluated then this should be performed on a nongradient system or the pH of interest should be used in order to mimic the region in the gut. If absorption in the distal parts of the small intestine,

e.g., ileum, are to be mimicked, then a nongradient system would be better (e.g., 7.4/7.4). Similarly, if the colon permeability is to be studied, a nongradient system of 7.4/7.4 could also be used.

Suggested examples for quick evaluation of the pH effect on transport in different regions of the intestine include:

- For jejunal transport = 6.0/7.4
- For ileal transport = 7.4/7.4
- For colon transport = 7.4/7.4

For weak acids, e.g., salicylic acid, the dependency on a pH gradient becomes complex since both the passive diffusion and the active transport process will be dependent on the proton concentration in the apical solution [61, 63, 98, 105] and a lowering of the pH from 7.4 to 6.5 will increase the apical to basolateral transport more than 20-fold. Similarly, for weak bases such as alfentanil or cimetidine, a lowering of the pH to 6.5 will decrease the passive transport towards the basolateral side [105]. The transport of the ionizable compound will, due to the pH partition hypothesis, follow the pK_a curve.

In a recent report by Neuhoff *et al.* [106], additional information on the complexity of applying a pH gradient, i.e., a "false efflux" for weak bases using Caco-2 cells when a physiological pH gradient is applied, is presented. This "false efflux" was not due to efflux protein interaction but rather to the lowering of transport for the weak bases, metoprolol and atenolol, from apical to the basolateral chamber. The results indicate that caution should be taken for interpretation of early screen data from such a gradient system since a substantial efflux would generate compounds to be excluded as false negatives. In an early screening situation when the transport process is unknown, it can be difficult to distinguish a passive asymmetric uptake or efflux due to the pH effect on ionization from a true carrier-mediated uptake or efflux. The following assays are therefore suggested:

- If screening for general intestinal absorption = pH gradient system, only report to projects a → b direction
- If screening for carrier-mediated transport in any direction = both a nongradient and a pH gradient system should be used and bidirectional transport data should be reported

5.4.6
Optimizing Experimental Conditions: Solubility and BSA

Optimizing the permeability measurements to avoid adsorption to plastic, filters or accumulation within the cell monolayer seems highly relevant for increasing the predictivity of the screening model in early screening of highly lipophilic drugs [98, 99]. The additional problem of low solubility of these compounds adds a substantial complexity and error to the determination of permeability values. For sparingly soluble compounds, much effort is spent on finding optimal solubilizing

vehicles and/or formulations. In general, DMSO solutions are the most commonly used vehicle in the early stages as the parallel syntheses made by combinatorial chemistry use 100% DMSO as the end solvent. Even if solubility at this stage is not usually of the same degree as at the stage of formulation development, solubility data are vital in order to improve the quality from the biological assays. To perform high-quality permeability measurements, using a cell culture-based model, a limit for low solubility has to be drawn. If the drug is not soluble within the experimental system then the data will be of low quality and affect the recovery estimates from the permeability assay. The solubility limit to be set is dependent upon several factors, e.g., analytical, enzymatic and whether (or not) transporters are involved. Therefore, a balance between solubility, analytical and permeability issues must be considered before conducting a large number of assays with lipophilic drugs.

Several attempts have been made to estimate the dose required in humans in relation to a drug's potency, and to put this into the context of solubility and permeability for an optimal oral drug [2, 3]. A relatively simple example of this is where a 1.0 mg kg^{-1} dose is required in humans, then 52 μg mL^{-1} solubility is needed if the permeability is intermediate (20–80%) [3]. This solubility corresponds approximately to 100 μM of a compound with a MW of 400 g mol^{-1}. Most screening activities for permeability determinations in, e.g., Caco-2, are made at a concentration of 10 μM or lower due to solubility restrictions. The first implication of this is that the required potency for these compounds needs to correspond to a dose of <0.1 mg kg^{-1} in humans if the drug should be considered orally active. Another implication would be the influence of carrier-mediated transport (uptake or efflux), which is more evident at low concentrations. This could result in low permeability coefficients for compounds interacting with efflux transporters at the intestinal membrane and which could either be saturated or of no clinical relevance at higher concentrations or doses.

The adsorption of compounds to plastic surfaces and accumulation of compounds within the cell membrane is related to the lipophilicity of the compound. Highly lipophilic drugs most likely have high intrinsic permeabilities, but it may be difficult to make a correct determination due to low recoveries in the *in vitro* system, and limits for accepted recoveries are needed to increase the quality of the data reported back to the projects. Many authors have suggested using BSA to increase sink conditions and to reduce the adsorption phenomenon [98, 107]. However, there seems to be a concentration-dependent effect of BSA, which has been tested between 0 to 4% [98]. The effect of the presence of BSA will be determined by both the protein binding capacity of the drug to be tested and its intrinsic permeability, i.e., high protein binding and high permeability values will increase the response to the presence of BSA in the basolateral chamber [98, 99].

There are several positive factors using BSA in the basolateral medium. First, it mimics the *in vivo* situation where the circulating blood provides an excellent base for sink conditions due to a large volume and content of serum proteins such as albumin (serum protein content and alpha-glycoproteins) [108]. Second, serum albumin hinders adsorption onto plastic surfaces and filters and thereby stops the

loss of compound in the experimental system, as well as in the different steps of dilution before the analysis of drug content. Third, the accumulation of a lipophilic drug within the cell monolayer is reduced due to increased sink conditions. These factors result in many cases that the recovery is substantially improved and permeability values from a larger number of compounds can be reported back to projects. For high-permeability compounds the impact of this on interpretation of the data is not substantial, but for low and moderately absorbed compounds the increased recovery can change the interpretation from a compound being excluded as a potential 'no-drug' to a potential 'yes-drug'. This phenomenon has a huge impact on the de-novo synthesis, since the SPR information from as many structural fragments as possible provides a better understanding of the requirements for good permeability. Hence, if information from several of these fragments is missing, the data may mislead the chemist in the synthesis of new analogues. It is therefore of utmost importance to rule out the "falsely" from "truly" poorly absorbed compounds [106].

BSA within the samples provides a complex bioanalytical matrix with suppression of the analytical response, especially during LC/MS analysis. Often, the BSA has to be separated before the analysis, and unfortunately some polar drugs can thereby be lost [98]. Precipitation and dilution with cold acetonitrile can improve the analysis, but this is strongly dependent on the compound to be analyzed. A general use of BSA for high-throughput screening using automated systems for both the transport experiment and the analytical part cannot be recommended.

5.5 Mechanistic Use of Cell Models

For the evaluation of a possible relationship between the molecular structure of a potential candidate and its transport abilities to cross the epithelial membrane of the gut, the mechanism or route of transport must be known [1, 4]. This is due to the structural requirements for the transcellular route being different from the paracellular route. During the lead optimization phase – when many mechanistically based studies are performed – the cell culture-based models can also be used with great confidence.

5.5.1 Paracellular Pathway

The paracellular pathway, between the epithelial cells, is both size- (MW, volume) and charge-dependent [60, 109, 110]. In general, compounds that are limited to paracellular transport are not efficiently absorbed due to the small available absorptive area and the restriction by tight junctions. The molecular weight cut-off seems to be around 400 g mol^{-1} and 300 g mol^{-1} for the small and large intestine respectively, and 300 g mol^{-1} for the Caco-2 cell monolayers [60], which shows the more colonic nature of the Caco-2 monolayer model. Compounds with a

value larger than 3.5 Å, described as the molecular radius, exhibit permeability coefficients similar to that of mannitol, which corresponds to a low fraction absorbed of 15–50% [85]. This is true for neutral compounds, but for charged molecules the cations seem to penetrate the tight junctional system much more easily than anions [109]. This means that a cation can be larger in size than a neutral or an anion, yet still penetrate the membrane successfully if the size does not exceed 4–5 Å.

In the screening procedure using Caco-2 cells or other cell lines with higher tight junctional resistance, a low P_{app} might be misleading if the compound is absorbed through the paracellular pathway. Evaluation of the paracellular component, which is especially noticeable when *in vivo* data obtained for example from rats is high and Caco-2 permeation data is low, can be studied using Caco-2 cells and opening the tight junctions by using EDTA, by omitting Ca^{2+} from the medium [111–114], or by using a pharmacological tool such as tight junction disruption with cytochalasin D, as has been investigated with MDCK cell monolayers [112]. This will open the way for a polar compound to penetrate the membrane via the tight junctional system, but will not affect the transcellularly more lipophilic compounds (Fig. 5.5). Mannitol can be used as a positive control for the paracellular pathway [115]. A continuous fluorescence measurement of transcellular and paracellular pathways, and evaluation of directionally dependent transport with respect to efflux studies, has been proposed [111]. It is possible that Caco-2

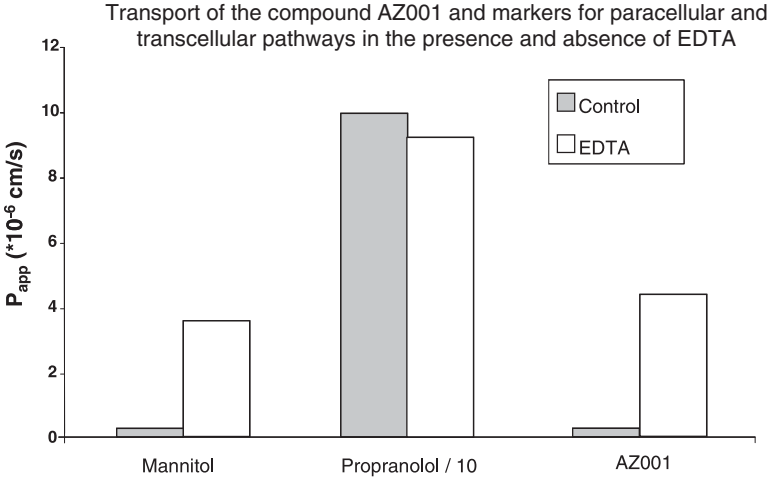

Fig. 5.5. Example of using the Caco-2 monolayers to evaluate paracellular transport of an unknown compound. Two markers, mannitol and propranolol are added together with the unknown compound to the apical side and transport of each of the molecules is measured both in the absence and in the presence of 5 mM EDTA (on both sides of the monolayer). The transport of the paracellularly transported mannitol is enhanced by the presence of EDTA, but not the transcellularly transported propranolol. The compound AZ001 is also enhanced by the presence of EDTA, which resembles the mannitol transport.

cells possess lower permeability towards polar molecules than does the small intestine *in vivo* because the monolayer has a much smaller effective surface area than the small intestine villi, due to the tight junctional resistance *per se* [63, 75, 116].

5.5.2 Transcellular Pathway

Molecules with a large molecular weight or size are confined to the transcellular route and its requirements related to the hydrophobicity of the molecule. The transcellular pathway has been evaluated for many years and is thought to be the main route of absorption of many drugs, both with respect to carrier-mediated transport and passive diffusion. The most well-known requirement for the passive part of this route is hydrophobicity, and a relationship between permeability coefficients across cell monolayers such as the Caco-2 versus log P and log D 7.4 or 6.5 have been established [102, 117]. However, this relationship appears to be nonlinear and reaches a plateau at around log P of 2, while higher lipophilicities result in reduced permeability [102, 117, 118]. Because of this, much more attention has recently been paid towards molecular descriptors other than lipophilicity [86, 119–125] (see section 5.5.6.). The relative contribution between the paracellular and transcellular components has also been evaluated using Caco-2 cells, and for a variety of compounds with different charges [110, 112] and sizes [112] (see Section 5.4.5).

The oral administration of large proteins and peptides is limited due to their low membrane permeability. These compounds are mainly restricted to the paracellular pathway, but because of their polar characteristics and their size the pore of the tight junctional system is also highly restrictive. An additional transcellular pathway has therefore been suggested for these peptides, i.e., the transcytotic pathway, which involves a receptor-mediated endocytosis in Caco-2 cells [126].

5.5.3 Carrier-mediated Transport

In addition to the passive diffusional processes over lipid membranes or between cells, substances can be transferred through the lipid phase of biological membranes through specialized systems, i.e., active transport and facilitated diffusion. Until recently, the active transport component has been discussed only for nutrients or endogenous substances (e.g., amino acids, sugars, bile acids, small peptides), and seemed not to play any major role in the absorption of pharmaceuticals. However, sufficient evidence has now been gathered to recognize the involvement of transporters in the disposition of pharmaceuticals in the body [50, 127].

The relevance of transporter system involvement *in vivo* in humans to the selection of a new drug for development has been debated within the industry, and in time might well become the rationale behind the decision to select a new com-

pound, or not. This finding is due mainly to the increased number of studies performed on "old" substances that are currently available, as well as to the increased knowledge of interactions with transporters that might explain the drug's pharmacokinetic behavior *in vivo*. In addition, in the same way that knowledge has been acquired about interactions with the cytochrome P450 enzyme system, the inhibition, induction and polymorphisms of transporters have also received increased attention in recent years. Consequently, screening tools to evaluate the involvement of transporters have been developed, the aim being to satisfy the need for more information before a potential candidate is selected.

Cell lines, such as the Caco-2 and MDCK cells [27, 35, 47, 49, 57, 67, 128–133], have been used frequently to study different transporters in the GI tract. These cell lines have been evaluated for transport both in absorptive and secretory direction and in addition also been transfected with specified transporter systems of interests to yield new clones [23, 31, 72, 79, 80, 134] or co-cultures [135]. Some of the uptake transporters belonging to the organic cation transporter (OCT) family have also been identified in cell lines such as the pig kidney cell line LLC-PK1, and MDCK [67, 136]. In fact, its presence in Caco-2 cells needs to be further elucidated as reports have shown both the absence and presence of transporters from this family of transporters [136–138].

In cell lines, the organic anion transporters (OAT and OATP) have been identified and cloned into cells of kidney origin such as LLC-PK1, MDCK, HK-2, and Caco-2 [129]. The most well-known uptake transporters, which transport the substrate over the membrane into the organism are the amino acid- [35, 42, 139] and oligopeptide-carriers (PepT1 and PepT2) [139–142]. These two transporter families are abundantly expressed in the small intestine of most animals, and can therefore be involved in the absorption process of pharmaceutical drugs. The PepT1 is expressed in the cell lines Caco-2 and HT-29 [140–142].

From an industrial perspective, quantitative knowledge of the existence of different transporters within the cellular system used in screening procedures is of major importance as it can influence both the predictive value of the permeability coefficients and interpretation of the results. In addition, information on species differences or similarities or discrepancies between cell culture models and animals now provide an important basis for the scaling of data during the early phases of drug discovery for animals or humans [48].

Both active and passive transport occur simultaneously, and their quantitative roles differ at different concentration gradients. At low substrate concentrations, active transport plays a major role, whilst above the concentration of saturation passive diffusion is the major transport process. This very simple rule can be studied in an experimental system using cell culture-based models, and the concentration dependency of the transport of a compound as well as asymmetric transport over the membrane are two factors used to evaluate the presence and influence of transporters. Previous data have indicated that the permeability of actively absorbed compounds may be underestimated in the Caco-2 model due to a lack of (or low) expression of some uptake transporters. However, many data which show a lack of influence of transporters are usually derived from experiments

carried out at saturable concentrations. Rather, if transport studies are performed at low concentrations, e.g., 10 μM or lower, then transport will not be saturated and the P_{app} values may correlate better with the fraction absorbed *in vivo*. The applied concentration is also important when the compound is a substrate for efflux transport.

Information from experiments with cell lines can generate data for:

- SPR for transporter interaction/binding.
- Affinity for a transporter and ranking of compounds.
- Correlations to the *in vivo* human situation for predictivity evaluation.
- Possible interactions between drugs (DDI).
- To determine if a compound is a substrate, or an inhibitor or inducer.

The importance from an industrial perspective is the possibility of testing compounds for interaction with transporters, and to obtain suggestions as to how the structure of the compound may be changed to either increase or decrease the interaction potential (to build a SPR). Functional and specific assays are therefore needed.

In general, the first choice is to use the standard screening model, e.g., Caco-2 cell monolayers and to:

- determine transport in both directions over the membrane (a to b, b to a); from these data an uptake (a to b/b to a) or efflux ratio (b to a/a to b) can be calculated;
- determine if a concentration dependency exists over a broad interval, e.g., 1 μM to 5000 μM, and to calculate K_m and V_{max} values;
- use different known inhibitors or substrates to the transporter of choice (usually test in two different concentrations) and to determine K_i values;
- test if there is a dependency towards ions such as Na^+, K^+, Cl^-, H^+ (this is especially relevant for interaction with the dipeptide carrier (PePT1) (H^+) or large neutral amino acid transporter (LNAA) (Na^+);
- evaluate temperature dependency (is there still an asymmetric transport at 4°C); and
- monitor pH dependency for acids and bases in order to study pseudo uptake/efflux.

A very simple technique is to use a radiolabeled ligand (usually a well-known substrate) of the specific transporter of interest. A recent suggestion for functional quantitation of the apparent affinities (K_i values) to P-gp using Caco-2 cells and the substrate taxol has been published [143]. The method can be described simply as: (1) determination of b → a transport of ^{3}H-taxol in normal, untreated Caco-2 cells; and (2) determination of b → a transport of ^{3}H-taxol in the presence of verapamil (0.2 mM). The difference between these two components represents the active transport via P-gp. The two concentrations of the test compound are chosen as approximately $0.25 \times K_i$ and $4.0 \times K_i$ and for the inhibition of taxol transport, and in the study of Gao *et al.* [143], 16 μM and 250 μM of the test compound were used

as first choices. For verapamil, vinblastine, daunorubicin, and etoposide the K_i values determined were very similar to those reported elsewhere in the literature. The method can in general offer a standard procedure for interactions with transporters, as only changes in the radioactivity of the ligand needs to be measured. Interactions with the LNAA and the dipeptide carrier (PepT1) have been studied in a similar manner using radiolabeled substrates and Caco-2 cells [35]. However, more assays and identification of specific probes for intestinal transporters for evaluation of drug–drug interactions and their relevance for human *in vivo* pharmacokinetics are needed – a suggestion which is also strongly emphasized by regulatory authorities [127].

It is, without doubt, difficult to utilize the information relating to NCE–transporter interaction during the early stages of a drug discovery project. Some companies have attempted to evaluate compounds with the aim of filtering them out at an early stage, by suggesting a limit to the efflux ratio (e.g., ER = 5). By contrast, if a structural group of compounds is rejected at too early a stage on the basis of a high ER value, this might restrict the variation in synthesis that might be used to obtain an optimal compound during the later phases.

Interestingly, transporter expression – like the expression of enzymes – can be regulated at both the RNA and protein levels. Induction of the P-gp transporter has been evaluated by Nuti *et al.* [58], who found that trypsin – when used to detach the cells from their support – seems to up-regulate MDR1. Efflux via MDR1 has also been proposed to be regulated by a nuclear receptor, SXR [144]. However, this area in transporters and drug–drug interaction is still in its very early stages of development, and substantial advances in the creation of specific cellular-based models are required before it can be incorporated into industrial screening processes.

5.5.4
Evaluation of Metabolism During Transport

Cell culture models can be used to evaluate the importance of metabolism in gut membranes, both with respect to oxidative metabolism via the cytochrome P450 system and Phase II reactions [16, 27, 100]. Recently, a graphical model for the visualization of oral drug bioavailability of drugs based on Caco-2 permeability and *in vitro* metabolic stability rates was presented [145]. Such tools are informative in evaluating important factors for bioavailability in a series of compounds, as well as to interpret large quantities of data. Enzymes (e.g., the conjugating enzymes) are also abundant, and important enzymes in the intestinal mucosa have been found in cellular models (e.g., UDP-glucuronosyltransferases, glutathione-S-transferase, and sulfotransferase), and metabolic inactivation due to conjugation has been studied using Caco-2 cells [51, 100]. Hence, these cells serve as a good model for studying Phase II conjugation during transport across the intestinal epithelium.

In addition to oxidative and conjugative metabolism, other enzymes are also present in the Caco-2 model, though at lower levels than in the human enterocyte *in vivo*. These are mainly apical cell surface peptidases, such as aminopeptidases

N, P and W dipeptidylpeptidase IV, endopeptidase-24, 11, and gamma-glutamyltranspeptidase [146]. In addition, esterase activity has been reported in Caco-2 [147, 148]. The bioactivation of prodrugs, such as the ester prodrugs of bis (POC)-PMPA [147], ethyl and isopropyl esters of a matrix metalloprotease inhibitor [100], thrombin inhibitor prodrugs [56, 132], acyl derivatives of tetragastrin [146] and inhibition of esterase activity using fruit extracts [147], has been successfully studied using Caco-2 cells.

The presence of enzymes within the cellular model makes it more complicated than serving only as a permeation/transport model. The evaluation of experimental data should include this as a possible source of error, recovery problems or variability when evaluating large compound sets during the early screening stages. The two main implications are first, the low-permeability drug, which has a different structure–activity relationship if the low permeability is due to metabolism rather than low passive diffusion. The second implication is the false-positive results of monolayer permeability data if the enzyme responsible for the drug's degradation in the human gut is absent from the cell-based model. In general, these implications are of less importance, and the Caco-2 model can in fact serve as an excellent model to investigate both permeation and first-pass metabolism. Due to the fact that Caco-2 cells also contain many important transporters (e.g., efflux transporters such as P-gp), this cell culture model has been – and will be – used to evaluate the relative role of oxidative metabolism versus carrier-mediated efflux in the limited oral bioavailability of drugs [100].

5.5.5 Evaluation of Toxicity

The intestinal epithelium constitutes both a physical and enzymatic barrier for the absorption of orally administered drugs. The physical barrier comprises the lipid bilayer of each cell facing the intestinal lumen, as well as the tight junctional complex that joins the cells into a single layer. A fully functional barrier is necessary in all experiments using cell culture models, or the results might be misinterpreted. In general, paracellular markers such as mannitol, Na- or carboxyfluorescein, lucifer yellow or rhodamine 123 [4, 149] are used to evaluate the integrity of the monolayer in combination with measurements of TER before and after the experiments are conducted [100, 150]. Further recommendations include validation of the cell monolayer integrity by passage and age, as well as restriction of the number of passages in the screening procedure. Care should also be taken when using the fluorescent markers fluorescein and rhodamine 123, both of which are thought to be transported via efflux processes [136].

Solvents used to increase solubility for compounds during screening of permeability across the cell monolayers, together with commonly used excipients for formulations, can also affect the barrier as they contain ingredients which enhance drug absorption [100, 151]. There are different mechanisms by which these compounds can modulate the barrier [4, 149, 150]; for example, they may increase the tight junctional pathway inhibiting carrier-mediated transport, or cholesterol

extraction out of the lipid bilayer, thereby increasing its fluidity. Toxicity screening of various absorption enhancers using Caco-2 cell monolayers has been reported [152]. Well-known dosage form excipients which affect cell monolayer integrity include polyethylene glycol (e.g., PEG-400), propylene glycol (PG), cyclodextrin, SDS, Tween 80, and inhibitory effects of surfactants on the apically polarized efflux system [100, 153]. Hence, care should be taken when using high concentrations of surfactants in the testing media. Cell monolayers such as Caco-2 appear to be the most sensitive model to different enhancer systems compared with animal *ex vivo* or *in vivo* models of drug absorption [149], and the exact correlation between concentration used in the monolayer experiment might differ greatly from that to be used either *in vivo* in the animal or in the formulation development.

Cell monolayers and integrity measurements can be used to:

- evaluate the toxicity of compounds;
- evaluate the toxicity of excipients in formulations;
- establish test solutions for optimal screening; and
- evaluate formulations containing enhancers of intestinal permeability.

Apart from using paracellular or transcellular markers of the functional epithelium, other techniques can be used to evaluate toxicity, e.g., MTT test, lactate dehydrogenase (LDH), morphology and confocal laser scanning [149, 154, 155]. The MTT test is based on the binding of the colored compound MTT to intracellular dehydrogenases; the compound is fluorescent only if the cell membrane is intact and cells are viable. The LDH method involves measuring the release of LDH (an intracellular soluble enzyme); if the lipid membrane is damaged, the resultant LDH leakage leads to increased enzyme levels in the extracellular fluid [155].

A lowering of the permeability coefficients of compounds has been reported during the screening procedure using cell monolayers and commonly used excipients [98] (e.g., using PEG 400, DMSO), and it is also known that both DMSO and ethanol affect the general metabolic capacity of the cells, leading to an overestimation of permeability [156].

5.5.6
Computational Models for Prediction of Intestinal Permeability

Passive diffusion through the lipid bilayer of the epithelium can be described using the partition coefficient between octanol/water (log P) and Δ log P (the difference between the partition into octanol/water and heptane/ethylene glycol or heptane/octanol) [157, 158]. The lipophilicity of the drug (log P) (or rather log D at a certain pH) can easily be either measured or calculated, and is therefore generally used as a predictor of drug permeability. Recently, a method using artificial membrane permeation (PAMPA) has also been found to describe the passive diffusion in a similar manner to the Caco-2 cell monolayers [159].

The direct relationship between permeability and lipophilicity appears to reach a plateau at around log P of 2 [102, 117]. Therefore, permeation through the lipid

bilayer is dependent not only on partition into the membrane but also on how the drug can diffuse within the lipid core of the membrane. Hence, other descriptors of the molecule also need to be accounted for. These additional descriptors were suggested to be molecular weight and volume, polar surface area (PSA, units $Å^2$), nonpolar surface area (NPSA, $Å^2$), hydrogen-bonding capacity, number of hydrogen bonds, polarizability, and number of rotatable bonds [86, 119–125, 160, 161]. Cell monolayers (e.g., Caco-2, MDCK) have frequently been used to establish QSAR/QSPR for the optimization of drug permeability across the intestinal membrane and to describe SPR for affinity towards transporters [1, 2, 86, 119–125, 132, 161–166].

Carrier systems can display a narrow specificity (SPR) for substrates, but transporter systems with a broad specificity also exist; for example, oligopeptide transporter (PePT1) [130, 140, 141, 167], and the efflux transporter MDR1 gene product, P-gp [168]. SPR for the efflux protein P-gp has been suggested for newly synthesized compounds of the thrombin inhibitor family [56, 132], for a small set of peptidomimetics [157], and also for generally known substrates and inhibitors for evaluation of a general structural pattern for recognition as a P-gp substrate [162, 168]. The structural characterization of substrates for the anion-exchange transporter has also been reported [129]. Many of these reported SPRs were assessed using the Caco-2 cell monolayer as the experimental system for collecting affinity data, and show the usefulness of cell monolayers also in this respect.

The power of using computed predictions of intestinal permeability during the early screening phase of drug discovery has a major impact within drug companies. An excellent recent review by Egan and Lauri describes several of these computational methods for prediction presented in the literature [161]. The early predictions serve as a general tool to reduce the time and cost to select potential candidates as well as to complement the biological screening and optimization processes because there is no need to synthesize compounds. Within the industry, specific QSPR models of intestinal permeability for each of the specific compound classes need to be generated, and each has their place in both the LI and LO phases. The computational models in the early phases are usually of a more general character and are built from a large diversity of compounds, whilst in the later LO phase a more restricted model for each project or structural group of compounds needs to be generated. Data obtained from cell culture models should be of high quality and low variability (see above) in both cases, as mixing of reported data from different laboratories may not yield a model of good accuracy.

Several commercially available tools/software using Caco-2 cells as a model for intestinal permeability have also been established, e.g., VolSurf (Tripos Inc.) and LION's iDEA (LION Bioscience, Inc.). Simulation Plus, which have generated the GastroPlus module to predict a human drug plasma profile for a potential drug candidate late in the LO phase use human intestinal perfusion data (P_{eff}) as permeability input, and transformation from Caco-2 data to human P_{eff} data is therefore required and also offered by the program (for a description see Ref. [169]). In general, these models can provide a good estimate of oral drug absorption and its relation to either the molecular surface descriptors, to permeability, or other important factors of oral drug absorption such as solubility and metabolic stability.

5.6 Concluding Remarks

In this chapter we have provided information and experience relating to the use of cell culture-based absorption models within the pharmaceutical industry. These cell-based models are well suited as high-capacity screening models and for mechanistic evaluation of transport route or mechanism. Ensured high quality during culturing and during the transport experiments is recommended, as differences can cause major variability among the data acquired.

References

1 Zamora, I., Oprea, T. I., Ungell, A.-L., Prediction of oral drug permeability, in: *Rational Approaches to Drug Design*. Höltje, H.-D., Sippl, W. (eds), Prous Science Press, Barcelona, **2001**, 271–280.

2 Oprea, T., Zamora, I., Ungell, A.-L., Pharmacokinetically based mapping device for chemical space navigation, *J. Comb. Chem.* **2002**, *4*, 258–266.

3 Lipinski, C. A., Drug-like properties and the causes of poor solubility and poor permeability, *J. Pharmacol. Toxicol. Methods* **2000**, *44*, 235–249.

4 Muranishi, S., Yamamoto, A., Mechanisms of absorption enhancement through gastrointestinal epithelium, in: *Drug Absorption Enhancement*. de Boer, A. G. (ed.), Harwood Academic Publishers, **1994**, 67–100.

5 Ungell, A.-L., *In vitro* absorption studies and their relevance to absorption from the GI tract, *Drug Dev. Indust. Pharmacy* **1997**, *23*, 879–892.

6 Ungell, A.-L., Abrahamsson, B., Biopharmaceutical support in candidate drug selection, in: *Pharmaceutical Preformulation and Formulation. A Practical Guide from Candidate Drug Selection to Commercial Dosage Formulation*. Gibson, M. (ed.), Interpharm Press, **2001**.

7 Balimane, P. V., Chong, S., Morrison, R. A., Current methodologies used for evaluation of intestinal permeability and absorption, *J. Pharmacol. Toxicol. Methods* **2000**, *44*, 301–312.

8 Stevenson, C. L., Augustijns, P. F., Hendren, R. W., Use of Caco-2 cells and LC/MS/MS to screen a peptide combinatorial library for permeable structures, *Int. J. Pharm.* **1999**, *177*, 103–115.

9 Taylor, E. W., Gibbons, J. A., Braeckman, R. A., Intestinal absorption screening of mixture from combinatorial libraries in the Caco-2 model, *Pharm. Res.* **1997**, *14*, 572–577.

10 Hillgren, K. M., Kato, A., Borchardt, R. T., *In vitro* systems for studying intestinal drug absorption, *Med. Res. Rev.* **1995**, *15*, 83–109.

11 Fogh, J., Fogh, J. M., Orfeo, T., One hundred and twenty-seven cultured human cell lines producing tumors in nude mice, *J. Natl. Cancer Inst.* **1977**, *59*, 221–225.

12 Artursson, P., Cell cultures as models for drug absorption across the intestinal mucosa, *Crit. Rev. Ther. Drug Carrier Syst.* **1991**, *8*, 305–330.

13 Hidalgo, I. J., Li, J., Carrier-mediated transport and efflux mechanisms in Caco-2 cells, *Adv. Drug Delivery Rev.* **1996**, *22*, 53–66.

14 Hidalgo, I. J., Raub, T. J., Borchardt, R. T., Characterization of the human colon carcinoma cell line (Caco-2) as a model for intestinal epithelial permeability, *Gastroenterology* **1989**, *96*, 736–749.

15 Walter, E., Kissel, T., Heterogeneity in the human intestinal cell line Caco-2 leads to differences in transepithelial transport, *Eur. J. Pharm. Sci.* **1995**, *3*, 215–230.

16 Delie, F., Rubas, W. A., Human colonic cell line sharing similarities with enterocytes as a model to examine oral absorption: advantages and limitations of the Caco-2 model, *Crit. Rev. Ther. Drug Carrier Syst.* **1997**, *14*, 221–286.

17 Hidalgo, I. J., Assessing the absorption of new pharmaceuticals, *Curr. Top. Med. Chem.* **2001**, *1*, 385–401.

18 Pinto, M., Robin-Léon, S., Appay, M. D., Kedinger, M., Triadou, N., Dussaulx, E., Lacroix, B., Simon-Assman, P., Haffen, K., Fogh, J., Zweibaum, A., Enterocyte-like differentiation and polarization of the human colon carcinoma cell line Caco-2 in culture, *Biol. Cell* **1983**, *47*, 323–330.

19 Hauri, H.-P., Sterchi, E. E., Bienz, D., Fransen, J. A. M., Marxer, A., Expression and intracellular transport of microvillus hydrolases in human intestinal epithelial cells, *J. Cell Biol.* **1985**, *101*, 838–851.

20 Chantret, I., Barbat, A., Dussaulx, E., Brattain, M. G., Zweibaum, A., Epithelial polarity, villin expression, and enterocytic differentiation of cultured human colon carcinoma cells: a survey of twenty cell lines, *Cancer Res.* **1988**, *48*, 1936–1942.

21 Howell, D., Kenny, A. J., Turner, J., A survey of membrane peptidases in two human colonic cell lines, Caco-2 and HT29, *Biochem. J.* **1992**, *284*, 595–601.

22 Bjorge, S., Hamelehle, K. L., Homa, R., Rose, S.-E., Turluck, D. A., Wright, D. S., Evidence for glucuronide conjugation of *p*-nitrophenol in the Caco-2 cell model, *Pharm. Res.* **1991**, *8*, 1441–1443.

23 Carriére, V., Chambaz, J., Rousset, M., Intestinal responses to xenobiotics, *Toxicol. In Vitro* **2001**, *15*, 373–378.

24 Baranczyk-Kuzma, A., Garren, J. A., Hidalgo, I. J., Borchardt, R. T., Substrate specificity and some properties of phenol sulphotransferase from human intestinal Caco-2 cells, *Life Sci.* **1991**, *49*, 1197–1206.

25 Pruesaritanont, T., Gorham, L. M., Hochman, J. H., Tran, L. O., Vyas, K. P., Comparative studies of drug-metabolising enzymes in dog, monkey, and human small intestine, and in Caco-2 cells, *Drug Metab. Dispos.* **1996**, *24*, 634–642.

26 Gervot, L., Carrière, V., Costet, P., Cugnenc, P.-H., Berger, A., Beaune, P. H., Waziers, I. de, CYP3A5 is the major cytochrome P450 3A expressed in human colon and colonic cell lines, *Environ. Toxicol. Pharmacol.* **1996**, *2*, 381–388.

27 Raeissi, S. D., Hidalgo, I., Segura-Aguilar, J., Artursson, P., Interplay between CYP3A-mediated metabolism and polarized efflux of terfenadine and its metabolites in intestinal epithelial Caco-2 (TC-7) cell monolayers, *Pharm. Res.* **1999**, *16*, 625–632.

28 Crespi, C. L., Penman, B. W., Hu, M., Development of Caco-2 cells expressing high levels of CDNA-derived cytochrome P450 3A4, *Pharm. Res.* **1996**, *16*, 1635–1641.

29 Schmiedlin-Ren, P., Thummel, K. E., Fisher, J. M., Paine, M. F., Lown, K. S., Watkins, P. B., Expression of enzymatically active CYP3A4 by Caco-2 cells grown on extracellular matrix-coated permeable supports in the presence of 1-alpha,25-dihydroxyvitamin D3, *Mol. Pharmacol.* **1997**, *51*, 741–754.

30 Engman, H. A., Lennernäs, H., Taipalensuu, J., Charlotta, O., Leidvik, B., Artursson, P., CYP3A4, CYP3A5, and MDR1 in human small and large intestinal cell lines suitable for drug transport studies, *J. Pharm. Sci.* **2001**, *90*, 1736–1751.

31 Cummins, C. L., Mangravite, L. M., Benet, L. Z., Characterizing the expression of CYP3A4 and efflux transporters (P-gp, MRP, and MRP2) in CYP3A4-transfected Caco-2 cells

after induction with sodium butyrate and the phorbol ester 12-O-tetradecanoylphorbol-13-acetate, *Pharm. Res.* **2001**, *18*, 1102–1109.

32 Blais, A., Bissonnette, P., Berteloot, A., Common characteristics for Na^+-dependent sugar transport in Caco-2 cells and human fetal colon, *J. Membr. Biol* **1987**, *99*, 113–125.

33 Riley, S. A., Warhurst, G., Crowe, P. T., Turnberg, L. A., Active hexose transport across cultured human Caco-2 cells: characterisation and influence of culture conditions, *Biochim. Biophys. Acta* **1991**, *1066*, 175–182.

34 Hidalgo, I. J., Borchardt, R. T., Transport of large neutral amino acid (phenylalanine, in a human intestinal cell line: Caco-2) *Biochim. Biophys. Acta* **1990**, *1028*, 25–30.

35 Hu, M., Borchardt, R. T., Transport of a large neutral amino acid in a human intestinal epithelial cell line (Caco-2): uptake and efflux of phenylalanine, *Biochim. Biophys. Acta* **1992**, *1135*, 233–244.

36 Nicklin, P., Irwin, B., Hassan, I., Williamson, I., MacKay, M., Permeable support type influence the transport of compounds across Caco-2 cells, *Int. J. Pharm.* **1992**, *83*, 197–209.

37 Nicklin, P. L., Irwin, W. J., Hassan, I. F., MacKay, M., Proline uptake by monolayers of human intestinal absorptive (Caco-2) cells in vitro, *Biochim. Biophys. Acta* **1992**, *1104*, 283–292.

38 Thwaites, D. T., McEwan, G. T. A., Hirst, B. H., Simmons, N. L., H^+-coupled a-methylaminoisobutyric acid transport in human intestinal Caco-2 cells, *Biochim. Biophys. Acta* **1995**, *1234*, 111–118.

39 Brandsch, M., Miyamoto, Y., Ganapathy, V., Leibach, F. H., Expression and protein C-dependent regulation of peptide/H^+ co-transport system in the Caco-2 human colon carcinoma cell line, *Biochem. J.* **1994**, *299*, 253–260.

40 Ganapathy, M. E., Brandsch, M., Prasad, P. D., Ganapathy, V., Leibach, F. H., Differential recognition of β-lactam antibiotics by intestinal and renal peptide transporters, PEPT1 and PEPT2, *J. Biol. Chem.* **1995**, *270*, 25672–25677.

41 Dix, C. J., Hassan, I. F., Obray, H. Y., Shah, R., Wilson, G., The transport of vitamin B12 through polarized monolayers of Caco-2 cells, *Gastroenterology* **1990**, *98*, 1272–1279.

42 Hidalgo, I. J., Borchardt, R. T., Transport of bile acids in a human intestinal epithelial cell line, Caco-2, *Biochim. Biophys. Acta* **1990**, *1035*, 97–103.

43 Wilson, G., Hassan, I. F., Dix, C. J., Williamson, I., Shah, R., MacKay, M., Artursson, P., Transport and permeability properties of human Caco-2 cells: an in vitro model of the intestinal epithelial cell barrier, *J. Controlled Release* **1990**, *11*, 25–40.

44 Hunter, J., Jepson, M. A., Tsuruo, T., Simmons, N. L., Hirst, B. H., Functional expression of P-glycoprotein in apical membranes of human intestinal epithelial Caco-2 cells: kinetics of vinblastine secretion and interaction with modulators, *J. Biol. Chem.* **1993**, *268*, 14991–14997.

45 Hunter, J., Hirst, B. H., Simmons, N. L., Drugs absorption limited by P-glycoprotein-mediated secretory drug transport in human intestinal epithelial Caco-2 cell layers, *Pharm. Res.* **1993**, *10*, 743–749.

46 Hunter, J., Hirst, B. H., Intestinal secretion of drugs: the role of P-glycoprotein and related drug efflux systems in limiting oral drug absorption, *Adv. Drug Del. Rev.* **1997**, *25*, 129–157.

47 Taipalensuu, J., Törnblom, H., Lindberg, G., Einarsson, C., Sjöqvist, F., Melhus, H., Garberg, P., Sjöström, B., Lundgren, B., Artursson, P., Correlation of gene expression of ten efflux proteins of the ATP-binding cassette transporter family in normal human jejunum and in human intestinal epithelial Caco-2 cell monolayers, *J. Pharmacol. Exp. Ther.* **2001**, *299*, 164–170.

48 Stephens, R. H., O'Neill, C. A., Warhurst, A., Carlson, G. L., Rowland, M., Warhurst, G., Kinetic profiling of P-glycoprotein-mediated drug efflux in rat and human intestinal epithelia, *J. Pharmacol. Exp. Ther.* **2001**, *296*, 584–591.

49 Kool, M., Haas, M. de, Scheffer, G. L., Scheper, R. J., van Eijk, M. J. T., Juijn, J. A., Baas, F., Borst, P., Analysis of expression of cMoat (MRP2), MRP3, MRP4, and MRP5, homologues of the multidrug resistance-associated protein gene (MRP1), in human cancer cell lines, *Cancer Res.* **1997**, *57*, 3537–3547.

50 Suzuki, H., Sugiyama, Y., Role of metabolic enzymes and efflux transporters in the absorption of drugs from the small intestine. Mini review, *Eur. J. Pharm. Sci.* **2000**, *12*, 3–12.

51 Walle, U. K., Galijatovic, A., Walle, T., Transport of the flavonoid chrysin and its conjugated metabolites by the human intestinal cell line Caco-2, *Biochem. Pharmacol.* **1999**, *58*, 431–438.

52 Hirohashi, T., Suzuki, H., Chu, X. Y., Tamai, I., Tsuji, A., Sugiyama, Y., Function and expression of multidrug resistance-associated protein family in human colon adenocarcinoma cells (Caco-2), *J. Pharmacol. Exp. Ther.* **2000**, *292*, 265–270.

53 Hu, M., Borchardt, R. T., Mechanism of L-α-methyldopa transport through a monolayer of polarized human intestinal epithelial cells (Caco-2), *Pharm. Res.* **1990**, *7*, 1313–1319.

54 Peters, W. H. N., Roelofs, H. M. J., Time-dependent activity and expression of glutathione S-transferases in the human colon adenocarcinoma cell line Caco-1, *Biochem. J.* **1989**, *264*, 613–616.

55 Yu, H., Cook, T. J., Sinko, P. J., Evidence for diminished functional expression of intestinal transporters in Caco-2 cell monolayers at high passages, *Pharm. Res.* **1997**, *14*, 757–762.

56 Walter, E., Kissel, T., Reers, M., Dickneite, G., Hoffmann, D., Stuber, W., Transepithelial transport properties of peptidomimetic thrombin inhibitors in monolayers of a human intestinal cell line (Caco-2) and their correlation to *in vivo* data, *Pharm. Res.* **1995**, *12*, 360–365.

57 Anderle, P., Niederer, E., Rubas, W., Hilgendorf, C., Spahn-Langguth, H., Wunderli-Allenspach, H., Merkle, H. P., Langguth, P., P-glycoprotein (P-gp) mediated efflux in Caco-2 cell monolayers: the influence of culturing conditions and drug exposure on P-gp expression levels, *J. Pharm. Sci.* **1998**, *87*, 757–762.

58 Nuti, S. L., Mehdi, A., Rao, S. U., Activation of the human P-glycoprotein ATPase by trypsin, *Biochemistry* **2000**, *39*, 3424–3432.

59 Artursson, P., Epithelial transport of drugs in cell culture I: a model for studying the passive diffusion of drugs over intestinal epithelia, *J. Pharm. Sci.* **1990**, *79*, 476–482.

60 Artursson, P., Ungell, A.-L., Löfroth, J.-E., Selective paracellular permeability in two models of intestinal absorption: cultured monolayers of human intestinal epithelial cells and rat intestinal segments, *Pharm. Res.* **1993**, *10*, 1123–1129.

61 Adson, A., Raub, T. J., Burton, P. S., Barsuhn, C. L., Hilgers, A. R., Audus, K. L., Ho, N. F. H., Quantitative approaches to delineate paracellular diffusion in cultured epithelial cell monolayers, *J. Pharm. Sci.* **1994**, *83*, 1529–1536.

62 Grasset, E., Pinto, M., Dussaulx, E., Zweibaum, A., Desjeux, J.-F., Epithelial properties of human colonic carcinoma cell line Caco-2: electrical parameters, *Am. J. Physiol.* **1984**, *247*, C260–C267.

63 Tanaka, Y., Taki, Y., Sakane, T., Nadai, T., Sezaki, H., Yamashita, S., Characterization of drug transport through tight-junctional pathway in Caco-2 monolayer: comparison with

isolated rat jejunum and colon, *Pharm. Res.* **1995**, *12*, 523–528.

64 Irvine, J. D., Takahashi, L., Lockhart, K., Cheong, J., Tolan, J. W., Selick, H. E., Grove, J. R., MDCK (Madin-Darby Canine Kidney) cells: a tool for membrane permeability screening, *J. Pharm. Sci.* **1999**, *88*, 28–33.

65 Cho, M. J., Thompson, D. P., Cramer, C. T., Vidmar, T. J., Scieszka, J. F., The Madin Darby canine kidney (MDCK) epithelial cell monolayer as a model cellular transport barrier, *Pharm. Res.* **1989**, *6*, 71–77.

66 Horio, M., Chin, K.-V., Currier, S. J., Goldenberg, S., Wiliams, C., Pasatan, I., Gottesman, M. M., Handler, J., Transepithelial transport of drugs by the multidrug transporter in cultured Madin-Darby canine kidney cell epithelia, *J. Biol. Chem.* **1989**, *264*, 14880–14884.

67 Shu, Y., Bello, C. L., Mangravite, L. M., Feng, B., Giacomini, K. M., Functional characteristics and steroid hormone-mediated regulation of an organic cation transporter in Madin-Darby Canine Kidney cells, *J. Pharmacol. Exp. Ther.* **2001**, *299*, 392–398.

68 Lentz, K. A., Polli, J. W., Wring, S. A., Humphreys, J. E., Polli, J. E., Influence of passive permeability on apparent P-glycoprotein kinetics, *Pharm. Res.* **2000**, *17*, 1456–1460.

69 Smith, B. J., Doran, A. C., Mclean, S., Tingley III, F. D., O'Neil, C. A., Kajiji, S. M., P-glycoprotein efflux at the blood-brain barrier mediates differences in brain disposition and pharmacodynamics between two structurally related neurokinin-1 receptor antagonists, *J. Pharmacol. Exp. Ther.* **2001**, *298*, 1252–1259.

70 Schipper, N. G. M., Österberg, T., Wrange, U., Westberg, C., Sokolowski, A., Rai, R., Young, W., Sjöström, B., In vitro intestinal permeability of factor Xa inhibitors: influence of chemical structure on passive transport and susceptibility to efflux, *Pharm. Res.* **2001**, *18*, 1735–1741.

71 Adachi, Y., Suzuki, H., Sugiyama, Y., Comparative studies on in vitro methods for evaluating in vivo function of MDR1 P-glycoprotein, *Pharm. Res.* **2001**, *18*, 1660–1668.

72 Hämmerle, S. P., Rothen-Rutishauser, B., Kramer, S. D., Gunthert, M., Wunderli-Allenspach, H., P-glycoprotein in cell cultures: a combined approach to study expression, localisation, and functionality in the confocal microscope, *Eur. J. Pharm. Sci.* **2000**, *12*, 69–77.

73 Brimer, C., Dalton, J. T., Zhu, Z., Schuetz, J., Yasuda, K., Vanin, E., Relling, M. V., Lu, Yi, Schuetz, E. G., Creation of polarized cells coexpressing CYP3A4, NADPH cytochrome P450 reductase and MDR1/P-glycoprotein, *Pharm. Res.* **2000**, *17*, 803–810.

74 Tavelin, S., Milovic, V., Ocklind, G., Olsson, S., Artursson, P. A., Conditionally immortalized epithelial cell line for studies of intestinal drug transport, *J. Pharmacol. Exp. Ther.* **1999**, *290*, 1212–1221.

75 Collett, A., Sims, E., Walker, D., He, L. H., Ayrton, J., Rowland, M., Warhurst, G., Comparison of HT29-18-C1 and Caco-2 cell lines as models for studying intestinal paracellular drug absorption, *Pharm. Res.* **1996**, *13*, 216–221.

76 Wils, P., Warnery, A., Phung-Ba, V., Scherman, D., Differentiated intestinal epithelial cell lines as in vitro models for predicting the intestinal absorption of drugs, *Cell Biol. Toxicol.* **1994**, *10*, 393–397.

77 Wikman, A., Karlsson, J., Carlstedt, I., Artursson, P., A drug absorption model based on the mucus layer producing human intestinal goblet cell line HT29-H, *Pharm. Res.* **1993**, *10*, 843–852.

78 Karlsson, J., Wikman, A., Artursson, P., The mucus layer as a barrier to drug absorption in monolayers of human intestinal epithelial HT29-H

goblet cells, *Int. J. Pharm.* **1993**, *99*, 209–218.

79 Hilgendorf, C., Spahn-Langguth, H., Regård, C. G., Lipka, E., Amidon, G. L., Langguth, P., Caco-2 versus Caco-2/HT29-MTX co-cultured cell lines: permeabilities via diffusion, inside- and outside-directed carrier-mediated transport, *J. Pharm. Sci.* **2001**, *89*, 63–75.

80 Behrens, I., Stenberg, P., Artursson, P., Kissel, T., Transport of lipophilic drug molecules in a new mucus-secreting cell culture model based on HT29-MTX cells, *Pharm. Res.* **2001**, *18*, 1138–1145.

81 Wikman-Larhed, A., Arursson, P., Co-cultures of human intestinal goblet (HT29-H) and absorptive (Caco-2) cells for studies of drug and peptide absorption, *Eur. J. Pharm. Sci.* **1995**, *3*, 171–183.

82 Laboisse, C. L., Jarry, A., Bou-Hanna, C., Merlin, D., Vallette, G., Intestinal cell culture models, *Eur. J. Pharm. Sci.* **1994**, *2*, 36–38.

83 Brayden, D. J., Human intestinal epithelial cell monolayers as prescreens for oral drug delivery, *Pharm. News* **1997**, *4*, 11–15.

84 Duizer, E., Penninks, A. H., Stenhuis, W. H., Groten, J. P., Comparison of permeability characteristics of the human colonic Caco-2 and rat small intestinal IEC-18 cell lines, *J. Controlled Release* **1997**, *49*, 39–49.

85 Artursson, P., Karlsson, J., Correlation between oral drug absorption in humans and apparent drug permeability coefficients in human intestinal epithelial (Caco-2) cells, *Biochem. Biophys. Res. Commun.* **1991**, *175*, 880–885.

86 Artursson, P., Palm, K., Luthman, K., Caco-2 monolayers in experimental and theoretical predictions of drug transport, *Adv. Drug Deliv. Rev.* **1996**, *22*, 67–84.

87 Rothen-Rutishauser, B., Brain, A., Günthert, M., Wunderli-Allenspach, H., Formation of multilayers in the Caco-2 cell culture model: a confocal laser scanning microscopy study, *Pharm. Res.* **2000**, *17*, 460–465.

88 Hilgers, A. R., Conradi, R. A., Burton, P. S., Caco-2 cell monolayers as a model for drug transport across the intestinal mucosa, *Pharm. Res.* **1990**, *7*, 902–910.

89 Karlsson, J., Artursson, P., A method for the determination of cellular permeability coefficients and aqueous boundary layer thickness in monolayers of intestinal epithelial (Caco-2) cells grown in permeable filter chambers, *Int. J. Pharm.* **1991**, *71*, 51–64.

90 Chong, S., Dando, S. A., Morrison, R. A., Evaluation of BIOCOAT® intestinal epithelium differentiation environment (3-day cultured Caco-2 cells) as an absorption screening model with improved productivity, *Pharm. Res.* **1997**, *14*, 1835–1837.

91 Liang, E., Chessic, K., Yazdanian, M., Evaluation of an accelerated Caco-2 cell permeability model, *J. Pharm. Sci.* **2000**, *89*, 336–345.

92 Lentz, K. A., Hayashi, J., Lucisani, L. J., Polli, J. E., Development of a more rapid, reduced serum culture system for Caco-2 monolayers and application to the biopharmaceutics classification system, *Int. J. Pharm.* **2000**, *200*, 41–51.

93 Garberg, P., Eriksson, P., Schipper, N., Sjöström, B., Automated absorption assessment using Caco-2 cells cultivated on both sides of polycarbonate membranes, *Pharm. Res.* **1999**, *16*, 441–445.

94 Lu, S., Gough, A. W., Bobrowski, W. F., Stewart, B. H., Transport properties are not altered across Caco-2 cells with heightened TEER despite underlying physiological and ultrastructural changes, *J. Pharm. Sci.* **1996**, *85*, 270–273.

95 Hosoya, K.-I., Kim, K.-J., Lee, V. H. L., Expression of P-glycoprotein, a drug efflux pump, in Caco-2 cell monolayers as a function of age, *Pharm. Res.* **1996**, *13*, 885–890.

96 Yazdanian, M., Glynn, S. L.,

Wright, J. L., Hawi, H., Correlating partitioning and Caco-2 cell permeability of structurally diverse small molecular weight compounds, *Pharm. Res.* **1997**, *15*, 1490–1494.

97 Yee, S., In vitro permeability across Caco-2 cells (colonic) can predict in vivo (small intestinal) absorption in man – Fact or myth? *Pharm. Res.* **1997**, *14*, 763–766.

98 Yamashita, S., Furubayashi, T., Kataoka, M., Sakane, T., Sezaki, H., Tokuda, H., Optimized conditions for prediction of intestinal drug permeability using Caco-2 cells, *Eur. J. Pharm. Sci.* **2000**, *10*, 195–204.

99 Krishna, G., Chen, K.-J., Lin, C.-C., Nomeir, A. A., Permeability of lipophilic compounds in drug discovery using in-vitro human absorption model, Caco-2, *Int. J. Pharm.* **2001**, *222*, 77–89.

100 Gan, L.-S. L., Thakker, D. R., Applications of the Caco-2 model in the design and development of orally active drugs: elucidation of biochemical and physical barriers posed by the intestinal epithelium, *Adv. Drug Deliv. Rev.* **1997**, *23*, 77–98.

101 Fallingborg, J., Christensen, L. A., Ingelman-Nielsen, M., Jacobsen, B. A., Abildgaard, K., Rasmussen, H. H., PH-profile and regional transit times of the normal gut measured by radiotelemetry device, *Aliment. Pharmacol. Ther.* **1989**, *3*, 605–613.

102 Taylor, D. C., Pownall, R., Burke, W., The absorption of beta adrenoceptor antagonists in rat in-situ small intestine: the effect of lipophilicity, *J. Pharm. Pharmacol.* **1985**, *37*, 280–283.

103 Lucas, M. L., Determination of acid surface pH in vivo in rat proximal jejunum, *Gut* **1983**, *24*, 734–739.

104 Nugent, S. G., Kumar, D., Rampton, D. S., Evans, D. F., Intestinal luminal pH in inflammatory bowel disease: possible determinants and implications for therapy with aminosalicylates and other drugs, *Gut* **2001**, *48*, 571–577.

105 Palm, K., Luthman, K., Ros, J., Grasjo, J., Artursson, P., Effect of molecular charge on intestinal epithelial drug transport: pH-dependent transport of cationic drugs, *J. Pharmacol. Exp. Ther.* **1999**, *291*, 435–443.

106 Neuhoff, S., Zamora, I., Ungell, A.-L., Artursson, P., pH-dependent bidirectional transport of weak basic drugs across Caco-2 cell monolayers, implications for drug–drug interactions, **2002** *Pharm. Res.* (submitted).

107 Walgren, R. A., Walle, T., The influence of plasma binding on absorption/exsorption in the Caco-2 model of human intestinal absorption, *J. Pharm. Pharmacol.* **1999**, *51*, 1037–1040.

108 *Scientific Tables*, 7th edition. Diem, K., Lentner, C. (eds), Ciba-Geigy Limited, Basel, Switzerland, **1970**.

109 Karlsson, J., Ungell, A.-L., Gråsjö, J., Artursson, P., Paracellular drug transport across intestinal epithelia: influence of charge and induced water flux, *Eur. J. Pharm. Sci.* **1999**, *9*, 47–56.

110 Pade, V., Stavchansky, S., Estimation of the relative contribution of the transcellular and paracellular pathway to the transport of passively absorbed drugs in the Caco-2 cell culture model, *Pharm. Res.* **1997**, *14*, 1210–1215.

111 Wielinga, P., De Waal, E., Westerhoff, H. V., Lankelma, J., In vitro transepithelial drug transport by on-line measurement: cellular control of paracellular and transcellular transport, *J. Pharm. Sci.* **1999**, *88*, 1340–1347.

112 Adson, A., Burton, P. S., Raub, T. J., Barsuhn, C. L., Audus, K. L., Ho, N. F. H., Passive diffusion of weak organic electrolytes across Caco-2 cell monolayers: uncoupling of the contributions of hydrodynamic, transcellular and paracellular barriers, *J. Pharm. Sci.* **1995**, *84*, 1197–1204.

113 Knipp, G. T., Ho, N. F. H., Barsuhn, C. L., Borchardt, R. T., Paracellular diffusion in Caco-2 cell monolayers: effect of perturbation on the transport of hydrophilic compounds that vary in

charge and size, *J. Pharm. Sci.* **1997**, *86*, 1105–1110.

114 Artursson, P., Magnusson, C., Epithelial transport of drugs in cell culture. II. Effect of extracellular calcium concentration on the paracellular transport of drugs of different lipophilicities across monolayers of intestinal epithelial (Caco-2) cells, *J. Pharm. Sci.* **1990**, *79*, 595–600.

115 Lazarova, L., Gråsjö, J., Artursson, P., Bergström, M., Wu, F., Petterman-Bergström, E., Ögren, M., Långström, B., Quantification and imaging of mannitol transport through Caco-2 cell monolayers using a positron-emitting tracer, *Pharm. Res.* **1998**, *15*, 1141–1144.

116 Yamashita, S., Tanaka, Y., Endoh, Y., Taki, Y., Sakane, T., Nadai, T., Sezaki, H., Analysis of drug permeation across Caco-2 monolayer: implications for predicting in vivo drug absorption, *Pharm. Res.* **1997**, *14*, 486–491.

117 Martin, Y. C., A practitioner's perspective of the role of quantitative structure-activity analysis in medicinal chemistry, *J. Med. Chem.* **1981**, *24*, 229–237.

118 Wils, P., Warnery, A. A., Phung-Ba, V., Llegrain, S., Scherman, D., High lipophilicity decreases drug transport across intestinal epithelial cells, *J. Pharmacol. Exp. Ther.* **1994**, *269*, 654–658.

119 Van de Waterbeemd, H., Camenisch, G., Folkers, G., Raevsky, O., Estimation of Caco-2 cell permeability using calculated molecular descriptors, *Quant. Struct. Act. Relat.* **1996**, *15*, 480–490.

120 Van de Waterbeemd, H., Smith, D. A., Beaumont, K., Walker, D. K., Property-based design: optimization of drug absorption and pharmacokinetics, *J. Med. Chem.* **2001**, *44*, 1313–1333.

121 Palm, K., Luthman, K., Ungell, A.-L., Strandlund, G., Artursson, P., Correlation of drug absorption with molecular surface properties, *J. Pharm. Sci.* **1996**, *85*, 32–39.

122 Palm, K., Stenberg, L. P., Luthman, K., Artursson, P., Polar molecular surface properties predict the intestinal absorption of drugs in humans, *Pharm. Res.* **1997**, *14*, 568–571.

123 Stenberg, P., Luthman, K., Artursson, P., Prediction of membrane permeability to peptides from calculated dynamic molecular surface properties, *Pharm. Res.* **1999**, *16*, 205–212.

124 Stenberg, P., Luthman, K., Ellens, H., Lee, C. P., Smith, P. L., Lago, A., Elliot, J. D., Artursson, P., Prediction of the intestinal absorption of endothelin receptor antagonists using three theoretical methods of increasing complexity, *Pharm. Res.* **1999**, *16*, 1520–1526.

125 Lipinski, C. A., Lombardo, F., Dominy, B. W., Feeney, P., Experimental and computational approaches to estimate solubility and permeability in drug discovery and development settings, *Adv. Drug Deliv. Rev.* **1996**, *23*, 3–25.

126 Sai, Y., Kajita, M., Tamai, I., Wakama, J., Wakamiya, T., Tsuji, A., Adsorptive-mediated transcytosis of a basic peptide, 001-C8 in Caco-2 cells, *Pharm. Res.* **1998**, *15*, 1305–1309.

127 Tukker, G., Houston, J. B., Huang, S.-M., Optimizing drug development: strategies to assess drug metabolism/transporter interaction potential – toward a consensus, *Clin. Pharmacol. Ther.* **2001**, *70*, 103–114.

128 Ohashi, R., Tamai, I., Yabuuchi, H., Ezu, J.-I., Oku, A., Sai, Y., Shimane, M., Tjuji, A., Na^+-dependent carnitine transport by organic cation transporter (OCTN2): its pharmacological and toxicological relevance, *J. Pharmacol. Exp. Ther.* **1999**, *291*, 778–784.

129 Ogihara, T., Tamai, I., Tsuji, A., Structural characterization of substrates for the anion exchange transporter in Caco-2 cells, *J. Pharm. Sci.* **1999**, *88*, 1217–1221.

130 Dantzig, A. H., Bergin, L., Uptake of cephalosporin, cephalexin, by a dipeptide transport carrier in the human intestinal cell line, Caco-2,

Biochim. Biophys. Acta **1990**, *1027*, 211–217.

131 Gutmann, H., Fricker, G., Török, M., Michael, S., Beglinger, C., Drewe, J., Evidence for different ABC-transporters in Caco-2 cells modulating drug uptake, *Pharm. Res.* **1999**, *16*, 402–407.

132 Kamm, W., Hauptmann, J., Behrens, I., Stürzebecher, J., Dullweber, F., Gohlke, H., Stubbs, M., Klebe, G., Kissel, T., Transport of peptidomimetic thrombin inhibitors with a 3-amidino-phenylalanine structure: permeability and efflux mechanism in monolayers of a human intestinal cell line (Caco-2), *Pharm. Res.* **2001**, *18*, 1110–1118.

133 Twaites, D. T., Basterfield, L., McCleave, P. M. J., Carter, S. M., and Simmons, N. L., Gamma-aminobutyric acid (GABA) transport across human intestinal epithelial (Caco-2) cell monolayers, *Brit. J. Pharmacol.* **2000**, *129*, 457–464.

134 Woodcock, S., Williamson, I., Hassan, I., MacKay, M., Isolation and characterization of clones from the Caco-2 cell line displaying increased taurocholic acid transport, *J. Cell Sci.* **1991**, *98*, 323–332.

135 Walter, E., Janich, S., Roessler, B. J., Hilfinger, J. M., Amidon, G., HT29-MTX/Caco-2 cocultures as an in vitro model for the intestinal epithelium: in vitro-in vivo correlation with permeability data from rats and humans, *J. Pharm. Sci.* **1996**, *85*, 1070–1076.

136 Van der Sandt, I. C. J., Blom-Roosemalen, M. C. M., Boer, A. G. de, Breimer, D. D., Specificity of doxorubicin versus rhodamine-123 in assessing P-glycoprotein functionality in the LLC-PK1, LLC-PK1:MDR1 and Caco-2 cell lines, *Eur. J. Pharm. Sci.* **2000**, *11*, 207–214.

137 Bleasby, K., Chauhan, S., Brown, C. D., Characterization of MMP^+ secretion across human intestinal Caco-2 cell monolayers: role of P-glycoprotein and a novel Na^+-dependent organic cation transport mechanism, *Br. J. Pharmacol.* **2000**, *129*, 619–625.

138 O'Neil, C. A., Stephens, R., Rowland, M., Warhurst, G., Molecular expression polyspecific drug transporters in human intestine, *J. Physiol.* **1999**, 517P, 53P.

139 Tsuji, A., Tamai, I., Carrier-mediated intestinal transport of drugs, *Pharm. Res.* **1996**, *13*, 963–977.

140 Guo, A., Hu, P., Balimane, P., Leibach, F. H., Sinko, P. J., Interactions of a nonpeptidic drug, valacyclovir, with the human intestinal peptide transporter (hPePT1) expressed in a mammalian cell line, *J. Pharmacol. Exp. Ther.* **1999**, *289*, 448–454.

141 Wenzel, U., Gebert, I., Weintraut, H., Weber, W.-M., Clauss, W., Daniel, H., Transport characteristics of differently charged cephalosporin antibiotics in oocytes expressing the cloned intestinal peptide transporter PepT1 and in human intestinal Caco-2 cells, *J. Pharmacol. Exp. Ther.* **1996**, *277*, 831–839.

142 Mrsny, R. J., Oligopeptide transporters as putative therapeutic targets for cancer cells, *Pharm. Res.* **1998**, *15*, 816–818.

143 Gao, J., Murase, O., Chowen, R. L., Aubé, J., Borchardt, R., A functional assay for quantitation of the apparent affinities of ligands of P-glycoprotein in Caco-2 cells, *Pharm. Res.* **2001**, *18*, 171–176.

144 Synold, R. W., Dussault, I., Forman, B. M., The orphan nuclear receptor SXR coordinately regulates drug metabolism and efflux, *Nature Med.* **2001**, *7*, 584–590.

145 Mandagere, A. K., Thompson, T. N., Hwang, K.-K., Graphical model for estimating oral bioavailability of drugs in humans and other species from their Caco-2 permeability and in vitro liver enzyme metabolic stability rates, *J. Med. Chem.* **2002**, *45*, 304–311.

146 Fujita, T., Kawahara, I., Quan, Y.-S., Hattori, K., Takenaka, K., Muranishi, S., Yamamoto, A., Permeability characteristics of

tetragastrins across intestinal membranes using the Caco-2 monolayer system: comparison between acylation and application of protease inhibitors, *Pharm. Res.* **1998**, *15*, 1387–1392.

147 Gelder, van J., Annaert, P., Naesens, L., Clercq, E. de, Van den Mooter, G., Kinget, R., Augustijns, P., Inhibition of intestinal metabolism of the antiviral ester prodrug bis(POC)-PMPA by nature-identical fruit extracts as a strategy to enhance its oral absorption: an in vitro study, *Pharm. Res.* **1999**, *16*, 1035–1040.

148 Augustijns, P., Annaert, P., Heylen, P., van den Mooter, G., Kinget, R., Drug absorption studies of prodrugs esters using the Caco-2 model: evaluation of ester hydrolysis and transepithelial transport, *Int. J. Pharm.* **1998**, *166*, 45–53.

149 Anderberg, E. K., Artursson, P., Cell cultures to access drug absorption enhancement, in: *Drug Absorption Enhancement*. de Boer. A. G. (ed.), Harwood Academic Publishers, **1994**, pp. 101–118.

150 Hochman, J., Artursson, P., Mechanisms of absorption enhancement and tight junction regulation, *J. Controlled Release* **1994**, *29*, 253–267.

151 Swenson, E. S., Milisen, W. B., Curatolo, W., Intestinal permeability enhancement: efficacy, acute toxicity and reversibility, *Pharm. Res.* **1994**, *11*, 1132–1142.

152 Quan, Y. S., Hattori, K., Lundborg, E., Fujita, T., Murakami, M., Muranishi, S., Yamamoto, A., Effectiveness and toxicity screening of various absorption enhancers using Caco-2 cell monolayers, *Biol. Pharm. Bull.* **1998**, *21*, 615–620.

153 Nerurkar, M. M., Burton, P. S., Borchardt, R. T., The use of surfactants to enhance the permeability of peptides through Caco-2 cells by inhibition of an apically polarized efflux system, *Pharm. Res.* **1996**, *13*, 528–534.

154 Sakai, M., Imai, T., Ohtake, H., Azuma, H., Otagiri, M., Effects of absorption enhancers on the transport of model compounds in Caco-2 cell monolayers: assessment by confocal laser scanning microscopy, *J. Pharm. Sci.* **1997**, *86*, 779–785.

155 Oberle, R. L., Moore, T. J., Krummel, D. A. P., Evolution of mucosal damage of surfactants in rat jejunum and colon, *J. Pharmacol. Toxicol. Methods* **1995**, *33*, 75–81.

156 Hanisch, G., Corswant, C. von, Breitholtz, K., Bergstrand, S., Ungell, A.-L., Can mucosal damage be minimised during permeability measurements of sparingly soluble compounds? *Fourth International Conference On Drug Absorption: Towards Prediction and Enhancement of Drug Absorption*. Edinburgh, **1998**.

157 Burton, P. S., Conradi, R. A., Hilgers, A. R., Ho, N. F. H., Maggiora, L. L., The relationship between peptide structure and transport across epithelial cell monolayers, *J. Controlled Release* **1992**, *19*, 87–97.

158 Goodwin, J. T., Burton, P. S., Hilgers, A. R., Conradi, R. A., Ho, N. N. F., Relationships between physicochemical properties for a series of peptides and membrane permeability in Caco-2 cells, *Pharm. Res.* **1996**, *13*, S243.

159 Camenisch, G., Folkers, G., van de Waterbeemd, H., Comparison of passive drug transport through Caco-2 cells and artificial membranes, *Int. J. Pharmaceut.* **1997**, *147*, 61–70.

160 Raevsky, O. A., Schaper, K.-J., Quantitative estimation of hydrogen bond contribution to permeability and absorption processes of some chemicals and drugs, *Eur. J. Med. Chem.* **1998**, *33*, 799–807.

161 Egan, W. J., Lauri, G., Prediction of intestinal permeability, *Adv. Drug. Del. Rev.* **2002**, *54*, 273–289.

162 Ekins, S., Kim, R. B., Leake, B. F., Danzig, A. H., Schuetz, E. G., Lan, L.-B., Yasuda, K., Shepard, R. L., Winter, M. A., Schuetz, J. D., Wikel, J. H., Wrighton, S. A.,

Three-dimensional quantitative structure–activity relationships of inhibitors of P-glycoprotein, *Molec. Pharmacol.* **2002**, *61*, 964–973.

163 Hjort-Krarup, L., Christensen, I. T., Hovgaard, L., Frökjaer, S., Predicting drug absorption from molecular surface properties based on molecular dynamics simulations, *Pharm. Res.* **1998**, *15*, 972–978.

164 Norinder, U., Österberg, T., Artursson, P., Theoretical calculation and prediction of Caco-2 cell permeability using MolSurf parametrization and PLS statistics, *Pharm. Res.* **1997**, *14*, 1786–1791.

165 Österberg, T., Norinder, U., Theoretical calculation and prediction of P-glycoprotein-interacting drugs using MolSurf parametrization and PLS statistics, *Eur. J. Pharmaceut. Sci.* **2000**, *10*, 295–303.

166 Clark, D. E., Pickett, S. D., Computational methods for the prediction of 'drug-likeness', *Drug Discov. Today* **2000**, *5*, 49–58.

167 Hidalgo, I. J., Bhatnagar, P., Lee, C.-P., Miller, J., Cucullino, G., Smith, P. L., Structural requirements for interaction with the oligopeptide transporter in Caco-2 cells, *Pharm. Res.* **1995**, *12*, 317–319.

168 Seelig, A., A general pattern for substrate recognition by P-glycoprotein, *Eur. J. Biochem.* **1998**, *251*, 252–261.

169 Algoram, B., Woltosz, W. S., Bolger, M. B., Predicting the impact of physiological and biochemical processes on oral drug bioavailability, *Adv. Drug Del. Rev.* **2001**, *50*, S41–S67.

170 References in Table 5.1.

1. Jacobson, M. A., de Miranda, P., Cederberg, D. M., Burnette, T., Cobb, E., Brodie, H. R., Mills, J., Human pharmacokinetics and tolerance of oral ganciclovir, *Antimicrob. Agents Chemother.* **1987**, *25*, 247–252.
2. Spencer, H. K., Cody, R. J., Clinical pharmacokinetics of the angiotensin converting enzyme inhibitors, *Clin. Pharmacokinet.* **1985**, *10*, 377–399.
3. Palm, K., Stenberg, P., Luthman, K., Artursson, P., Polar molecular surface properties predict the intestinal absorption of drugs in humans, *Pharm. Res.* **1997**, *14*, 568–571.
4. Dressman, J. B., Amidon, G. L., Fleisher, D., Absorption potential: estimating the fraction absorbed, *J. Pharm. Sci.* **1985**, *74*, 588–589.
5. de Miranda, P., Blum, R., Pharmacokinetics of acyclovir after intravenous and oral administration, *J. Antimicrob. Ther.* **1983**, *12*, 29–37.
6. Welling, P. G., Barbhaiya, R. H., Patel, R. B., Forster, J. S., Shah, V. P., Thiazides X: lack of dose proportionality in plasma chlorothiazide levels following oral solution doses, *Curr. Ther. Res.* **1982**, *31*, 379–385.
7. Munkholm, P., Langholz, E., Hollander, D., Thornberg, K., Orholm, M., Katz, K. D., Binder, V., Intestinal permeability in patients with Crohn's disease and ulcerative colitis and their first degree relatives, *Gut* **1994**, *35*, 68–72.
8. Mason, W. D., Winer, N., Kochak, G., Cohen, I., Bell, R., Kinetics and absolute bioavailability of atenolol, *Clin. Pharmacol. Ther.* **1979**, *25*, 408–415.
9. Garg, D. C., Weidler, D. J., Eshelman, F. N., Ranitidine bioavailability and kinetics in normal male subjects, *Clin. Pharmacol. Ther.* **1983**, *33*, 445–452.
10. Hinderling, P. H., Hartman, D., Pharmacokinetics of digoxin and main metabolites/derivatives in healthy humans, *Ther. Drug Monit.* **1991**, *13*, 381–401.
11. Henderson, E. S., Adamson, R. H., Oliverio, V. T., The metabolic fate of tritiated methotrexate II. Absorption and excretion in man, *Cancer Res.* **1965**, *25*, 1018–1024.
12. Rakhit, A., Holford, N. H., Guentert, T. W., Maloney, K., Riegelman, S., Pharmacokinetics of quinidine and three of its metabolites in man, *J. Pharmacokinet. Biopharm.* **1984**, *12*, 1–21.

13. Eichelbaum, M., Ochs, H. R., Roberts, G., Somogyi, A., Pharmacokinetics and metabolism of antipyrine (phenazone) after intravenous and oral administration, *Drug Res.* **1982**, *32*, 575–578.
14. Blanchard, J., Sawers, S. J. A., The absolute bioavailability of caffeine in man, *Eur. J. Clin. Pharmacol.* **1983**, *24*, 93–98.
15. Regård, C. G., Borg, K. O., Johansson, R., Johansson, G., Pharmacokinetic studies on the selective β1-receptor antagonist metoprolol in man, *J. Pharmacokinet. Biopharm.* **1974**, *2*, 347–364.
16. Hardman, J. G., Limbird, L. E., Molinoff, P. B., Ruddon, R. W., Gilman, G. A., *Goodman & Gilman's the pharmacological basis of therapeutics.* 9th edition, McGraw-Hill, New York, **1996**.
17. Borgström, L., Johansson, C.-G., Larsson, H., Levander, R., Pharmacokinetics of propranolol, *J. Pharmacokinet. Biopharm.* **1981**, *9*, 419–429.
18. Shinohara, Y., Baba, S., Kasuya, Y., Absorption, metabolism, and excretion of oral testosterone in humans by mass fragmentography, *J. Clin. Endocrinol. Metab.* **1980**, *51*, 1459–1462.
19. Taburet, A. M., Schmit, B., Pharmacokinetic optimisation of asthma treatment, *Clin. Pharmacokinet.* **1994**, *26*, 396–418.
20. McTavish, D., Sorkin E. M., Verapamil: an updated review of its pharmacodynamic and pharmacokinetic properties, and therapeutic use in hypertension, *Drugs* **1989**, *38*, 19–76.

6
Use of Animals for the Determination of Absorption and Bioavailability

Chris Logan

Abbreviations

ADME/PK	Absorption, distribution, metabolism, and excretion/pharmacokinetics
AUC	Area under the plasma concentration–time curve
Caco-2	Adenocarcinoma cell line derived from human colon
DMPK	Drug metabolism and pharmacokinetics
GIT	Gastrointestinal tract
HPLC	High-pressure liquid chromatography
hpv	Hepatic portal vein
HTS	High-throughput screen
i.v.	Intravenous
i.t.	Intra-tracheal
MDCK	Madin–Darby canine kidney cells
PAMPA	Parallel artificial membrane permeation assay
P_{app}	Apparent permeability coefficient
PB/PK	Physiologically based pharmacokinetics
PK	Pharmacokinetics
p.o.	Oral (per os)

Symbols

$C_{min,ss}$	Minimum plasma concentration at steady state
fu	Fraction unbound in plasma
k	Elimination rate constant
log D	Logarithm of the distribution coefficient in octanol/water (usually at pH 7.4)
τ	(Tau) dosing interval
Vd	Volume of distribution

Drug Bioavailability: Estimation of Solubility, Permeability, Absorption and Bioavailability.
Edited by Han van de Waterbeemd, Hans Lennernäs and Per Artursson

ISBN: 3-527-30438-X

6.1 Introduction

This chapter will review some of the important methods for carrying out *in vivo* absorption and bioavailability studies, as well as attempt to provide an overview of how the information may be used in the drug discovery process. The chapter is aimed at medicinal chemists and thus will focus on the use of animals in discovery phase absorption, distribution, metabolism, and excretion/pharmacokinetic (ADME/PK) studies, rather than the design of studies that are for regulatory submission, or part of a development safety package.

6.1.1 ADME/PK in Drug Discovery

The need to carry out ADME/PK studies prior to the start of drug development has only recently become widely accepted. The very high failure rate of drug development has been well known for a long time, but the key publication of Prentis *et al.* in 1988 [1] highlighted that a significant proportion of the failures (39%) for the seven major UK pharmaceutical companies could be attributed to "inappropriate pharmacokinetics". In a more recent report [2], the failure rate attributed to the same cause was 25%. Whether this apparent improvement is due to the variability in the reporting system or a very rapid change due to the incorporation of DMPK into discovery is not clear. However, it is often very difficult to attribute a failure to a single cause; is the failure due to the toxicity of the compound or to poor PK, which leads to excessive exposures at the peak concentrations that are necessary to achieve the required pharmacological effect over the whole dosing period? Our own experience, like that of others [3], is that there are often several aspects that contribute to the decision not to progress a development project.

Nonetheless, it is now generally accepted that it is worthwhile "front-loading" projects with ADME/PK and toxicology information in order to improve the chances of compounds achieving registration and becoming "best in class" [4].

The incorporation of ADME/PK into the discovery process has required a complete re-evaluation of the approach to the science. Drug discovery can be seen as a cyclical process (Fig. 6.1), with chemists making compounds that are screened for biological activity. The biological data are fed back to the chemists who use it to improve the design of the next compounds, which are then used to initiate the next revolution of the cycle. The incorporation of ADME/PK into drug discovery means that there is now a second, often orthogonal, make/test cycle. For this cycle to be productive it is essential for it to operate at the same rate as the biological testing, otherwise the chemistry will have moved on, and the ADME/PK data will have been generated on compounds that are no longer of interest.

Of course, as the generation of biological information has moved towards high-throughput approaches, ADME/PK has also needed to aspire to similar expectations. This has led to significant automation and simplification of the ADME

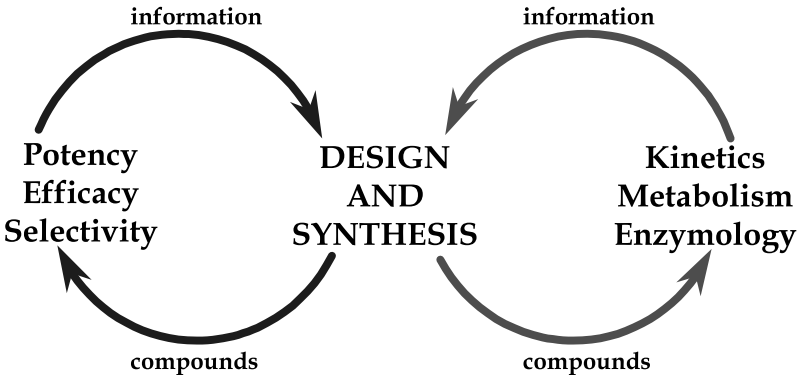

Fig. 6.1. Research optimization process.

screens, as will be seen elsewhere in this book. Even so, few projects have had ready access to truly high-throughput screening (HTS) ADME/PK, and so it is more usual for DMPK considerations to be taken on when projects are at the ''Hit to Lead'' stage, or later [4].

6.1.2 The Need for Prediction

As ADME/PK has become incorporated into drug discovery it has become necessary to reconsider the purpose of the studies. If the science is really going to reduce the attrition rate in development, then it is essential for the studies to allow predictions of the PK in man to be made. This means predicting the likely size and frequency of the dose. A review of the top 10 medicines of 1999 (Table 6.1) shows all of them to be once-a-day compounds. It is clear that to be ''best in class'', and to be able to maintain that position as follow-up compounds come along, it seems probable that a compound will need to be suitable for once a day dosing.

Although the pressure to screen large numbers of compounds quickly has led to the rapid development of *in silico* and *in vitro* assays, the sheer number and complexity of the processes involved in determining the disposition of any particular compound means that *in vivo* studies are still required to provide assurance that the important processes are modeled with sufficient accuracy [4–6], and indeed, that the potential contribution of processes for which there are no good *in vitro* models (e.g., biliary secretion) are adequately assessed.

Although prediction of ADME/PK in man may be the primary purpose for the pre-clinical studies, it is also important that potential new drugs have acceptable properties in toxicology species. Without these it can be very difficult to generate adequate safety margins to allow studies in man to start. It is also likely that the development safety assessment program will be difficult and hence slow.

Tab. 6.1. The top 10 best-selling drugs in 1999.

Product	*Indications*	*1999 sales [$billion]*	*%Global Sales*	*Launched*	*Dosing regime*
Losec (omeprazole)	Duodenal ulcer Gastro-oesophageal reflux *Helicobacter* infections	5.7	1.9	1989 – UK and US	Once daily, except when used as part of combination therapy
Zocor (Simvastatin)	Hypercholesterolemia Hyperlipoproteinemia Hypertriglyceridemia	3.9	1.3	1989 – UK 1991 – US	Once daily
Lipitor (Atorvastatin)	Atherosclerosis Dyslipidemia Hypercholesterolemia	3.8	1.3	1997 – UK and US	Once daily
Norvasc (Amlodipine Besilate)	Hypertension	3.0	1.0	1990 – UK 1992 – US	Once daily
Prozac (Fluoxetine)	Depression Obsessive-compulsive disorders Panic Post-traumatic stress disorder	2.9	1.0	1988 – US 1989 – UK	Once daily
Ogasrtro (Lansoprazole)	Duodenal ulcer Gastro-oesophageal reflux *Helicobacter* infections	2.3	0.8	1994 – UK 1995 – US	Once daily, except when used as part of combination therapy for *H. pylori* and for hypersectetory conditions. Twice-daily when dose $\geq$120 mg.
Seroxat (Paroxetine)	Depression Obsessive-compulsive disorders Panic Post-traumatic stress disorder	2.1	0.7	1991 – UK 1993 – US	Once daily
Zoloft (Sertraline)	Depression Obsessive-compulsive disorders Panic Post traumatic stress disorder	2.0	0.7	1996 – EU and US	Once daily
Claritin (Loratadine)	Allergy Rhinitis	2.0	0.7	1989 – UK 1993 – US	Once daily
Zyprexa (Olanzapine)	Bipolar disorders Gilles de la Tourette's syndrome Psychotic disorders	1.9	0.6	1996 – UK and US	Once daily

Data from Scrip 2001 Yearbook, 17th edition, Table 2.7 p. 69. Sales of top 10 products worldwide 1999.

6.2
Consideration of Absorption and Bioavailability

There are two methods of dosing that are of primary interest to medicinal chemists: the oral and intravenous routes. Oral is important because it is generally the most convenient method of administration for patients, and the one most likely to result in high patient compliance. Again, this is confirmed by inspection of Table 6.1, showing the best-selling drugs in 1999. All of the top 10 compounds are for oral administration. Thus, oral administration is likely to be the desired route for any compound to be developed. However, intravenous dosing is also important because it allows determination of both rate of clearance and volume of distribution. These two are the primary parameters that determine the half-life. Clearance can be modulated in a series of compounds by altering rates of metabolism, whilst altering partition properties may change volume. Thus, it is important for medicinal chemists to know how these two parameters vary within their chemical series in order to be able to optimize the chemistry.

The important stages in delivering a drug to its desired target after an oral dose can be summarized as shown in Fig. 6.2. Initially the formulation has to be swallowed and survive the transition to the site of absorption – the gastrointestinal tract (GIT). The time required for this to happen will depend on the stomach emptying time, which in turn will be a function of the fed/fasted state of the subject or animal that is being studied (see for example Ref. [7]). This kind of information can only be obtained from *in vivo* studies.

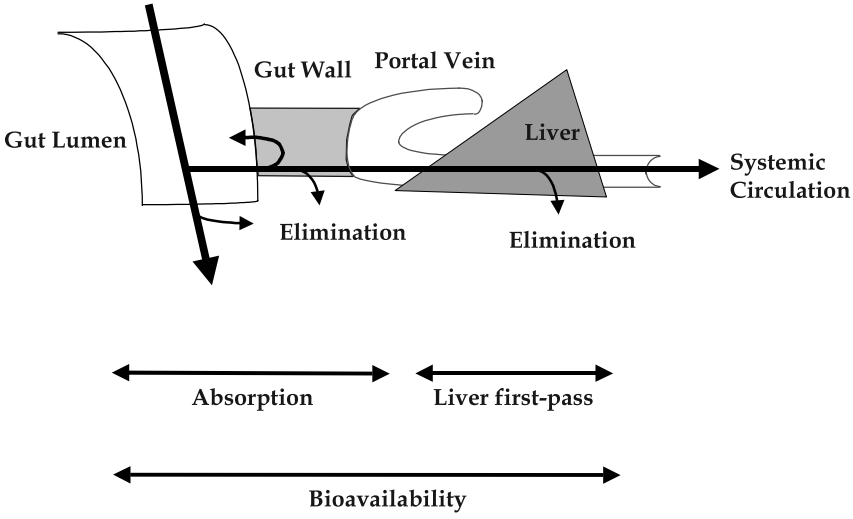

Fig. 6.2. Absorption and bioavailability.

Once in the GIT, when the drug has been released from the formulation into solution, the process of absorption may begin. In this phase the compound has to pass across the wall of the GIT. This can be either by passive diffusion, which is commonly thought to be the most predominant route for the majority of drugs with molecular weights below 1000 Daltons, or it can be by paracellular absorption, or by active uptake. The paracellular route avoids passing through the cells, and instead the drug gains access to the portal blood by either passing through the tight junctions between the cells or through the nonrestrictive junctions. This method of absorption can be important for compounds of a smaller size (and hence lower molecular weight), and higher polarity than the norm. Active uptake mechanisms are most common for naturally occurring compounds such as sugars, amino acids and di- and tri-peptides.

The compound in the portal blood is transported to the liver, which usually is the major site of metabolism for pharmaceuticals. In the liver there is usually one, or more, of three principal fates for the drug: either metabolism; excretion into the bile; or return to the blood for distribution to the other tissues of the body. These other tissues may also be sites of metabolism or, particularly in the case of the kidney, sites of excretion.

There is often confusion as to the meaning of absorption, as opposed to bioavailability. For the purposes of this chapter, absorption will be taken to mean the processes that are involved in transferring the drug in solution from the site of administration to the venous blood. In the case of oral absorption this will be to the hepatic portal vein (see Fig. 6.2). Bioavailability is the ratio of the AUC after administration by the route of interest, and after administration of the same amount of drug direct into the systemic circulation, usually by intravenous injection. Thus bioavailability, after oral dosing, differs from absorption by also including the effects due to such processes as metabolism and/or biliary secretion during the first pass of the compound through the liver.

Bioavailability is an important parameter in drug screening cascades. It gives a good indication of the efficiency of the delivery of the compound to the systemic circulation by the chosen route. It can only be measured *in vivo* but, as will be described below, it can be predicted for man using a number of methods.

Measurement of absorption can be complicated by efflux mechanisms. It is clear that many compounds are actively transported back into the GIT, into the bile or into the urine by efflux proteins. In the case of those in the GIT these may have an impact on the apparent absorption of a compound. Some understanding of the substrate specificity for one of these proteins, P-glycoprotein, is becoming apparent [8, 9], but currently the understanding is limited. At the moment there are no published reliable methods either *in vivo* or *in vitro* for predicting the importance of efflux mechanisms for a particular compound in man [10–12].

Absorption studies can be carried out using a variety of dosing routes, and although this chapter will focus on oral dosing, analogous stages can be envisioned after other methods of dosing.

6.3 Choice of Animal Species

The main pre-clinical species used for pharmacokinetic studies are the rat, mouse and dog. An examination of the Biosys database for 2000 and 2001 shows that of the abstracted papers, 6334 mapped to the subject heading "Pharmacokinetics". Of these, the vast majority (70%) were studies on humans. Studies on rats constituted 14% of the reports, mice 7.5% and dogs 3.4% (Table 6.2). Nonhuman primates can also be important pharmacokinetic models, but ethical and practical considerations severely limit studies in these animals such that, within the same period, they represented less than 0.5% of the abstracted reports on PK.

The initial choice of the rat as the primary species for pharmacokinetic studies arose because of their use in pharmacology and toxicology studies. However, there is now such a large database of information about the relative pharmacokinetics of the same compounds in rats and man that, as described below, useful predictions to man can be made.

The importance of the mouse as a species for pharmacokinetics will probably increase as genetically modified mice become more important in producing humanized models for *in vivo* pharmacology. The mouse presents a particular challenge to pharmacokineticists, because of the very small volumes of blood that can be obtained, and the difficulties this presents for bioanalysis. However, there are now published methods for obtaining repetitive samples from mice [13], and this means that, provided a statistically appropriate experimental design is used (essentially a Latin Square – see Ref. [14]) the numbers of animals used in a study can be limited. This same approach can be used for studies in larger animals when

Tab. 6.2. Numbers of pharmacokinetic studies by animal. Numbers of papers abstracted into Biosys Previews and mapping to the Subject Heading Pharmacokinetics.

Species	*Total no. of studies**	*Percentage**
All species	6334	100
Human	4411	69.6
Rat	862	13.6
Mouse	478	7.5
Dog	215	3.4
Rabbit	199	3.1
Guinea pig	38	0.6
Hamster	23	0.4
Non-human primate	21	0.3[+]

* Numbers given against individual species sum to more than the total given for all studies as some studies included more than one species.

[+] Many primate studies are on human antibodies that cannot be tested with other species due to problems of antigenicity.

the analytical method requires plasma samples that are so large that a complete PK profile cannot be determined in a single animal.

6.4 Methods

There are a number of important methods that are worthy of discussion before consideration of how the data are used to predict human ADME/PK.

6.4.1 Radiolabels

An approach that can be used in determining ADME/PK parameters that is simple to execute and gives confidence that the whole dose is accounted for, is to use a radiolabel. This has been the standard approach for development ADME studies for many years. The common isotopes used are ^{14}C or ^{3}H (tritium).

Of course, it is important to ensure that the site of labeling is chosen carefully so that it is not readily lost by metabolism. For example, CH_3–N and CH_3–O groups, although perhaps amenable to simple synthetic approaches, are often major sites of metabolism, and could lead to significant portions of the dose being converted to $^{14}CO_2$ or $^{3}H_2O$. Even though it is possible to trap and count the exhaled gas, from a practical point of view these kinds of labels poor choices.

The incorporation of ^{14}C into compounds at a suitable site often requires extensive and complicated syntheses, and thus a relatively long time. This usually means that ^{14}C-labeled compounds are unsuitable for studies to be carried out during discovery. There are however, very rapid methods for incorporating ^{3}H into compounds. The newer methods, generally involving metal-catalyzed exchange reactions [15–18], in our experience, mean that suitable labels can often be prepared in 2 or 3 weeks. These time scales make the approach viable for discovery support. Additionally, and importantly, these methods can lead to *specific* incorporation of tritium.

There is a general prejudice among drug metabolism scientists against using tritiated compounds. This is because such labels have often given rise to the formation of $^{3}H_2O$. Tritiated water has a remarkably long half-life in the body of between 6 and 9 days [19–22], and this is probably much longer than the half-life of the compound of interest, or its metabolites. In any studies, significant production of $^{3}H_2O$ is an unwanted complication. However, we have found that *specifically* labeled compounds often lose only small amounts of radioactivity as $^{3}H_2O$, and most of this can be readily removed by freeze-drying the samples. Hence, it is usually possible to gain comprehensive information about the fate of the bulk of the dose. We have often found the use of a ^{3}H-labeled compound has significantly improved our knowledge of a compound, and hence its chemical series, and given clear information on the major pathways of clearance, or extent of absorption. This then allows the data from *in vitro* screens to be used with greater confidence.

6.4.2 *Ex vivo* Methods for Absorption

6.4.2.1 Static Method

There are several approaches to estimating absorption using *in vitro* methods, notably Caco-2 and MDCK cell-based methods or using methods that assess passive permeability, for example the parallel artificial membrane permeation assay (PAMPA) method. These are reviewed elsewhere in this book. The assays are very useful, and usually have an important role in the screening cascades for drug discovery projects. However, as discussed below, the cell-based assays are not without their drawbacks, and it is often appropriate to use *ex vivo* and/or *in vivo* absorption assays.

The simplest *ex vivo* assay consists of isolating segments of the GIT in an anesthetized rat, whilst leaving the blood and nervous supply intact as far as possible [23]. Hence, the segments continue to receive a blood supply, and any absorbed compound is carried away. The compound of interest is injected into segments, and at the end of the study the isolated segments are collected, and analyzed for remaining compound. Absorption is estimated by loss. By injecting the compound into different segments at different times, a time course for the loss may be established. The approach has the advantage of simplicity, but suffers from the need to obtain good recoveries from what is often a difficult matrix to analyze. For poorly absorbed compounds – often the ones where reliable estimation of absorption is wanted – the method suffers from needing to determine accurately small differences from 100%.

6.4.2.2 Perfusion Methods

Because of these problems, perfusion assays have been developed. Success in predicting absorption in man using in-situ single-pass perfusion of the rat intestine has been reported [24–26]. In this model the animal is anesthetized, and a segment of the gut is exposed and cannulated. A formulation of the drug is perfused through the gut segment and the concentration before and after perfusion is determined. This approach has the advantage of being able to make several estimations of the concentration of the perfusate, and of allowing measurements to be made from a cleaner matrix.

For a series of renin inhibitors a good correlation between the measured membrane permeability and log D was found ($r^2 = 0.8$). The model has been validated against a human perfusion model [10], as well as being extended by including molecular weight as a third parameter [27]. A further development of the model is to chronically cannulate the animals so that they can be allowed to recover [28]. This model should avoid any effects from the anesthetic on the absorption process.

Using the single-pass in-situ absorption model in the anesthetized rat, a study of nine compounds found a good correlation between rat and man as to whether compounds were subject to active up-take or absorbed by simple passive diffusion [29].

However, because of the significant surgical alterations that are necessary, studies using isolated perfused gut loops do not always accurately predict the

results in whole animals, and there can be significant advantages in whole animal models for absorption.

6.4.3 *In vivo* Methods

There are several possible *in vivo* approaches to the determination of the absorption of a compound after oral dosing. Probably the simplest and most direct is to use a radiolabel. For the vast majority of studies, this means either a ^{14}C or ^{3}H label. The approach used can be quite simple: the labeled version of the drug is administered to an animal that is then housed in a ''metabolism cage'' for the separate, and complete, collection of both urine and feces. The samples of excreta are collected for as long as is necessary to obtain a full recovery of radioactivity. They are then analyzed for radioactive content. At its simplest, it can usually be assumed that, after an oral dose, at least all of the radioactivity that appears in the urine must have been absorbed, thus giving an assessment of the minimum absorption of the compound. Collecting the feces and subjecting them to chromatographic analysis with radiodetection can refine the study. This allows the identification of the proportion of the dose that has been absorbed but then excreted in the bile as metabolites (as opposed to the dose that has not been absorbed and has passed straight through the GIT as the parent compound). This approach should be supported with further studies to ensure that the parent compound is not metabolized directly in the GIT by the microflora. However, it is possible to be misled if the parent compound is absorbed but excreted unchanged in the bile.

Another refinement, that avoids the necessity of developing suitable fecal extraction and chromatographic methods, is to dose the radiolabeled compound by both the i.v. and p.o. routes in two separate studies. Knowing that, by definition, the whole of the i.v. dose must have been bioavailable, a comparison of the proportion of the dose in the urine after the two different routes allows estimation of the percent absorbed. An analogous approach can be used without the use of a radiolabel, when the urine from the two studies is analyzed either for the parent compound or, more usually, for a major common metabolite. Assuming quantitatively identical clearance after both the i.v. and p.o. doses, the ratio of the amounts of analyte in the two experiments gives the absorption.

6.5 *In vivo* Methods for Determining Bioavailability

6.5.1 Cassette Dosing

Cassette dosing or ''N into 1'' dosing was one of the first techniques used to enhance the throughput of ADME/PK studies. It has the advantage of reducing the number of animals used, and increasing the number of compounds that can be

tested in a set time. This method involves dosing each animal with several compounds at the same time [30]. The selectivity and sensitivity of analytical methods now available, usually HPLC/mass spectrometry [31], mean that it is possible to analyze for each of the compounds in the presence of others [32, 33]. Although reports on cassettes of up to 22 compounds have been made [34], it is more usual to limit the number to between three and six. There are significant benefits to this approach, as animals are only dosed once and the same number of plasma samples is collected as would be for a single compound study. However, the dose levels must be limited in order to minimize possible stress to the animals and possible compound–compound interactions.

The potential for the metabolites that are formed to have the same masses as other parent compounds is another factor that limits the number of compounds that may be included in the cassette, as does the potential for drug–drug interactions [35]. Other limitations are the total dose that can be administered without saturating important pathways of metabolism or distribution, and the solubility of the compounds in the dosing formulation. However, there is a balance to be achieved as, if the dose of each component given is very low, it is likely that the analytical method will not have sufficient sensitivity to provide an accurate assessment of the pharmacokinetics.

Nonetheless the approach can provide – both routinely and rapidly – large amounts of pharmacokinetic or other distribution information on several compounds without significantly increasing the burden on the animals, whilst also minimizing the number of animals used. It is common to include a compound of known pharmacokinetics that acts as a control in each of these studies. This can help in identifying when the co-administered compounds have changed the kinetics. However, such marker compounds will not necessarily highlight problems with compounds that are subject to different clearance mechanisms [35].

6.5.2 Semi-simultaneous Dosing

An approach that can bring benefits by reducing variability and increasing the speed of generating results is to use ''semi-simultaneous dosing'' pharmacokinetic studies [36]. In these studies, animals are dosed by the two different routes of interest, a short period apart, often 4–6 hours, and usually less than 48 hours. Blood samples are collected in the usual way following the dosing, and analyzed for the parent compound. The pharmacokinetic profiles are then constructed, subtracting out, if necessary, any part of the profile from the first dose that is still present during the profile from the second dose [37]. These studies allow both profiles to be determined in the same animals at essentially the same time (''semi-simultaneous''). This has the advantage of reducing variability in the pharmacokinetic profiles from the two doses, and allowing a more reliable comparison of the two profiles. To ensure that there is not a significant increase in the number of samples that are taken to determine the two profiles, the samples can be withdrawn through an indwelling catheter, or the total number of venepunctures

restricted to the same number that would be used for single-dosing studies. The total amount of blood taken need not be significantly greater than is taken in a normal pharmacokinetic study, and so there is little increase in the stress on the animals. These studies have the advantage of eliminating a second procedure for the animals, whilst retaining the advantage of a crossover design with little chance for significant alteration in the factors that control the pharmacokinetics between the two doses. The approach also generates information more rapidly than when there is a ''wash-out'' period between the two doses.

The original proposal of the approach, supported by a Monte Carlo simulation study [36], has been further validated with both pre-clinical [38, 39] and clinical studies [40]. It has been shown to be robust and accurate, and is not highly dependent on the models used to fit the data. The method can give poor estimates of absorption or bioavailability in two sets of circumstances: (i) when the compound shows nonlinear pharmacokinetics, which may happen when the plasma protein binding is nonlinear, or when the compound has cardiovascular activity that changes blood flow in a concentration-dependent manner; or (ii) when the rate of absorption is slow, and hence 'flip-flop' kinetics are observed, i.e., when the apparent terminal half-life is governed by the rate of drug input.

6.5.3
Hepatic Portal Vein Cannulation

The use of hepatic portal vein-cannulated animals can be helpful in determining specific causes of poor bioavailability. After oral dosing, the total bioavailability of a compound is normally calculated as:

$$\text{Bioavailability} = \frac{\text{AUC}_{\text{po}}}{\text{AUC}_{\text{iv}}} \times \frac{\text{Dose}_{\text{iv}}}{\text{Dose}_{\text{po}}} \tag{1}$$

where AUC is the area under the drug concentration–time curve to infinite time and po and iv indicate oral or intravenous routes. The oral bioavailability can also be considered from the perspective of loss at different stages of the process of reaching the systemic circulation, i.e.,

$$F_{\text{oral}} = (1 - f_G)(1 - f_H)(1 - f_{\text{abs}}) \tag{2}$$

where f_{abs} is the fraction not absorbed from the GIT, and f_G and f_H are the fractions of drug cleared (e.g., metabolized) in the gut wall and the liver, respectively. It is possible to measure the relative contributions of these processes by carrying out dosing and or sampling of the hepatic portal vein [41] in addition to the normal methods of p.o. and i.v. dosing coupled with i.v. sampling. Thus,

$$f_G = 1 - \text{AUC}_{\text{po}}/\text{AUC}_{\text{hpv}} \tag{3}$$

and

$$f_H = 1 - AUC_{hpv}/AUC_{iv} \quad (4)$$

These multiple input experiments can be carried out in a crossover fashion.

6.6 Inhalation

There are many ways of administering compounds to man or pre-clinical safety species, and it is not possible to review them all within the scope of this chapter. However, the inhalation route is worthy of some consideration as it can be important. This is usually when the target organ is the lung, in diseases such as asthma or chronic obstructive pulmonary disorder (COPD), or when the lung may be a suitable route of administration for the systemic delivery of macromolecular peptide or protein biopharmaceuticals – compounds that would neither survive passage through, nor be absorbed from, the GIT [42, 43]. The absorption of these molecules is thought to occur by diffusion in the conducting airways [44] and by diffusion and transcytosis in the alveolar region of the lungs [42]. Even with the lower metabolic activity in the lung [45], direct administration can be a useful way of delivering compounds to their site of action, whilst limiting systemic side effects.

However, it is rarely possible to carry out inhalation studies during the research phase. Compared with intra-tracheal (i.t.) dosing, inhalation dosing is perhaps physiologically more similar to the clinical dosing method, is noninvasive, results in lower dose rates, and may well provide more even and representative distribution within the lungs. Nonetheless, i.t. instillation is often a worthwhile alternative as it allows accurately quantified doses to be administered, and does not require the complex dosing systems needed in inhalation studies. Inhalation dosing invariably leads to significant oral exposure, either due to direct ingestion of the aerosol or by the animal grooming particles from its pelt after dosing has finished (see Ref. [46] and references cited therein). Although i.t. administration has been shown to produce a very nonuniform distribution within the lungs, it has also been possible to obtain remarkably consistent, dose-proportional absorption over a wide range of doses (up to two and four orders of magnitude) [47], suggesting that absorption from the lung will not necessarily be saturated. Compounds given by the i.t. route can give rise to pharmacokinetics that closely mimic those of an i.v. dose [48, 49] with apparently very rapid and extensive absorption. However, i.t. dosing can also give indications of differing rates of absorption from the lung, depending on the compound and its physico-chemical properties [45, 47, 50] or formulation [51, 52]. It has been reported that for a series of drugs the absorption after aerosol administration was approximately twice as fast as through i.t. dosing [53], suggesting that absorption from the deeper alveolar region may be more rapid than from the tracheobronchial region of the lung.

Although the usual animal model for i.t. studies is the rat [45, 47, 48, 54], studies on dogs [50, 54], rabbits [49] and guinea pigs [55] have also been reported.

A detailed review of i.t. dosing has recently been published [46], which provides practical details of the technique.

6.7 Relevance of Animal Models

6.7.1 Models for Prediction of Absorption

Measurement of the fraction absorbed, as described elsewhere in this book, can be carried out using *in vitro* systems. However, for Caco-2 cells for example, the relationship between the apparent rate of permeability that is measured and the percentage of the dose absorbed in man is often very steep. Thus, small changes in the measured rate of permeation result in a compound going from being predicted to have low human absorption to having good absorption [6, 56]. Other model systems, such as those based on the use of gut tissue in Ussing chambers, are highly dependent on the supply of good quality tissue. Because of these kinds of issues, *in vivo* models can have significant advantages over the *in vitro* systems. Although the rate of absorption can be highly variable, the extent has often been shown to be similar between species including man (see for example Ref. [57] and references cited therein), the similarity has recently been analyzed and the correlation between percentage dose absorbed in rat and man shown to be reliable and quantitative [58]. The relationship was analyzed for a group of 64 drugs, which covered a wide range of physical properties (acids, bases, neutrals and zwitterions) and molecular weights (138–1202 Da). Also included were compounds for which absorption may involve carrier-mediated mechanisms. Excluded were compounds thought to be unstable in the GIT, or which are affected by particle size or are polymorphic. The ratio between percent absorbed in human and rat was found to be very close to 1, with a correlation coefficient of 0.97.

The other principal pre-clinical PK model – the dog – is not thought to be such a useful model for prediction of absorption in man, because of larger pore size and greater pore frequency in the paracellular pathway of dog compared with rat [59].

6.7.2 Models for Prediction of Volume

Estimation of the volume of distribution in man may be carried out in a number of ways. These methods have recently been reviewed by Obach *et al.* [60], who carried out a wide-ranging evaluation of a large number of different ways of predicting the human pharmacokinetics of 50 compounds that entered development at Pfizer. One of the simplest methods was reported to be the most reliable. It is based on the assumption that the free-fraction of drug in the plasma in dog and human and

the volume of distribution are proportional, i.e., free $Vd_{(human)}$ = free $Vd_{(dog)}$. This allows a prediction for Vd in man to be generated:

$$Vd_{(predicted\ in\ man)} = fu_{(man)} \times Vd_{(dog)}/fu_{(dog)} \quad (5)$$

Both human and dog volumes are in units of L kg^{-1}, and fu is the fraction of the drug unbound in plasma. The method was found to predict within 2-fold for about 80% of the compounds, which spanned about three orders of magnitude in their Vd. Although the dog has been recommended as the best model for predicting volume in man [60], there are also reports indicating that the rat may also be a suitable model [61].

6.8 Prediction of Dose in Man

6.8.1 Allometry

One of the most frequently used methods for predicting human pharmacokinetics from animal data is allometry. This technique was initially used to explain the relationship between body size and organ weights in animals [62–67]. The approach is based on finding a correlation between a physiological and the pharmacokinetic parameter of interest. Generally the relationship takes the form of:

$$y = a \times B^x \quad (6)$$

where y is the dependent variable, e.g., clearance; B is the independent variable, e.g., body weight, brain size or maximum life span; and a and x are the allometric coefficient and exponent, respectively.

The allometric coefficient and exponent are determined empirically, and are not thought to have any physiological correlate.

The drawback of this approach is that it is essentially empirical, and does not allow for differences in metabolic clearance between the species, i.e., it assumes that clearance is proportional to blood flow. This works well for compounds that are highly extracted in the liver, and/or where passive renal clearance is the major pathway [5, 68]. An approach for compounds that are actively secreted into the urine has also been proposed [69], although the precise values of some of the physiological scaling factors have been questioned [70].

Unfortunately, when clearance is largely metabolic and low, allometry can significantly over-predict the human value [71]. Recent investigations have attempted to address this by combining allometric approaches with *in vitro* metabolism data [5].

A recent debate on allometric scaling has suggested that a great deal of further work is necessary before allometry can be used with confidence in a prospective

manner. It is claimed that it is not possible to know in advance when allometry will not be suitable, and indeed the accuracy of the predictions may not be as reliable as assumed [72–74].

6.8.2 Physiologically Based Pharmacokinetics

Another method of predicting human pharmacokinetics is physiologically based pharmacokinetics (PB-PK). The normal pharmacokinetic approach is to try to fit the plasma concentration–time curve to a mathematical function with one, two or three compartments, which are really mathematical constructs necessary for curve fitting, and do not necessarily have any physiological correlates. In PB-PK, the model consists of a series of compartments that are taken to actually represent different tissues [75–77] (Fig. 6.3). In order to build the model it is necessary to know the size and perfusion rate of each tissue, the "partition coefficient" of the compound between each tissue and blood, and the rate of clearance of the compound in each tissue. Although different sources of errors in the models have been

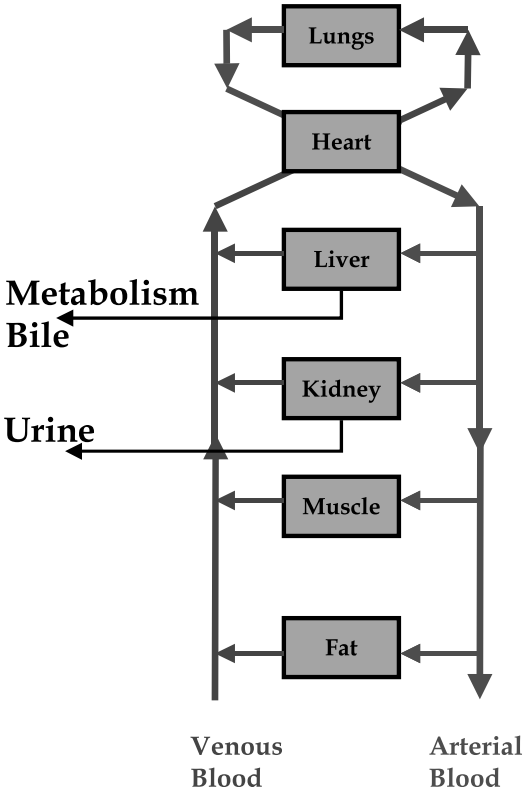

Fig. 6.3. Physiological pharmacokinetic model.

described [78–80], these kinds of models are extremely appealing to kineticists, because they should lead to a fuller understanding of the factors that determine the pharmacokinetics of any compound. However, they require many experimental determinations to be made for each compound, and thus they are unlikely to become the method of choice during the routine design, make/test cycle (see Fig. 6.1). They may however, become an important contributor to the decision about the suitability of a compound to progress into development.

6.8.3 Prediction of Human Dose

As stated in the Section 6.1, one of the principal purposes of carrying out DMPK studies during the discovery phase is to reduce the failure rate during development. For DMPK this logically means predicting the pharmacokinetics that will be observed and hence the dose that will be required in man when clinical studies are carried out.

It is possible to predict the steady-state minimum plasma concentration (Fig. 6.4) using the equation:

$$C_{min,ss} = \frac{fa.Dose}{V(e^{kt} - 1)} \tag{7}$$

where:

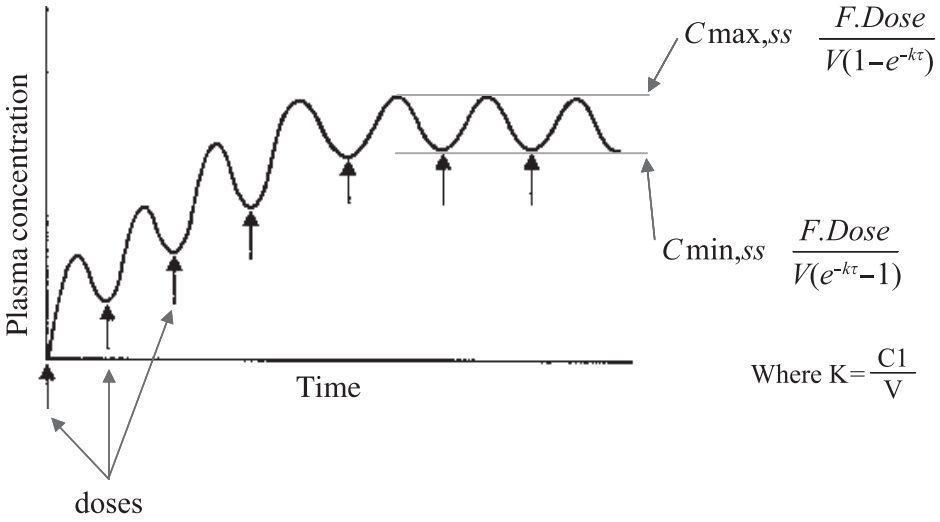

Fig. 6.4. Dose prediction.

$C_{min,ss}$ is the minimum plasma concentration at steady state;
f_a is the fraction absorbed in man;
Dose is the dose (in mg kg^{-1});
V is the volume of distribution at steady state (in L kg^{-1});
k is the elimination constant (this is given by clearance divided by volume);

and

τ is the dosing interval given in $hours^{-1}$.

The equation is an approximation, adapted from that for intravenous dosing [81], corrected by addition of a term for absorption. Essentially it assumes instantaneous absorption of the dose, but for compounds with reasonable physico-chemical and PK properties that are expected to be suitable for once-a-day dosing, this approximation makes little difference to the predicted value of $C_{min,ss}$. Use of the relationship can provide a simple approach for estimating the required dose in man for a compound in the discovery phase.

Equation (7) can be re-arranged to allow the prediction of the dose and dose interval, provided that the following can be estimated: human potency, absorption, clearance, and volume.

Estimation of the potency can be made in a several ways and will be highly dependent on the nature of the target. If a purified system is used it is normal to correct for the effect of plasma protein binding (which can be measured directly in human plasma) as it is usual for the effect to be proportional to the unbound concentration [82]. This can be used to set a value for the minimum plasma concentration at steady state.

As described above, it will be normal to assume that the dose interval is 24 hours, i.e., once-a-day dosing. Absorption can be estimated with good confidence from absorption in the rat (see Section 6.1). Clearance is the sum of the predicted hepatic, renal, biliary and extrahepatic clearance. Hepatic clearance can be derived from *in vitro* studies with the appropriate human system, using either microsomes or hepatocytes. We prefer to use an approach based on that described by Houston and Carlile [83]. Renal clearance can be predicted allometrically (see section 6.8.1). The other two potential methods of clearance are difficult to predict. To minimize the risks, animal studies can be used to select compounds that show little or no potential for clearance by these routes. As volume can be predicted from that measured in the dog, after correction for human and dog plasma protein binding (see Section 6.2), it is possible to make predictions for all of the important parameters necessary.

We believe that this approach brings together the best combination of *in vitro* to *in vivo* and allometric approaches, and can provide useful estimates of likely human doses, provided that sufficient attention is paid to the errors associated with all of the measurements [4].

6.9 Conclusion

The purpose of this chapter has been to illustrate the potential role of animal studies in ADME/PK in drug discovery. Given that one of the major objectives for ADME/PK is to predict PK in man, it must be concluded that much work is still to be done in the development of reliable and accurate models. Although, quite rightly, many studies have focused on *in silico* and *in vitro* approaches, there is still a general agreement that, with current knowledge, we are still highly dependent on animal models [3, 5, 6, 84]. Indeed, their use in predicting important parameters such as absorption and volume of distribution has been highlighted in this chapter.

References

1 Prentis, R. A., *et al.* Pharmaceutical innovation by the seven UK-owned pharmaceutical companies (1964–1985), *Br. J. Clin. Pharmacol.* **1988**, *25*, 387–396.

2 McAuslane, N., 'Accelerating pre-clinical development by successful integration into drug discovery'. Vision in Business, Conference 25–26 February, **1999**, Nice, France.

3 Eddershaw, P. J., Beresford, A. P., Bayliss, M. K., ADME/PK as part of a rational approach to drug discovery, *Drug Discov. Today* **2000**, *5*, 409–414.

4 Davis, A. M., Dixon, J., Logan, C. J., Payling, D. W., Accelerating the process of drug discovery, in: *Pharmacokinetic Challenges in Drug Discovery*. Pelkonen, O., Baumann, A., Reichel, A. (eds), Springer, Berlin **2002**, pp. 1–32.

5 Lavé, T., Coassolo, P., Reigner, B., Prediction of hepatic metabolic clearance based on interspecies allometric scaling techniques and *in vitro-in vivo* correlations, *Clin. Pharmacokinet.* **1999**, *36*, 211–321 and references cited therein.

6 van de Waterbeemd, H., Smith, D. A., Beaumont, K., Walker, D. A., Property based design: optimisation of drug absorption and pharmacokinetics, *J. Med. Chem.* **2001**, *44*, 1313–1333.

7 Davis, S. S., Hardy, J. G., Fara, J. W., Transit of pharmaceutical dosage forms through the small intestine, *Gut* **1986**, *27*, 886–892.

8 Seelig, A., How does P-glycoprotein recognise its substrates? *Int. J. Clin. Pharmacol. Ther.* **1998**, *36*, 50–54.

9 Seelig, A., Landwojtowicz, E., Structure-activity relationship of P-glycoprotein substrates and modifiers, *Eur. J. Pharm. Sci.* **2000**, *12*, 31–40.

10 Fagerholm, U., Johansson, M., Lennernäs, H., Comparison between permeability coefficients in rats and human jejunum, *Pharm. Res.* **1996**, *13*, 1336–1341.

11 Schwarz, U. I., Gramatté, T., Krappweis, J., Berndt, A., Oertel, R., von Richter, O., Kirch, W., Unexpected effect of verapamil on oral bioavailability of the beta-blocker talinolol in humans, *Clin. Pharmacol. Ther.* **1999**, *65*, 283–290.

12 Sandersträm, R., Knutson, L., Knutson, T., Jannson, B., Lennernäs, H., The effect of ketoconazole on jejunal permeability and CYP 3A4 metabolism of *R*/*S* verapamil in humans, *Br. J. Clin. Pharmacol.* **1999**, *48*, 180–189.

13 Hem, A., Smith, A. J., Solberg, P., Saphenous vein puncture for blood sampling of the mouse, rat, hamster, gerbil, guinea-pig, ferret and mink, *Lab. Animals* **1998**, *32*, 364–368. and http://www.uib.no/vivariet

14 Cochran, W. G., Cox, G. M., in *Experimental Designs*, 2nd edition, John Wiley and Sons, Inc. **1964**.

15 Kingston, L. P., Lockley, W. J. S., Mather, A. N., Spink, E., Thompson,

S. P., Wilkinson, D. J., Parallel chemistry investigations of ortho-directed hydrogen isotope exchange between substituted aromatics and isotopic water: novel catalysis by cyclooctadienyliridium(I)pentan-1,3-dionates, *Tetrahedron Lett.* **2000**, *41*, 2705–2708.

16 Kingston, L. P., Lockley, W. J. S., Mather, A. N., Spink, E., Thompson, S. P., Wilkinson, D. J., Hydrogen isotope labelling: novel applications of parallel chemistry techniques, International Isotope Society Symposium, Dresden, June **2000**.

17 Shu, A. Y. L., Saunders, D., Levinson, S. H., Landvatter, S. W., Mahoney, A., Senderoff, S. G., Mack, J. F., Heys, J. R., Direct tritium labelling of multifunctional compounds using organoiridium catalysis 2, *J. Label. Comp. Radiopharm.* **1999**, *42*, 797–807.

18 Chen, W., Garnes, K. T., Levinson, S. H., Saunders, D., Senderoff, S. G., Shu, A. Y. L., Villani, A. J., Heys, J. R., Direct tritium labelling of multifunctional compounds using organoiridium catalysis, *J. Label. Comp. Radiopharm.* **1997**, *39*, 291–298.

19 Trivedi, A., Galeriu, D., Richardson, R. B., Dose contribution from metabolized organically bound tritium after acute tritiated water intakes in humans, *Health Physics* **1997**, *73*, 579–586.

20 Foy, J. M., Schnieden, H., Estimation of total body water (virtual tritium space) in the rat, cat, rabbit, guinea-pig, and man, and of the biological half-life of tritium in man, *J. Physiol.* **1960**, *154*, 169–176.

21 Wylie, K. F., Bigler, W. A., Grove, G. R., Biological half-life of tritium, *Health Physics* **1963**, *9*, 911–914.

22 Cawley, C. N., Spitzberg, D. B., Cale, W. G., Jr., Fenyves, E. J., A model to estimate the biological half-life of tritium in man, *Proc. Summer Comput. Simul. Conf.* **1978**, 629–635.

23 Doluisio, J. T., Billups, N. F., Dillert, L. W., Sugita, E. T., Swintosky, J. V., Drug absorption I: an *in situ* rat gut technique yielding realistic absorption techniques, *J. Pharm. Sci.* **1969**, *58*, 1196–1200.

24 Amidon, G. L., Lennernäs, H., Shah, V. P., Crison, J., A theoretical basis for a biopharmaceutical drug classification: the correlation of *in vitro* drug product dissolution and *in vivo* bioavailability, *Pharm Res.* **1995**, *12*, 413–420.

25 Steffansen, B., Lepist, E.-I., Frökjaer, S., Taub, M., Lennernäs, H., Stability, metabolism and transport of D-ASP(OBZL) – a model prodrug with affinity for the oligopeptide transporter, *Eur. J. Pharm. Sci.* **1999**, *8*, 67–73.

26 Abrahamsson, B., Alpsten, M., Hugosson, M., Jonsson, U. E., Sundgren, M., Svenheden, A., Tolli, J., Absorption, gastrointestinal transit, and tablet erosion of felodipine extended release (ER) tablets, *Pharm. Res.* **1993**, *10*, 709–714.

27 Artursson, P., Ungell, A.-L., Löfroth, J.-E., Selective paracellular permeability in two models of intestinal absorption: cultured monolayers of human intestinal epithelial cells and rat intestinal segments, *Pharm. Res.* **1993**, *10*, 1123–1129.

28 Poelma, F. G. J., Tukker, J. J., Evaluation of the chronically isolated internal loop in the rat for the study of drug absorption kinetics, *J. Pharm. Sci.* **1987**, *76*, 433–436.

29 Amidon, G. L., Sinko, P. J., Fleisher, D., Estimating human oral fraction dose absorbed: a correlation using rat intestinal membrane permeability for passive and carrier-mediated compounds, *Pharm. Res.* **1988**, *5*, 651–654.

30 Toon, S., Rowland, M., Structure-pharmacokinetic relationships among the barbiturates in the rat, *J. Pharmacol. Exp. Ther.* **1983**, *225*, 752–763.

31 Bryant, M. S., Korfmacher, W. A., Wang, S., Nardo, C., Nomeir, A. A., Lin, C.-C., Pharmacokinetic screening for the selection of new drug discovery candidates is greatly enhanced

through the use of liquid chromatography-atmospheric pressure ionization tandem mass spectrometry, *J. Chromatogr. A.* **1997**, *777*, 61–66.

32 Berman, J., Halm, K., Adkinson, K., Shaffer, J., Simultaneous pharmacokinetic screening of a mixture of compounds in the dog using API LC/MS/MS analysis for increased throughput, *J. Med. Chem.* **1997**, *40*, 827–829.

33 Olah, T. V., McLoughlin, D. A., Gilbert, J. D., The simultaneous determination of mixtures of drug candidates by liquid chromatography/atmospheric pressure chemical ionisation mass spectrometry as an *in vivo* drug screening procedure, *Rapid Commun. Mass Spec.* **1997**, *11*, 17–23.

34 Shaffer, J. E., Adkison, K. K., Halm, K., Hedeen, K., Berman, J., Use of 'N-in-One' dosing to create an in vivo pharmacokinetics database for use in developing structure-pharmacokinetic relationships, *J. Pharm. Sci.* **1999**, *88*, 313–318.

35 White, R. E., Manitpisitkul, P., Pharmacokinetic theory of cassette dosing in drug discovery screening, *Drug Metab. Dispos.* **2001**, *29*, 957–966.

36 Karlsson, M. O., Bredberg, U., Bioavailability estimation by semi-simultaneous drug administration: a Monte Carlo simulation study, *J. Pharmacokinet. Biopharm.* **1990**, *18*, 103–120.

37 Gabrielsson, J., Weiner, D., in: *Pharmacokinetic and Pharmacodynamic Data Analysis: Concepts and Applications*, 2nd edition. Swedish Pharmaceutical Society, Swedish Pharmaceutical Press, Stockholm, **1997**, pp. 412–418.

38 Karlsson, M. O., Bredberg, U., Estimation of bioavailability on a single occasion after semisimultaneous drug administration, *Pharm. Res.* **1989**, *6*, 817–821.

39 Bredberg, U., Karlsson, M. O., *In vivo* evaluation of the semi-simultaneous method for bioavailability estimation using controlled intravenous infusion as an 'extravascular' route of administration, *Biopharm. Drug Dispos.* **1991**, *12*, 583–597.

40 Karlsson, M. O., Lindberg-Freijs, A., Comparison of methods to calculate cyclosporine A bioavailability from consecutive oral and intravenous doses, *J. Pharmacokinet. Biopharm.* **1990**, *18*, 293–311.

41 Griffiths, R., Lewis, A., Jeffrey, P., Models for drug absorption in situ and in conscious animals, in: *Models for Assessing Drug Absorption and Metabolism*. Borchard, R. T., Smith, P. L., Wilson, G. (eds), Plenum Press, New York, **1996**, pp. 67–84.

42 Patton, J. S., Platz, R. M., Routes of delivery: case studies (2) Pulmonary delivery of peptides and proteins for systemic action, *Adv. Drug Delivery Rev.* **1992**, *8*, 179–196.

43 Byron, P. R., Determinants of drug and polypeptide bioavailability from aerosols delivered to the lung, *Adv. Drug Delivery Rev.* **1990**, *5*, 107–132.

44 Taylor, A. E., Gaar., K. A., Estimation of pore radii of pulmonary and alveolar membranes, *Am. J. Physiol.* **1970**, *218*, 1133–1140.

45 Chanoine, F., Grenot, C., Heidmann, P., Junien, J. L., Pharmacokinetics of butixocort 21-proprionate, budesonide, and beclomethazone diproprionate in the rat after intratrachael, intravenous and oral treatments, *Drug Metab. Dispos.* **1991**, *19*, 546–553.

46 Driscoll, K. E., Costa, D. L., Hatch, G., Henderson, R., Oberdorster, G., Salem, H., Schlesinger, R. B., Intratracheal instillation as an exposure technique for the evaluation of respiratory tract toxicity: uses and limitations, *Toxicol. Sci.* **2000**, *55*, 24–35.

47 Enna, S. J., Schanker, L. S., Absorption of saccharides and urea from the rat lung, *Am. J. Physiol.* **1972**, *222*, 409–414.

48 Lizio, R., Klenner, T., Borchard, G., Romeis, P., Sarlikiotis, A. W., Reissmann, T., Lehr, C.-M., Systemic delivery of the GnRH antagonist

cetrorelix by intratracheal instillation in anaesthetized rats, *Eur. J. Pharm. Sci.* **2000**, *9*, 253–258.

49 Irazuzta, J. E., Ahmad, U., Gancayaco, A., Ahmed, S. T., Zhang, J., Anand, K. J. S., Intratracheal administration of fentanyl: pharmacokinetics and local tissue effects, *Intensive Care Med.* **1996**, *22*, 129–133.

50 Bennett, D. B., Tyson, E., Nerenberg, C. A., Mah, S., de Groot, J. S., Teitelbaum, Z., Pulmonary delivery of detirelix by intratracheal instillation and aerosol inhalation in the briefly anaesthetized dog, *Pharm. Res.* **1994**, *11*, 1048–1054.

51 Smith, S. A., Pillers, D.-A. M., Gilhooly, J. T., Wall, M. A., Olsen, G. D., Furosemide pharmacokinetics following intratracheal instillation in the guinea pig, *Biol. Neonate* **1995**, *68*, 191–199.

52 Klyashchitsky, B. A., Owen, A. J., Nebulizer-compatible liquid formulations for aerosol pulmonary delivery of hydrophobic drugs: glucocorticoids and cyclosporine, *J. Drug Targeting* **1999**, *7*, 79–99.

53 Schanker, L. S., Mitchell, E. W., Brown, R. A., Jr., Species comparison of drug absorption from the lung after aerosol inhalation or intratracheal injection, *Drug Metab. Dispos.* **1986**, *14*, 79–88.

54 Leusch, A., Eichhorn, B., Müller, G., Rominger, K.-L., Pharmacokinetics and tissue distribution of the anticholinergics tiotropium and ipratropium in the rat and the dog, *Biopharm. Drug Dispos.* **2001**, *22*, 199–212.

55 Trnovec, T., Durisova, M., Bezek, S., Kallay, Z., Navarova, J., Tomcikova, O., Kettner, M., Faltus, F., Erichleb, M., Pharmacokinetics of gentamicin administered intratracheally or as an inhalation aerosol to guinea pigs, *Drug Metab. Dispos.* **1984**, *12*, 641–614.

56 Stewart, B. H., Chan, O. H., Lu, R. H., Reyner, E. L., Schmid, H. L., Hamilton, H. W., Steinbaugh, B. A., Taylor, M. D., Comparison of intestinal permeabilities determined in multiple *in vitro* and *in situ* models: relationship to absorption in humans, *Pharm. Res.* **1995**, *12*, 693–699.

57 Clarke, B., Smith, D. A., Pharmacokinetics and toxicity testing, *CRC Crit. Rev. Toxicol.* **1984**, *12*, 343–385.

58 Chiou, W. L., Barve, A., Linear correlation of the fraction of oral dose absorbed of 64 drugs between humans and rats, *Pharm. Res.* **1998**, *15*, 1792–1795.

59 He, Y.-L., Murby, S., Warhurst, G., Gifford, L., Walker, D., Ayrton, J., Eastmond, R., Rowland, M., Species differences in size discrimination in the paracellular pathway reflected by oral bioavailability of poly(ethylene glycol) and D-peptides, *J. Pharm. Sci.* **1998**, *87*, 626–633.

60 Obach, R. S., Baxter, J. G., Liston, T. E., Silber, M., Jones, B. C., MacIntyre, F., Rance, D. J., Wastall, P., The prediction of human pharmacokinetic parameters from preclinical and *in vitro* metabolism data, *J. Pharmacol. Exp. Ther.* **1997**, *283*, 46–58.

61 Bachman, K., Pardoe, D., White, D., Scaling basic toxicokinetic parameters from rat to man, *Environ. Health Perspect.* **1996**, *104*, 400–407.

62 Dedrick, R. L., Bishoff, K. B., Zaharko, D. S., Interspecies correlation of plasma concentration history of methotrexate (NSC-740), *Cancer Chemother. Rep. Part 1* **1970**, *54*, 95–101.

63 Mordenti, J., Man vs. beast: pharmacokinetic scaling in mammals, *J. Pharm. Sci.* **1986**, *75*, 1028–1040.

64 Boxenbaum, H., Interspecies scaling, allometry, physiological time, and the ground plan of pharmacokinetics, *J. Pharmacokinet. Biopharm.* **1982**, *10*, 201–227.

65 Boxenbaum, H., Interspecies pharmacokinetic scaling and the evolutionary-comparative paradigm, *Drug Metab. Rev.* **1984**, *15*, 1071–1121.

66 Boxenbaum, H., DiLea, C., First-time-in-human dose selection: allometric

thoughts and perspectives, *J. Clin. Pharmacol.* **1995**, *35*, 957–966.

67 Mahmood, I., Balian, J. D., Interspecies scaling: a comparative study for the prediction of clearance and volume using two or more species, *Life Sci.* **1996**, *59*, 579–585.

68 Jezequel, S. G., Fluconazole: interspecies scaling and allometric relationships of pharmacokinetic properties, *J. Pharm. Pharmacol.* **1994**, *46*, 196–199.

69 Mahmood, I., Interspecies scaling of renally secreted drugs, *Life Sci.* **1998**, *63*, 2356–2371.

70 Ward, K. W., Proksch, P. D., Gorycki, P. D., Yu, C.-P., Ho, M. Y. K., Bush, B. D., Levy, M. A., Smith, B. R., SB-242235, a selective inhibitor of p-38 mitogen-activated protein kinase. II: *in vitro* and *in vivo* metabolism studies and pharmacokinetic extrapolation to man, *Xenobiotica* **2002**, *32*, 235–250.

71 Boxenbaum, H., D'Souza, R. W., Interspecies pharmacokinetic scaling, biological design and neoteny, in: *Advances in Drug Research*, Volume 19. Testa, B. (ed.), Academic Press Ltd., London, **1990**, pp. 139–196.

72 Bonate, P. L., Howard D., Critique of prospective allometric scaling: does the emperor have clothes? *J. Clin. Pharmacol.* **2000**, *40*, 335–340.

73 Mahmood, I., Prospective allometric scaling: does the emperor have clothes? *J. Clin. Pharmacol.* **2000**, *40*, 341–344.

74 Bonate, P. L., Howard D., Rebuttal to Mahmood, *J. Clin. Pharmacol.* **2000**, *40*, 345–346.

75 Himmelstein, K. J., Lutz, R. J., A review of the applications of physiologically based pharmacokinetic modelling, *J. Pharmacokinet. Biopharm.* **1979**, *7*, 127–145.

76 Rowland, M., Physiologic pharmacokinetic models: relevance, experience and future trends, *Drug Metab. Rev.* **1984**, *15*, 55–74.

77 Balant, L. P., Gex-Fabry, M., Review: Physiological pharmacokinetic modelling, *Xenobiotica* **1990**, *20*, 1241–1257.

78 Jang, J.-Y., Droz, P. O., Chung, H. K., Uncertainties in physiologically based pharmacokinetic models caused by several input parameters, *Int. Arch. Occup. Environ. Health* **1999**, *72*, 247–254.

79 Khor, S. P., Mayersohn, M., Potential error in the measurement of tissue to blood distribution coefficients in physiological pharmacokinetic modeling: residual tissue blood. 1. Theoretical considerations, *Drug Metab. Dispos.* **1991**, *19*, 478–485.

80 Khor, S. P., Bozigian, H., Mayersohn, M., Potential error in the measurement of tissue to blood distribution coefficients in physiological pharmacokinetic modeling: residual tissue blood. II. Distribution of phencyclidine in the rat, *Drug Metab. Dispos.* **1991**, *19*, 486–490.

81 Rowland, M., Tozer, T. N., *Clinical Pharmacokinetics: Concepts and Applications*, 3rd edition. Lippincott, Williams & Wilkins, Philadelphia, USA, **1994**, p. 99.

82 Ross, E. M., Pharmacodynamics: mechanism of drug action and the relationship between drug concentration and effect, in: *Goodman and Gilman's The Pharmacological Basis of Therapeutics*, 9th edition. Hardman, J. G., Limbird, L. E., Gilman, A. G. (eds), McGraw-Hill, New York, **1995**, pp. 29–41.

83 Houston, J. B., Carlile, D. J., Prediction of hepatic clearance from microsomes, hepatocytes and liver slices, *Drug Metab. Rev.* **1997**, *29*, 891–922.

84 Balant, L. P., Gex-Fabry, M., Modelling during drug development, *Eur. J. Pharmaceut. Biopharm.* **2000**, *50*, 13–26.

7
In vivo Permeability Studies in the Gastrointestinal Tract of Humans

Niclas Petri and Hans Lennernäs

Abbreviations

P_{eff}	Effective intestinal permeability
F	Bioavailability
fa	Fraction dose absorbed
E_G	Gut wall extraction
E_H	Hepatic extraction
fu	Fraction drug unbound in plasma
Cl_{int}	Intrinsic clearance
Qh	Hepatic blood flow
P-gp	P-glycoprotein
MRP	Multidrug resistance-related protein family
LRP	Lung cancer-resistance protein
BCRP	Breast cancer-resistance protein
hPepT1	Oligo peptide carrier for di- and tripeptides
MCT	Monocarboxylic acid cotransporter
OCT	Organic cation transporter
LNAA	Large neutral amino acid
CYP 3A4	Cytochrome P450 3A4
HBD	Number of hydrogen bond donors
PSA	Polar molecular surface area

Symbols

CLOGP	Logarithm of the calculated octanol/water partition coefficient (for neutral species)
log $D_{6.5}$	Logarithm of the distribution coefficient in octanol/water at pH 6.5
MW	Molecular weight

Drug Bioavailability: Estimation of Solubility, Permeability, Absorption and Bioavailability.
Edited by Han van de Waterbeemd, Hans Lennernäs and Per Artursson

ISBN: 3-527-30438-X

7.1 Introduction

The predominant way to deliver drugs to the systemic circulation in order to generate pharmacological and clinical effects is the oral route. Self-administration of drugs to the gastrointestinal (GI) tract is considered to be safe, efficient and easily accessible, with minimal discomfort to the patient in comparison with other routes of drug administration. The design and composition of the pharmaceutical dosage formulation as well as the physico-chemical properties of the drug itself will certainly affect the *in vivo* performance, and hence the therapeutic outcome. Bioavailability (F) of drugs following oral administration is determined by several factors such as solubility and dissolution, transit time, GI stability, intestinal permeability and first-pass extraction in the gut and/or by the liver [1–4]. Among these, the effective intestinal permeability (P_{eff}) is a major determinant of fraction dose absorbed (fa) [1, 3, 5]. It is a recognized fact that some drugs may be transported by multiple mechanisms, by passive diffusion and by various carrier-mediated transporters both via the absorptive and via the secretory route (Fig. 7.1) [1, 3, 6–8].

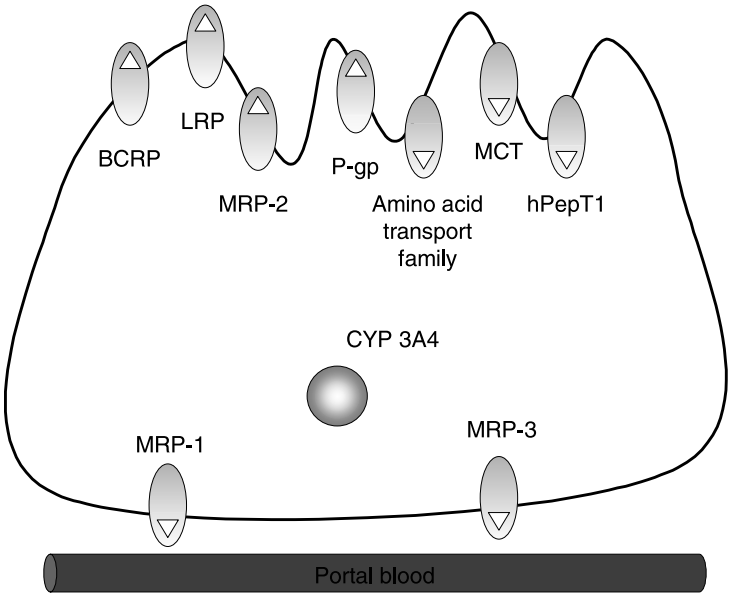

Fig. 7.1. The intestinal permeability of drugs *in vivo* is the total transport parameter that may be affected by several parallel transport mechanisms in both absorptive and secretory directions. Some of the most important transport proteins that may be involved in the intestinal transport of drugs and their metabolites across intestinal epithelial membrane barriers in humans are displayed. P-gp = P-glycoprotein; BCRP = breast cancer-resistance protein; LRP = lung-resistant protein; MRP1–5 = multidrug-resistant protein family; hPepT1 = oligopeptide carrier for di- and tripeptides; MCT = $H^{(+)}$-monocarboxylic acid cotransporter. CYP34A4 is the important intracellular oxidation CYP P450 enzyme for which ~50–60% of all clinically used drugs serve as substrates.

The expression and functional activity of the intestinal transport proteins and enzymes are currently under examination, and the future will reveal the extent to which various transporters will contribute to intestinal absorption and presystemic metabolism of drugs (Fig. 7.1) [9]. Undoubtedly, such knowledge will increase our understanding of the basis of inter-individual variability and regulation in drug response, both from a genomic and from a nongenomic perspective [9, 10]. However, the *in vivo* measured drug transport kinetics (P_{eff}) represents the total transport (i.e., the macroscopic transport rate) of all parallel processes.

Direct measurements of intestinal absorption, secretion and metabolism of drugs in humans are possible by regional intestinal perfusion techniques [6, 11, 12]. In general, three different clinical tools have been employed in the small intestine: (i) a triple-lumen tube including a mixing segment; (ii) a multilumen tube with a proximal occluding balloon; and (iii; and a multilumen tube (Loc-I-Gut®) with two balloons occluding a 10 cm-long intestinal segment (Fig. 7.2) [5, 6, 11, 13–15]. The advantages and disadvantages of the various intestinal perfusion techniques are discussed elsewhere [3, 16]. The complete Loc-I-Gut concept is displayed in Fig. 7.3 [11, 13]. This intestinal perfusion technique, Loc-I-Gut, has been widely applied to investigate drug absorption, presystemic metabolism, drug dissolution, *in vitro–in vivo* correlation, drug–drug interactions, inter-individual variability, GI physiology and disease mechanisms (Fig. 7.4) [3, 11, 16–36]. The Loc-I-Gut approach provides the possibility of investigating and predicting the integrated *in vivo* processes in the human intestine where genetic, biochemical, physiological, pathophysiological, and environmental influences are present to affect the trans-

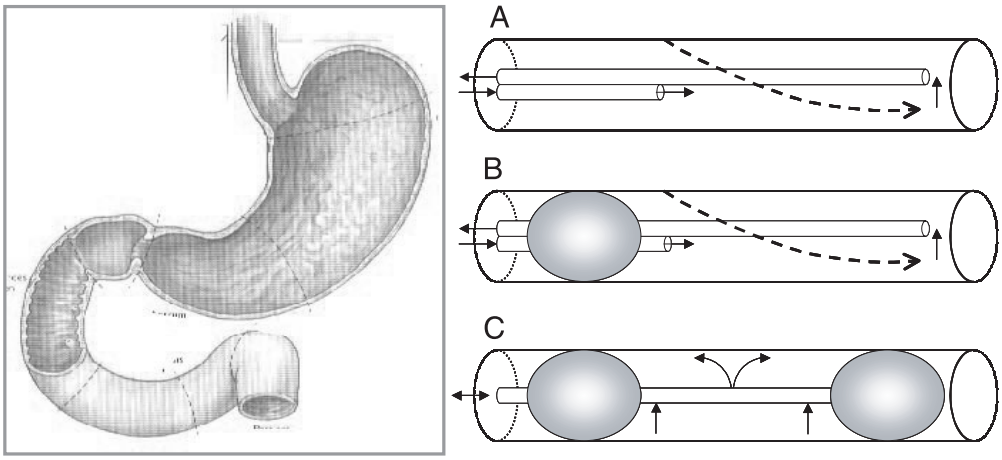

Fig. 7.2. Schematic diagram of three different intestinal perfusion methodologies for human use. (A) Open; (B) semi-open; (C) double balloon. For the open and semi-open systems, the hydrodynamics are best described by the parallel tube model (the dotted line indicates the concentration profile over the intestinal length). The well-stirred model is the best hydrodynamic model for the double balloon perfusion technique.

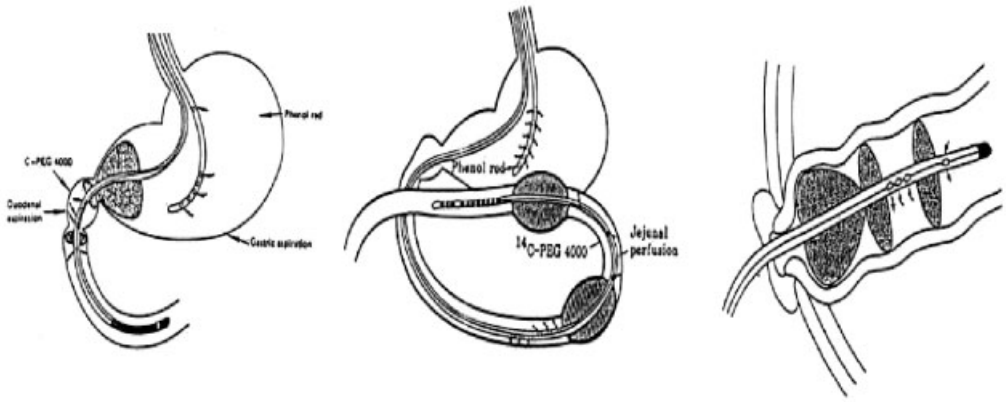

Fig. 7.3. The total Loc-I-Gut concept. Left: a perfusion system of the duodenal segment. Center: a tube system with double balloons which allow a segmental single-pass perfusion of jejunum. Right: a perfusion system of the small intestinal stomi.

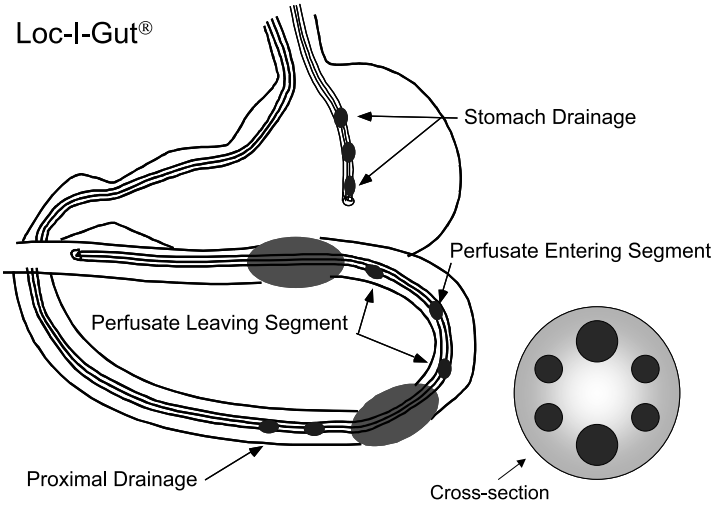

Fig. 7.4. The Loc-I-Gut perfusion technique for the proximal region of the human jejunum. The multichannel tube is made from polyvinyl chloride and is 175 cm long, with an external diameter of 5.3 mm. It contains six channels and is provided distally with two 40 mm-long, elongated latex balloons, placed 10 cm apart; each of these is separately connected to one of the smaller channels. The two wider channels in the center of the tube are for infusion and aspiration of perfusate. The two remaining peripheral smaller channels are used for administration of marker substances and/or drainage. A tungsten weight is attached to the distal end of the tube to facilitate passage of the tube into the jejunum. The balloons are filled with air when the proximal balloon has passed the ligament of Treitz. Gastric suction is obtained using a separate tube. ^{14}C-PEG 4000 is used as a volume marker to detect water flux across the intestinal barrier.

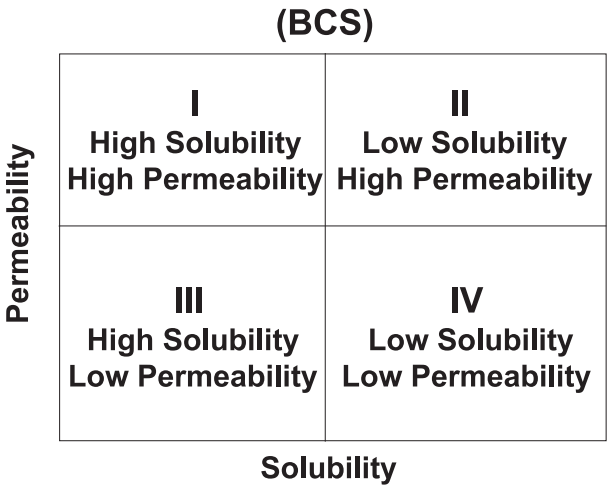

Fig. 7.5. The Biopharmaceutics Classification System (BCS) provides a scientific basis for predicting intestinal drug absorption and for identifying the rate-limiting step based on primary biopharmaceutical properties such as: solubility and effective intestinal permeability (P_{eff}). BCS serves as a product control instrument. The BCS divides drugs into four different classes based on their solubility and intestinal permeability. Drug regulation aspects related to *in vivo* performance of pharmaceutical dosage forms have been the driving force in the development of BCS. Guidance for industry based on BCS mainly indicates when bioavailability/bioequivalence (BA/BE) studies can be replaced by *in vitro* bioequivalence testing (www.fda.gov/cder/guidance/3618fnl.htm).

port/metabolism of drugs [3, 11]. In addition, the Loc-I-Gut technique has been used to establish an *in vivo* human permeability database for the proposed Biopharmaceutical Classification system (BCS) for oral immediate-release products (Fig. 7.5) [1, 31, 37]. The human *in vivo* P_{eff} values, obtained during appropriate physiological conditions, provide the basis for establishing *in vitro–in vivo* correlation, which can be used in making predictions about oral absorption as well as in setting bioequivalence standards for drug approval [1, 16, 21, 28, 29, 31]. Recently, this single-pass perfusion approach has been used for measurements of the expression and function of enzymes and transporters in human-shed enterocytes in combination with determination of transport and presystemic metabolism in the same individuals [38, 39]. All together, this clearly indicates that intestinal perfusion techniques are very useful in increasing our understanding of intestinal absorption and secretion and the metabolism of drugs. The purpose of the present chapter is to describe the usefulness of human *in vivo* perfusion studies in oral drug delivery research and to summarize reports based on these *in vivo* techniques.

7.2 Pharmacokinetic Definition of Intestinal Absorption (fa), Presystemic Metabolism (E_G and E_H) and Absolute Bioavailability (F) of Drugs Administered Orally to Humans

The most useful pharmacokinetic variable for describing the quantitative aspects of all processes influencing the absorption (fa) and first-pass metabolism and excretion (E_G and E_H) in the gut and liver is the absolute bioavailability (F) [40]. This pharmacokinetic parameter is used to illustrate the fraction of the dose that reaches the systemic circulation, and relate it to pharmacological and safety effects for oral pharmaceutical products in various clinical situations. The bioavailability is dependent on three major factors: the fraction dose absorbed (fa) and the first-pass extraction of the drug in the gut wall (E_G) and/or the liver (E_H) (Eq. (1)) [2–4, 15, 35]:

$$F = fa \times (1 - E_G) \times (1 - E_H) \quad (1)$$

There exist several factors that may affect the intestinal absorption (i.e., fa) and gut wall metabolism (i.e., E_G) of drugs. These can be divided into three general categories: (i) pharmaceutical factors; (ii) physico-chemical factors of the drug molecule itself; and (iii) physiological, genetic, biochemical and pathophysiological factors in the intestine [3, 5–8, 11, 15, 27, 32, 41–46]. The fa is the fraction of the dose transported (absorbed) across the apical cell membrane into the cellular space of the enterocyte according to scientific and regulatory definitions [3, 11, 16, 25–31, 47, 48]. Once the drug has reached the intracellular site, it may be subjected to cytochrome P450 (CYP P450)-mediated metabolism, predominantly CYP3A4, as well as other enzymatic steps [2–4, 15, 34, 35, 38, 49]. The enzymatic capacity of the small intestine to metabolize drugs can, in pharmacokinetic terms, be expressed as the extraction ratio of the intestine (E_G) [40]. It is important to realize that CYP3A4 is not expressed in the colon [50, 51]. Instead, drug metabolism by colonic microflora may play a crucial role in colonic drug absorption, especially with regard to drugs given in extended-release dosage forms, which may be subjected to predominantly hydrolytic and other reductive reactions [52, 53]. The fraction that escapes metabolism in the small intestine ($1 - E_G$) may undergo additional metabolism and/or biliary secretion in the liver (E_H) before reaching the systemic circulation. The E_H is dependent on the blood flow (Qh), the protein binding (fu), and the intrinsic clearance of the enzymes and/or transporters (Cl_{int}) [40]. Recently, it has also been recognized that membrane transport into the hepatocyte has to be included in the models for predicting and explaining liver extraction.

7.3 Methodological Aspects on *in vivo* Intestinal Perfusion Techniques

Clinical studies of effective intestinal permeability (P_{eff}), secretion and metabolism of various compounds, such as drugs, environmental pollutants and nutrients are

rarely performed *in vivo* in humans, even if experimental techniques are available (Figs. 7.2–7.4) [3, 11, 13, 16, 17, 24–31]. Direct measurements of compound transport and metabolism in the mesenteric vein and portal vein in humans are not possible for obvious reasons. Perfusion techniques do, however, offer great possibilities of measuring intestinal processes. Over the past 70 years, different *in vivo* intestinal perfusion techniques have been developed and the importance of such *in vivo* studies has been clearly demonstrated [3, 5, 6, 11, 13–16, 25–31]. The fundamental principle of an *in vivo* intestinal perfusion experiment is that the absorption (i.e., P_{eff}) is calculated from the rate at which the compound disappears from the perfused intestinal segment. An accurate determination of the P_{eff} requires knowledge of the hydrodynamics, perfusion rate and the surface area of the perfused intestinal segment [3, 11, 16, 25–31]. Fluid hydrodynamics are dependent on the perfusion technique applied, flow rate and GI motility [11, 30]. The major advantages in using P_{eff} as the absorption parameter are that it is possible to measure regardless of the transport mechanism(s) across the intestinal mucosa, predicts the fa and can be used to assess *in vitro–in vivo* correlations which validates the use of different intestinal absorption models [1, 22, 28, 29] commonly applied in discovery and preclinical development (Fig. 7.6a–c). It is important to recognize that such *in vivo* studies of intestinal absorption and function provide the fully integrated response in humans, with a relevant combination of genetic, biochemical, physiological, pathological and environmental factors [54]. We have established a good correlation between *in vivo* determined P_{eff} and historical data on fa for a large number of structurally diverse drugs (Figs. 7.7 and 7.8).

The enterocyte is the most common cell type (>90%) in the small intestinal barrier, which also contains a significant number of lymphocytes, mast cells, and macrophages [59]. The intestinal P_{eff} for passive transcellular diffusion is considered to reflect the diffusion across the complex apical membrane into the cytosol, which is situated close to the cytoplasmic leaflet of the apical enterocyte membrane [3, 5, 7, 11, 16, 25–31, 47, 49, 55]. Consequently, intestinal perfusion models, that measure the disappearance of the drug from the perfused segment, directly describe its quantitative uptake into epithelial cells. The apical enterocyte membrane is very complex and apparently represents the rate-limiting step in the diffusion across the barrier. In addition, it has been speculated that the exofacial leaflet is responsible for the low permeability of the apical membrane [47, 55, 56]. Molecular dynamics simulations have identified four separate regions in the membrane, although the biological membrane containing multiple components can be considered to be more complex [56]. More studies are required to establish the role of bilayer asymmetry and membrane proteins in determining the unique permeability properties of the barrier epithelial apical membrane [47, 55, 56].

Assessing the effect of the intestinal metabolism in the P_{eff} as a membrane transport rate parameter is a methodological issue [7, 26, 34, 35, 49]. An evaluation of its influence has to include a study to establish which enzyme(s) is (are) involved and the site of metabolism in relation to the site of the measurements. Intracellular metabolism in the enterocyte, for instance by CYP 3A4 and di- and tri-

a

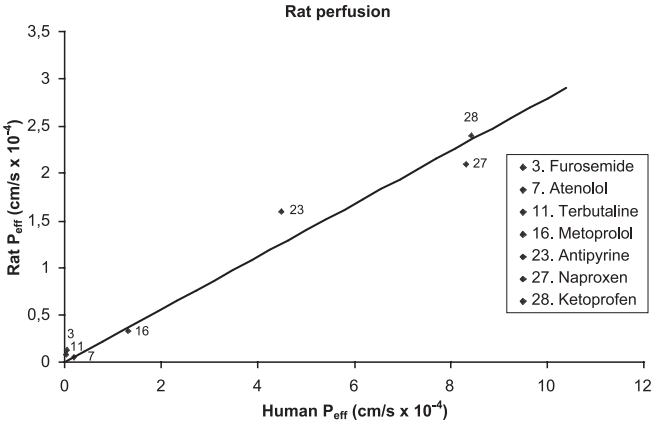
Rat perfusion
Rat P_{eff} (cm/s x 10^{-4})
Human P_{eff} (cm/s x 10^{-4})
3. Furosemide
7. Atenolol
11. Terbutaline
16. Metoprolol
23. Antipyrine
27. Naproxen
28. Ketoprofen

b

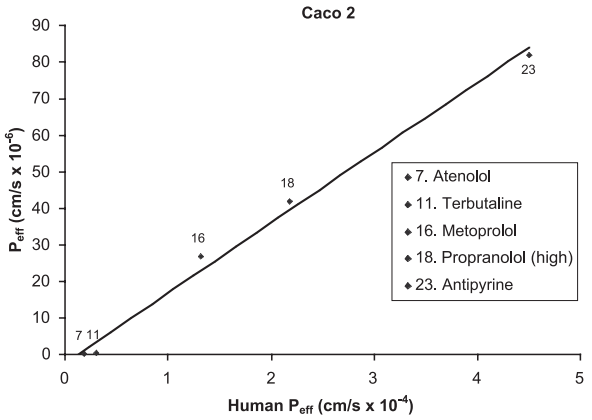
Caco 2
P_{eff} (cm/s x 10^{-6})
Human P_{eff} (cm/s x 10^{-4})
7. Atenolol
11. Terbutaline
16. Metoprolol
18. Propranolol (high)
23. Antipyrine

c

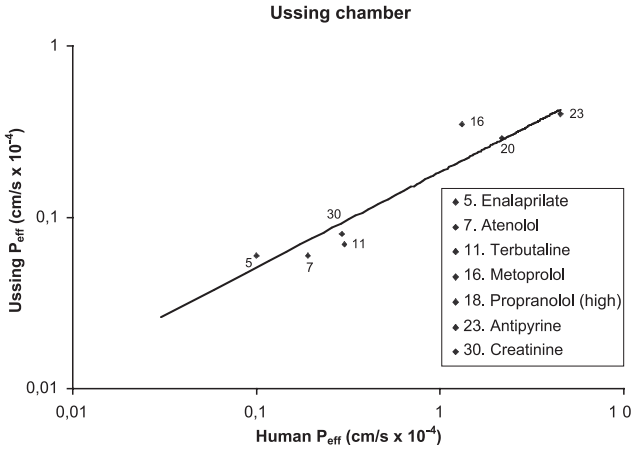
Ussing chamber
Ussing P_{eff} (cm/s x 10^{-4})
Human P_{eff} (cm/s x 10^{-4})
5. Enalaprilate
7. Atenolol
11. Terbutaline
16. Metoprolol
18. Propranolol (high)
23. Antipyrine
30. Creatinine

Fig. 7.6. a–c. Human *in vivo* permeabilities are a cornerstone of the BCS; the correlation of fraction dose absorbed and permeability with other models enables drugs to be classified according to BCS, and for bioequivalence to be defined for pharmaceutical product approval. These human *in vivo* P_{eff} were determined with a regional double-balloon perfusion system (Loc-I-Gut®) (see Fig. 7.4). The major advantage of using P_{eff} is that it can be measured irrespective of transport mechanism(s) across the intestinal mucosa. It can also be used to predict the fa and to assess *in vitro-in vivo* correlations that validate the intestinal absorption models [21, 22, 28, 29] used in discovery and preclinical development.

peptidases, does not occur in the vicinity of the outer leaflet of the apical membrane, and is therefore not considered to affect the P_{eff} determined by the disappearance approach (single-pass perfusion) [7, 15, 26, 34, 35, 38, 49]. By contrast, drug metabolism in the lumen and/or at the brush border will directly interfere with the determination of the P_{eff}, since here, the drug is metabolized before it is absorbed [57, 58]. It has also been suggested that intracellular metabolism may indirectly affect intestinal permeability by providing a further sink boundary condition across the apical membrane. However, we have shown that a specific inhibition of the enterocyte CYP 3A4 by ketoconazole does not change the P_{eff} of *R*/*S*-

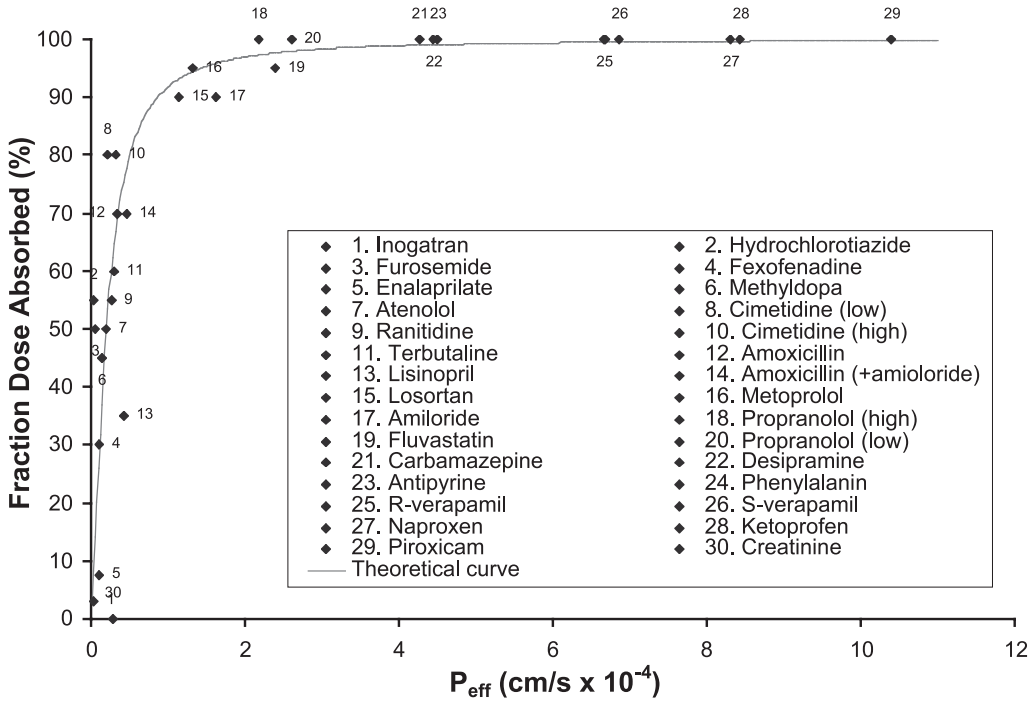

Fig. 7.7. Human *in vivo* permeability values (P_{eff}) can be determined using a single-pass perfusion technique (Loc-I-Gut) in humans. These human P_{eff} values correlated very well with the fraction dose absorbed (fa) after oral administration of many drugs in different pharmacological classes and which represent structural diversity.

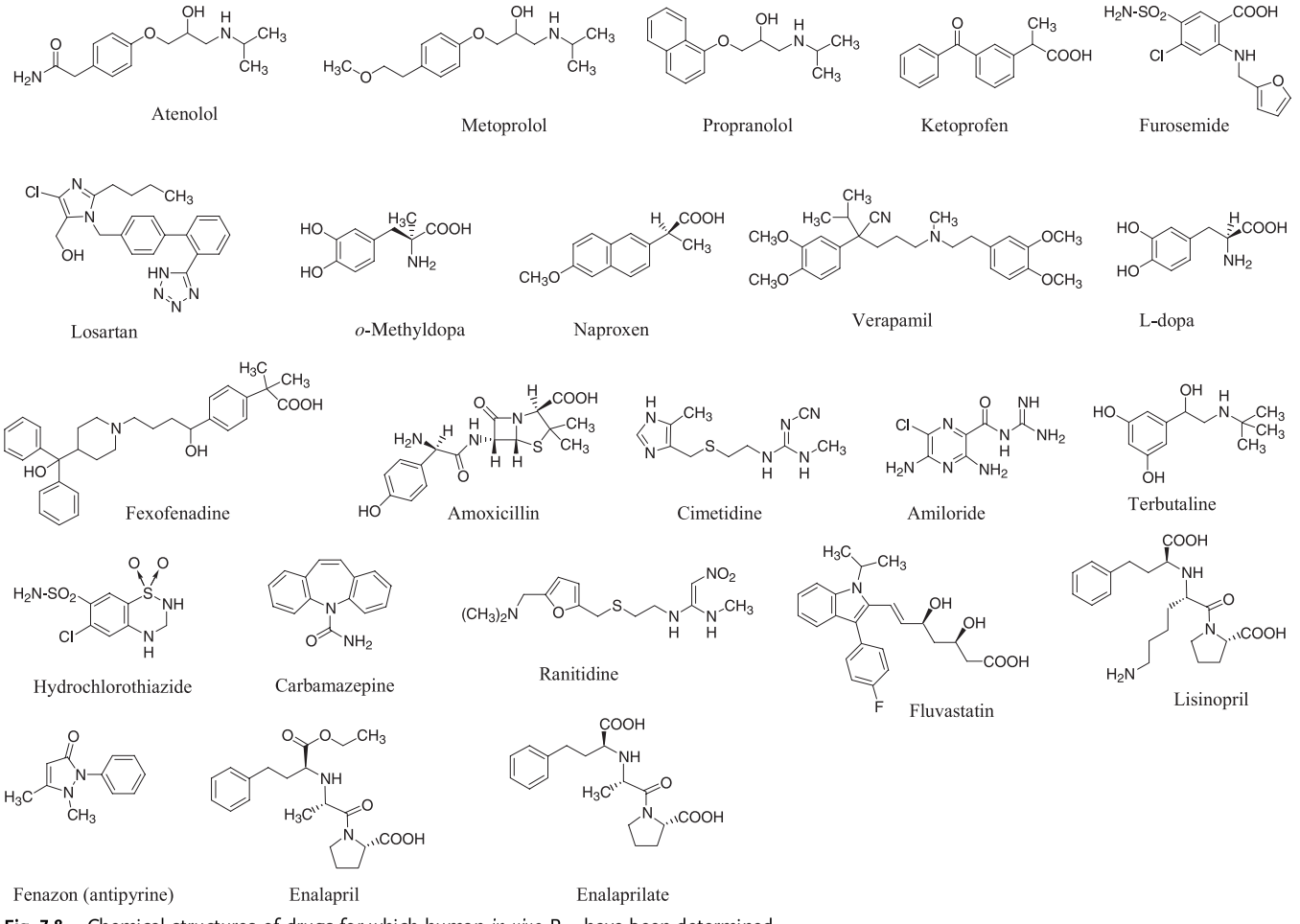

Fig. 7.8. Chemical structures of drugs for which human *in vivo* P_{eff} have been determined.

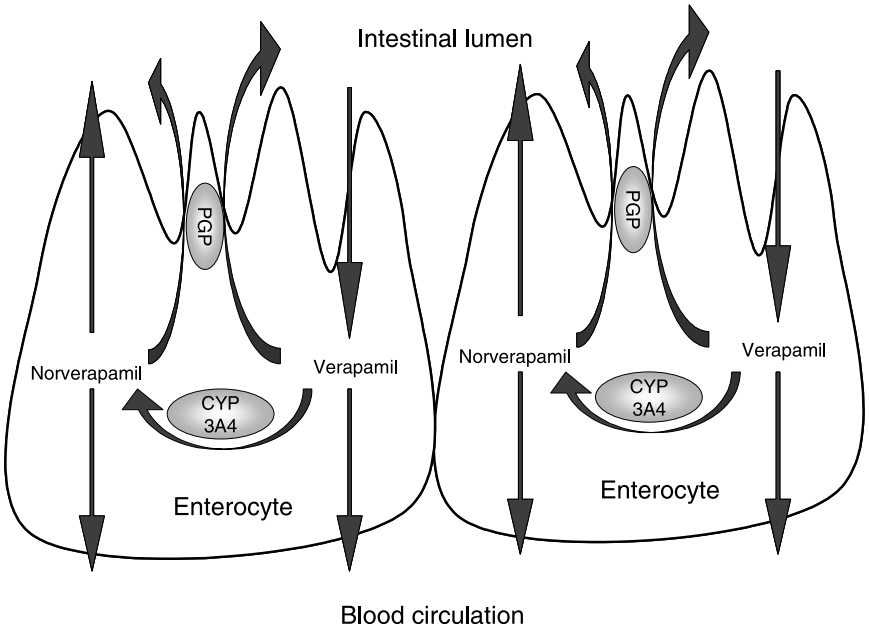

Fig. 7.9. Schematic illustration of P-glycoprotein (P-gp) transport and CYP 3A4 metabolism of *R*/*S*-verapamil in the human jejunum. It is assumed that the drug must be absorbed before being metabolized by CYP 3A4 in the human enterocyte. Both the parent drug and its metabolite, *R*/*S*-norverapamil, can be transported into the blood or back into the intestinal lumen.

verapamil, which suggests that the sink condition *in vivo* is already provided by the highly perfused mesenteric blood vessels (Fig. 7.9) [34, 35].

7.4 Paracellular Passive Diffusion

The enterocytes are sealed together by negatively charged tight junctions, and the intracellular space formed is considered to be the paracellular route [59, 60]. The available surface area for paracellular intestinal absorption has been estimated to be about 0.01% of the total surface area of the small intestine [59, 60]. The quantitative importance of the paracellular route for the macroscopic intestinal absorption of hydrophilic compounds *in vivo* is not yet fully clear. There have been several *in vitro* investigations demonstrating that the paracellular route is important for the intestinal absorption of various hydrophilic compounds [48, 61–63]. However, *in vivo* studies have suggested that this route has only a minor contribution to the overall intestinal absorption of drugs [20, 23, 25, 27, 64, 65]. In other *in vitro* studies, it has been reported that the tight junctions between enterocytes are regu-

lated by nutrients to induce solvent drag and thereby increase the intestinal absorption [62, 66–68].

We have assumed in previous reports that water transport during solvent drag is largely paracellular. Based on this assumption, we have suggested that compounds with a molecular weight (MW) of over approximately 200 Da (radius > 4.0 Å) are too large for the limited intercellular space between the enterocytes, and therefore not sensitive to solvent drag in terms of quantitative absorption [20, 23, 25, 27]. This hypothesis is supported by our observation that in humans, small hydrophilic compounds such as urea (MW 60 Da, molecular radius 2.6 Å) and creatinine (MW 113 Da, molecular size 7.2–8.0 Å) are affected by solvent drag in humans, whereas other hydrophilic compounds with a MW > 180 Da, such as D-glucose (180 Da), antipyrine (188 Da), L-dopa (197 Da), terbutaline (225 Da), atenolol (266 Da) and enalaprilate (348 Da) are not [20, 23, 25, 27]. Further support for passive transcellular transport of fairly hydrophilic drugs are the observations that atenolol ($\log D_{6.5} < -2$, PSA 88 Å^2, HBD 4) inhibits P-glycoprotein (P-gp)-mediated efflux and that terbutaline ($\log D_{6.5} < -1.3$, PSA 76 Å^2, HBD 4) is extensively metabolized in the gut wall during first-pass extraction following oral administration. Both these compounds have been suggested to be largely absorbed by the paracellular route due to their hydrophilic properties [61]. However, atenolol has been reported to decrease the basal apical transport of celiprolol – a P-gp substrate that does not undergo CYP 3A4 metabolism, in Caco-2 cells [69]. This transport inhibition is a competitive interaction at the binding sites of the P-gp, which are suggested to be located at the transmembrane region of the P-gp. Terbutaline undergoes extensive sulfate conjugation after oral administration, which appears to occur predominantly in the gut wall [70, 71]. This particular conjugation enzyme is located in the cytosolic fraction of the enterocyte, which indicates that terbutaline must be transported via the transcellular route even if it is a hydrophilic drug with low intestinal permeability. Our human *in vivo* perfusion data – together with this discussion on two hydrophilic drugs, atenolol and terbutaline – support the hypothesis that small and fairly hydrophilic drugs are mainly absorbed via the transcellular route if passive diffusion is the predominant intestinal absorption mechanism. In addition, Soergel suggests that the intestinal mucosa is nearly impermeable to paracellular transport of hexoses, and Amelsberg *et al.* (1996) hypothesize that paracellular absorption in mammals is unlikely to make a major contribution to small intestinal absorption of bile acids (i.e., of MW 500–600 Da) [60, 72].

7.5 Transcellular Passive Diffusion

Previously, the unstirred water layer (UWL) adjacent to the intestinal lining was considered to be the rate-limiting step for intestinal P_{eff} of high-permeability compounds [27, 73]. However, several *in vivo* studies have clearly reported that the thickness of this UWL is significantly thinner than was previously assumed, since

there is an instantaneous mixing of intestinal fluids [43, 74]. For instance, in 1995, Fagerholm and Lennernäs observed no significant changes in estimated P_{eff} of two high-permeability compounds, D-glucose (10×10^{-4} cm s^{-1}) and antipyrine (4×10^{-4} cm s^{-1}), or UWL thickness over a four-fold range of perfusion rates (1.5 to 6.0 mL min^{-1}) when using the Loc-I-Gut technique in humans [73]. Therefore, it is currently accepted that the epithelial membrane controls the transport rate for both low- and high-permeability compounds, regardless of the transport mechanism *in vivo* [43, 73, 74].

The main intestinal absorption mechanism for drugs *in vivo* is considered to be passive transcellular membrane diffusion with the apical membrane as the rate-limiting step [3, 27, 36, 61, 75]. This is consistent with most drugs as the majority of them are fairly lipophilic in nature. For instance, in a pharmacokinetic database of a total of 472 drugs, it was found that 235 (50%) had a log P-value > 2, while 379 (80%) had log P-values > 0 [76]. Even if a drug is a substrate for an intestinal transport protein, passive diffusion will probably be the main absorption mechanism if the drug has suitable lipophilic physico-chemical properties. On the other hand, intestinal carrier-mediated membrane transport will dominate for hydrophilic drugs and polar metabolites if they are substrates for any transporter, since the passive membrane diffusion is then expected to be slow for such compounds [31, 36].

In a detailed multivariate data analysis report of the structure–permeability relationship we have shown that the *in vivo* jejunal human P_{eff} for 22 compounds, determined by the Loc-I-Gut technique, with diversified structures was correlated with both experimentally determined lipophilicity values using a pH-metric technique and calculated molecular descriptors [36] (Figs 7.8, 7.10 and 7.11). Some of these 22 investigated compounds were omitted from the final analysis as they are carrier-mediated (amoxicillin, D-glucose, L-leucine, L-dopa, and α-methyldopa) or paracellularly transported (urea and creatinine). The remaining 15 drugs were included in the multivariate analysis for passive membrane diffusion, even if some of them (e.g., verapamil, losartan, furosemide, fluvastatin) have been considered to be substrates for efflux proteins, such as P-gp and multidrug-resistant protein (MRP), located in the enterocyte membrane [7, 36, 46, 77]. The relationships shown in Figs 7.7 and 7.10–7.11 strongly suggest that the intestinal absorption mechanism for these drugs is probably expected to be dominated by passive transcellular diffusion, and this is supported by the fact that for these drugs a linear relationship exists between the fraction dose absorbed and the clinical dose range. The theoretical models based on these *in vivo* permeability data from healthy volunteers can be used to predict passive intestinal membrane diffusion in humans for compounds that fit into the defined property space [36]. We used one of the models obtained from this multivariate analysis to predict the log P_{eff} values for an external validation set consisting of 34 compounds. A good correlation was found with the absorption data of these compounds, which further validates our *in vivo* permeability dataset, as does the observation that passive diffusion is a dominating mechanism for the *in vivo* intestinal absorption of many drugs [36].

In accordance with its polar nature, furosemide (log $D_{6.5}$ −0.5, PSA 124 $Å^2$, HBD 4) has a low jejunal P_{eff} of 0.05 ± 0.014 cm s^{-1} (Loc-I-Gut), and is classified

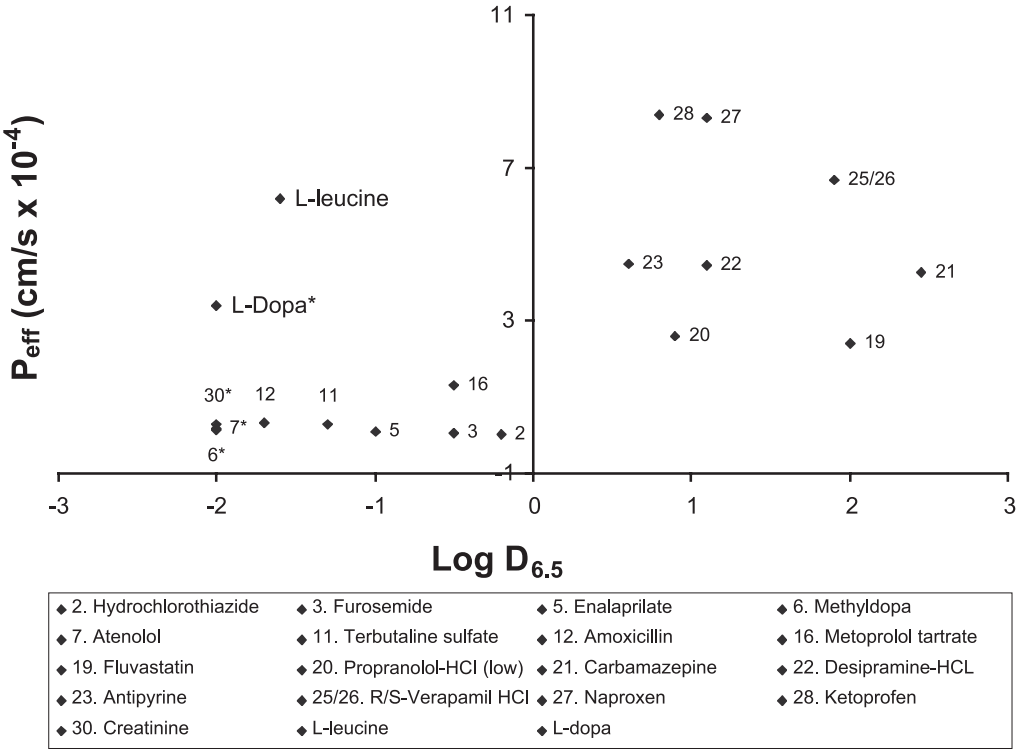

Fig. 7.10. Correlation between *in vivo* P_{eff} (determined with the Loc-I-Gut technique in humans) and octanol/buffer (pH 6.5) distribution coefficients for several common drugs. Drugs with octanol/buffer (pH 6.5) distribution coefficients >0 are highly permeable and well absorbed in humans (fa > 90%).

as a low-permeability compound according to the BCS [1, 16]. Interestingly, after oral administration the absorption and bioavailability (35–75%) of furosemide are highly variable [78, 79]. There are several hypotheses for this high variability, including active intestinal secretion, low passive diffusion, highly pH-dependent dissolution and permeability [80]. Figures 7.10 and 7.11 suggest that drugs with octanol/buffer partitioning coefficients higher than 0 and a PSA $< 100\,Å^2$ will be highly permeable ($P_{eff} >\approx 1.0 \times 10^{-4}$ cm s^{-1} and fa > 90%) across the human jejunum, and suggest that a strong influence of pH on physico-chemical properties which will most certainly influence the passive intestinal permeability *in vivo*. At pH 7.4, 6.5, and 5.5 the experimentally determined partitioning coefficients for furosemide at different pH were −0.9, −0.5 and 0.4, respectively [36]. In addition, the uncharged furosemide has an experimentally determined partitioning coefficient (i.e., log P-value) of 2.53 ± 0.01. Finally, a recent *in vitro* study showed that active intestinal secretion process is important for the transport of furosemide across the Caco-2 monolayer [80]. However, these *in vitro* results must be further

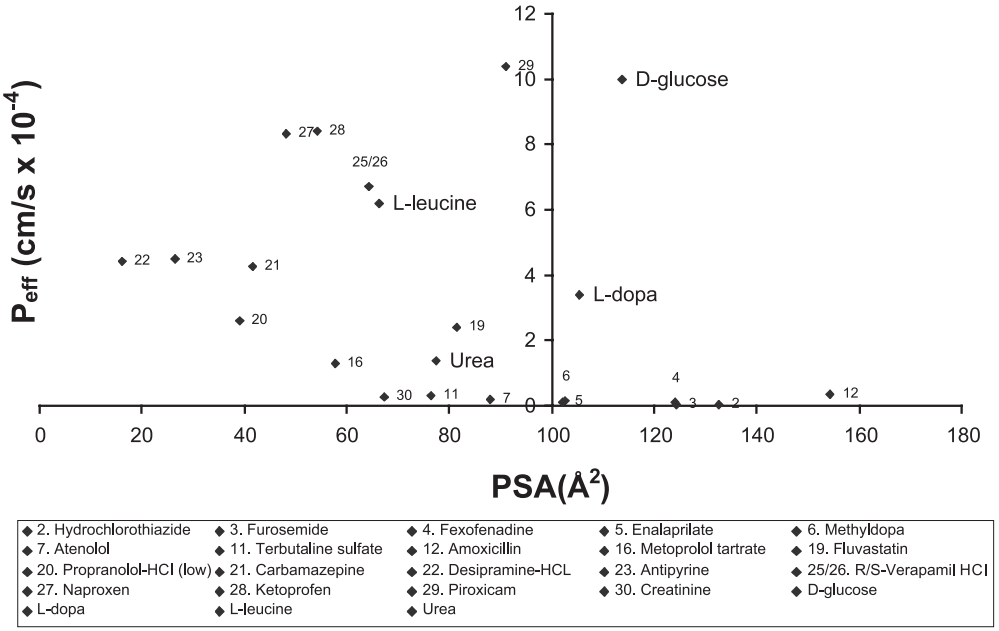

Fig. 7.11. Correlation between *in vivo* P_{eff} (determined with the Loc-I-Gut technique in humans) and polar surface area (PSA) for several common drugs. Drugs with a PSA $>100\,Å^2$ are highly permeable and well absorbed in humans (fa $>$ 90%).

investigated *in vivo* before any conclusion can be drawn regarding the mechanisms involved in the intestinal absorption of furosemide in humans.

7.6 Carrier-mediated Intestinal Absorption

The region where the major part of nutrients are absorbed is the proximal jejunum. Accordingly, a very large number of carrier proteins, channels and enzymes are expressed in this highly absorptive part of the GI tract. Carrier-mediated intestinal absorption of drugs becomes the dominating absorption mechanism of drugs with a reasonably high affinity to any intestinal transport protein, whereas the passive permeability contribution is small due to the polar nature of the compound [3, 27, 36, 61, 75]. The intestinal epithelium is polarized, and many transport proteins are located in the apical membrane and maintained there because of the tight junctions, which prevents proteins from diffusing within the membrane. Tight junctions also prevent backflow of nutrients from the basal side of the enterocytes into the gut lumen.

Targeting poorly absorbed drugs to nutrient transport system is a successful approach to increasing oral bioavailability [7]. The two most important nutrient

absorption proteins that can be utilized for drug transport in the absorptive direction are the oligopeptide carrier and the amino acid transport family. These proteins are only expressed in the small intestine to any significant degree and drugs, which are mainly absorbed through these carriers, will not be absorbed in the colon. By using the Loc-I-Gut technique in the proximal jejunum in humans, we investigated the transport of drugs that are substrates for any of these two proteins, namely amoxicillin, cephalexin, enalapril, lisinopril, α-methyldopa, and L-dopa [3, 16, 31, 81, 82].

The oligopeptide carrier (hPepT1) is a symport carrier, which transports a substrate with a proton across the apical enterocyte membrane. The access to protons of the oligopeptide carrier is a result of a sodium carrier, the Na^+/H^+ exchanger, which is located in the brush border membrane of the enterocytes [83]. In humans, the intestinal absorption of amoxicillin on average decreases from 72 ± 9% to 45 ± 11% if the oral dose is increased from 500 mg to 3000 mg [84]. This confirms that hPepT1 has a high transport capacity, since amoxicillin is fairly well absorbed despite such large doses. The *in vivo* jejunal P_{eff} for amoxicillin has been reported to be 0.4×10^{-4} cm s^{-1} at a perfusate concentration of 300 mg L^{-1} (0.82 mM), which corresponds to an oral dose of 1200 mg [31]. This jejunal P_{eff} value predicts that fa is <90%, which classifies amoxicillin as a low-permeability drug according to the BCS. The P_{eff} measured *in vivo* by Winiwarter *et al.* in 1999, was higher than that predicted for amoxicillin from the physico-chemical properties (log $D_{6.5}$ −1.7, CLOGP = 0.33, PSA 154 $Å^2$, MW 365 Da) [36]. This observation supports earlier pharmacokinetic reports, which suggested that amoxicillin has a higher intestinal absorption (~50–75%) than would be expected based on its low lipophilicity and amphoteric nature [84, 85]. The large inter-individual variability in the *in vivo* P_{eff} for amoxicillin may be due to polymorphism in the expression of hPepT1. Another possible explanation might be variation in nutritional status, as it has been reported that transcriptional activation of the PepT1 gene occurs by selective amino acids and dipeptides in the diet [86]. It has also been reported that the integrated response to a certain stimulus may increase PepT1 activity by translocation from a preformed cytoplasmic pool [87]. We reported that enalaprilate, the diacid and active form, has a low P_{eff} and consequently, a low fa in humans (Fig. 7.12). The prodrug approach of esterifying enalaprilate to enalapril has increased the human *in vivo* P_{eff} as well as the fa after oral administration (Fig. 7.12), this being most likely due to the higher transport activity of hPepT1 with the ester prodrug enalapril than the diacid form enalaprilate [88]. In the human jejunum, we determined the *in vivo* P_{eff} for amoxicillin, cephalexin, enalapril and lisinopril. These compounds have physico-chemical properties that predict low passive diffusion across the human intestine. It has also been shown that, in Caco-2 cells, the *in vitro* permeability is low, and this is in accordance with the poor expression of hPepT1 in that absorption model. The passive diffusion is low due to the polar nature of the compounds [89]. However, *in vivo* the intestinal permeability has been reported to be significantly higher. This is in accordance with a higher expression of hPepT1, which is the main mechanism for intestinal absorption of these drugs.

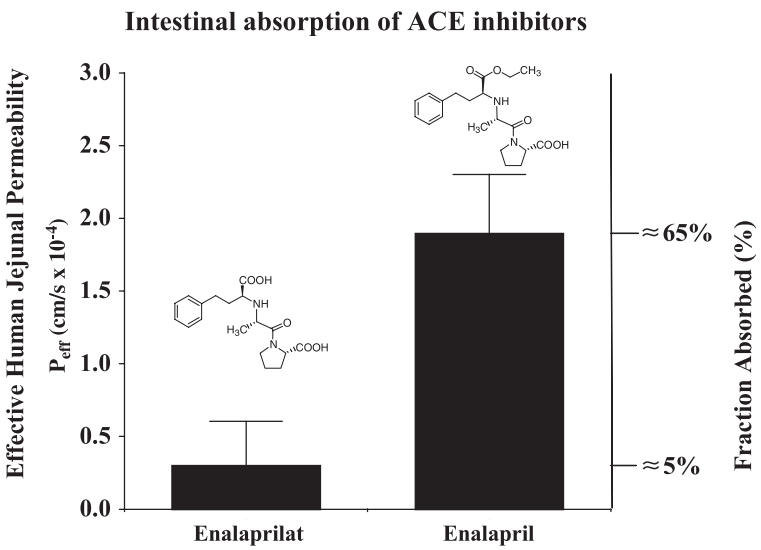

Fig. 7.12. Effective permeability (P_{eff}) of enalapril and enalaprilate in human jejunum *in vivo*. The P_{eff}-values predict the fraction dose absorbed for both drugs in human pharmacokinetic studies. The higher jejunal P_{eff} of enalapril most likely results from significantly higher transport due to the peptide carrier.

The *in vivo* P_{eff} in healthy volunteers of drugs transported by the amino acid transporter for large neutral amino acid (LNAA) was determined for L-dopa and α-methyldopa. α-Methyldopa was classified as a low P_{eff} drug ($0.1 \pm 0.1 \times 10^{-4}$ cm s^{-1}, at a perfusate concentration of 6.0–6.5 mM (Fig. 7.13) [16, 36, 81]. The corresponding *in vivo* P_{eff} for L-dopa was about 30-fold higher, namely $3.4 \pm 1.0 \times 10^{-4}$ cm s^{-1}, at a luminal concentration of 2.0–2.5 mM (Fig. 7.13) [3, 16, 36]. The difference regarding *in vivo* P_{eff} between α-methyldopa and L-dopa is probably due to a lower affinity to and/or transport capacity for α-methyldopa of the LNNA transporter. The low *in vivo* P_{eff} of α-methyldopa indicates that the passive diffusion is also low, which is in accordance with the physico-chemical properties (MW 211 Da, log $D_{6.5} < -2$, PSA 103 $Å^2$, HBD 5) [36]. Figure 7.13 illustrates that a small change in the chemical structure of a substrate for the LNAA transporter significantly alters its *in vivo* permeability. This is due to the narrow substrate specificity of this carrier protein. Two nutrient substrates for this carrier family, L-leucine and L-phenylalanine, have high *in vivo* P_{eff} in humans, despite these being determined at two widely different perfusate concentrations in this study (Fig. 7.13). This observation confirms that the amino transport family also exhibit a high in vivo transport capacity in the human jejunum.

The rate and extent of intestinal absorption of cimetidine has been widely discussed previously, and a reasonable value of fa for this drug has been estimated as 75% [90, 91]. It has been reported that cimetidine is a substrate for both P-gp and/or organic cation transporters (OCNT1 and OCNT2) [82, 92]. We determined the

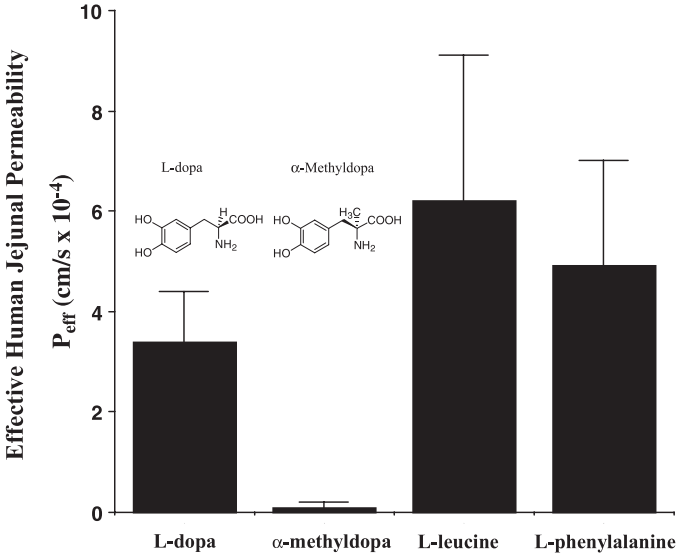

Fig. 7.13. Effective permeability (P_{eff}) of L-dopa, α-methyldopa, L-leucine and L-phenylalanine in human jejunum *in vivo*. P_{eff} were measured using a single-pass perfusion technique at concentrations of 2.5 mM, 6.7 mM, 40 mM and 0.06 mM for L-dopa, α-methyldopa, L-leucine and L-phenylalanine, respectively.

human jejunal *in vivo* P_{eff} at two different clinically relevant concentrations in order to investigate saturation in any carrier-mediated transport across the intestinal epithelium (Fig. 7.14). There was no difference between the two concentrations, and together with the observation that the human permeability correlates well with that of the Caco-2 model (which has a low expression of carrier proteins), this suggests that passive diffusion is a dominating mechanism even for cimetidine [82]. If organic cation transporters were the dominating mechanism, it might have been expected that the human intestinal *in vivo* permeability would have been significantly higher than the Caco-2 permeability, as the expression of OCNT1 and OCNT2 is higher in the human small intestine than in the Caco-2 model [82].

7.7
Jejunal Transport and Metabolism

Cytochrome P450 (EC 1.14.14.1) enzymes are well known for their ability to metabolize the majority of drugs, to detoxify environmental pollutants, and to activate some classes of carcinogens [93]. The most highly expressed subfamily is CYP 3A, which includes the isoforms CYP 3A4, CYP 3A5, CYP 3A7, and CYP 3A43 [93, 94]. The most abundant isoform is CYP 3A4, which corresponds to 30% of the total P450 content in the liver and about 70% of the total P450 content in the

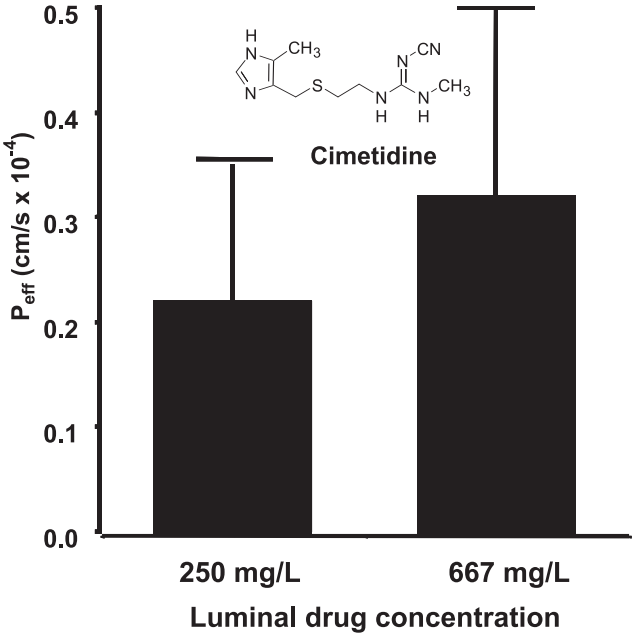

Fig. 7.14. Effective permeability (P_{eff}) of cimetidine in human jejunum at two clinically relevant luminal concentrations. A reasonable fa value for cimetidine has been estimated to 75% [90, 91]. Cimetidine may be a substrate for both P-gp and/or organic cation transporters (OCNT1 and OCNT2) [82, 92]. This investigation was performed to determine saturation in carrier-mediated transport across the intestinal epithelium. No difference was seen between the two cimetidine concentrations, and human permeability correlated well with that of the Caco-2 model (which has a low expression of carrier proteins). Hence, passive diffusion is a dominating mechanism for cimetidine [82].

intestine [93–95]. The CYP 3A4 isoform is one of the most important enzymes for oxidative drug metabolism, with about 50–60% of clinically used drugs being metabolized by this particular isoenzyme [93, 96]. Despite the higher enzymatic capacity in the liver than in the small intestine, it has been shown that the human intestine contributes significantly to the first-pass extraction of drugs subjected to metabolism by CYP 3A4 [4, 97–99]. The proposed apical recycling hypothesis is one attempt to explain this fairly high gut wall extraction despite relatively low intestinal CYP 3A4 activity in comparison with the liver. This hypothesis suggests that P-gp and CYP 3A4 act synergistically to prolong the intracellular residence time and thereby repeatedly expose the drug to the CYP 3A4 enzyme [49, 77, 100, 101]. In addition, the process may provide an active transport of formed metabolites towards the intestinal lumen which may prevent product inhibition of the enzyme [102–104]. Further evidence of the metabolism–efflux interplay is the close vicinity of P-gp and CYP 3A4 in the enterocyte [100, 105] and the overlapping substrate specificity [106]. However, strong *in vivo* evidence to support this elegant hypothesis is still lacking, and its validity *in vivo* is not evident as CYP 3A4 sub-

strates (e.g., midazolam and felodipine) undergo extensive gut wall metabolism, even though they are not subjected to any intestinal efflux [46, 107].

The intestinal epithelium has a carrier-mediated efflux system for limiting the uptake of xenobiotics, which is in turn mediated by ATP-binding cassette (ABC) transport proteins [3, 7, 108–110]. These proteins are also expressed in numerous cell types in tissues such as the liver, kidney, testes, placenta and blood–brain barrier, and may also play a role in the pharmacokinetics of drugs [108]. The multidrug-resistance transporter gene MDR1 (HUGO nomenclature: ATP-binding cassette transporter gene ABCB1) codes for P-gp and is the most extensively studied. Other multidrug transporters which are also currently under investigation include the multidrug-resistant protein family (MRP1–6) and breast cancer-resistant protein (BCRP) [46, 111, 112]. In normal situations, these proteins limit the cellular entrance and increase the excretion of agents from the cells where they are expressed [108]. Despite extensive research having been conducted to identify the importance of efflux proteins with regard to intestinal drug absorption, relatively few examples have been reported in humans [6, 107, 113, 114]. Greiner *et al.*, in 1999, reported a good example of their clinical significance, stating that the plasma concentration–time profile (i.e., bioavailability) of oral digoxin was significantly lower during rifampin treatment – a finding which was attributed to an increased expression of intestinal P-gp [8]. It has also been shown that a polymorphism in exon 26 (C34 35T) can result in a decreased intestinal expression level of P-gp, along with an increased oral bioavailability of digoxin [115, 116]. Atorvastatin (80 mg once daily) has likewise been shown to affect the steady-state pharmacokinetics of digoxin in humans [117], with the C_{max} and plasma AUC having been reported to increase by 20% and 15%, respectively. However, the renal clearance was unaffected, which suggests that this drug–drug interaction is due to increased intestinal absorption and/or decreased biliary secretion of digoxin, mediated through P-gp inhibition [117]. This was also confirmed *in vitro* (i.e., in Caco-2 cells) where atorvastatin decreased digoxin secretion by 58%; this was equivalent to the extent of inhibition seen with verapamil, a well-known P-gp inhibitor [117, 118]. Recently, several clinical studies have also claimed that an inhibition of intestinal efflux (especially of P-gp) was the major factor behind an increased bioavailability when certain drugs were co-administered [100, 119]. However, in many of these reports the most likely main mechanism was still the inhibition of CYP 3A4, and the role of the cellular efflux *in vivo* at the intestinal level remains unclear. The reason for this over-interpretation of the role of enterocyte efflux activity on intestinal drug absorption may be due to the overlapping specificities of both the substrates and inhibitors to both CYP 3A4 and P-gp [106]. Additional factors may be saturation of the efflux carrier due to high drug concentration in the intestinal lumen and/or a fairly high passive permeability component [34, 35].

A direct *in vivo* assessment of the quantitative importance of gut wall metabolism and transport of drugs and metabolites in humans is difficult and consequently has been attempted only rarely [3, 6, 11, 12, 15, 16, 23, 25–32, 34, 35, 81]. The most direct *in vivo* approach to investigating these processes in drugs with variable and incomplete bioavailability was intestinal perfusion by single-pass per-

fusion or an instillation approach (see Fig. 7.2) [3, 6, 11, 12, 15, 16, 25–32, 34, 35, 81]. In general, traditional pharmacokinetic studies may have limitations in their ability to distinguish intestinal from hepatic extraction, as is discussed by Lin *et al.* [120]. However, the obtained values of metabolic extraction of *R*/*S*-verapamil in the human gut (≈50%) and liver (≈50%) have been reported to be similar using the steady-state single-pass perfusion approach and the instillation technique [15, 34, 35], and also agree with findings in traditional pharmacokinetic studies [2, 121].

A direct *in vivo* assessment was carried out with the single-pass perfusion approach in the human jejunum by using the Loc-I-Gut technique with *R*/*S*-verapamil (log $D_{6.5}$ 2.7, octanol/water; pH 7.4; MW 455 Da) as the model compound for CYP 3A4 and P-gp-mediated local intestinal kinetics [2, 34, 35, 122] (see Figs. 7.7 and 7.9). The P_{eff} for both enantiomers at each of the concentrations (4.0, 40, 120, and 400 mg L^{-1}) was 2.5×10^{-4}, 4.7×10^{-4}, 5.5×10^{-4} and 6.7×10^{-4} cm s^{-1}, respectively (Fig. 7.15) [34, 35]. A luminal concentration of 400 mg L^{-1} is expected to be achieved in the upper part of the small intestine after oral administration of a 100-mg dose of verapamil in an immediate-release dosage form [1, 34, 35]. The three other perfusate concentrations represent fractions of the dose when 30%, 10%, and 1%, respectively are left to be absorbed [34, 35]. The increased *in vivo* jejunal P_{eff} of *R*/*S*-verapamil, along with its increased luminal perfusate concentration, is in accordance with a saturable efflux mechanism mediated by

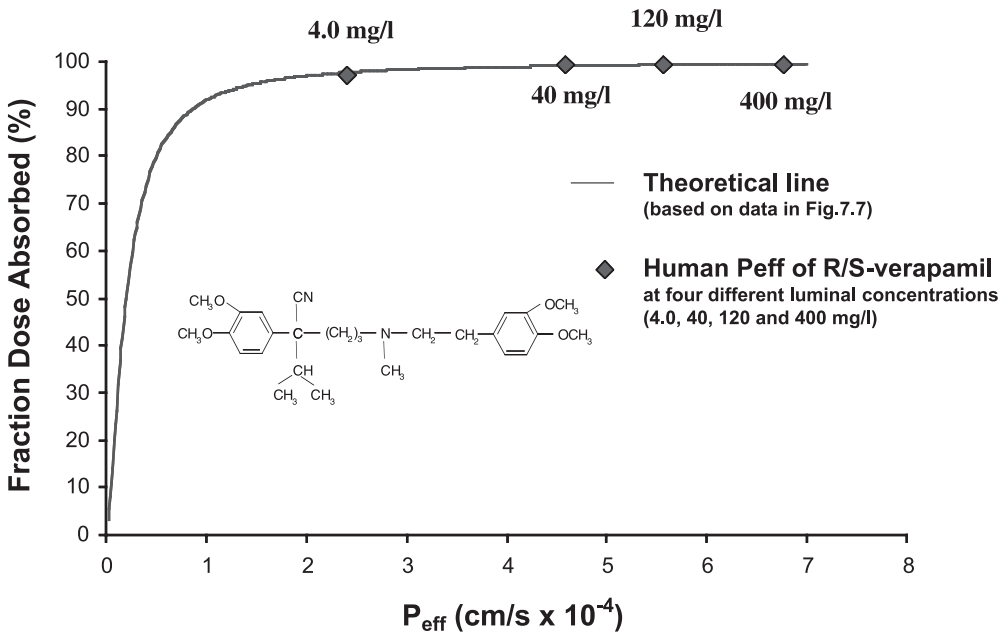

Fig. 7.15. Effective permeability (P_{eff}) of *R*/*S*-verapamil in human jejunum at four clinically relevant luminal concentrations. The measured in-vivo jejunal P_{eff} was sufficient at all perfusate concentrations (>2.0×10^{-4} cm s^{-1}) to predict complete intestinal fa following oral administration. (See text for details.)

P-gp (Fig. 7.15). Furthermore, there was no difference in P_{eff} between the *R*- and *S*-forms of verapamil at any luminal concentration, which suggests that the efflux transport cannot discriminate between the enantiomers. However, the measured *in vivo* jejunal P_{eff} was sufficient at all four perfusate concentrations ($>2.0 \times 10^{-4}$ cm s^{-1}) to predict complete intestinal fa following oral dosing (Figs. 7.7 and 7.15) [34, 35]. Together with the fact that P_{eff} and fa are excellent – as predicted for the physico-chemical properties of *R*/*S* verapamil – this suggests that passive diffusion is the dominating transport mechanism for this drug in the human intestine [34–36].

Ketoconazole, a well-known potent inhibitor of CYP 3A4 metabolism and a less potent P-gp modulator, acutely inhibited the CYP 3A4 metabolism but did not affect the P_{eff} of *R*/*S*-verapamil when they were coperfused through the human jejunal segment, with ketoconazole at 40 mg L^{-1} and *R*/*S*-verapamil at 120 mg L^{-1} (Figs. 7.9, 7.15 and 7.16) [35]. This confirms that, *in vivo*, ketoconazole is less potent as an inhibitor of P-gp in humans than is CYP 3A4, since even if verapamil is transported by passive diffusion to large extent, an increased P_{eff} would have been expected for P-gp inhibition [35, 123–125]. These findings also demonstrate that intracellular metabolism has no effect on apical drug permeability (Figs. 7.9 and 7.16). In this regard, it has been proposed that an intracellular CYP 3A4

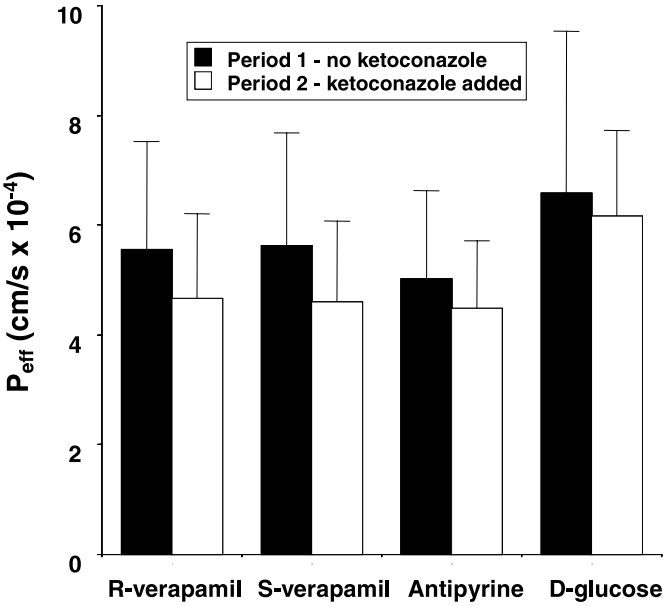

Fig. 7.16. Ketoconazole had no effect on human effective *in vivo* permeability (P_{eff}) of *R*/*S*-verapamil, antipyrine, and D-glucose. The data suggest that extensive intracellular metabolism (in the enterocyte; mediated by CYP 3A4) of substrates such as *R*/*S*-verapamil has no direct or indirect effect on P_{eff}; this was supported by the similarity in P_{eff} between *R*- and *S*-verapamil. Otherwise, the stereoselective CYP 3A4 metabolism (*S*-verapamil is more readily metabolized) would be reflected in the P_{eff} values measured *in vivo*.

metabolism may provide a more pronounced concentration gradient across the apical enterocyte membrane, which in theory should increase the intestinal permeability [120, 126, 127]. Since verapamil is transported mainly via passive diffusion and is subjected to extensive CYP 3A4 metabolism in the gut, it is considered to be a good model drug to investigate this issue in humans [2, 15, 34–36]. However, an inhibition of small intestinal metabolism did not result in a decreased jejunal P_{eff}. In addition, if intracellular CYP 3A4 metabolism would have had a pronounced effect on jejunal P_{eff}, then *S*-verapamil should have had a significantly higher intestinal permeability, as its gut wall metabolism is more extensive than is that of *R*-verapamil. However, we have shown with the Loc-I-Gut technique that the human jejunal P_{eff} for *S*- and *R*-verapamil is identical, though *S*-verapamil was subjected to a significantly higher degree of intestinal first-pass metabolism [35]. Altogether, this suggests that an extensive CYP 3A4 metabolism in the enterocyte in humans does not affect drug permeability across the apical membrane by increasing the concentration gradient across the apical enterocyte membrane (Figs. 7.9 and 7.15). A more plausible explanation may be that the concentration gradient *in vivo* across the intestinal barrier is provided by the extensive mesenteric blood flow. This would emphasize an important methodological aspect for intestinal perfusion techniques, in which a determined P_{eff} based on the disappearance rate from a perfused segment, is not affected by extensive intracellular metabolism.

The jejunal permeability and intestinal and hepatic extraction of fluvastatin, a drug which is completely metabolized by CYP 2C9, were investigated in humans by using the Loc-I-Gut technique [32]. It was shown that the contribution of the intestine to the total first-pass effect is negligible for fluvastatin. This observation agrees with the observation that CYP 2C enzymes are expressed in low amounts in the enterocytes [8, 128]. *In vitro* (i.e., in Caco-2 cells), fluvastatin showed a significant efflux ratio of about five, at clinically relevant concentrations, which was probably mediated by MRP 2. The human *in vivo* P_{eff} was high ($2.4 \pm 1.4 \times 10^{-4}$ cm s^{-1}, which demonstrates that despite a significant *in vitro* intestinal efflux fluvastatin will have a complete intestinal absorption *in vivo* (Fig. 7.7) [3, 16, 32]. This is most likely due to the significant contribution of passive intestinal permeability to the overall absorption of fluvastatin, which is in accordance with its lipophilic properties (acid pK_a 4.3, log $D_{6.5}$ 2.0, PSA 81 $Å^2$, HBD 3) (Figs. 7.10 and 7.11) [32, 36]. A similar pattern has been shown for many drugs. For instance, the determined jejunal P_{eff} for cyclosporine, a well-known CYP 3A4 and P-gp substrate, has been reported to be high and to predict a complete intestinal absorption even if the drug is subjected to significant efflux in *in vitro* cell models [2, 15, 34, 35, 129, 130]. Altogether, these directly determined *in vivo* human P_{eff} values suggest that in humans, drugs with a high passive intestinal permeability contribution to the overall absorption rate, will be completely absorbed from the gut even if they are substrates (such as verapamil, fluvastatin, losartan, and cyclosporine) for one and/or several efflux transporters. The values also suggest that drugs with a sufficiently high lipophilicity will be absorbed from the gut by passive transcellular diffusion as their main mechanism. Finally, *in vivo* data suggest that for many drugs, there

is a limited effect of intestinal active efflux on fa even if they are efflux substrates, which is in accordance with the limited number of reports that shows its clinical significance [8, 115, 116]. This may be due to a high contribution of passive diffusion as well as to the fact that these intestinally located efflux proteins may be easily saturated due to high concentrations adjacent to the intestinal membrane of the orally administered drug.

Model drugs and direct *in vivo* methods are needed in order to perform accurate investigations of the clinical significance and the pharmacogenetics of transporters and their influence on pharmacokinetics. Such model compounds should not be subjected to any metabolism, which would make the assessment of the role of transporter possible. For instance, digoxin and fexofenadine have been suggested to be model compounds to assess the phenotype for P-gp significance [8, 115, 116, 131]. We investigated the effect of ketoconazole on the measured P_{eff} for fexofenadine because concomitant oral administration of these drugs led to an increase in the C_{max} and AUC, which would be consistent with inhibition of P-gp-mediated transport [132, 133]. Fexofenadine has indeed been shown to be a substrate for P-gp in Caco-2 and L-MDR1 cells, and its disposition is altered in knockout mice lacking the gene for mdr1a [134, 135]. Hence, an expected acute effect of ketoconazole when added to the jejunal perfusion would have been an increase in jejunal P_{eff} and the plasma AUC of fexofenadine, but there was no acute effect on the jejunal P_{eff} of fexofenadine. The jejunal P_{eff} was low ($0.1–0.2 \times 10^{-4}$ cm s^{-1}) and variable which, according to the BCS, classifies it among the low-permeability compounds (Figs. 7.5 and 7.7) [1]. The reported absence of an effect of ketoconazole on fexofenadine permeability means that further *in vivo* studies are needed in order to fully understand the interaction between these two drugs. It also means that a fuller understanding of the mechanisms involved is needed before the general conclusion – that fexofenadine is a typical *in vivo* probe for P-gp activity in humans – can be drawn. Our understanding of the expression of transporters and their functional activity in different human tissues is at an early stage, and there is a need for more *in vivo* pharmacokinetic data to be acquired in order validate *in vitro* methods of studying drug transport in terms of both quantitative and qualitative aspects [107].

In a recent publication, Glaeser *et al.* have shown that the majority of shed human enterocytes collected from an intestinal perfusion were still functionally active and did not show signs of apoptosis [38]. Based on a validation of the Loc-I-Gut system for the study of gene expression during perfusion, changes of mRNA levels in shed enterocytes before and after perfusion of a 10 cm-long jejunal segment were studied in parallel to the intestinal permeability, metabolism of selected compounds in the gut wall and the excretion of their metabolites back into the lumen (see Fig. 7.4) [39]. Sulforaphane and quercetin-3,4′-diglucoside were rapidly effluxed back into the lumen as sulforaphane-glutathione and quercetin-3′-glucuronide conjugates, respectively. Gene expression analysis in exfoliated enterocytes showed 1.8 ± 0.5-fold (range 1.1–2.3) induction of glutathione transferase A1 (GST) mRNA and 2.1 ± 1.3 (range 0.7–4.0) induction of UDP-glucuronosyltransferase 1A1 (UGT1A1) mRNA after only 90-min exposure to these two com-

pounds. The technique demonstrates it usefulness to elucidate intracellular processes and relate to temporal changes in gene expression (see Fig. 7.4) [38, 39].

7.8 Regional Differences in Transport and Metabolism of Drugs

Regional differences in the transport and metabolism of drugs, especially in the colon, have not been investigated thoroughly in humans by using intestinal perfusion techniques. Therefore, there is a need to develop clinical techniques that make it possible to directly investigate the transport and metabolism *in vivo* of drugs in various regions of the GI tract. This would certainly improve our understanding of regional differences of the transport and metabolism of drugs – an understanding that is crucial for the development of orally controlled release systems, which have received increased attention as they create new therapeutic opportunities. In addition, regional absorption and metabolism may also affect the local effect of a drug, which is targeted to a certain region where diseases such as inflammatory bowel disease (IBD) and colon cancer are localized [136].

Investigations of regional differences in permeability and metabolism have been carried out using a variety of animal models [22, 29, 75, 102, 109, 112, 137]. Animal tissues (mainly from rats) are widely used in the Ussing chamber to investigate intestinal transport of drugs, and regional aspects [29, 75, 138], whereas few studies have been conducted with human tissues due to their limited availability.

Regional differences regarding functional activity of P-gp have been reported in only very few cases, and are mainly based on animal studies [22, 75, 109, 112, 137]. For instance, one of the few systemic kinetic analyses of efflux activity showed that marked differences exist along the different regions of the rat GI tract [112], with maximal transporter activity varying over a four- to five-fold range in the order ileum > jejunum > colon. Previous studies have claimed that MDR1 mRNA levels should be highest in the human colon [129]; however, recent investigations have reported that P-gp is more readily expressed in the small intestine than in the colorectal region [50, 109]. Interestingly, Nakamura *et al.* in 2002 reported that in their study, MDR1, MRP1 and CYP 3A mRNA levels were higher in human duodenal tissue than in normal colorectal tissue and colorectal adenocarcinoma tissue [50]. Although there are inconsistencies among reported MDR1 mRNA levels and P-gp-mediated efflux activity in the small intestine and colon, these may be attributed to wide species differences, as well as to variations in methodology and study design [107, 109, 112, 129, 137, 144].

It has also been shown *in vitro*, by using rat small intestinal and colonic tissue in an Ussing chamber, that the low-permeability drugs (BCS classes III–IV) have an even lower permeability in the colon, whereas high-permeability drugs (BCS classes I–II) show a slightly higher permeability in the colon when passive diffusion is the dominating mechanism (see Fig. 7.5) [75]. This intestinal permeability pattern has also been shown to be relevant for small and large intestinal specimens from humans applied to the Ussing chamber model [104]. A regional difference

in permeability for five different compounds has been reported from a study that applied an open triple-lumen tube and perfused an 80 cm-long segment of human jejunum and ileum (see Fig. 7.2) [139]. The P_{eff} for hydrochlorothiazide, atenolol, furosemide and cimetidine – all of which are classified as low-permeability drugs according to the BCS – decreased in the ileum in comparison with the jejunum [3, 139]. This *in vivo* observation is in agreement with the regional Ussing chamber studies in rats for low-permeability compounds [75]. Salicylic acid, which is highly permeable, was well absorbed throughout the small intestine. The small intestinal regional permeability pattern has also been demonstrated for ranitidine (low-permeability) and paracetamol (acetaminophen) and griseofulvin (two high-permeability compounds), using a similar open intestinal perfusion technique [140–142]. *In vivo* permeability measurements of drugs in the colonic/rectal region in humans are difficult to perform, and this most likely explains why so few data have been published. However, we developed and validated a new technique for the perfusion of a defined and closed segment in the colon/rectum [143]. We observed that the permeability of antipyrine in the rectal region was high, while D-glucose was not absorbed – which is in accordance with the fact that passive diffusion is the dominating drug absorption mechanism in this specific intestinal region. However, we found the present technique valuable for studying drug absorption from the human rectum, and this encouraged us to investigate the influence of a penetration enhancer, sodium caprate, on the rectal absorption of phenoxymethyl penicillin and antipyrine [12]. The data generated suggest that sodium caprate alone has a limited effect on the permeability *in vivo* across the rectal epithelium when it is presented in solution. Interestingly, there was a correlation between P_{eff} for sodium caprate and the individual plasma AUC and C_{max} of phenoxymethyl penicillin, which indicates that the permeability of an enhancer in the tissue upon which it should act is crucial if an effect is to be achieved.

7.9 Conclusion

Overall, in this chapter we have attempted to emphasize the need for more *in vivo* studies to be conducted to clarify the dynamic interplay between mechanisms of drug transport and metabolism in the human intestine under *in vivo* conditions. There is also a need to develop additional *in vivo* techniques for direct measurements of these processes in regions along the GI tract in humans, and to relate the findings to various physiological/pathophysiological conditions. This would clearly increase our knowledge of the mechanisms involved, and provide *in vivo* data to help develop and validate rapid and reliable *in vitro* intestinal models.

References

1 Amidon, G. L., Lennernäs, H., Shah, V. P., Crison, J. R., A theoretical basis for a biopharmaceutic drug classification: the correlation of

in vitro drug product dissolution and in vivo bioavailability, *Pharm. Res.* **1995**, *12*, 413–420.

2 Fromm, M. F., Busse, D., Kroemer, H. K., Eichelbaum, M., Differential induction of prehepatic and hepatic metabolism of verapamil by rifampin, *Hepatology* **1996**, *24*, 796–801.

3 Lennernäs, H., Human intestinal permeability, *J. Pharm. Sci.* **1998**, *87*, 403–410.

4 Wu, C. Y., Benet, L. Z., Hebert, M. F., Gupta, S. K., Rowland, M. *et al.*, Differentiation of absorption and first-pass gut and hepatic metabolism in humans: studies with cyclosporine, *Clin. Pharmacol. Ther.* **1995**, *58*, 492–497.

5 Csáky, T. Z., Methods for investigation of intestinal permeability, in: *Pharmacology of Intestinal Permeability I*, Springer-Verlag, Berlin, **1984**, pp. 91–112.

6 Gramatte, T., Oertel, R., Terhaag, B., Kirch, W., Direct demonstration of small intestinal secretion and site-dependent absorption of the beta-blocker talinolol in humans, *Clin. Pharmacol. Ther.* **1996**, *59*, 541–549.

7 Zhang, Y., Benet, L. Z., The gut as a barrier to drug absorption: combined role of cytochrome P450 3A and P-glycoprotein, *Clin. Pharmacokinet.* **2001**, *40*, 159–168.

8 Greiner, B., Eichelbaum, M., Fritz, P., Kreichgauer, H. P., von Richter, O. *et al.*, The role of intestinal P-glycoprotein in the interaction of digoxin and rifampin, *J. Clin. Invest.* **1999**, *104*, 147–153.

9 Roden, D. M., George, A. L. J., The genetic basis of variability in drug responses, *Nature Rev. Drug Discov.* **2002**, *1*, 37–44.

10 Evans, W. E., Relling, M. V., Pharmacogenomics: translating functional genomics into rational therapeutics, *Science* **1999**, *286*, 487–491.

11 Lennernäs, H., Ahrenstedt, O., Hallgren, R., Knutson, L., Ryde, M. *et al.*, Regional jejunal perfusion, a new in vivo approach to study oral drug absorption in man, *Pharm. Res.* **1992**, *9*, 1243–1251.

12 Lennernäs, H., Gjellan, K., Hallgren, R., Graffner, C., The influence of caprate on rectal absorption of phenoxymethyl-penicillin: experience from an in-vivo perfusion in humans, *J. Pharm. Pharmacol.* **2002**, *54*, 499–508.

13 Knutson, L., Odlind, B., Hallgren, R., A new technique for segmental jejunal perfusion in man, *Am. J. Gastroenterol.* **1989**, *84*, 1278–1284.

14 Phillips, S. F., Summerskill, W. H., Occlusion of the jejunum for intestinal perfusion in man, *Mayo Clin. Proc.* **1966**, *41*, 224–231.

15 von Richter, O., Greiner, B., Fromm, M. F., Fraser, R., Omari, T. *et al.*, Determination of in vivo absorption, metabolism, and transport of drugs by the human intestinal wall and liver with a novel perfusion technique, *Clin. Pharmacol. Ther.* **2001**, *70*, 217–227.

16 Lennernäs, H., Human jejunal effective permeability and its correlation with preclinical drug absorption models, *J. Pharm. Pharmacol.* **1997**, *49*, 627–638.

17 Ahrenstedt, O., Knutson, L., Nilsson, B., Nilsson-Ekdahl, K., Odlind, B. *et al.*, Enhanced local production of complement components in the small intestines of patients with Crohn's disease, *N. Engl. J. Med.* **1990**, *322*, 1345–1349.

18 Bonlokke, L., Hovgaard, L., Kristensen, H. G., Knutson, L., Lennernäs, H., Direct estimation of the in vivo dissolution of spironolactone, in two particle size ranges, using the single-pass perfusion technique (Loc-I-Gut) in humans, *Eur. J. Pharm. Sci.* **2001**, *12*, 239–250.

19 Bonlokke, L., Christensen, F. N., Knutson, L., Kristensen, H. G., Lennernäs, H., A new approach for direct in vivo dissolution studies of poorly soluble drugs, *Pharm. Res.* **1997**, *14*, 1490–1492.

20 Fagerholm, U., Borgstrom, L., Ahrenstedt, O., Lennernäs, H., The

lack of effect of induced net fluid absorption on the in vivo permeability of terbutaline in the human jejunum, *J. Drug Target.* **1995**, *3*, 191–200.

21 Fagerholm, U., Johansson, M., Lennernäs, H., Comparison between permeability coefficients in rat and human jejunum, *Pharm. Res.* **1996**, *13*, 1336–1342.

22 Fagerholm, U., Lindahl, A., Lennernäs, H., Regional intestinal permeability in rats of compounds with different physicochemical properties and transport mechanisms, *J. Pharm. Pharmacol.* **1997**, *49*, 687–690.

23 Fagerholm, U., Nilsson, D., Knutson, L., Lennernäs, H., Jejunal permeability in humans in vivo and rats in situ: investigation of molecular size selectivity and solvent drag, *Acta Physiol. Scand.* **1999**, *165*, 315–324.

24 Knutson, L., Ahrenstedt, O., Odlind, B., Hallgren, R., The jejunal secretion of histamine is increased in active Crohn's disease. *Gastroenterology* **1990**, *98*, 849–854.

25 Lennernäs, H., Ahrenstedt, O., Ungell, A. L., Intestinal drug absorption during induced net water absorption in man; a mechanistic study using antipyrine, atenolol and enalaprilat, *Br. J. Clin. Pharmacol.* **1994**, *37*, 589–596.

26 Lennernäs, H., Crison, J. R., Amidon, G. L., Permeability and clearance views of drug absorption: a commentary, *J. Pharmacokinet. Biopharm.* **1995**, *23*, 333–343.

27 Lennernäs, H., Does fluid flow across the intestinal mucosa affect quantitative oral drug absorption? Is it time for a reevaluation?, *Pharm. Res.* **1995**, *12*, 1573–1582.

28 Lennernäs, H., Palm, K., Fagerholm, U., Artursson, P., Comparison between active and passive drug transport in human intestinal epithelial (Caco-2) cells in vitro and human jejunum in vivo, *Int. J. Pharm.* **1996**, *127*, 103–107.

29 Lennernäs, H., Nylander, S., Ungell, A. L., Jejunal permeability: a comparison between the Ussing chamber technique and the single-pass perfusion in humans, *Pharm. Res.* **1997**, *14*, 667–671.

30 Lennernäs, H., Lee, I. D., Fagerholm, U., Amidon, G. L., A residence-time distribution analysis of the hydrodynamics within the intestine in man during a regional single-pass perfusion with Loc-I-Gut: in-vivo permeability estimation, *J. Pharm. Pharmacol.* **1997**, *49*, 682–686.

31 Lennernäs, H., Knutson, L., Knutson, T., Hussain, A., Lesko, L. *et al.*, The effect of amiloride on the in vivo effective permeability of amoxicillin in human jejunum: experience from a regional perfusion technique, *Eur. J. Pharm. Sci.* **2002**, *15*, 271–277.

32 Lindahl, A., Sandstrom, R., Ungell, A. L., Abrahamsson, B., Knutson, T. W. *et al.*, Jejunal permeability and hepatic extraction of fluvastatin in humans, *Clin. Pharmacol. Ther.* **1996**, *60*, 493–503.

33 Lindahl, A., Ungell, A. L., Knutson, L., Lennernäs, H., Characterization of fluids from the stomach and proximal jejunum in men and women, *Pharm. Res.* **1997**, *14*, 497–502.

34 Sandstrom, R., Karlsson, A., Knutson, L., Lennernäs, H., Jejunal absorption and metabolism of *R*/*S*-verapamil in humans, *Pharm. Res.* **1998**, *15*, 856–862.

35 Sandstrom, R., Knutson, T. W., Knutson, L., Jansson, B., Lennernäs, H., The effect of ketoconazole on the jejunal permeability and CYP3A metabolism of (*R*/*S*)-verapamil in humans, *Br. J. Clin. Pharmacol.* **1999**, *48*, 180–189.

36 Winiwarter, S., Bonham, N. M., Ax, F., Hallberg, A., Lennernäs, H. *et al.*, Correlation of human jejunal permeability (in vivo) of drugs with experimentally and theoretically derived parameters. A multivariate data analysis approach, *J. Med. Chem.* **1998**, *41*, 4939–4949.

37 CDER Waiver of in vivo bioavailability and bioequivalence studies for

immediate-release solid oral dosage forms based on a biopharmaceutics classification system, Food and Drug Administration, **2000**.

38 Glaeser, H., Drescher, S., van der Kuip, H., Behrens, C., Geick, A. *et al.*, Shed human enterocytes as a tool for the study of expression and function of intestinal drug-metabolizing enzymes and transporters, *Clin. Pharmacol. Ther.* **2002**, *71*, 131–140.

39 Petri, N., Tannergren, C., Bennett, R. N., Holst, B., Bao, Y. *et al.*, Intestinal absorption and metabolism of sulforaphane and quercetin as well as regulation of phase II enzymes in human jejunum in vivo and in Caco-2 cells, *Drug Metab. Dispos.* **2003** (in press).

40 Rowland, M., Tozer, T. N., *Clinical Pharmacokinetics: Concepts and Applications*, 3rd edition, Williams & Wilkins, Media, **1995**.

41 Dressman, J. B., Amidon, G. L., Reppas, C., Shah, V. P., Dissolution testing as a prognostic tool for oral drug absorption: immediate release dosage forms, *Pharm. Res.* **1998**, *15*, 11–22.

42 Komiya, I., Park, J. Y., Kamani, A., Higuchi, W. I., Quantitative mechanistic studies in simultaneous fluid flow and intestinal absorption using steroids as model solutes, *Int. J. Pharm.* **1980**, *4*, 249–262.

43 Levitt, M. D., Furne, J. K., Strocchi, A., Anderson, B. W., Levitt, D. G., Physiological measurements of luminal stirring in the dog and human small bowel, *J. Clin. Invest.* **1990**, *86*, 1540–1547.

44 Oberle, R. L., Chen, T. S., Lloyd, C., Barnett, J. L., Owyang, C. *et al.*, The influence of the interdigestive migrating myoelectric complex on the gastric emptying of liquids, *Gastroenterology* **1990**, *99*, 1275–1282.

45 Sandberg, A., Abrahamsson, B., Sjogren, J., Influence of dissolution rate on the extent and rate of bioavailability of metoprolol, *Int. J. Pharm.* **1991**, *68*, 167–177.

46 Suzuki, H., Sugiyama, Y., Role of metabolic enzymes and efflux transporters in the absorption of drugs from the small intestine, *Eur. J. Pharm. Sci.* **2000**, *12*, 3–12.

47 Lande, M. B., Donovan, J. M., Zeidel, M. L., The relationship between membrane fluidity and permeabilities to water, solutes, ammonia, and protons, *J. Gen. Physiol.* **1995**, *106*, 67–84.

48 Artursson, P., Epithelial transport of drugs in cell culture. I: a model for studying the passive diffusion of drugs over intestinal absorptive (Caco-2) cells, *J. Pharm. Sci.* **1990**, *79*, 476–482.

49 Benet, L. Z., Cummins, C. L., The drug efflux-metabolism alliance: biochemical aspects, *Adv. Drug Deliv. Rev.* **2001**, *50* (Suppl. 1), S3–S11.

50 Nakamura, T., Sakaeda, T., Ohmoto, N., Tamura, T., Aoyama, N. *et al.*, Real-time quantitative polymerase chain reaction for MDR1, MRP1, MRP2, and CYP3A-mRNA levels in Caco-2 cell lines, human duodenal enterocytes, normal colorectal tissues, and colorectal adenocarcinomas, *Drug Metab. Dispos.* **2002**, *30*, 4–6.

51 de Waziers, I., Cugnenc, P. H., Yang, C. S., Leroux, J. P., Beaune, P. H., Cytochrome P 450 isoenzymes, epoxide hydrolase and glutathione transferases in rat and human hepatic and extrahepatic tissues, *J. Pharmacol. Exp. Ther.* **1990**, *253*, 387–394.

52 Lindahl, A., Borestrom, C., Landin, A., Ungell, A. L., Abrahamsson, B., In vitro Metabolism in the Colonic Lumen. EUFEPS World Conference on Drug Absorption and Drug Delivery Benefiting from the New Biology and Informatics, Copenhagen, **2001**.

53 Goldin, B. R., Intestinal microflora: metabolism of drugs and carcinogens, *Ann. Med.* **1990**, *22*, 43–48.

54 The fall and rise of in vivo pharmacology, *Trends Pharmacol. Sci.* **2002**, *23*, 13–18.

55 Lande, M. B., Priver, N. A., Zeidel, M. L., Determinants of apical membrane permeabilities of barrier

epithelia, *Am. J. Physiol.* **1994**, *267*, C367–C374.

56 Mouritsen, O. G., Jorgensen, K., A new look at lipid-membrane structure in relation to drug research, *Pharm. Res.* **1998**, *15*, 1507–1519.

57 Krondahl, E., Orzechowski, A., Ekstrom, G., Lennernäs, H., Rat jejunal permeability and metabolism of mu-selective tetrapeptides in gastrointestinal fluids from humans and rats, *Pharm. Res.* **1997**, *14*, 1780–1785.

58 Langguth, P., Bohner, V., Heizmann, J., Merkle, H. P. *et al.*, The challenge of proteolytic enzymes in intestinal peptide delivery, *J. Controlled Release* **1997**, *46*, 29–57.

59 Madara, J. L., Pappenheimer, J. R., Structural basis for physiological regulation of paracellular pathways in intestinal epithelia, *J. Membr. Biol.* **1987**, *100*, 149–164.

60 Soergel, K. H., Showdown at the tight junction, *Gastroenterology* **1993**, *105*, 1247–1250.

61 van De Waterbeemd, H., Smith, D. A., Beaumont, K., Walker, D. K., Property-based design: optimization of drug absorption and pharmacokinetics, *J. Med. Chem.* **2001**, *44*, 1313–1333.

62 Pappenheimer, J. R., Reiss, K. Z., Contribution of solvent drag through intercellular junctions to absorption of nutrients by the small intestine of the rat, *J. Membr. Biol.* **1987**, *100*, 123–136.

63 Smith, D. A., Jones, B. C., Walker, D. K., Design of drugs involving the concepts and theories of drug metabolism and pharmacokinetics, *Med. Res. Rev.* **1996**, *16*, 243–266.

64 Nilsson, D., Fagerholm, U., Lennernäs, H., The influence of net water absorption on the permeability of antipyrine and levodopa in the human jejunum, *Pharm. Res.* **1994**, *11*, 1540–1547.

65 Uhing, M. R., Kimura, R. E., The effect of surgical bowel manipulation and anesthesia on intestinal glucose absorption in rats, *J. Clin. Invest.* **1995**, *95*, 2790–2798.

66 Sadowski, D. C., Meddings, J. B., Luminal nutrients alter tight-junction permeability in the rat jejunum: an in vivo perfusion model, *Can. J. Physiol. Pharmacol.* **1993**, *71*, 835–839.

67 Fine, K. D., Santa Ana, C. A., Porter, J. L., Fordtran, J. S., Mechanism by which glucose stimulates the passive absorption of small solutes by the human jejunum in vivo, *Gastroenterology* **1994**, *107*, 389–395.

68 Pappenheimer, J. R., Dahl, C. E., Karnovsky, M. L., Maggio, J. E., Intestinal absorption and excretion of octapeptides composed of D amino acids, *Proc. Natl. Acad. Sci. USA* **1994**, *91*, 1942–1945.

69 Karlsson, J., Kuo, S. M., Ziemniak, J., Artursson, P., Transport of celiprolol across human intestinal epithelial (Caco-2) cells: mediation of secretion by multiple transporters including P-glycoprotein, *Br. J. Pharmacol.* **1993**, *110*, 1009–1016.

70 Walle, U. K., Pesola, G. R., Walle, T., Stereoselective sulphate conjugation of salbutamol in humans: comparison of hepatic, intestinal and platelet activity, *Br. J. Clin. Pharmacol.* **1993**, *35*, 413–418.

71 Nyberg, L., Pharmacokinetic parameters of terbutaline in healthy man. An overview, *Eur. J. Respir. Dis. Suppl.* **1984**, *134*, 149–160.

72 Amelsberg, A., Schteingart, C. D., Ton-Nu, H. T., Hofmann, A. F., Carrier-mediated jejunal absorption of conjugated bile acids in the guinea pig, *Gastroenterology* **1996**, *110*, 1098–1106.

73 Fagerholm, U., Lennernäs, H., Experimental estimation of the effective unstirred water layer thickness in the human jejunum, and its importance in oral drug absorption. *Eur. J. Pharm. Sci.* **1995**, *3*, 247–253.

74 Anderson, B. W., Levine, A. S., Levitt, D. G., Kneip, J. M., Levitt, M. D., Physiological measurement of luminal stirring in perfused rat jejunum, *Am. J. Physiol.* **1988**, *254*, G843–G848.

75 Ungell, A. L., Nylander, S., Bergstrand, S., Sjoberg, A., Lennernäs, H., Membrane transport of drugs in different regions of the intestinal tract of the rat, *J. Pharm. Sci.* **1998**, *87*, 360–366.

76 Jack, D. B., *Handbook of Clinical Pharmacokinetic Data*, Macmillan Publishers Ltd, Basingstoke, **1992**.

77 Johnson, B. M., Charman, W. N., Porter, C. J., The impact of P-glycoprotein efflux on enterocyte residence time and enterocyte-based metabolism of verapamil, *J. Pharm. Pharmacol.* **2001**, *53*, 1611–1619.

78 Hammarlund-Udenaes, M., Benet, L. Z., Furosemide pharmacokinetics and pharmacodynamics in health and disease – an update, *J. Pharmacokinet. Biopharm.* **1989**, *17*, 1–46.

79 Ponto, L. L., Schoenwald, R. D., Furosemide (frusemide). A pharmacokinetic/pharmacodynamic review (Part I), *Clin. Pharmacokinet.* **1990**, *18*, 381–408.

80 Flanagan, S. D., Takahashi, L. H., Liu, X., Benet, L. Z., Contributions of saturable active secretion, passive transcellular, and paracellular diffusion to the overall transport of furosemide across adenocarcinoma (Caco-2) cells, *J. Pharm. Sci.* **2002**, *91*, 1169–1177.

81 Lennernäs, H., Nilsson, D., Aquilonius, S. M., Ahrenstedt, O., Knutson, L. *et al.*, The effect of L-leucine on the absorption of levodopa, studied by regional jejunal perfusion in man, *Br. J. Clin. Pharmacol.* **1993**, *35*, 243–250.

82 Sun, D., Lennernäs, H., Welage, L. S., Barnett, J., Landowaki, C. P. *et al.*, A Comparison of human and Caco-2 gene expression profiles for 12,000 genes and the permeabilities of 26 drugs in the human intestine and Caco-2 cells, *Pharm. Res.* **2002**, *19*, 1400–1416.

83 Adibi, S. A., The oligopeptide transporter (Pept-1) in human intestine: biology and function, *Gastroenterology* **1997**, *113*, 332–340.

84 Paintaud, G., Alvan, G., Dahl, M. L., Grahnen, A., Sjovall, J. *et al.*, Nonlinearity of amoxicillin absorption kinetics in human, *Eur. J. Clin. Pharmacol.* **1992**, *43*, 283–288.

85 Chulavatnatol, S., Charles, B. G., Determination of dose-dependent absorption of amoxycillin from urinary excretion data in healthy subjects, *Br. J. Clin. Pharmacol.* **1994**, *38*, 274–277.

86 Shiraga, T., Miyamoto, K., Tanaka, H., Yamamoto, H., Taketani, Y. *et al.*, Cellular and molecular mechanisms of dietary regulation on rat intestinal H^+/Peptide transporter PepT1, *Gastroenterology* **1999**, *116*, 354–362.

87 Thamotharan, M., Bawani, S. Z., Zhou, X., Adibi, S. A., Hormonal regulation of oligopeptide transporter pept-1 in a human intestinal cell line, *Am. J. Physiol.* **1999**, *276*, C821–C826.

88 Swaan, P. W., Koops, B. C., Moret, E. E., Tukker, J. J., Mapping the binding site of the small intestinal peptide carrier (PepT1) using comparative molecular field analysis, *Receptors Channels* **1998**, *6*, 189–200.

89 Chu, X. Y., Sanchez-Castano, G. P., Higaki, K., Oh, D. M., Hsu, C. P. *et al.*, Correlation between epithelial cell permeability of cephalexin and expression of intestinal oligopeptide transporter, *J. Pharmacol. Exp. Ther.* **2001**, *299*, 575–582.

90 Grahnen, A., The impact of time dependent phenomena on bioequivalence studies in: *Topics in Pharmaceutical Sciences*, Elsevier, Amsterdam, **1985**, pp. 179–190.

91 Grahnen, A., von Bahr, C., Lindstrom, B., Rosen, A., Bioavailability and pharmacokinetics of cimetidine, *Eur. J. Clin. Pharmacol.* **1979**, *16*, 335–340.

92 Collett, A., Higgs, N. B., Sims, E., Rowland, M., Warhurst, G., Modulation of the permeability of H2 receptor antagonists cimetidine and ranitidine by P-glycoprotein in rat intestine and the human colonic cell line Caco-2, *J. Pharmacol. Exp. Ther.* **1999**, *288*, 171–178.

93 Guengerich, F. P., Cytochrome P-450 3A4: regulation and role in drug

metabolism, *Annu. Rev. Pharmacol. Toxicol.* **1999**, *39*, 1–17.

94 Eichelbaum, M., Burk, O., CYP3A genetics in drug metabolism, *Nature Med.* **2001**, *7*, 285–287.

95 Paine, M. F., Khalighi, M., Fisher, J. M., Shen, D. D., Kunze, K. L. *et al.*, Characterization of interintestinal and intraintestinal variations in human CYP3A-dependent metabolism. *J. Pharmacol. Exp. Ther.* **1997**, *283*, 1552–1562.

96 Shimada, T., Yamazaki, H., Mimura, M., Inui, Y., Guengerich, F. P., Interindividual variations in human liver cytochrome P-450 enzymes involved in the oxidation of drugs, carcinogens and toxic chemicals: studies with liver microsomes of 30 Japanese and 30 Caucasians, *J. Pharmacol. Exp. Ther.* **1994**, *270*, 414–423.

97 Regardh, C. G., Edgar, B., Olsson, R., Kendall, M., Collste, P. *et al.*, Pharmacokinetics of felodipine in patients with liver disease, *Eur. J. Clin. Pharmacol.* **1989**, *36*, 473–479.

98 Paine, M. F., Shen, D. D., Kunze, K. L., Perkins, J. D., Marsh, C. L. *et al.*, First-pass metabolism of midazolam by the human intestine, *Clin. Pharmacol. Ther.* **1996**, *60*, 14–24.

99 Thummel, K. E., O'Shea, D., Paine, M. F., Shen, D. D., Kunze, K. L. *et al.*, Oral first-pass elimination of midazolam involves both gastrointestinal and hepatic CYP3A-mediated metabolism, *Clin. Pharmacol. Ther.* **1996**, *59*, 491–502.

100 Watkins, P. B., The barrier function of CYP3A4 and P-glycoprotein in the small bowel, *Adv. Drug Deliv. Rev.* **1997**, *27*, 161–170.

101 Ito, K., Kusuhara, H., Sugiyama, Y., Effects of intestinal CYP3A4 and P-glycoprotein on oral drug absorption – theoretical approach, *Pharm. Res.* **1999**, *16*, 225–231.

102 Lampen, A., Zhang, Y., Hackbarth, I., Benet, L. Z., Sewing, K. F. *et al.*, Metabolism and transport of the macrolide immunosuppressant sirolimus in the small intestine, *J. Pharmacol. Exp. Ther.* **1998**, *285*, 1104–1112.

103 Hochman, J. H., Chiba, M., Nishime, J., Yamazaki, M., Lin, J. H., Influence of P-glycoprotein on the transport and metabolism of indinavir in Caco-2 cells expressing cytochrome P-450 3A4, *J. Pharmacol. Exp. Ther.* **2000**, *292*, 310–318.

104 Berggren, S., Lennernäs, P., Ekelund, M., Westrom, B., Hoogstraate, J. *et al.*, Regional difference in permeability and metabolism of ropivacaine and its CYP 3A4 metabolite PPX in human intestine, *J. Pharm. Pharmol.* **2003** (in press).

105 Cummins, C. L., Mangravite, L. M., Benet, L. Z., Characterizing the expression of CYP3A4 and efflux transporters (P-gp, MRP1, and MRP2) in CYP3A4-transfected Caco-2 cells after induction with sodium butyrate and the phorbol ester 12-*O*-tetradecanoylphorbol-13-acetate, *Pharm. Res.* **2001**, *18*, 1102–1109.

106 Wacher, V. J., Wu, C. Y., Benet, L. Z., Overlapping substrate specificities and tissue distribution of cytochrome P450 3A and P-glycoprotein: implications for drug delivery and activity in cancer chemotherapy, *Mol. Carcinogen.* **1995**, *13*, 129–134.

107 Tucker, G. T., Houston, J. B., Huang, S. M., Optimizing drug development: strategies to assess drug metabolism/transporter interaction potential – towards a consensus, *Br. J. Clin. Pharmacol.* **2001**, *52*, 107–117.

108 Klein, I., Sarkadi, B., Varadi, A., An inventory of the human ABC proteins, *Biochim. Biophys. Acta* **1999**, *1461*, 237–262.

109 Makhey, V. D., Guo, A., Norris, D. A., Hu, P., Yan, J. *et al.*, Characterization of the regional intestinal kinetics of drug efflux in rat and human intestine and in Caco-2 cells, *Pharm. Res.* **1998**, *15*, 1160–1167.

110 Martin, C., Berridge, G., Higgins, C. F., Mistry, P., Charlton, P. *et al.*, Communication between multiple drug binding sites on P-glycoprotein, *Mol. Pharmacol.* **2000**, *58*, 624–632.

111 Jonker, J. W., Smit, J. W., Brinkhuis, R. F., Maliepaard, M., Beijnen, J. H. *et al.*, Role of breast cancer resistance protein in the bioavailability and fetal penetration of topotecan, *J. Natl. Cancer Inst.* **2000**, *92*, 1651–1656.

112 Stephens, R. H., O'Neill, C. A., Warhurst, A., Carlson, G. L., Rowland, M. *et al.*, Kinetic profiling of P-glycoprotein-mediated drug efflux in rat and human intestinal epithelia, *J. Pharmacol. Exp. Ther.* **2001**, *296*, 584–591.

113 Schwarz, U. I., Gramatte, T., Krappweis, J., Oertel, R., Kirch, W., P-glycoprotein inhibitor erythromycin increases oral bioavailability of talinolol in humans, *Int. J. Clin. Pharmacol. Ther.* **2000**, *38*, 161–167.

114 Gramatte, T., Oertel, R., Intestinal secretion of intravenous talinolol is inhibited by luminal *R*-verapamil, *Clin. Pharmacol. Ther.* **1999**, *66*, 239–245.

115 Hoffmeyer, S., Burk, O., von Richter, O., Arnold, H. P., Brockmoller, J. *et al.*, Functional polymorphisms of the human multidrug-resistance gene: multiple sequence variations and correlation of one allele with P-glycoprotein expression and activity in vivo, *Proc. Natl. Acad. Sci. USA* **2000**, *97*, 3473–3478.

116 Sakaeda, T., Nakamura, T., Horinouchi, M., Kakumoto, M., Ohmoto, N. *et al.*, MDR1 genotype-related pharmacokinetics of digoxin after single oral administration in healthy Japanese subjects, *Pharm. Res.* **2001**, *18*, 1400–1404.

117 Boyd, R. A., Stern, R. H., Stewart, B. H., Wu, X., Reyner, E. L. *et al.*, Atorvastatin coadministration may increase digoxin concentrations by inhibition of intestinal P-glycoprotein-mediated secretion. *J. Clin. Pharmacol.* **2000**, *40*, 91–98.

118 Bogman, K., Peyer, A. K., Torok, M., Kusters, E., Drewe, J., HMG-CoA reductase inhibitors and P-glycoprotein modulation, *Br. J. Pharmacol.* **2001**, *132*, 1183–1192.

119 Floren, L. C., Bekersky, I., Benet, L. Z., Mekki, Q., Dressler, D. *et al.*, Tacrolimus oral bioavailability doubles with coadministration of ketoconazole, *Clin. Pharmacol. Ther.* **1997**, *62*, 41–49.

120 Lin, J. H., Chiba, M., Baillie, T. A., Is the role of the small intestine in first-pass metabolism overemphasized?, *Pharmacol. Rev.* **1999**, *51*, 135–158.

121 Fromm, M. F., Dilger, K., Busse, D., Kroemer, H. K., Eichelbaum, M. *et al.*, Gut wall metabolism of verapamil in older people: effects of rifampicin-mediated enzyme induction, *Br. J. Clin. Pharmacol.* **1998**, *45*, 247–255.

122 Loo, T. W., Clarke, D. M., Defining the drug-binding site in the human multidrug resistance P-glycoprotein using a methanethiosulfonate analog of verapamil, MTS-verapamil, *J. Biol. Chem.* **2001**, *276*, 14972–14979.

123 Zhang, Y., Hsieh, Y., Izumi, T., Lin, E. T., Benet, L. Z., Effects of ketoconazole on the intestinal metabolism, transport and oral bioavailability of K02, a novel vinylsulfone peptidomimetic cysteine protease inhibitor and a P450 3A, P-glycoprotein dual substrate, in male Sprague-Dawley rats, *J. Pharmacol. Exp. Ther.* **1998**, *287*, 246–252.

124 von Moltke, L. L., Greenblatt, D. J., Duan, S. X., Harmatz, J. S., Shader, R. I., In vitro prediction of the terfenadine-ketoconazole pharmacokinetic interaction, *J. Clin. Pharmacol.* **1994**, *34*, 1222–1227.

125 Gibbs, M. A., Thummel, K. E., Shen, D. D., Kunze, K. L., Inhibition of cytochrome P-450 3A (CYP3A) in human intestinal and liver microsomes: comparison of Ki values and impact of CYP3A5 expression, *Drug Metab. Dispos.* **1999**, *27*, 180–187.

126 Paine, M. F., Leung, L. Y., Lim, H. K., Liao, K., Oganesian, A. *et al.*, Identification of a novel route of extraction of sirolimus in human small intestine: roles of metabolism and secretion, *J. Pharmacol. Exp. Ther.* **2002**, *301*, 174–186.

127 Li, L. Y., Amidon, G. L., Kim, J. S., Heimbach, T., Kesisoglou, F. *et al.*, Intestinal metabolism promotes regional differences in apical uptake of indinavir: coupled effect of P-glycoprotein and cytochrome P450 3A on indinavir membrane permeability in rat, *J. Pharmacol. Exp. Ther.* **2002**, *301*, 586–593.

128 Obach, R. S., Zhang, Q. Y., Dunbar, D., Kaminsky, L. S., Metabolic characterization of the major human small intestinal cytochrome p450s, Drug Metab. Dispos. **2001**, *29*, 347–352.

129 Fricker, G., Drewe, J., Huwyler, J., Gutmann, H., Beglinger, C., Relevance of p-glycoprotein for the enteral absorption of cyclosporin A: in vitro–in vivo correlation, *Br. J. Pharmacol.* **1996**, *118*, 1841–1847.

130 Lown, K. S., Mayo, R. R., Leichtman, A. B., Hsiao, H. L., Turgeon, D. K. *et al.*, Role of intestinal P-glycoprotein (mdr1) in interpatient variation in the oral bioavailability of cyclosporine, *Clin. Pharmacol. Ther.* **1997**, *62*, 248–260.

131 Hamman, M. A., Bruce, M. A., Haehner-Daniels, B. D., Hall, S. D., The effect of rifampin administration on the disposition of fexofenadine, *Clin. Pharmacol. Ther.* **2001**, *69*, 114–121.

132 Davit, B., Reynolds, K., Yuan, R., Ajayi, F., Conner, D. *et al.*, FDA evaluations using in vitro metabolism to predict and interpret in vivo metabolic drug–drug interactions: impact on labeling, *J. Clin. Pharmacol.* **1999**, *39*, 899–910.

133 Simpson, K., Jarvis, B., Fexofenadine: a review of its use in the management of seasonal allergic rhinitis and chronic idiopathic urticaria, *Drugs* **2000**, *59*, 301–321.

134 Cvetkovic, M., Leake, B., Fromm, M. F., Wilkinson, G. R., Kim, R. B., OATP and P-glycoprotein transporters mediate the cellular uptake and excretion of fexofenadine, *Drug Metab. Dispos.* **1999**, *27*, 866–871.

135 Soldner, A., Christians, U., Susanto, M., Wacher, V. J., Silverman, J. A. *et al.*, Grapefruit juice activates P-glycoprotein-mediated drug transport, *Pharm. Res.* **1999**, *16*, 478–485.

136 Farrell, R. J., Murphy, A., Long, A., Donnelly, S., Cherikuri, A. *et al.*, High multidrug resistance (P-glycoprotein 170) expression in inflammatory bowel disease patients who fail medical therapy, *Gastroenterology* **2000**, *118*, 279–288.

137 Sababi, M., Borga, O., Hultkvist-Bengtsson, U., The role of P-glycoprotein in limiting intestinal regional absorption of digoxin in rats, *Eur. J. Pharm. Sci.* **2001**, *14*, 21–27.

138 Ussing, H. H., Anomalous transport of electrolytes and sucrose through the isolated frog skin induced by hypertonicity of the outside bathing solution, *Ann. N. Y. Acad. Sci.* **1966**, *137*, 543–555.

139 Sutcliffe, F. A., Riley, S. A., Kaser-Liard, B., Turnberg, L. A., Rowland, M., Absorption of drugs from the human jejunum and ileum, *Br. J. Clin. Pharmacol.* **1988**, *26*, 206P–207P.

140 Gramatte, T., Griseofulvin absorption from different sites in the human small intestine, *Biopharm. Drug Dispos.* **1994**, *15*, 747–759.

141 Gramatte, T., Richter, K., Paracetamol absorption from different sites in the human small intestine, *Br. J. Clin. Pharmacol.* **1994**, *37*, 608–611.

142 Gramatte, T., el Desoky, E., Klotz, U., Site-dependent small intestinal absorption of ranitidine, *Eur. J. Clin. Pharmacol.* **1994**, *46*, 253–259.

143 Lennernäs, H., Fagerholm, U., Raab, Y., Gerdin, B., Hallgren, R., Regional rectal perfusion: a new in vivo approach to study rectal drug absorption in man, *Pharm. Res.* **1995**, *12*, 426–432.

144 Brady, J. M., Cherrington, N. J., Hartley, D. P., Buist, S. C., Li, N., Klaassen, C. D., Distribution and chemical induction of multiple drug resistance genes in rats, *Drug Metab. Dispos.* **2002**, *30*, 838–844.

II
Drug Dissolution and Solubility

Drug Bioavailability: Estimation of Solubility, Permeability, Absorption and Bioavailability.
Edited by Han van de Waterbeemd, Hans Lennernäs and Per Artursson

ISBN: 3-527-30438-X

8
Gastrointestinal Dissolution and Absorption of Drugs

Gladys E. Granero, Chandrasekharan Ramachandran, and Gordon L. Amidon

Abbreviations

BCS	Biopharmaceutics classification system
CMC	Critical micelle concentration
EIT	Electrical impedance tomography
FaSSIF	Fasted state simulating intestinal fluid
GE	Gastric emptying
GI	Gastrointestinal
IR	Immediate release
MMC	Migrating motor complex
MR	Modified release
NSAID	Non-steroidal anti-inflammatory drug
SI	Small intestine

Symbols

An	Absorption number
C_s	Equilibrium solubility
D	Diffusion coefficient
d_{crit}	Critical diameter
Dn	Dissolution number
Do	Dose number
F	Fraction of drug absorbed
G	Surface specific dissolution rate
h	Diffusion boundary layer thickness
h_{app}	Apparent diffusional distance
I_s	Initial saturation
k_a	Absorption rate constant
M_0	Dose
P	Permeability
P	Distribution coefficient

Drug Bioavailability: Estimation of Solubility, Permeability, Absorption and Bioavailability.
Edited by Han van de Waterbeemd, Hans Lennernäs and Per Artursson

ISBN: 3-527-30438-X

r Particle radius
S Surface area
V Gastrointestinal volume

8.1 General Dissolution

Mechanisms of dissolution kinetics of crystals have been intensively studied in the pharmaceutical domain, because the rate of dissolution affects the bioavailability of drug crystals. Many efforts have been made to describe the crystal dissolution behavior. A variety of empirical or semi-empirical models have been used to describe drug dissolution or release from formulations [1–6]. Noyes and Whitney published the first quantitative study of the dissolution process in 1897 [7]. They found that the dissolution process is diffusion controlled and involves no chemical reaction. The Noyes-Whitney equation simply states that the dissolution rate is directly proportional to the difference between the solubility and the solution concentration:

$$\frac{dm}{dt} = \frac{D}{V}\frac{S}{h}(C_s - C_t) \tag{1}$$

where dm/dt is the dissolution rate, expressed as the change in the amount of drug dissolved (m) per unit time (t); D is the diffusion coefficient; S is the surface area; h is the thickness of the diffusion film adjacent to the dissolving surface; C_s is the saturation solubility of the drug molecule; C_t is the concentration of the dissolved solute; and V the volume of the dissolution medium.

Although the Noyes-Whitney equation has been used widely, it has been shown to be inadequate in modeling either S-shape experimental data or data with a steeper initial slope. Therefore, a more general function, based on the Weibull distribution [8], was proposed [9] and applied empirically and successfully to all types of dissolution curves [10]:

$$M = 1 - exp(-\alpha t^{\beta}) \tag{2}$$

where M is the accumulated fraction of the material in solution at time t, α is a scale parameter and β is a shape parameter which characterizes the curve as either typical exponential ($\beta = 1$), S-shaped ($\beta > 1$), or exponential with a steeper initial slope ($\beta < 1$). Two steps are involved in solid particle dissolution: the first step is the detachment of molecules from the solid surface to form hydrated molecules at the solid-liquid interface; the second step is the mass transport from this interface to the bulk solution. Most dissolution processes are controlled by the second step, which is diffusion-convection-controlled. Modifications of the Noyes-Whitney dissolution model by Nernst [11] and Brunner [12] assume that a rapid equilibrium (i.e., saturation) is achieved at the solid-liquid interface followed by diffusion across

a thin layer of solution, termed the diffusion layer, into the solution. Diffusion across this diffusion layer is rate controlling in most cases. Diffusional transport is affected by degree of agitation, viscosity of the medium, temperature of the medium, and particle size of the drug particles. The total interfacial surface area involved in the dissolution process is not always easily determined for suspensions, especially with strongly agglomerating materials. In these cases, calculations based on the surface area of the primary particles may lead to an overestimation of the effective solid surface area participating in the dissolution.

The velocity of liquid flow around suspended solid particles is reduced by frictional resistance and results in a region characterized by a velocity gradient between the surface of the solid particle and the bulk fluid. This region is termed the hydrodynamic boundary layer and the stagnant layer within it that is diffusion-controlled is often known as the effective diffusion boundary layer. The thickness of this stagnant layer has been suggested to be about 10 times smaller than the thickness of the hydrodynamic boundary layer [13].

It has been demonstrated that the surface specific dissolution rate increases as a function of time due to a decrease in particle size of the dissolution materials. Thus, Niebergall et al. concluded that the hydrodynamic boundary layer thickness is a function of the square root of the diameter of the dissolving particle [14]. Higuchi and Hiestand have stated that the diffusion boundary layer thickness is comparable to or greater than the particle radius [15]. Also, other authors [16–18] have demonstrated that the thickness of the diffusional layer is a function of the particle size of the drug. Thus, for particle sizes below 5 μm, dramatic increases in surface specific dissolution rates were observed [18]. The authors also reported that the surface specific dissolution rates of particles < 5 μm were not significantly affected by increased agitation intensities; however, particles of the same drug with size ranges of 25–35 μm were affected by agitation.

Bisrat et al. concluded that for sparingly soluble, suspended drugs, diffusional transport plays a major role in the dissolution kinetics [19]. They studied the effect of particle size and viscosity on dissolution rate and apparent diffusional distance (h_{APP}) of oxazepam and griseofulvin. The term apparent diffusional distance was used as a simplified measure of the distance over which diffusion dominates and was calculated as follows:

$$h_{APP} = \frac{DC_s}{G} \tag{3}$$

where D is the diffusion coefficient, C_s is the equilibrium solubility, and G is the surface specific dissolution rate. The authors concluded that a decrease in particle size corresponded to a reduced diffusion layer thickness and a shorter diffusional distance for dissolved molecules. The correlation between particle size and diffusion layer thickness is depicted in Figure 8.1. It is seen that the increase in the diffusional layer thickness is less pronounced for particles exceeding 10 μm in radius. As the particle radius increases, the diffusion layer thickness becomes small relative to the particle size and tends to level off to a constant value.

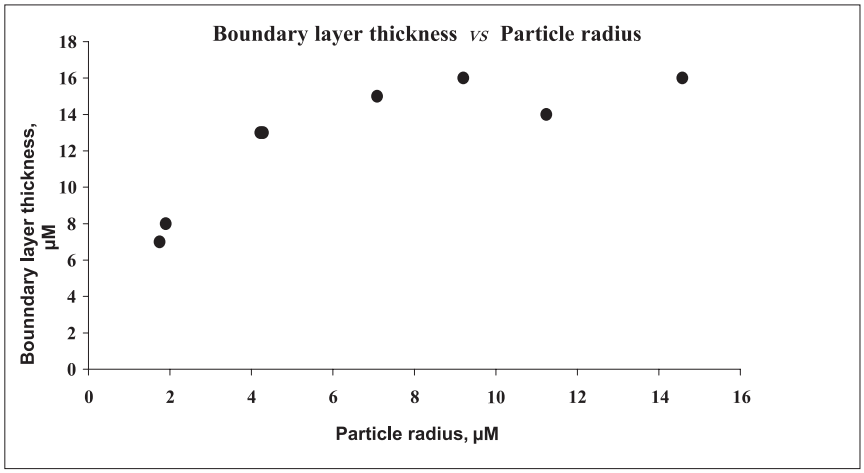

Fig. 8.1. Effect of particle radius on the boundary layer thickness of digoxin and oxazepam. Graph constructed from data in Bisrat et al. [19].

The viscosity of the medium also affects the dissolution kinetics of drugs. Apart from increasing the viscosity, the addition of viscosity enhancing agents affects solubility, diffusibility and thus the diffusion layer thickness. The diffusion layer thickness is affected by both the direct increases in viscosity and the change in the diffusion coefficient due to the addition of viscosity enhancing agents. Bisrat et al. [19] found that the apparent diffusional distance, h_{APP}, increased with increasing viscosity for two sieve fractions of oxazepam with widely different particle size ranges. However, the increase in apparent diffusional distance for the smaller particles (<5 μm) was about two-fold lower than that observed for the larger particle size fraction (25–35 μm).

For a drug of low aqueous solubility, particle size and the resulting surface area could have a significant effect on the rate of dissolution over the time interval during which gastrointestinal absorption occurs, and therefore, affects the bioavailability of the drug. The importance of diffusional transport in dissolution kinetics of drugs has been examined extensively. In this regard, the thickness of the diffusion boundary layer plays a pivotal role and derivations of dissolution rate expressions often include boundary layer thickness considerations. Thus, Hixson and Crowell [20], for example, assumed the diffusion boundary layer thickness (h) to be a constant, while others, such as Higuchi et al. [15], considered h to be proportional to the particle diameter (approximately equal to the particle radius). Hintz and Johnson [21] extended the mixing-tank model to predict dissolution rate-controlled oral absorption of monodisperse powders to polydisperse mixtures of a drug under non-sink conditions. The authors derived a Noyes-Whitney type equation to simulate drug dissolution and absorption in terms of spherical particle geometry, time-dependent diffusion layer thickness, initial dosage and percent weight particle size distribution;

$$\frac{dX_{si}}{dt} = -\frac{3DX_{oi}^{2/3}X_{si}^{1/3}}{\rho h_i r_{oi}}\left|Cs - \frac{X_{dt}}{V}\right| \tag{4}$$

where X_{si} is the amount of solid drug in the i^{th} particle size group at any time, D is the drug diffusion coefficient, X_{oi} the initial amount of solid drug in the i^{th} particle size group, ρ is the drug density, h_i is the diffusion layer thickness of the i^{th} particle size group, r_{oi} is the initial particle radius of the i^{th} particle size group, C_s is the drug solubility, X_{dt} is the total amount of dissolved drug at any time, and V is the estimated volume of fluid present in the gastrointestinal tract. A simulation of the percent dose absorbed based on the above equation was reported by Johnson et al. [24];

$$\frac{dX_{di}}{dt} = +\frac{3DX_{oi}^{2/3}X_{si}^{1/3}}{\rho h_i r_{oi}}\left|Cs - \frac{X_{dt}}{V}\right| - k_a X_{di}; \quad \frac{dX_{ai}}{dt} = k_a X_{di} \tag{5}$$

where X_{di} is the amount of dissolved drug in the i^{th} particle size group at any time, k_a is a first-order absorption rate constant, and X_{ai} is the amount of absorbed drug in the i^{th} particle size group at any time. In this simulation, the diffusion layer thickness h_i was set equal to radius r_{0i} for all particle size groups with r_{0i} less than 30 μm and equal to 30 μm for all larger groups. The gastrointestinal tract was treated as a well-stirred tank; thus colonic absorption is ignored in the analysis. The authors concluded that in general, the relative effect of particle size on percent dose absorbed decreased with increasing solubility and that particle size was practically irrelevant for drugs at a solubility of 1 mg/ml. The authors also found that the greatest effect of particle size was for low-solubility low-dose drugs. Thus, there was little effect of particle size on a low-solubility drug at high dose or on a high-solubility drug at low dose. Also, there was an increased absorption rate constant for drugs in the solubility range of roughly 0.001–0.01 mg/ml with doses in range of 10–100 mg.

Amidon et al. have developed drug dissolution and absorption models for water insoluble drugs [22, 23]. These models suggest that the key parameters controlling drug absorption can be expressed by three dimensionless numbers; an absorption number (An), a dissolution number (Dn) and a dose number (Do); representing the fundamental processes of membrane permeation, drug dissolution and dose, respectively. The three important dimensionless groups are:

$$Do = DoseNumber = \frac{M_0/V_0}{C_s} \tag{6}$$

$$Dn = DissolutionNumber = \frac{DCs}{r_o}\frac{4\pi r_o^2}{\frac{3}{4}\pi r_o^3 \rho}t_{res} = t_{res}3DC_s/\rho r_o^2 = t_{res}/t_{Diss} \tag{7}$$

$$An = AbsorptionNumber = \frac{P_{eff}}{R}t_{res} = t_{abs}^{-1}t_{res} \tag{8}$$

$$t_{ress} = \pi R^2 L/Q = mean\ residence\ time \tag{9}$$

$$t_{Diss} = \frac{r_o^2 \rho}{3DC_s} = \textit{time required for a particle of the drug to dissolve} \tag{10}$$

$$t_{abs}^{-1} = k_{abs} = (S/V)P_{eff} = 2\frac{P_{eff}}{R} = \textit{the effective absorption rate constant} \tag{11}$$

where S is surface area, V is volume, R is the intestinal radius, M_0 is the dose, and r_0 is the initial particle radius.

Combining the above expressions with equation (4) and setting h equal to r_0 for small particles results in an expression for dissolution rate in terms of Do and Dn;

$$\frac{dX_{st}}{d_t} = \frac{X_{oi}^{1/3} X_{si}^{2/3} Dn}{t_{res} C_s} \left(\frac{M_0/V_0}{Do} - \frac{X_{dt}}{V} \right) \tag{12}$$

The Johnson dissolution models described above postulate that h varies linearly with particle size up to a certain value, beyond which h remains unaltered. This assumption encompasses the differences in the release kinetics for both small and large particles.

The classical diffusional models are generally based on the Noyes-Whitney type equation and assume that the diffusion coefficient is independent of concentration and time and that the particle shape is spherical. Further, the assumption of particle monodispersity (or collections of monodisperse particles in polydisperse mixtures) and constancy of particle number leads to the interfacial area being related to the weight of solids in a simple manner (S is proportional to $w^{2/3}$) (Table 8.1). Also, the major differences between such classical models are inherent in the interdependency of the diffusion layer thickness, h, and particle size, r. It has been suggested that the invalidity of the assumptions implicit in classical models may be more important than the interdependence of h and particle size. Indeed, accounting for factors such as the change in the number of suspended particles throughout dissolution, their departure from sphericity, or the polydispersity degree, can result in a significant improvement in the dissolution model fitting.

Tab. 8.1. Classical Dissolution Models.

h	*Integrated Equation*	*Rate Dissolution Constant*
constant	$w_0^{1/3} - w^{1/3} = K_{1/3}t$	$K_{1/3} = \frac{1}{3} N^{1/3} \frac{D}{h} \pi \left(\frac{6}{\pi\rho} \right)^{2/3} C_s$
kd	$w_0^{2/3} - w^{2/3} = K_{2/3}t$	$K_{2/3} = \frac{2}{3} N^{2/3} \frac{D}{k} \pi \left(\frac{6}{\pi\rho} \right)^{1/3} C_s$
$k\sqrt{d}$	$w_0^{1/2} - w^{1/2} = K_{1/2}t$	$K_{1/2} = \frac{1}{2} N^{1/2} \frac{D}{k} \pi \left(\frac{6}{\pi\rho} \right)^{1/2} C_s$

k = constant, d = particle diameter, N = particle number, w_0 = weight of suspended solids at time $t = 0$, and w = weight of suspended solids at time $t = t$.

A dissolution model that takes in account the change in particle number and the polydisperse nature of the powder was proposed by de Almeida et al. [25]. The following dissolution equations were used to calculate the decrease in weight of solids with time:

$$w_{t+\Delta t,\,i}^{2/3} = w_{t,\,i}^{2/3} - N_i^{2/3} Kt \quad \text{when} \quad di < d_{crit} \tag{13}$$
$$K = \frac{2D}{3k}\alpha_{s,\,dv}\left(\frac{6}{\pi\rho}\right)^{1/3} C_s$$

and

$$w_{t+\Delta t,\,i}^{1/3} = w_{t,\,i}^{1/3} - N_i^{1/3} Kt \quad \text{when} \quad di \geq d_{crit} \tag{14}$$
$$K = \frac{1D}{3kd_{crit}}\alpha_{s,\,dv}\left(\frac{6}{\pi\rho}\right)^{2/3} C_s,$$

where $w_{t+\Delta t,\,i}$ = suspended particles weight at time $t + \Delta t$ for size class i, k = constant (see Table 8.1), $\alpha_{s,\,dv}$ = particle shape factor, d_{crit} = critical diameter.

These equations are similar to those shown in Table 8.1. The only difference is the experimental particle shape factor ($\boldsymbol{\alpha_{s,\,dv}}$) used instead of π (only valid for spheres). In their model, the better fit was achieved considering a constant value for h, above a certain particle size.

Heterogeneous conditions both in terms of hydrodynamics and composition prevails in the GI tract. Parameters such as D, C_s, V, and h are influenced by the conditions in the GI tract which change with time. Thus, time dependent rate coefficients govern the dissolution process under *in vivo* conditions. One of the major sources of variability for poorly soluble drugs can be associated with the time dependent character of the rate coefficient, which governs drug dissolution under *in vivo* conditions.

8.2 Absorption Models

One of the original concepts governing oral absorption of organic molecules is the 'pH partition hypothesis'. This hypothesis states that only the nonionized form of the drug is able to permeate the membranes of epithelial cells lining the GI tract [26]. According to the classical pH-partition theory, permeability is expected to correlate not with the intrinsic partition coefficient but with the so-called distribution coefficient D of the solute [27], where D is defined as:

$$\log D = \log P + \log f_U = \log P + \log(1 - f_I) \tag{15}$$

where f_U is the unionized and f_I the ionized fraction, respectively. The correction terms f_U and $\log(1 - f_I)$ describe the pH dependence of log D. The fraction

absorbed is often higher than expected from the pH-partition hypothesis. Two types of deviation from the classical pH-absorption curves may be observed. The lower part of the curve may be shifted upward, probably due to a substantial permeation of the ionic form of the drug through the membrane. In this case, the permeation correlates not with the distribution coefficient D but with the effective distribution coefficient P_{eff} of the solute [28–30]. Alternatively, a parallel shift of the pH-absorption curve from the pH-dissociation curve (to the right for acids and to the left for bases) may occur, especially for very lipophilic compounds. The presence of pH differences at the surface of the membrane (microclimate pH), binding of drug to the membrane surface or the presence of an unstirred aqueous diffusion layer adjacent to the lipid membrane [31–33] are a few factors that can be responsible for parallel shifts.

Although, the pH-partition hypothesis has not been found to be universally applicable, it has resulted in the recognition of the important contribution of GI pH to permeability and to the dissolution rate of solid dosage forms. This theory does not consider the solubility of the drug, which is a critical physicochemical parameter in the oral absorption process. Dressman et al. [34] developed an absorption potential concept that takes the two parameters into account. The absorption potential is defined as

$$AP = \log\left(\frac{PF_{un}}{Do}\right) \tag{16}$$

where AP is the absorption potential as a predictor of the extent of drug absorption, P is the partition coefficient, and F_{un} is the fraction in unionized form at pH 6.5. Do is the dimensionless dose number defined earlier in equation (6);

$$Do = \frac{C_0}{C_s} = \frac{M_0/V_0}{C_s}$$

where C_s is the physiological solubility, M_0 is the dose, and V_0 is the volume of water taken with the dose, which is generally set to be 250 mL.

A number of theoretical transport and absorption models have been developed to describe mathematically, the passive transport of drug from its site of absorption to its site of action [35–40]. In spite of the complex nature of GI transit and *in vivo* drug dissolution, the derivation of the equations used in linear compartment modeling rely on the hypothesis that absorption takes place from a homogeneous drug solution in the GI fluids and proceeds uniformly throughout the GI tract. The homogeneous GI absorption is routinely described by the following equation [41]:

$$\text{Absorption rate} = FDk_a\, exp(-k_a t) \tag{17}$$

where F is the fraction of dose (D) absorbed and k_a is the first-order absorption rate constant. The initial absorption rate (FDk_a) predicted by equation (17), however, is not in accord with the principles of the transport of the drug molecules in the

absorption process, where the absorption rate must be zero initially and increase to reach a maximum over a finite period of time. These models cannot predict the often complicated plasma concentration profiles attributable to time and site dependence of permeability, to variable dissolution environment due to pancreatic and bile secretions, to time-dependent gastric emptying and intestinal transit, to changes of pH from stomach to intestine and to time-dependence of pH in the intestinal lumen. Several models have been proposed for the analyses of these irregular profiles [42–44]. Oberle and Amidon [45] suggested that gastric emptying and intestinal transit rates may be responsible for the double peaks of cimetidine in plasma concentration profiles following oral dosing and developed a time-dependent absorption and transit model. Yu and Amidon [46] developed a compartmental absorption and transit (CAT) model to simulate the rate and extent of drug absorption. The CAT model is described by a set of differential equations that considers simultaneous movement of a drug in solution through the GI tract and absorption of the dissolved material from each compartment into the portal vein. The rate constant for absorption from each compartment is based on measured values of P_{eff}. A good correlation was found between the fraction of dose absorbed and the effective permeability for ten drugs covering a wide range of absorption characteristics. The model was also able to explain the oral plasma concentration profiles of atenolol. Higaki and Amidon [47] using a time-dependent absorption rate coefficient, $k_a(t)$, wherein the time dependence was varied to account for the dynamic processes such as changes in fluid absorption or secretion, developed six new models. They found that the TPLAG model (Two-phase Model Including Lag Time) was the most efficient in prediction of irregular absorption kinetics. A microscopic mass balance approach was developed by Oh and Amidon [48] to predict the fraction of dose absorbed of suspensions of poorly soluble compounds by calculating four dimensionless parameters: initial saturation (I_s), absorption number (An), dose number (Do), and dissolution number (Dn).

Based on their solubility and intestinal permeability characteristics, drugs have been classified into one of four categories according to the Biopharmaceutics Classification System (BCS) proposed by Amidon et al. [49].

BCS Class I: High-solubility, high-permeability drugs. These compounds are generally very well absorbed. For Class I compounds formulated as immediate release products, dissolution rates generally exceed gastric emptying rates. Therefore, nearly 100% absorption can be expected if at least 85% of a product dissolves within 30 min of *in vitro* dissolution testing across a range of pH values. Accordingly, *in vivo* bioequivalence data are not necessary to assure product comparability.

BCS Class II: Low-solubility, high-permeability drugs. The bioavailability of products containing these compounds is likely to be dissolution-rate limited. For this reason, a correlation between *in vivo* bioavailability and *in vitro* dissolution rate (IVIVC) may be observed.

BCS Class III: High-solubility, low-permeability drugs. Absorption is permeability-rate limited but dissolution will most likely occur very rapidly. For this reason,

there has been some suggestion that as long as the test and reference formulations do not contain agents that can modify drug permeability or GI transit time, waiver criteria similar to those associated with Class I compounds may be appropriate.

BCS Class IV: Low-solubility, low-permeability drugs. These compounds have very poor oral bioavailability. They are not only difficult to dissolve but often exhibit limited permeability across the GI mucosa. These drugs tend to be very difficult to formulate and can exhibit very large intersubject and intrasubject variability.

For Class I compounds (where $Dn > 1$), the fraction absorbed (F) can be expressed as:

$$F = 1 - exp(-2An) \tag{18}$$

As *An* increases, the fraction of drug absorbed increases, with 90% absorption (highly permeable compounds) occurring when $An = 1.15$. For Class II drugs, dissolution number $Dn < 1$. In these cases, the relationship between Do and Dn is critical in determining the fraction of drug absorbed, and the rate of drug dissolution tends to be the rate-limiting step. Accordingly, factors that increase the rate and extent of *in vivo* dissolution will also increase the bioavailability of that compound.

GastroPlus™ is a simulation software product based on a new model, which is called the advanced CAT (ACAT) [50]. This model assumes that drug passing through the small intestine will have equal transit time in each of the seven compartments. To satisfy the equal transit time constraint in the duodenum and jejunum (since the volume of fluid entering the small intestine, 8–9 liters/day, is more than the 0.5–1 liters/day that exits the small intestine) the model considers largest volumes and transit rates in the upper small intestine (SI) compartments. This model uses the concentration gradient across the apical and basolateral membranes to calculate the rate of drug transfer into and out of an enterocyte compartment for each GI tract lumen compartment assuming drug transfer to be unidirectional (lumen to central compartment). Thus, drug can move in either direction depending on the concentration gradient. It can be passively secreted back into the lumen, even from an intravenous dose.

8.3 Gastrointestinal Variables

Orally administered dosage forms are absorbed into the systemic circulation following dissolution in the GI tract. Because substances must be in solution for the absorption from the GI lumen, the absorption rate of poorly water-soluble drugs is limited by their rate of dissolution. The dissolution rate is affected by the unique physicochemical properties of the drug and by physiological factors: the pH, composition, and hydrodynamics of the GI medium.

8.3.1 Bile Salts

Solubility is a thermodynamic parameter, and is closely related to dissolution, a kinetic parameter. Bile acids affect both solubility and dissolution, by a micellization effect. The natural bile salts are amphipathic molecules. The natural bile salts are surface active and self-associate above a narrow concentration range to form multimers (usually termed micelles) [51]. Although variable, typical bile salt concentrations in the fasted intestine in humans are 4–6 mM compared with postprandial levels of 10–20 mM. Approximately 40% of the bile salts are conjugates of cholic acid, 40% are conjugates of chenodeoxycholic acid, and the remaining 20% are conjugates of deoxycholic acid [52]. In addition, phospholipids are present in the bile. Additionally, bile contains cholesterol and lecithin excreted into intestine is significantly hydrolyzed by pancreatic phospholipase A_2 to lysolecithin. The composition of the fed state upper intestine is complex because of additional secretions during digestion, and the contributions of components from food and its subsequent digestion. The composition of intestinal fluids is likely to vary considerably due to meal ingestion, meal composition, gastric emptying, and other physiologic factors. The major components, in fed state, of upper GI lumen are tri-, di-, and monoglycerides, fatty acids, cholesterol, and lysolecithin. The contents of upper GI tract in the fed state has been characterized as an emulsion, although more detailed examination has shown that it consists of multiple phases [53]. Consequently, both emulsions and micellar solutions represent the fed state. The secretion of bile in response to food is responsible for an overall increase in solubilizing capacity of the GI tract by increasing micelle numbers rather than increasing bile salt levels to supramicellar concentrations. The presence of bile may improve the bioavailability of poorly water-soluble drugs by enhancing the rate of dissolution and/or solubility. The increase of solubility by micellar solubilization or the increase in the effective surface area of the solid by a decrease in the interfacial energy (*via* enhanced wetting) could be responsible for the improved dissolution. A consequence of drug solubilization within the bile salt micelle is a decrease in the apparent diffusion coefficient of the drug. In general, enhanced wetting predominates at bile salt concentrations below the CMC, whereas enhanced solubility is dominant at concentrations above the CMC [54].

8.3.2 Gastric Emptying

Discontinuous input rates following oral drug administration are often attributed to gastric emptying (GE). The rate of stomach emptying can determine the rate of absorption after oral drug administration, particularly for drugs with a high intestinal membrane permeability or when potentially rate-limiting process such as dissolution are relatively fast [55]. Gastric emptying is totally controlled by the two patterns of upper GI motility i.e. the inter-digestive and the digestive motility pattern. The inter-digestive pattern, termed the migrating motor complex (MMC)

dominates in the fasted state and is organized into alternating phases of activity and quiescence [56]. Previous studies suggest that factors such as meal types including the volume, osmolarity, pH, and calorific values as well as gender, age, body mass, psychological states, and acid secretion may influence the gastric emptying process.

8.3.2.1 Effect of Volume

Gastric emptying rates not only depend on the existing MMC phase but also on the volume of liquid co-administered with the dose. Luminal fluid volume is a critical variable in determining the time for gastric emptying. Greater fluid volumes tended to increase the initial rate of gastric transit, although the time for 100% emptying of particles was completed more rapidly at smaller fluid volumes. With both high and low fluid volumes, particles with densities closet to that of the gastric contents emptied the fastest. Very light or very heavy particles emptied with greater difficulty. In part, the slower emptying of large particles may be due to retropulsion induced by gastric contraction. Oberle et al. [57] measured the gastric emptying rates of 50 and 200 ml volumes of phenol red solution while monitoring contractile activity (Fig. 8.2). They found that there was a statistically significant difference in the overall mean emptying rate between the 50 and 200 ml volumes. Also, during phase I, the emptying rate was faster for the 200 ml volume. They observed that the emptying of small volumes was more dependent on motility phase than of large volumes. In addition, emptying may deviate from log lin-

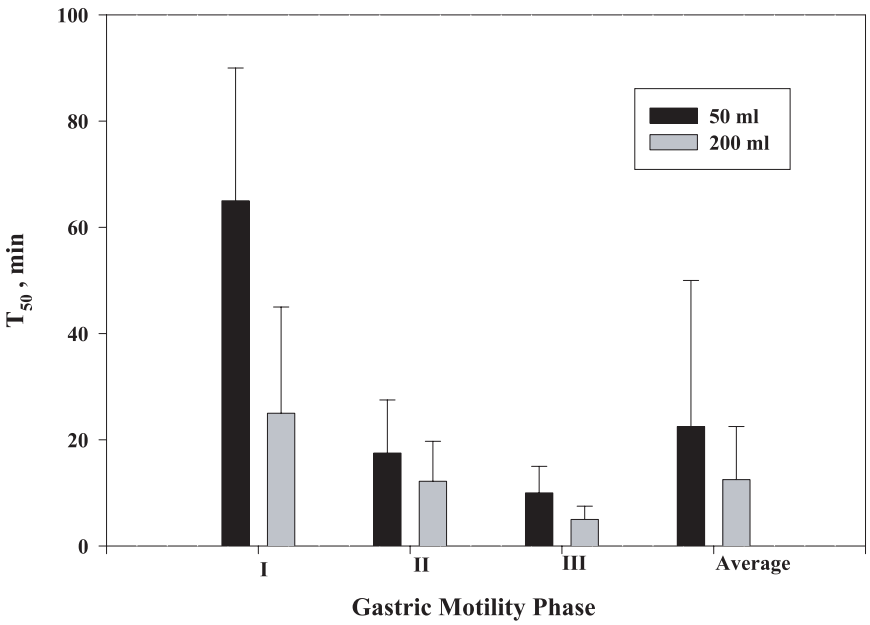

Fig. 8.2. Gastric emptying time for 50% fluid emptying, T_{50} in humans in various motility phases. Data from reference [57].

earity because of fluctuations in contractile activity. The gastric emptying (GE) of volumes > 200 ml is governed by stomach volume, while phase I and phase II activity in the stomach influences the emptying of smaller volumes.

8.3.2.2 Effect of Size and Density of the Drug Particle

In humans, particle density has been demonstrated to significantly impact gastric residence, with heavier particles (e.g. 2.8 g/cm^3) being retained substantially longer than smaller particles (e.g. 1.5 g/cm^3) [58]. Fed state motility is characterized by a pattern of low amplitude contractions, which results in the relatively consistent GE of small solids through the pylorus. The fed state size cut-off for non-digestible solids is controversial with reports ranging from 2 mm to 7 mm. Particles beyond this margin empty during the stronger contractions associated with Phase II and III of the fasted state cycle. Rhie et al. [59] concluded that the fed state size cut-off vary according to meal composition and motility. Phase II governs the emptying of the larger pellets, while the smallest pellets were able to empty during the fed state. On the other hand, they found that the altered drug absorption associated with meals appears to be attributable primarily to altered fluid flow dynamics rather than to GI motility alterations.

8.3.2.3 Effect of pH

Chaw et al. [60] evaluated the pH and volume effects of liquid citrate phosphate buffers of varying pH on the gastric emptying rate by electrical impedance tomography (EIT) and simultaneous pH monitoring using pH-sensitivity radiotelemetry capsule in fasted state in humans. The authors obtained a positive correlation between the two methods. The authors concluded that the effect of pH of the administered test liquid on gastric emptying predominates over the effects of volume. A significant delay in the onset of gastric emptying and the mean gastric residence time of the pH 3 buffer liquid (34.7–46.7 min) was found compared with pH 7 buffer liquid (14.4–22.5 min). These data are explained by a higher negative feedback gastrin release response to acidity of the liquid.

8.3.3 Gastrointestinal Transit

The GI-transit, depending on the drug characteristics and dosage form characteristics, may have a significant impact on rate and extension of orally drugs absorption. As a generalization, gastric transit time influences the systemic appearance of rapidly dissolved, well-absorbed drugs. Intestinal transit time impacts the absorption of drugs with limited mucosal permeability, or those transported by carrier-mediated pathways or subject to intestinal degradation or products whose dissolution is the rate-limiting step for systemic absorption. Transit through the small intestine is largely independent of the feeding conditions and physical properties of the system (Fig. 8.3). The average transit time is around 3 hours. The band of contractions of the migrating motor complex (MMC) usually begins in the duodenum and migrates caudally to the ileocolonic junction. In dogs and humans, this

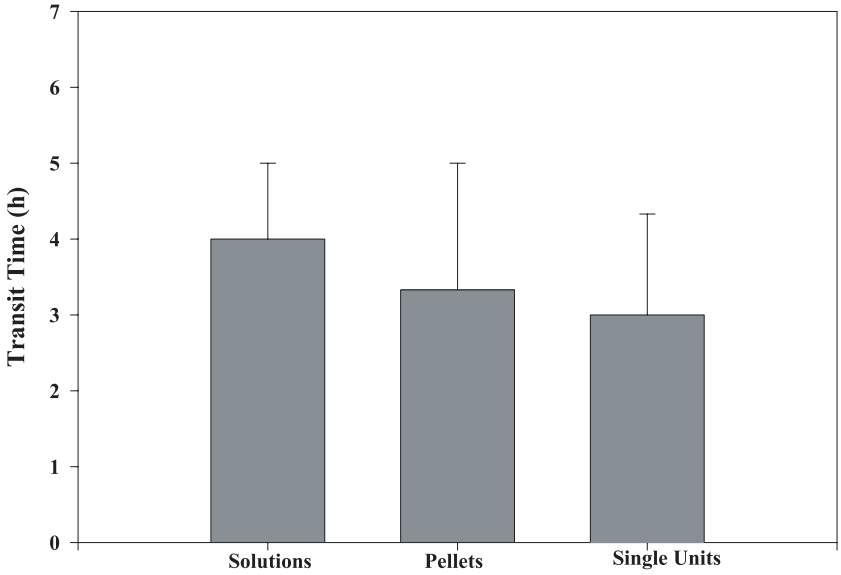

Fig. 8.3. Average transit time in the small intestine measured using γ-scintigraphy following administration of various pharmaceutical dosage forms to humans. Data from reference [61].

phenomenon occurs continuously at a cycle length of 90–150 min until food is ingested [61, 62].

8.3.4 Gastrointestinal pH

Gastrointestinal pH can affect dosage-form performance and drug absorption in several ways. For drugs that are passively absorbed, the nonionized form is generally better absorbed than the ionized species. An alteration in the effective fraction available in the nonionized form as a function of the pH may therefore dictate the rate of absorption of drugs with dissociation constants in the physiological pH range. Upon ingestion of a meal, the gastric pH increases initially because of the buffering effects of food components. After 3–4 h following meal intake, the fasted state pH is usually reestablished. On the other hand, the small intestine pH at first decreases in response to a meal until the fasted state pH is reestablished as a result of pancreatic bicarbonate output.

During its passage through the GI tract, a dosage form experiences a pH range in the fasted state of 1–3 in the stomach, 5–7 in the duodenum, and a slightly higher pH (around 7.5) in the jejunum and ileum. A pH value of 5 to 6.5 is representative of the upper small intestine in the fasted state [63]. Youngberg et al. [64] monitored the fasting small-intestinal pH data over a 3 h period of intestinal tran-

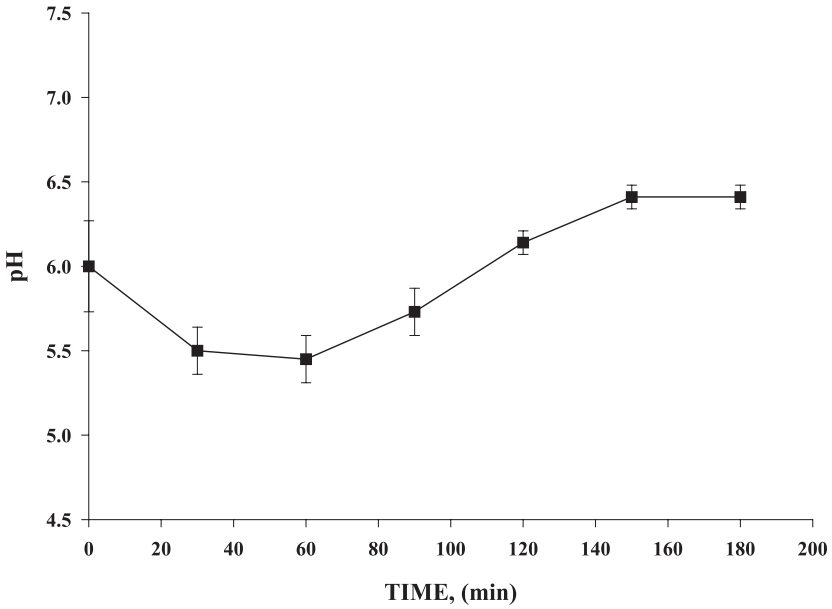

Fig. 8.4. Fasting small-intestinal pH data over a 3 h period of intestinal transit. Graph constructed from data in Youngberg et al. [63].

sit in healthy humans (Fig. 8.4). They found that in healthy subjects, mean intestinal pH climbed to 6.4 within 2.5 h after an untethered Heidelberg capsule, used to continuously monitor pH, was emptied from the stomach.

8.4 Solubilization and Dissolution

Dissolution testing is an integral part of the development of solid dosage forms and has become one of the most important tests for assuring product uniformity and batch-to-batch bioequivalence. Bile salts and lipids are implicated in the differences observed in absorption between the fed and fasted states for some drugs. A variety of lipids are present throughout the upper GI tract in both fed and fasted states; therefore it is important to evaluate their effects on wetting in combination with bile salts. More recently, the industry began a search for dissolution media that not only reflects the dosage form's *in vitro* performance regarding manufacturing variability but also, if it is possible, one that reflects the *in vivo* performance. Given the complex nature of the dissolution process for solid dosage forms, it is important that factors that influence this process are accounted for by the composition of the media. Wetting is an important factor in the dissolution process, both *in vitro* and *in vivo*. The wetting terms are directly related to pro-

cesses involved in the disintegration and dissolution of tablets and capsules. Also, highly hydrophobic drugs that exhibit low solubility and poor wetting properties generally require the inclusion of surfactants in the dissolution media.

8.4.1 Surfactants

The *in vivo* dissolution of many poorly soluble drugs is enhanced by the action of surfactants secreted into the upper GI tract. Bile salts, the physiological surfactants secreted into the GI tract, act to solubilize these otherwise insoluble molecules by incorporating them into micelles. Different drugs interact uniquely with any particular surfactant, depending on the ionic nature and chemical properties of both entities. Therefore, any quantitative *in vitro* dissolution simulation for this type of drug *in vivo* would necessarily include surfactants in the dissolution medium. Many researchers have extensively investigated the effect of pH and the effect of surfactant on the dissolution of drugs. Higuchi [65] developed a one-dimensional diffusion layer theory describing the effect of surfactant on the dissolution of a solid. Singh et al. [66] investigated the influence of micelle-drug-solubilization on the dissolution rate for the benzocaine-plolysorbate 80 system using different hydrodynamic models. Most frequently, a rotating disk apparatus is used as the dissolution apparatus. The film equilibrium model assumes simultaneous diffusive transport of the free solute and micelle in equilibrium within a common stagnant film at the surface of the solid. An effective diffusivity is defined to describe the total diffusion component of the micelle and free solute. This model has been adapted to include convective diffusion transport, substituting the effective diffusivity of the free solute and drug-loaded micelle for the diffusion term in the Levich equation. Gibaldi et al. [67] examined the influence of polyoxyethylene lauryl ether on the dissolution of benzoic acid and salicylic acid by the rotating disk and the static disk method. De Smidt et al. [68] reported the effect of sodium lauryl sulfate on the dissolution of griseofulvin, a poorly water-soluble drug. Recently, Granero et al. [69] examined the dissolution behavior of fenofibrate, a unionizable water-insoluble drug, in sodium lauryl sulfate solutions at pH of 6.8 using rotating disk experiments.

8.4.2 Effect of Surfactants and pH on Dissolution Rate

Mooney et al. [70] investigated the effect of pH on the solubility and dissolution of ionizable drugs based on a film model with total component material balances for reactive species, proposed by Olander. McNamara and Amidon [71] developed a convective diffusion model that included the effects of ionization at the solid-liquid surface and irreversible reaction of the dissolved species in the hydrodynamic boundary layer. Jinno et al. [72], and Kasim et al. [73] investigated the combined effects of pH and surfactants on the dissolution of the ionizable, poorly water-soluble BCS Class II weak acid NSAIDs piroxicam and ketoprofen, respectively.

The results of these studies suggest that ketoprofen would be completely ionized and highly soluble in the intestinal environment (an average pH ~ 6.5).

8.4.3 Effect of pH

Earlier dissolution studies have shown that solubility-limited acidic drugs dissolve in buffer solutions at much higher rates than their intrinsic dissolution rates [74]. This is attributable to the equilibrium conversion of the unionized drug to the more soluble ionized form as soon as it dissolves, allowing more drugs to dissolve. A compound's solubility is a function of its ability to form hydrogen bonds with water molecules. Generally, aqueous solubility is directly proportional to the number of hydrogen bonds that can be formed with water, and ionized compounds exhibit greater aqueous solubility than do the unionized counterparts. Consequently, the rate of solute dissolution can be markedly affected by the pH of the aqueous solvent. Weak bases dissolve more slowly at higher pH values (since above its pK_a, more drug exists in its unionized form), whereas weak acids dissolve faster at a higher pH (since above its pK_a, more drug exist in its ionized form). Li et al. [75] showed that the use of pH along with other methods such as co-solvency, micellization or complexation, could significantly enhance the solubility of poorly soluble drugs that are ionizable. Also, Jain et al. [76] suggested a similar strategy.

8.4.4 Bio-relevant Dissolution Media

Most pharmacopoeias describe four different dissolution test apparatuses: basket, paddle, reciprocating cylinder and flow-through cell. The two former methods are recommended because of their precise and simple set-up and handling. In addition to the apparatus and its influence on the dissolution of a substance, the choice of a suitable dissolution medium is a critical parameter. National pharmacopoeias describe various test media such as SIF or SGF to cover the physiological pH range between 1.2 and 7.5. But for many drugs, which are poorly water-soluble over this pH range, these media are not very useful. In such cases, surfactants such as sodium lauryl sulfate, emulsions, higher pH values, or even organic solvents are added to the dissolution media to improve the solubility of the drug. The use of cosolvents can be problematic particularly for modified-release (MR) dosage forms, since they can interact with the release controlling mechanism of the formulation; thus, regulatory agencies tend to discourage their use. Several researchers have investigated new biorelevant dissolution media. Luner et al. [53] evaluated the effect of various individual lipids and composition of physiologically representative media estimated on the basis of physiologic data. They concluded that in micellar systems, both the type and concentration of lipid present in the bile salt solution have influence on wetting. On the other hand, for the fed state compositions, alteration of the solution pH from 7.5 to 5.0 resulted in a significant change in wetting, because the pH will affect the ionization of the fatty acid, concomitantly

influencing the characteristics of the micelle. Thus, the surface tension of the medium representative of the fasted state was higher than that of the fed state. From the analysis of the wetting behavior of individual lipids as a function of concentration in bile salt solutions, they concluded that the lipids adsorb in a manner that progressively reduces the expected wetting of the surface. Löbenberg et al. [77] investigated the dissolution behavior of two formulations of glibenclamide in various media for predicting the *in vivo* performance of the two formulations. They found that the dissolution of the two drug powders was highly dependent on wetting, particle size, pH, and the composition of the medium. Of the various media tested, FaSSIF (Fasted State Simulating Intestinal Fluid) seems to be the most suitable medium for showing differences between formulations. Strong correlations were observed between dissolution in FaSSIF and absorption for both glibenclamide products. Kostewicz et al. [78] used two physiologically relevant media to predict the *in vivo* absorption behavior of dipyridamole, BIMT 17 BS and BIBU 104 XX, three poorly soluble weak bases.

8.4.5 Particle Size

Particle size may be a critical formulation variable. Both size and density can modify *in vivo* particle dispersion, with greater dispersion resulting in improved dissolution of poorly soluble and slowly dissolving drugs. This consideration may be particularly important when formulating BCS Class II compounds or sustained release preparations. For highly insoluble drugs, the limiting factor is more often the rate of dissolution than the passage across the intestinal barrier, and one way to better control the dissolution process is to reduce the size of the drug product particles, since surface area increases with decreasing particle size. The dissolution rate is expected to increase proportionally with an increase in surface area. However, it is the effective surface area that is important (i.e. the surface area available to the dissolution fluid) rather than the actual particle size. Consequently, if the drug is hydrophobic and if the dissolution medium has poor wetting properties, a decrease in particle size may retard dissolution rate [79]. If the powder characteristics are adequate (structure, hardness, and chemical stability), micronization is a well-established technique to attain this objective. Aungst et al. [80] evaluated the effects of drug substance and formulation variables on DPC 961, a low-solubility, high-permeability second-generation non-nucleoside reverse transcriptase inhibitor, oral absorption in fasted and fed states in dogs. The authors demonstrate that absolute oral bioavailability of DPC 961 was greater in the fed state compared to the fasted state. They also found that particle size had a major effect on oral absorption in the fasted state and in *in vitro* dissolution tests; however, it had no effect on oral absorption in the fed state. The authors suggest that these differences may be related to differences in the solubilization capacities in the fed and fasted states. Garner et al. [81] evaluated the influence of particle size on the overall absorption of micronized and non-micronized ^{14}C-diosmin tablets after oral administration to humans. The authors found that a reduction of the particle size increased the

duration of absorption of diosmin. Bønløkke et al. [82] investigated the *in vivo* dissolution rate of two particle sizes of spironolactone, a poorly soluble drug, by perfusing a semi-open segment in the proximal jejunum in humans. They found a difference in *in vivo* dissolution rate of the two different particle sizes, although this difference did not affect relative bioavailability.

8.4.6 Biopharmaceutics Classification System: Redefining BSC Solubility Class Boundary

Solubility, dissolution rate, and intestinal permeability, are the major biopharmaceutic factors that affect the rate and extent of absorption of an oral drug product. Particularly for water insoluble drugs that have generally high membrane permeability (BCS Class II), dissolution, and dose are the most critical factors affecting the rate and the extent of oral absorption.

The proposed Biopharmaceutics Classification system (BCS) [49] is based on determining the underlying process that is controlling the drug absorption rate and extent, namely, drug solubility and intestinal membrane permeability. The goal of the BCS is to function as a tool for developing *in vitro* dissolution specifications for drug products that are predictive of their *in vivo* performance. Low solubility dissolution-rate limited drugs can be regulated based on an *in vitro* dissolution test that reflects the *in vivo* dissolution process (Table 8.2). The initial implementation of the BCS is generally considered to be conservative with respect to the class boundaries of solubility, permeability, and the dissolution criteria. The solubility classification of a drug in the BCS is based on the highest dose strength in the immediate-release (IR) product. The solubility class is determined by calculating the volume of an aqueous medium sufficient to dissolve the highest dose strength in the pH range of 1–7.5. A drug substance should be classified as highly soluble when the highest dose strength is soluble in $\leq$250 ml of aqueous media over the pH range of 1–7.5. The dose volume of 250 ml is a conservative estimate of what actually is available *in vivo* for solubilization and dissolution. The solid drug, if it were not in solution on emptying, would dissolve in the fluids in the

Tab. 8.2. Biopharmaceutics Classification System (BCS). BCS is a permeability and solubility classification.

Class	*Permeability*	*Solubility*	*IVIV correlation expectation*
Class I	High	High	IVIV correlation not expected if dissolution is rapid. Gastric emptying is rate determining.
Class II	Low	High	IVIV correlation expected if *in vitro* dissolution rate is similar to *in vivo* dissolution rate (unless dose is very high).
Class III	High	Low	Same as Class I. Correlation will depend on intestinal permeability profile along the gastrointestinal tract.
Class IV	Low	Low	Limited or no IVIV correlation expected.

small intestine. Experimental estimates of small intestinal volumes exhibit a wide variability ranging from 50 to 1100 ml with an average of 500 ml. Thus, an appropriate definition of the volume for solubility classification is difficult to set.

Effective permeability (P_{eff}) is generally described in terms of units of distance of molecular movement per unit time (10^{-4} cm/s). A drug is defined as a high permeability drug if the extent of oral absorption is greater than or equal to 90% and provided that it is not associated with any documented instability in the GI tract.

Weak acid Class II BCS drugs possess low solubility but are highly permeable and well absorbed from the GI tract. Thus, the effective human jejunal permeability of ketoprofen was found to be quite high (8.7×10^{-4} cm/s) and its oral bioavailability in humans is estimated to be >90%. However, its intrinsic aqueous solubility is ~0.119 mg/ml. The *in vitro* solubilities of ketoprofen at pH 6.0 and pH 7.8 were determined to be 3.68 ± 0.18 mg/ml and 19.90 ± 0.06 mg/ml, respectively [73]. Thus, it is expected that at an average intestinal pH of around 6.5, the highest oral dose strength administered would be in the dissolved state. For example, at the highest dose strength of ketoprofen (75 mg, Wyeth-Ayerst Pharmaceuticals, PA), the estimated dose number according to equation (6) would be 0.059 ($V_0 = 250$ ml; $C_s = 5.068$ mg/ml at pH ~ 6.5), suggesting that the absorption of ketoprofen in the intestinal lumen is not dissolution rate-limited. The presence of moderate bile salt and lecithin concentrations in the upper intestine is also expected to contribute to this process. Granero et al. [83] studied the disposition of ketoprofen administered as solutions and as suspensions into the stomach of dogs using an intubation method. The authors demonstrated the rapid disappearance of ketoprofen from the intestinal lumen following gastric emptying, suggesting that absorption of ketoprofen is not dissolution rate-limited. The conclusions drawn from monitoring of ketoprofen amounts in the dog intestine were confirmed by pharmacokinetic studies in dogs. The authors suggest that a Class II BCS weak acid ionizable drug such as ketoprofen behaves in a manner essentially equivalent to Class I drugs and could be considered for a waiver of bioavailability and bioequivalence testing [84].

References

1 E. L. Parrot, D. E. Wurster, T. Higuchi. Investigation of drug release from solids. I. Some factors influencing the dissolution rate. *Am. J. Pharm. Assoc. Sci Ed.* **1995**, *44*, 269.

2 A. Djorjevic and I. Mendas. Method for modelling in vitro dissolution profiles of drug using gamma distribution. *Eur. J. Pharm. Biopharm.* **1997**, *44*, 215–217.

3 J. B. Dressman, G. L. Amidon, C. Reppas, V. Shah. Dissolution testing as a prognostic tool for oral drug absorption: Immediate release dosage forms. *Pharm. Res.* **1998**, *15*, 11–21.

4 P. Macheras, A. Dokoumetzidis. On the heterogeneity of drug dissolution and release. *Pharm. Res.* **2000**, *17*, 108–112.

5 P. Lánský, M. Weiss. Modeling heterogeneity of particles and random effects in drug dissolution. *Pharm. Res.* **2001**, *18*, 1061–1067.

6 G. Shan, K. Igarashi, H. Ooshima. Dissolution kinetics of crystal in suspension and its application to L-aspartic acid crystals. *Chem. Eng. J.* **2002**, *88*, 53–58.

7 A. A. Noyes, W. R. Whitney. The rate of solution of solid substances in their own solutions. *J. Am. Chem. Soc.* **1897**, *19*, 930–934.

8 W. Weibull. A statistical distribution of wide applicability. *J. Appl. Mechan.* **1951**, *18*, 293–297.

9 F. Langenbucher. Linearization of dissolution rate curves by the Weibull distribution. *J. Pharm. Pharmacol.* **1972**, *24*, 979–981.

10 P. M. Sathe, Y. Tsong, V. Shah. *In vitro* dissolution profile comparison: Statistics and analysis, model dependent approach. *Pharm. Res.* **1996**, *13*, 1799–1803.

11 E. Brunner. Reaktionsgeschwindigkeit in heterogenen Systemen. *Z. Phys. Chem.* **1904**, *47*, 56–102.

12 W. Nernst. Theorie der Reaktionsgeschwindigkeit in heterogenen Systemen. *Z. Phys. Chem.* **1904**, *47*, 52–55.

13 H. Grijseels, D. J. A. Crommelin, C. J. De Blaey. Hydrodynamic approach to dissolution rate. *Pharm. Weekbl.* **1981**, *3*, 129–144.

14 P. J. Niebergall, G. Milsovich, J. E. Goyan. Dissolution rate studies. II. Dissolution of particles under conditions of rapid agitation. *J. Pharm. Sci.* **1963**, *52*, 236–241.

15 W. I. Higuchi, E. N. Hiestand. Dissolution rates of finely divided drug powders. I. Effect of distribution of particle sizes in a diffusion-controlled process. *J. Pharm. Sci.* **1963**, *52*, 67–71.

16 C. Nyström, J. Mazur, M. I. Barnett, M. Glazer. Dissolution rate measurements of sparingly soluble compounds with the Coulter Counter model TAII. *J. Pharm. Pharmacol.* **1985**, *37*, 217–221.

17 E. K. Anderberg, M. Bisrat, C. Nyström. Physicochemical aspects of drug release. VII. The effect of surfactant concentration and drug particle size on solubility and dissolution rate of felodipine, a sparingly soluble drug. *Int. J. Pharm.* **1988**, *47*, 67–77.

18 M. Bisrat, C. Nyström. Physicochemical aspects of drug release. VIII. The relation between particle size and surface specific dissolution rate in agitated suspensions. *Int. J. Pharm.* **1988**, *47*, 223–231.

19 M. Bisrat, E. K. Anderberg, M. I. Barnett, C. Nyström. Physicochemical aspects of drug release. XV. Investigation of diffusional transport in dissolution of suspended, sparingly soluble drugs. *Int. J. Pharm.* **1992**, *80*, 191–201.

20 A. W. Hixson, J. H. Crowell. Dependence of reaction velocity upon surface and agitation. I. Theoretical considerations. *Ind. Eng. Chem.* **1931**, *51*, 923–931.

21 R. J. Hintz, K. C. Johnson. The effect of particle size distribution on dissolution rate and oral absorption. *Int. J. Pharm.* **1989**, *51*, 9–17.

22 D.-M. Oh, R. L. Curl, G. L. Amidon. Estimating the fraction dose absorbed from suspensions of poorly soluble compounds in humans: A mathematical model. *Pharm. Res.* **1993**, *10*, 264–270.

23 J. R. Crison. Estimating the dissolution and absorption of water insoluble drugs in the small intestine. Ph.D. Thesis, The University of Michigan, Ann Arbor, MI, **1993**.

24 K. C. Johnson, A. C. Swindell. Guidance in the setting of drug particle size specifications to minimize variability in absorption. *Pharm. Res.* **1996**, *13*, 1795–1798.

25 L. Pereira de Almeida, S. Simões, P. Brito, A. Portugal, M. Figueredo. Modeling dissolution of sparingly soluble multisized powders. *J. Pharm. Sci.* **1997**, *86*, 726–732.

26 D. E. Leahy, J. Lynch, D. C. Taylor. Mechanisms of absorption of small molecules. In: eds. L. F. Prescott and W. S. Nimmo, Novel Drug Delivery and its Therapeutic Application. Wiley, New York **1989**, 33–44.

27 A. Avdeef. Assessment of distribution-pH profiles. In: eds. V. Pliska, B. Testa and H. van de Waterbeemd, Lipophilicity in drug action and toxicology. VCH, Weinheim **1996**, 109–137.

28 H. Nogami, T. Matsuzawa. Studies

on absorption and excretion of drugs. I. Kinetics of penetration of acidic drug, salicylic acid, through the intestinal barrier in vitro. *Chem. Pharm. Bull.* **1961**, *9*, 532–540.

29 H. Nogami, T. Matsuzawa. Studies on absorption and excretion of drugs. II. Kinetics of penetration of basic drugs, aminopyrine, through the intestinal barrier in vitro. *Chem. Pharm. Bull.* **1962**, *10*, 1055–1060.

30 W. G. Crouthamel, G. H. Tan. Drug absorption IV – Influence of pH on absorption kinetics of weakly acidic drugs. *J. Pharm. Sci.* **1971**, *60*, 1160–1163.

31 C. A. M. Hogben, D. J. Tocco, B. B. Brodie, L. S. Schanker. On the mechanism of intestinal absorption of drugs. *J. Pharm. Exp. Ther.* **1959**, *125*, 275–282.

32 J. A. Blair, A. J. Matty. Acid microclimate in intestinal absorption. *Clin. Gastroenterol.* **1974**, *5*, 183–197.

33 J. A. Blair, M. L. Lucas, A. J. Matty. Acidification in the rat proximal jejunum. *J. Physiol.* **1975**, *245*, 333–350.

34 J. B. Dressman, G. L. Amidon, D. Fleisher. Absorption potential: Estimating the fraction absorbed for orally administered compounds. *J. Pharm. Sci.* **1985**, *74*, 588–589.

35 B. C. Goodacre, R. J. Murray. A mathematical model of drug absorption. *J. Clin. Hosp. Pharm.* **1981**, *6*, 117–133.

36 N. F. H. Ho, H. P. Merkle, W. I. Higuchi. Quantitative, mechanistic and physiologically realistic approach to the biopharmaceutical design of oral drug delivery systems. *Drug. Dev. Ind. Pharm.* **1983**, *9*, 1111–1184.

37 J. B. Dressman, D. Fleisher, G. L. Amidon. Physicochemical model for dose-dependent drug absorption. *J. Pharm. Sci.* **1984**, *73*, 1274–1279.

38 J. B. Dressman, D. Fleisher. Mixing-tank model for predicting dissolution rate control of oral absorption. *J. Pharm. Sci.* **1986**, *75*, 109–116.

39 P. J. Sinko, G. D. Leesman, G. L. Amidon. Predicting fraction dose absorbed in humans using a macroscopic mass balance approach. *Pharm. Res.* **1991**, *8*, 979–988.

40 D.-M. Oh, P. J. Sinko, G. L. Amidon. Predicting oral drug absorption in humans: A macroscopic mass balance approach for passive and carrier-mediated compounds. In: ed. D. Z. D'Argenio, Advanced Methods of Pharmacokinetic and Pharmacodynamic Systems Analysis. Plenum Press, New York **1991**, 3–11.

41 P. Veng-Pedersen, N. B. Modi. Optimal extravascular dosing intervals. *J. Pharmacokin. Biopharm.* **1991**, *19*, 405–412.

42 R. Süverkrüp. Discontinuous absorption processes in pharmacokinetic models. *J. Pharm. Sci.* **1979**, *68*, 1395–1400.

43 J. J. Zimmerman. Use of Metzler's NONLIN program for fitting discontinuous absorption profiles. *J. Pharm. Sci.* **1983**, *72*, 138–142.

44 K. Murata, K. Noda, K. Kohno, M. Samejima. Pharmacokinetic analysis of concentration data of drugs with irregular absorption profiles using multi-function absorption models. *J. Pharm. Sci.* **1987**, *76*, 109–113.

45 R. L. Oberle, G. L. Amidon. The influence of variable gastric emptying and intestinal transit rates on the plasma level curve of cimetidine: An explanation for the double peak phenomenon. *J. Pharmacokin. Biopharm.* **1987**, *15*, 529–544.

46 L. X. Yu, G. L. Amidon. A compartmental absorption and transit model for estimating oral drug absorption. *Int. J. Pharm.* **1999**, *186*, 119–125.

47 K. Higaki, S. Yamashita, G. L. Amidon. Time-dependent oral absorption models. *J. Pharmacokin. Pharmacodyn.* **2001**, *28*, 109–128.

48 D.-M. Oh, R. L. Curl, G. L. Amidon. Estimating the fraction dose absorbed from suspensions of poorly soluble compounds in humans: A mathematical model. *Pharm. Res.* **1993**, *10*, 264–270.

49 G. L. Amidon, H. Lennernäs, V. P. Shah, J. R. Crison. A theoretical basis for a biopharmaceutic classification, the correlation of in vitro

drug product dissolution and in vivo bioavailability. *Pharm. Res.* **1995**, *12*, 413–420.

50 B. Agoram, W. S. Woltosz, M. B. Bolger. Predicting the impact of physiological and biochemical processes on oral drug bioavailability. *Adv. Drug Deliv. Rev.* **2001**, *50*, S41–S67.

51 A. F. Hofmann, K. J. Mysels. Bile salts as biological surfactants. *Colloids and Surfaces*, **1988**, *30*, 145–173.

52 W. N. Charman, C. J. H. Porter, S. Mithani, J. B. Dressman. Physicochemical and physiological mechanisms for the effects of food on drug absorption: the role of lipids and pH. *J. Pharm. Sci.* **1997**, *86*, 269–282.

53 P. E. Luner, D. V. Kamp. Wetting behavior of bile salt-lipid dispersions and dissolution media patterned after intestinal fluids. *J. Pharm. Sci.* **2001**, *90*, 348–358.

54 D. Hörter, J. B. Dressman. Influence of physicochemical properties on dissolution of drugs in the gastrointestinal tract. *Adv. Drug. Deliv. Revs.* **2001**, *46*, 75–87.

55 P. Langguth, K. M. Lee, H. Spahn-Langguth, G. L. Amidon. Variable gastric emptying and discontinuities in drug absorption profiles: dependence of rates and extent of cimetidine absorption on motility phase and pH. *Biopharm. Drug Disposit.* **1994**, *15*, 719–746.

56 S. K. Sarna. Cyclic motor activity; migrating motor complex. *Gastroenterol.* **1985**, *89*, 894–913.

57 R. L. Oberle, T.-S. Chen, C. Lloyd, J. L. Barnett, C. Owyang, J. H. Meyer, G. L. Amidon. The influence of the interdigestive migrating myoelectric complex on the gastric emptying of liquids. *Gastroenterol.* **1990**, *99*, 1275–1282.

58 J. E. Devereux, J. M. Newton, M. B. Short. The influence of density of the gastrointestinal transit of pellets. *J. Pharm. Pharmacol.* **1990**, *7*, 500–501.

59 J. K. Rhie, Y. Hayashi, L. S. Welage, J. Frens, R. J. Wald, J. L. Barnett, G. E. Amidon, L. Putcha, G. L. Amidon. Drug marker absorption in relation to pellet size, gastric motility and viscous meals in humans. *Pharm. Res.* **1998**, *15*, 233–237.

60 C. S. Chaw, E. Yazaki, D. F. Evans. The effect of pH change on the gastric emptying of liquids measured by electrical impedance tomography and pH-sensitive radiotelemetry capsule. *Int. J. Pharm.* **2001**, *227*, 167–175.

61 S. S. Davis, J. G. Hardy, J. W. Fara. The intestinal transit of pharmaceutical dosage forms. *Gut* **1986**, *27*, 886–892.

62 L. X. Yu, J. R. Crison, G. L. Amidon. Compartmental transit and dispersion model analysis of small intestinal transit flow in humans. *Int. J. Pharm.* **1996**, *140*, 111–118.

63 C. A. Youngberg, R. R. Berardi, W. F. Howatt, M. L. Hyneck, G. L. Amidon, J. H. Meyer, J. B. Dressman. Comparison of gastrointestinal pH in cystic fibrosis and healthy subjects. *Dig. Dis. Sci.* **1987**, *32*, 472–480.

64 S. Chakrabarti, M. Z. Southard. Control of poorly soluble drug dissolution in conditions simulating the gastrointestinal tract flow. 1. Effect of tablet geometry in buffered medium. *J. Pharm. Sci.* **1996**, *85*, 313–319.

65 W. I. Higuchi. Effects of interacting colloids on transport rates. *J. Pharm. Sci.* **1964**, *53*, 532–535.

66 P. Singh, S. J. Desai, D. R. Flanagan, A. P. Simonelli, W. I. Higuchi. Mechanistic study of the influence of micelle solubilization and hydrodynamic factors on the dissolution rate of solid drugs. *J. Pharm. Sci.* **1968**, *57*, 959–965.

67 J. R. Crison, V. P. Shah, J. P. Skelly, G. L. Amidon. Drug dissolution into micellar solutions: Development of a convective diffusion model and comparison to the film equilibrium model with application to surfactant-facilitated dissolution of carbamazepine. *J. Pharm. Sci.* **1996**, *85*, 1005–1011.

68 M. Gibaldi, S. Feldman, N. D. Weiner. Hydrodynamic and diffusional considerations in assessing effects of surface active agents on the

dissolution rate of drugs. *Chem. Pharm. Bull.* **1970**, *18*, 715–723.

69 J. H. de Smidt, J. C. Offringa, D. J. Crommelin. Dissolution kinetics of griseofulvin in sodium docecylsulfate soltuions. *J. Pharm. Sci.* **1987**, *76*, 711–714.

70 G. E. Granero, C. Ramachandran, G. L. Amidon. Dissolution and solubility behavior of fenofibrate in sodium lauryl sulfate solutions: potential in vivo performance implications (Unpublished).

71 K. G. Mooney, M. A. Mintun, K. J. Himmelstein, V. J. Stella. Dissolution kinetics of carboxylic acids II; effect of buffers. *J. Pharm. Sci.* **1981**, *70*, 22–32.

72 D. P. McNamara, G. L. Amidon. Dissolution of acidic and basic compounds from the rotating disk: influence of convective diffusion and reaction. *J. Pharm. Sci.* **1986**, *75*, 858–868.

73 J. Jinno, D.-M. Oh, J. R. Crison, G. L. Amidon. Dissolution of ionizable water-insoluble drugs: The combined effect of pH and surfactant. *J. Pharm. Sci.* **2000**, *89*, 268–274.

74 N. A. Kasim, A. H. Nada, Y. E. Hammouda, A. Hussain, J. R. Crison, G. L. Amidon. pH and surfactant-facilitated in vitro solubilization and dissolution of ketoprofen, a class II drug. Implications for waiver of bioavailability and bioequivalence studies (Unpublished).

75 P. Li, E. Tabibi, S. H. Yalkowsky. Combined effect of complexation and pH on solubilization. *J. Pharm. Sci.* **1998**, *87*, 1535–1537.

76 N. Jain, G. Yang, S. E. Tabibi, S. H. Yalkowsky. Solubilization on NSC-639829. *Int. J. Pharm.* **2001**, *225*, 41–47.

77 R. Löbenberg, K. Krämer, V. P. Shah, G. L. Amidon, J. B. Dressman. Dissolution testing as a prognostic tool for oral drug absorption: dissolution behavior of glibenclamide. *Pharm. Res.* **2000**, *17*, 439–444.

78 P. Finholt. Influence of formulation on dissolution rate, In: eds. L. J. Leeson, J. T. Carstensen, Dissolution Technology, Whitlock Press, Washington, DC **1974**, 106–146.

79 E. S. Kostewicz, U. Brauns, R. Becker, J. B. Dressman. Forecasting the oral absorption behavior of poorly soluble weak bases using solubility and dissolution studies in biorelevant media. *Pharm. Res.* **2002**, *19*, 345–349.

80 B. J. Aungst, N. H. Nguyen, N. J. Taylor, D. S. Bindra. Formulation and food effects on the oral absorption of a poorly water soluble, highly permeable antiretroviral agent. *J. Pharm. Sci.* **2002**, *91*, 1390–1395.

81 R. C. Garner, J. V. Garner, S. Gregory, M. Whattam, A. Calam, D. Leong. Comparison of the absorption of micronized (daflon 500® mg) and nonmicronized ^{14}C-diosmin tablets after oral administration to healthy volunteers by accelerator mass spectrometry and liquid scintillation counting. *J. Pharm. Sci.* **2002**, *91*, 32–40.

82 L. Bønløkke, L. Hovgaard, H. G. Kristensen, L. Knutson, H. Lennernäs. Direct estimation of the in vivo dissolution of spironolactone, in two particle size ranges, using the single-pass perfusion technique (Loc-I-Gut®) in humans. *Eur. J. Pharm. Sci.* **2001**, *12*, 239–250.

83 G. E. Granero, C. Ramachandran, G. L. Amidon. Rapid *in vivo* dissolution of ketoprofen in dogs (Unpublished).

84 Guidance for industry, waiver for in vivo bioavailability and bioequivalence studies for immediate release solid oral dosage forms based on a biopharmaceutics classification system. August **2000**, CDER/FDA.

9
Aqueous Solubility in Discovery, Chemistry, and Assay Changes

Chris Lipinski

Abbreviations

DMSO	Dimethyl sulfoxide
ELSD	Evaporative light scattering detection
EPA	Environmental Protection Agency
FDA	Food and Drug Administration
HPLC	High-performance liquid chromatography
HTS	High-throughput screening
MW	Molecular weight
NMR	Nuclear magnetic resonance
R&D	Research and development
sd	Structure data (file type)
TPN	Total parental nutrition
UV	Ultraviolet

Symbols

pH	Acidity/basicity
pK_a	Ionization constant

9.1 Introduction

This chapter is not simply a treatise on the highest capacity methods for measuring aqueous solubility in a discovery setting that most closely approximate a lower capacity thermodynamic solubility measurement. Rather it is the author's viewpoint that dealing with the problem of poor drug solubility in an early discovery setting requires an appreciation of recent changes in three related but distinct areas. The areas to be considered are:

1. Changes in the chemistry method of synthesis and therefore in resultant physical form and aqueous solubility.

Drug Bioavailability: Estimation of Solubility, Permeability, Absorption and Bioavailability.
Edited by Han van de Waterbeemd, Hans Lennernäs and Per Artursson

ISBN: 3-527-30438-X

2. Changes in the method of compound distribution for biological assays and therefore changes in apparent aqueous solubility and compound concentration.
3. Changes in screening technologies and changes in biological targets and their resulting impact on aqueous solubility.

These three areas will be discussed as they relate to aqueous solubility. This will be followed by a general discussion of experimental approaches to measuring aqueous solubility in a discovery setting. Detailed descriptions of varied discovery solubility assays can be found in the excellent review by Kerns [1].

9.2 Compound Synthesis

Combinatorial chemistry and parallel synthesis are now the dominant methods of compound synthesis at the lead discovery stage [2]. The method of chemistry synthesis is important because it dictates compound physical form and therefore compound aqueous solubility. As the volume of chemistry synthetic output increases due to combinatorial chemistry and parallel synthesis, there is an increasing probability that resultant chemistry physical form will be amorphous or a ''neat'' material of indeterminate solid appearance. There are two major styles of combinatorial chemistry – solid-phase and solution-phase synthesis. There is some uncertainty as to the true relative contribution of each method to chemistry output in the pharmaceutical/biotechnology industry. Published reviews of combinatorial library synthesis suggest that solid-phase synthesis is currently the dominant style contributing to about 80% of combinatorial libraries [3]. In solid-phase synthesis the mode of synthesis dictates that relatively small quantitities of compounds are made.

9.3 Compound Physical Form

The most commonly encountered physical form of compounds in current early drug discovery is noncrystalline. This is important because noncrystalline materials are almost always more soluble in all solvents, including aqueous media. In traditional chemistry, the melting point was used a criterion of compound identity and purity. For example, if the compound being made had previously been reported in the scientific literature, one would look for an identical or perhaps higher melting point for the newly synthesized material. A lower melting point was viewed as problematic because of the observation that a contaminant usually causes a melting point depression. A sharp melting point was an indication of compound purity. A broad melting point was an indicator of an impure compound. In the modern era, there is an emphasis on the use of solution spectra such as proton or carbon NMR as an indicator of compound identity or purity.

Mass spectral analysis serves to confirm identity. So, in terms of compound identity or purity, melting point is less important than in previous eras. When chemists face pressure to increase chemistry synthetic output they do so by initially deleting noncritical steps in the synthesis/isolation process. Repeated compound crystallization to a sharply-melting crystalline solid is very time consuming, is noncritical to compound identity and purity, and is therefore eliminated. This has occurred even if the chemistry is the traditional single compound at a time synthesis. For example, at the Pfizer Global R&D Groton laboratories the percentage of early discovery stage traditionally made compounds with melting point measured was close to zero in 2000, as opposed to a decade earlier where some 80% of compounds intended for biological screening were registered with melting point information.

9.4 Compound Distribution

Compounds intended for biological screening are increasingly being distributed as solutions in dimethyl sulfoxide (DMSO) rather than as ''neat'' materials. There are two effects of this trend on the apparent compound solubility in DMSO, each with different implications. Over relatively short time scales (up to perhaps a day), compounds may appear more soluble in DMSO than thermodynamic solubility would suggest. Over longer time scales, compounds may precipitate, and this may lead to uncertainty as to the actual concentration of the drug in the DMSO stock solution. As far as aqueous solubility is concerned, compounds will appear to be more soluble than a thermodynamic assay would suggest if initial dissolution in aqueous medium occurs from a DMSO stock solution. This is especially so if the time scale for the solubility assay is short (on the order of tens of minutes). Why are compounds distributed as DMSO solutions? The reason is that it is far easier to automate the distribution of solutions of compound solubilized in DMSO than it is to distribute compounds as ''neat'' materials. Robots efficiently pipette measured volumes of liquids. One cannot nearly as efficiently quantitate and transfer a neat (solid) compound. When a compound in DMSO solution is added to an aqueous medium, it is being delivered in a very high energy state relative to the thermodynamically most stable polymorph. The compound is in DMSO solution, so there is no compound crystal lattice to disrupt as part of the aqueous solubilization process. The effect is that the compound's initial apparent aqueous solubility is almost invariably higher than in a thermodynamic solubility experiment. This phenomenon occurs irrespective of any solubilization advantage attendant to the amount (often quite small) of DMSO that may be present in the aqueous medium. The apparent increase in solubility tends to be time-dependent, i.e., the solubility difference tends to decline with time. Exceptions to the phenomenon of higher apparent solubility when compound is added in DMSO solution to aqueous media have been observed when solubility is quantitated by very sensitive particle scattering methodology, as in the use of cell sorting technology to detect particulate (undissolved solid) by light scattering. The causes of this counter-intuitive behavior

are unknown, but it would be reasonable to conjecture that the phenomenon of apparently higher solubility could be due to light scattering caused by aggregates with sizes in the micron to sub-micron size range.

9.5 Compound Physical Form: Ostwald's Rule of Stages

When a newly synthesized compound is first isolated, it frequently may exist in an amorphous form. As experience is gained in compound isolation, the amorphous form is gradually successively replaced by polymorphs (crystalline forms) of increasing thermodynamic stability. This process occurs so frequently that it has been given a name ''Ostwald's rule of stages''. The process occurs because in the isolation/crystallization process there is a tension between the importance of kinetic and thermodynamic factors in the crystallization/isolation process. When the knowledge base in the chemistry crystallization process is low, i.e., early in the history of the compound isolation process, it is unlikely that the crystallization conditions are the optimum to produce the thermodynamically most stable form. Rather, kinetic processes determine the crystalline form and thermodynamically less stable polymorphs are likely to be encountered. With increasing isolation experience, control of crystallization conditions such as compound concentration, solvent choice, cooling rate, etc., become better known and the probability of isolating the thermodynamically most stable polymorph is much increased [4].

9.6 Polymorph Form and Aqueous Solubility

Process changes in chemistry which increase the probability that new compounds will be isolated in amorphous or thermodynamically unstable polymorphic form will have the effect of increasing the apparent aqueous solubility of newly synthesized compounds. Ostwald's rule of stages explains the common phenomenon that the physical form that is first isolated for a newly synthesized compound has a low melting point. This low-melting point material corresponds to amorphous material or a thermodynamically unstable polymorph. The initially isolated material is in a high-energy state relative to the thermodynamically most stable (highest melting point) polymorph. The consequence of the high-energy state is that when dissolution in a solvent is attempted, less energy is required to disrupt the crystalline/solid state and the compound is therefore more soluble. In general, there are only a few exceptions to the rule that the highest-melting point polymorph is the most insoluble. The types of polymorphs that might have a lower melting point but higher solubility (enantiotropic polymorphs) are seldom encountered in a pharmaceutical setting. These exceptions typically occur when the solubility is measured at a temperature moderately close to the compound melting point. Most pharmaceutical organizations select against compounds with a melting point of

less than 100 or 110° Celsius because the low melting point is associated with problems in accelerated stability testing and with problems in formulation development. As a result, the rule that the highest-melting point polymorph is the least soluble generally holds for solubility measured either at room temperature or body temperature.

9.6.1 Implications for *in vitro* Assays

Process changes in chemistry which increase the probability that new compounds will be isolated in amorphous or thermodynamically unstable polymorphic form have profound implications for *in vitro* assays, and in particular for high-throughput screening (HTS). In the case of libraries of hundreds or thousands of compounds, the reader can approximate the thermodynamic aqueous solubility that might be expected by performing a calculation using any of the commercially available solubility calculation programs. A discussion of solubility calculation is outside the scope of this chapter. An aqueous solubility calculator that operates in batch mode using Molecular Design Limited (MDL) format structure data (sd) files as input can be obtained as a free download from a United States Environmental Protection Agency (EPA) web site [5]. Generally, a molar solubility of 10 μM or poorer is incompatible with appreciable oral activity for the average permeability, average potency (typically 1 mg kg^{-1}) drug [6]. It is not unusual to find that one half of compounds in a suboptimal combinatorial library are predicted to have a thermodynamic solubility at or below 10 μM when examining sd files of commercially available combinatorial compounds. When noncrystalline combinatorial compounds are screened in HTS assays, the results are far better than might be predicted from solely thermodynamic solubility considerations, and it is quite possible to detect fairly insoluble active compounds in the HTS screen. Success in detecting a poorly soluble compound in an in-vitro screen depends very much on the assay conditions. For example, does the assay contain components likely to solubilize the compound? Success in the HTS assay in detecting activity in an insoluble compound is also dependent on the initial physical form of the compound. An amorphous compound (the predominant physical form in combinatorial chemistry compounds) is far more likely to dissolve to give a concentrated DMSO stock solution than is a crystalline compound. For many amorphous compounds, the solubility in DMSO will be supersaturated relative to the thermodynamic DMSO solubility of a more stable crystalline form. Some compounds will stay in solution indefinitely, even though the solutions are supersaturated. These are compounds whose concentration lies in a thermodynamically unstable but kinetically stable so-called ''metastable zone''. This phenomenon is encountered only when a supersaturated solution is created in the absence of crystalline solid; it does not occur if dissolution starts from the crystalline solid.

Compounds will precipitate from a DMSO stock solution if the kinetic conditions are appropriate; for example, if enough time passes or enough freeze–thaw cycles are encountered as part of the compound in DMSO storage process. Opera-

tionally, the present author has encountered the phenomenon of a ''working day'' solubility window. Amorphous compounds generally dissolve fairly easily at 30 or even at 60 mM in DMSO, but noticeable precipitation can be detected after about a day. This occurs even at room temperature and even in the absence of any freeze–thaw cycle. The one working-day window phenomenon for solubility in DMSO has implications for the detection of HTS actives. For example, suppose an HTS assay results in a number of actives. A similarity search is then conducted on the actives and, based on the search, compounds are submitted to an HTS re-screen. We have frequently found compounds active in the re-screen that were inactive in the original HTS assay. The likely reason is the kinetic phenomenon of compound precipitation from medium time length storage of DMSO master plates. Active compounds were not detected in the primary screen because these compounds were not available to the primary screen; clearly, they had precipitated from the stored master DMSO plates. The re-screen is performed with freshly DMSO solubilized samples (within the one working-day window), thereby allowing a better detection of a truly active compound.

Process changes in chemistry which increase the probability that new compounds will be isolated in amorphous or thermodynamically unstable polymorphic form have profound implications for *in vitro* assays in traditional biology laboratories. This author anticipates an increase in the noise level of traditional biology *in vitro* assays in particular as compounds are increasingly distributed as DMSO stock solutions, and also anticipates a resultant very negative reaction from traditional biology personnel. The reason for the increased noise level is the increased degree of uncertainty as to the actual concentration of a compound being screened when compounds are distributed as DMSO stock solutions. The purely technical considerations relating to compound physical form and resultant precipitation from DMSO stocks are similar in HTS assays and traditional biology *in vitro* assays, but the people considerations are very different. Personnel involved in HTS assays have long been tolerant of the problems attendant to HTS screens. They are not particularly upset because active compounds may be missed in an HTS screen because of poor aqueous or DMSO solubility. To people familiar with HTS assays, this is just part of the cost of doing business – an inevitable trade-off between the greatly enhanced screening capacity of HTS versus an inevitable loss of accuracy. This type of mindset is very different from that likely to be encountered among traditional biologists. Traditional biologists place a premium on *in vitro* screen accuracy and take pride in assay reproducibility. Uncertainty as to compound concentration is minimized when stock solutions are freshly prepared from a ''neat'' amorphous material or a freshly prepared DMSO stock. In essence with respect to compound distribution a traditional biology laboratory mostly works within the one working-day scenario. However, all this changes if the method of compound distribution changes towards an automated dispensing of drug in DMSO stocks. Compound concentration in an *in vitro* assay becomes an important noise factor if the compound has precipitated from DMSO as part of the compound storage process. The biologist may interpret assay results as reflective of compound aqueous insolubility. However, the problem may have occurred at an even earlier stage in

that precipitation actually occurred from the DMSO stock solution. In addition, compound loss from DMSO may be interpreted as a chemical instability (degradation) problem. Considerable semantic confusion can result from the term ''instability''. To a biologist, it may mean compound loss from solution, whereas a chemist might interpret ''instability'' as a change in chemical structure, i.e., as a chemical degradation problem. These differences are meaningful because different strategies might be chosen to deal with compound loss from a DMSO stock, depending on whether the problem is precipitation or chemical degradation.

9.6.2 Implications for *in vivo* Assays

Process changes in chemistry which increase the probability that new compounds will be isolated in amorphous or thermodynamically unstable polymorphic form enhance the probability that *in vivo* activity will be detected if aqueous solubilization of the compound is performed fairly rapidly. This is likely to be the case, since a biologist or drug metabolism worker will likely want to ensure oral exposure of a solution to an animal fairly quickly so that dosing occurs before the compound precipitates. Alternately, dosing might be performed with ''neat'' amorphous solid materials as a suspension. In either of these scenarios the oral dosing with amorphous solid will appear more efficacious than if the oral dosing is started with a suspension of the less-soluble, thermodynamically more stable crystalline product form. The oral activity improvement attendant to the amorphous form of the compound may not be detected until a serious attempt is made to obtain crystalline material. This could come as late as the clinical candidate nomination stage. What should be avoided at all costs is the choice of the ''best'' orally active compound by a comparison of the oral bioavailability of poorly characterized solid forms. The oral absorption component of oral bioavailability (but not the metabolism factor) is extremely dependent on crystalline form. Making a choice using poorly characterized solid forms risks choosing a nonoptimum compound. In fact, this error may not even be noticed if only the clinical candidate has been crystallized. Critical to these arguments is the presumption that most *in vivo* assays will not be conducted with stored compound in DMSO stock solutions.

9.7 Solubility, Potency and Permeability Inter-relationships

Aqueous solubility, potency and permeability are three factors under medicinal chemistry control that must be optimized to achieve a compound with acceptable oral absorption. Typically, a lead (chemistry starting point) is deficient in all three parameters. The inter-relationships of these three parameters has been described in a series of publications from Pfizer researchers [7, 8]. Figure 9.1 depicts graphically the minimum acceptable solubility as a function of projected clinical potency and intestinal permeability. A minimum thermodynamic aqueous solubility of 52

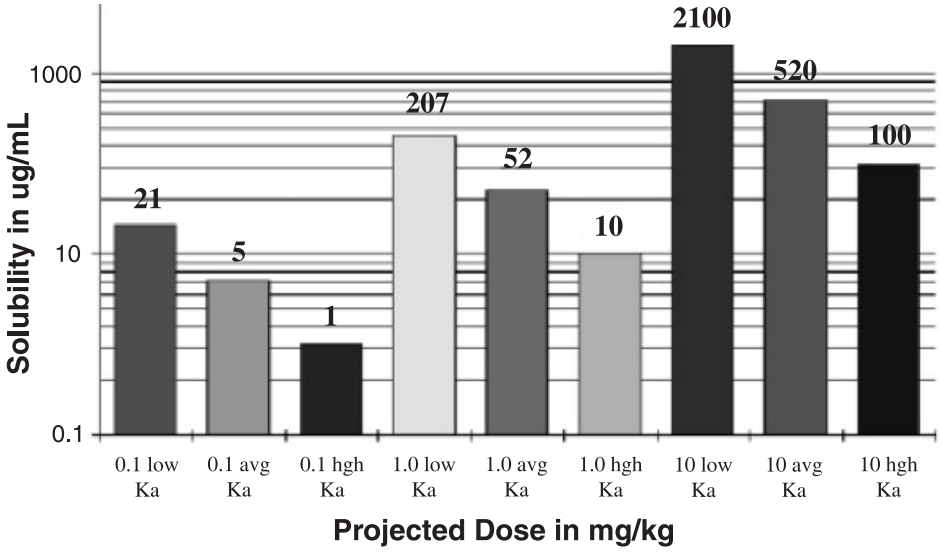

Fig. 9.1. Minimum acceptable solubility (in μg mL^{-1}). The bars show the minimum solubility for low, medium, and high permeability (Ka) at a clinical dose. The middle three bars are for a 1 mg kg^{-1} dose. With medium permeability, a solubility of 52 μg mL^{-1} is required.

μg mL^{-1} is required in the most commonly encountered situation where the projected clinical potency is 1 mg kg^{-1} and the permeability is in the average range. If the permeability is in the lower tenth percentile – as might be found for a peptidomimetic – the minimum acceptable solubility is 207 μg mL^{-1}. The minimum acceptable solubility is 2100 μg mL^{-1} if the potency is poor (and the dose high), as for example occurs among some HIV protease inhibitors.

9.8 Acceptable Aqueous Solubility for Oral Activity

9.8.1 Traditional Definition

A classic pharmaceutical science textbook might have defined poor solubility as anything below a solubility of 1 g mL^{-1} (2 mol L^{-1} solution for a molecular weight of 500 Da) at pH 6.5 (or pH 7). This classic view is reflected in the Chemical Abstracts SciFinder 2001® solubility range definitions for solubility calculated using Advanced Chemistry Development (ACD) Software Solaris V4.67. These semiquantitative ranges for molar solubility are: very soluble, 1 mol L^{-1} < solubility; soluble, 0.1 mol L^{-1} < solubility < 1 mol L^{-1}; slightly soluble, 0.01 mol L^{-1} <

solubility < 0.1 mol L^{-1}; sparingly soluble, solubility < 0.01 mol L^{-1}. The traditional definition is reasonable for the time frame where many drugs had clinical potency in the 10–20 mg kg^{-1} per day range. This type of very poor potency (high doses in the gram range) is seldom encountered today, except for therapy with some infectious disease and antiviral drugs. The likely reason is the use of mechanism as opposed to phenomenological screening (*in vivo* screening) and the improved potency attendant to leads resulting from high-throughput screening.

9.8.2
Current Era Definition

In the current era with widespread problems of poor solubility [4] a compound (drug) with average permeability and a projected clinical potency of 1 mg kg^{-1} needs a minimum aqueous solubility of 50–100 μg mL^{-1} to avoid the use of nonstandard solubility fixing formulation technology. The guidelines published by Pfizer's Curatolo on maximum absorbable dose are an excellent guide for the combination of permeability, solubility and potency required in an orally active drug [8].

9.9
Solubility in Practice: Development versus Discovery

9.9.1
Development Thermodynamic Solubility as a Benchmark

The quantitation of solubility in the current discovery setting differs markedly from that of a traditional aqueous solubility assay. In the traditional solubility assay, crystalline well-characterized solid is equilibrated in aqueous solution for sufficient time to reach equilibrium (generally 24–48 hours). The solution composition is important in the comparison with a discovery solubility assay. The traditional thermodynamic solubility experiment is performed in the absence of any organic co-solvent. By way of comparison, the discovery solubility assay is frequently performed in the presence of a co-solvent, usually DMSO. The physical state of the starting solid in the development thermodynamic assay is relevant to the comparison with discovery solubility assays. As previously mentioned, solids in discovery in the current era are frequently noncrystalline and therefore invariably more water-soluble. The thermodynamic assay time duration is important to the comparison of the time scale of discovery solubility assays where the time scale is frequently much shorter. The development thermodynamic solution experiment is filtered through a filter, typically in the micron size range. For example, filters of 1.2 μm are recommended for lipid-containing total parenteral nutrition (TPN) solutions, and filters of 0.22 μm for nonlipid TPN. The particle size that would be considered as constituting a ''solution'' in a thermodynamic solubility measurement is important in the context of discovery solubility measured by particle-based

light scattering. After separating the solid from the liquid phase by filtration (or possibly by centrifugation), the quantity of compound in the aqueous phase is measured by a quantitative technique, for example by HPLC with ultraviolet (UV) detection. Positive standards are used to bracket the aqueous concentration of soluble drug. Care is taken that the positive standards reflect the ionization state of the drug in solution, since substantial changes in UV extinction coefficient frequently occur as a function of solution pH for an ionizable drug. This latter point is important in the context of discovery solubility measured by UV spectroscopy. In the developmental thermodynamic solubility assay, the compound purity is typically quite high. This is important to the comparison with the discovery solubility assay where the compound purity is typically lower. At the time of writing, typical compound purity criteria for combinatorial chemistry compounds from the better chemistry sources were 90% pure by evaporative light scattering detection (ELSD) or 80% pure by UV detection (typically ELSD is a less sensitive detector than UV of compound impurities). The compound purity issue is particularly important to the issue of discovery solubility assays using a UV quantitation end point.

9.9.2 Turbidimetric/Particle-based Solubility

The presence of a precipitate of insoluble material can be used as an indicator that the solubility limit of a compound has been exceeded. There are two general methods to instrumentally detect the presence of a precipitate: (i) the precipitation can be detected using UV absorbance; or (ii) it can be detected by directly measuring light scattering using a type of nephelometric light-scattering detector. Light scattering can also be detected visually by taking advantage of the Tyndall effect. The UV absorbance method uses the fact that particles in the path of the light beam scatter light away from the light detector, or actually block the light from reaching the detector. The light-scattering ''absorption'' curve has the properties of an inverse power curve with the absorption predicted by a curve of the form (constant divided by wavelength raised to the power n). In any particular solubility experiment the constant term and power n tend to be constant until a significant change in the particles occurs (e.g., from agglomeration). In our experiments we encountered values of n ranging from 2.5 to 4.5. Because of the inverse power curve form of the absorption curve, the absorption due to light scattering is greatest at short wavelengths. The presence of a confounding UV absorbance from soluble drug is the major disadvantage of measuring particle-based light scattering by UV absorbance. For compounds with an aqueous solution that is not visibly colored, this is generally not a problem as one can measure absorbance due to light scattering at about 500 nm, which is outside of the typical soluble chromophore absorption range. However, colored compounds or compounds with colored impurities can absorb due to soluble chromophore in this range. The problem can be circumvented by using a UV diode array detector and performing a Fourier transform analysis on an absorbance data array, for example a range of 64 or 128 absorbance readings at evenly spaced wavelength increments. The Fourier trans-

form analysis relies on the fact that the apparent band width of the absorption light-scattering curve is very much broader than the band width of any soluble absorbance chromophore. The successive terms of the absorbance data Fourier transform can be interpreted in terms of contributions of gradually decreasing bandwidth. The first term of the Fourier transform essentially defines a baseline shift of very broad bandwidth and is a very sensitive measure of the absorbance due to light scattering. A plot of the first Fourier transform term versus amount of compound added works much better as an index of precipitation than a simple plot of absorbance versus amount of compound added. The UV absorbance method is also somewhat dependent on the instrumental design and works best when there is a large distance between the sample cell and the UV detector.

The presence of a precipitate of insoluble material can be directly detected by an instrument specifically designed to detect a light-scattering signal. Instruments are available that operate in single-cell or plate-reader format. Single-cell instruments can be used as is, or adapted to automated measurement. For example, we were able to develop an automated assay using a modified HACH AN2100 nephelometric turbidity detector. Instrument costs are quite reasonable because simple, robust light-scattering detectors are widely sold for use by water quality engineers to test for clarity in water treatment plants. It transpires that water clarity is a very good indication of the absence of a variety of pathogenic intestinal parasites that might be found in contaminated water. These types of organisms have effective sizes of about 1 μm and are reliably detected by visible light scattering using a detector at 90° to the visible light path. Most mammals (including humans) have, through evolution, developed a keen ability to detect light scattering (cloudiness) in water. In our benchmarking, we discovered that this author's ability to detect light scattering using the Tyndall effect was only about one order of magnitude less sensitive than that using a HACH instrument. A nephelometric turbidity detector can be calibrated against a set of commercially available turbidity standards. The detector response is nonlinear to the quantity of compound precipitated, so what is measured is essentially binary data, i.e., the solution is clear (no precipitation) or turbidity (precipitation) is detected outside of the baseline (clear) nephelometric turbidity signal.

Two extremes of turbidity signal are detected as compound in DMSO solution is added stepwise to an aqueous medium. In one pattern, a gentle steady increase in signal is observed as the solubility limit is exceeded. We find that this pattern most often corresponds to a compound that precipitates because it is excessively lipophilic. In the second pattern, a very marked steep increase in turbidity signal is encountered as the solubility limit is exceeded. We find that this pattern most often corresponds to a compound that precipitates because of crystalline packing considerations. We also find that compounds generating the second type of pattern tend to give far more reproducible results in replicate assays. We interpret this as reflecting a very quick precipitation when the solubility limit is surpassed for a compound precipitating because of crystal packing reasons. Large signals are generated with these types of compounds because particle sizes are small and in the optimum size range (~1 μm) for detection with a visible light source. Lipophilic

compounds tend to precipitate as larger particles, which also generate a weaker light-scattering signal. Reproducibility is poorer for the detection of precipitates of lipophilic compounds, presumably because of kinetic considerations, i.e., there is more variability in the time it takes for precipitation of the lipophilic compound to occur. The precipitation behavior has similarity to the crystallization behavior of compounds in a chemistry synthesis laboratory. The more lipophilic compounds are more difficult to crystallize than the high-melting point compounds. A fluorescent compound can generate a false-positive signal in a nephelometric turbidity assay, whilst a soluble drug with good fluorescent properties absorbs unpolarized light and emits unpolarized light with a good Stokes shift, i.e., at higher wavelength in all directions. This behavior could then be confused with a light-scattering signal. The potential problem is easily solved by introducing a low-wavelength cutoff filter in front of the off axis detector. In our assays at Pfizer we introduced a cutoff filter that prevented detection of soluble fluorescein up to the upper concentration limit in our assay. The filter had no discernable effect on reducing sensitivity to the detection of scattered visible light. Fortunately, for pharmaceutical drug solubility screening there are very few drugs that fluoresce above the fluorescein emission range as these soluble compounds would generate a false-positive signal.

9.9.3 UV Detector-based Solubility

The solubility of a compound can be quantitated by measuring the compound solution concentration by UV spectroscopy. This method requires the use of some type of positive standard because there are no reliable computational techniques to predict UV absorbance and extinction coefficient from structure alone. The factors that need to be considered in a reliable UV-based method include the following. A method must be in place to correct for any UV spectral absorbance changes between reference and test samples that occur as a result of: (i) solvent medium changes between reference and test sample; (ii) pH changes between reference and test sample; and (iii) confounding UV absorbances between reference and test samples that may result from UV-absorbent impurities in the compound whose solubility is being tested. The order of importance of these possible problems and the need for their correction is listed from least to most important. Very detailed discussions of these issues in solubility profiling can be found in the excellent review by Avdeef [9].

The least problematic issues are UV spectral changes as a function of different solvents between the reference and the test sample. Solvent effects on UV spectra in solvents of decreased dielectric constant compared with water parallel solvent effects on apparent pK_a. The changes are most marked for acids, for example, leading to a numerical increase of up to two pK_a units – an apparent decrease in the acidity of the carboxylic acid. Effects on bases are considerably less. The apparent pK_a of a base in a reduced dielectric constant solvent might be up to about half a pK_a unit numerically lower (less basic). The UV spectra of neutral compounds

are generally not markedly affected by changes in solvent dielectric properties. As a result, solvent corrections are generally not critical for UV quantitation of libraries of neutral or weakly basic or acidic compounds (frequently combinatorial). The most problematical functional group, namely a carboxylic acid, does not pose a major concern. Among known Phase II drugs, only about 14% are carboxylic acids and these are frequently under-represented relative to this 14% figure in combinatorial libraries.

The issue of UV spectral absorbance changes resulting from pH changes between the reference and test sample is more important. The UV spectra of compounds containing ionizable moieties located on or near chromophoric groups can be markedly changed (both in absorption maxima and extinction coefficient) by differences in medium pH. This phenomenon is well known, and is the basis of methods for determining compound pK_a by plotting spectral absorbance changes versus pH. Correction requires experimental data, i.e., UV spectra captured at several pH values. Alternatively, batch mode pK_a calculations can be used to bin compounds into the neutral and weakly basic and acidic materials for which there is unlikely to be a potential problem, as opposed to the strong acid and base classes for which the ionization state can markedly affect the UV quantitation.

9.9.4
Other Methods-based Solubility

Aqueous solubility can be measured by potentiometric titration. The theory behind this method and its practical implementation has been pioneered by Avdeef. A solution of the compound in the pH range where the compound is soluble is titrated towards the pH region where the compound is insoluble. In the soluble region, the normal type of data from a potentiometric titration are collected, namely millivolt versus volume of titrant added. This data range serves to define the compound pK_a. At and past the compound precipitation point, data corresponding to millivolt versus volume of titrant added data continues to be collected. However, the data obtained past the precipitation point defines not the pK_a but the compound solubility product. In favorable cases where the precipitation point occurs about halfway through the titration it is possible to obtain both compound pK_a and compound solubility product from a single titration experiment. The theory is very well worked out for this method for almost every reasonable combination of ionizable groups likely to be present in a drug molecule. The analysis of the change in titration data once precipitation occurs requires very high-quality potentiometric titration equipment, excellent protection against carbon dioxide uptake, and very sophisticated curve analysis software – all of which are commercially available. The method requires the compound in low-milligram quantities, and works best for very insoluble compounds – which also are the most difficult to quantitate by other methods. The method is relatively slow, since for best results the titration rate is greatly slowed as the precipitation point is reached. Compound in the assay is solubilized at the beginning of the assay, either by pH dissolution of solid or by dissolution of a concentrated DMSO stock solution in aqueous media

of appropriate pH. As a result, there is no control as to which polymorphic form of the compound corresponds to the solubility product. The method is likely to be particularly useful in the solubility classification of compounds according to the FDA bioavailability waiver system because of the extensive validation of the method, its reproducibility and its particular applicability to compounds with the poorest solubility.

9.10 Solids not Characterized in Early Discovery

As previously discussed, compound form differs markedly between early discovery and the late discovery/development interface. The early discovery compound is poorly characterized as to its crystalline form – it may be nonsolid, amorphous, or possibly crystalline but uncharacterized as to polymorphic form. The late discovery/development interface compound is crystalline as defined by phase-contract microscopy or powder X-ray diffraction, and its polymorphic and salt form is frequently characterized. This difference has profound implications for the design of a discovery solubility assay. The key question is this: Is it better to design an early discovery solubility assay as a separate type of experiment, or is it better to try to automate a traditional thermodynamic solubility assay to handle the very large number of compounds likely to be encountered in early discovery? Another way to state this question is this: Does it make sense to run a thermodynamic solubility assay on poorly crystalline early discovery compounds? This is the type of question about which reasonable people could disagree. However, this author does have a distinct opinion. It is much better to set up a distinctively different solubility assay in early discovery and to maintain a clear distinction between the assay type appropriate in early discovery and the assay type appropriate at the late discovery/development interface. Two issues are relevant to this opinion: One relates to the need for a solubility assay to reflect/predict early discovery stage oral absorption; and the other relates to people/chemistry issues.

An early discovery solubility assay is most useful to chemists at the stage where oral absorption structure–activity relationship (SAR) is not present or poorly defined. This typically might occur after reasonable *in vitro* activity has been discovered and attempts are underway in drug metabolism to establish oral absorption, or in biology to demonstrate oral activity. The early discovery solubility assay is most likely to predict the early drug metabolism or biology studies when the solubility protocol mimics the manner of dosing in drug metabolism and biology. Typically, this means that starting compound is dissolved in DMSO solution and short read times in the low tens of minutes are used in the solubility assay. These solubility assay conditions mimic the dosing conditions in early drug metabolism and biology. This type of reasoning is a very hard sell for a scientist with a strong development or analytical background, because it means setting up a solubility assay that breaks every pharmaceutical sciences textbook rule about the qualities of a ''proper'' solubility assay.

Chemists have the primary responsibility of altering the compound chemical structure so as to improve on a solubility problem. Anything that undermines this primary responsibility of the chemist is harmful to overall research productivity. In my experience, chemists (perhaps unconsciously) are always eager to obtain data that make their compounds look better. For example, chemists might seek solubility data in simulated intestinal contents in order to obtain better (higher) solubility values. This exercise is of no value if it does not somehow result in compounds with better properties being made. Unfortunately, this search for better-appearing solubility data can actually be counterproductive. This happens if the new solubility data does not solve a solubility problem and takes the pressure of the chemist to change the chemical structure towards a better profile. The chemist ''people'' factor is a major reason for avoiding a ''thermodynamic'' solubility assay on early discovery compounds. The term ''thermodynamic assay'' has a connotation associated with developmental rigor and accuracy. There is a grave danger that the chemist will uncritically accept the solubility value from a ''thermodynamic assay'' in early discovery on amorphous material or on material in a DMSO solution. As previously discussed, solubility assays on compounds in high-energy forms (DMSO solution or amorphous) almost always overestimate the aqueous solubility. If the chemist uncritically accepts an inflated early stage solubility as the gospel truth, there will be little pressure to produce an acceptable solubility compound once the material is characterized in the crystalline form. It is much better to keep the solubility assays distinct: an early assay for prediction of absorption SAR; and an efficient thermodynamic assay for the late discovery/development interface. In our discovery organization in Groton, Connecticut, USA, we force this distinction by refusing to run our automated thermodynamic solubility assay on compounds that are not crystalline. The traditional ''thermodynamic'' solubility assay starting from crystalline material can be considerably improved by applying more modern dissolution technology with particular care to reducing the aqueous volume and hence the sample size requirement [10].

9.11
Solids Solubilized in DMSO in Early Discovery

Adding compounds solubilized in DMSO to aqueous medium as part of a discovery solubility assay can lead to two types of solubility assay with different uses. At one extreme, the quantity of DMSO is kept very low (<1%). At this low level of DMSO, the solubility is only slightly affected by the DMSO content. For example, data from a poster by Ricerca Ltd. [11] suggest that a DMSO content of 1% should not elevate apparent solubility by more than about 65%. At 5% DMSO, this group reported an average solubility increase of 145% due to the DMSO content. Solubility in an early discovery assay containing one percent DMSO can however exceed ''thermodynamic'' solubility by much more than 65%. However, this is very likely due to the time scale. Studies by the Avdeef (pIon Inc.) group show a close approximation of early discovery solubility (quantitated by UV) to literature ther-

modynamic solubility if the early discovery assay is allowed to approach equilibrium, for example by being left overnight. The availability of DMSO stock solutions places limitations on the concentration range that can be achieved without exceeding the 1% DMSO limit. For example, if the DMSO stock is 30 mM, a 1 to 100 dilution achieves a final concentration of 300 μM. This corresponds to a concentration of 150 μg mL^{-1} (for MW = 500), which is above the solubility limit required for oral activity in an average permeability, average 1 mg kg^{-1} potency heterocycle. However, the upper concentration range will not be high enough at 1% DMSO if something like an HTS DMSO stock is used with a concentration of 4 mM. The resulting aqueous concentration at 1 to 100 dilution is only 40 μM (which corresponds to 20 μg mL^{-1} solubility (for MW = 500). This is not high enough a solubility to ensure oral activity for the average permeability, average potency heterocycle – a minimum solubility of 50 μg mL^{-1} is required.

At the other extreme of adding compounds dissolved in DMSO in an early discovery assay, the goal is to maximize assay throughput and to generate a relative solubility ranking, and so the DMSO content is allowed to exceed 1%. For example, workers at Glaxo have employed an HTS solubility assay keeping the DMSO content at a fixed 5% [12]. If the addition is of aqueous medium to DMSO stock, a series of increasing dilutions can be performed with a plate-reader nephelometric assay being run at each dilution stage. In this way, very high throughputs can be obtained, and the assay is completely compound-sparing if it is implemented as part of a normal process of compound preparation for assay testing. The disadvantages are fairly clear. It may be difficult to compare compound solubility across chemical series. At high DMSO percentages, the link to thermodynamic solubility is lost and it may be difficult to conclude whether a compound has sufficient solubility to have the potential for oral activity.

References

1 Kerns, E. H., High throughput physicochemical profiling for drug discovery, *J. Pharm. Sci.* **2001**, *90*, 1838–1858.

2 Wards, R. A., Zhang, K., Firth, L., Benchmarking chemistry functions within pharmaceutical drug discovery and preclinical development, *Drug Discovery World* Summer **2002**, 67–71.

3 Dolle, R. E., Comprehensive survey of combinatorial library synthesis: 2000, *J. Comb. Chem.* **2001**, *3*, 477–517.

4 Bernstein, J., Davey, R. J., Henck, J., Concomitant polymorphs, *Angew. Chem. Int. Ed.* **1999**, *38*, 3440–3461.

5 Syracuse Research Corporation's EPI suite of software that includes the KowWin aqueous solubility calculator is available at http://www.epa.gov/oppt/exposure/docs/episuitedl.htm.

6 Lipinski, C. A., Drug-like properties and the causes of poor solubility and poor permeability, *J. Pharmacol. Toxicol. Methods* **2000**, *44*, 235–249.

7 Johnson, K. C., Swindell, A. C., Guidance in the setting of drug particle size specifications to minimize variability in absorption, *Pharm. Res.* **1996**, *13*, 1795–1798.

8 Curatolo, W., Physical chemical properties of oral drug candidates in the discovery and exploratory development settings, *Pharm. Sci. Tech Today* **1998**, *1*, 387–393.

9 Avdeef, A., Physicochemical profiling (solubility, permeability and charge

state), *Curr. Top. Med. Chem.* **2001**, *1*, 277–351.

10 Bergstrom, C. A. S., Norinder, U., Luthman, K., Artursson, P., Experimental and computational screening models for prediction of aqueous drug solubility, *Pharm. Res.* **2002**, *19*, 182–188.

11 Estimated from poster data presented in "Rapid screening of aqueous solubility by a nephelometric assay", Hill, J. R., Curran, C. M., Dow, N. S., Halloran, K., Ramachandran, V., Rose, K. G., Shelby, D. J., Hartman, D. A., Ricerca Ltd., AAPS **2001**, Denver, CO.

12 Bevan, C. D., Lloyd, R. S., A high-throughput screening method for the determination of aqueous drug solubility using laser nephelometry in microtiter plates, *Anal. Chem.* **2000**, *72*, 1781–1787.

10
Factors Influencing the Water Solubilities of Crystalline Drugs

James W. McFarland, Chau M. Du, and Alex Avdeef

Abbreviations

ANN	Artificial neural network
MLR	Multiple linear regression (Statistica)
PLS	Partial least squares (SIMCA-S)
VIP	Variable importance in the projection (SIMCA-S)

Symbols

A	Overall H-bond acidity (Absolv); also as $\Sigma\alpha_2^H$ [8]
ALOGP	Calculated log P (Absolv)
AB	Product of overall H-bond acidity and basicity (Absolv)
α	Molecular polarizability in Å^3 (HYBOT) [23]; also Alpha
B	Overall H-bond basicity (Absolv); also as $\Sigma\beta_2^H$ [8]
C_{a_max}	Largest H-bond acceptor value in molecule (HYBOT) [23]; also Ca_max
$C_{a\_max} + \lvert C_{d\_max}\rvert$	Sum of the absolute values of C_{a_max} and C_{d_max} (HYBOT) [23]; also SumCmax
C_{d_max}	Largest H-bond donor value in molecule (HYBOT) [23]; also Cd_max[1]
CLOGP	Calculated log P (MEDCHEM) [26]
CMR	Calculated molecular refractivity (MEDCHEM) [26]
E	Excess molar refractivity (Absolv); also as R_2 [8]
log P	Experimental logarithm of the partition coefficient, octanol/water
log S_o	Logarithm of intrinsic solubility (mol L^{-1}) experimentally determined (*p*SOL); also logSexp
mp	Melting point
MW	Molecular weight
q^+_{max}	Maximum positive partial atomic charge (HYBOT) [23]; also Qposmax
$q^+_{max} + \lvert q^-_{min}\rvert$	Absolute sum of q^+_{max} and q^-_{min} (HYBOT) [23]; also SumQmax

Drug Bioavailability: Estimation of Solubility, Permeability, Absorption and Bioavailability.
Edited by Han van de Waterbeemd, Hans Lennernäs and Per Artursson

ISBN: 3-527-30438-X

q^-_{min}	Minimum negative partial atomic charge (HYBOT) [23]; also Qnegmin
S	Dipolarity/polarizability (Absolv); also as π_2^H [8]
ΣC_a	Sum of H-bond acceptor factors (HYBOT) [23]; also SumCa
$\Sigma C_a/\alpha$	Sum of H-bond acceptor factors/molecular polarizability (HYBOT) [23]; also SCa_A
ΣC_{ad}	Absolute sum of H-bond acceptor, donor factors (HYBOT) [23]; also SumCad
$\Sigma C_{ad}/\alpha$	Absolute sum of H-bond acceptor, donor factors/molecular polarizability (HYBOT) [23]; also SCad_A
ΣC_d	Sum of H-bond donor factors (HYBOT) [23]; also SumCd
$\Sigma C_d/\alpha$	Sum of H-bond donor factors/molecular polarizability (HYBOT) [23]; also SCd_A
Σq^+	Sum of positive partial atomic charges (HYBOT) [23]; also SumQpos
$\Sigma q^+/\alpha$	Sum of positive partial atomic charges/molecular polarizability. (HYBOT) [23]; also SQpos_A
V	McGowan's characteristic volume (Absolv); also as V_x [8]

10.1 Introduction

Water solubility is an important property of all chemical compounds as it plays a major role in their distribution in the environment. Thus, sodium chloride will likely end up dissolved in the ocean, and silicon dioxide as sand on the beach. Because of the theme of this volume, it is the water solubilities of drugs that will concern us here. Generally, the more water-soluble drugs are, the more likely they will be well absorbed when administered orally. So it is an advantage in designing new drugs to be able to estimate their solubilities in advance of their actual preparation. In this way, potential new compounds can be eliminated from consideration if their predicted solubilities make them hopeless drug candidates. Many studies have been made to predict water solubility. Owing to the limited space allotted here, it will not be possible to refer to them all, but some of the more recent ones and those relevant to our discussion are listed (see Refs [1–20]). Additional discussion and some more recent references are found in 1.3.

10.2 Crystallinity

At least two correlation studies on the aqueous solubilities of liquid organic compounds have been published [18, 19], and in each case an excellent correlation ($r > 0.9$) was obtained. For both liquid and solid compounds, log P or CLOGP accounts for a major portion of variance in water solubility [3, 4, 20]. However, the

correlations are better with just liquids. To improve the results with solids, Yalkowsky and Valvani [20] used an equation of the form:

$$\log S_w = -a \times \log P - b \times mp + c \quad (1)$$

For crystalline compounds, they noted that an important factor to consider is the crystal lattice energy. From theoretical considerations and subsequent empirical studies, they discovered that melting point (mp) serves as an excellent proxy for this factor. While this is a significant advance in our understanding of water solubility, it falls short as a means to predict solubility from the chemical structure alone; a compound must be made and a mp determined experimentally.

10.3 Solubility Datasets

Many successful correlation studies [2, 6–10, 12–15, 17 among others] have been reported using: (i) large datasets containing both liquid and solid compounds; and (ii) only descriptors calculated from chemical structural information. Except for the results from two of these investigations, no terms were needed to account for differences in physical state. Abraham and Le [8] used an interaction term containing descriptors related to H-bond acceptors and H-bond donors to account for such differences. The term used by Jorgensen and Duffy [6] was similar. While the results of these studies are impressive, there is the question of whether the high percentage of liquid compounds in the datasets tends to blur the distinction between liquids and crystals, and thereby help to assure good results.

Huuskonen and coworkers [11] published a study on 211 drugs, all of which were solids. The solubility data were taken from the literature. We will discuss this work further in 10.7. Klopman et al. [16] published a water-solubility study on 483 literature compounds, but unless one orders the accompanying Supplementary Material it is difficult to know the physical states of the substances they studied.

McFarland *et al.* recently [1] published the results of studies carried out on 22 crystalline compounds. Their water solubilities were determined using *p*SOL [21], an automated instrument employing the pH-metric method described by Avdeef and coworkers [22]. This technique assures that it is the thermodynamic equilibrium solubility that is measured. While only ionizable compounds can be determined by this method, their solubilities are expressed as the molarity of the unionized molecular species, the intrinsic solubility, S_o. This avoids confusion about a compound's overall solubility dependence on pH. Thus, S_o, is analogous to P, the octanol/water partition coefficient; in both situations, the ionized species are implicitly factored out. In order to use *p*SOL, one must have knowledge of the various pK_as involved; therefore, in principle, one can compute the total solubility of a compound over an entire pH range. However, the intrinsic solubility will be our focus here. There was one zwitterionic compound in this dataset. To obtain best results, this compound was formulated as the zwitterion rather than the neutral form in the HYBOT [23] calculations.

10.4 MLR Analyses

Forward step-wise MLR [24] was used to analyze the data obtained from the solubility investigations that follow. To compute Q^2, we used MODDE software [25]. The results from the study reported in [1] are summarized in Eq. (2):

$$\begin{aligned} -\log S_o &= 1.10(\pm 0.16)\mathrm{CLOGP} + 4.95(\pm 0.99)(q^+_{max} + |q^-_{min}|) \\ &\quad + 6.44(\pm 2.10)\Sigma C_{ad}/\alpha - 3.93(\pm 1.21) \qquad (2) \\ n = 22 \qquad & R = 0.90 \qquad s = 0.70 \qquad F_{3,18} = 26.946 \\ & R^2 = 0.82 \qquad Q^2 = 0.64 \qquad p = 0.000001 \end{aligned}$$

The negative logarithm of S_o is used here; hence, a positive coefficient indicates that increases in the value of the associated descriptor will result in lower solubility. In developing Eq. (2), McFarland *et al.* [1] considered the MEDCHEM [26] descriptors CLOGP and CMR and the HYBOT [23] descriptors listed in the table of symbols at the beginning of this chapter. Thus, the important factors discovered here are lipophilicity (CLOGP), the largest difference between positive and negative partial atomic charges found in the molecule ($q^+_{max} + |q^-_{min}|$), and the density of H-bond acceptors and donors ($\Sigma C_{ad}/\alpha$) in the molecule. Each of these factors tends to reduce water solubility.

With only 22 compounds available, there was only enough information to support a three-term correlation equation. Since this work was published, the solubilities of an additional 36 compounds have been reported to us. Many of these were determined [27] in the same laboratories as those cited in [1], but 21 were determined in the laboratory of Artursson [28], and six in the laboratories of Faller and Wohnsland [29]. While this introduced some inter-laboratory variability, we believe that this is minimal because the same automated method on comparable, commercial *p*SOL instruments was employed. This new dataset now contains six zwitterionic compounds; as before, their structures were entered in their zwitterionic forms to do the HYBOT calculations. When they were entered in their neutral forms, poorer results were obtained in the subsequent MLR analysis.

Using the solubilities of these compounds and the same set of descriptors as given in [1], the correlation summarized in Eq. (3) was obtained:

$$\begin{aligned} -\log S_o &= 0.79(\pm 0.10)\mathrm{CLOGP} + 1.65(\pm 0.59)(q^+_{max} + |q^-_{min}|) \\ &\quad + 3.40(\pm 1.25)\Sigma C_{ad}/\alpha - 0.29(\pm 0.76) \qquad (3) \\ n = 58 \qquad & R = 0.83 \qquad s = 0.90 \qquad F_{3,54} = 39.135 \\ & R^2 = 0.69 \qquad Q^2 = 0.63 \qquad p < 0.000001 \end{aligned}$$

Whilst it was gratifying to see that the same descriptors were selected in the analysis and that the signs of the coefficients were all positive as in Eq. (2), the magni-

tudes of the coefficients and intercept are all different. More importantly, the strength of the correlation is diminished: the standard error of the estimate, *s*, is larger and R^2 is smaller. Clearly, at least one other important factor has been overlooked.

10.5 The Absolv Approach

To see if we could gather additional insights, we investigated Absolv [8, 30]. This is a commercial software product that is used to predict, among other things, the aqueous solubilities of compounds based on chemical structures in their neutral forms. From the chemical structure alone Absolv calculates the descriptors A (the overall H-bond acidity), B (the overall H-bond basicity), E (the excess molar refraction), S (dipolarity/polarizability) and V (McGowan characteristic volume); these are defined in more detail elsewhere [8, 31]. Absolv uses these descriptors and an amended general solvation equation to predict aqueous solubilities. We tried this approach to predict the water solubilities of the 58 compounds mentioned above. The results were rather disappointing. The correlation between the observed and predicted values are shown in Eq. (4):

$$-\log S_o = 0.21(\pm 0.07)(-\log S_{absolv}) + 2.58(\pm 0.40) \quad (4)$$

$$n = 55 \qquad R = 0.37 \qquad s = 1.45 \qquad F_{1,53} = 8.5289$$

$$R^2 = 0.14 \qquad p < 0.0051$$

Bromocriptine, erythromycin and terfenadine had to be omitted from this correlation because Absolv does not calculate the water solubilities of compounds with McGowan volumes, V, greater than 4.0. This is because the solubility training set used in Absolv, Eq. (6), does not contain compounds with V values greater than 4; hence predictive power for such compounds are not reliable.

The dataset upon which Absolv is founded [8] mostly consists of liquids. The crystalline compounds are mainly hydrocarbons such as naphthalene. Only about 100 out of the 659 compounds could be said to be ''drug-like''. So it is perhaps no wonder that Absolv did not perform well when only crystalline compounds challenged it. Using the 58-compound dataset generated by *p*SOL and descriptors calculated by Absolv, we recalculated Abraham and Le's amended general solubility equation:

$$-\log S_o = -0.54(\pm 0.74)A - 2.13(\pm 0.35)B + 0.28(\pm 0.32)AB + 1.17(\pm 0.31)E + 0.27(\pm 0.36)S + 1.28(\pm 0.23)V + 1.22(\pm 0.73) \quad (5)$$

$$n = 58 \qquad R = 0.86 \qquad s = 0.84 \qquad F_{3,54} = 24.982$$

$$R^2 = 0.75 \qquad Q^2 = 0.68 \qquad p < 0.000001$$

The coefficients of descriptors A, AB and S are not statistically significant, but the terms are left in the equation for comparison with Abraham and Le's [8] water-solubility equation, modified here to conform to the mathematical conventions used in this chapter:

$$-\log S_o = -2.17A - 4.24B + 3.36AB + 1.00E - 0.77S + 3.99V + 0.52 \quad (6)$$

$$n = 659 \qquad R^2 = 0.92 \qquad s = 0.56 \qquad F_{6,652} = 1256$$

Clearly, Eq. (5) and Eq. (6) are not exactly the same. In Abraham and Le's equation [8], the H-bond and volume terms have much larger coefficients than the corresponding ones in Eq. (5). This helps to explain why Eq. (6) did not predict the solubilities of the 58 compounds well.

Nevertheless, Absolv gave us five additional parameters to work with. What is more, we used ALOGP, the predicted octanol/water partition coefficient also calculated by Absolv. We combined these descriptors with CLOGP, CMR and those from HYBOT. Forward step-wise regression gave Eq. (7):

$$-\log S_o = 0.37(\pm 0.05)\text{CLOGP} + 1.20(\pm 0.20)\text{E} - 1.51(\pm 0.27)\text{B} + 1.17(\pm 0.26)\Sigma q^+ + 0.98(\pm 0.36) \quad (7)$$

$$n = 58 \qquad R = 0.89 \qquad s = 0.73 \qquad F_{4,53} = 52.915$$

$$R^2 = 0.80 \qquad Q^2 = 0.76 \qquad p < 0.000001$$

Comparing these results to those of Eq. (2), we find that they are nearly as good in terms of s and R^2 and superior in Q^2.

In Eq. (7), CLOGP is the first term accepted in the step-wise MLR analysis and accounts for 60% of the variance in $-\log S_o$. The other terms are accepted in the order: E (8%), B (4%) and Σq^+ (8%). Clearly, lipophilicity is the dominant factor in the aqueous solubilities of these 58 crystalline substances. This is consistent with work of Yalkowski's group [3, 4, 20]. By inference, the other three factors together could be interpreted as a proxy for mp.

How is Eq. (7) different from Eq. (3)? CLOGP plays the dominant role in both equations; also, each has a term related to H-bonding, although they take somewhat different forms. Each has a term related to partial atomic charge, again each taking a somewhat different form. Equation (7) has an additional term, E, the excess molar refraction. Abraham [31] interprets E as representing the contribution of dispersion forces in solute-condensed phase interactions. Thus, E, which has the dimensions of volume, represents something new to our analysis of crystalline compounds.

When examining other work published in this field [1–20], one sees that in different forms, in different combinations and not always together, lipophilicity, H-bonding, partial atomic charge and volume have been identified as determinants of aqueous solubility. Even lipophilicity represents a combination of volume and H-bonding as shown by El Tayar and Testa [32] and by Raevsky *et al.* [33]. Thus,

it appears that aqueous solubility can be reduced to terms involving just volume, H-bonding and partial atomic charge. This makes sense from the point of view that they are all related to intermolecular interaction energies: volume is identified with dispersion, dipole-induced dipole and endoergic cavity effects [31]; H-bonding takes into account attractive forces between molecules within crystals and in solvent-solute conditions; and partial atomic charge is related to electrostatic attractions between molecules in the crystalline and solution states.

Unfortunately, the descriptors used to express these conditions are inextricably correlated to each other to various degrees. For example, the correlation coefficient, r, for ΣC_a and Σq^+ is 0.92. This is further demonstrated by the PLS study that follows.

10.6 The PLS Approach

Using our dataset which includes all of the descriptors mentioned so far, we conducted a PLS analysis using SIMCA software [34]. In the initial PLS model, MW, V, and α (Alpha) were removed because they are in each case highly correlated with CMR ($r > 0.95$). SIMCA's VIP function selected only q^-_{min} (Qnegmin) for removal on the basis of it making no important contribution to the model. In the second model, $\Sigma q^+/\alpha$ (SQpos_A) and $\Sigma Ca/\alpha$ (SCa_A) coincided nearly exactly in the three-component space; of these two, we decided to keep only $\Sigma Ca/\alpha$ in the third and final model. This model consisted of three components and accounted for 75% of the variance in log S_o; the Q^2 value was 0.66.

Figures 10.1 and 10.2 show the variable loadings for this model in the first and second component and in the first and third component directions, respectively. As is evident from their distances from the origin and by the VIP function, all of these descriptors play significant roles in the model.

10.7 Discussion

Excellent predictive models for the solubilities of organic compounds have been made using datasets or training and test sets each consisting largely of liquids [2–10, 12–20]. We demonstrated that application of a predictive model derived from a training set containing a high proportion of liquids did not work well for a test set of compounds that contains only crystalline compounds. To make a truly useful method to predict the aqueous solubilities of organic compounds, in particular potential drugs, further studies need to be carried out on much larger datasets comprising only crystalline compounds.

We report here studies conducted with 58 crystalline drug-like compounds. The solubilities are of high quality, having been determined in only three laboratories using the same automated potentiometric method. However, the set is too small to

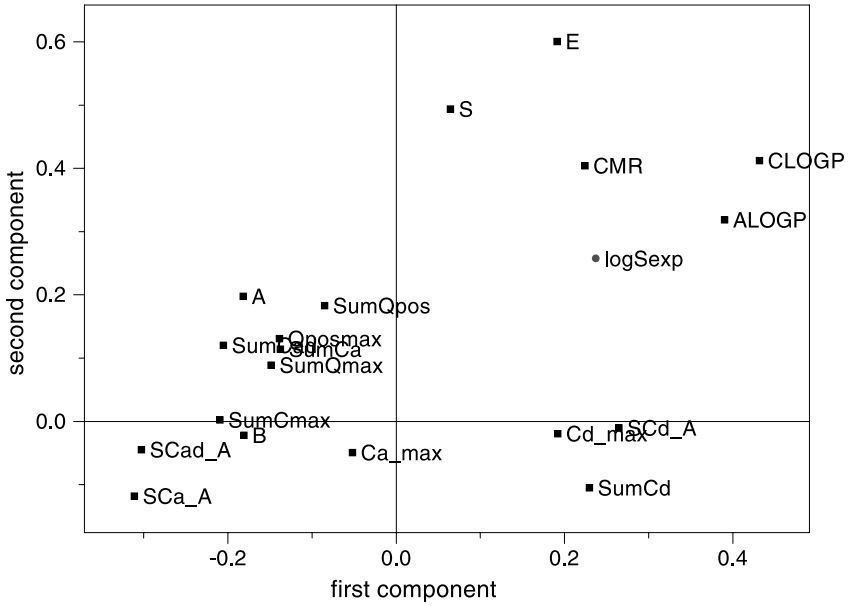

Fig. 10.1. Loadings plot for the variables in the partial least squares (PLS) analysis. Abscissa: first component; ordinate: second component.

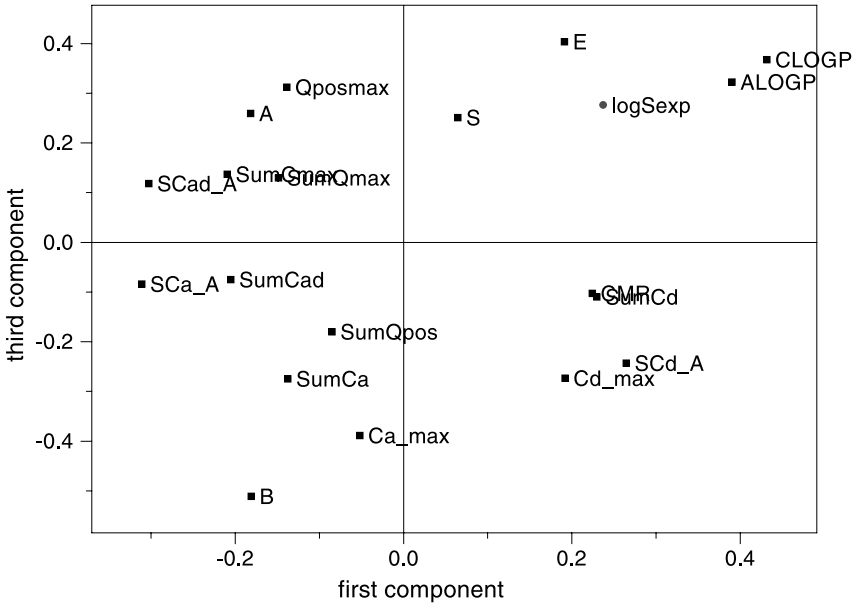

Fig. 10.2. Loadings plot for the variables in the partial least squares (PLS) analysis. Abscissa: first component; ordinate: second component.

divide into a training set and a test set for the types of predictive studies reported so far. Such studies require large datasets to cover the broadest possible solubility range and to get good representations of structural types. Perhaps over 300 well-chosen compounds would be required for a good study.

Huuskonen et al. [11] made a good start by compiling from the literature the aqueous solubilities of 211 solid, drug-like compounds. These were divided into a training set of 160 and a test set of 51 compounds. These authors used topological descriptors and an ANN to make a predictive model of the data, and obtained excellent results for the training set ($r^2 = 0.90$) and the test set ($r^2 = 0.86$). However, because of the nature of the ANN analysis it is was not possible to quantify the significance of the various descriptors, and to interpret their meaning in the model. Our preference is to work with descriptors that have a physical significance to the processes involved in solution.

Although the dataset we used was small, we were nevertheless able to construct models in which the roles of lipophilicity, hydrogen bonding, partial atomic charge and volume were quantitatively determined. When one considers that lipophilicity is itself explained by H-bonding and volume, then the explanatory descriptors can be reduced to simply H-bonding, partial atomic charge and volume. Further studies should be carried out to increase the accuracy and precision in predicting the aqueous solubilities of crystalline organic compounds.

Acknowledgments

We thank Professor Per Artursson of Uppsala University for allowing us to use the intrinsic solubilities reported in reference [28] prior to their publication, and Suzanne Tilton and Alexis Foreman of pION INC. for some of the *p*SOL solubility measurements.

References

1 McFarland, J. W., Avdeef, A., Berger, C. M., Raevsky, O. A., Estimating the water solubilities of crystalline compounds from their chemical structures alone, *J. Chem. Inf. Comput. Sci.* **2001**, *41*, 1355–1359.

2 McElroy, N. R., Jurs, P. C., Prediction of aqueous solubility of hetero-containing organic compounds from molecular structure, *J. Chem. Inf. Comput. Sci.* **2001**, *41*, 1237–1247.

3 Ran, Y., Yalkowsky, S. H., Prediction of drug solubility by the general solubility equation (GSE), *J. Chem. Inf. Comput. Sci.* **2001**, *41*, 354–357.

4 Jain, N., Yalkowsy, S. H., Estimation of the aqueous solubility I: Application to organic nonelectrolytes, *J. Pharm. Sci.* **2001**, *90*, 234–252.

5 Klamt, A., Eckert, F., COSMO-RS: a novel way from quantum chemistry to free energy, solubility, and general QSAR-descriptors for partitioning, in: *Rational Approaches to Drug Design (Proceedings of the 13th European Symposium on Quantitative Structure–Activity Relationships)*. Holtje, H.-D., Sippl, W. (eds), Prous Science, Barcelona, **2001**, pp. 195–205.

6 Jorgensen, W. L., Duffy, E. M., Prediction of drug solubility from Monte Carlo simulations, *Bioorg. Med. Chem. Lett.* **2000**, *10*, 1155–1158.

7 Huuskonen, J., Estimation of aqueous solubility for a diverse set of

organic compounds based on molecular topology, *J. Chem. Inf. Comput. Sci.* **2000**, *40*, 773–777.

8 Abraham, M. H., Le, J., The correlation and prediction of the solubility of compounds in water using an amended solvation energy relationship, *J. Pharm. Sci.* **1999**, *88*, 868–880.

9 Katritzky, A. R., Wang, Y., Sild, S., Tamm, T., QSPR studies on vapor pressure, aqueous solubility, and the prediction of water-air partition coefficients, *J. Chem. Inf. Comput. Sci.* **1998**, *38*, 720–725.

10 Mitchell, B. E., Jurs, P. C., Prediction of aqueous solubility of organic compounds from molecular structure, *J. Chem. Inf. Comput. Sci.* **1998**, *38*, 489–496.

11 Huuskonen, J., Salo, M., Taskinen, J., Aqueous solubility prediction of drugs based on molecular topology and neural network modeling, *J. Chem. Inf. Comput. Sci.* **1998**, *38*, 450–456.

12 Huibers, P. D. T., Katritzky, A. R., Correlation of the aqueous solubility of hydrocarbons and halogenated hydrocarbons with molecular structure, *J. Chem. Inf. Comput. Sci.* **1998**, *38*, 283–292.

13 Ruelle, P., Kesselring, U. W., Prediction of the aqueous solubility of proton-acceptor oxygen-containing compounds by the mobile order solubility model, *J. Chem. Soc., Faraday Trans.*, **1997**, *93*, 2049–2052.

14 Sutter, J. M., Jurs, J. C., Prediction of aqueous solubility for a diverse set of heteroatom-containing organic compounds using a quantitative structure–property relationship, *J. Chem. Inf. Comput. Sci.* **1996**, *36*, 100–107.

15 Nelson, T. M., Jurs, P. C., Prediction of aqueous solubility of organic compounds, *J. Chem. Inf. Comput. Sci.* **1994**, *34*, 601–609.

16 Klopman, G., Wang, S., Balthasar, D. M., Estimation of aqueous solubility of organic molecules by the group contribution approach. Application to the study of biodegradation, *J. Chem. Inf. Comput. Sci.* **1992**, *32*, 474–482.

17 Bodor, N., Huang, M.-J., A new method for the estimation of the aqueous solubility of organic compounds, *J. Pharm. Sci.* **1992**, *81*, 954–960.

18 Raevsky, O. A., Quantification of non-covalent interactions on the basis of the thermodynamic hydrogen bond parameters, *J. Phys. Org. Chem.* **1997**, *10*, 405–413.

19 Hansch, C., Quinlan, J. E., Lawrence, G. L., The linear free energy relationship between partition coefficients and the aqueous solubility of organic liquids, *J. Org. Chem.* **1968**, *33*, 347–350.

20 Yalkowsky, S. H., Valvani, S. C., Solubilities and partitioning I: solubility of nonelectrolytes in water, *J. Pharm. Sci.* **1980**, *69*, 912–922.

21 *p*SOL, pION INC., 5 Constitution Way, Woburn, MA 01801. E-mail: pion@pion-inc.com.

22 Avdeef, A., Berger, C. M., Brownell, C., pH-Metric solubility. 2: Correlation between the acid-base titration and the saturation shake-flask solubility pH methods, *Pharm. Res.* **2000**, *17*, 85–89.

23 HYBOTPLUS-2000 is available from the MolPro Project. Contact Professor O. A. Raevsky, Institute of Physiologically Active Compounds, Chernogolovka, Moscow Region, 142432, Russia; e-mail: raevsky@ipac.ac.ru or Dr. J. W. McFarland, reckon.dat consulting, 217 Blood Street, Lyme, CT 06371-3509; e-mail: reckon.dat@attglobal.net.

24 Statistica (Release 5, '97 Edition), Statsoft, 2300 East 14th Street, Tulsa, OK 74104.

25 Modde 4.0, Graphical Software for Design of Experiments, Umetri AB, Box 7960, S-907 19 Umeå, Sweden, 1997.

26 MEDCHEM, Daylight Chemical Information Systems, Inc., 18500 Von Karman Ave., Suite 450, Irvine, CA 92715.

27 Unpublished data from pION Inc.

28 Bergström, C. A. S., Strafford, M., Lazorova, L., Avdeef, A., Luthman, K., Artursson, P., Absorption Classification of Oral Drugs Based on Molecular Surface Properties. *J. Med. Chem.* **2003**, *46*, 558–570.

29 Faller, B., Wohnsland, F., Physicochemical parameters as tools in drug discovery and lead optimization, in: *Pharmacokinetic Optimization in Drug Research; Biological, Physicochemcial and Computational Strategies.* Testa, B., Van de Waterbeemd, H., Folkers, G., Guy, R. (eds), Wiley-VCH, Weinheim and Verlag HCA, Zurich, **2001**, pp. 257–274.

30 Absolv, Sirius Analytical Instruments, Ltd., Riverside, Forest Row Business Park, Forest Row, East Sussex, RH18 5DW, UK, Tel. +44 (0)1342 820720, Fax +44 (0)1342 820725, e-mail sirius@sirius-analytical.com, website www.siriur-analytical.com.

31 Abraham, M. H., Scales of solute hydrogen bonding: their construction and applications to physicochemical and biochemical processes, *Chem. Soc. Rev.* **1993**, *22*, 73–83.

32 El Tayar, N., Testa, B., Polar intermediate interactions encoded in partition coefficients and their interest in QSAR, in: *Trends in QSAR and Molecular Modelling 92.* Wermuth, C. G. (ed.), ESCOM, Leiden, **1993**, pp. 101–108.

33 Raevsky, O. A., Schaper, K.-J., Seydel, J. K., H-bond contribution to octanol-water partition coefficients of polar compounds, *Quant. Struct.-Act. Relat.* **1995**, *14*, 433–436.

34 SIMCA-S for Windows, Version 6.0, Umetri AB, Box 7960, S-907 19 Umeå, Sweden, tel. +46 (0)90 154840, fax +46 (0)90 197685, e-mail info@umetri.se.

III
Role of Transporters and Metabolism in Oral Absorption

Drug Bioavailability: Estimation of Solubility, Permeability, Absorption and Bioavailability.
Edited by Han van de Waterbeemd, Hans Lennernäs and Per Artursson

ISBN: 3-527-30438-X

11
Transporters in the GI Tract

Ho-Chul Shin, Christopher P. Landowski, Duxin Sun, and Gordon L. Amidon

Abbreviations

ABC	ATP-binding cassette
ACE	Angiotensin-converting enzyme
cAMP	Cyclic adenosine monophosphate
ATP	Adenosine triphosphate
AZT	Azidothymidine
CAT	Cationic amino acid transporter
CNS	Central nervous system
CNT	Concentrative nucleoside transporter
DNA	Deoxyribonucleic acid
ENT	Equilibrative nucleoside transporter
FATP	Fatty acid transport protein
GABA	Gamma-aminobutyric acid
GI	Gastrointestinal
GLUT	Sodium-independent facilitated diffusion transporter
hPT	Human peptide transporter
HUGO	Human genome organization
LAT	L-amino acid transporter
MCT	Monocarboxylate transporter
MDR	Multidrug resistance
MRP	Multidrug resistance accociated protein
NADC	Sodium-dependent dicarboxylate transporter
NTCP	Sodium-dependent taurocholate cotransporting polypeptide
OAT	Organic anion transporter
OATP	Organic anion transporting polypetide
OCT	Organic cation transporter
OCTN	Organic cation/carnitine transporter
PEPT	Peptide transporter
P-gp	P-glycoprotein
PHT	Peptide/histidine transporter

Drug Bioavailability: Estimation of Solubility, Permeability, Absorption and Bioavailability.
Edited by Han van de Waterbeemd, Hans Lennernäs and Per Artursson

ISBN: 3-527-30438-X

RFC	Reduced folate transporter
SGLT	Sodium dependent secondary active transporter
SLC	Solute carrier
SMVT	Sodium-dependent multivitamin transporter
SVCT	Sodium-dependent vitamin C transporter
THTR	High affinity thiamine transporter

11.1 Introduction

Membrane transporters play a key role in determining exposure of a cell or organism to a variety of solutes including nutrients, cellular by-products, drugs, and other xenobiotics. It has been thought that intestinal absorption of most drugs proceeds by passive diffusion, in which the lipid solubility of the drug molecule is a determining factor. However, many water-soluble compounds can move across cell membranes through specialized carrier-mediated transport mechanisms [1]. These compounds include peptide analogues, nucleosides, amino acids, sugars, monocarboxylic acids, bile acids, fatty acids, organic cations and anions, phosphates, and water-soluble vitamins.

Membrane transporter research is rapidly progressing due to the advances in molecular biology. The human genome contains numerous genes encoding more than 800 transporters [2]. So far, the Human Genome Organization (HUGO) has approved 229 solute carrier (SLC) family genes and 52 ATP-binding cassette (ABC) genes. Of the transporter genes, more than 200 genes have been cloned and characterized. These transporters include nucleoside transporters, amino acid transporters, peptide transporters, vitamin transporters, ion transporters, carriers, and neurotransmitter transporters [2]. It would be interesting to know which transporters play a role in drug absorption, but information about the relevant transporters is very limited at present. To facilitate the study of drug transporters on a broad scale, some research groups [3, 4] have constructed gene transcription databases for human membrane transporters. Our recent GeneChip® data has revealed that various types of transporters including peptide, amino acid, nucleoside, glucose, phosphate, and ATP-binding cassette transporters are highly expressed in human intestine [4] (Fig. 11.1–11.4). These transporters include peptide transporter HPT1, cationic amino acid transporter LAT1, taurine transporter, concentrative purine nucleoside transporter CNT2, Na^+/glucose cotransporter SGLT1, glucose/fructose transporter GLUT5, mitochondrial phosphate carrier protein SLC25A3, and ABC transporter ABCD3 (Fig. 11.1–11.4). A catalog of intestinal membrane transporter mRNA expression will be helpful in the utilization of these transporters for enhancing oral delivery of poorly absorbed drugs.

As shown in Table 11.1, there are various membrane transporters and isoforms. Many of these transporters are expressed in the GI tract. Among them, the peptide transport systems have received the most attention. Di-, tri-peptide trans-

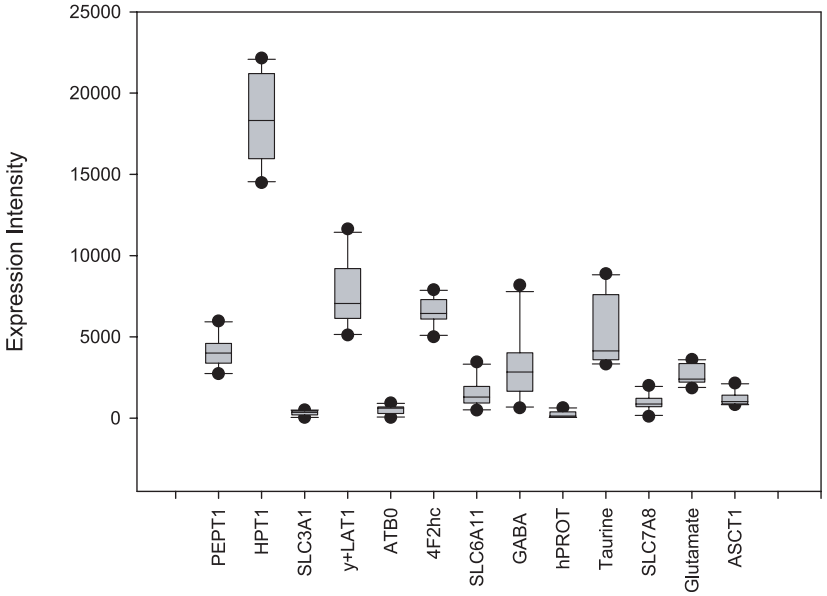

Fig. 11.1. Human duodenal expression variability of peptide and amino acid transporters (our unpublished data). Shaded box indicates 25–75% of expression range, the line within the box marks the median, and error bars indicate 10–90% of expression range. PEPT1, di-, tri-peptide transporter; HPT1 (LI-cadherin), peptide transporter; SLC3A1, cystine, dibasic and neutral amino acid transporter; y+LAT1, cationic amino acid transporter; ATB_0, neutral amino acid transporter; 4F2hc, activator of dibasic and neutral amino acid transport; SLC6A11, gamma-aminobutyric acid transporter; GABA (SLC6A8), GABA/noradrenaline transporter; hPROT, L-proline transporter; Taurine, taurine transporter; Glutamate, neuronal/epithelial high affinity glutamate transporter; ASCT1, glutamate/neutral amino acid transporter.

porters, localized at the intestinal epithelia brush-border membrane, are proton-coupled transporters that are known to play an essential role in the oral absorption of β-lactam antibiotics, angiotensin-converting enzyme (ACE) inhibitors, renin inhibitors, antitumor drugs, thrombin inhibitors, and a dopamine receptor antagonist. Moreover, the utility of this transporter as a platform for improving the oral bioavailability of drugs such as zidovudine and acyclovir has well been demonstrated. Nucleosides and their analogues depend on the nucleoside transporters to be taken up in the intestine. Nucleoside analog drugs including azidothymidine (AZT), zalcitabine, cladribine, cytarabine, and gemcitabine are widely used for the treatment of various conditions including cancer and viral infections by interfering with nucleotide metabolism and DNA replication. There are many different amino acid transporters in the intestine and they have highly restrictive substrate specificities. Amino acid analogues including L-4-chlorokynurenine, abapentin, baclofen, and gabapentin seem to be absorbed by the amino acid transporters. Organic cation and anion transporters have also shown to be a specific transport system for

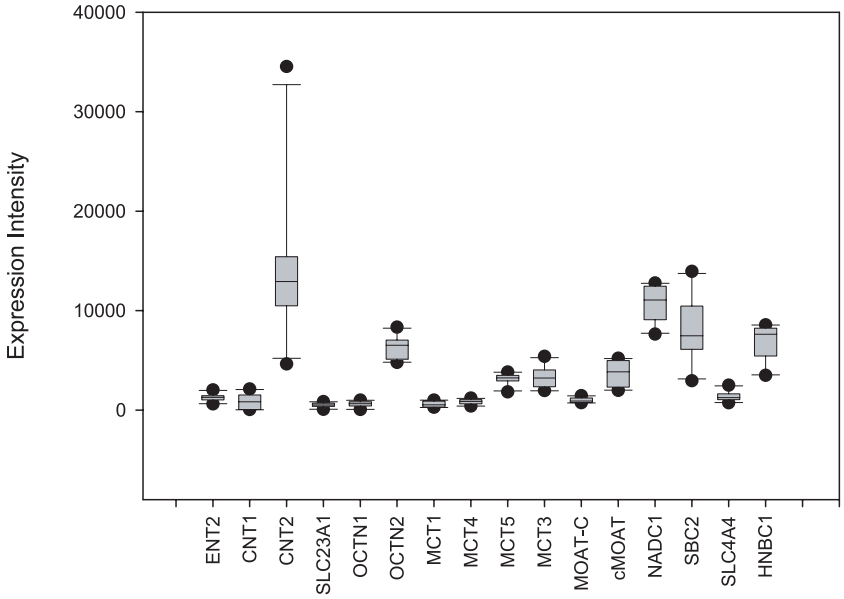

Fig. 11.2. Human duodenal expression variability of nucleoside, organic cation ion, and anion transporters (unpublished data). Shaded box indicates 25–75% of expression range, the line within the box marks the median, and error bars indicate 10–90% of expression range. ENT2, equilibrative nucleoside transporter; CNT1, concentrative pyrimidine nucleoside transporter; CNT2, concentrative purine nucleoside transporter; SLC23A1, nucleobase transporter; OCTN1, organic cation transporter 1; OCTN2, organic cation transporter 2; MCT(1,3,4,5), monocarboxylic acid transporters; MOAT-c (ABCC5), organic anion transporter; cMOAT (ABCC2), organic anion transporter; NADC1, sodium-dependent dicarboxylate transporter; SBC2, sodium bicarbonate cotransporter; SLC4A4, pancreas sodium bicarbonate cotransporter; HNBC1, sodium bicarbonate cotransporter.

many endogenous amines as well as xenobiotic drugs. The bile acid transport system has been utilized for improving oral drug delivery by coupling active peptides to bile acids. P-glycoprotein, as a primary active transporter in the intestinal brush-border membrane, leads to net secretion of drugs such as anticancer agents in the blood-to-luminal direction. This transporter serves as a detoxifying mechanism and as a part of the absorption barrier in the intestine [5]. Many other transporters have been known to transport several water-soluble vitamins, monocarboxylic acids, phosphates, bicarbonates, fatty acids, sugars, and ions.

The transporter-mediated uptake of drugs into epithelial cells is emerging as a new trend in biopharmaceutics [6]. Utilization of the intestinal epithelial transporters to facilitate the absorption of drugs or prodrugs appears to be an attractive delivery approach. The purpose of this chapter is to describe the pharmaceutical and medicinal relevances of intestinal transporters. This will provide new knowledge for strategies to enhance intestinal absorption of drugs.

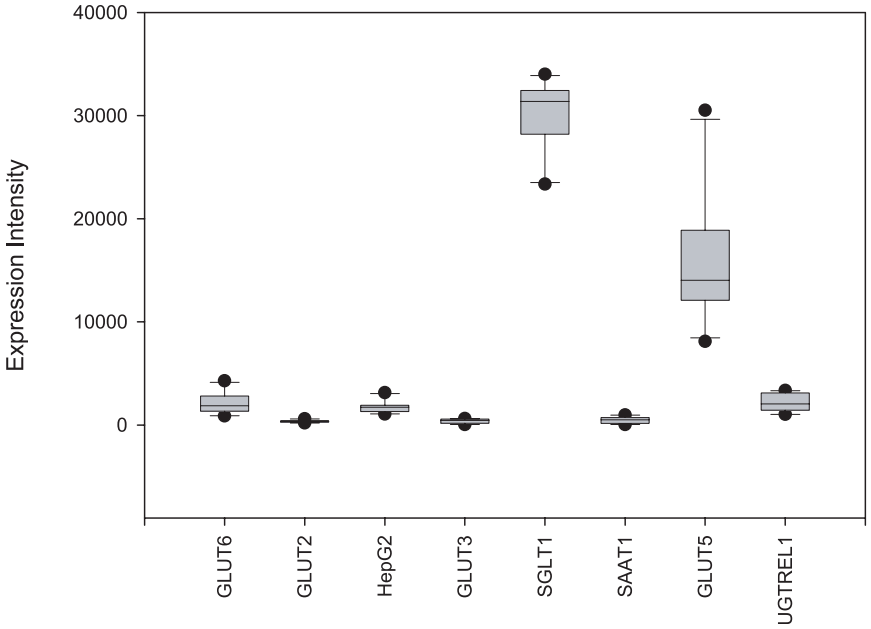

Fig. 11.3. Human duodenal expression variability of glucose transporters (unpublished data). Shaded box indicates 25–75% of expression range, the line within the box marks the median, and error bars indicate 10–90% of expression range. GLUT6, glucose transporter pseudogene; GLUT2, glucose transporter-like protein; HepG2, glucose transporter; GLUT3, glucose transporter-like protein; SGLT1, Na+/glucose co-transporter; SAAT1, low affinity sodium glucose cotransporter; GLUT5, glucose/fructose transporter; UGTREL1, UDP-galactose transporter.

11.2 Intestinal Transporters

11.2.1 Peptide Transporters

A number of peptide transporters such as peptide transporter-1 (PEPT1, SLC15A1), peptide transporter-2 (PEPT2, SLC15A2), peptide transporter-3 (PTR3), human peptide transporter-1 (hPT-1), peptide/histidine transporter-1 (PHT1), and ATP-binding cassette peptide transporter family have been identified from the various mammalian tissues [7–17]. PEPT1 and hPT-1 are localized predominantly in the brush border membrane of human intestine, but do not share significant cDNA homology to each other [10, 17–21]. PEPT2 does show approximately 50% sequence identity with PEPT1 and occurs abundantly in the kidney [17, 19, 22–25].

During the past 10 years, one of the most exciting developments in the oral peptide drug delivery was the identification of PEPT1. This is a significant finding because this carrier protein is known to play a critical role in the absorption of

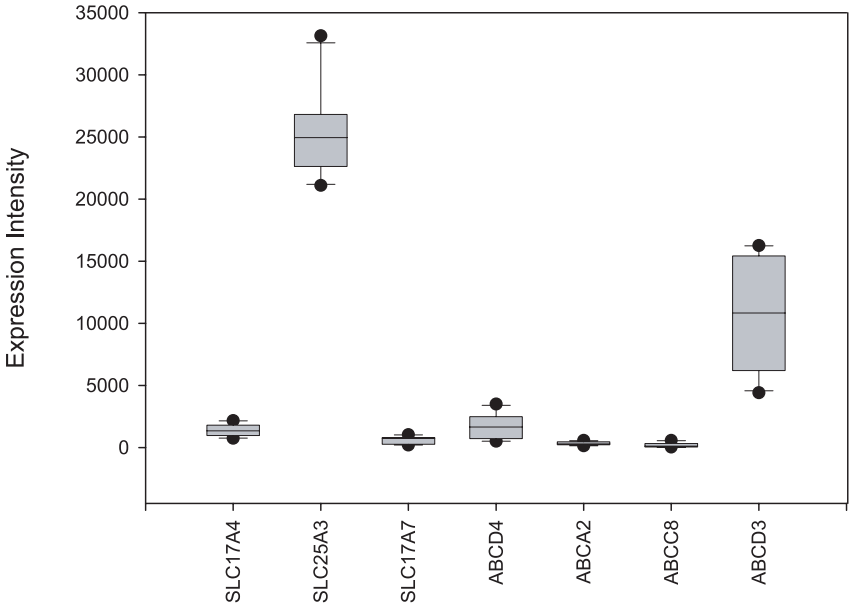

Fig. 11.4. Human duodenal expression variability of phosphate and ABC transporters (unpublished data). Shaded box indicates 25–75% of expression range, the line within the box marks the median, and error bars indicate 10–90% of expression range. SLC17A4, sodium phosphate cotransporter; SLC25A3, mitochondrial phosphate carrier protein; SLC17A7, sodium-dependent inorganic phosphate cotransporter; ABCD4, ATP-binding cassette (ABC) transporter; ABCA2, ABC transporter; ABCC8, ABC transporter; ABCD3, ABC transporter.

peptidomimetic compounds from the intestinal tract [7, 10–12, 15, 26–28]. This transporter uses an electrochemical proton gradient as its driving force [29]. The PEPT1 transporter has been cloned from the intestine in a variety of species such as rabbit, human, rat, ovine, and chicken [21, 30–34]. PEPT1 contains 708 amino acids that produce 12 membrane-spanning domains (Fig. 11.5). The transporter is functionally expressed in *Xenopus laevis* oocytes, human cell lines Caco-2 and HeLa, Chinese hamster ovary cell line CHO, and yeast *Pichia pastoris* [10, 21, 31, 33–42].

The PEPT1 carrier protein is stereoselective, with peptides that contain L-amino acid residues having a higher affinity for binding and transport than peptides that contain one or more D-amino acids [11, 43]. In addition, this transporter absorbs many peptide-like drugs, including β-lactam antibiotics, angiotensin converting enzyme inhibitors, renin inhibitors, antitumor or antiviral agents, thrombin inhibitors, a dopamine receptor antagonist, and amino acid prodrugs. The β-lactam antibiotics have a similar basic structure compared to peptides and their oral bioavailability is due to their affinity for peptide transporters such as PEPT1 [11, 44]. Cephalosporins including cephradine, cefadroxil, cephalexin, cephradin, cefadroxil, cephaloglycine, cefaclor, cefixime, and ceftibuten are substrates for the peptide

Tab. 11.1. Membrane transporters

Transporters	*Family (no. of isoforms)*	*Gene symbol*
Peptide transporters	PEPT1, PEPT2	SLC15A members
	PTR3, hPT-1, PHT1	
Nucleoside transporters	CNTs (3)	SLC28A
	ENTs (3)	SLC29A
Amino acid transporters	CATs (4), LATs (3), $b^{(0,+)}AT$	SLC7A
	EAATs (5), ASCTs (2), ATB^o	SLC1A
	rBAT, 4F2hc	SLC3A
	GATs (3), BGT, GLYTs (3), TAUT, PROT	SLC6A
	CT, HTT, DAT1, NAT1	SLC6A
Organic cation transporters	OCTs (3), OCTNs (3)	SLC22A
Organic anion transporters	OATs (4)	SLC22A
	OATPs (8)	SLC21A
Glucose transporters	SGLTs (3)	SLC5A
	GLUTs (13)	SLC2A
Vitamin transporters	SVCTs (2)	SLC23A
	Folate transporters (3)	SLC19A
	SMVT	SLC5A6
	Nicotinic acid transporters (2)	
Bile acid transporters	NTCP, ISBT	SLC10A
Fatty acid transporters	FATPs (6)	SLC27A
Phosphate transporters	SLC17As (4)	SLC17A
	SLC34As (2)	SLC34A
Monocarboxylic acid transporters	MCTs (6)	SLC16A
Bicarbonate transporters	SBC2, HNBC1	SLC4A
ABC transporters	ABCAs (12), ABCBs (10), ABCCs (12)	ABC
	ABCDs (8), ABCEs (1), ABCFs (13)	ABC
	ABCGs (6)	ABC
Other transporters	NADC1	SLC13A2
	Ion transporters	

PEPT1: peptide transporter-1, PEPT2: peptide transporter-2, PTR3: peptide transporter-3, hPT-1: human peptide transporter-1, PHT1: peptide/histidine transporter-1, ENT: Na^+-independent equilibrative transporter, CNT: Na^+-dependent concentrative transporter, CAT: cationic amino acid transport, LAT: L amino acid transporter, EAAT: excitatory amino acid transporter, ASCT: alanine, serine, and cysteine transporter, RBAT: basic amino acid transporter, 4F2hc: 4F2 heavy chain, GAT: GABA transporter, BGT: betaine/GABA transporter BGT, GLYT: glycine transporter, TAUT: taurine transporter, PROT: proline transporter, CT: creatine transporter, HTT: serotonin transporter, DAT1: dopamine transporter, NAT1: N-system amino acid transporter, OCT: organic cation transporter, OCTN: organic cation/carnitine transporter, OAT: organic anion transporters, OATP: organic anion transporting polypeptide, SGLT: Na^+-dependent secondary active transporter, GLUT: Na^+-independent facilitated diffusion transporter, SVCT: vitamin C transporter, SMVT: Na^+-dependent multivitamin transporter, NTCP: Na^+-dependant taurocholate cotransporting polypeptide, ISBT: Na^+-dependant bile salt transporter, FATP: fatty acid transport protein, MCT: monocarboxylate transporter, SBC2: Na^+-dependent bicarbonate transporter 2, HNBC1: Na^+-dependent bicarbonate transporter, NADC1: Na^+-dependent dicarboxylate transporter HNBC1, ABC: ATP-binding cassette family, SLC: solute carrier family.

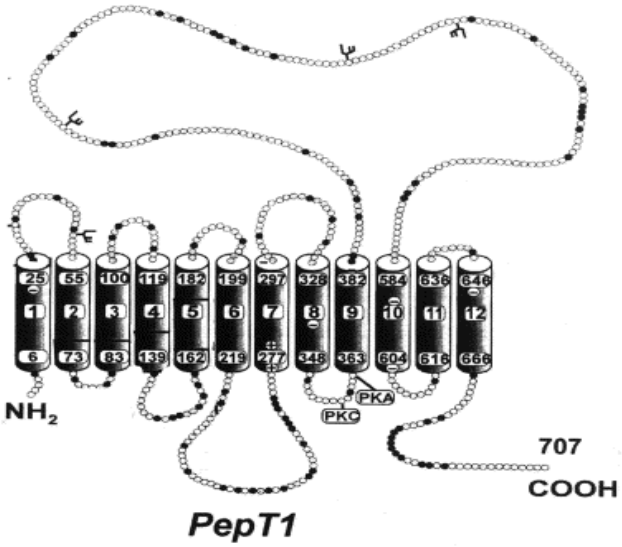

Fig. 11.5. A schematic model of PEPT1 (Adapted from Reference [31])

transporter [32, 38, 44–50]. Aminopenicillins such as ampicillin, amoxicillin, and cyclacillin are also absorbed by the peptide transporter [30, 35, 47, 50–52]. Angiotensin-converting enzyme (ACE) inhibitors are used in hypertension treatment. Widely used ACE inhibitors, captopril and enalapril are good PEPT1 substrates, while lisinopril, quinapril, benazepril, and fosinopril also show good affinity for this transporter [30, 45, 53–62]. The peptide transporter is also involved in uptake of renin inhibitors such as CH3-18, S86,2033, and S86,3390 [63–65], peptidomimetic thrombin inhibitors derived from L-Asp-D-Phe [66], the dipeptide-like anticancer drug bestatin [67, 68], a dopamine receptor antagonist sulpiride [69], a NMDA-antagonist PD158473 [70], and a new antihepatitis agent JBP923 [71].

It has been shown that the presence of a peptide bond is not essential for the rapid transport of substrates by the intestinal peptide transporter PEPT1 [72–74]. Various substrates lacking a peptide bond including acyclovir produgs, 4-aminophenylacetic acid (4-APAA) [74], arphamenine-A [75] and 5-aminolevulinic acid (δ-ALA) [76] have been shown to interact with this transporter. Coupling an amino acid residue to a drug currently appears to be an effective approach to make a PEPT1 substrate. The L-valine prodrugs of antiviral nucleosides, acyclovir, gancyclovir and zidovudine, are favorably transported by this carrier [72, 77–81]. The affinity of the prodrugs for PEPT1 is surprising because the molecules have nucleoside structural features rather than peptide-like features. Valacyclovir, the L-valyl ester of acyclovir, shows 3–5 fold higher oral bioavailability than free acyclovir [82–85]. An analogue of valacyclovir that has its guanine moiety substituted with a purine also exhibited PEPT1 associated transcellular transport [86]. The amino acid prodrugs of 3,4-dihydroxy-L-phenylalanine (L-Dopa), pamidronate, tetrahydrofuranyl-carbapenems, methyl ester val-Ome are also good examples of

PEPT1-mediated transport [72, 80, 81, 86–88]. In Caco-2 cells expressing PEPT1, L-dopa-L-Phe enhanced uptake 40-fold compared to free L-dopa [87].

The mRNA expression of PEPT1 varies significantly in response to several chemical factors. The expression of the transporter was upregulated by substrates [89, 90], diet [91, 92], insulin [93], α2-adrenergic agonists [93], and pentazocine [94]. While it has been reported that intestinal transplantation [89, 95], cAMP [96], epidermal growth factor [97], and thyroid hormone [98] inhibited the expression of PEPT1.

Another type of intestinal peptide transporter, hPT1, which is significantly different in sequence from PEPT1, was identified using a functionally inhibitory monoclonal antibody [99]. This transporter is widely expressed in the human GI tract and facilitates the oral absorption of β-lactam antibiotics and ACE inhibitors from the intestine [18, 99]. Interestingly, we recently reported that hPT1 gene expression is approximately 4-fold higher than PEPT1 in the human duodenum [4] (Fig. 11.1).

As the number of new peptide and peptidomimetic drugs rapidly increase, the peptide transport system has gained increasing attention as a potential drug delivery system for small peptides and peptide-like compounds. The peptide transporters can accommodate a wide range of molecules of differing sizes, hydrophobicity, and charge thereby allowing chemical modification for making prodrugs.

11.2.2 Nucleoside Transporters

Nucleoside analogues are widely used for the treatment of cancers and viral infections. Although there have been considerable advances in the development of new nucleoside analogs, little is known about the transport mechanisms involved in the intestinal absorption of these compounds. Nucleoside transporters have been subdivided into two major classes by Na^+-independent equilibrative transporters (ENT family) and Na^+-dependent concentrative transporters (CNT family) [77, 100–103].

Tab. 11.2. Nucleoside transporters

Transporter family	*Subtype*	*Substrate drugs*
Concentrative nucleoside transporters (CNTs)	CNT1	azidothymidine(AZT), zalcitabine, cladribine, cytarabine, gemcitabine, 5'deoxy-5-fluorouridine
	CNT2	cladribine, didanosine (ddI)
	CNT3	5-fluorouridine, floxuridine, zebularine, gemcitabine, AZT, cladribine, fludarabine, ddI
Equilibrative nucleoside transporters (ENTs)	ENT1	cladribine, cytarabine, fludarabine, gemcitabine, zalcitabine, ddI
	ENT2	AZT, ddI, gemcitabine
	ENT3	–

Mammalian equilibrative nucleoside transporters are typically divided into two classes, ENT1 and ENT2, based on their sensitivity or resistance respectively to inhibition by nitrobenzylthioinosine (NBMPR). In 1997, both ENT1 and ENT2 were first cloned from human placenta [104, 105] and rat intestine [106]. Characterization of other equilibrative transporters, such as human ENT3 and mouse ENT3, has also been reported recently [102]. Based on substrate selectivity, the concentrative nucleoside transporters can be divided into three major subtypes, CNT1, CNT2, and CNT3. CNT1 has been cloned from rat intestine (rCNT1) [107], human kidney, and bile duct (hCNT1) [108, 109]. The CNT2 transporter has been cloned from human intestine and kidney (hCNT2 or hSPNT2) [110, 111], rabbit intestine (rbSPNT2) [112], rat brain (rCNT2) [113], and mouse spleen [114]. More recently, CNT3 was cloned from human mammary gland (hCNT3) and mouse liver (mCNT3) (Fig. 11.6) [115]. These nucleoside transporters have been functionally expressed in *Xenopus laevis* oocytes, human cell lines HeLa, CEM, L1210, L37, the rat cell line C6 and the monkey cell line COS-1 [105, 106, 111, 112, 114, 116–126].

The concentrative nucleoside transporters appear to be restricted in their distribution within intestinal cells and tissues and also in their substrate selectivity. In contrast, the equilibrative nucleoside transporters appear to be widely distributed and have broad substrate specificities. CNT1, CNT2 and CNT3 are all expressed in human intestine [110, 127–129]. It has been demonstrated that ENT1 and ENT2 are also present in human or rodent intestine [106, 115, 130], however, the tissue expression of the different nucleoside transporters shows considerable variability among individuals or experimentals [131]. Of the nucleoside transporters, CNT2 is most predominantly expressed in the human intestine [131]. Our GeneChip® expression data [4] shows significantly higher CNT2 expression in human intestine compared to ENT1, ENT2, or CNT1 (Fig. 11.2). These results may suggest that CNT2 has a critical role in the uptake of nucleoside drugs from the intestine.

The ENT transporters show wide substrate specificity accepting both purine and pyrimidine nucleosides, whereas the CNTs show more limited substrate specificity. CNT1 prefers pyrimidine substrates, CNT2 prefers purines, and CNT3 shows broad specificity [132]. In addition to natural nucleoside substrates such as adenosine, guanosine, inosine, uridine, cytidine, and thymidine, many nucleoside drugs have also been known to interact with the nucleoside transporters. CNT1 mediates the active transport of several anticancer drugs including azidothymidine (AZT), zalcitabine (ddC) [108, 123], cladribine (2CdA), cytarabine (Ara-C) [100], gemcitabine [133], and 5'deoxy-5-fluorouridine (DFUR) [119]. It is known that CNT2 participates in the transmembrane transport of 2CdA [116] and didanosine (ddI) [110, 123, 134]. While the CNT3 transporter is known to exhibit broad selectivities for compounds such as 5-fluorouridine, floxuridine, zebularine, gemcitabine, AZT, 2CdA, fludarabine, ddI, but not ganciclovir [115]. ENT1 has been shown to transport anticancer drugs such as cladribine, cytarabine, fludarabine, gemcitabine, zalcitabine, ddI, but not the antiviral drug AZT. The equilibrative transporter, ENT2, transports AZT, didanosine, and gemcitabine [102, 105, 133, 135]. The substrate selectivity of the newly isolated ENT3 has not yet been estab-

Fig. 11.6. Predicted amino acid sequence homologies of human CNT1, CNT2, and CNT3. Shaded box indicates a similar amino acid match and a black box indicates an identical amino acid match between the CNT transporters. The alignments were done with Clustal W and shaded with Boxshade.

lished [102]. In humans, these nucleoside transporters are potentially inhibited by the coronary vasodilator drugs dilazep, and dipyridamole [136] [104–106, 122, 137].

Although there has been very poor information about the activity relationships of different nucleoside transporters for oral drug absorption, many current publications support that each nucleoside transporter has a specific role in the intestinal absorption of nucleoside drugs. Molecular cloning studies over the past 5 years have provided a wealth of information about the nucleoside transporters with a diverse range of substrate selectivities. Therefore, these transporters will be good targets to design improved nucleoside drugs for antiviral and anticancer therapies.

11.2.3 Amino Acid Transporters

Amino acids, especially essential amino acids, are required for protein synthesis and as energy sources in all living cells. Since most amino acid compounds are hydrophilic, special membrane proteins are necessary for their membrane transport. The classification of amino acid transporters is well defined according to their substrate specificity and tissue distribution [138, 139]. Neutral amino acid transporters involve sodium-dependent systems A, ASC, N, BETA, GLY, IMINO, PHE, and B^o, and sodium-independent system L. Cationic amino acid transporters include sodium-dependent system $B^{o,+}$ and sodium-independent systems b^+, y^+, y^+L, and $b^{o,+}$. Anionic amino acid transporters are divided into system X^-_{AG} and system X^-_C. Although the amino acid transporters have been extensively studied since 1960, their molecular characterization did not begin until 1991 [140, 141]. So far, about 30 amino acid transporters have been cloned from mammalian cells. However, it is difficult to precisely classify cloned cDNA into the defined transporter system based on amino acid sequence. According to their sequence similarity, these cloned amino acid transporters could be classified into several subfamilies including CAT family, glutamate family, rBAT/4F2hc family, and GABA transporter family [138, 139]. Also in some cases transporters from well-defined systems, such as A, N, $B^{o,+}$ and X^-_C amino acid transporters, have not been cloned yet.

The CAT family for sodium-independent cationic amino acid transport are CAT(1–4) (fit into system y^+), LAT(1–3) (fit into system L or y^+L) and $b^{(0,+)}$AT (fit into $b^{(0,+)}$ system). The glutamate family for potassium- and sodium-dependent anionic and zwitterionic amino acid transport are EAAT(1–5) (fit into system X^-_{AG}), ASCT(1–2) (fit into system ASC) and ATB^o (fit into B^o system). The rBAT/4F2hc family for sodium-independent cationic and zwitterrionic amino acid transport are rBAT (fit into $b^{o,+}$ system) and 4F2hc (fit into y^+L system). The GABA transporter family are GABA transporter GAT(1–3), BGT-1 (fit into BETA system), glycine transporter GLYT(1–3) (fit into GLY system), taurine and proline transporter TAUT (fit into BETA system), PROT (might fit into IMINO system), and other members such as CT-1, CT-2, HTT, DAT1, and NAT1.

In this section, we focus on the amino acid transporters expressed in the GI tract. The cationic amino acid transporter CAT family, CAT-1 and LAT-1, are abun-

dantly expressed in intestine. CAT-1 was the first cloned amino acid transporter [140, 141], while hLAT-1 and hy$^+$LAT-1 were most recently cloned [142, 143]. The b$^{(0,+)}$AT is also expressed in small intestine [144]. From the glutamate family, EAAC1 (EAAT3) was first isolated through expression cloning from a rabbit intestine cDNA library [145–147]. EAAC1 mediates sodium-dependent glutamate and aspartate transport and is widely expressed in rabbit intestine and various other organs. The human ATB^0 transporter was isolated from placental carcinoma cells [148] and the rabbit ATB^0 was cloned from a jejunum cDNA library [149]. From the rBAT/4F2hc family, rBAT was cloned from rat intestine and rat and human kidney [150, 151]. This transporter is highly expressed in human intestine [152–157]. Expression of rBAT in Xenopus oocytes showed the activity of a sodium-independent cationic and neutral amino acid transporter. The human 4F2hc cDNA which has high sequence similarity with rBAT has been cloned from human 4F2 cells [158]. Another group of amino acid transporters is the GABA transporter family, which mediates sodium- and chloride-dependent neurotransmitter transport. All these transporters are expressed in the CNS with exception to the intestinally expressed TAUT transporter. Human TAUT was first cloned from thyroid cells and contains 619 amino acids [159]. The transporter TAT1 subserving the system T, which has not been identified in any of the already known amino acid transporter families, is also strongly expressed in human and rat intestine [160, 161].

The amino acid transporters have highly restrictive substrate specificities. Intestinal uptake of the antiepileptic agent gabapentin is likely mediated by system L (LAT1) and b$^{0,+}$. The uptake of pregabalin (isobutyl gamma-aminobutyric acid, isobutyl GABA) is also mediated by B^0 and/or B$^{0,+}$ [162–164]. The hLAT1 carrier transports the amino acid-related anticancer agent melphalan [165–167]. Several amino acid analogues such as L-methyl-dopa, 3-O-methyl-dopa, L-dopa, and baclofen seem to be absorbed by the neutral amino acid transporters including LAT1, LAT2, and TAT1 [161, 163, 168–172]. D-cycloserine is transported by a proton-coupled amino acid transporter [173]. A neurotoxicant methyl-mercury-L-cysteine complex was a good substrate for human LAT1 and LAT2 [174]. It was shown that the thyroid hormones triiodothyronine and thyroxine are also transported by LAT1, although the transport rate was low [167]. Recently new EAAT substrates, termed Glu-1a and Asp-3, have been developed as potential neuroprotective agents [175]. In general, information about amino acid transporter mediated drug uptake in the intestine has been scarce. Further molecular identification, including substrate recognition for the various subtypes of amino acid transporters or related proteins, is required in order to use these transporters to improve the bioavailability of amino acid related drugs.

11.2.4 Organic Cation Transporters

Recently, considerable progress has been made in the cloning and functional characterization of organic cation transporters (OCTs) from many species and

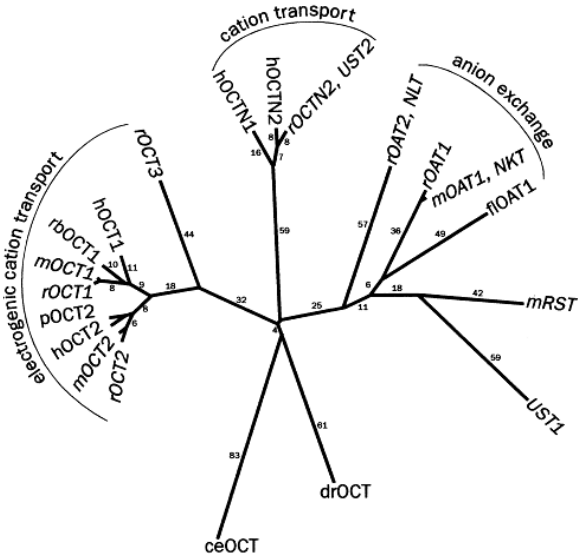

Fig. 11.7. Phylogenetic tree of OCTs and OATs isoforms. (Adapted from Reference [177])

various tissues [176–181]. The OCTs expressed in the liver, kidney, and intestine are critical for absorption and elimination of many endogenous amines as well as a wide array of drugs and environmental toxins. The organic cation transporter family has been classified into the two main groups, OCT1–3 and OCTN1–3 (Fig. 11.7).

In 1994, Grundemann *et al.* [182] cloned the first organic cation transporter OCT1 from a rat kidney. Subsequently, OCT2 and OCT3 were also cloned from rat kidney [183] and rat placenta [184], respectively. Human OCT1 and OCT2 homologs have also been cloned and functionally characterized [185, 186]. However, so far there is no report for the cloning of human OCT3. Sequence homology in the OCT family predicts similar molecular structures that contain 12 transmembrane domains and a large extracellular hydrophilic loop [177]. The functional properties of OCT have been examined after OCT expression in *Xenopus laevis* oocytes, human kidney cell line HEK293, and carcinoma HeLa cells [180]. Recently, new members of the OCT family having the ability to transport carnitine, called OCTN1, OCTN2, and OCTN3 were found in human and animal tissues. OCTN1 was originally cloned from human fetal kidney by Dr. Tsuji's group [187] and also isolated from rat [188] and mouse [189]. OCTN2 was first cloned from human kidney [190] and placenta cells [191]. OCTN2 shows 76% sequence homology with OCTN1. Very recently, OCTN3 which is expressed highly in testis was also isolated from mice [192], but its functional characterization and distribution pattern from different species such as human are not yet clear.

Organic cation drugs are widely used as therapeutic agents. This drug class makes up approximately 50% of all drugs including antiarrhythmics, antihistamines, opoid analgesics, β-adrenergic blocking agents, and skeletal muscle relax-

Tab. 11.3. Organic cation transporters

Transporter family	*Subtype*	*Substrate drugs*
Organic cation transporters (OCTs)	OCT1/2	tetraethylammonium (TEA), thiamine, tyramine, tryptamine, N-methylnicotineamide (NMN), choline, spermine, spermidine quinine, d-tubocurarine, procanamide, dopamine, noradrenaline, serotonin, histamine, corticosterone, 1-methyl-4-phenylpyridinium (MPP), despramine
	OCT3	dopamine, MPP, TEA and guanidine
Organic cation/carnitine transporters (OCTNs)	OCTN1	TEA, pyrilamine, quinidine and verapamil
	OCTN2	carnitine derivatives, betaine, cephaloridine, choline, emetine, pyrilamine, quinidine, TEA, valproate verapamil
	OCTN3	carnitine

ants, as well as some endogenous compound such as choline, dopamine, and histamine. Substrates of OCTs include many cationic drugs, xenobiotics, some vitamins, and various endogenous compounds. OCT1 and OCT2 over-expressed in oocytes or cell lines mediate the uptake of tetraethylammonium (TEA), N-methylnicotineamide (NMN), thiamine, tyramine, tryptamine, choline, spermine, spermidine quinine, d-tubocurarine, procanamide, dopamine, noradrenaline, serotonin, histamine, corticosterone, 1-methyl-4-phenylpyridinium (MPP) and despramine [186, 193, 194]. OCT3 transports dopamine, MPP, TEA and guanidine [184, 195]. OCTN1 appears to mediate TEA, pyrilamine, quinidine and verapamil [188, 196]. It has been demonstrated that OCTN2 has many drug substrates such as carnitine derivatives, betaine, cephaloridine, choline, emetine, pyrilamine, quinidine, TEA, valproate and verapamil [188, 197–199]. There has been no report of OCTN3 substrates besides carnitine [192].

Although there are differences in substrate specificity and affinity, the organic cation transporters are widely expressed in the various tissues such as kidney, liver, placenta and intestine [180, 181]. OCTN1 and OCTN2 were detected at higher levels in the human small intestine and Caco-2 cells [4]. This indicates that the basolateral organic cation transporters may act as a critical mediator for transporting their substrates, absorbed from the GI tract *via* other apical transporters, into the systemic circulation. The OCTNs are generally distributed in intestinal area and mediate the transport of many cation drugs, indicating that these transporters might be good targets for effective oral cation drug delivery.

11.2.5 Organic Anion Transporters

Organic anion transporters play important roles in the elimination of a variety of endogenous anionic substances, xenobiotics, and their metabolites from the body

[200]. Organic anion transporters can be divided into three major families: organic anion transporters (OATs), organic anion transporting polypeptides (OATPs), and multidrug resistance associated proteins (MRPs) [201].

The first OAT1 was cloned from rat kidney [202, 203], and various isoforms including OAT2 and OAT3 in rats and OAT3 and OAT4 in humans have been identified by several research groups [200, 204–207]. Since the first cloning of OATP1 from rat liver by Jacquemin [208], at least six rodent OATPs and eight human OATPs have been identified so far [209]. A convention has been established to name the human OATPs alphabetically in capital letters (that is OATP-A, B, C, etc.). The OATP-A transporter was originally isolated from human liver in 1995 [210]. Many isomers of OCTPs including OATP-A, OATP-B, OATP-C, OATP-D, OATP-E, OATP-F, OATP-8, and OATPRP4 (GenBank NM030958) have been identified in various human tissues by several groups [189, 210–220]. The MRP family, belonging to the ATP-binding cassette (ABC) superfamily also mediates the uptake of many organic anions. Recent publications demonstrate that there are various isoforms in this family, designed MRPs [201, 221–223].

OAT1 substrates are organic anions such as PAH, methotrexate, β-lactam antibiotics, non-steroidal anti-inflammatory drugs, and antiviral nucleoside analogues [200]. OAT2 is mainly expressed in the liver and transports methotrexate, PAH, and salicylate [204, 205]. OAT3 is predominantly expressed in the kidney and accepts more lipophilic organic anions such as estrone sulfate, ochratoxin A, and cimetidine [201, 206]. Substrates of rodent OATP1 and OATP2 include amphipathic organic anions such as bromosulfophthalein (BSP), estradiol 17β-glucuronide (E217G), and bile acids, as well as drugs such as a HMG-CoA reductase inhibitor pravastatin, temocaprilat, an angiotensin converting enzyme inhibitor enalapril, a thrombin inhibitor CRC-220, an endothelin receptor antagonist BQ-123, gadoxetate, and dehydroepiandrosterone sulfate [224–231]. The human OATPs have also shown a broad substrate spectrum including BSP, taurocholate, glycocholate, estrone sulfate, E217G, dehydroepiandrostane sulfate, oubain, *N*-methyl-quinidine, prostaglandin E_2, triiodothyronine, thyroxine, deltorphin II, *d*-penicillamine, enkephalin, BQ-123, fexofenadine, rocuronium, quinidine, benzylpenicillin, rifampin, leukotriene C_4; methotrexate, pravastatin, cholecystokinin, and digoxin [189, 210, 211, 213–215, 217, 219, 232–237]. Cumulative studies revealed that MRP2 (cMOAT) accepts glutathione conjugates, sulfate conjugates, glucuronides and non-conjugated organic anions, pravastatin, vinblastine, temocaprilat, BQ-123, methotrexate, irinotecan and HIV protease inhibitors such as saquinavir, ritonavir, and indinavir [238–246]. MRP3 mediates the transport of glucuronide conjugates, taurocholate, glycocholate, and methotrexate [247–251].

The major functional relevance of the multispecific organic anion transporters is to function as an efflux system for a number of endogenous compounds, various anionic drugs, environmental substances, and their metabolic products. Since many of the anion compounds are harmful to the body, it is a normal physiological response to export them rapidly from the body *via* the liver and kidney. It is well known that OATP-B, OATP-C, and OATP-8 have good capacity for solute uptake in the human hepatocytes [189, 200, 211], while the MRP2 and MRP3 secret anionic

Tab. 11.4. Organic anion transporters

Transporter family	*Subtype*	*Substrate drugs*
Organic anion transporters (OATs)	OAT1	PAH, methotrexate, β-lactam antibiotics, non-steroidal anti-inflammatory drugs, antiviral nucleoside analogues
	OAT2	methotrexate, PAH, salicylate
	OAT3	estrone sulfate, ochratoxin A, cimetidine
Organic anion transporting polypeptides (OATPs)	OATP1/2	bromosulfophthalein (BSP), pravastatin, temocaprilat, estradiol 17β-glucuronide (E217G), enalapril, BQ-123, thrombin inhibitor CRC-220, gadoxetate, dehydroepiandrosterone sulfate
	hOATPs	BSP, taurocholate, glycocholate, estrone sulfate, E217G, dehydroepiandrostane sulfate, oubain, *N*-methyl-quinidine, prostaglandin E_2, triiodothyronine, thyroxine, deltorphin II, d-penicillamine, enkephalin, BQ-123, fexofenadine, rocuronium, quinidine, benzylpenicillin, rifampin, leukotriene C_4; methotrexate, pravastatin, cholecystokinin, digoxin
Multidrug resistance associated proteins (MRPs)	MRP2	pravastatin, vinblastine, temocaprilat, BQ-123, methotrexate, irinotecan, saquinavir, ritonavir, indinavir
	MRP3	methotrexate

compounds from the small intestine [201, 252]. The OATs, OATPs, and MRPs are mainly expressed in the liver and kidney, but some isoforms including OAT2, OATP-B, MRP1, and MRP2 are also expressed in the small intestine [189, 211, 252, 253]. Despite significant efflux characterization, the pharmaceutical role of organic anion transporters in the intestinal absorption relating to anionic drugs remains unclear. Molecular characterization and identifying substrate structure relationships among the organic acid transporters may be necessary to target these transporters for drug absorption.

11.2.6 Glucose Transporters

Final products of digested carbohydrate are absorbed from the small intestine *via* glucose transporters. Glucose transport processes involve two different transporter families, Na^+-dependent secondary active transporters (SGLTs) and Na^+-independent facilitated diffusion transporters (GLUTs). The SGLTs transport glucose across the brush border membranes of intestinal and renal epithelia using a sodium electrochemical gradient as a driving force. In 1987, the intestinal SGLT1

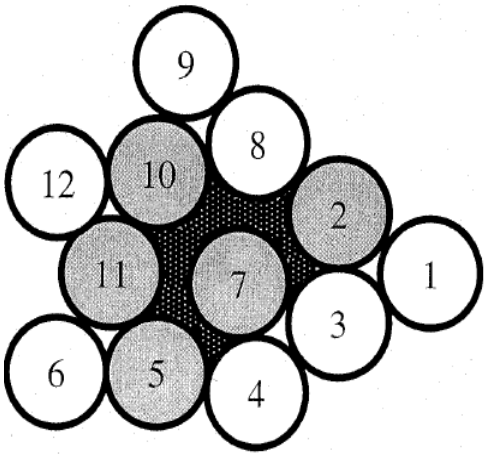

Fig. 11.8. Proposed model for GLUT1 helix packing. (Adapted from Reference [380])

transporter was cloned as the first member of a new gene family (Fig. 11.8) [254] and SGLT2 was isolated from human and rat kidney [255–259]. The third type, SGLT3 (SAAT1), was also identified from pig [260]. Mammalian cells also have a large family of facilitative hexose transport systems GLUT proteins. Over the past 20 years more than 13 GLUT isoforms have been identified through modern cDNA and genomic sequencing technology. On the basis of sequence similarities and characteristic elements, the GLUT family can be divided into three subfamilies, namely class I (GLUT1–4), class II (GLUT5, GLUT7, GLUT9 and GLUT11), and class III (GLUT6, 8, 10, 12, and the myo-inositol transporter HMIT1) [261]. GLUT1–5 were identified between 1985 and 1990 [262–266]. More recently several new members, GLUT6–12 and HMIT1 [261, 267–278], were cloned from various tissues and have been shown to transport glucose with different affinity and capacity. The rapidly increasing number of GLUT family members may allow us to obtain more information to sort out the functional differences amoung GLUT proteins.

In general, the SGLTs are located in the brush-border membrane, while the GLUTs are located in the basolateral membrane. Of the glucose transporters, several members have been shown to be expressed in the GI tract as detected by immunohistochemistry and western blot studies. SGLT1 is primarily localized in the apical membrane of intestine [254]. Just like SGLT1, the SGLT3 transporter is also located in intestinal brush border membrane [260]. Following intestinal absorption by glucose apical transporters, the accumulated glucose in enterocytes can be transported into the systemic circulation *via* basolateral glucose transporters such as GLUT2, a low-affinity glucose transporter [264]. Another GLUT transporter, GLUT5, also shows high expression on the brush border membrane of human small intestine and seems to be localized on both the apical and basolateral membranes [266, 279–282].

The sugar transporters are specific for D-forms of glucose, galactose and fruc-

tose. Moreover, L-forms of sugars have about 1,000 times less affinity for the transporter than D-forms. SGLT1 transports both glucose and galactose, whereas the SGLT3 transport glucose but not galactose [283]. SGLT2 has high selectivity for glucose over galactose [256]. GLUT2 mediates the transport of glucose and fructose. Among the GLUT family members, GLUT5 most prefers to transport fructose over glucose [282, 284], although it is very similar to other GLUTs in both amino acid sequence and secondary structural features. Interestingly, GLUT5 shows a particularly higher distribution in the GI tract [4].

Little is known about the transport of drugs by these transporters. The SGLT family transports sugars, inositol, proline, pantothenate, iodide, urea, myoinositol, and glucose derivatives [285]. Modification of parent compounds to glucose analogues like p-nitrophenyl-b-D-glucopyranoside or b-D-galactopyranoside was a strategy employed to facilitate intestinal absorption [286, 287]. GLUT2-expressing cells transported streptozotocin, a glucose analog, used as a tool for creating experimental diabetes [288]. Overexpression of GLUT11 in cells specifically showed a binding affinity for cytochalasin B. All the glucose transporters have significant homologies to each other, but they function differently to transport different sugars or sugar related compounds into various tissues.

11.2.7
Vitamin Transporters

The water-soluble vitamins generally function as cofactors for metabolism enzymes such as those involved in the production of energy from carbohydrates and fats. Their members consist of vitamin C and vitamin B complex which include thiamine, riboflavin (vitamin B_2), nicotinic acid, pyridoxine, pantothenic acid, folic acid, cobalamin (vitamin B_{12}), inositol, and biotin. A number of recent publications have demonstrated that vitamin carriers can transport various types of water-soluble vitamins, but the carrier-mediated systems seem negligible for the membrane transport of fat-soluble vitamins such as vitamin A, D, E, and K.

The water-soluble vitamin C is essential for many enzymatic reactions and also acts as a free radical scavenger [289]. Tsukaguchi *et al.* [290] cloned two different Na^+-dependent vitamin C transporters SVCT1 and SVCT2 from rat kidney and brain, in which exhibit only 65% amino acid sequence homology. Human SVCT1 and SVCT2 have been isolated from placenta [291] and kidney [292]. However, expression studies show that SVCT1 is predominantly expressed in epithelial tissues such as intestine, liver, and kidney, while SVCT2 is mainly expressed in brain, eye, and other organs [290, 293]. These two transporters reveal exquisite stereospecific substrate selectivity for ascorbic acid. The SVCT1 transporter intensely favors L-ascorbic acid over its isomers D-isoascorbic acid, dehydroascorbic acid, and 2- or 6-substituted analogues [294].

Another important vitamin is folate, which is required for purine and pyrimidine nucleotide synthesis. Since folate and its derivatives are generally lipophobic anions, they do not traverse biological membranes *via* simple diffusion but rather have to be taken up into the cells by specific transport processes

Tab. 11.5. Vitamin transporters

Transporter family	*Subtype*	*Substrate drugs*
Vitamin C transporters (SVCTs)	SVCT1/2	ascorbic acid derivatives
Folate transporters	RFC-1	reduced folate derivatives, methotrexate
	THTR-1/-2	thiamine
Na^+-dependent multivitamin transporter (SMVT)	SMVT	pantothenate, biotin, lipoate
Nicotinic acid transporter		nicotinic acid, valproic acid, salicylic acid, penicillins
Riboflavin transporter		riboflavin

[295]. The three members of the folate transporter family are the reduced folate transporter RFC-1 (SLC19A1), the high affinity thiamine transporter THTR-1 (SLC19A2), and the THTR-2 (SLC19A3) gene [296, 297]. The human RFC-1 transporter, which interacts with reduced folates much more efficiently than with oxidized folates, was cloned from lymphoblast, placenta, and small intestine libraries [298–301]. In addition, northern blot analysis revealed that the RFC-1 gene was expressed in small and large intestine [300]. Molecular characterization then uncovered that several folate derivatives and MTX showed typical substrate characteristics for this transporter [300, 302, 303]. The second member, THTR-1, is most closely related to RFC-1 at the level of amino acid sequence, however this transporter is specific to thiamine [297, 304]. Even though thiamine is an organic cation, this vitamin is not a substrate for the known members of the mammalian OCTs family [304]. A newly identified folate transporter, THTR-2, was recently identified from human and mouse tissue and is functionally similar to SLC19A2 (THTR-1) [296, 297]. THTR-2 is widely expressed in the tissues including placenta, kidney, liver and intestine, and mediates thiamine uptake.

Recently, Prasad *et al.* cloned a mammalian Na^+-dependent multivitamin transporter (SMVT) from rat placenta [305]. This transporter is very highly expressed in intestine and transports pantothenate, biotin, and lipoate [305, 306]. Additionally, it has been suggested that there are other specific transport systems for more water-soluble vitamins. Takanaga *et al.* [307] demonstrated that nicotinic acid is absorbed by two independent active transport mechanisms from small intestine; one is a proton cotransporter and the other an anion antiporter. These nicotinic acid related transporters are capable of taking up monocarboxylic acid-like drugs such as valproic acid, salicylic acid, and penicillins [5]. Also, more water-soluble transporters were discovered as Huang and Swann [308] reported the possible occurrence of high-affinity riboflavin transporter(s) on the microvillous membrane.

11.2.8
Bile Acid Transporters

Bile acids secreted into the small intestine facilitate absorption of fat-soluble vitamins and cholesterol. The majority of bile acids are reabsorbed from the intes-

tine and returned to the liver *via* portal circulation [309–312]. Sodium/bile acid cotransporters are integral membrane glycoproteins that participate in the enterohepatic circulation of bile acids. Two homologous transporters are involved in the membrane transport of bile acids. One transporter is the Na^+-dependant taurocholate cotransporting polypeptide NTCP (LBAT, SLC10A1) that is present on the basolateral membrane of hepatocytes. Hagenbuch and Meier [313] cloned the NTCP from a human liver cDNA library so that it could be characterized. Transcription of NTCP cDNA in Xenopus oocytes resulted in the expression and Na^+-dependent taurocholate uptake in those cells. The NTCP-mediated taurocholate uptake in oocytes was inhibited by major bile acid derivatives and by bromosulfophthalein. The second bile acid transporter, the ileal Na^+-dependent bile salt transporter ISBT (ASBT, SLC10A2), is apically localized in order to absorb bile acids from the intestinal lumen, the bile duct, and the kidney. In addition to human ileum, the ISBT was also identified in hamster, rat, mouse, and rabbit ileum [314–319].

The cloned NTCP mediated uptake of many physiological bile salts such as taurocholate, cholate, glycocholate, taurochenodeoxycholate, and tauroursodeoxycholate, as well as of the steroid conjugate estrone 3-sulfate [320]. A multispecific hepatic bile acid transport system has been described for a variety of cholephilic compounds (steroids and steroid conjugates), cyclic peptides (phalloidin, antamanide, and somatostatin analogues) and numerous drugs (BSP, ICG, bumetanide, and others) [321–324]. In comparison, ISBT exhibited a narrower substrate specificity compared to the related NTCB [315]. The fact that ISBT is primarily expressed on the ileum brush border membrane but not the jejunum indicates that the ileum is the major site of active bile acid uptake from the intestine. Therefore, there have been attempts to target the bile acid transport system for improving oral drug delivery. Bile acids can be conjugated with peptide, oligonucleotide, or other hydrophilic compounds. This may be of great importance for the design and development of orally active peptide drugs [325]. Coupling peptides to cholic acid, such as ChEAAA, resulted in decreased metabolism and increased intestinal absorption by the intestinal bile acid transporter [326].

To decrease serum cholesterol, some research groups have attempted to develop ISBT inhibitors. Using an inhibitor, S-8921, lead to a decrease in serum cholesterol in the normal condition [327] and a potent cholesterol lowering agent, 264W94, also showed a therapeutic effect by inhibition of ISBT [328]. Non-bile acid-derived inhibitors of ISBT have been reported [329]. Primary bile acid malabsorption is an idiopathic intestinal disorder associated with the interruption of the enterohepatic bile acid circulation [330]. Several investigators [330–332] suggested that the bile acid malabsorption resulted from ISBT mutations.

11.2.9
Fatty Acid Transporters

Long-chain fatty acids are an important energy source for cells. It is a general concept that fatty acids are absorbed by passive diffusion, but evidence suggests that

transporters are involved in the fatty acid transport [333–335]. Shaffer and Lodish [336] identified a fatty acid transport protein, designated FATP, from a mouse adipocyte library in 1994. Expression studies showed that FATP increased oleic acid uptake and similar effects were observed with other long-chain fatty acids. Hirsch *et al.* [337] identified 5 distinct FATPs in mouse and 6 different FATPs in human, designated FATP1–6 (SLC27A1–6). The FATPs have unique expression patterns and are found in major organs of fatty acid metabolism such as adipose tissue, liver, heart, and kidney.

One of the most important fatty acid transporters, FATP4, is expressed at high levels on the apical side of enterocytes in the small intestine [338, 339]. Furthermore, overexpression of FATP4 in 293 cells facilitated uptake of long chain fatty acids including palmitate, oleate, linolate, butyrate, and cholesterol with the similar specificity as enterocytes [338]. These results suggest that FATP4 is the principal fatty acid transporter in enterocytes and may constitute a novel target for anti-obesity therapy. In addition to the FATP4, FATP1 is also detected in the small intestine [340]. FAT/CD36 is another transporter candidate for oral absorption [341]. It shows 73% sequence similarity to FATP1 and was highly expressed in the jejunum. Its substrates are long chain fatty acid such as myristate, oleate, palmitate, stearate, arachidonate, and linoleate.

11.2.10
Phosphate Transporters

Inorganic phosphates are absorbed from the small intestine and renal tubule by sodium-dependent phosphate transporters. Although functionally related, these phosphate transporters are structurally distinct and can be broadly grouped into 2 major types, SLC17 and SLC34 family, based on HUGO gene nomenclature. The SLC17 members are NPT1 (SLC17A1), NPT3 (SLC17A2), NPT4 (SLC17A3), and KAIA2138 (SLC17A4). NPT1 is found mainly in kidney [342, 343] with PAH and faropenem being typical substrates [344, 345]. A similar sodium/phosphate cotransporter SLC17A4 was isolated from human intestinal mucosa cDNA library [346]. The SLC34 members include NAPI3 (SLC34A1) and NAPI3B (SLC34A2). NAPI3 is found almost exclusively in the renal proximal tubule [347, 348] whereas NAPI3B was identified in human small intestine [349]. The intestinal phosphate transporters are located in the brush border membrane. It has been reported that the intestinal phosphate transporters mediate absorption of drugs such as foscarnet and fosfomycin [350–353]. Phosphate-mimic drugs containing a phosphate moiety may be utilized as substrates for the intestinal sodium-dependent phosphate transporters for enhancing intestinal absorption.

11.2.11
Monocarboxylic Acid Transporters

Monocarboxylates such as lactic acid and pyruvate are transported across plasma membranes by members of the proton-linked monocarboxylate transporter (MCT)

family [354, 355]. The MCT family includes MCT1–6 [356–359]. These transporters are mainly expressed in erythrocytes, muscle, intestine, and kidney. Each MCT appears to have slightly different substrate/inhibitor specificities and transport kinetics. Valproic and pyruvic acid are typical substrates of the MCT [360]. The HMG-CoA reductase inhibitor atorvastatin and benzoic acid appear to be absorbed across the apical membrane by the intestinal MCT1 [361, 362].

11.2.12 ATP-Binding Cassette Transporters

The ATP-binding cassette (ABC) transporters are a family of large membrane proteins and are able to transport a variety of compounds through membranes using ATP hydrolysis energy [363–366]. The name ABC transporter was first introduced in 1992 by Higgins [367], although ATPases and P-glycoproteins (P-gps) are other names used for this family. The genes that encode ABC transporters are widely dispersed in the genome and show a high degree of amino acid sequence identity. These proteins translocate a wide variety of substrates including sugars, amino acids, nucleosides, lipids, bile salts, metal ions, peptides, proteins, a large number of hydrophobic compounds, and metabolites across extra- and intracellular membranes. To date, there are 52 characterized human ABC genes approved by HUGO. These genes can be divided into seven distinct subfamilies, ABCA-ABCG, based on domain organization and amino acid homology. The ABCA family contains 12 members such as ABC1 (ABCA1), ABC2 (ABCA2), ABC3 (ABCA3), and AMCR (ABCA4). The ABCB family has 10 members including MDR1 (P-gp, ABCB1), MDR2/3 (ABCB4), and ABC7 (ABCB7). The ABCC family has 12 members including MRP1 (ABCC1), MRP2 (cMOAT, ABCC2), MRP3 (cMOAT2, ABCC3), MOAT-C (ABCC5), CFTR (ABCC7), and MRP7 (ABCC10). The ABCD family consists of 8 members, while ABCE has only one member named OABP (ABCE1). The ABCF family contains 3 members such as ABC50 (ABCF1), and the final family, ABCG, contains 6 members such as ABC8 (ABCG1) and ABCP (ABCG2).

Many of the ABC transporters including MDR1 (P-gp), MRP1, MRP2, MRP3, MOAT-C, and ABCG family members are expressed in the intestinal tissues. Various investigators have studied MDR1 in the intestine as a potentially limiting factor in drug absorption [368–374]. Substrate drugs secreted into the intestinal lumen *via* MDR1 are colchicines, doxorubicin, adriamycin, vinblastine, paclitaxel, dexamethasone, digoxin, PSC833, ofloxacin, ciprofloxacin, quinidine, etoposide, pristinamycin, peptide drugs, celiprolol, saquinivir, cytokines, as well as toxins and other organic cations [28, 365, 375]. Some MDR1 inhibitors such as verapamil, 1,9-dideoxyforskolin, nifedipine, cyclosporin-A, taxotere, SDZ PSC 833, vanadate, and quinidine can increase drug bioavailability by blocking the transporter [373, 376–378]. MRP1 and MRP2 also transport many drugs such as pravastatin, MTX, anioiconjugates, toxic compounds, and other organic anions. ABCG2 transports anthracycline, topotecan, mitoxantrone, doxorubicin, and several dyes. The ABCG5 and ABCG8 genes appear to be related to absorption of dietary sterols [375, 379]. Over 50 different ABC proteins have been detected in the human genome,

although the function and expression profiles of these transporters in the intestine are far from being entirely elucidated. Yet, it is clear that many of the ABC members are involved in the translocation of various substrate drugs across the intestinal membrane.

11.2.13 Other Transporters

Some transporters such as Na^+-dependent dicarboxylate transporter (NADC1), Na^+-dependent bicarbonate transporter 2 (SBC2), Na^+-dependent bicarbonate transporter HNBC1, several ion transporters, and channels are also expressed in the intestinal tissues [4].

11.3 Summary

Intestinal transporters play an important role in the membrane transport of drugs and nutrients. They are mainly located in the brush border membrane with variable distribution along the GI tract. It is of interest to know which transporters are highly expressed and which drugs are preferentially absorbed *via* the intestinal transporters. Even though the expression levels vary significantly by transporter type, it is known that the transporters expressed in the intestine include peptide transporters (such as PEPT1 and hPT1), nucleoside transporters (ENT1, ENT2, CNT1, and CNT2), amino acid transporters (CAT-1, LAT-1, $b^{(0,+)}$AT, EAAC1, ATB^o, HLAT, BAT, 4F2hc, TAUT, and TAT1), organic cation transporters (OCT1, OCTN1, and OCTN2), organic anion transporters (OAT2 and OATP-B), glucose transporters (SGLT1, SGLT3, GLUT2, and GLUT5), vitamin transporters (SVCT1, RFC-1, THTR1, THTR2, and SMVT), bile acid transporter (ISBT), fatty acid transporters (FATP1 and FATP4), phosphate transporters (SLC17A3, SLC17A4, and NAPI3B), monocarboxylic acid transporter (MCT1), ATP-binding cassette transporters (MDR1, MRP1, MRP2, MRP3, MOAT-C, and ABCG family members), and some other transporters (NADC1, SBC2, NBC2, and HNBC1). These intestinal transporters show diverse substrate specificities. PEPT1 is known to play an essential role in the oral absorption of peptidomimetic drugs such as angiotensin-converting enzyme inhibitors, β-lactam antibiotics and ester prodrugs of zidovudine and acyclovir. The nucleoside transporters transport many nucleoside drugs. There are many different amino acid transporters in the intestine and they have highly restrictive substrate specificities. Organic cation and anion transporters have been shown to be specific transport systems for many endogenous amines and ionic xenobiotics. MDR1 serves as an absorption barrier in the intestine. A number of transporters have been known to transport bile acids, several water-soluble vitamins, monocarboxylic acids, phosphates, bicarbonates, fatty acids, sugars, and ions. Recent advances in gene cloning and molecular biology techniques have made it possible to find and classify specific substrate drugs. There are several

examples where the bioavailability of poorly absorbed drugs has been improved through using transporters. Therefore, this review will provide information for new strategies in oral drug discovery, development, and targeting.

References

1 Tamai, I. [Molecular characterization of intestinal absorption of drugs by carrier-mediated transport mechanisms]. *Yakugaku Zasshi* **1997**, *117*, 415–434.

2 Venter, J. C., et al. The sequence of the human genome. *Science* **2001**, *291*, 1304–13051.

3 Yan, Q. and W. Sadee. Human membrane transporter database: a Web-accessible relational database for drug transport studies and pharmacogenomics. *AAPS PharmSci*. **2000**, *2*, E20.

4 Sun, D., et al. Comparison of human duodenum and Caco-2 gene expression profiles for 12,000 gene sequences tags and correlation with permeability of 26 drugs. *Pharm. Res.* **2002**, *19*, 1400–1416.

5 Tsuji, A. and I. Tamai. Carrier-mediated intestinal transport of drugs. *Pharm. Res.* **1996**, *13*, 963–977.

6 Alper, J. Drug delivery. Breaching the membrane. *Science* **2002**, *296*, 838–839.

7 Yang, C. Y., A. H. Dantzig, and C. Pidgeon. Intestinal peptide transport systems and oral drug availability. *Pharm. Res.* **1999**, *16*, 1331–1343.

8 Lee, V. H., et al. Biopharmaceutics of transmucosal peptide and protein drug administration: role of transport mechanisms with a focus on the involvement of PepT1. *J. Control. Release* **1999**, *62*, 129–140.

9 Lipka, E., J. Crison, and G. L. Amidon. Transmembrane transport of peptide type compounds: prospects for oral delivery. *J. Control. Release* **1996**, *39*, 121–129.

10 Adibi, S. A. The oligopeptide transporter (Pept-1) in human intestine: biology and function. *Gastroenterology* **1997**, *113*, 332–340.

11 Rubio-Aliaga, I. and H. Daniel. Mammalian peptide transporters as targets for drug delivery. *Trends Pharmacol. Sci.* **2002**, *23*, 434–440.

12 Daniel, H. Function and molecular structure of brush border membrane peptide/H+ symporters. *J. Membr. Biol.* **1996**, *154*, 197–203.

13 Detmers, F. J., F. C. Lanfermeijer, and B. Poolman. Peptides and ATP binding cassette peptide transporters. *Res. Microbiol.* **2001**, *152*, 245–258.

14 Inui, K., et al. Physiological and pharmacological implications of peptide transporters, PEPT1 and PEPT2. *Nephrol. Dial. Transplant.* **2000**, *15*, 11–13.

15 Meredith, D. and C. A. Boyd. Structure and function of eukaryotic peptide transporters. *Cell. Mol. Life Sci.* **2000**, *57*, 754–778.

16 Ganapathy, V. and F. H. Leibach. Peptide transporters. *Curr. Opin. Nephrol. Hypertens.* **1996**, *5*, 395–400.

17 Leibach, F. H. and V. Ganapathy. Peptide transporters in the intestine and the kidney. *Annu. Rev. Nutr.* **1996**, *16*, 99–119.

18 Herrera-Ruiz, D., et al. Spatial expression patterns of peptide transporters in the human and rat gastrointestinal tracts, Caco-2 *in vitro* cell culture model, and multiple human tissues. *AAPS PharmSci.* **2001**, *3*, E9.

19 Shen, H., et al. Localization of PEPT1 and PEPT2 proton-coupled oligopeptide transporter mRNA and protein in rat kidney. *Am. J. Physiol.* **1999**, *276*, F658–665.

20 Ogihara, H., et al. Immunolocalization of H+/peptide cotransporter in rat digestive tract. *Biochem. Biophys. Res. Commun.* **1996**, *220*, 848–852.

21 Liang, R., et al. Human intestinal H+/peptide cotransporter. Cloning, functional expression, and

chromosomal localization. *J. Biol. Chem.* **1995**, *270*, 6456–6463.

22 Fei, Y. J., V. Ganapathy, and F. H. Leibach. Molecular and structural features of the proton-coupled oligopeptide transporter superfamily. *Prog. Nucleic Acid. Res. Mol. Biol.* **1998**, *58*, 239–261.

23 Saito, H., et al. Molecular cloning and tissue distribution of rat peptide transporter PEPT2. *Biochim. Biophys. Acta* **1996**, *1280*, 173–177.

24 Liu, W., et al. Molecular cloning of PEPT 2, a new member of the H+/peptide cotransporter family, from human kidney. *Biochim. Biophys. Acta* **1995**, *1235*, 461–466.

25 Botka, C. W., et al. Human proton/oligopeptide transporter (POT) genes: identification of putative human genes using bioinformatics. *AAPS PharmSci.* **2000**, *2*, E16.

26 Brodin, B., et al. Transport of peptidomimetic drugs by the intestinal Di/tri-peptide transporter, PepT1. *Pharmacol. Toxicol.* **2002**, *90*, 285–296.

27 Lee, V. H. Membrane transporters. *Eur. J. Pharm. Sci.* **2000**, *11*, S41–S50.

28 Oh, D. M., H. K. Han, and G. L. Amidon. Drug transport and targeting. Intestinal transport. *Pharm. Biotechnol.* **1999**, *12*, 59–88.

29 Ganapathy, V. and F. H. Leibach. Role of pH gradient and membrane potential in dipeptide transport in intestinal and renal brush-border membrane vesicles from the rabbit. Studies with L-carnosine and glycyl-L-proline. *J. Biol. Chem.* **1983**, *258*, 14189–14192.

30 Boll, M., et al. Expression cloning of a cDNA from rabbit small intestine related to proton-coupled transport of peptides, beta-lactam antibiotics and ACE-inhibitors. *Pflugers Arch.* **1994**, *429*, 146–149.

31 Fei, Y. J., et al. Expression cloning of a mammalian proton-coupled oligopeptide transporter. *Nature* **1994**, *368*, 563–566.

32 Saito, H., et al. Cloning and characterization of a rat H+/peptide cotransporter mediating absorption of beta-lactam antibiotics in the intestine and kidney. *J. Pharmacol. Exp. Ther.* **1995**, *275*, 1631–1637.

33 Chen, H., et al. Molecular cloning and functional expression of a chicken intestinal peptide transporter (cPepT1) in *Xenopus* oocytes and Chinese hamster ovary cells. *J. Nutr.* **2002**, *132*, 387–393.

34 Pan, Y., et al. Expression of a cloned ovine gastrointestinal peptide transporter (oPepT1) in *Xenopus* oocytes induces uptake of oligopeptides *in vitro*. *J. Nutr.* **2001**, *131*, 1264–1270.

35 Covitz, K. M., G. L. Amidon, and W. Sadee. Human dipeptide transporter, hPEPT1, stably transfected into Chinese hamster ovary cells. *Pharm. Res.* **1996**, *13*, 1631–1634.

36 Han, H. K., et al. CHO/hPEPT1 cells overexpressing the human peptide transporter (hPEPT1) as an alternative *in vitro* model for peptidomimetic drugs. *J. Pharm. Sci.* **1999**, *88*, 347–350.

37 Hsu, C. P., et al. Function and immunolocalization of overexpressed human intestinal H+/peptide cotransporter in adenovirus-transduced Caco-2 cells. *AAPS PharmSci.* **1999**, *1*, E12.

38 Tamai, I., et al. The predominant contribution of oligopeptide transporter PepT1 to intestinal absorption of beta-lactam antibiotics in the rat small intestine. *J. Pharm. Pharmacol.* **1997**, *49*, 796–801.

39 Hsu, C.-P., et al. Overexpression of human intestinal oligopeptide transporter in mammalian cells via adenoviral transduction. *Pharm. Res.* **1998**, *15*, 1376–1381.

40 Han, H.-K., D.-M. Oh, and G. L. Amidon. Cellular uptake mechanism of amino acid ester prodrugs in Caco-2/hPEPT1 cells overexpressing a human peptide transporter. *Pharm. Res.* **1998**, *15*, 1382–1386.

41 Doring, F., S. Theis, and H. Daniel. Expression and functional characterization of the mammalian intestinal peptide transporter PepT1 in the methylotropic yeast Pichia pastoris. *Biochem. Biophys. Res. Commun.* **1997**, *232*, 656–662.

42 Covitz, K.-M. Y., G. L. Amidon, and W. Sadee. Human dipeptide transporter, hPEPT1, stably transfected into Chinese hamster ovary cells. *Pharm. Res.* **1996**, *113*, 1631–1634.

43 Wenzel, U., D. T. Thwaites, and H. Daniel. Stereoselective uptake of beta-lactam antibiotics by the intestinal peptide transporter. *Br. J. Pharmacol.* **1995**, *116*, 3021–3027.

44 Bretschneider, B., M. Brandsch, and R. Neubert. Intestinal transport of beta-lactam antibiotics: analysis of the affinity at the H+/peptide symporter (PEPT1), the uptake into Caco-2 cell monolayers and the transepithelial flux. *Pharm. Res.* **1999**, *16*, 55–61.

45 Bai, J. P. and G. L. Amidon. Structural specificity of mucosal-cell transport and metabolism of peptide drugs: implication for oral peptide drug delivery. *Pharm. Res.* **1992**, *9*, 969–978.

46 Chu, X. Y., et al. Correlation between epithelial cell permeability of cephalexin and expression of intestinal oligopeptide transporter. *J. Pharmacol. Exp. Ther.* **2001**, *299*, 575–582.

47 Terada, T., et al. Recognition of beta-lactam antibiotics by rat peptide transporters, PEPT1 and PEPT2, in LLC-PK1 cells. *Am. J. Physiol.* **1997**, *273*, F706–F711.

48 Terada, T., et al. Identification of the histidine residues involved in substrate recognition by a rat H+/peptide cotransporter, PEPT1. *FEBS Lett.* **1996**, *394*, 196–200.

49 Tomita, Y., et al. Transport of oral cephalosporins by the H+/dipeptide cotransporter and distribution of the transport activity in isolated rabbit intestinal epithelial cells. *J. Pharmacol. Exp. Ther.* **1995**, *272*, 63–69.

50 Ganapathy, M. E., et al. Differential recognition of beta-lactam antibiotics by intestinal and renal peptide transporters, PEPT 1 and PEPT 2. *J. Biol. Chem.* **1995**, *270*, 25672–25677.

51 Oh, D. M., P. J. Sinko, and G. L. Amidon. Characterization of the oral absorption of some beta-lactams: effect of the alpha-amino side chain group. *J. Pharm. Sci.* **1993**, *82*, 897–900.

52 Poschet, J. F., S. M. Hammond, and P. D. Fairclough. Characterisation of penicillin-G uptake in rabbit small-intestinal brush-border membrane vesicles. *Biochim. Biophys. Acta* **1996**, *1278*, 233–240.

53 Moore, V. A., et al. A rapid screening system to determine drug affinities for the intestinal dipeptide transporter 2: affinities of ACE inhibitors. *Int. J. Pharm.* **2000**, *210*, 29–44.

54 Swaan, P. W. and J. J. Tukker. Molecular determinants of recognition for the intestinal peptide carrier. *J. Pharm. Sci.* **1997**, *86*, 596–602.

55 Yee, S. and G. L. Amidon. Oral absorption of angiotensin-converting enzyme inhibitors and peptide prodrugs. In: Peptide-based Drug Design. G. L. Amidon (ed), American Chemistry Society, Washington DC 1995, 137–147.

56 Zhu, T., et al. Differential recognition of ACE inhibitors in *Xenopus* laevis oocytes expressing rat PEPT1 and PEPT2. *Pharm. Res.* **2000**, *17*, 526–532.

57 Kitagawa, S., J. Takeda, and S. Sato. pH-dependent inhibitory effects of angiotensin-converting enzyme inhibitors on cefroxadine uptake by rabbit small intestinal brush-border membrane vesicles and their relationship with hydrophobicity and the ratio of zwitterionic species. *Biol. Pharm. Bull.* **1999**, *22*, 721–724.

58 Kitagawa, S., et al. Inhibitory effects of angiotensin-converting enzyme inhibitor on cefroxadine uptake by rabbit small intestinal brush border membrane vesicles. *Biol. Pharm. Bull.* **1997**, *20*, 449–451.

59 Hu, M., et al. Mechanisms of transport of quinapril in Caco-2 cell monolayers: comparison with cephalexin. *Pharm. Res.* **1995**, *12*, 1120–1125.

60 Friedman, D. I. and G. L. Amidon. Passive and carrier-mediated intestinal absorption components of two angiotensin converting enzyme (ACE) inhibitor prodrugs in rats: enalapril and fosinopril. *Pharm. Res.* **1989**, *6*, 1043–1047.

61 Hu, M. and G. L. Amidon. Passive and carrier-mediated intestinal absorption components of captopril. *J. Pharm. Sci.* **1988**, *77*, 1007–1011.

62 Shu, C., et al. Mechanism of intestinal absorption and renal reabsorption of an orally active ace inhibitor: uptake and transport of fosinopril in cell cultures. *Drug Metab. Dispos.* **2001**, *29*, 1307–1315.

63 Hashimoto, N., et al. Renin inhibitor: relationship between molecular structure and oral absorption. *Pharm. Res.* **1994**, *11*, 1443–1447.

64 Hashimoto, N., et al. Renin inhibitor: transport mechanism in rat small intestinal brush-border membrane vesicles. *Pharm. Res.* **1994**, *11*, 1448–1451.

65 Kramer, W., et al. Interaction of renin inhibitors with the intestinal uptake system for oligopeptides and beta-lactam antibiotics. *Biochim. Biophys. Acta* **1990**, *1027*, 25–30.

66 Walter, E., et al. Transepithelial transport properties of peptidomimetic thrombin inhibitors in monolayers of a human intestinal cell line (Caco-2) and their correlation to *in vivo* data. *Pharm. Res.* **1995**, *12*, 360–365.

67 Takano, M., et al. Bestatin transport in rabbit intestinal brush-border membrane vesicles. *Biochem. Pharmacol.* **1994**, *47*, 1089–1090.

68 Inui, K., et al. H+ coupled active transport of bestatin via the dipeptide transport system in rabbit intestinal brush-border membranes. *J. Pharmacol. Exp. Ther.* **1992**, *260*, 482–486.

69 Watanabe, K., et al. Studies on intestinal absorption of sulpiride (2): transepithelial transport of sulpiride across the human intestinal cell line Caco-2. *Biol. Pharm. Bull.* **2002**, *25*, 1345–1350.

70 Surendran, N., et al. Evidence for overlapping substrate specificity between large neutral amino acid (LNAA) and dipeptide (hPEPT1) transporters for PD 158473, an NMDA antagonist. *Pharm. Res.* **1999**, *16*, 391–395.

71 Liu, K. X., et al. Hydroxyprolylserine derivatives JBP923 and JBP485 exhibit the antihepatitis activities after gastrointestinal absorption in rats. *J. Pharmacol. Exp. Ther.* **2000**, *294*, 510–515.

72 Balimane, P. V., et al. Direct evidence for peptide transporter (PepT1)-mediated uptake of a nonpeptide prodrug, valacyclovir. *Biochem. Biophys. Res. Commun.* **1998**, *250*, 246–251.

73 Brandsch, M., et al. Evidence for the absolute conformational specificity of the intestinal H+/peptide symporter, PEPT1. *J. Biol. Chem.* **1998**, *273*, 3861–3864.

74 Temple, C. S., et al. Peptide mimics as substrates for the intestinal peptide transporter. *J. Biol. Chem.* **1998**, *273*, 20–22.

75 Enjoh, M., et al. Inhibitory effect of arphamenine A on intestinal dipeptide transport. *Biosci. Biotechnol. Biochem.* **1996**, *60*, 1893–1895.

76 Doring, F., et al. Delta-aminolevulinic acid transport by intestinal and renal peptide transporters and its physiological and clinical implications. *J. Clin. Invest.* **1998**, *101*, 2761–2767.

77 Balimane, P. V. and P. J. Sinko. Involvement of multiple transporters in the oral absorption of nucleoside analogues. *Adv. Drug Deliv. Rev.* **1999**, *39*, 183–209.

78 Han, H., et al. 5′-Amino acid esters of antiviral nucleosides, acyclovir, and AZT are absorbed by the intestinal PEPT1 peptide transporter. *Pharm. Res.* **1998**, *15*, 1154–1159.

79 Han, H. K., D. M. Oh, and G. L. Amidon. Cellular uptake mechanism of amino acid ester prodrugs in Caco-2/hPEPT1 cells overexpressing a human peptide transporter. *Pharm. Res.* **1998**, *15*, 1382–1386.

80 Sugawara, M., et al. Transport of valganciclovir, a ganciclovir prodrug, via peptide transporters PEPT1 and PEPT2. *J. Pharm. Sci.* **2000**, *89*, 781–789.

81 Ganapathy, M. E., et al. Valacyclovir: a substrate for the intestinal and renal peptide transporters PEPT1 and PEPT2. *Biochem. Biophys. Res. Commun.* **1998**, *246*, 470–475.

82 Acosta, E. P. and C. V. Fletcher. Valacyclovir. *Ann. Pharmacother.* **1997**, *31*, 185–191.

83 Peyriere, H., et al. [Neurologic toxicity caused by zelitrex (valaciclovir) in 3 patients with renal failure. Is overdose associated with improvement of product bioavailability improvement?]. *Rev. Med. Interne* **2001**, *22*, 297–303.

84 Poirier, J. M., N. Radembino, and P. Jaillon. Determination of acyclovir in plasma by solid-phase extraction and column liquid chromatography. *Ther. Drug Monit.* **1999**, *21*, 129–133.

85 Steingrimsdottir, H., et al. Bioavailability of aciclovir after oral administration of aciclovir and its prodrug valaciclovir to patients with leukopenia after chemotherapy. *Antimicrob. Agents Chemother.* **2000**, *44*, 207–209.

86 Friedrichsen, G. M., et al. Synthesis of analogs of L-valacyclovir and determination of their substrate activity for the oligopeptide transporter in Caco-2 cells. *Eur. J. Pharm. Sci.* **2002**, *16*, 1–13.

87 Tamai, I., et al. Improvement of L-dopa absorption by dipeptidyl derivation, utilizing peptide transporter PepT1. *J. Pharm. Sci.* **1998**, *87*, 1542–1546.

88 Sawada, K., et al. Recognition of L-amino acid ester compounds by rat peptide transporters PEPT1 and PEPT2. *J. Pharmacol. Exp. Ther.* **1999**, *291*, 705–709.

89 Thamotharan, M., et al. Mechanism of dipeptide stimulation of its own transport in a human intestinal cell line. *Proc. Assoc. Am. Physicians* **1998**, *110*, 361–368.

90 Walker, D., et al. Substrate upregulation of the human small intestinal peptide transporter, hPepT1. *J. Physiol.* **1998**, *507*, 697–706.

91 Shiraga, T., et al. Cellular and molecular mechanisms of dietary regulation on rat intestinal H+/ Peptide transporter PepT1. *Gastroenterology* **1999**, *116*, 354–362.

92 Ihara, T., et al. Regulation of PepT1 peptide transporter expression in the rat small intestine under malnourished conditions. *Digestion* **2000**, *61*, 59–67.

93 Thamotharan, M., et al. Hormonal regulation of oligopeptide transporter pept-1 in a human intestinal cell line. *Am. J. Physiol.* **1999**, *276*, C821–C826.

94 Fujita, T., et al. sigma Receptor ligand-induced up-regulation of the H(+)/peptide transporter PEPT1 in the human intestinal cell line Caco-2. *Biochem. Biophys. Res. Commun.* **1999**, *261*, 242–246.

95 Motohashi, H., et al. Expression of peptide transporter following intestinal transplantation in the rat. *J. Surg. Res.* **2001**, *99*, 294–300.

96 Muller, U., et al. Inhibition of the H+/peptide cotransporter in the human intestinal cell line Caco-2 by cyclic AMP. *Biochem. Biophys. Res. Commun.* **1996**, *218*, 461–465.

97 Nielsen, C. U., et al. Epidermal growth factor inhibits glycylsarcosine transport and hPepT1 expression in a human intestinal cell line. *Am. J. Physiol.* **2001**, *281*, G191–G199.

98 Ashida, K., et al. Thyroid hormone regulates the activity and expression of the peptide transporter PEPT1 in Caco-2 cells. *Am. J. Physiol.* **2002**, *282*, G617–G623.

99 Dantzig, A. H., et al. Association of intestinal peptide transport with a protein related to the cadherin superfamily. *Science* **1994**, *264*, 430–433.

100 Wang, J., et al. Functional and molecular characteristics of Na(+)-dependent nucleoside transporters. *Pharm. Res.* **1997**, *14*, 1524–1532.

101 Ritzel, M. W., et al. Recent molecular advances in studies of the concentrative Na+-dependent nucleoside transporter (CNT) family: identification and characterization of novel human and mouse proteins (hCNT3 and mCNT3) broadly selective for purine and pyrimidine nucleosides (system cib). *Mol. Membr. Biol.* **2001**, *18*, 65–72.

102 Hyde, R. J., et al. The ENT family of eukaryote nucleoside and nucleobase transporters: recent advances in the investigation of structure/function

relationships and the identification of novel isoforms. *Mol. Membr. Biol.* **2001**, *18*, 53–63.

103 Pastor-Anglada, M., et al. Complex regulation of nucleoside transporter expression in epithelial and immune system cells. *Mol. Membr. Biol.* **2001**, *18*, 81–85.

104 Griffiths, M., et al. Cloning of a human nucleoside transporter implicated in the cellular uptake of adenosine and chemotherapeutic drugs. *Nat. Med.* **1997**, *3*, 89–93.

105 Griffiths, M., et al. Molecular cloning and characterization of a nitrobenzylthioinosine-insensitive (ei) equilibrative nucleoside transporter from human placenta. *Biochem. J.* **1997**, *328*, 739–743.

106 Yao, S. Y., et al. Molecular cloning and functional characterization of nitrobenzylthioinosine (NBMPR)-sensitive (es) and NBMPR-insensitive (ei) equilibrative nucleoside transporter proteins (rENT1 and rENT2) from rat tissues. *J. Biol. Chem.* **1997**, *272*, 28423–28430.

107 Huang, Q. Q., et al. Cloning and functional expression of a complementary DNA encoding a mammalian nucleoside transport protein. *J. Biol. Chem.* **1994**, *269*, 17757–17760.

108 Ritzel, M. W., et al. Molecular cloning and functional expression of cDNAs encoding a human Na+-nucleoside cotransporter (hCNT1). *Am. J. Physiol.* **1997**, *272*, C707–C714.

109 Che, M., D. F. Ortiz, and I. M. Arias. Primary structure and functional expression of a cDNA encoding the bile canalicular, purine-specific Na(+)-nucleoside cotransporter. *J. Biol. Chem.* **1995**, *270*, 13596–13599.

110 Ritzel, M. W., et al. Molecular cloning, functional expression and chromosomal localization of a cDNA encoding a human Na+/nucleoside cotransporter (hCNT2) selective for purine nucleosides and uridine. *Mol. Membr. Biol.* **1998**, *15*, 203–211.

111 Wang, J., et al. Na(+)-dependent purine nucleoside transporter from human kidney: cloning and functional characterization. *Am. J. Physiol.* **1997**, *273*, F1058–F1065.

112 Gerstin, K. M., et al. Molecular cloning of a Na+-dependent nucleoside transporter from rabbit intestine. *Pharm. Res.* **2000**, *17*, 906–910.

113 Li, J. Y., R. J. Boado, and W. M. Pardridge. Cloned blood-brain barrier adenosine transporter is identical to the rat concentrative Na+ nucleoside cotransporter CNT2. *J. Cereb. Blood Flow Metab.* **2001**, *21*, 929–936.

114 Patel, D. H., et al. Cloning, genomic organization and chromosomal localization of the gene encoding the murine sodium-dependent, purine-selective, concentrative nucleoside transporter (CNT2). *Gene* **2000**, *242*, 51–58.

115 Ritzel, M. W., et al. Molecular identification and characterization of novel human and mouse concentrative Na+-nucleoside cotransporter proteins (hCNT3 and mCNT3) broadly selective for purine and pyrimidine nucleosides (system cib). *J. Biol. Chem.* **2001**, *276*, 2914–2927.

116 Schaner, M. E., et al. Transient expression of a purine-selective nucleoside transporter (SPNTint) in a human cell line (HeLa). *Pharm. Res.* **1997**, *14*, 1316–1321.

117 Dragan, Y., et al. Selective loss of nucleoside carrier expression in rat hepatocarcinomas. *Hepatology* **2000**, *32*, 239–246.

118 Lu, X., et al. Correlation of nucleoside and nucleobase transporter gene expression with antimetabolite drug cytotoxicity. *J. Exp. Ther. Oncol.* **2002**, *2*, 200–212.

119 Mata, J. F., et al. Role of the human concentrative nucleoside transporter (hCNT1) in the cytotoxic action of 5[Prime]-deoxy-5-fluorouridine, an active intermediate metabolite of capecitabine, a novel oral anticancer drug. *Mol. Pharmacol.* **2001**, *59*, 1542–1548.

120 Crawford, C. R., et al. Stable expression of a recombinant sodium-dependent, pyrimidine-selective nucleoside transporter (CNT1) in a

transport-deficient mouse leukemia cell line. *Biochem. Cell. Biol.* **1998**, *76*, 843–851.

121 Schaner, M. E., et al. Functional characterization of a human purine-selective, Na+-dependent nucleoside transporter (hSPNT1) in a mammalian expression system. *J. Pharmacol. Exp. Ther.* **1999**, *289*, 1487–1491.

122 Crawford, C. R., et al. Cloning of the human equilibrative, nitrobenzylmercaptopurine riboside (NBMPR)-insensitive nucleoside transporter ei by functional expression in a transport-deficient cell line. *J. Biol. Chem.* **1998**, *273*, 5288–5293.

123 Yao, S. Y., C. E. Cass, and J. D. Young. Transport of the antiviral nucleoside analogs 3′-azido-3′-deoxythymidine and 2′,3′-dideoxycytidine by a recombinant nucleoside transporter (rCNT) expressed in *Xenopus* laevis oocytes. *Mol. Pharmacol.* **1996**, *50*, 388–393.

124 Fang, X., et al. Functional characterization of a recombinant sodium-dependent nucleoside transporter with selectivity for pyrimidine nucleosides (cNT1rat) by transient expression in cultured mammalian cells. *Biochem. J.* **1996**, *317*, 457–465.

125 Boumah, C. E., et al. Functional expression of the nitrobenzylthioinosine-sensitive nucleoside transporter of human choriocarcinoma (BeWo) cells in isolated oocytes of *Xenopus* laevis. *Biochem. J.* **1994**, *299*, 769–773.

126 Sinclair, C. J., et al. Nucleoside transporter subtype expression: effects on potency of adenosine kinase inhibitors. *Br. J. Pharmacol.* **2001**, *134*, 1037–1044.

127 Patil, S. D., L. Y. Ngo, and J. D. Unadkat. Structure-inhibitory profiles of nucleosides for the human intestinal N1 and N2 Na+-nucleoside transporters. *Cancer Chemother. Pharmacol.* **2000**, *46*, 394–402.

128 Patil, S. D. and J. D. Unadkat. Sodium-dependent nucleoside transport in the human intestinal brush-border membrane. *Am. J. Physiol.* **1997**, *272*, G1314–G1320.

129 Ngo, L. Y., S. D. Patil, and J. D. Unadkat. Ontogenic and longitudinal activity of Na(+)-nucleoside transporters in the human intestine. *Am. J. Physiol.* **2001**, *280*, G475–G481.

130 Chandrasena, G., et al. Functional expression of human intestinal Na+-dependent and Na+-independent nucleoside transporters in *Xenopus* laevis oocytes. *Biochem. Pharmacol.* **1997**, *53*, 1909–1918.

131 Pennycooke, M., et al. Differential expression of human nucleoside transporters in normal and tumor tissue. *Biochem. Biophys. Res. Commun.* **2001**, *280*, 951–959.

132 Xiao, G., et al. A novel proton-dependent nucleoside transporter, CeCNT3, from Caenorhabditis elegans. *Mol. Pharmacol.* **2001**, *59*, 339–348.

133 Mackey, J. R., et al. Gemcitabine transport in *Xenopus* oocytes expressing recombinant plasma membrane mammalian nucleoside transporters. *J. Natl. Cancer Inst.* **1999**, *91*, 1876–1881.

134 Li, J. Y., R. J. Boado, and W. M. Pardridge. Differential kinetics of transport of 2′,3′-dideoxyinosine and adenosine via concentrative Na^+ nucleoside transporter CNT2 cloned from rat blood-brain barrier. *J. Pharmacol. Exp. Ther.* **2001**, *299*, 735–740.

135 Mackey, J. R., et al. Functional nucleoside transporters are required for gemcitabine influx and manifestation of toxicity in cancer cell lines. *Cancer Res.* **1998**, *58*, 4349–4357.

136 Griffith, D. A. and S. M. Jarvis. Nucleoside and nucleobase transport systems of mammalian cells. *Biochim. Biophys. Acta* **1996**, *1286*, 153–181.

137 Ward, J. L., et al. Kinetic and pharmacological properties of cloned human equilibrative nucleoside transporters, ENT1 and ENT2, stably expressed in nucleoside transporter-deficient PK15 cells. Ent2 exhibits a low affinity for guanosine and cytidine but a high affinity for inosine. *J. Biol. Chem.* **2000**, *275*, 8375–8381.

138 Oxender, D. L. Membrane transport. *Annu. Rev. Biochem.* **1972**, *41*, 777–814.

139 Palacin, M., et al. Molecular biology of mammalian plasma membrane amino acid transporters. *Physiol. Rev.* **1998**, *78*, 969–1054.

140 Wang, H., et al. Cell-surface receptor for ecotropic murine retroviruses is a basic amino-acid transporter. *Nature* **1991**, *352*, 729–731.

141 Kim, K. H., et al. Slow inward current induced by achatin-I, an endogenous peptide with a D-Phe residue. *Eur. J. Pharmacol.* **1991**, *194*, 99–106.

142 Verrey, F., et al. New glycoprotein-associated amino acid transporters. *J. Membr. Biol.* **1999**, *172*, 181–192.

143 Pfeiffer, R., et al. Luminal heterodimeric amino acid transporter defective in cystinuria. *Mol. Biol. Cell* **1999**, *10*, 4135–4147.

144 Feliubadalo, L., et al. Non-type I cystinuria caused by mutations in SLC7A9, encoding a subunit (bo,+AT) of rBAT. International Cystinuria Consortium. *Nat. Genet.* **1999**, *23*, 52–57.

145 Kanai, Y. and M. A. Hediger. Primary structure and functional characterization of a high-affinity glutamate transporter. *Nature* **1992**, *360*, 467–471.

146 Kanai, Y., et al. Expression of mRNA (D2) encoding a protein involved in amino acid transport in S3 proximal tubule. *Am. J. Physiol.* **1992**, *263*, F1087–F1092.

147 Kanai, Y., et al. Electrogenic properties of the epithelial and neuronal high affinity glutamate transporter. *J. Biol. Chem.* **1995**, *270*, 16561–16568.

148 Kekuda, R., et al. Cloning of the sodium-dependent, broad-scope, neutral amino acid transporter Bo from a human placental choriocarcinoma cell line. *J. Biol. Chem.* **1996**, *271*, 18657–18661.

149 Kekuda, R., et al. Molecular and functional characterization of intestinal Na(+)-dependent neutral amino acid transporter B0. *Am. J. Physiol.* **1997**, *272*, G1463–G1472.

150 Lee, W. S., et al. Cloning and chromosomal localization of a human kidney cDNA involved in cystine, dibasic, and neutral amino acid transport. *J. Clin. Invest.* **1993**, *91*, 1959–1963.

151 Wells, R. G. and M. A. Hediger. Cloning of a rat kidney cDNA that stimulates dibasic and neutral amino acid transport and has sequence similarity to glucosidases. *Proc. Natl. Acad. Sci. U. S. A.* **1992**, *89*, 5596–5600.

152 Yan, N., et al. Distribution of mRNA of a Na(+)-independent neutral amino acid transporter cloned from rat kidney and its expression in mammalian tissues and *Xenopus* laevis oocytes. *Proc. Natl. Acad. Sci. U. S. A.* **1992**, *89*, 9982–9985.

153 Palacin, M. A new family of proteins (rBAT and 4F2hc) involved in cationic and zwitterionic amino acid transport: a tale of two proteins in search of a transport function. *J. Exp. Biol.* **1994**, *196*, 123–137.

154 Tate, S. S., N. Yan, and S. Udenfriend. Expression cloning of a Na(+)-independent neutral amino acid transporter from rat kidney. *Proc. Natl. Acad. Sci. U. S. A.* **1992**, *89*, 1–5.

155 Wells, R. G., et al. The 4F2 antigen heavy chain induces uptake of neutral and dibasic amino acids in *Xenopus* oocytes. *J. Biol. Chem.* **1992**, *267*, 15285–15288.

156 Bertran, J., et al. Stimulation of system y(+)-like amino acid transport by the heavy chain of human 4F2 surface antigen in *Xenopus* laevis oocytes. *Proc. Natl. Acad. Sci. U. S. A.* **1992**, *89*, 5606–5610.

157 Bertran, J., et al. Expression of Na(+)-independent amino acid transport in *Xenopus* laevis oocytes by injection of rabbit kidney cortex mRNA. *Biochem. J.* **1992**, *281*, 717–723.

158 Quackenbush, E., et al. Molecular cloning of complementary DNAs encoding the heavy chain of the human 4F2 cell-surface antigen: a type II membrane glycoprotein involved in normal and neoplastic cell growth. *Proc. Natl. Acad. Sci. U. S. A.* **1987**, *84*, 6526–6530.

159 Jhiang, S. M., et al. Cloning of the human taurine transporter and

characterization of taurine uptake in thyroid cells. *FEBS Lett.* **1993**, *318*, 139–144.

160 Kim do, K., et al. The human T-type amino acid transporter-1: characterization, gene organization, and chromosomal location. *Genomics* **2002**, *79*, 95–103.

161 Kim, D. K., et al. Expression cloning of a Na+-independent aromatic amino acid transporter with structural similarity to H+/monocarboxylate transporters. *J. Biol. Chem.* **2001**, *276*, 17221–17228.

162 Stewart, B. H., et al. A saturable transport mechanism in the intestinal absorption of gabapentin is the underlying cause of the lack of proportionality between increasing dose and drug levels in plasma. *Pharm. Res.* **1993**, *10*, 276–281.

163 Uchino, H., et al. Transport of amino acid-related compounds mediated by L-type amino acid transporter 1 (LAT1): insights into the mechanisms of substrate recognition. *Mol. Pharmacol.* **2002**, *61*, 729–737.

164 Piyapolrungroj, N., et al. Mucosal uptake of gabapentin (neurontin) vs. pregabalin in the small intestine. *Pharm. Res.* **2001**, *18*, 1126–1130.

165 Takada, Y., et al. Affinity of antineoplastic amino acid drugs for the large neutral amino acid transporter of the blood-brain barrier. *Cancer Chemother. Pharmacol.* **1991**, *29*, 89–94.

166 Yanagida, O., et al. Human L-type amino acid transporter 1 (LAT1): characterization of function and expression in tumor cell lines. *Biochim. Biophys. Acta* **2001**, *1514*, 291–302.

167 Kim, D., et al. Characterization of the system L amino acid transporter in T24 human bladder carcinoma cells. *Biochim. Biophys. Acta* **2002**, *1565*, 112.

168 Amidon, G. L., A. E. Merfeld, and J. B. Dressman. Concentration and pH dependency of alpha-methyldopa absorption in rat intestine. *J. Pharm. Pharmacol.* **1986**, *38*, 363–368.

169 Hu, M. and R. T. Borchardt. Mechanism of L-alpha-methyldopa transport through a monolayer of polarized human intestinal epithelial cells (Caco-2). *Pharm. Res.* **1990**, *7*, 1313–1319.

170 Cercos-Fortea, T., et al. Influence of leucine on intestinal baclofen absorption as a model compound of neutral alpha-aminoacids. Biopharm. *Drug. Dispos.* **1995**, *16*, 563–577.

171 Shindo, H., T. Komai, and K. Kawai. Studies on the metabolism of D- and L-isomers of 3,4-dihydroxyphenylalanine (DOPA). V. Mechanism of intestinal absorption of D- and L-DOPA-14C in rats. *Chem. Pharm. Bull.* **1973**, *21*, 2031–2038.

172 Fraga, S., M. P. Serrao, and P. Soares-da-Silva. The L-3,4-dihydroxyphenylalanine transporter in human and rat epithelial intestinal cells is a type 2 hetero amino acid exchanger. *Eur. J. Pharmacol.* **2002**, *441*, 127–135.

173 Thwaites, D. T., et al. D-cycloserine transport in human intestinal epithelial (Caco-2) cells: mediation by a H(+)-coupled amino acid transporter. *Br. J. Pharmacol.* **1995**, *115*, 761–766.

174 Simmons-Willis, T. A., et al. Transport of a neurotoxicant by molecular mimicry: the methylmercury-l-cysteine complex is a substrate for human L-type large neutral amino acid transporter (LAT) 1 and LAT2. *Biochem. J.* **2002**, *367*, 239–246.

175 Campiani, G., et al. A rational approach to the design of selective substrates and potent nontransportable inhibitors of the excitatory amino acid transporter EAAC1 (EAAT3). New glutamate and aspartate analogues as potential neuroprotective agents. *J. Med. Chem.* **2001**, *44*, 2507–2510.

176 Kamisako, T., et al. Molecular aspects of organic compound transport across the plasma membrane of hepatocytes. *J. Gastroenterol. Hepatol.* **1999**, *14*, 405–412.

177 Koepsell, H., V. Gorboulev, and P. Arndt. Molecular pharmacology of organic cation transporters in kidney. *J. Membr. Biol.* **1999**, *167*, 103–117.

178 Zhang, L., C. M. Brett, and K. M. Giacomini. Role of organic cation

transporters in drug absorption and elimination. *Annu. Rev. Pharmacol. Toxicol.* **1998**, *38*, 431–460.

179 Koepsell, H. Organic cation transporters in intestine, kidney, liver, and brain. *Annu. Rev. Physiol.* **1998**, *60*, 243–266.

180 Burckhardt, G. and N. A. Wolff. Structure of renal organic anion and cation transporters. *Am. J. Physiol.* **2000**, *278*, F853–F866.

181 Lahjouji, K., G. A. Mitchell, and I. A. Qureshi. Carnitine transport by organic cation transporters and systemic carnitine deficiency. *Mol. Genet. Metab.* **2001**, *73*, 287–297.

182 Grundemann, D., et al. Drug excretion mediated by a new prototype of polyspecific transporter. *Nature* **1994**, *372*, 549–552.

183 Okuda, M., et al. cDNA cloning and functional expression of a novel rat kidney organic cation transporter, OCT2. *Biochem. Biophys. Res. Commun.* **1996**, *224*, 500–507.

184 Kekuda, R., et al. Cloning and functional characterization of a potential-sensitive, polyspecific organic cation transporter (OCT3) most abundantly expressed in placenta. *J. Biol. Chem.* **1998**, *273*, 15971–15979.

185 Zhang, L., et al. Cloning and functional expression of a human liver organic cation transporter. *Mol. Pharmacol.* **1997**, *51*, 913–921.

186 Gorboulev, V., et al. Cloning and characterization of two human polyspecific organic cation transporters. DNA *Cell. Biol.* **1997**, *16*, 871–881.

187 Tamai, I., et al. Cloning and characterization of a novel human pH-dependent organic cation transporter, OCTN1. *FEBS Lett.* **1997**, *419*, 107–111.

188 Wu, X., et al. Structural and functional characteristics and tissue distribution pattern of rat OCTN1, an organic cation transporter, cloned from placenta. *Biochim. Biophys. Acta* **2000**, *1466*, 315–327.

189 Tamai, I., et al. Molecular identification and characterization of novel members of the human organic anion transporter (OATP) family. *Biochem. Biophys. Res. Commun.* **2000**, *273*, 251–260.

190 Tamai, I., et al. Molecular and functional identification of sodium ion-dependent, high affinity human carnitine transporter OCTN2. *J. Biol. Chem.* **1998**, *273*, 20378–20382.

191 Wu, X., et al. cDNA sequence, transport function, and genomic organization of human OCTN2, a new member of the organic cation transporter family. *Biochem. Biophys. Res. Commun.* **1998**, *246*, 589–595.

192 Tamai, I., et al. Molecular and functional characterization of organic cation/carnitine transporter family in mice. *J. Biol. Chem.* **2000**, *275*, 40064–40072.

193 Busch, A. E., et al. Electrogenic properties and substrate specificity of the polyspecific rat cation transporter rOCT1. *J. Biol. Chem.* **1996**, *271*, 32599–32604.

194 Busch, A. E., et al. Monoamine neurotransmitter transport mediated by the polyspecific cation transporter rOCT1. *FEBS Lett.* **1996**, *395*, 153–156.

195 Wu, X., et al. Identity of the organic cation transporter OCT3 as the extraneuronal monoamine transporter (uptake2) and evidence for the expression of the transporter in the brain. *J. Biol. Chem.* **1998**, *273*, 32776–32786.

196 Yabuuchi, H., et al. Novel membrane transporter OCTN1 mediates multispecific, bidirectional, and pH-dependent transport of organic cations. *J. Pharmacol. Exp. Ther.* **1999**, *289*, 768–773.

197 Wang, Y., et al. Functional analysis of mutations in the OCTN2 transporter causing primary carnitine deficiency: lack of genotype-phenotype correlation. *Hum. Mutat.* **2000**, *16*, 401–407.

198 Ohashi, R., et al. Na(+)-dependent carnitine transport by organic cation transporter (OCTN2): its pharmacological and toxicological relevance. *J. Pharmacol. Exp. Ther.* **1999**, *291*, 778–784.

199 Wagner, C. A., et al. Functional and pharmacological characterization of human Na(+)-carnitine cotransporter hOCTN2. *Am. J. Physiol.* **2000**, *279*, F584–F591.

200 Sekine, T., S. H. Cha, and H. Endou. The multispecific organic anion transporter (OAT) family. *Pflugers Arch.* **2000**, *440*, 337–350.

201 Kusuhara, H. and Y. Sugiyama. Role of transporters in the tissue-selective distribution and elimination of drugs: transporters in the liver, small intestine, brain and kidney. *J. Control. Release* **2002**, *78*, 43–54.

202 Sweet, D. H., N. A. Wolff, and J. B. Pritchard. Expression cloning and characterization of ROAT1. The basolateral organic anion transporter in rat kidney. *J. Biol. Chem.* **1997**, *272*, 30088–30095.

203 Sekine, T., et al. Expression cloning and characterization of a novel multispecific organic anion transporter. *J. Biol. Chem.* **1997**, *272*, 18526–18529.

204 Simonson, G. D., et al. Molecular cloning and characterization of a novel liver-specific transport protein. *J. Cell Sci.* **1994**, *107*, 1065–1072.

205 Sekine, T., et al. Identification of multispecific organic anion transporter 2 expressed predominantly in the liver. *FEBS Lett.* **1998**, *429*, 179–182.

206 Kusuhara, H., et al. Molecular cloning and characterization of a new multispecific organic anion transporter from rat brain. *J. Biol. Chem.* **1999**, *274*, 13675–13680.

207 Race, J. E., et al. Molecular cloning and characterization of two novel human renal organic anion transporters (hOAT1 and hOAT3). *Biochem. Biophys. Res. Commun.* **1999**, *255*, 508–514.

208 Jacquemin, E., et al. Expression cloning of a rat liver Na(+)-independent organic anion transporter. *Proc. Natl. Acad. Sci. U. S. A.* **1994**, *91*, 133–137.

209 Tirona, R. G. and R. B. Kim. Pharmacogenomics of organic anion-transporting polypeptides (OATP). *Adv. Drug Deliv. Rev.* **2002**, *54*, 1343–1352.

210 Kullak-Ublick, G. A., et al. Molecular and functional characterization of an organic anion transporting polypeptide cloned from human liver. *Gastroenterology* **1995**, *109*, 1274–1282.

211 Kullak-Ublick, G. A., et al. Organic anion-transporting polypeptide B (OATP-B) and its functional comparison with three other OATPs of human liver. *Gastroenterology* **2001**, *120*, 525–533.

212 Abe, T., et al. Identification of a novel gene family encoding human liver-specific organic anion transporter LST-1. *J. Biol. Chem.* **1999**, *274*, 17159–17163.

213 Hsiang, B., et al. A novel human hepatic organic anion transporting polypeptide (OATP2). Identification of a liver-specific human organic anion transporting polypeptide and identification of rat and human hydroxymethylglutaryl-CoA reductase inhibitor transporters. *J. Biol. Chem.* **1999**, *274*, 37161–37168.

214 Konig, J., et al. A novel human organic anion transporting polypeptide localized to the basolateral hepatocyte membrane. *Am. J. Physiol.* **2000**, *278*, G156–G164.

215 Abe, T., et al. LST-2, a human liver-specific organic anion transporter, determines methotrexate sensitivity in gastrointestinal cancers. *Gastroenterology* **2001**, *120*, 1689–1699.

216 Konig, J., et al. Localization and genomic organization of a new hepatocellular organic anion transporting polypeptide. *J. Biol. Chem.* **2000**, *275*, 23161–23168.

217 Fujiwara, K., et al. Identification of thyroid hormone transporters in humans: different molecules are involved in a tissue-specific manner. *Endocrinology* **2001**, *142*, 2005–2012.

218 Ismair, M. G., et al. Hepatic uptake of cholecystokinin octapeptide by organic anion-transporting polypeptides OATP4 and OATP8 of rat and human liver. *Gastroenterology* **2001**, *121*, 1185–1190.

219 Pizzagalli, F., et al. Identification of a novel human organic anion transporting polypeptide as a high affinity thyroxine transporter. *Mol. Endocrinol.* **2002**, *16*, 2283–2296.

220 St-Pierre, M. V., et al. Characterization of an organic anion-transporting polypeptide (OATP-B) in human placenta. *J. Clin. Endocrinol. Metab.* **2002**, *87*, 1856–1863.

221 van Leeuwen, F., et al. Tandemly repeated DNA is a target for the partial replacement of thymine by beta-D-glucosyl-hydroxymethyluracil in Trypanosoma brucei. *Mol. Biochem. Parasitol.* **2000**, *109*, 133–145.

222 Hopper, E., et al. Analysis of the structure and expression pattern of MRP7 (ABCC10), a new member of the MRP subfamily. *Cancer Lett.* **2001**, *162*, 181–191.

223 Kruh, G. D., et al. MRP subfamily transporters and resistance to anticancer agents. *J. Bioenerg. Biomembr.* **2001**, *33*, 493–501.

224 Meier, P. J., et al. Substrate specificity of sinusoidal bile acid and organic anion uptake systems in rat and human liver. *Hepatology* **1997**, *26*, 1667–1677.

225 Muller, M. and P. L. Jansen. Molecular aspects of hepatobiliary transport. *Am. J. Physiol.* **1997**, *272*, G1285–G1303.

226 Abu-Zahra, T. N., et al. Uptake of enalapril and expression of organic anion transporting polypeptide 1 in zonal, isolated rat hepatocytes. *Drug Metab. Dispos.* **2000**, *28*, 801–806.

227 Ishizuka, H., et al. Transport of temocaprilat into rat hepatocytes: role of organic anion transporting polypeptide. *J. Pharmacol. Exp. Ther.* **1998**, *287*, 37–42.

228 Reichel, C., et al. Localization and function of the organic anion-transporting polypeptide Oatp2 in rat liver. *Gastroenterology* **1999**, *117*, 688–695.

229 Isern, J., et al. Functional analysis and androgen-regulated expression of mouse organic anion transporting polypeptide 1 (Oatp1) in the kidney. *Biochim. Biophys. Acta* **2001**, *1518*, 73–78.

230 Hagenbuch, B., I. D. Adler, and T. E. Schmid. Molecular cloning and functional characterization of the mouse organic-anion-transporting polypeptide 1 (Oatp1) and mapping of the gene to chromosome X. *Biochem. J.* **2000**, *345*, 115–120.

231 Eckhardt, U., et al. Polyspecific substrate uptake by the hepatic organic anion transporter Oatp1 in stably transfected CHO cells. *Am. J. Physiol.* **1999**, *276*, G1037–G1042.

232 Bossuyt, X., M. Muller, and P. J. Meier. Multispecific amphipathic substrate transport by an organic anion transporter of human liver. *J. Hepatol.* **1996**, *25*, 733–738.

233 Cui, Y., et al. Hepatic uptake of bilirubin and its conjugates by the human organic anion transporter SLC21A6. *J. Biol. Chem.* **2001**, *276*, 9626–9630.

234 Cvetkovic, M., et al. OATP and P-glycoprotein transporters mediate the cellular uptake and excretion of fexofenadine. *Drug Metab. Dispos.* **1999**, *27*, 866–871.

235 Gao, B., et al. Organic anion-transporting polypeptides mediate transport of opioid peptides across blood-brain barrier. *J. Pharmacol. Exp. Ther.* **2000**, *294*, 73–79.

236 Kullak-Ublick, G. A., et al. Dehydroepiandrosterone sulfate (DHEAS): identification of a carrier protein in human liver and brain. *FEBS Lett.* **1998**, *424*, 173–176.

237 Nakai, D., et al. Human liver-specific organic anion transporter, LST-1, mediates uptake of pravastatin by human hepatocytes. *J. Pharmacol. Exp. Ther.* **2001**, *297*, 861–867.

238 Borst, P., et al. A family of drug transporters: the multidrug resistance-associated proteins. *J. Natl. Cancer Inst.* **2000**, *92*, 1295–1302.

239 Keppler, D. and J. Konig. Hepatic secretion of conjugated drugs and endogenous substances. *Semin. Liver Dis.* **2000**, *20*, 265–272.

240 Konig, J., et al. Conjugate export pumps of the multidrug resistance protein (MRP) family: localization, substrate specificity, and MRP2-mediated drug resistance. *Biochim. Biophys. Acta* **1999**, *1461*, 377–394.

241 Buchler, M., et al. cDNA cloning of the hepatocyte canalicular isoform of the multidrug resistance protein, cMrp, reveals a novel conjugate export pump deficient in hyperbilirubinemic mutant rats. *J. Biol. Chem.* **1996**, *271*, 15091–15098.

242 Huisman, M. T., et al. Multidrug resistance protein 2 (MRP2) transports HIV protease inhibitors, and transport can be enhanced by other drugs. *AIDS* **2002**, *16*, 2295–2301.

243 Williams, G. C., et al. Direct Evidence that Saquinavir Is Transported by Multidrug Resistance-Associated Protein (MRP1) and Canalicular Multispecific Organic Anion Transporter (MRP2). *Antimicrob. Agents Chemother.* **2002**, *46*, 3456–3462.

244 Tang, F., K. Horie, and R. T. Borchardt. Are MDCK cells transfected with the human MRP2 gene a good model of the human intestinal mucosa? *Pharm. Res.* **2002**, *19*, 773–779.

245 Suzuki, H. and Y. Sugiyama. Transporters for bile acids and organic anions. *Pharm. Biotechnol.* **1999**, *12*, 387–439.

246 Shin, H. C., et al. Hepatobiliary transport mechanism for the cyclopentapeptide endothelin antagonist BQ-123. *Am. J. Physiol.* **1997**, *272*, G979–G986.

247 Hirohashi, T., H. Suzuki, and Y. Sugiyama. Characterization of the transport properties of cloned rat multidrug resistance-associated protein 3 (MRP3). *J. Biol. Chem.* **1999**, *274*, 15181–15185.

248 Hirohashi, T., et al. ATP-dependent transport of bile salts by rat multidrug resistance-associated protein 3 (Mrp3). *J. Biol. Chem.* **2000**, *275*, 2905–2910.

249 Zeng, H., et al. Transport of amphipathic anions by human multidrug resistance protein 3. *Cancer Res.* **2000**, *60*, 4779–4784.

250 Oleschuk, C. J., R. G. Deeley, and S. P. Cole. Substitution of Trp1242 of Transmembrane Segment 17 Alters Substrate Specificity of Human Multidrug Resistance Protein, MRP3. *Am. J. Physiol.* **2002**, *284*, G280–289.

251 Akita, H., et al. Transport activity of human MRP3 expressed in Sf9 cells: comparative studies with rat MRP3. *Pharm. Res.* **2002**, *19*, 34–41.

252 Gotoh, Y., et al. Involvement of an organic anion transporter (canalicular multispecific organic anion transporter/multidrug resistance-associated protein 2) in gastrointestinal secretion of glutathione conjugates in rats. *J. Pharmacol. Exp. Ther.* **2000**, *292*, 433–439.

253 Pavlova, A., et al. Developmentally regulated expression of organic ion transporters NKT (OAT1), OCT1, NLT (OAT2), and Roct. *Am. J. Physiol.* **2000**, *278*, F635–F643.

254 Hediger, M. A., et al. Expression cloning and cDNA sequencing of the Na+/glucose co-transporter. *Nature* **1987**, *330*, 379–381.

255 Cramer, S. C., et al. Colocalization of GLUT2 glucose transporter, sodium/glucose cotransporter, and gamma-glutamyl transpeptidase in rat kidney with double-peroxidase immunocytochemistry. *Diabetes* **1992**, *41*, 766–770.

256 Kanai, Y., et al. The human kidney low affinity Na+/glucose cotransporter SGLT2. Delineation of the major renal reabsorptive mechanism for D-glucose. *J. Clin. Invest.* **1994**, *93*, 397–404.

257 Wells, R. G., T. K. Mohandas, and M. A. Hediger. Localization of the Na+/glucose cotransporter gene SGLT2 to human chromosome 16 close to the centromere. *Genomics* **1993**, *17*, 787–789.

258 Wells, R. G., et al. Cloning of a human kidney cDNA with similarity to the sodium-glucose cotransporter. *Am. J. Physiol.* **1992**, *263*, F459–F465.

259 You, G., et al. Molecular characteristics of Na(+)-coupled glucose transporters in adult and embryonic rat kidney. *J. Biol. Chem.* **1995**, *270*, 29365–29371.

260 Kong, C. T., S. F. Yet, and J. E. Lever. Cloning and expression of a mammalian Na+/amino acid cotransporter with sequence similarity to Na+/glucose cotransporters. *J. Biol. Chem.* **1993**, *268*, 1509–1512.

261 Joost, H. G. and B. Thorens. The extended GLUT-family of sugar/polyol transport facilitators: nomenclature, sequence characteristics, and potential function of its novel members (review). *Mol. Membr. Biol.* **2001**, *18*, 247–256.

262 Fukumoto, H., et al. Cloning and characterization of the major insulin-responsive glucose transporter expressed in human skeletal muscle and other insulin-responsive tissues. *J. Biol. Chem.* **1989**, *264*, 7776–7779.

263 Mueckler, M., et al. Sequence and structure of a human glucose transporter. *Science* **1985**, *229*, 941–945.

264 Fukumoto, H., et al. Sequence, tissue distribution, and chromosomal localization of mRNA encoding a human glucose transporter-like protein. *Proc. Natl. Acad. Sci. U. S. A.* **1988**, *85*, 5434–5438.

265 Kayano, T., et al. Evidence for a family of human glucose transporter-like proteins. Sequence and gene localization of a protein expressed in fetal skeletal muscle and other tissues. *J. Biol. Chem.* **1988**, *263*, 15245–15248.

266 Kayano, T., et al. Human facilitative glucose transporters. Isolation, functional characterization, and gene localization of cDNAs encoding an isoform (GLUT5) expressed in small intestine, kidney, muscle, and adipose tissue and an unusual glucose transporter pseudogene-like sequence (GLUT6). *J. Biol. Chem.* **1990**, *265*, 13276–13282.

267 Doege, H., et al. Activity and genomic organization of human glucose transporter 9 (GLUT9), a novel member of the family of sugar-transport facilitators predominantly expressed in brain and leucocytes. *Biochem. J.* **2000**, *350*, 771–776.

268 Phay, J. E., H. B. Hussain, and J. F. Moley. Cloning and expression analysis of a novel member of the facilitative glucose transporter family, SLC2A9 (GLUT9). *Genomics* **2000**, *66*, 217–220.

269 Doege, H., et al. Characterization of human glucose transporter (GLUT) 11 (encoded by SLC2A11), a novel sugar-transport facilitator specifically expressed in heart and skeletal muscle. *Biochem. J.* **2001**, *359*, 443–449.

270 Doege, H., et al. GLUT8, a novel member of the sugar transport facilitator family with glucose transport activity. *J. Biol. Chem.* **2000**, *275*, 16275–16280.

271 Carayannopoulos, M. O., et al. GLUT8 is a glucose transporter responsible for insulin-stimulated glucose uptake in the blastocyst. *Proc. Natl. Acad. Sci. U. S. A.* **2000**, *97*, 7313–7318.

272 Ibberson, M., M. Uldry, and B. Thorens. GLUTX1, a novel mammalian glucose transporter expressed in the central nervous system and insulin-sensitive tissues. *J. Biol. Chem.* **2000**, *275*, 4607–4612.

273 McVie-Wylie, A. J., D. R. Lamson, and Y. T. Chen. Molecular cloning of a novel member of the GLUT family of transporters, SLC2a10 (GLUT10), localized on chromosome 20q13.1: a candidate gene for NIDDM susceptibility. *Genomics* **2001**, *72*, 113–117.

274 Dawson, P. A., et al. Sequence and functional analysis of GLUT10: a glucose transporter in the Type 2 diabetes-linked region of chromosome 20q12–13.1. *Mol. Genet. Metab.* **2001**, *74*, 186–199.

275 Uldry, M., et al. Identification of a mammalian H(+)-myo-inositol symporter expressed predominantly in the brain. *EMBO J.* **2001**, *20*, 4467–4477.

276 Joost, H. G., et al. Nomenclature of the GLUT/SLC2A family of sugar/polyol transport facilitators. *Am. J. Physiol.* **2002**, *282*, E974–E976.

277 Schurmann, A., et al. The glucose transport facilitator GLUT8 is predominantly associated with the acrosomal region of mature spermatozoa. *Cell Tissue Res.* **2002**, *307*, 237–242.

278 Wu, X., et al. Cloning and characterization of glucose transporter 11, a novel sugar transporter that is alternatively spliced in various tissues. *Mol. Genet. Metab.* **2002**, *76*, 37–45.

279 Takata, K. Glucose transporters in the transepithelial transport of glucose. *J. Electron Microsc.* **1996**, *45*, 275–284.

280 Davidson, N. O., et al. Human intestinal glucose transporter expression and localization of GLUT5. *Am. J. Physiol.* **1992**, *262*, C795–C800.

281 Blakemore, S. J., et al. The GLUT5 hexose transporter is also localized to the basolateral membrane of the human jejunum. *Biochem. J.* **1995**, *309*, 7–12.

282 Burant, C. F., et al. Fructose transporter in human spermatozoa and small intestine is GLUT5. *J. Biol. Chem.* **1992**, *267*, 14523–14526.

283 Mackenzie, B., et al. Biophysical characteristics of the pig kidney Na+/glucose cotransporter SGLT2 reveal a common mechanism for SGLT1 and SGLT2. *J. Biol. Chem.* **1996**, *271*, 32678–32683.

284 Olson, A. L. and J. E. Pessin. Structure, function, and regulation of the mammalian facilitative glucose transporter gene family. *Annu. Rev. Nutr.* **1996**, *16*, 235–256.

285 Wright, E. M. Renal Na(+)-glucose cotransporters. *Am. J. Physiol.* **2001**, *280*, F10–18.

286 Mizuma, T., et al. Intestinal active absorption of sugar-conjugated compounds by glucose transport system: implication of improvement of poorly absorbable drugs. *Biochem. Pharmacol.* **1992**, *43*, 2037–2039.

287 Mizuma, T., K. Ohta, and S. Awazu. The beta-anomeric and glucose preferences of glucose transport carrier for intestinal active absorption of monosaccharide conjugates. *Biochim. Biophys. Acta* **1994**, *1200*, 117–122.

288 Schnedl, W. J., et al. STZ transport and cytotoxicity. Specific enhancement in GLUT2-expressing cells. *Diabetes* **1994**, *43*, 1326–1333.

289 Liang, W. J., D. Johnson, and S. M. Jarvis. Vitamin C transport systems of mammalian cells. *Mol. Membr. Biol.* **2001**, *18*, 87–95.

290 Tsukaguchi, H., et al. A family of mammalian Na+-dependent L-ascorbic acid transporters. *Nature* **1999**, *399*, 70–75.

291 Rajan, D. P., et al. Human placental sodium-dependent vitamin C transporter (SVCT2): molecular cloning and transport function. *Biochem. Biophys. Res. Commun.* **1999**, *262*, 762–768.

292 Daruwala, R., et al. Cloning and functional characterization of the human sodium-dependent vitamin C transporters hSVCT1 and hSVCT2. *FEBS Lett.* **1999**, *460*, 480–484.

293 Wang, H., et al. Human Na(+)-dependent vitamin C transporter 1 (hSVCT1): primary structure, functional characteristics and evidence for a non-functional splice variant. *Biochim. Biophys. Acta* **1999**, *1461*, 1–9.

294 Wang, Y., et al. Human vitamin C (L-ascorbic acid) transporter SVCT1. *Biochem. Biophys. Res. Commun.* **2000**, *267*, 488–494.

295 Sirotnak, F. M. and B. Tolner. Carrier-mediated membrane transport of folates in mammalian cells. *Annu. Rev. Nutr.* **1999**, *19*, 91–122.

296 Eudy, J. D., et al. Identification and characterization of the human and mouse SLC19A3 gene: a novel member of the reduced folate family of micronutrient transporter genes. *Mol. Genet. Metab.* **2000**, *71*, 581–590.

297 Rajgopal, A., et al. SLC19A3 encodes a second thiamine transporter ThTr2. *Biochim. Biophys. Acta* **2001**, *1537*, 175–178.

298 Williams, F. M. and W. F. Flintoff. Isolation of a human cDNA that complements a mutant hamster cell defective in methotrexate uptake. *J. Biol. Chem.* **1995**, *270*, 2987–2992.

299 Prasad, P. D., et al. Molecular cloning of the human placental folate transporter. *Biochem. Biophys. Res. Commun.* **1995**, *206*, 681–687.

300 Nguyen, T. T., et al. Human intestinal folate transport: cloning, expression, and distribution of complementary RNA. *Gastroenterology* **1997**, *112*, 783–791.

301 Said, H. M., et al. Intestinal folate transport: identification of a cDNA involved in folate transport and the functional expression and distribution of its mRNA. *Biochim. Biophys. Acta* **1996**, *1281*, 164–172.

302 Roy, K., et al. Chromosomal localization of the murine RFC-1 gene encoding a folate transporter and its amplification in an antifolate resistant variant overproducing the transporter. *Cancer Genet. Cytogenet.* **1998**, *105*, 29–38.

303 Itoh, T., et al. Stereoselectivity of the folate transporter in rabbit small intestine: studies with amethopterin enantiomers. *Chirality* **2001**, *13*, 164–169.

304 Dutta, B., et al. Cloning of the human thiamine transporter, a member of the folate transporter family. *J. Biol. Chem.* **1999**, *274*, 31925–31929.

305 Prasad, P. D., et al. Cloning and functional expression of a cDNA encoding a mammalian sodium-dependent vitamin transporter mediating the uptake of pantothenate, biotin, and lipoate. *J. Biol. Chem.* **1998**, *273*, 7501–7506.

306 Wang, H., et al. Human placental Na+-dependent multivitamin transporter. Cloning, functional expression, gene structure, and chromosomal localization. *J. Biol. Chem.* **1999**, *274*, 14875–14883.

307 Takanaga, H., et al. Nicotinic acid transport mediated by pH-dependent anion antiporter and proton cotransporter in rabbit intestinal brush-border membrane. *J. Pharm. Pharmacol.* **1996**, *48*, 1073–1077.

308 Huang, S. N. and P. W. Swaan. Riboflavin uptake in human trophoblast-derived BeWo cell monolayers: cellular translocation and regulatory mechanisms. *J. Pharmacol. Exp. Ther.* **2001**, *298*, 264–271.

309 Shneider, B. L. Intestinal bile acid transport: biology, physiology, and pathophysiology. *J. Pediatr. Gastroenterol. Nutr.* **2001**, *32*, 407–417.

310 Bahar, R. J. and A. Stolz. Bile acid transport. *Gastroenterol. Clin. North Am.* **1999**, *28*, 27–58.

311 Erlinger, S. [Bile acid transport by the liver]. *Gastroenterol. Clin. Biol.* **1998**, *22*, 144–148.

312 Love, M. W. and P. A. Dawson. New insights into bile acid transport. *Curr. Opin. Lipidol.* **1998**, *9*, 225–229.

313 Hagenbuch, B. and P. J. Meier. Molecular cloning, chromosomal localization, and functional characterization of a human liver Na+/bile acid cotransporter. *J. Clin. Invest.* **1994**, *93*, 1326–1331.

314 Shneider, B. L., et al. Cloning and molecular characterization of the ontogeny of a rat ileal sodium-dependent bile acid transporter. *J. Clin. Invest.* **1995**, *95*, 745–754.

315 Craddock, A. L., et al. Expression and transport properties of the human ileal and renal sodium-dependent bile acid transporter. *Am. J. Physiol.* **1998**, *274*, G157–G169.

316 Christie, D. M., et al. Comparative analysis of the ontogeny of a sodium-dependent bile acid transporter in rat kidney and ileum. *Am. J. Physiol.* **1996**, *271*, G377–G385.

317 Alpini, G., et al. Functional expression of the apical Na+-dependent bile acid transporter in large but not small rat cholangiocytes. *Gastroenterology* **1997**, *113*, 1734–1740.

318 Hagenbuch, B., et al. Functional expression cloning and characterization of the hepatocyte Na+/bile acid cotransport system. *Proc. Natl. Acad. Sci. U. S. A.* **1991**, *88*, 10629–10633.

319 Wong, M. H., P. Oelkers, and P. A. Dawson. Identification of a mutation in the ileal sodium-dependent bile acid transporter gene that abolishes transport activity. *J. Biol. Chem.* **1995**, *270*, 27228–27234.

320 Schroeder, A., et al. Substrate specificity of the rat liver Na(+)-bile salt cotransporter in *Xenopus* laevis oocytes and in CHO cells. *Am. J. Physiol.* **1998**, *274*, G370–G375.

321 Kramer, W., et al. Substrate specificity of the ileal and the hepatic Na(+)/bile acid cotransporters of the rabbit. I. Transport studies with membrane vesicles and cell lines expressing the cloned transporters. *J. Lipid Res.* **1999**, *40*, 1604–1617.

322 Frimmer, M. and K. Ziegler. The transport of bile acids in liver cells. *Biochim. Biophys. Acta* **1988**, *947*, 75–99.

323 Zimmerli, B., J. Valantinas, and P. J. Meier. Multispecificity of Na+-dependent taurocholate uptake in basolateral (sinusoidal) rat liver plasma membrane vesicles. *J. Pharmacol. Exp. Ther.* **1989**, *250*, 301–318.

324 Wieland, T., et al. Identity of hepatic membrane transport systems for bile salts, phalloidin, and antamanide by photoaffinity labeling. *Proc. Natl. Acad. Sci. U. S. A.* **1984**, *81*, 5232–5236.

325 Kramer, W., et al. Intestinal absorption of peptides by coupling to bile acids. *J. Biol. Chem.* **1994**, *269*, 10621–10627.

326 Swaan, P. W., et al. Enhanced transepithelial transport of peptides by conjugation to cholic acid. *Bioconjug. Chem.* **1997**, *8*, 520–525.

327 Hara, S., et al. S-8921, an ileal Na+/bile acid cotransporter inhibitor decreases serum cholesterol in hamsters. *Life Sci.* **1997**, *60*, 365–370.

328 Root, C., et al. Ileal bile acid transporter inhibition, CYP7A1 induction, and antilipemic action of 264W94. *J. Lipid Res.* **2002**, *43*, 1320–1330.

329 Root, C., et al. Inhibition of ileal sodium-dependent bile acid transport by 2164U90. *J. Lipid Res.* **1995**, *36*, 1106–1115.

330 Oelkers, P., et al. Primary bile acid malabsorption caused by mutations in the ileal sodium-dependent bile acid transporter gene (SLC10A2). *J. Clin. Invest.* **1997**, *99*, 1880–1887.

331 Small, D. M. Point mutations in the ileal bile salt transporter cause leaks in the enterohepatic circulation leading to severe chronic diarrhea and malabsorption. *J. Clin. Invest.* **1997**, *99*, 1807–1808.

332 Shneider, B. L. A new era in bile acid transport pathophysiology. *J. Pediatr. Gastroenterol. Nutr.* **1998**, *26*, 236–237.

333 Abumrad, N., C. Harmon, and A. Ibrahimi. Membrane transport of long-chain fatty acids: evidence for a facilitated process. *J. Lipid Res.* **1998**, *39*, 2309–2318.

334 Abumrad, N., C. Coburn, and A. Ibrahimi. Membrane proteins implicated in long-chain fatty acid uptake by mammalian cells: CD36, FATP and FABPm. *Biochim. Biophys. Acta* **1999**, *1441*, 4–13.

335 Hamilton, J. A. and F. Kamp. How are free fatty acids transported in membranes? Is it by proteins or by free diffusion through the lipids? *Diabetes* **1999**, *48*, 2255–2269.

336 Schaffer, J. E. and H. F. Lodish. Expression cloning and characterization of a novel adipocyte long chain fatty acid transport protein. *Cell* **1994**, *79*, 427–436.

337 Hirsch, D., A. Stahl, and H. F. Lodish. A family of fatty acid transporters conserved from mycobacterium to man. *Proc. Natl. Acad. Sci. U. S. A.* **1998**, *95*, 8625–8629.

338 Stahl, A., et al. Identification of the major intestinal fatty acid transport protein. *Mol. Cell* **1999**, *4*, 299–308.

339 Herrmann, T., et al. Mouse fatty acid transport protein 4 (FATP4): characterization of the gene and functional assessment as a very long chain acyl-CoA synthetase. *Gene* **2001**, *270*, 31–40.

340 Martin, G., et al. The human fatty acid transport protein-1 (SLC27A1; FATP-1) cDNA and gene: organization, chromosomal localization, and expression. *Genomics* **2000**, *66*, 296–304.

341 Harmon, C. M. and N. A. Abumrad. Binding of sulfosuccinimidyl fatty acids to adipocyte membrane proteins: isolation and amino-terminal sequence of an 88-kD protein implicated in transport of long-chain fatty acids. *J. Membr. Biol.* **1993**, *133*, 43–49.

342 Chong, S. S., et al. Molecular cloning of the cDNA encoding a human renal sodium phosphate transport protein and its assignment to chromosome 6p21.3–p23. *Genomics* **1993**, *18*, 355–359.

343 Kos, C. H., et al. Comparative mapping of Na+-phosphate cotransporter genes, NPT1 and NPT2, in human and rabbit. Cytogenet. *Cell. Genet.* **1996**, *75*, 22–24.

344 Uchino, H., et al. Faropenem transport across the renal epithelial luminal membrane via inorganic phosphate transporter Npt1. *Antimicrob. Agents Chemother.* **2000**, *44*, 574–577.

345 Uchino, H., et al. p-aminohippuric acid transport at renal apical membrane mediated by human inorganic

phosphate transporter NPT1. *Biochem. Biophys. Res. Commun.* **2000**, *270*, 254–259.

346 Shibui, A., et al. Isolation and chromosomal mapping of a novel human gene showing homology to Na+/PO4 cotransporter. *J. Hum. Genet.* **1999**, *44*, 190–192.

347 Magagnin, S., et al. Expression cloning of human and rat renal cortex Na/Pi cotransport. *Proc. Natl. Acad. Sci. U. S. A.* **1993**, *90*, 5979–5983.

348 Hartmann, C. M., et al. Structure of murine and human renal type II Na+-phosphate cotransporter genes (Npt2 and NPT2). *Proc. Natl. Acad. Sci. U. S. A.* **1996**, *93*, 7409–7414.

349 Feild, J. A., et al. Cloning and functional characterization of a sodium-dependent phosphate transporter expressed in human lung and small intestine. *Biochem. Biophys. Res. Commun.* **1999**, *258*, 578–582.

350 Tsuji, A. and I. Tamai. Na+ and pH dependent transport of foscarnet via the phosphate carrier system across intestinal brush-border membrane. *Biochem. Pharmacol.* **1989**, *38*, 1019–1022.

351 Swaan, P. W. and J. J. Tukker. Carrier-mediated transport mechanism of foscarnet (trisodium phosphonoformate hexahydrate) in rat intestinal tissue. *J. Pharmacol. Exp. Ther.* **1995**, *272*, 242–247.

352 Ishizawa, T., et al. Mechanisms of intestinal absorption of the antibiotic, fosfomycin, in brush-border membrane vesicles in rabbits and humans. *J. Pharmacobiodyn.* **1992**, *15*, 481–489.

353 Ishizawa, T., et al. Sodium and pH dependent carrier-mediated transport of antibiotic, fosfomycin, in the rat intestinal brush-border membrane. *J. Pharmacobiodyn.* **1990**, *13*, 292–300.

354 Tamai, I., et al. Participation of a proton-cotransporter, MCT1, in the intestinal transport of monocarboxylic acids. *Biochem. Biophys. Res. Commun.* **1995**, *214*, 482–489.

355 Garcia, C. K., et al. Molecular characterization of a membrane transporter for lactate, pyruvate, and other monocarboxylates: implications for the Cori cycle. *Cell* **1994**, *76*, 865–873.

356 Kim, C. M., J. L. Goldstein, and M. S. Brown. cDNA cloning of MEV, a mutant protein that facilitates cellular uptake of mevalonate, and identification of the point mutation responsible for its gain of function. *J. Biol. Chem.* **1992**, *267*, 23113–23121.

357 Price, N. T., V. N. Jackson, and A. P. Halestrap. Cloning and sequencing of four new mammalian monocarboxylate transporter (MCT) homologues confirms the existence of a transporter family with an ancient past. *Biochem. J.* **1998**, *329*, 321–328.

358 Lafreniere, R. G., L. Carrel, and H. F. Willard. A novel transmembrane transporter encoded by the XPCT gene in Xq13.2. *Hum. Mol. Genet.* **1994**, *3*, 1133–1139.

359 Takanaga, H., et al. cDNA cloning and functional characterization of rat intestinal monocarboxylate transporter. *Biochem. Biophys. Res. Commun.* **1995**, *217*, 370–377.

360 Ackley, D. C. and R. A. Yokel. Aluminum citrate is transported from brain into blood via the monocarboxylic acid transporter located at the blood-brain barrier. *Toxicology* **1997**, *120*, 89–97.

361 Wu, X., L. R. Whitfield, and B. H. Stewart. Atorvastatin transport in the Caco-2 cell model: contributions of P-glycoprotein and the proton-monocarboxylic acid co-transporter. *Pharm. Res.* **2000**, *17*, 209–215.

362 Tamai, I., et al. Immunohistochemical and functional characterization of pH-dependent intestinal absorption of weak organic acids by the monocarboxylic acid transporter MCT1. *J. Pharm. Pharmacol.* **1999**, *51*, 1113–1121.

363 Geourjon, C., et al. A common mechanism for ATP hydrolysis in ABC transporter and helicase superfamilies. *Trends Biochem. Sci.* **2001**, *26*, 539–544.

364 Dean, M., A. Rzhetsky, and R. Allikmets. The human ATP-binding cassette (ABC) transporter superfamily. *Genome Res.* **2001**, *11*, 1156–1166.

365 Borst, P. and R. O. Elferink. Mammalian ABC transporters in health and disease. *Annu. Rev. Biochem.* **2002**, *71*, 537–592.

366 Dassa, E. and E. Schneider. The rise of a protein family: ATP-binding cassette systems. *Res. Microbiol.* **2001**, *152*, 203.

367 Higgins, C. F. ABC transporters: from microorganisms to man. *Annu. Rev. Cell Biol.* **1992**, *8*, 67–113.

368 Sababi, M., O. Borga, and U. Hultkvist-Bengtsson. The role of P-glycoprotein in limiting intestinal regional absorption of digoxin in rats. *Eur. J. Pharm. Sci.* **2001**, *14*, 21–27.

369 Smit, J. W., et al. Contribution of the murine mdr1a P-glycoprotein to hepatobiliary and intestinal elimination of cationic drugs as measured in mice with an mdr1a gene disruption. *Hepatology* **1998**, *27*, 1056–1063.

370 Luo, F. R., et al. Intestinal transport of irinotecan in Caco-2 cells and MDCK II cells overexpressing efflux transporters Pgp, cMOAT, and MRP1. *Drug Metab. Dispos.* **2002**, *30*, 763–770.

371 Fromm, M. F. P-glycoprotein: a defense mechanism limiting oral bioavailability and CNS accumulation of drugs. *Int. J. Clin. Pharmacol. Ther.* **2000**, *38*, 69–74.

372 Wacher, V. J., et al. Role of P-glycoprotein and cytochrome P450 3A in limiting oral absorption of peptides and peptidomimetics. *J. Pharm. Sci.* **1998**, *87*, 1322–1330.

373 Hunter, J., B. H. Hirst, and N. L. Simmons. Drug absorption limited by P-glycoprotein-mediated secretory drug transport in human intestinal epithelial Caco-2 cell layers. *Pharm. Res.* **1993**, *10*, 743–749.

374 Aungst, B. J. and H. Saitoh. Intestinal absorption barriers and transport mechanisms, including secretory transport, for a cyclic peptide, fibrinogen antagonist. *Pharm. Res.* **1996**, *13*, 114–119.

375 Dean, M., Y. Hamon, and G. Chimini. The human ATP-binding cassette (ABC) transporter superfamily. *J. Lipid Res.* **2001**, *42*, 1007–1017.

376 Hooiveld, G. J., et al. Function and regulation of ATP-binding cassette transport proteins involved in hepatobiliary transport. *Eur. J. Pharm. Sci.* **2000**, *12*, 13–30.

377 van Asperen, J., et al. Enhanced oral bioavailability of paclitaxel in mice treated with the P-glycoprotein blocker SDZ PSC 833. *Br. J. Cancer* **1997**, *76*, 1181–1183.

378 Leu, B. L. and J. D. Huang. Inhibition of intestinal P-glycoprotein and effects on etoposide absorption. *Cancer Chemother. Pharmacol.* **1995**, *35*, 432–436.

379 Klucken, J., et al. ABCG1 (ABC8), the human homolog of the Drosophila white gene, is a regulator of macrophage cholesterol and phospholipid transport. *Proc. Natl. Acad. Sci. U. S. A.* **2000**, *97*, 817–822.

380 Hruz, P. W. and M. M. Mueckler. Structural analysis of the GLUT1 facilitative glucose transporter. *Mol. Membr. Biol.* **2001**, *18*, 183–193.

12
Hepatic Transport

Hiroshi Suzuki and Yuichi Sugiyama

Abbreviations

ABC	ATP-binding cassette
ATP	Adenosine triphosphate
AUC	Area under the (plasma concentration–time) curve
BCRP	Breast cancer-resistant protein
BSEP	Bile salt export pump
Caco-2	Cell line: human colon carcinoma cells
cAMP	Cyclic adenosine monophosphate
HMG-CoA	3-Hydroxyl-3-methylglutaryl-coenzyme A
LLC-PK1	Cell line
MDCK	Madin–Darby canine kidney cells
MDR	Gene coding for P-gp
MRP	Multidrug resistance-associated protein
NTCP (Ntcp)	Na^+-taurocholate cotransporting polypeptide
OAT (Oat)	Organic anion transporter
OATP (Oatp)	Organic anion transporting polypeptide
OCT (Oct)	Organic cation transporter
P-gp	P-glycoprotein
SNP	Single nucleotide polymorphism

12.1
Introduction

The liver plays an important role in determining the oral bioavailability of drugs. Drug molecules absorbed into the portal vein are taken up by hepatocytes, and then metabolized and/or excreted into the bile. For hydrophilic drugs, transporters located on the sinusoidal membrane are responsible for the hepatic uptake [1, 2]. Biliary excretion of many drugs is also mediated by the primary active transporters, referred to as ATP-binding cassette transmembrane (ABC) transporters, located on the bile canalicular membrane [1, 3–5]. Recently, many molecular biological

Drug Bioavailability: Estimation of Solubility, Permeability, Absorption and Bioavailability.
Edited by Han van de Waterbeemd, Hans Lennernäs and Per Artursson

ISBN: 3-527-30438-X

studies of these transporters have been performed and, therefore, it is now possible to use recombinant transporters to predict the *in vivo* hepatic disposition of substrate drugs. In this chapter, we will focus on the transporter mediated hepatobiliary excretion of clinically important drugs, concentrating particularly on the quantitative prediction of *in vivo* disposition from *in vitro* data.

12.2 Hepatic Uptake

12.2.1 Hepatic Uptake of Organic Anions

12.2.1.1 Quantitative Prediction of *in vivo* Disposition from *in vitro* Data

Hepatic uptake has been determined in *in vivo*, *in situ* and *in vitro* experiments with isolated hepatocytes and/or sinusoidal membrane vesicles. A comparison of *in vivo* and *in vitro* results will be discussed using pravastatin, a 3-hydroxyl-3-methylglutaryl-coenzyme A (HMG-CoA) reductase inhibitor, as a model drug. Unlike other statins, pravastatin is hydrophilic; hence after administration its distribution is restricted to tissues where the transporters for uptake are expressed (such as the liver and kidney) [6]. This is in marked contrast to the much more hydrophobic statins such as simvastatin, which are distributed to almost all tissues in the body. The efficient hepatic uptake of pravastatin has been characterized by using isolated rat hepatocytes [7]. Pravastatin is taken up by isolated hepatocytes in an Na^+-independent manner, with a K_m of 29 μM [7]. These *in vitro* results have been compared with the *in vivo* disposition whereby rats received an intravenous bolus injection of several doses of pravastatin [8]. Kinetic analysis indicated that the *in vivo* K_m value was 23 μM, which is similar to that determined *in vitro* [8]. Moreover, by considering the hepatocyte content per gram of liver, it was possible to extrapolate the *in vitro* uptake data to the *in vivo* situation in rats [8, 9]. From this point of view, it may also be possible to predict human *in vivo* disposition from human isolated and/or cryopreserved hepatocytes, although the viability of human hepatocytes needs to be evaluated. Several reports on drug transport in human hepatocytes have also been published [10–13].

12.2.1.2 Transporter Molecules Responsible for Hepatic Uptake of Organic Anions

Recently, molecular biology studies have been carried out on hepatic uptake transporters. With regard to the Na^+-dependent hepatic uptake of bile acids, Na^+-taurocholate cotransporting polypeptide (Ntcp/NTCP) has been cloned from both rodents and humans [14–17]. Ntcp/NTCP accepts bile salts, such as taurocholate and glycocholate, as well as some anionic compounds such as dehydroepiandrosterone sulfate and bromosulfophthalein [16, 18]. However, the presence of unidentified Na^+-dependent transporters for anionic drugs (e.g., bumetanide) has also been suggested [19, 20].

Although the Na^+-dependent mechanism is largely responsible for the hepatic

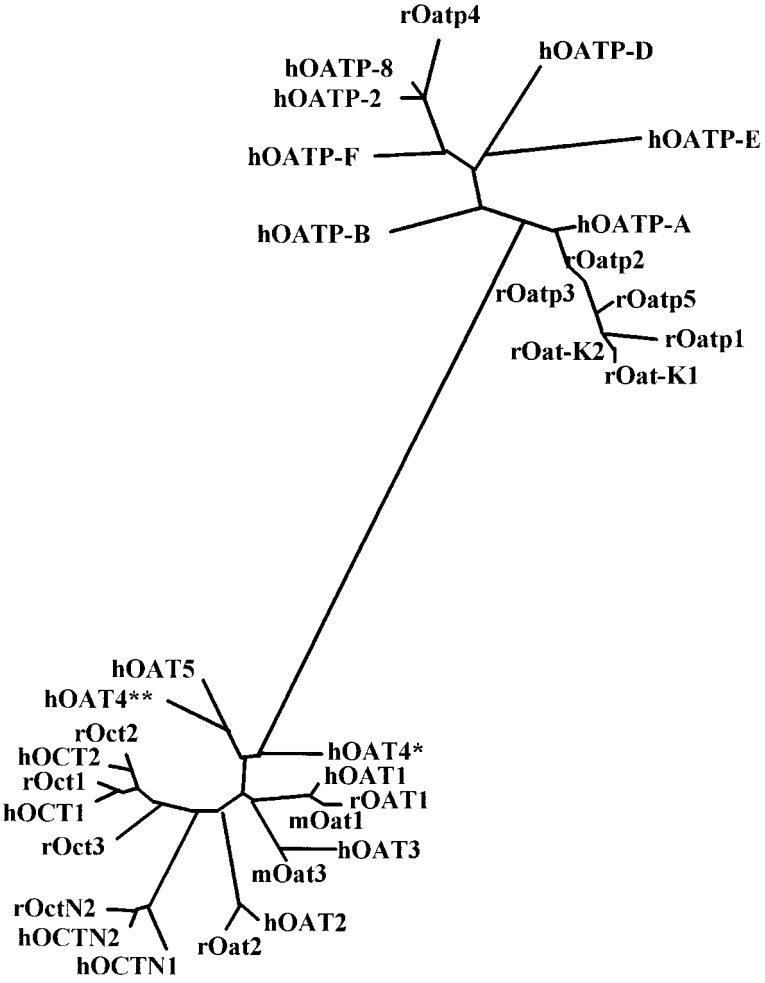

Fig. 12.1. Phylogenic trees for uptake transporters. *hOAT4 reported in Ref. [39]. **hOAT4 reported in Ref. [37].

uptake of certain types of bile acids (e.g., taurocholate) and non-bile acid organic anions, the Na^+-independent transport mechanism is responsible for many types of anionic drugs. As transporters responsible for the Na^+-independent hepatic uptake, organic anion transporting polypeptides (Oatps/OATPs) and organic anion transporters (Oats/OATs) have been identified, although the nomenclature of Oatp/OATP family proteins has not yet been established (Fig. 12.1). In rats, Oatp1 (gene symbol Slc21a1; see Ref. [21]), Oatp 2 (Slc21a5; Ref. [22]) and Oatp 4 (Slc21a10; Ref. [23]) are largely responsible for the hepatic uptake, whereas in humans, OATP2 (OATP-C/LST-1/SLC21A6; Refs. [24–26]) and OATP8 (SLC21A15;

Tab. 12.1. List of substrates for human OATP-B, 2 and 8.

Substrate	*OATP-B*	*OATP2*	*OATP8*
Taurocholate	NT [29]	10.0 [31], 13.6 [24], 33.8 [25]	+ [29]
Glycocholate	NT [29]	+ [29]	+ [29]
Cholate	–	11.4 [31]	NT [31]
Dehydroepiandrosterone sulfate	+ [29]	21.5 [31]	>30 [31]
Estrone-3-sulfate	9.04 [33]	0.068–0.094 (high affinity) [33] and 5.34–7.00 (low affinity) [33]	
		12.5 [31]	+ [29]
Taurolithocholate sulfate	–	+ [93]	–
17β-estradiol-17β-D-glucuronide	NT [29]	3.71 [33], 8.2 [31], 9.7 [12]	5.4 [31]
3,5,3′-Triiodo-L-thyronine	NT [29]	2.7 [24]	+ [29]
Thyroxine	NT [29]	3.0 [24]	+ [29]
Prostaglandin E_2	NT [29]	+ [29]	NT [29]
Thromboxane B_2	–	+ [24]	–
Leukotriene C_4	NT [29]	+ [29]	+ [29]
Leukotriene E_4	–	+ [24]	–
Monoglucuronosyl bilirubin	–	0.10 [31]	0.50 [31]
Bisglucuronosyl bilirubin	–	0.28 [31]	NT [31]
Bromosulfophthalein	0.7 [29]	0.14 [31], 0.3 [29]	0.4 [29], 3.3 [31]
Benzylpenicillin	–	+ [32]	–
Pravastatin	–	13.7 [12], 33.7 [25]	–
BQ-123	NT [29]	+ [29]	+ [29]
Cholesystokinin 8	NT [30]	NT [30]	11.1 [30]
[D-penicillamine^{2,5}]enkephalin	NT [29]	+ [29]	+ [29]
Ouabain	NT [29]	NT [29]	+ [29]
Digoxin	NT [29]	NT [29]	+ [29]

Numbers in the table represent K_m values (μM).
+, significant transport observed.
NT, no significant transport observed.
Results taken from Refs. [12, 24, 25, 29–33].

Ref. [27]) may be the most important hepatic uptake transporters. Rat Oatp 2 is not a homologue of human OATP2 as it has only 46% amino acid identity with human OATP2. Rat Oatp4 has the highest amino acid similarity with human OATP2 and 8, the amino acid identity for these human transporters being 64%. The substrate specificity of rat Oatps is summarized elsewhere [2, 28]. The substrate specificity of human OATP2 and 8 has been determined in a number of studies [24, 25, 29–33] and is summarized in Table 12.1. In contrast to the hepatic selective expression of OATP2 and 8, OATP-B (SLC2A9), OATP-D (SLC2A11) and OATP-E (SLC2A12) are expressed in a wide range of tissues [29, 32], whereas OATP-A is predominantly expressed in the brain [34, 35].

In addition to OATP/Oatp family proteins, some of the organic anion transporter (OAT) family proteins may be responsible for hepatic uptake. Although many OAT family proteins are expressed in the kidney [36], human and rat OAT2 is also expressed in the liver [37, 38]. Human OAT2 transports *p*-amino-

hippuric acid, methotrexate, cAMP, α-ketoglutarate and prostaglandin F2α [37, 39], while rat OAT2 transports salicylate, acetylsalicylate, progstaglandin E2, α-ketoglutarate, *p*-aminohippuric acid, indomethacin, 3′-azido-3′-deoxythymidine and 2′,3′-dideoxycytidine [38, 40]. Although OAT3 is expressed in male rat liver and transports organic anions such as *p*-aminohippuric acid, ochratoxin A and estrone-3-sulfate and organic cations such as cimetidine [41, 42], its hepatic expression is minimal in mice and humans [42–44]. Indeed, the uptake of OAT3 substrates (such as estrone-3-sulfate and *p*-aminohippuric acid) was not different between normal and OAT3(−/−) mice [42].

Contribution of each transporter to hepatic drug uptake Since it is possible that the substrate specificity of different transporters overlap, we need to determine the contribution of each transporter. One possible method is to extrapolate the transport activity in cRNA-injected oocytes and/or cDNA-transfected cultured cells to that of hepatocytes, after correcting for the expression level of transporter protein using Western blot analysis [45–47]. If ligands specific to each transporter are identified in future, it may also be possible to use such ligands as reference compounds to normalize the expression level of each transporter between the transfected cells and hepatocytes [45–48]. Alternatively, selective inhibitors for each transporter may also be used as a useful tool to determine the contribution of each transporter. However, such selective inhibitors have not yet been identified, although it has been suggested that digoxin may be selective for Oatp2 rather than Oatp1 [49].

With regard to the uptake of pravastatin into rat hepatocytes, Oatp1 and 2 have each been shown to play a role. Pravastatin was transported into Oatp1 and Oatp2 cRNA-injected *Xenopus laevis* oocytes with K_m values of 30 μM and 38 μM, respectively [25, 50]. It is also possible that rat Oatp4 is involved in the uptake of pravastatin, though this hypothesis has yet to be clarified. The uptake of pravastatin into human hepatocytes has been studied in detail; using cryopreserved human hepatocytes, pravastatin has been shown to be taken up with a K_m of 12 μM [12]. Pravastatin was also taken up by oocytes injected with human OATP2 cRNA, with a K_m of 34 μM [25]. In addition, the uptake of pravastatin into oocytes was stimulated by the injection of poly A^+ RNA from human liver, and this stimulation was abolished by the simultaneous administration of OATP2 antisense [12]. It is thus suggested that the human hepatic uptake of pravastatin may be predominantly mediated by OATP2.

12.2.2 Hepatic Uptake of Organic Cations

By analyzing the uptake into the isolated rat hepatocytes, it has been suggested that organic cations may be classified into two groups as follows:

- Type I drugs: these consist of hydrophilic compounds, including tetraethylammonium, tributylmethylammonium, and procainamide.

- Type II drugs: these consist of bulky hydrophobic compounds, such as *d*-tubocurarine, metocurine, vecuronium, and rocuronium [51, 52].

Type II cations are sensitive to inhibition by bile salts and cardiac glycosides (e.g., digoxin) [51, 52]. The results of recent molecular biology studies support these previous hypotheses, namely that Type I and II drugs are transported by rat organic cation transporter Oct1 (Slc22a1) and rat Oatp2, respectively [53], as discussed below. It has been shown that the rat organic cation transporter 1 (Oct1, Slc22a1), located on the basolateral membrane of hepatocytes, transports hydrophilic compounds, including 1-methyl-4-phenylpyridinium (a neurotoxin), N^1-methylnicotinamide, cimetidine, choline, dopamine, serotonin, adrenaline, noradrenaline, and histamine [2, 54–56]. Human OCT1 (SLC22A1) also significantly transports 1-methyl-4-phenylpyridinium and tetraethylammonium and N^1-methylnicotinamide, but not cimetidine [2, 57–60]. Moreover, by examining the hepatic uptake in Oct1 (−/−) mice, it was shown that the transport of tetraethylammonium, metaiodobenzylguanidine (an anticancer drug) and 1-methyl-4-phenylpyridinium (a neurotoxin), but not that of cimetidine or choline, is largely mediated by Oct1 [61]. It is noteworthy that the hepatic uptake of cimetidine or choline was not affected by knocking out the mouse Oct1 gene [61], although these two compounds are significantly transported by rat Oct1 [60]. It is plausible that the uptake of cimetidine into isolated rat hepatocytes [62] is mediated by an, as yet, unidentified transporter. Clinically important cationic compounds, such as a series of biguanides which are used for the treatment of diabetes, are transported by Oct1, and the hepatic uptake of metformin has been shown to be abolished in oct1 (−/−) mice [63].

In contrast, some Type II cations, such as *N*-(4,4-azo-*n*-pentyl)-21-deoxyajmalinium and rocuronium, have been shown to be transported by rat Oatp 2 [64–66]. Since human OATP2 or OATP8 cannot transport organic cations [53], the molecular mechanism for the uptake of Type II cations (e.g., rocuronium) into isolated human hepatocytes [11] remains to be clarified. Although human OATP-A transports rocuronium, its hepatic expression is minimal [66].

12.2.3
Utilization of Transporters as a Target for the Drug Delivery

Because bile salts are selectively taken up by hepatocytes after systemic administration, attempts have been made to use the bile salt transporters as a target for their drug delivery to the liver. For example, HMG-CoA reductase inhibitors, cytostatic compounds, and oligonucleotides have been conjugated with bile salts to improve delivery to the liver [1, 67–70]. In particular, platinum conjugates with bile salts have been shown to be effective in the treatment of liver tumors implanted into experimental animals [71]. Both *cis*-diammine-chloro-cholylglycinate-platinum (II) and *cis*-diammine-bisursodeoxycholate-platinum (II) have been found to be substrates for human OATP-C, NTCP and OCT1 [70]. Effective hepatic targeting of these conjugates may be expected in human liver.

12.3 Biliary Excretion

12.3.1 Biliary Excretion Mediated by P-Glycoprotein

The biliary excretion of drugs is largely mediated by ABC transporters located on the bile canalicular membrane. Among the ABC transporters, P-glycoprotein (P-gp), which is encoded by the mdr1/MDR1 gene (gene symbol ABCB1), is responsible for the biliary excretion of many types of substrates. Although mdr1a and 1b genes are present in rodents, humans have only one MDR1 gene. A difference in the substrate specificity among mouse mdr1a, 1b and human MDR1 has also been documented [72–74].

The role of mdr1 on the bile canalicular membrane has been demonstrated by comparing the biliary excretion between normal and mdr1 gene knockout mice [75, 76]. Since mdr1b is induced in mdr1a knockout mice, comparison should be performed between normal and mdr1a/1b (−/−) mice [75, 76]. Typical type I cations, such as tri-butylmethyl ammonium and azidoprocainamide methoiodide, and type II cations, such as vecuronium, are excreted into the bile via mdr1 [77]. In particular, the role of P-gp may be emphasized for vecuronium as more than 40% of the administered dose is excreted into the bile, largely mediated by this transporter [77]. This is in marked contrast to the finding that the urinary excretion of tri-butylmethyl ammonium and azidoprocainamide exceeds the biliary excretion [77]. In addition, doxorubicin and vinblastine are also excreted into the bile by mdr1a, although only a limited amount of vinblastine was excreted into the bile as a result of hepatic metabolism [78]. As indicated for vinblastine, the substrate specificity of P-gp overlaps that of the drug-metabolizing enzymes (such as cytochrome P450 3A) [79], and hence only a limited amount of many P-gp substrate drugs is excreted into the bile.

MDR3, a homologue of MDR1, is responsible for the biliary excretion of phospholipids, and a hereditary defect in this gene results in the acquisition of progressive familial intrahepatic cholestasis Type 3 [80–82].

12.3.2 Biliary Excretion Mediated by Multidrug Resistance-Associated Protein 2 (MRP2)

Although P-gp accepts many neutral and cationic compounds, MRP2 (gene symbol ABCC2) has a critical role in determining the biliary excretion of many anionic compounds and conjugated metabolites [1–5, 83–86]. The substrate specificity of MRP2 has been determined by comparing transport across the bile canalicular membrane between normal and MRP2-deficient rats (such as transport-deficient rats and Eisai hyperbilirubinemic rats) (Table 12.2) [1, 2, 5, 51]. MRP2 substrates include many clinically important anionic drugs such as pravastatin [87], and it has also been found that the uptake (OATP2) and efflux transporters (MRP2) synergistically support efficient biliary excretion and, consequently, the efficient

Tab. 12.2. List of typical substrates excreted into the bile via MRP2.

Glutathione conjugates of organic anions:
oxidized glutathione; LTC_4 and its subsequent metabolites; 2,4-dinitrophenyl-*S*-glutathione
Glutathione conjugates of metals:
antimony; arsenic; bismuth; cadmium; zinc
Glucuronide conjugates:
bilirubin glucuronides; 17β estradiol-17β-D-glucuronide, E3040 glucuronide; SN-38 glucuronide; grepafloxacin glucuronide; telmisaltan glucuronide; acetaminophen glucuronide; indomethacin glucuronide; liquiritigenin glucuronide; glycyrrhizin
Glucuronide and sulfate conjugates of bile salts:
cholate-3-glucuronide; lithocholate-3-*O*-glucuronide; chenodeoxycholate-3-*O*-glucuronide; nordeoxycholate-3-*O*-glucuronide; nordeoxycholate-3-sulfate; lithocholate-3-sulfate; taurolithocholate-3-sulfate; glycolithocholate-3-sulfate; taurochenodeoxycholate-3-sulfate
Non-conjugated organic anions:
reduced folates; methotrexate; dibromosulfophthalein; CPT-11 (carboxylate); SN-38 (carboxylate); ampicillin; cefodizime; pravastatin; temocaprilat; BQ-123

Modified from Refs. [1, 5, 89].

enterohepatic circulation of pravastatin [1]. The impact of MRP2 in determining the drug disposition and, consequently, the pharmacological and adverse effects of substrate drugs, has been previously summarized in detail [1]. It is also reported that the impaired biliary excretion of S3025 (1-[2-(4-chlorophenyl)-cyclopropylmethoxy]-3,4-dihydroxy-5-(3-imidazo-[4,5]b pyridine-1-3-yl-3-[4-carboxy]-phenyl-acryloyloxy)-cyclohexancarboxylic acid), a chlorogenic acid derivative, in Mrp2-deficient mutant rats resulted in the prolonged pharmacological action (inhibition of hepatic glucose production) compared with normal rats [88].

In addition to anionic drugs, many glutathione- and glucuronide-conjugates of xenobiotics, and sulfate conjugates of bile salts (but not sulfate conjugates of xenobiotics) are transported by MRP2 [1–5]. An hereditary defect in MRP2 expression results in the acquisition of Dubin–Johnson syndrome in humans; this exhibits hyperbilirubinemia due to a lack in biliary excretion of bilirubin glucuronides mediated by MRP2 [3, 4, 81, 82, 89].

It is important to establish an *in vitro* system which will allow *in vivo* transport across the bile canalicular membrane to be predicted quantitatively. By comparing the transport activity between *in vivo* and *in vitro* situations in isolated bile canalicular membrane vesicles, it has been shown that there is a significant correlation for nine types of substrates [90]. Here, *in vivo* transport activity was defined as the biliary excretion rate, divided by the unbound hepatic concentration at steady-state, whereas *in vitro* transport activity was defined as the initial velocity for the transport into the isolated bile canalicular membrane vesicles divided by the medium concentration [90]. Collectively, it is possible to predict *in vivo* canalicular transport from *in vitro* experiments with the isolated bile canalicular membrane vesicles.

From this viewpoint, it is interesting to examine ligand transport in isolated bile

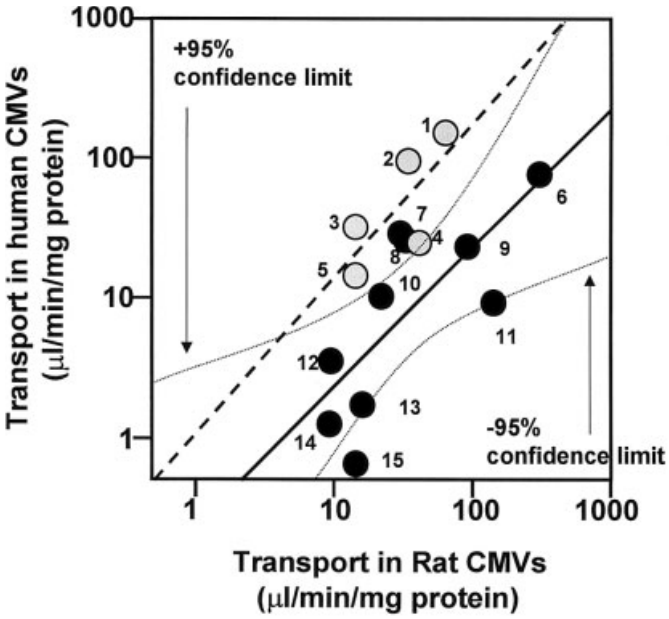

Fig. 12.2. Comparison of ATP-dependent transport activity between rats and humans determined in isolated bile canalicular membrane vesicles. Key; 1, SN-38 glucuronide (carboxylate); 2, SN-38 glucuronide (lactone); 3, E3040 (6-hydroxy-5,7-dimethyl-2-methyl-amino-4-(3-pyridylmethyl) benzothiazole) glucuronide; 4, 17β estradiol-17β-D-glucuronide; 5, grepafloxacin glucuronide; 6, leukotriene C_4; 7, SN-38 (carboxylate); 8, CPT-11 (carboxylate); 9, taurocholic acid; 10, sandostatin; 11, 2,4-dinitrophenyl-S-glutathione; 12, pravastatin; 13, BQ-123; 14, temocaprilat; 15, methotrexate. The broken line represents the regression line for glucuronide conjugates, whereas the solid line represents the regression line for other compounds with 95% confidence limits. (Modified from Ref. [91].)

canalicular membrane vesicles from human liver [91]. As shown in Fig. 12.2, it has been shown that the transport activity per mg membrane vesicle protein is virtually identical between humans and rats for glucuronide conjugates. In contrast, the transport of nonconjugated organic anions and glutathione-conjugates in humans was between 10% and 20% of that in rats, indicating a species difference in the substrate specificity of MRP2. It might be possible also to predict transport across the human bile canalicular membrane *in vivo* from the transport activity determined in isolated membrane vesicles from cDNA-transfected cells.

It is also important to predict the *in vivo* biliary excretion clearance in humans, and for this purpose MDCK II cell lines expressing both uptake and efflux transporters may be used (Fig. 12.3) [92, 93]. It has been shown that MRP2 is expressed on the apical membrane, whereas OATP2 and 8 are expressed on the basolateral membrane after cDNA transfection (Fig. 12.3) [92, 93]. The transcellular transport across such double-transfected cells may correspond to the excretion of ligands from blood into bile across hepatocytes. Indeed, the vectorial transport from the basal to apical side was observed for pravastatin only in OATP2- and MRP2-expressing

MDCK II cells (Fig. 12.3) [93]. Kinetic analysis revealed that the K_m value for transcellular transport (24 μM) was similar to the K_m for OATP2 (34 μM) [93]. Moreover, the efflux across the bile canalicular membrane was not saturated under these experimental conditions. These *in vitro* observations are consistent with *in vivo* experimental results in rats which showed that the rate-determining process for the biliary excretion of pravastatin is uptake across the sinusoidal membrane. By normalizing the expression level between the double transfectant and human hepatocytes, it might be possible to predict *in vivo* hepatobiliary excretion.

12.3.3
Biliary Excretion Mediated by Breast Cancer-Resistant Protein (BCRP)

In addition to P-gp and MRP2, BCRP (gene symbol ABCG2) might also be involved in the biliary excretion of certain types of drugs. BCRP accepts many kinds of antitumor drugs, and its substrate specificity overlaps that of P-gp and MRP2 [94]. A contribution by BCRP to the biliary excretion of topotecan has been suggested by examining the inhibitory effect of a BCRP inhibitor (GF120918) in the disposition of topotecan in normal and mdr1a/1b (−/−) mice [95]. Although BCRP also transports sulfated conjugates of steroids and xenobiotics (e.g., estrone-3-sulfate and 4-methylumbelliferone sulfate), its contribution to biliary excretion remains to be determined [96].

12.3.4
Biliary Excretion of Monovalent Bile Salts

Bile salt export pump (BSEP; gene symbol ABCB11) mediates the biliary excretion of nonconjugated bile salts, such as taurocholic acid, glycocholic acid and cholic acid, and therefore is responsible for the formation of the bile acid-dependent bile flow [97, 98]. Its hereditary defect results in the acquisition of PFIC2, a potentially lethal disease which requires liver transplantation [17, 81, 82, 99]. As discussed in Section 12.5.2, the inhibition of BSEP following drug administration may result in cholestasis.

12.4
Inter-individual Differences in Transport Activity

Recently, the presence of single nucleotide polymorphisms (SNPs) has been reported for several types of transporter. Extensive studies have been performed on the SNPs of OATP2 [100, 101], and the SNPs identified in African- and European-Americans are indicated in Fig. 12.3. Moreover, the frequency of SNPs differed among the African-American, European-Americans and Japanese, indicating the presence of an ethnic difference in the allelic mutation of this transporter [100, 101]. In addition, some of the mutations were associated with reduced transporter function and/or abnormalities in membrane targeting [100, 102] (Fig. 12.3). It is

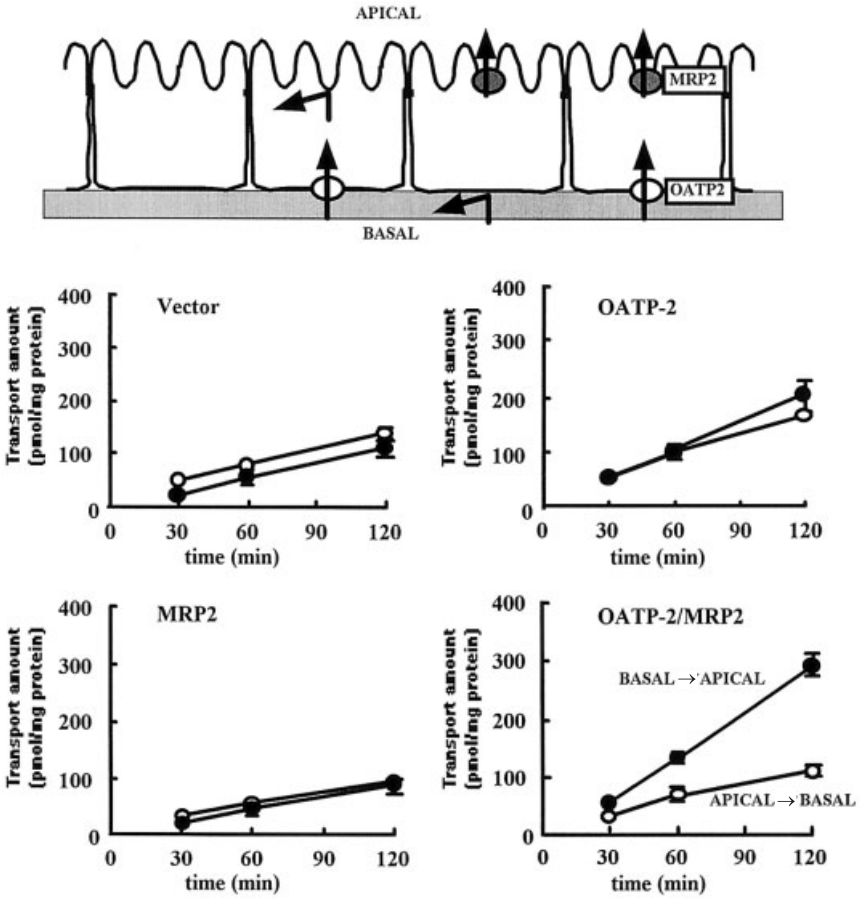

Fig. 12.3. Transcellular transport of pravastatin across MDCK II cells. Upper panel: schematic diagram illustrating the expression of transporters in MDCK II cells after transfection of OATP2 and MRP2 cDNAs. Lower panels: transcellular transport of pravastatin across MDCK II cells transfected with plasmid vector, OATP2 cDNA, MRP2 cDNA and cDNAs for both OATP2 and MRP2. (From Ref. [93].)

possible that the subjects with these mutations have a lower transport activity; hence the plasma concentration may be increased. Moreover, it is plausible that for drugs whose target is within the hepatocytes (e.g., pravastatin), the SNPs in OATP2 might account for inter-individual differences in pharmacological action.

In the same manner, SNPs have been reported for ABC transporters on the bile canalicular membrane. Although the results are controversial, the C3435T mutation in the MDR1 gene (silent mutation, Ile1145Ile), closely linked with the G2677T/Ala893Ser mutation, has been suggested to be associated with altered expression level and/or the transport function of P-gp in some tissues [103]. The impact of these mutations on the biliary excretion of substrate drugs remains to be

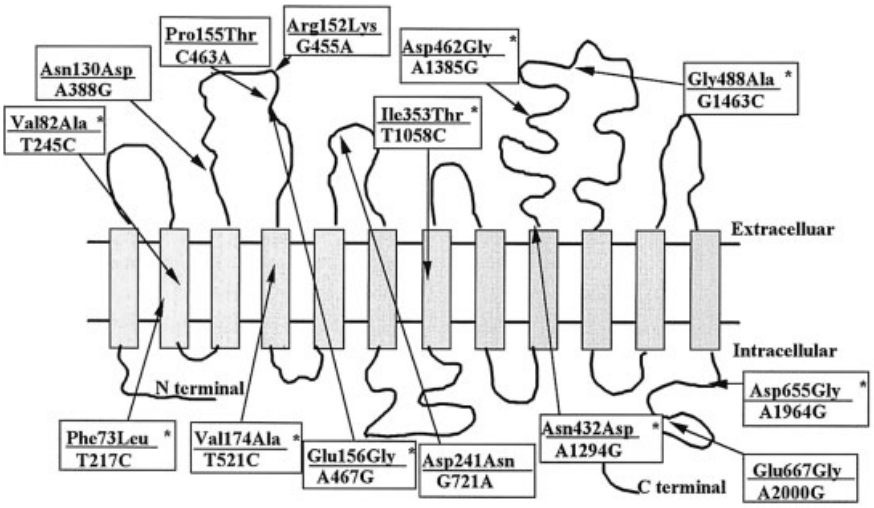

Fig. 12.4. Single nucleotide polymorphisms in OATP2 gene found in African- and European Americans. Asterisks represent the mutations associated with the altered transport function. (Prepared from data reported in Ref. [100].)

clarified. In addition, mutations in MRP2 have been reported in healthy volunteers, along with the cell lines established for tumor specimens dissected during surgery [89, 104, 105]. The effect of the frequently observed G1249A/Val417Ile mutation should be examined in both *in vitro* and *in vivo* situations.

12.5 Drug–Drug Interactions

12.5.1 Effect of Drugs on the Activity of Transporters Located on the Sinusoidal Membrane

If the unbound drug concentrations in plasma are higher than their K_i values on the transporters, then transporter function may be significantly affected [106]. Following a pharmacokinetic analysis of the effect of probenecid on the hepatobiliary excretion of methotrexate, it has been shown the extent of an *in vivo* drug–drug interaction can be quantitatively predicted from the kinetic parameters for transport across the sinusoidal and bile canalicular membranes determined *in vitro* [107].

As far as sinusoidal uptake is concerned, drug–drug interactions have also been reported between antituberculosis agents (rifamycin SV and rifampicin) and bromosulfophthalein in humans; both drugs reduce the clearance of bromosulfophthalein and also induce hyperbilirubinemia [108]. These results may be ac-

counted for by considering the fact that the K_i values of rifamycin are 2 and 3 μM for OATP2 and OATP8, respectively, whereas those of rifampicin are 17 and 5 μM for these transporters, respectively, and the peak unbound plasma concentrations of rifamycin SV and rifampicin may be 5–10 μM [108]. The fact that rifamycin SV induces a more potent increase in plasma unconjugated bilirubin concentrations than rifampicin may also be accounted for by these kinetic considerations [108].

The interaction between cerivastatin and gemfibrozil has also been highlighted, due to the appearance of severe side effects, including death [109]. An increase in cerivastatin blood concentration is also produced following the administration of cyclosporin A [110]. Indeed, in subjects given cyclosporin A, the plasma AUC of cerivastatin was 3.8-fold higher than that in untreated subjects [110]. *In vitro* experiments revealed that the uptake of cerivastatin into isolated rat and human hepatocytes is inhibited by cyclosporin A in a highly concentration-dependent manner, with K_i values of 0.20 and 0.28–0.69 μM, respectively [111]. Moreover, OATP2-mediated cerivastatin uptake into cDNA-transfected LLC-PK1 cells was also inhibited by cyclosporin A, with a K_i value of 0.24 μM [111]. In contrast, cerivastatin metabolism was not affected by cyclosporin A at concentrations up to 30 μM [111]. These results suggest that the inhibition of cerivastatin transport into hepatocytes results in an increased blood level of this drug, with the subsequent appearance of side effects.

12.5.2 Effect of Drugs on the Activity of Transporters Located on the Bile Canalicular Membrane

A variety of inhibitory effects of drugs on the function of bile canalicular membrane transporters has also been reported. Although much of the severe drug-induced cholestasis results from immune reactions, part may also be caused by the inhibition of BSEP [17, 112]. Cyclosporin A, glibenclamide, rifamycin SV and rifampicin have also been reported to induce cholestasis [113]. *In vitro* experiments with isolated bile canalicular membrane vesicles have shown that cyclosporin A, glibenclamide, rifamycin SV, rifampicin and bosentan and its metabolite Ro-47-8634 each inhibit BSEP, with respective K_i values of 0.2, 5.7, 0.9, 6.4, 12, and 8.5 μM [113]. It is possible that the cholestatic effect of these drugs is a result of the inhibition of BSEP, and this inhibitory effect might also be predicted from *in vitro* experiments with isolated bile canalicular membrane vesicles [114]. Recently, it has been shown that troglitazone and its sulfated conjugate inhibit BSEP function, with K_i values of 1.3 μM and 0.23 μM, respectively [115]. Male rats were shown to have higher troglitazone sulfate levels than females (due to a higher sulfotransferase activity in males); hence the more profound cholestasis seen in males after troglitazone administration might be caused by an inhibition of BSEP by troglitazone sulfate [116].

More recently, a much more complex mechanism has been suggested for BSEP inhibition. By comparing the inhibitory effect of Mrp2 substrates on BSEP func-

tion in isolated bile canalicular membrane vesicles in normal and MRP2-deficient rats, and also in membrane vesicles expressing only BSEP and those expressing both MRP2 and BSEP, it has been suggested that some Mrp2 substrates *trans*-inhibit the function of BSEP [117, 118]. Thus, MRP2 substrates may inhibit the function of BSEP from the bile side of this transporter. Although this suggestion remains controversial, the finding that MRP2 substrates with a cholestatic nature do not cause cholestasis in MRP2-deficient rats might be consistent with this hypothesis [119].

Drug–drug interactions may also be used to alter the disposition of substrate drugs. SN-38, which is an active metabolite, is formed within hepatocytes following the hydrolysis of irrinotecan, a campthothecin analogue, and then excreted into the bile [1]. Although the severe intestinal toxicity of the antitumor drug irrinotecan adversely limits its dose, this effect may be ascribed to inter-individual differences in UGT1A1 due to SNPs in the promoter region [120], and it is also possible that enterocytes are exposed to the biliary excreted SN-38. Inhibition of the biliary excretion of SN-38 by probenecid, an inhibitor for MRP2, causes a reduction in the incidence of diarrhea, but does not affect SN-38 plasma levels. Thus, it is possible to control adverse reactions to this drug by using the effect of a drug–drug interaction on the bile canalicular membrane [121, 122].

12.6 Concluding Remarks

The information summarized within this chapter describes how transporters may play an important role in the hepatobiliary excretion of drugs. Moreover, it may also be possible to alter the disposition of ligands by changing their affinity for uptake and efflux transporters by chemical modification. For example, BQ-123 (cyclo[D-Trp-D-Asp-L-Pro-D-Val-L-Leu]), an anionic cyclic peptide with an antagonist activity at the endothelin receptor, is taken up by hepatocytes via OATP2 and efficiently excreted into the bile via MRP2, resulting in extensive first-pass elimination in the liver [123]. In contrast, cyclo[D-Trp-D-Asp-L-Hyp(L-Arg)-D-Val-L-Leu], a derivative of BQ-123, undergoes lower transport activity by both uptake and efflux transporters and, consequently, its bioavailability is significantly higher than that of BQ-123 [123]. The *in vitro* experimental systems described in this chapter may be useful for identifying such compounds with the desired transport properties during the screening of drug candidates. Such an *in vitro* model might also be useful for predicting possible drug–drug interactions, as well as inter-individual differences in transport activity due to single nucleotide polymorphisms.

References

1 Suzuki, H., Sugiyama, Y., Transporters for bile acids and organic anions, in: *Membrane Transporters as Drug Targets*. Amidon, X., Sadee, X. (eds), Kluwer Academic Publishers, New York, **1999**, pp. 387–439.

2 Suzuki, H., Sugiyama, Y., Transport of drugs across the hepatic sinusoidal membrane: sinusoidal drug influx and efflux in the liver, *Semin. Liver Dis.* **2000**, *20*, 251–263.

3 König, J., Nies, A. T., Cui, Y., Leier, I., Keppler, D., Conjugate export pumps of the multidrug resistance protein (MRP) family: localization, substrate specificity, and MRP2-mediated drug resistance, *Biochim. Biophys. Acta* **1999**, *1461*, 377–394.

4 Keppler, D., König, J., Hepatic secretion of conjugated drugs and endogenous substances, *Semin. Liver Dis.* **2000**, *20*, 265–272.

5 Suzuki, H., Sugiyama, Y., Excretion of GSSG and glutathione conjugates mediated by MRP1 and cMOAT/MRP2, *Semin. Liver Dis.* **1998**, *18*, 359–376.

6 Yamazaki, M., Tokui, T., Ishigami, M., Sugiyama, Y., Tissue-selective uptake of pravastatin in rats: contribution of a specific carrier-mediated uptake system, *Biopharm. Drug Dispos.* **1996**, *17*, 775–789.

7 Yamazaki, M., Suzuki, H., Hanano, M., Tokui, T., Komai, T., Sugiyama, Y., Na(+)-independent multispecific anion transporter mediates active transport of pravastatin into rat liver, *Am. J. Physiol.* **1993**, *264*, G36–G44.

8 Yamazaki, M., Akiyama, S., Nishigaki, R., Sugiyama, Y., Uptake is the rate-limiting step in the overall hepatic elimination of pravastatin at steady-state in rats, *Pharm. Res.* **1996**, *13*, 1559–1564.

9 Miyauchi, S., Sawada, Y., Iga, T., Hanano, M., Sugiyama, Y., Comparison of the hepatic uptake clearances of fifteen drugs with a wide range of membrane permeabilities in isolated rat hepatocytes and perfused rat livers, *Pharm. Res.* **1993**, *10*, 434–440.

10 Sandker, G. W., Weert, B., Olinga, P., Wolters, H., Slooff, M. J., Meijer, D. K., Groothuis, G. M., Characterization of transport in isolated human hepatocytes. A study with the bile acid taurocholic acid, the uncharged ouabain and the organic cations vecuronium and rocuronium, *Biochem. Pharmacol.* **1994**, *47*, 2193–2200.

11 Olinga, P., Merema, M., Hof, I. H., Slooff, M. J., Proost, J. H., Meijer, D. K., Groothuis, G. M., Characterization of the uptake of rocuronium and digoxin in human hepatocytes: carrier specificity and comparison with in vivo data, *J. Pharmacol. Exp. Ther.* **1998**, *285*, 506–510.

12 Nakai, D., Nakagomi, R., Furuta, Y., Tokui, T., Abe, T., Ikeda, T., Nishimura K., Human liver-specific organic anion transporter, LST-1, mediates uptake of pravastatin by human hepatocytes, *J. Pharmacol. Exp. Ther.* **2001**, *297*, 861–867.

13 Shitara, Y., Lu, C., Li, A. P., Y. Kato, Y., Suzuki, H., Ito, K., Itoh, T., Sugiyama, Y., Cryopreserved human hepatocytes as a tool for the prediction of in vivo transport and transporter-mediated drug–drug interactions, *Abstract of International Conference on Drug Interaction*, Hamamatsu, October 21–23, **1999**, p. 87.

14 Hagenbuch, B., Stieger, B., Foguet, M., Lubbert, H., Meier, P. J., Functional expression cloning and characterization of the hepatocyte Na^+/bile acid cotransport system, *Proc. Natl. Acad. Sci. USA* **1991**, *88*, 10629–10633.

15 Hagenbuch, B., Meier, P. J., Molecular cloning, chromosomal localization, and functional characterization of a human liver Na^+/bile acid cotransporter, *J. Clin. Invest.* **1994**, *93*, 1326–1331.

16 Meier, P. J., Eckhardt, U., Schroeder, A., Hagenbuch, B., Stieger, B., Substrate specificity of sinusoidal bile acid and organic anion uptake systems in rat and human liver, *Hepatology* **1997**, *26*, 1667–1677.

17 Meier, P. J., Stieger, B., Bile salt transporters, *Annu. Rev. Physiol.* **2002**, *64*, 635–661.

18 Kullak-Ublick, G. A., Regulation of organic anion and drug transporters of the sinusoidal membrane, *J. Hepatol.* **1999**, *31*, 563–573.

19 Petzinger, E., Blumrich, M., Bruhl, B., Eckhardt, U., Follmann, W., Honscha, W., Horz, J. A., Muller, N., Nickau, L., Ottallah-Kolac, M., Platte, H. D., Schenk, A., Schuh, K., Schulz, K., Schulz, S., What we have learned about bumetanide and the concept of multispecific bile acid/drug transporters from the liver, *J. Hepatol.* **1996**, *24* (Suppl. 1), 42–46.

20 Schroeder, A., Eckhardt, U., Stieger, B., Tynes, R., Schteingart, C. D., Hofmann, A. F., Meier, P. J., Hagenbuch, B., Substrate specificity of the rat liver Na(+)-bile salt cotransporter in *Xenopus laevis* oocytes and in CHO cells, *Am. J. Physiol.* **1998**, *274*, G370–G375.

21 Jacquemin, E., Hagenbuch, B., Stieger, B., Wolkoff, A. W., Meier, P. J., Expression cloning of a rat liver Na(+)-independent organic anion transporter, *Proc. Natl. Acad. Sci. USA* **1994**, *91*, 133–137.

22 Noé, B., Hagenbuch, B., Stieger, B., Meier, P. J., Isolation of a multispecific organic anion and cardiac glycoside transporter from rat brain, *Proc. Natl. Acad. Sci. USA* **1997**, *94*, 10346–10350.

23 Cattori, V., Hagenbuch, B., Hagenbuch, N., Stieger, B., Ha, R., Winterhalter, K. E., Meier, P. J., Identification of organic anion transporting polypeptide 4 (Oatp4) as a major full-length isoform of the liver-specific transporter-1 (rlst-1) in rat liver, *FEBS Lett.* **2000**, *474*, 242–245.

24 Abe, T., Kakyo, M., Tokui, T., Nakagomi, R., Nishio, T., Nakai, D., Nomura, H., Unno, M., Suzuki, M., Naitoh, T., Matsuno, S., Yawo, H., Identification of a novel gene family encoding human liver-specific organic anion transporter LST-1, *J. Biol. Chem.* **1999**, *274*, 17159–17163.

25 Hsiang, B., Zhu, Y., Wang, Z., Wu, Y., Sasseville, V., Yang, W. P., Kirchgessner, T. G., A novel human hepatic organic anion transporting polypeptide (OATP2). Identification of a liver-specific human organic anion transporting polypeptide and identification of rat and human hydroxymethylglutaryl-CoA reductase inhibitor transporters, *J. Biol. Chem.* **1999**, *274*, 37161–37168.

26 König, J., Cui, Y., Nies, A. T., Keppler, D., A novel human organic anion transporting polypeptide localized to the basolateral hepatocyte membrane, *Am. J. Physiol.*, **2000**, *278*, G156–G164.

27 König, J., Cui, Y., Nies, A. T., Keppler, D., Localization and genomic organization of a new hepatocellular organic anion transporting polypeptide, *J. Biol. Chem.* **2000**, *275*, 23161–23168.

28 Cattori, V., van Montfoort, J. E., Stieger, B., Landmann, L., Meijer, D. K., Winterhalter, K. H., Meier, P. J., Hagenbuch, B., Localization of organic anion transporting polypeptide 4 (Oatp4) in rat liver and comparison of its substrate specificity with Oatp1, Oatp2 and Oatp3, *Pflügers Arch.* **2001**, *443*, 188–195.

29 Kullak-Ublick, G. A., Ismair, M. G., Stieger, B., Landmann, L., Huber, R., Pizzagalli, F., Fattinger, K., Meier, P. J., Hagenbuch, B., Organic anion-transporting polypeptide B (OATP-B) and its functional comparison with three other OATPs of human liver, *Gastroenterology* **2001**, *120*, 525–533.

30 Ismair, M. G., Stieger, B., Cattori, V., Hagenbuch, B., Fried, M., Meier, P. J., Kullak-Ublick, G. A., Hepatic uptake of cholecystokinin octapeptide by organic anion-transporting polypeptides OATP4 and OATP8 of rat and human liver, *Gastroenterology* **2001**, *121*, 1185–1190.

31 Cui, Y., König, J., Leier, I., Buchholz, U., Keppler, D., Hepatic uptake of bilirubin and its conjugates by the human organic anion transporter SLC21A6, *J. Biol. Chem.* **2001**, *276*, 9626–9630.

32 Tamai, I., Nezu, J., Uchino, H., Sai, Y., Oku, A., Shimane, M., Tsuji, A., Molecular identification and characterization of novel members of the human organic anion transporter

(OATP) family, *Biochem. Biophys. Res. Commun.* **2000**, *273*, 251–260.

33 Tamai, I., Nozawa, T., Koshida, M., Nezu, J., Sai, Y., Tsuji, A., Functional characterization of human organic anion transporting polypeptide B (OATP-B) in comparison with liver-specific OATP-C, *Pharm. Res.* **2001**, *18*, 1262–1269.

34 Kullak-Ublick, G. A., Hagenbuch, B., Stieger, B., Schteingart, C. D., Hofmann, A. F., Wolkoff, A. W., Meier, P. J., Molecular and functional characterization of an organic anion transporting polypeptide cloned from human liver, *Gastroenterology* **1995**, *109*, 1274–1282.

35 Gao, B., Hagenbuch, B., Kullak-Ublick, G. A., Benke, D., Aguzzi, A., Meier, P. J., Organic anion-transporting polypeptides mediate transport of opioid peptides across blood–brain barrier, *J. Pharmacol. Exp. Ther.* **2000**, *294*, 73–79.

36 Sekine, T., Cha, S. H., Endou, H., The multispecific organic anion transporter (OAT) family, *Pflügers Arch.* **2000**, *440*, 337–350.

37 Sun, W., Wu, R. R., van Poelje, P. D., Erion, M. D., Isolation of a family of organic anion transporters from human liver and kidney, *Biochem. Biophys. Res. Commun.* **2001**, *283*, 417–422.

38 Sekine, T., Cha, S. H., Tsuda, M., Apiwattanakul, N., Nakajima, N., Kanai, Y., Endou, H., Identification of multispecific organic anion transporter 2 expressed predominantly in the liver, *FEBS Lett.* **1998**, *429*, 179–182.

39 Enomoto, A., Takeda, M., Shimoda, M., Narikawa, S., Kobayashi, Y., Kobayashi, Y., Yamamoto, T., Sekine, T., Cha, S. H., Niwa, T., Endou, H., Interaction of human organic anion transporters 2 and 4 with organic anion transport inhibitors, *J. Pharmacol. Exp. Ther.* **2002**, *301*, 797–802.

40 Morita, N., Kusuhara, H., Sekine, T., Endou, H., Sugiyama, Y., Functional characterization of rat organic anion transporter 2 in LLC-PK1 cells, *J. Pharmacol. Exp. Ther.* **2001**, *298*, 1179–1184.

41 Kusuhara, H., Sekine, T., Utsunomiya-Tate, N., Tsuda, M., Kojima, R., Cha, S. H., Sugiyama, Y., Kanai, Y., Endou, H., Molecular cloning and characterization of a new multispecific organic anion transporter from rat brain, *J. Biol. Chem.* **1999**, *274*, 13675–13680.

42 Sweet, D. H., Miller, D. S., Pritchard, J. B., Fujiwara, Y., Beier, D. R., Nigam, S. K., Impaired organic anion transport in kidney and choroid plexus of organic anion transporter 3 (Oat3 (Slc22a8)) knockout mice, *J. Biol. Chem.* **2002**, *277*, 26934–26943.

43 Race, J. E., Grassl, S. M., Williams, W. J., Holtzman, E. J., Molecular cloning and characterization of two novel human renal organic anion transporters (hOAT1 and hOAT3), *Biochem. Biophys. Res. Commun.* **1999**, *255*, 508–514.

44 Cha, S. H., Sekine, T., Fukushima, J. I., Kanai, Y., Kobayashi, Y., Goya, T., Endou, H., Identification and characterization of human organic anion transporter 3 expressing predominantly in the kidney, *Mol. Pharmacol.* **2001**, *59*, 1277–1286.

45 Kouzuki, H., Suzuki, H., Ito, K., Ohashi, R., Sugiyama, Y., Contribution of sodium taurocholate co-transporting polypeptide to the uptake of its possible substrates into rat hepatocytes, *J. Pharmacol. Exp. Ther.* **1998**, *286*, 1043–1050.

46 Kouzuki, H., Suzuki, H., Ito, K., Ohashi, R., Sugiyama, Y., Contribution of organic anion transporting polypeptide to uptake of its possible substrates into rat hepatocytes, *J. Pharmacol. Exp. Ther.* **1999**, *288*, 627–634.

47 Ishizuka, H., Konno, K., Naganuma, H., Nishimura, K., Kouzuki, H., Suzuki, H., Stieger, B., Meier, P. J., Sugiyama Y., Transport of temocaprilat into rat hepatocytes: role of organic anion transporting polypeptide, *J. Pharmacol. Exp. Ther.* **1998**, *287*, 37–42.

48 Venkatakrishnan, K., von Moltke, L. L., Court, M. H., Harmatz, J. S.,

Crespi, C. L., Greenblatt, D. J., Comparison between cytochrome P450 (CYP) content and relative activity approaches to scaling from cDNA-expressed CYPs to human liver microsomes: ratios of accessory proteins as sources of discrepancies between the approaches, *Drug Metab. Dispos.* **2000**, *28*, 1493–1504.

49 Shitara, Y., Sugiyama, D., Kusuhara, H., Kato, Y., Abe, T., Meier, P. J., Itoh, T., Sugiyama, Y., Comparative inhibitory effects of different compounds on rat Oatp1 (slc21a1)- and Oatp2 (Slc21a5)-mediated transport, *Pharm. Res.* **2002**, *19*, 147–153.

50 Tokui, T., Nakai, D., Nakagomi, R., Yawo, H., Abe, T., Sugiyama, Y., Pravastatin, an HMG-CoA reductase inhibitor, is transported by rat organic anion transporting polypeptide, oatp2, *Pharm. Res.* **1999**, *16*, 904–908.

51 Oude Elferink, R. P., Meijer, D. K., Kuipers, F., Jansen, P. L., Groen, A. K., Groothuis, G. M., Hepatobiliary secretion of organic compounds; molecular mechanisms of membrane transport, *Biochim. Biophys. Acta* **1995**, *1241*, 215–268.

52 Meijer, D. K. F., Jansen, P. L. M., Groothuis, G. M. M., Hepatobiliary disposition and targeting of drugs and genes, in: *Oxford Textbook of Clinical Hepatology.* Bircher, J., Benhamou, J. P., McIntyre, N. *et al.* (eds), 2nd edition, Volume 1. Oxford, Oxford University Press, **1999**, pp. 87–144.

53 van Montfoort, J. E., Muller, M., Groothuis, G. M., Meijer, D. K., Koepsell, H., Meier, P. J., Comparison of "type I" and "type II" organic cation transport by organic cation transporters and organic anion-transporting polypeptides, *J. Pharmacol. Exp. Ther.* **2001**, *298*, 110–115.

54 Grundemann, D., Gorboulev, V., Gambaryan, S., Veyhl, M., Koepsell, H., Drug excretion mediated by a new prototype of polyspecific transporter, *Nature* **1994**, *372*, 549–552.

55 Zhang, L., Brett, C. M., Giacomini, K. M., Role of organic cation transporters in drug absorption and elimination, *Annu. Rev. Pharmacol. Toxicol.* **1998**, *38*, 431–460.

56 Koepsell, H., Organic cation transporters in intestine, kidney, liver, and brain, *Annu. Rev. Physiol.* **1998**, *60*, 243–266.

57 Zhang, L., Dresser, M. J., Gray, A. T., Yost, S. C., Terashita, S., Giacomini, K. M., Cloning and functional expression of a human liver organic cation transporter, *Mol. Pharmacol.* **1997**, *51*, 913–921.

58 Zhang, L., Schaner, M. E., Giacomini, K. M., Functional characterization of an organic cation transporter (hOCT1) in a transiently transfected human cell line (HeLa), *J. Pharmacol. Exp. Ther.* **1998**, *286*, 354–361.

59 Gorboulev, V., Ulzheimer, J. C., Akhoundova, A., Ulzheimer-Teuber, I., Karbach, U., Quester, S., Baumann, C., Lang, F., Busch, A. E., Koepsell, H., Cloning and characterization of two human polyspecific organic cation transporters, *DNA Cell Biol.* **1997**, *16*, 871–881.

60 Grundemann, D., Liebich, G., Kiefer, N., Koster, S., Schomig, E., Selective substrates for non-neuronal monoamine transporters, *Mol. Pharmacol.* **1999**, *56*, 1–10.

61 Jonker, J. W., Wagenaar, E., Mol, C. A., Buitelaar, M., Koepsell, H., Smit, J. W., Schinkel, A. H., Reduced hepatic uptake and intestinal excretion of organic cations in mice with a targeted disruption of the organic cation transporter 1 (Oct1 [Slc22a1]) gene, *Mol. Cell. Biol.* **2001**, *21*, 5471–5477.

62 Nakamura, H., Sano, H., Yamazaki, M., Sugiyama Y., Carrier-mediated active transport of histamine H2 receptor antagonists, cimetidine and nizatidine, into isolated rat hepatocytes: contribution of type I system, *J. Pharmacol. Exp. Ther.* **1994**, *269*, 1220–1227.

63 Wang, D. S., Jonker, J. W., Kato, Y., Kusuhara, H., Schinkel, A. H., Sugiyama, Y., Involvement of organic cation transporter 1 in hepatic and intestinal distribution of metformin,

J. Pharmacol. Exp. Ther. **2002**, *302*, 510–515.

64 Bossuyt, X., Müller, M., Hagenbuch, B., Meier, P. J., Polyspecific drug and steroid clearance by an organic anion transporter of mammalian liver, *J. Pharmacol. Exp. Ther.* **1996**, *276*, 891–896.

65 Bossuyt, X., Müller, M., Meier, P. J., Multispecific amphipathic substrate transport by an organic anion transporter of human liver, *J. Hepatol.* **1996**, *25*, 733–738.

66 van Montfoort, J. E., Hagenbuch, B., Fattinger, K. E., Müller, M., Groothuis, G. M., Meijer, D. K., Meier, P. J., Polyspecific organic anion transporting polypeptides mediate hepatic uptake of amphipathic type II organic cations, *J. Pharmacol. Exp. Ther.* **1999**, *291*, 147–152.

67 Kramer, W., Wess, G., Schubert, G., Bickel, M., Girbig, F., Gutjahr, U., Kowalewski, S., Baringhaus, K. H., Enhsen, A., Glombik, H. *et al.*, Liver-specific drug targeting by coupling to bile acids, *J. Biol. Chem.* **1992**, *267*, 18598–18604.

68 Wess, G., Kramer, W., Han, X. B., Bock, K., Enhsen, A., Glombik, H., Baringhaus, K. H., Boger, G., Urmann, M., Hoffmann, A. *et al.*, Synthesis and biological activity of bile acid-derived HMG-CoA reductase inhibitors. The role of 21-methyl in recognition of HMG-CoA reductase and the ileal bile acid transport system, *J. Med. Chem.* **1994**, *37*, 3240–3246.

69 Petzinger, E., Wickboldt, A., Pagels, P., Starke, D., Kramer, W., Hepatobiliary transport of bile acid amino acid, bile acid peptide, and bile acid oligonucleotide conjugates in rats, *Hepatology* **1999**, *30*, 1257–1268.

70 Briz, O., Serrano, M. A., Rebollo, N., Hagenbuch, B., Meier, P. J., Koepsell, H., Marin, J. J., Carriers involved in targeting the cytostatic bile acid-cisplatin derivatives cis-diammine-chloro-cholylglycinate-platinum(II) and cis-diammine-bisursodeoxycholate-platinum(II) toward liver cells, *Mol. Pharmacol.* **2002**, *61*, 853–860.

71 Dominguez, M. F., Macias, R. I., Izco-Basurko, I., de La Fuente, A., Pascual, M. J., Criado, J. M., Monte, M. J., Yajeya, J., Marin, J. J., Low in vivo toxicity of a novel cisplatin-ursodeoxycholic derivative (Bamet-UD2) with enhanced cytostatic activity versus liver tumors, *J. Pharmacol. Exp. Ther.* **2001**, *297*, 1106–1112.

72 Smit, J. W., Weert, B., Schinkel, A. H., Meijer, D. K., Heterologous expression of various P-glycoproteins in polarized epithelial cells induces directional transport of small (type 1) and bulky (type 2) cationic drugs, *J. Pharmacol. Exp. Ther.* **1998**, *286*, 321–327.

73 Yamazaki, M., Neway, W. E., Ohe, T., Chen, I., Rowe, J. F., Hochman, J. H., Chiba, M., Lin, J. H., In vitro substrate identification studies for p-glycoprotein-mediated transport: species difference and predictability of in vivo results, *J. Pharmacol. Exp. Ther.* **2001**, *296*, 723–735.

74 Hooiveld, G. J., Heegsma, J., van Montfoort, J. E., Jansen, P. L., Meijer, D. K., Müller, M., Stereoselective transport of hydrophilic quaternary drugs by human MDR1 and rat Mdr1b P-glycoproteins, *Br. J. Pharmacol.* **2002**, *135*, 1685–1694.

75 Schinkel, A. H., Smit, J. J., van Tellingen, O., Beijnen, J. H., Wagenaar, E., van Deemter, L., Mol, C. A., van der Valk, M. A., Robanus-Maandag, E. C., te Riele, H. P. *et al.*, Disruption of the mouse mdr1a P-glycoprotein gene leads to a deficiency in the blood–brain barrier and to increased sensitivity to drugs, *Cell* **1994**, *77*, 491–502.

76 Schinkel, A. H., Mayer, U., Wagenaar, E., Mol, C. A., van Deemter, L., Smit, J. J., van der Valk, M. A., Voordouw, A. C., Spits, H., van Tellingen, O., Zijlmans, J. M., Fibbe, W. E., Borst, P., Normal viability and altered pharmacokinetics in mice lacking mdr1-type (drug-transporting) P-glycoproteins, *Proc. Natl. Acad. Sci USA* **1997**, *94*, 4028–4033.

77 Smit, J. W., Schinkel, A. H., Weert, B., Meijer, D. K., Hepatobiliary and intestinal clearance of amphiphilic cationic drugs in mice in which both mdr1a and mdr1b genes have been disrupted, *Br. J. Pharmacol.* **1998**, *124*, 416–424.

78 van Asperen, J., van Tellingen, O., Beijnen, J. H., The role of mdr1a P-glycoprotein in the biliary and intestinal secretion of doxorubicin and vinblastine in mice, *Drug Metab. Dispos.* **2000**, *28*, 264–267.

79 Benet, L. Z., Cummins, C. L., The drug efflux-metabolism alliance: biochemical aspects, *Adv. Drug Deliv. Rev.* **2001**, *50* (Suppl. 1), S3–S11.

80 Smit, J. J. M., A. H. Schinkel, R. P. J. Oude, Elferink, A. K. Groen, E. Wagenaar, L. Van Deemter, C. A. A. M. Mol, R. Ottenhoff, N. M. T. Van der Lugt, M. A. Van Roon *et al.*, Homozygous disruption of the murine *mdr2* P-glycoprotein gene leads to a complete absence of phospholipid from bile and to liver disease. *Cell* **1993**, *75*, 451–462.

81 Thompson, R., Jansen, P. L. M., Genetic defects in hepatocanalicular transport, *Semin. Liv. Dis.* **2000**, *20*, 365–372.

82 Oude Elferink, R., Groen, A. K., Genetic defects in hepatobiliary transport, *Biochim. Biophys. Acta* **2002**, *1586*, 129–145.

83 Paulusma, C. C., Bosma, P. J., Zaman, G. J., Bakker, C. T., Otter, M., Scheffer, G. L., Scheper, R. J., Borst, P., Oude Elferink, R. P., Congenital jaundice in rats with a mutation in a multidrug resistance-associated protein gene, *Science* **1996**, *271*, 1126–1128.

84 Buchler, M., König, J., Brom, M., Kartenbeck, J., Spring, H., Horie, T., Keppler, D., cDNA cloning of the hepatocyte canalicular isoform of the multidrug resistance protein, cMrp, reveals a novel conjugate export pump deficient in hyperbilirubinemic mutant rats, *J. Biol. Chem.* **1996**, *271*, 15091–15098.

85 Taniguchi, K., Wada, M., Kohno, K., Nakamura, T., Kawabe, T., Kawakami, M., Kagotani, K., Okumura, K., Akiyama, S., Kuwano, M., A human canalicular multispecific organic anion transporter (cMOAT) gene is overexpressed in cisplatin-resistant human cancer cell lines with decreased drug accumulation, *Cancer Res.* **1996**, *56*, 4124–4129.

86 Ito, K., Suzuki, H., Hirohashi, T., Kume, K., Shimizu, T., Sugiyama, Y., Molecular cloning of canalicular multispecific organic anion transporter defective in EHBR, *Am. J. Physiol.* **1997**, *272*, G16–G22.

87 Yamazaki, M., Akiyama, S., Ni'inuma, K., Nishigaki, R., Sugiyama Y., Biliary excretion of pravastatin in rats: contribution of the excretion pathway mediated by canalicular multispecific organic anion transporter, *Drug Metab. Dispos.* **1997**, *25*, 1123–1129.

88 Herling, A. W., Schwab, D., Burger, H. J., Maas, J., Hammerl, R., Schmidt, D., Strohschein, S., Hemmerle, H., Schubert, G., Petry, S., Kramer, W., Prolonged blood glucose reduction in mrp-2 deficient rats (GY/TR(−)) by the glucose-6-phosphate translocase inhibitor S 3025, *Biochim. Biophys. Acta* **2002**, *1569*, 105–110.

89 Suzuki, H., Sugiyama, Y., Single nucleotide polymorphisms in Multidrug Resistance Associated Protein 2 (MRP2/ABCC2): its impact on drug disposition, *Adv. Drug Deliv. Rev.* **2002**, *54*, 1311–1331.

90 Aoki, J., Suzuki, H., Sugiyama, Y., Quantitative prediction of in vivo biliary excretion clearance across the bile canalicular membrane from in vitro transport studies with isolated membrane vesicles. Abstract of Millennial World Congress of pharmaceutical Sciences, San Francisco, April 16–20, **2000**, p. 92.

91 Niinuma, K., Kato, Y., Suzuki, H., Tyson, C. A., Weizer, V., Dabbs, J. E., Froehlich, R., Green, C. E., Sugiyama, Y., Primary active transport of organic anions on bile canalicular membrane in humans, *Am. J. Physiol.* **1999**, *276*, G1153–G1164.

92 Cui, Y., König, J., Keppler, D., Vectorial transport by double-transfected cells expressing the human uptake transporter SLC21A8 and the apical export pump ABCC2, *Mol. Pharmacol.* **2001**, *60*, 934–943.

93 Sasaki, M., Suzuki, H., Ito, K., Abe, T., Sugiyama, Y., Transcellular transport of organic anions across a double-transfected Madin-Darby canine kidney II cell monolayer expressing both human organic anion-transporting polypeptide (OATP2/SLC21A6) and Multidrug resistance-associated protein 2 (MRP2/ABCC2), *J. Biol. Chem.* **2002**, *277*, 6497–6503.

94 Litman, T., Druley, T. E., Stein, W. D., Bates, S. E., From MDR to MXR: new understanding of multidrug resistance systems, their properties and clinical significance, *Cell Mol. Life Sci.* **2001**, *58*, 931–959.

95 Jonker, J. W., Smit, J. W., Brinkhuis, R. F., Maliepaard, M., Beijnen, J. H., Schellens, J. H., Schinkel, A. H., Role of breast cancer resistance protein in the bioavailability and fetal penetration of topotecan, *J. Natl. Cancer Inst.* **2000**, *92*, 1651–1656.

96 Suzuki, M., Suzuki, H., Sugimoto, Y., Sugiyama, Y., Identification of BCRP/ABCG2 as an ABC transporter capable of transporting sulfated conjugates, *Hepatology* **2002**, *36*, 218A.

97 Gerloff, T., Stieger, B., Hagenbuch, B., Madon, J., Landmann, L., Roth, J., Hofmann, A. F., Meier, P. J., The sister of P-glycoprotein represents the canalicular bile salt export pump of mammalian liver, *J. Biol. Chem.* **1998**, *273*, 10046–10050.

98 Wang, R., Salem, M., Yousef, I. M., Tuchweber, B., Lam, P., Childs, S. J., Helgason, C. D., Ackerley, C., Phillips, M. J., Ling, V., Targeted inactivation of sister of P-glycoprotein gene (spgp) in mice results in nonprogressive but persistent intrahepatic cholestasis, *Proc. Natl. Acad. Sci. USA* **2001**, *98*, 2011–2016.

99 Strautnieks, S. S., Bull, L. N., Knisely, A. S., Kocoshis, S. A., Dahl, N., Arnell, H., Sokal, E., Dahan, K., Childs, S., Ling, V., Tanner, M. S., Kagalwalla, A. F., Nemeth, A., Pawlowska, J., Baker, A., Mieli-Vergani, G., Freimer, N. B., Gardiner, R. M., Thompson, R. J., A gene encoding a liver-specific ABC transporter is mutated in progressive familial intrahepatic cholestasis, *Nature Genet.* **1998**, *20*, 233–238.

100 Tirona, R. G., Leake, B. F., Merino, G., Kim, R. B., Polymorphisms in OATP-C: identification of multiple allelic variants associated with altered transport activity among European- and African-Americans, *J. Biol. Chem.* **2001**, *276*, 35669–35675.

101 Nozawa, T., Nakajima, M., Tamai, I., Noda, K., Nezu, J., Sai, Y., Tsuji, A., Yokoi, T., Genetic polymorphisms of human organic anion transporters OATP-C (SLC21A6) and OATP-B (SLC21A9): allele frequencies in the Japanese population and functional analysis, *J. Pharmacol. Exp. Ther.* **2002**, *302*, 804–813.

102 Michalski, C., Cui, Y., Nies, A. T., Nuessler, A. K., Neuhaus, P., Zanger, U. M., Klein, K., Eichelbaum, M., Keppler, D., König, J., A naturally occurring mutation in the SLC21A6 gene causing impaired membrane localization of the hepatocyte uptake transporter, *J. Biol. Chem.* **2002**, *277*, 43058–43063.

103 Brinkmann, U., Eichelbaum, M., Polymorphisms in the ABC drug transporter gene MDR1, *Pharmacogenomics J.* **2001**, *1*, 59–64.

104 Ito, S., Ieiri, I., Tanabe, M., Suzuki, A., Higuchi, S., Otsubo, K., Polymorphism of the ABC transporter genes, MDR1, MRP1 and MRP2/cMOAT, in healthy Japanese subjects, *Pharmacogenetics* **2001**, *11*, 175–184.

105 Itoda, M., Saito, Y., Soyama, A., Saeki, M., Murayama, N., Ishida, S., Sai, K., Nagano, M., Suzuki, H., Sugiyama, Y., Ozawa, S., Sawada, J., Polymorphisms in the ABCC2 (cMOAT/MRP2) gene found in 72 established cell lines derived from Japanese individuals: an association between single nucleotide polymor-

phisms in the 5′-untranslated region and exon 28, *Drug Metab Dispos.* **2002**, *30*, 363–364.

106 Kusuhara, H., Sugiyama, Y., Drug–drug interaction involving the membrane transport process, in: *Drug–drug Interactions.* Rodrigues, A. D. (ed.), Marcel Dekker, Basel, **2001**, pp. 123–188.

107 Ueda, K., Kato, Y., Komatsu, K., Sugiyama, Y., Inhibition of biliary excretion of methotrexate by probenecid in rats: quantitative prediction of interaction from in vitro data, *J. Pharmacol. Exp. Ther.* **2001**, *297*, 1036–1043.

108 Vavricka, S. R., Van Montfoort, J., Ha, H. R., Meier, P. J., Fattinger, K., Interactions of rifamycin SV and rifampicin with organic anion uptake systems of human liver, *Hepatology* **2002**, *36*, 164–172.

109 Muck, W., Frey, R., Boix, O., Voith, B., Gemfibrozil/Cerivastatin Interaction, *AAPS PharmSci.* **2001**, *3* (Suppl.), abstract No. 3566.

110 Muck, W., Mai, I., Fritsche, L., Ochmann, K., Rohde, G., Unger, S., Johne, A., Bauer, S., Budde, K., Roots, I., Neumayer, H.-H., Kuhlmann, J., Increase in cerivastatin systemic exposure after single and multiple dosing in cyclosporin-treated kidney transplant recipients, *Clin. Pharmacol. Ther.* **1999**, *65*, 251–261.

111 Shitara, Y., Li, A., Kato, Y., Itoh, T., Sato, H., Sugiyama, Y., Transporter-mediated drug–drug interaction. Abstract of 14th International symposium on microsomes and drug oxidations, July 22–26, **2002**, Sapporo, Japan, Abstract No. P24-B-35.

112 Bohan, A., Boyer, J. L., Mechanism of hepatic transport of drugs: implications for cholestatic drug reactions, *Semin. Liv. Dis.* **2002**, *22*, 123–136.

113 Fattinger, K., Funk, C., Pantze, M., Weber, C., Reichen, J., Stieger, B., Meier, P. J., The endothelin antagonist bosentan inhibits the canalicular bile salt export pump: a potential mechanism for hepatic adverse reactions, *Clin. Pharmacol. Ther.* **2001**, *69*, 223–231.

114 Horikawa, M., Kato, Y., Sugiyama, Y., Drug–drug interaction at the biliary excretion process: prediction of the potential cholestatic activity using bile canalicular membrane vesicles, *Jpn. J. Pharmacol. Ther.* **2001**, *29S*, S243–S245.

115 Funk, C., Pantze, M., Jehle, L., Ponelle, C., Scheuermann, G., Lazendic, M., Gasser, R., Troglitazone-induced intrahepatic cholestasis by an interference with the hepatobiliary export of bile acids in male and female rats. Correlation with the gender difference in troglitazone sulfate formation and the inhibition of the canalicular bile salt export pump (Bsep) by troglitazone and troglitazone sulfate, *Toxicology* **2001**, *167*, 83–98.

116 Funk, C., Ponelle, C., Scheuermann, G., Pantze, M., Cholestatic potential of troglitazone as a possible factor contributing to troglitazone-induced hepatotoxicity: in vivo and in vitro interaction at the canalicular bile salt export pump (Bsep) in the rat, *Mol. Pharmacol.* **2001**, *59*, 627–635.

117 Stieger, B., Fattinger, K., Madon, J., Kullak-Ublick, G. A., Meier, P. J., Drug- and estrogen-induced cholestasis through inhibition of the hepatocellular bile salt export pump (Bsep) of rat liver, *Gastroenterology* **2000**, *118*, 422–430.

118 Akita, H., Suzuki, H., Ito, K., Kinoshita, S., Sato, N., Takikawa, H., Sugiyama, Y., Characterization of bile acid transport mediated by multidrug resistance associated protein 2 and bile salt export pump, *Biochim. Biophys. Acta* **2001**, *1511*, 7–16.

119 Huang, L., Smit, J. W., Meijer, D. K., Vore, M., Mrp2 is essential for estradiol-17beta(beta-D-glucuronide)-induced cholestasis in rats, *Hepatology* **2000**, *32*, 66–72.

120 Ando, Y., Saka, H., Ando, M., Sawa, T., Muro, K., Ueoka, H., Yokoyama, A., Saitoh, S., Shimokata, K., Hasegawa, Y., Polymorphisms of

UDP-glucuronosyltransferase gene and irinotecan toxicity: a pharmacogenetic analysis, *Cancer Res.* **2000**, *60*, 6921–6926.

121 Horikawa, M., Kato, Y., Tyson, C. A., Sugiyama, Y., The potential for an interaction between MRP2 (ABCC2) and various therapeutic agents: probenecid as a candidate inhibitor of the biliary excretion of irinotecan metabolites, *Drug Metab. Pharmacokinet.* **2002**, *17*, 23–33.

122 Horikawa, M., Kato, Y., Tyson, C. A., Sugiyama, Y., Reduced gastrointestinal toxicity following inhibition of the biliary excretion of irinotecan and its metabolites by probenecid in rats, *Pharm. Res.* **2002**, *19*, 1342–1350.

123 Kato, Y., Akhteruzzaman, S., Hisaka, A., Sugiyama, Y., Hepatobiliary transport governs overall elimination of peptidic endothelin antagonists in rats, *J. Pharmacol. Exp. Ther.* **1999**, *288*, 568–574.

13
The Importance of Gut Wall Metabolism in Determining Drug Bioavailability

Kevin Beaumont

Abbreviations

GIT	Human gastrointestinal tract
UDP	Uridine diphosphate
V_{max}	Maximum rate of metabolism by an enzyme
F_a	Fraction absorbed from the GIT
F_g	Fraction escaping gut wall first-pass extraction
F_h	Fraction escaping hepatic first-pass extraction
cDNA	Complementary DNA
CYP1A1/2	Cytochrome P450 isoforms 1A1 and 1A2
CYP2C8/9	Cytochrome P450 isoforms 2C8 and 2C9
CYP2C19	Cytochrome P450 isoform 2C19
CYP3A4	Cytochrome P450 isoform 3A4
CYP2D6	Cytochrome P450 isoform 2D6
C_{max}	Maximum plasma concentration
AUC	Area under the plasma concentration–time curve
Caco-2	Adenocarcinoma cell line derived from human colon

13.1
Introduction

Most drugs are delivered at sites that are remote from their sites of action. Although the most convenient route of administration is the oral route, this presents significant challenges to the delivery of a drug molecule. Clearly, in order to be effective, an orally delivered drug must avoid several potential barriers. For example, it must:

- avoid degradation by stomach acid and gut lumen digestive enzymes;
- dissolve in the aqueous environment of the gut lumen;
- cross the lipophilic environment of the gut wall cell membrane;
- avoid metabolism by enzymes in the gut wall cell; and
- avoid first-pass extraction by the liver.

Drug Bioavailability: Estimation of Solubility, Permeability, Absorption and Bioavailability.
Edited by Han van de Waterbeemd, Hans Lennernäs and Per Artursson

ISBN: 3-527-30438-X

The extent to which the drug can overcome the barriers to its oral delivery is measured by the term "oral bioavailability", and this is one of the key determinants of compound quality as it is an indication of the ability of that drug to overcome the barriers to its delivery.

In order to understand the barriers confronting the oral delivery of a drug, it is necessary to understand the physiology of the human gut.

13.2 The Human Gastrointestinal Tract

The human gastrointestinal tract (GIT) is well adapted for its role in the digestion and absorption of food. Following ingestion, the first organ encountered is the stomach. It is here that the process of digestion starts with the breakdown of complex macromolecules into their constituent parts. The stomach contains many digestive enzymes and has the capacity to produce an acidic environment. Very few drugs are absorbed from the stomach, and as such it will not be considered further in this review.

The duodenum, jejunum and ileum (together termed the small intestine) are the major sites of nutrient (and drug) absorption. The human duodenum is approximately 20 cm long, and it is here where the acid in the stomach is neutralized to a more physiological pH. The jejunum and ileum together are approximately 700 cm long and are responsible for most drug absorption. The colon is approximately 1 m in length, and its main role is to reabsorb water from the digestive process. It is not a major absorptive site for drug molecules, although for extended release formulations it is important that a drug can be absorbed in the colon.

The gut wall within the small intestine is particularly well adapted for its role as an absorptive surface. Absorption rate is proportional to the area of the surface that is available for absorption. Thus, the internal surface of the small intestine is folded towards the lumen of the gut. This folding increases the surface area of the gut by approximately 3-fold. In this area, the gut wall is covered with many finger-like projections called villi, and these provide a further 10-fold increase in surface area. In addition, the gut wall epithelial cells are polarized such that on the luminal surface there are millions of microvilli providing a further 20-fold increase in surface area for absorption. In all, these surface area modifications provide an absorptive area which is some 600-fold higher than would be provided by a simple cylinder. Thus, the estimated surface area of the human gut is approximately 200 m^2 [1].

With such a large surface area available for the absorption of nutrients, there is the potential for the absorption of dietary constituents that could be harmful to the health of an individual. Thus, in order to protect against dietary toxins, there are a series of barriers, which must be overcome before a molecule can enter the systemic circulation. This applies equally to drug molecules.

The barriers confronting oral delivery of a drug molecule are summarized in Fig. 13.1. During the absorption process, the drug must cross the enterocyte cell apical

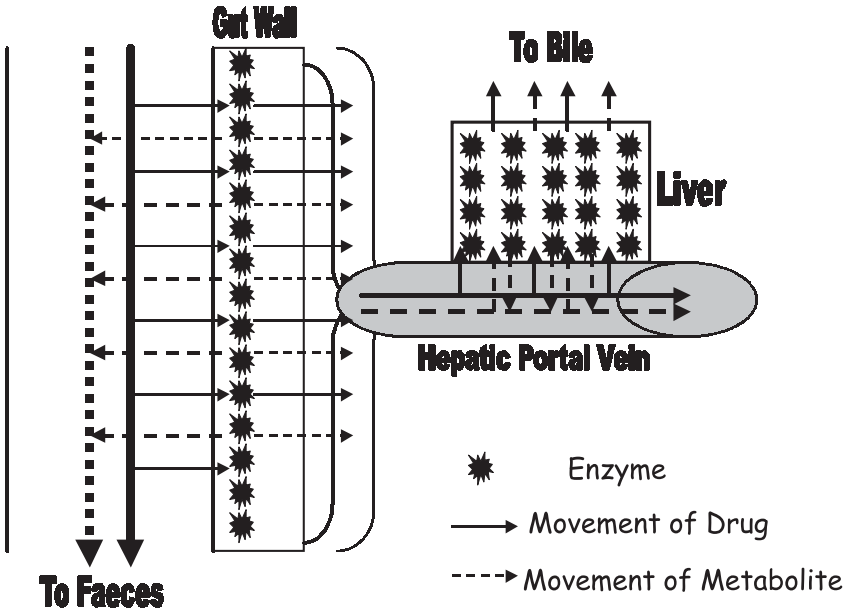

Fig. 13.1. Barriers to oral drug delivery.

membrane and move across the enterocyte before crossing the basolateral membrane into the blood in the mesenteries. On passage through the enterocyte membrane and the cell itself, the drug can be subject to potential metabolism and counter-transport processes. Counter-transport removes the drug from the enterocyte and places it back into the gut lumen from where it can be excreted in the feces. In addition, any metabolite that is produced by enzymes in the enterocyte can either be transported back into the lumen of the gut for excretion into the feces or removed across the basolateral membrane of the enterocyte into the blood in the mesenteries. Such metabolism and counter-transport of a drug on passage across the enterocyte is termed gut wall first-pass extraction.

The mesenteric blood empties into the hepatic portal vein from where it is transported to the liver. At the liver, drug and metabolites can also be extracted from the portal blood and either metabolized or excreted unchanged into the bile. This is termed hepatic first-pass extraction.

Thus, the oral bioavailability of a drug is determined by the amount absorbed from the GIT, the fraction escaping first-pass extraction by the gut, and the fraction escaping first-pass extraction by the liver. It is summarized by the following equation:

$$\text{Fraction bioavailable} = F_a \times F_g \times F_h \quad (1)$$

Consequently, the gut wall can exert a significant outcome on the overall oral bioavailability of a drug molecule. It is now time to consider the enzymes and transporters, which combine to express gut wall first-pass extraction.

Tab. 13.1. Relative rates of glucuronidation in human liver and intestinal microsomes.

Substrate	*V_{max} [nmol min^{-1} mg^{-1} microsomal protein]*	
	Intestine	*Liver*
p-Nitrophenol	0.8	–
1-Naphthol	1.3	5.86
Morphine	0.03	0.38
Ethinylestradiol	0.025	0.11

13.3 Enzymes Expressed at the Gut Wall

The enterocyte expresses many of the metabolic enzymes that are expressed in the liver. These include UDP-glucuronyltransferases, sulfotransferases, esterases and cytochromes P450.

13.3.1 UDP-Glucuronyltransferases

UDP-glucuronyltransferases catalyze the addition of glucuronic acid onto phenol, hydroxyl and carboxylic acid functions of molecules. They are expressed in many tissues of the body, including the liver and intestine [2–5]. Microsomes from human intestines have been shown to metabolize UDP-glucuronyltransferase substrates including *p*-nitrophenol [6], 1-naphthol, morphine, and ethinylestradiol [4]. The relative rates of metabolism of these substrates in liver and intestinal microsomes are shown in Table 13.1.

Overall, the human intestine is capable of metabolizing UDP-glucuronyltransferase substrates, although the rates of metabolism are between 5- and 10-fold lower than those observed in human liver microsomes. However, the presence of a metabolic capacity towards UDP-glucuronyltransferase substrates at the level of the enterocyte can exert a significant gut wall first-pass extraction on oral administration.

The level of *p*-nitrophenol glucuronidation activity was similar in human duodenum, jejunum and ileum-derived microsomes [7], indicating that expression of UDP-glucuronyltransferases does not change significantly throughout the small intestine. However, the level of glucuronidation in the colon was found to be significantly lower.

13.3.2 Sulfotransferases

Sulfotransferases are cytosolic enzymes that add sulfate to phenolic and hydroxyl functions as well as certain amines. The relative rates of sulfation of several sulfo-

Tab. 13.2. Relative rates of sulfation in human liver and intestinal cytosol.

Substrate	*Activity [pmol min^{-1} mg^{-1} protein]*		*Reference*
	Intestine	*Liver*	
2-Naphthol	640	1820	
(+)-Terbutaline	415	45	8
(+)-Isoproterenol	1400	30	9
Acetaminophen (paracetamol)	120	–	6

transferase substrates in cytosol from human liver and intestine are shown in Table 13.2.

Overall, the rates of sulfation in the intestine tend to be higher than the liver (up to 10-fold). In addition, for (+)-terbutaline, the relative rates of metabolism are reduced at sites lower down the GIT (i.e., activity values of 1195, 415 and 268 pmol min^{-1} mg^{-1} in the duodenum, ileum and colon, respectively). Thus, the intestine represents a considerable barrier to the oral bioavailability of sulfotransferase substrate drugs.

13.3.3 Esterases

Esterases form a wide family of enzymes that catalyze the hydrolysis of ester bonds. They are ubiquitously expressed in all tissues including the intestine, and are found in both microsomal and cytosolic fractions. Prueksaritonont *et al.* [6] have studied the metabolism of both *p*-nitrophenol acetate and acetylsalicylic acid by esterases from human intestinal microsomal and cytosolic systems, and the activity values were 2.76 μmol min^{-1} mg^{-1} and 0.96 nmol min^{-1} mg^{-1}, respectively. Thus, the activity for the hydrolysis of *p*-nitrophenol acetate in human intestine approaches that in the liver.

The presence of high activities of esterase activity in human intestine is an important consideration for the absorption of pro-drugs. Pro-drugs are often employed to improve the membrane permeation (and hence absorption) of poorly absorbed drugs. The rationale behind pro-drugs is to mask polar functions on the active principle and to increase overall lipophilicity. This is often achieved by attaching ester functionality to a carboxylic acid or alcohol function. Such esters are designed to be rapidly metabolized by esterases following absorption. However, with significant esterase activity in the human enterocyte, it is possible that hydrolysis will occur during the absorption process. The released active principle may then be transported back into the lumen of the gut. Thus, the esterase activity in the human intestine can act as a barrier to the oral absorption of ester pro-drugs.

A good example of this is the work completed on the fibrinogen receptor antagonist L-767,679 [10]. This compound exhibits extreme polarity due to its zwitter-

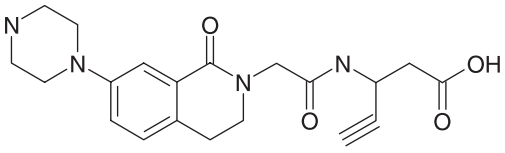

L-767,679

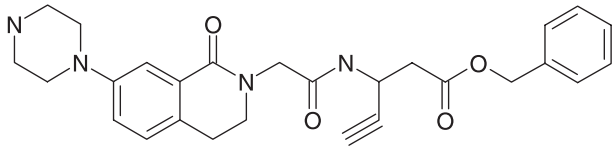

L-775,318

Fig. 13.2. Structures of fibrinogen receptor antagonists L-767,679 and L-775,318.

ionic nature. Consequently, its potential to cross membranes was limited, and this led to poor oral absorption characteristics.

In an effort to address the poor membrane permeation of L-767,679, the benzyl ester pro-drug, L-775,318 was synthesized (Fig. 13.2) The latter compound exhibited significant lipophilicity (log P = 0.7) that was consistent with improved potential to cross the enterocyte membrane. However, this did not lead to a marked improvement in absorption potential (in the rat), as intestinal hydrolysis and counter-transport combined to prevent significant passage of the compound across Caco-2 cells and the rat gut.

13.3.4 Cytochromes P450

The cytochromes P450 are a large super-family of enzymes that are responsible for the metabolism of the majority of drugs. The major drug-metabolizing cytochromes P450 in humans are CYP1A1/2, CYP2C8/9, CYP2C19, CYP3A4, and CYP2D6 [11], among which CYP3A4 is the major component [11].

Cytochromes P450 are expressed in the human intestine, although the mean amount of 20 pmol mg^{-1} microsomal protein [12] is significantly lower than that in the human liver (300–350 pmol mg^{-1} microsomal protein [13]). Prueksaritonont *et al.* (1996) have shown that human intestine expresses functional CYP2D6 (bufurolol hydroxylase activity 15 pmol min^{-1} mg^{-1} in human intestinal microsomes) and CYP2C (tolbutamide hydroxylase activity 5.1 pmol min^{-1} mg^{-1}). However, de Waziers *et al.* [14] suggest that the catalytic activity of these isoforms is some 100- to 200-fold lower than that in hepatic microsomes.

Tab. 13.3. Relative rates metabolism in human intestinal microsomes for a series of CYP3A substrates.

Substrate	*Activity [pmol min^{-1} mg^{-1} protein]*		*Reference*
	Intestine	*Liver*	
Sirolimus	89	–	17
Midazolam (1)	463	1004	18
Midazolam (2)	644	850	19
Erythromycin	1600	2800	14
Tacrolimus	54	96	20
Fentanyl	10–410	1440	21
Methadone	120	–	22
Lovastatin	155	1576	23
Terfenadine	61	370	24
Testosterone	1580	–	6

The most highly expressed cytochrome P450 in the human intestine is CYP3A4 [15]. Lown *et al.* [16] have shown that the sequences of hepatic and intestinal CYP3A4 cDNAs are identical, suggesting that both tissues express exactly the same isoform. Thus, the intestine expresses the major drug-metabolizing human cytochrome P450.

The metabolism of several CYP3A4 substrates in microsomes from the upper small intestine has been compared with liver microsomal metabolism. The results are summarized in Table 13.3. Thus, microsomes from the human upper small intestine can metabolize CYP3A4 substrates at rates approaching those found in human liver microsomes. However, the rate of metabolism in intestinal microsomes can be highly variable (8-fold for sirolimus [17] and 18- to 29-fold for midazolam [19]).

The expression of CYP3A4 exhibits a significant gradient at sites lower down the GIT. Thummel *et al.* [25] have shown that the expression levels of CYP3A4 in microsomal preparations were 31, 23 and 17 pmol mg^{-1} in human duodenum, jejunum and ileum, respectively, whereas de Waziers *et al.* [14] measured these values at 160, 120 and 70 pmol mg^{-1}, respectively. The differences between these estimates may reflect the difficulty of preparation of human intestinal microsomes. However, both studies suggest that the expression of CYP3A4 in human intestine is highest in the duodenum and jejunum where the oral absorption of most drugs occurs. Other studies [19] confirm this, as they suggest that the total amount of CYP3A4 in the duodenum and ileum is 9.7 nmol and 22 nmol, respectively. When the total length of each segment is considered (the duodenum length is one-tenth that of the ileum), it appears that the concentration of CYP3A4 is highest in the upper small intestine.

This has been confirmed in activity studies where the rates of metabolism of midazolam [19] and erythromycin [14] have been studied in microsomes from

Tab. 13.4. Metabolism of midazolam and erythromycin in microsomes from human duodenum, jejunum and ileum.

Tissue	*Activity [pmol min^{-1} mg^{-1} protein]*	
	Midazolam	*Erythromycin*
Duodenum	644	1600
Jejunum	426	1100
Ileum	68	150

human duodenum, jejunum, and ileum (Table 13.4). Thus, metabolism of CYP3A4 substrates decreases at distal sites in the human GIT.

The expression of CYP3A4 in the human intestine has significant implications for the oral delivery of its substrates. The most highly studied CYP3A4 substrate in this respect is midazolam. The pharmacokinetics of midazolam in humans has been studied following intravenous and oral administration [26, 27]. Following the oral administration of radiolabeled midazolam, up to 90% of the radioactivity was recovered in the urine, indicating essentially complete oral absorption [27]. Following intravenous administration of midazolam, mean systemic clearance was 6.4 and 4.6 ml min^{-1} kg^{-1} across the two studies. Thus, midazolam exhibits moderate clearance relative to hepatic blood flow ($\sim$25 mL min^{-1} kg^{-1}). Taken together, complete oral absorption and moderate systemic (hepatic) clearance would indicate an oral bioavailability of approximately 80%. However, the estimated oral bioavailability is significantly lower than this. Smith *et al.* [26] suggested that the oral bioavailability of midazolam was 36%, whereas Heizmann *et al.* [27] estimated this value to be approximately 50% (range 31–72%). Consequently, there is a significant nonhepatic component to the first-pass extraction of midazolam on oral administration, and this is most likely to occur in the intestine.

The gut wall first-pass extraction of midazolam has been extensively investigated in two studies [18, 28]. In the first study, Thummel *et al.* [18] administered 1 mg midazolam intravenously and 2 mg orally to human volunteers in a cross-over design. The mean systemic clearance was 5.3 mL min^{-1} kg^{-1} (corresponding with the above two studies), and showed a 3-fold variation. The mean oral bioavailability was calculated as 30% (range 12–50%) and the variability was significantly higher than after intravenous administration. In 18 out of the 20 subjects, the oral bioavailability was lower than would have been expected from systemic clearance relative to liver blood flow. Assuming complete oral absorption and that only the liver contributes to the systemic clearance of midazolam, these authors were able to estimate the contribution of the gut to the oral bioavailability of midazolam. The mean gut wall extraction ratio was 0.43 (range 0–0.77), whereas the mean hepatic extraction ratio was 0.44 (range 22–72%).

These findings were confirmed by Paine *et al.* [28] who administered 1 mg midazolam intravenously ($n = 5$) or 2 mg intraduodenally ($n = 5$) to liver transplant patients during the time that the liver had been removed. Thus, only the gut wall

extraction was examined in this study, thereby enabling the contribution of the gut to the systemic and oral clearance of midazolam to be determined. In this way, the gut wall extraction ratio following intraverous administration was calculated as 0.08 (range 0–0.26), suggesting that the intestine does not contribute significantly to the systemic clearance of midazolam. This is not unexpected since the CYP3A4 in the intestine is expressed predominantly at the villus tip where perfusion by the blood supply may be limited. The calculated gut wall first-pass extraction in this study was 0.43 (range 0.14–0.59), which is in good agreement with the study conducted by Thummel *et al.* [18].

The midazolam example shows that gut wall cytochrome P450 can contribute significantly to the attenuation of oral bioavailability of substrate drugs. In addition, the variability and site dependence of expression of the major intestinal CYPs can lead to significant effects on the disposition of orally delivered drugs.

13.4 Non-metabolic Barriers to Oral Absorption

In addition to the metabolic capacity of the enterocyte, there are further non-metabolic barriers to the passage of drug molecules. The enterocyte expresses a number of drug transport proteins, which are orientated in such a way as to intercept the drug as it passes through the enterocyte membrane, and actively transport it back into the gut lumen. This counter-absorptive mechanism is termed drug efflux. The best-characterized drug efflux transporter is P-glycoprotein.

13.4.1 P-glycoprotein

P-glycoprotein (P-gp) was first discovered in 1976 by Juliano and Ling [29], who suggested that it played a role in modulating cellular permeability. Interest in P-gp was heightened when it was implicated in multiple drug resistance of cancers. In response to various cytotoxic agents, tumors overexpress P-gp, which prevents entry of the drug into the tumor cell, and thus the tumor becomes resistant to the chemotherapeutic agent. For this reason, P-gp became known as the MDR-protein, and much research was aimed at producing P-gp inhibitors for co-administration with cytotoxic agents.

More recently, P-gp has been shown to be expressed in normal human tissues. In the gut, the expression is highly localized to the apical surfaces of the gut wall epithelium [30], where it is well placed to intercept its substrates and deposit them back into the lumen of the gut in a counter-absorptive manner.

Wacher *et al.* [31] have shown that, in contrast to CYP3A4, P-gp mRNA levels increase longitudinally along the intestine (lowest levels in the stomach and highest in the colon). Lown *et al.* [32] have shown using duodenal mucosal biopsies ($n = 20$) that there was a 10-fold variation in the P-gp mRNA level, suggesting that there will be variability in the expression of P-gp in the gut and this will lead to potential variability in oral bioavailability.

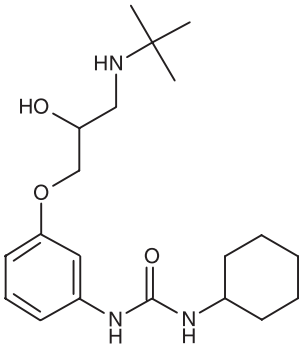

Fig. 13.3. Structure of the β-blocker talinolol.

The study of the role of P-gp in limiting oral absorption has been enhanced through the development of the Caco-2 cell monolayer model of absorption [33, 34]. Caco-2 cells are derived from a colon carcinoma cell and spontaneously form polarized monolayers in cell culture. These cells express P-gp only at their apical (absorptive) membrane. Consequently, P-gp substrates can show significantly greater passage (flux) across these cells when applied to the basolateral chamber than when applied to the apical chamber. Such asymmetry of flux is often termed the efflux ratio, and this suggests that P-gp is limiting the passage of its substrate across the cell membrane.

One of the most well-studied P-gp substrates is talinolol, an intermediate lipophilicity β-blocker (Fig. 13.3). The metabolic clearance of talinolol is negligible [35], and the compound is cleared almost exclusively unchanged in the urine and feces. Oral bioavailability is 54%, which has been ascribed to incomplete absorption from the GIT. The physico-chemical properties of talinolol (moderate lipophilicity and low molecular weight) would suggest that the compound should permeate membranes well. However, in the Caco-2 cell absorption model, talinolol exhibits asymmetric flux with approximately a 10-fold greater flux in the basolateral to apical direction [36]. This efflux ratio could be abolished by the addition of the P-gp inhibitor, verapamil. In addition, Gramatte *et al.* [37] studied the absorption of talinolol at several locations in the human gut using intubation methodology. These authors found that the talinolol AUC in blood decreased with increasing distance from the teeth, consistent with the assertion that the intestinal levels of P-gp increase along the length of the gut. Thus, it appears that the oral bioavailability of talinolol in man is limited by P-gp-mediated efflux rather than poor membrane permeation or first-pass metabolism.

The introduction of P-gp knockout mice [38] has enabled workers to study the role of P-gp in limiting the oral bioavailability of its substrates. An example of this is the NK_2 antagonist, UK-224,671 [39, 40] (Fig. 13.4).

In man, the oral bioavailability of UK-224,671 is less than 10% [39]. Since clearance of UK-224,671 is low relative to liver blood flow, the poor oral bioavailability is due to incomplete absorption of the compound from the GIT. Caco-2 flux experi-

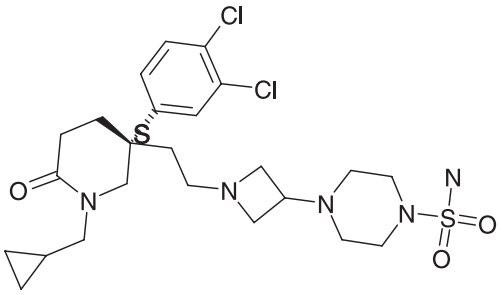

Fig. 13.4. Structure of NK_2 antagonist UK-224,671.

ments showed a poor apical to basolateral flux and a marked asymmetry (approximately 10-fold). In addition, UK-224,671 was shown to exhibit marked differences in oral bioavailability between wild-type (<5%) and P-gp knockout (22%) mice, indicating that P-gp plays a major role in limiting the oral absorption of this compound.

In addition to talinolol and UK-224,671, gut wall P-gp has been implicated in limiting the oral absorption of other drugs, including fexofenadine [41], digoxin [42] and paclitaxel [43]. Furthermore, there may be a mechanism by which P-gp and metabolizing enzymes in the gut wall cell may combine to limit the passage of drugs across the gut wall cell. This is most pronounced for CYP3A4.

13.4.2
A Combined Role for P-gp and CYP3A4 in the Gut Wall

Many authors have suggested that gut wall CYP3A4 and P-gp act in a concerted manner to control the absorption of their substrates [1, 17, 32, 44–47]. This is based on the large overlap of substrates between the two [48], and the proximity of their expression within the gut wall. Thus, it is proposed [44] that P-gp effectively recycles its substrates, thereby allowing CYP3A4 several opportunities to metabolize compounds in the gut. In this way, a small amount of CYP3A4 in the gut wall (relative to the liver content) can exert a profound extraction of the compound.

This certainly appears to be the case for cyclosporin, which is a substrate for both CYP3A4 and P-gp. Intestinal metabolism accounts for up to 50% of oral cyclosporin metabolism following oral administration. Lown *et al.* [46] have studied the expression of CYP3A4 and P-gp in the intestines of 25 kidney transplant patients and their effect on the oral clearance of cyclosporin. These authors found no correlation between the expression of CYP3A4 in the liver and intestine (i.e., a high expression in liver did not mean a high expression in gut), suggesting that the levels of CYP3A4 in these organs are not coordinately regulated. In addition, there was no correlation between the amount of P-gp and CYP3A4 in the gut. Interestingly, C_{max} and oral clearance of cyclosporin could be predicted by comparison of liver CYP3A4 and intestinal P-gp levels, but intestinal CYP3A4 levels could not be

implicated despite a 10-fold variability in enterocyte content. In addition, analysis revealed that 50% of the variability in oral clearance of cyclosporin was due to liver CYP3A4 and a further 17% to variability in intestinal P-gp. Variability in intestinal CYP3A4 did not produce any further variability in oral clearance of cyclosporin. These authors concluded that the rate-determining step in intestinal extraction of cyclosporin was cycling due to gut wall P-gp. These data were supported by information from Fricker *et al.* [49], who administered cyclosporin at various points in the GIT and showed that absorption was significantly inversely correlated with gut wall P-gp mRNA levels.

13.4.3 CYP Interactions

From the above, it appears that gut wall metabolism (particularly for CYP3A4 substrates) can be a major determinant of oral bioavailability in terms of extent and variability. Due to the position of the gut wall epithelial CYP3A4 (i.e., at the tip of the villus) the potential is there for this enzyme to come into contact with both inhibitors and inducers (possible dietary components or co-administered drugs). Under these circumstances, if gut wall CYP3A4 is important in determining oral bioavailability, a number of drug–drug interactions might be expected, and this indeed seems to be the case.

Ketoconazole (a potent inhibitor of CYP3A4) has been shown to increase the oral bioavailability of cyclosporin from 22 to 56% [50]. This consisted of a 1.8-fold decrease in systemic clearance combined with a 4.9-fold decrease in oral clearance. The authors estimated that hepatic extraction was decreased only 1.15-fold, whereas the oral bioavailability increased 2.6-fold and the observation was attributed to decreased intestinal metabolism. Erythromycin was also shown to increase the oral bioavailability of cyclosporin A 1.7-fold, while pre-treatment with rifampin (an inducer of CYP3A4) decreased oral bioavailability of cyclosporin from 27% to 10% due to a 4.2-fold increase in oral clearance but only a 1.2-fold increase in systemic clearance. Floren *et al.* [51] have also shown that ketoconazole can double the oral bioavailability of tacrolimus in man by inhibiting gut wall CYP3A4.

Perhaps the most interesting gut wall CYP3A4 interactions are caused by grapefruit juice. These have been reported for felodipine [52], midazolam [53], lovastatin [54], simvastatin [55], terfenadine [56], and buspirone [57]. The magnitude of these interactions ranges from 2-fold for felodipine to 16-fold for lovastatin; such variation reflects the relative oral bioavailabilities of these compounds and the contribution of gut wall first-pass metabolism. Schmedlin-Ren *et al.* [58] have speculated that the mechanism for this interaction is a loss of CYP3A4 from the small intestine. The reduction is rapid, with a 47% decrease within 4 hours of grapefruit juice ingestion. The juice has little effect on systemic clearance, and consequently does not affect intravenously dosed compounds. The juice contains many flavonoid compounds, in particular 6′,7′-dihydroxybergamottin, which appear to act at the transcriptional level to prevent the expression of CYP3A4 protein.

Lown *et al.* [59] have taken the felodipine–grapefruit juice interaction one stage further by giving 225 g (8 oz, one glass) of grapefruit juice three times daily for 6 days, during which time they challenged with felodipine on several occasions. Using biopsy material, they were able to show that ingestion of the juice caused a 62% reduction in small intestinal CYP3A4 content, with no effect on liver CYP3A4 levels. In addition, the ingestion of grapefruit juice did not affect the systemic clearance of felodipine; rather, its effect following oral administration was to increase C_{max}, with no significant change in elimination half-life. The effect appeared rapidly, with one glass of juice increasing C_{max} from 5.5 nM to 17.9 nM (225% increase) and AUC from 35 to 76 nM · h (116% increase). The effect of 6 days of ingestion of juice caused further 34% and 44% increases in C_{max} and AUC, respectively (to 24 nM and 110 nM · h). Also, the effect of grapefruit juice was to reduce the variability associated with oral felodipine plasma concentrations. The coefficient of variation for C_{max} was reduced from 61% to 18% with the first glass, and was 36% following the 16th glass. Subjects with the highest enterocyte CYP3A4 content pre-study showed the largest increases in C_{max}, whilst after juice ingestion these individuals showed comparable enterocyte CYP3A4 content to those observed in some subjects pre-study. Consequently, the effect of grapefruit juice appears to be to normalize the amount of CYP3A4 in the intestine, reduce the gut wall first-pass effect for felodipine and thus, to increase oral bioavailability and reduce variability.

These authors suggest that components of grapefruit juice damage CYP3A4 through suicide inhibition and accelerated degradation of the enzyme. Interestingly, there appears to be no effect on intestinal expression of P-gp. In addition, they suggest that the oral pharmacokinetics of felodipine are largely determined by the gut wall CYP3A4 content, and that once grapefruit juice reduces CYP3A4 in the gut, the oral pharmacokinetics of felodipine becomes more dependent on systemic clearance by liver CYP3A4. This is likely to be the case with other CYP3A4 substrates. In addition, studies with simvastatin [60] suggest that the effect on intestinal CYP3A4 dissipates between 3 and 7 days after the last glass of grapefruit juice.

13.4.4 P-gp Interactions

Pharmacokinetic interactions between P-gp substrates are becoming more apparent as the literature grows. A good example is the quinidine–digoxin interaction, which is common in clinical practice. When quinidine is administered to patients receiving digoxin, the plasma concentrations of digoxin can rise by up to 3-fold. Since digoxin has a low therapeutic index, this can lead to toxicity.

Fromm *et al.* [61] have shown in Caco-2 cells, that the apical to basolateral flux of digoxin is 1.2% per hour, and the basolateral to apical flux is 8.9% per hour. This polarized flux can be normalized by the addition of increasing concentrations of quinidine (with 100 μM quinidine, digoxin flux rates are 2.7% per hour apical to basolateral and 3% per hour basolateral to apical). Such a profile is indicative of

P-gp-mediated transport. These authors underlined their results with P-gp knockout mice studies. Co-administration of digoxin and quinidine to wild-type mice resulted in a 73% increase in digoxin concentrations, whereas the increase for the knockout mice was only 20%.

13.5 Summary and Conclusions

From the above, it is clear that the gut wall represents more than just a physical barrier to oral drug absorption. In addition to the requirement to permeate the membrane of the enterocyte, the drug must avoid metabolism by the enzymes present in the gut wall cell as well as counter-absorptive efflux by transport proteins in the gut wall cell membrane. Metabolic enzymes expressed by the enterocyte include the cytochrome P450, glucuronyltransferases, sulfotransferases and esterases. The levels of expression of these enzymes in the small intestine can approach that of the liver. The most well-studied efflux transporter expressed by the enterocyte is P-gp.

These enzymes (and transporters) exhibit differential expression at various sites throughout the GIT. For example, CYP3A4 expression is highest in the duodenum and lowest in the colon; conversely, the expression of P-gp is greatest in the colon. This has implications for the gut wall first-pass extraction of drugs delivered by modified-release formulations, where the majority of the drug must be absorbed from the colon.

The expression of metabolic enzymes in the enterocyte can lead to a profound gut wall first-pass extraction ratio for substrate drugs. In addition, efflux transporters can slow the passage of drugs across the enterocyte in a cycling fashion. This allows the metabolic enzymes several opportunities to metabolize their substrates, and in this way a low expression level of an enzyme can exhibit a significant extraction.

The expression of a significant gut wall first-pass extraction ratio has several implications for affected drugs. First, oral bioavailability is lower than would be expected from the extent of absorption and the hepatic first-pass extraction. Second, the variability in expression of gut wall metabolic enzymes and transporters can lead to significant variability in gut wall first-pass extraction and thus oral bioavailability. Finally, the site of expression of these enzymes and transporters (i.e., the villus tip) brings them into contact with potentially co-administered drugs or dietary constituents, which could be inhibitors or inducers. Thus, there is the potential for drug–drug interactions at the level of the gut wall.

The aim of oral drug delivery is almost exclusively to achieve as high an oral bioavailability as possible. Thus, the challenge to the medicinal chemist in drug discovery is to avoid the potential for a drug to exhibit a high gut wall first-pass extraction ratio. This can be achieved by balancing the physico-chemistry needed to maintain good transmembrane flux with an avoidance of the structural features that predispose compounds to metabolism by gut wall enzymes.

This chapter has provided only a short review of a very large subject, and for further details the reader is directed to excellent reviews on gut wall metabolism [62], transporter proteins [63], and cytochromes P450 [11].

References

1 van Asperen, J., van Tellingen, O., Beijnen, J. H., Pharmacological role of P-glycoprotein in the intestinal epithelium, *Pharmacol. Res.* **1998**, *37*, 429–435.

2 Pacific, G. M., Franchi, M., Bencini, F., Repetti, F., di Lascio, N., Muraro, G. B., Tissue distribution of drug metabolising enzymes in humans, *Xenobiotica* **1988**, *18*, 849–856.

3 Capiello, M., Franchi, M., Guiliani, L., Pacifici, G. M., Distribution of 2-naphthol sulphotransferase and its endogenous substrate adenosine 3-phosphate 5-phosphourate in human tissues, *Eur. J. Clin. Pharmacol.* **1989**, *37*, 317–320.

4 Capiello, M., Guiliani, L., Pacifici, G. M., Distribution of UDP-glucuronosyl transferase and its endogenous substrate uridine 5-diphosphoglucuronic acid in human tissues, *Eur. J. Clin. Pharmacol.* **1991**, *41*, 345–350.

5 Krishna, D. R., Klotz, U., Extrahepatic metabolism of drugs in humans, *Clin. Pharmacokinet.* **1997**, *26*, 144–160.

6 Prueksaritonont, T., Gorham, L. M., Hochman, J. H., Tran, L. O., Vyas, K. P., Comparative studies of drug metabolising enzymes in dog, monkey and human small intestines and in Caco-2 cells, *Drug Metab. Disp.* **1996**, *24*, 634–642.

7 Peters, W. H., Kock, L., Nagengast, F. M., Kremers, P. G., Biotransformation enzymes in human intestine: critical low levels in the colon? *Gut*, **1991**, *32*, 408–412.

8 Pacifici, G. M., Eligi, M., Guiliani, L., (+) and (–) terbutaline are sulphated at a higher rate in human intestine than in liver, *Eur. J. Clin. Pharmacol.* **1993**, *45*, 483–487.

9 Pesola, G. R., Walle, T., Stereoselective sulfate conjugation of isoproterenol in humans: comparison of hepatic, intestinal and platelet activity, *Chirality* **1993**, *5*, 602–609.

10 Prueksaritonont, T., Deluna, P., Gorham, L. M., Ma, B., Cohn, D., Pang, J., Xu, X., Leung, K., Lin, J. H., *In vitro* and *in vivo* evaluation of intestinal barriers for the zwitterions L-767,679 and its carboxyl ester prodrug L-775,318, *Drug Metab. Disp.* **1998**, *26*, 520–527.

11 Jones, B. C., Clark, S. E., Human cytochromes P450 and their role in metabolism based drug–drug interactions, in: *Drug–Drug Interactions.* Rodrigues, A. D. (ed.), **2001**, Chapter 3, 55–88. Marcel Dekker Inc. New York.

12 Peters, W. H., Kremers, P. G., Cytochromes P450 in the intestinal mucosa of man, *Biochem. Pharmacol.* **1989**, *38*, 1535–1538.

13 Shimada, T., Yamazaki, H., Mumura, M., Inui, Y., Guengerich, F. P., Interindividual variations in human liver cytochrome P450 enzymes involved in the oxidation of drugs, carcinogens and toxic chemicals: studies with liver microsomes of 30 Japanese and Caucasians, *J. Pharmacol. Exp. Ther.* **1994**, *270*, 414–423.

14 de Waziers, I., Cugenec, P. H., Yang, C. S., Lerous, J. P., Beaune, P. H., Cytochrome P450 isoenzymes, epoxide hydrolase and glutathione transferases in rat and human hepatic and extrahepatic tissues, *J. Pharmacol. Exp. Ther.* **1990**, *253*, 387–394.

15 Watkins, P. B., Wrighton, S. A., Schuetz, E. G., Molowa, D. T., Guzelian, P. S., Identification of glucocorticoid cytochrome P450 in the intestinal mucosa of rats and man, *J. Clin. Invest.* **1997**, *80*, 1029–1036.

16 Lown, K. S., Ghosh, M., Watkins, P. B., Sequences of intestinal and hepatic cytochrome P450 3A4 cDNAs are identical, *Drug Metab. Disp.* **1998**, *26*, 185–187.

17 Lampen, A., Zhang, Y., Hackbarth, I., Benet, L. Z., Sewing, K., Christians, U., Metabolism and transport of the macrolide immunosupressant sirolimus in the small intestine, *J. Pharmacol. Exp. Ther.* **1998**, *285*, 1104–1112.

18 Thummel, K. E., O'Shea, D., Paine, M. F., Shen, D. D., Kunze, K. L., Perkins, J. D., Wilkinson, G. R., Oral first-pass elimination of midazolam involves both gastrointestinal and hepatic CYP3A mediated metabolism, *Clin. Pharmacol. Ther.* **1996**, *59*, 491–502.

19 Paine, M. F., Khalighi, K., Fisher, J. M., Shen, D. D., Kunze, K. L., Marsh, C. L., Perkins, J. D., Thummel, K. E., Characterisation of interintestinal and intraintestinal variations in human CYP3A-dependent metabolism, *J. Pharmacol. Exp. Ther.* **1997**, *283*, 1552–1562.

20 Lampen, A., Christians, U., Guengerich, F. P., Watkins, P. B., Kolars, J. C., Bader, A., Dralle, H., Hackbarth, I., Sewing, K. F., Metabolism of the immunosuppressant tacrolimus in the small intestine: cytochrome P450 drug interactions, and interindividual variability, *Drug Metab. Disp.* **1995**, *23*, 1315–1324.

21 Labroo, R. B., Paine, M. F., Thummel, K. E., Kharasch, E. D., Fentanyl metabolism by human hepatic and intestinal cytochrome P4503A4. Implications for interindividual variability in disposition, efficacy and drug interactions, *Drug Metab. Disp.* **1997**, *25*, 1072–1080.

22 Oda, Y., Kharasch, E. D., Metabolism of methadone and levo-α-acetylmethadol (LAAM) by human intestinal cytochrome P450 3A4 (CYP3A4): potential contribution of intestinal metabolism to presystemic clearance and bioactivation, *J. Pharmacol. Exp. Ther.* **2001**, *298*, 1021–1032.

23 Jacobsen, W., Kirchner, G., Hallensleben, K., Mancinelli, L., Deters, M., Hackbarth, I., Baner, K., Benet, L. Z., Sewing, K. F., Christians, U., Small intestinal metabolism of the 3-hydroxy-3-methylglutaryl-coenzyme A reductase inhibitor lovastatin and comparison with pravastatin, *J. Pharmacol. Exp. Ther.* **1999**, *291*, 131–139.

24 Raeissi, S. D., Guo, Z., Dobson, G. L., Artursson, P., Hidalgo, I. J., Comparison of CYP3A activities in a subclone of Caco-2 cells (TC7) and human intestine, *Pharm. Res.* **1997**, *14*, 1019–1025.

25 Thummel, K. E., Kunze, K. L., Shen, D. D., Enzyme catalysed processes of first-pass hepatic and intestinal drug extraction, *Adv. Drug Del. Rev.* **1997**, *27*, 99–127.

26 Smith, M. T., Eadie, M. J., Brophy, T. O., Pharmacokinetics of midazolam in man, *Eur. J. Clin. Pharmacol.* **1981**, *19*, 271–278.

27 Heizmann, P., Eckert, M., Ziegler, W. H., Pharmacokinetics and bioavailability of midazolam in man, *Br. J. Clin. Pharmacol.* **1983**, *16*, 43S–49S.

28 Paine, M. F., Shen, D. D., Kunze, K. L., Perkins, J. D., Marsh, C. L., McVicar, J. P., Barr, D. M., Gillies, B. S., Thummel, K. E., First-pass metabolism of midazolam by the human intestine, *Clin. Pharm. Ther.* **1996**, *60*, 14–24.

29 Juliano, R. L., Ling, V., A surface glycoprotein modulating drug permeability in Chinese hamster ovary cell mutants, *Biochim. Biophys. Acta* **1976**, *455*, 152–162.

30 Thiebaut, F., Tsuruo, T., Hamada, H., Gottesman, M. M., Pastan, I., Willingham, M. C., Cellular localisation of the multidrug resistance gene product P-glycoprotein in normal human tissues, *Proc. Natl. Acad. Sci. USA* **1987**, *84*, 7735–7738.

31 Wacher, V. J., Silverman, J. A., Zhang, Y., Benet, L. Z., Role of P-glycoprotein and cytochrome P4503A in limiting oral absorption of peptides and peptidomimetics, *J. Pharm. Sci.* **1998**, *87*, 1322–1330.

32 Lown, K. S., Fontana, R. J., Schmiedlin-Ren, P., Turgeon, D. K., Watkins, P. B., Interindividual variation in intestinal MDR1 expression: lack of short term diet effects, *Gastroenterology* **1995**, *108*, A737.

33 Artursson, P., Epithelial transport of drugs in cell culture. I: a model for studying the passive diffusion of drugs over intestinal absorptive (Caco-2) cells, *J. Pharm. Sci.* **1990**, *79*, 476–482.

34 Yee, S., *In vitro* permeability across Caco-2 cells can predict in vivo absorption in man – Fact or myth? *Pharm. Res.* **1997**, *14*, 763–766.

35 Trausch, B., Oertel, R., Richter, K., Gramatte, T., Disposition and bioavailability of the β-adrenoceptor antagonist Talinolol in man, *Biopharmaceut. Drug Disp.* **1995**, *16*, 403–414.

36 Wetterich, U., Spahn-Langguth, H., Mutschler, E., Terhaag, B., Rosch, W., Langguth, P., Evidence for intestinal secretion as an additional clearance pathway of Talinolol enantiomers: concentration and dose dependent absorption in vitro and in vivo, *Pharm. Res.* **1996**, *13*, 514–522.

37 Gramatte, T., Oertel, R., Terhaag, B., Kirch, W., Direct demonstration of small intestinal secretion and site-dependent absorption of the β-blocker Talinolol in humans, *Clin. Pharmacol. Ther.* **1996**, *66*, 239–245.

38 Schinkel, A. H., Smit, J. J., van Tellingen, O., Beijnen, J. H., Wagenaar, E., van Deemter, L., Mol, C. A. A. M., van der Valk, M. A., RobanusMandaag, E. C., Borst, P., Disruption of the mouse mdr1a P-glycoprotein gene leads to a deficiency in the blood brain barrier and to increased sensitivity to drugs, *Cell* **1994**, *77*, 491–502.

39 Beaumont, K., Harper, A., Smith, D. A., Abel, S., Pharmacokinetics and metabolism of a sulphamide NK2 antagonist in rat, dog and human, *Xenobiotica* **2000**, *30*, 627–642.

40 Beaumont, K., Harper, A., Smith, D. A., Bennett, J., The role of P-glycoprotein in determining the oral absorption and clearance of the NK2 antagonist, UK-224,671, *Eur. J. Pharm. Sci.* **2000**, *12*, 41–50.

41 Cvetkovic, M., Leake, B., Fromm, M. F., Wilkinson, G. R., Kim, R. B., OATP and P-glycoprotein transporters mediate the cellular uptake and excretion of fexofenadine, *Drug Metab. Disp.* **1999**, *27*, 866–871.

42 Hoffmeyer, S., Burk, O., von Richter, O., Arnold, H. P., Brockmoller, J., Johne, A., Cascorbi, I., Gerlo, T., Roots, I., Eichelbaum, M., Brinkmann, U., Functional polymorphism of the human multidrug resistance gene: multiple sequence variations and correlation of one allele with P-glycoprotein expression and activity *in vivo*, *Proc. Natl. Acad. Sci. USA* **2000**, *97*, 3473–3478.

43 Sparreboom, A., van Asperen, J., Mayer, U., Schinkel, A. H., Smit, J. W., Meier, D. K. F., Borst, P., Nooijen, W. J., Beijnen, J. H., van Tellingen, O., Limited oral bioavailability and active epithelial excretion of paclitaxel (taxol) caused by P-glycoprotein in the intestine, *Proc. Natl. Acad. Sci. USA* **1997**, *94*, 2031–2035.

44 Hebert, M. F., Contributions of hepatic and intestinal P-glycoprotein to cyclosporine and tacrolimus oral drug delivery, *Adv. Drug. Del. Rev.* **1997**, *27*, 201–214.

45 Hall, S. D., Thummel, K. E., Watkins, P. B., Lown, K. S., Benet, L. Z., Paine, M. F., Mayo, R. R., Turgeon, D. K., Bailey, D. G., Fontana, R. J., Wrighton, S. A., Molecular and physical mechanisms of first-pass extraction, *Drug Metab. Disp.* **1999**, *27*, 161–166.

46 Lown, K. S., Mayo, R. R., Leichtman, A. B., Hsiao, H., Turgeon, D. K., Schmiedlin-Ren, P., Brown, M. B., Guo, W., Rossi, S. J., Benet, L. Z., Watkins, P. B., Role of intestinal P-glycoprotein in interpatient variation in the oral bioavailability of cyclosporin, *Clin. Pharmacol. Ther.* **1997**, *62*, 248–260.

47 Benet, L. Z., Izumi, T., Zhang, T., Silverman, J., Wacher, V. J.,

Intestinal MDR transport proteins and P-450 enzymes as barriers to oral drug delivery, *J. Controlled Release* **1999**, *62*, 25–31.

48 Wacher, V. J., Salphati, L., Benet, L. Z., Active secretion and enterocytic drug metabolism barriers to drug absorption, *Adv. Drug Del. Rev.* **1996**, *20*, 99–112.

49 Fricker, G., Drewe, J., Huwyler, J., Gutmann, H., Beglinger, C., Relevance of P-glycoprotein for the enteral absorption of cyclosporin A: *in vitro–in vivo* correlation, *Br. J. Pharmacol.* **1996**, *118*, 1841–1847.

50 Gomez, D. Y., Wacher, V. J., Tomlanovich, S. J., Hebert, M. F., Benet, L. Z., Effects of ketoconazole on intestinal metabolism and bioavailability of cyclosporine, *Clin. Pharmacol. Ther.* **1995**, *58*, 15–19.

51 Floren, L. C., Bekersky, I., Benet, L. Z., Mekki, Q., Dressler, D., Lee, J. W., Roberts, J. P., Hebert, M. F., Tacrolimus oral bioavailability doubles with co-administration of ketoconazole, *Clin. Pharmacol. Ther.* **1997**, *62*, 41–49.

52 Lundahl, J., Regardh, C. G., Edgar, B., Johnsson, G., Effects of grapefruit juice ingestion: pharmacokinetics and haemodynamics of intravenous and orally administered felodipine in healthy men, *Eur. J. Clin. Pharmacol.* **1997**, *52*, 139–145.

53 Kupferschmidt, H. H. T., Riem, H., Ziegler, W. H., Meier, P. J., Krahenbuhl, S., Interaction between grapefruit juice and midazolam in humans, *Clin. Pharmacol. Ther.* **1995**, *58*, 20–28.

54 Kantola, T., Kivisto, K. T., Neuvonen, P. J., Grapefruit juice greatly increases serum concentrations of lovastatin and lovastatin acid, *Clin. Pharmacol. Ther.* **1998**, *63*, 397–402.

55 Lilja, J. L., Kivisto, K. T., Backman, J. T., Lamberg, T. S., Neuvonen, P. J., Grapefruit juice substantially increases plasma concentrations of buspirone, *Clin. Pharmacol. Ther.* **1998**, *64*, 655–660.

56 Rau, S. E., Bend, J. R., Arnold, M. O., Tran, L. T., Spence, J. D., Bailey, D. G., Grapefruit juice terfenadine single dose interaction: magnitude, mechanism and relevance, *Clin. Pharmacol. Ther.* **1997**, *61*, 401–409.

57 Lilja, J. L., Kivisto, K. L., Neuvonen, P. J., Grapefruit juice–simvastatin interaction: effect on serum concentrations of simvastatin and HMG-CoA reductase inhibitors, *Clin. Pharmacol. Ther.* **1998**, *64*, 477–483.

58 Schmedlin-Ren, P., Edwards, D. J., Fitzsimmons, M. E., He, K., Lown, K. S., Woster, P. M., Rahman, A., Thummel, K. E., Fisher, J., Hollenberg, P. F., Watkins, P. B., Mechanisms of enhanced oral availability of CYP3A4 substrates by grapefruit juice constituents, *Drug Metab. Disp.* **1997**, *25*, 1228–1233.

59 Lown, K. S., Bailey, D. G., Fontana, R. R., Janarden, S. K., Adair, C. H., Fortlage, L. A., Brown, M. B., Guo, W., Watkins, P. B., Grapefruit juice increases felodipine oral availability in humans by decreasing intestinal CYP3A protein expression, *J. Clin. Invest.* **1997**, *99*, 2545–2553.

60 Lilja, J. J., Kivisto, K. T., Neuvonen, P. J., Duration of effect of grapefruit juice on the pharmacokinetics of the CYP3A4 substrate simvastatin, *Clin. Pharmacol. Ther.* **2000**, *68*, 384–390.

61 Fromm, M. F., Kim, R. B., Stein, M., Wilkinson, G. R., Roden, D. M., Inhibition of P-glycoprotein-mediated drug transport: a unifying mechanism to explain the interaction between digoxin and quinidine, *Circulation* **1999**, *99*, 552–557.

62 Linn, L. H., Chiba, M., Baillie, T. A., Is the role of the small intestine in first-pass metabolism overemphasised? *Pharm. Rev.* **1999**, *51*, 135–157.

63 Ayrton, A., Morgan, P., Role of transport proteins in drug absorption, distribution and excretion, *Xenobiotica* **2001**, *31*, 469–497.

14
Modified Cell Lines

Charles L. Crespi

Abbreviations

Caco-2	Human colon adenocarcinoma cell line used as absorption model
cDNA	Complementary DNA
CYP	Cytochrome P450
LLC-PK_1	Porcine kidney cell line used as absorption model
MDCK	Madin–Darby canine kidney cell line used as absorption model
MDR1	Multidrug resistance protein 1 (also designated P-gp and ABCB1).
MRP1	Multidrug resistance-associated protein 1 (also designated ABCC1).
MRP2	Multidrug resistance-associated protein 2 (also designated ABCC2).
OR	Cytochrome P450:NADPH oxidoreductase
TEER	Transepithelial electrical resistance

14.1
Introduction

The extent of oral absorption of a drug is dependent upon physical properties of the drug (e.g., solubility and membrane permeability), and also upon any interaction of the drug with various enzymatic processes of an organism. The two most prominent enzymatic systems are drug-metabolizing enzymes and drug transporters, both of which exist in many related forms that generally have distinct, yet potentially overlapping, substrate specificities.

The action of drug-metabolizing enzymes may reduce oral bioavailability by metabolizing a portion of the drug that has been absorbed before it enters circulation. Human drug-metabolizing enzymes have been extensively studied for decades and are now well characterized. Metabolic enzyme-specific substrate, inhibitor and antibody *in vitro* probe reagents, as well as authentic standards, are available for most of the major enzymes. These reagents allow the establishment of the relative and absolute amounts of metabolism by individual enzymes and prediction of drug–drug interactions. In addition, a number of *in vivo* probes are available, and

Drug Bioavailability: Estimation of Solubility, Permeability, Absorption and Bioavailability.
Edited by Han van de Waterbeemd, Hans Lennernäs and Per Artursson

ISBN: 3-527-30438-X

in vivo studies are essential to validate predictive models based upon *in vitro* measurements.

There are a number of drug transporters that are expressed in various tissues, including the intestine. The action of intestinal drug transporters can be either to increase or decrease oral bioavailability, depending upon whether the transporter facilitates or impedes drug uptake into the enterocyte (which is generally regarded as rate-limiting). The potential importance of transporters in drug disposition has only become evident during the past few years, and there is a clear need for a better understand of the substrate specificities and abundance of the individual forms. However, this research is currently hampered by a lack of comprehensive sets of reagents and standards, and consequently – as with the metabolizing enzymes – the goal for drug transporters is to develop predictive *in vitro* models.

In order to conduct basic research and address the need for reagents and standards, several cell lines have been modified to express individual transporters. These can serve as a source of active protein to validate a chemical as a substrate or inhibitor, or as a source of protein to validate the specificity of an antibody. In order for this approach to be sufficiently robust to establish specificity (and to minimize false-negative findings), all of the key proteins need to be available and active in the system. However, as specific probes are being increasingly identified and developed, valuable mechanistic studies can be performed with the transporters and substrates/inhibitors that are currently available.

There is also a need for cell systems that express a multiplicity of transporters. Cell line modification through cDNA-expression can be used to add missing functions to cells that are known to express only a subset of the enzymes or transporters that are needed and are known to be present *in vivo*. In this way, *in vitro* screening models can be improved.

This chapter describes some of the modified mammalian cell-based systems that have been developed to express intestinal cytochrome P450 enzymes and intestinal transporters. The reader should be aware that other experimental systems, such as transporter expression and drug uptake studies in *Xenopus laevis* oocytes, have also shown considerable promise [1].

14.2 Cell/Vector Systems

Modified mammalian cell systems for the study of the role of transporters and/or metabolism in oral absorption consists of two main components: the cell line; and the vector bearing a cDNA encoding the protein of interest. The cell line serves two roles: first, to support adequate expression of the cDNA; and second, to provide a barrier function which is generally critical in assays for transporter function.

The key function of the vector is to introduce the cDNA under control of a strong promoter and, if a stable cell line is to be developed, also to introduce resistance to a compound that is otherwise toxic to the host cell. This facilitates selection (of only vector-bearing cells grown in special media) of the minority of cells that have

incorporated the vector. Today, many adequate expression vectors are available commercially from a number of suppliers. Indeed, many vector systems appear appropriate for transporter expression, as integrating, episomal, retroviral, vaccinia virus and adenovirus-based systems have all been used successfully in the reports referred to herein.

The analysis of cytochrome P450 function is most commonly performed by monitoring metabolite formation in culture. However, this presents an analytical challenge as during the drug discovery/lead optimization phases, radiolabeled compounds or authentic metabolite standards are generally not available. While the extent of metabolism could in theory be measured by the loss of parent compound, this degree of loss is generally less than 20%. This low amount is difficult to detect reliably and therefore provides only a very narrow dynamic range by which compounds can be ranked.

The analysis of transporter functions is most commonly performed by analyzing rates of drug transport through cell monolayers grown on membrane support systems (e.g., microporous polycarbonate or polyethylene terephthalate membrane-containing cell culture inserts). Typically, efflux transporters such as MDR1 are preferentially expressed on the apical face of the cell, and the apparent permeability of a MDR1 substrate is substantially higher in the basolateral to apical direction relative to the apical to basolateral direction. In the transport assay, rates of drug permeation are measured in the two directions. A diagram of the assay is shown in Fig. 14.1. A polarization ratio is calculated as the apparent permeability in the basolateral to apical direction divided by the apparent permeability in the apical to basolateral direction. Polarization ratios greater than unity indicate active efflux

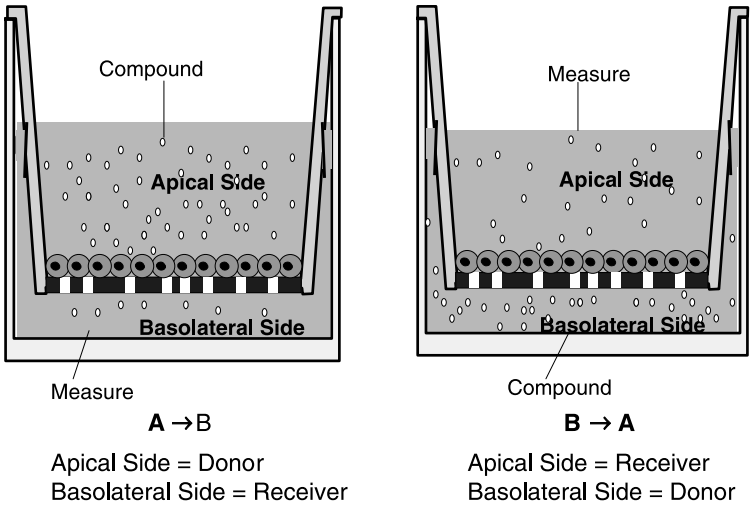

Fig. 14.1. Schematic representation of drug transport assay in cell monolayers cultured on a culture insert containing permeable membrane.

transport, whereas higher polarization ratios in cells modified to express a transporter, relative to control cells, indicate a role for the transporter. The parent compound is the analyte in these assays, and automation-compatible membrane insert systems (24-well) have been available for several years. More recently, 96-well insert systems have also been introduced.

For efflux transporters the functional interaction between the drug and transporter occurs in the intracellular space. Some substrates – particularly the negatively charged MRP2 substrates – are of very low permeability and, in the absence of an uptake transporter, may not produce detectable transport. In these cases, transport has been analyzed using membrane vesicles prepared from transfected (and control) cells [2, 3]. Generally, studies with membrane vesicles require the use of radiolabeled substrate material, but unfortunately this is generally not available for all compounds in a drug discovery/lead optimization program.

Two properties determine the value of a cell line as a particular host for cDNA expression:

1. The extent to which the cell line supports appropriate expression of the cDNA. The level of expression achieved is determined by interactions of the vector/expressed protein with the cell. These interactions include the strength of the promoter (weaker promoters can be compensated for by using a vector which is present at high copy number), the adequacy of the selective agent (not all agents are toxic to all cells), the stability of the expressed protein (some proteins may be rapidly degraded in some cells), and whether the expressed protein exerts any deleterious effects on the viability of host cells (some efflux transporters could deplete the cell of essential components). Finally, transporters must be expressed in a polarized manner in the host cell (i.e., preferentially on either the basolateral or apical side of the cell).
2. The extent to which the cell line is appropriate for drug metabolism and transport studies. If drug transport studies are to be performed, the cell line needs to form monolayers with tight cell–cell junctions. If cell–cell junctions are loose, background (or nontransporter-dependent) paracellular drug transport will be high. In addition, if a panel of cells expressing individual transporters is being developed, expression of any native drug-metabolizing enzymes or transporters should be low, as these native processes introduce background to the system.

Three cell lines, Caco-2, MDCK and LLC-PK_1, have been most commonly used for cDNA expression. All three of these cell lines have very low levels of oxidative drug metabolism, although variants of Caco-2, when cultured under appropriate conditions, have been reported to express significant levels of CYP3A subfamily enzymes [4, 5]. Caco-2 cells have been reported to express significant levels of a number of uptake and efflux transporters [6, 7]. Using putative MDR1 substrates, MDCK cells express substantially higher levels of native efflux transporters than LLC-PK_1 cells. All else being equal, the LLC-PK_1 model is preferred because it forms high-quality monolayers and has low levels of native transporters.

14.3 Expression of Individual Metabolizing Enzymes

Most interest has focused on the oxidative enzymes of the cytochrome P450 (CYP) class; these are expressed at highest levels in the liver, but are also expressed to a significant degree in the intestine. Conjugating enzymes are also expressed in the intestine [8]. Human intestine appears to be relatively rich in CYP3A4 (which is also abundant in the liver), and intestinal CYP3A4 can contribute significantly to the first-pass metabolism of drugs such as midazolam, cyclosporin A and verapamil [9]. Human intestine has also been reported to contain lower levels of CYP2D6 [10] and CYP1A1 [11]. However, because of low abundance, it appears unlikely that the presence of these latter two enzymes in the intestine significantly reduces oral bioavailability (relative to the impact of first-pass metabolism in the liver).

The catalytic activity of CYP enzymes requires functional coupling with its redox partners, cytochrome P450:NADPH oxidoreductase (OR) and cytochrome b_5. Measurable levels of these two proteins are natively expressed in most cell lines. Therefore, introduction of only the CYP cDNA is generally needed for detectable catalytic activity. However, the levels of expression of the redox partner proteins may not support maximal CYP catalytic activity, and therefore enhancement of OR levels may be desirable. This approach has been used successfully with an adenovirus expression system in LLC-PK_1 cells [12].

Because of its importance in first-pass metabolism, there has been considerable interest in introducing CYP3A4 into cell systems. This protein is not normally expressed in cell lines and was introduced into Caco-2 cells with the goal of improving this common screening model. The first reported expression of a drug-metabolizing enzyme in a drug permeability model was with CYP3A4 in Caco-2 cells [13]. CYP3A4 catalytic activities were increased about 100-fold relative to control cells, but were still well below that found in intestine. However, it was noted that expression of CYP3A4 markedly reduced the proliferative capacity of the Caco-2 cells (relative to CYP2A6-expressing and control cells). Nonetheless, expression of CYP3A4 did not alter transepithelial electrical resistance (TEER) values or the permeability of model compounds. Co-expressing OR did not substantially elevate CYP3A4 catalytic activity (on a milligram cellular protein basis) [14]. However, 4-fold and 16-fold higher catalytic activities were obtained using the same expression system with MDCK and LLC-PK_1 cells as hosts [15]. Similar, high levels of expression were obtained in the LLC-PK_1 model using an adenovirus vector [12].

The levels of CYP3A4 activity in LLC-PK_1 models appear to be comparable with those found in human intestine [15], and a significant first-pass effect has been observed as CYP3A4 substrates pass though monolayers. For example, in the LLC-PK_1 model, up to 19% of nifedipine was metabolized as it passed through the monolayer. The LLC-PK_1/CYP3A4 systems appear to be a reasonable model for assessing the extent of any first-pass effect during permeation through the intestine. However, given the modest amount of metabolite formed for nifedipine (a good CYP3A4 substrate), there appears to be little reason to adopt these cells as an

"improved" screening model. Alternative approaches, such as measuring the rates of parent compound loss in CYP3A4 microsomal incubations should be more informative.

Systems to study the role of intestinal oxidative metabolism (CYP3A4) have been developed and appear to have adequate enzyme activity levels. Although there appears to be a relatively limited need for additional system development in this area. there is still a fundamental question as to whether any synergistic interplay exists between metabolic enzymes and transporters (i.e., does the presence of an efflux transporter influence the extent of metabolism?) and co-expression of CYP3A4 and transporters provides a pivotal experimental model.

14.4 Expression of Transporters

14.4.1 Efflux Transporters

The identities and roles of many of the drug transporters are discussed in other chapters in this volume, and are not extensively reintroduced here. A goal is to develop a comprehensive panel of cells expressing individual, functional transporters as research reagents. To simplify data interpretation, the set of transporters should be expressed in the same host cell line and the abundance of functional proteins in the cell line should be known relative to the corresponding *in vivo* values. However, useful mechanistic data can be obtained from less comprehensive systems.

As stated earlier, there are many drug transporters expressed in the intestine (as determined at the mRNA level by polymerase chain reaction) [6, 7]. However, the protein levels have not yet been defined. The export proteins MDR1, MRP1 and MRP2 have been of particular interest because they are expressed at relatively high levels in the intestine [6, 7], and their known function is to efflux drugs. In addition, the peptide uptake transporter PepT1 also transports some drugs and can function to increase drug bioavailability (see Section 14.4.2).

The most extensively studied protein is MDR1, which is natively expressed in Caco-2 cells. MDCK and LLC-PK_1 cells expressing high levels of cDNA-derived human (and rodent) MDR1 have been developed in several laboratories [16, 17]. The development of these cell lines has been facilitated by the fact that MDR1 expression confers resistance to cytotoxic drugs such as vinblastine. This allows direct, growth selection of cells expressing high levels of MDR1.

MRP1 and MRP2 have been successfully expressed in MDCK cells [18]. Like MDR1, MRP1 expression can confer resistance to cytotoxic drugs, and this may facilitate the isolation of cells expressing high levels of functional protein. Many MRP2 substrates have very poor permeability, and when added to the extracellular space cannot reach the active site of the transporter. To overcome this issue, membrane vesicles were prepared from cDNA-expressing and control cells and

used to performed uptake studies [2, 3]. Vesicle preparation and vesicle assays are, however, labor-intensive. The issue of substrate access to the MRP2 active site has been addressed by co-expressing an uptake transporter, such as OATP2, which allows efficient access to the substrate within the intracellular space [19–21].

MDR1-expressing cells have been used extensively to study the extent and rates of drug transport. Generally, a larger polarization ratio (rate of drug permeation basolateral to apical divided by the rate of drug permeation apical to basolateral) in MDR1-expressing cells relative to control cells (or MDR1 cells incubated in the presence of a MDR1 inhibitor) is considered evidence for active transport by MDR1. Polarization ratio values are determined by both the drug-transporting activity of MDR1 in the system for transporting the drug of interest and the intrinsic permeability of the molecule. Compounds with higher intrinsic permeabilities give lower polarization ratios. Additionally, because transport processes are saturable, polarization ratios tend to decrease with increasing drug concentration. Therefore, care must be used in interpreting the significance of polarization ratio values.

There is a need to develop a framework to better understand the conditions under which efflux transporters will significantly modulate oral bioavailability. While it is clear that transport by MDR1 can reduce oral bioavailability, many successful, orally bioavailable drugs are *in vitro* substrates for efflux transporters such as MDR1 (e.g., digoxin, fexofenadine cyclosporin A, erythromycin). One *in vivo* indication of a role of MDR1 in oral bioavailability has been pharmacokinetic drug–drug interactions between MDR1 inhibitors and nonmetabolized MDR1 substrates such as digoxin and fexofenadine. Another *in vivo* manifestation may be nonproportional pharmacokinetics; for example, the high-affinity MDR1 substrate UK-343,664 (K_m 7.3 μM) shows no systemic exposure at doses below 10 mg, but between 30 and 800 mg the systemic exposure is increased about 250-fold [22]. It seems reasonable that there is a region defined by drug dose, drug permeability, efflux enzyme affinity and efflux enzyme activity where efflux transport will reduce oral bioavailability. Given that transporters are saturable, drugs administered at low doses and/or drugs with low intrinsic permeability are most likely to have lower oral bioavailability reduced by the action of efflux transporters. Data for more drug compounds are needed to define the combination of conditions that allow for the potential of MDR1 to significantly reduce oral bioavailability.

A clear priority remains to expand the panel of intestinal efflux transporters that are expressed individually in modified cell lines. These research tools will be instrumental in identifying and validating selective probe transporter substrates and inhibitors. The availability of such probes will allow for a better understanding of the influence of transporters on *in vivo* pharmacokinetics. A similar set of probes has been instrumental in increasing our understanding of the role that cytochrome P450 plays in human pharmacokinetics and in avoiding issues associated with these enzymes.

In addition, the availability of specific probes for transporters will allow the generation of data to create transporter structure activity models for the transporters [23], and this provide the ability to design rationally around any transporter-related

issues associated with a drug candidate series. There is a need to define the conditions (dose, intrinsic permeability, efflux transporter activity and affinity) which must be met in order for efflux transport to limit significantly the oral bioavailability. This will permit the analysis of transport and pharmacokinetic parameters for more compounds such as UK343,664.

14.4.2 Uptake Transporters

Some drugs with low intrinsic permeability achieve acceptable oral bioavailability because they are substrates for uptake transporters, which normally function in nutrient uptake. The most prominent example is the peptide transporter, PepT1, which is active toward peptidomimetic antibiotics such as cephalexin, the antiviral agent valacyclovir [24] and other drugs. PepT1 is natively expressed in Caco-2 cells, and adenovirus transduction has been used to increase PepT1 expression levels [25]. However, the expression of PepT1 was not polarized in this system and this expressed system appears to be of limited value as an ''improved'' screening model. PepT1 has also been expressed in Chinese hamster ovary cells and a variety of other mammalian systems [26, 27].

In addition to PepT1, there is a related renal transporter, PepT2. There are also a series of other uptake transporters (organic anion transporting polypeptides, organic anion transporters, organic cation transporters), which are expressed primarily in the liver and other tissues but are not known to affect oral bioavailability.

References

1 Nelson, J. A., Dutt, A., Allen, L. H., Wright, D. A., Functional expression of renal organic cation transporter and P-glycoprotein in *Xenopus laevis* oocytes, *Cancer Chemother. Pharmacol.* **1995**, *37*, 187–189.

2 Kinoshita, S., Suzuki, H., Ito, K., Shimizu, T., Sugiyama, Y., Transfected rat cMOAT is functionally expressed on the apical membrane of Madin–Darby canine kidney (MDCK) cells, *Pharm. Res.* **1998**, *15*, 1851–1856.

3 Evers, R., Kool, M., van Deemter, L., Janssen, H., Calafat, J., Oomen, L. C., Paulusma, C. C., Oude Elferink, R. P., Baas, F., Schinkel, A. H., Borst, P., Drug export activity of the human canalicular multispecific organic anion transporter in polarized kidney MDCK cells expression cMOAT (MRP2) cDNA, *J. Clin. Invest.* **1988**, *101*, 1310–1319.

4 Schmiedlin-Ren, P., Thummel, K. E., Fisher, J. M., Paine, M. F., Lown, K. S., Watkins, P. B., Expression of enzymatically active CYP3A4 in Caco-2 cells grown in extracellular matrix-coated permeable supports in the presence of 1-alpha,25-dihydroxyvitamin D3, *Mol. Pharmacol.* **1997**, *51*, 741–754.

5 Engman, H. A., Lennernas, H., Taipalensuu, J., Otter, C., Leidvik, B., Artursson, P., CYP3A4, CYP3A5 and MDR1 in human small and large intestine cell lines suitable for drug transport studies, *J. Pharm. Sci.* **2001**, *90*, 1736–1751.

6 Nakamura, T., Sakaeda, T., Ohomoto, N., Tamura, T., Aoyama, N., Shirakawa, T., Kamagaki, T., Nakamura, T., Kim, K. I., Kim, S. R., Kuroda, Y., Matsuo, M., Lasuga, M., Okumura, K., Real-time quantitative

polymerase chain reaction for MDR1, MRP1, MRP2m and CYP3A-mRNA levels in Caco-2 cell lines, human duodenal enterocytes, normal colorectal tissues and colorectal adenocarcinomas, *Drug Metab. Disp.* **2002**, *30*, 4–6.

7 Taipalensuu, J., Tornblom, H., Lindberg, G., Einarsson, C., Sjoqvist, F., Melhus, H., Garberg, P., Sjostrom, B., Lundgren, B., Artursson, P., Correlation of gene expression of ten efflux proteins of ATP-binding cassette transporter family in normal human jejunum and in human intestinal epithelial Caco-2 cell monolayers, *J. Pharmacol. Exp. Ther.* **2001**, *299*, 164–170.

8 Soars, M. G., Burchell, B., Riley, R. J., *In vitro* analysis of human drug glucuronidation and prediction of *in vivo* metabolic clearance, *J. Pharmacol. Exp. Ther.* **2002**, *301*, 382–390.

9 Paine, M. F., Khalighi, M., Fisher, J. M., Shen, D. D., Kunze, K. L., Marsh, C. L., Perkins, J. D., Thummel, K. E., Characterization of interintestinal and intraintestinal variations in human CYP3A-dependent metabolism, *J. Pharmacol. Exp. Ther.* **1997**, *283*, 1552–1562.

10 Madani, S., Paine, M. F., Lewis, L., Thummel, K. E., Shen, D. D., Comparison of CYP2D6 content and metoprolol oxidation between microsomes isolated from human livers and small intestines, *Pharm. Res.* **1999**, *16*, 1199–1205.

11 Paine, M. F., Schmiedlin-Ren, P., Watkins, P. B., Cytochrome P-450 1A1 expression in human small bowel: interindividual variation and inhibition by ketoconazole, *Drug. Metab. Disp.* **1999**, *27*, 360–364.

12 Brimer, C., Dalton, J. T., Zhu, Z., Schuetz, J., Yasuda, K., Vanin, E., Relling, M. V., Lu, Y., Schuetz, E. G., Creation of polarized cells coexpressing CYP3A4, NADPH cytochrome P450 reductase and MDR1/P-glycoprotein, *Pharm. Res.* **2000**, *17*, 803–810.

13 Crespi, C. L., Penman, B. W., Hu, M., Development of Caco-2 cells expressing high levels of cDNA-derived cytochrome P4503A4, *Pharm. Res.* **1996**, *13*, 1635–1641.

14 Hu, M., Li, Y., Davitt, C. M., Huang, S. M., Thummel, K., Penman, B. W., Crespi, C. L., Transport and metabolic characterization of Caco-2 cells expressing CYP3A4 and CYP3A4 plus oxidoreductase, *Pharm. Res.* **1999**, *16*, 1352–1359.

15 Crespi, C. L., Fox, L., Stocker, P., Hu, M., Steimel, D. T., Analysis of transport and metabolism in cell monolayer systems that have been modified by cytochrome P4503A4 cDNA-expression, *Eur. J. Pharm. Sci.* **2000**, *12*, 63–68.

16 Horio, M., Chin, K.-V., Currier, S. J., Goldenberg, S., Williams, C., Pastan, I., Gottesman, M. M., Handler, J., Transepithelial transport of drug by multidrug transporter in cultured Madin–Darby canine kidney cell epithelia, *J. Biol. Chem.* **1989**, *264*, 14880–14884.

17 Tanigawara, Y., Okamura, N., Hirai, M., Yasuhara, M., Ueda, K., Kioka, N., Komano, T., Hori, R., Transport of digoxin by human P-glycoprotein expressed in porcine kidney epithelial cell line (LLC-PK1), *J. Pharmacol. Exp. Ther.* **1992**, *263*, 840–845.

18 Guo, A., Marinaro, W., Hu, P., Sinko, P. J., Delineating the contribution of secretory transporters in the efflux of etoposide using Madin–Darby canine kidney (MDCK) cells overexpressing P-glycoprotein (Pgp), multidrug resistance-associate protein (MRP1) and canalicular multispecific organic anion transporter (cMOAT), *Drug Metab. Disp.* **2002**, *30*, 457–463.

19 Cvetkovic, M., Leake, B., Fromm, M. F., Wilkinson, G. R., Kim, R. B., OATP and P-glycoprotein transporters mediate the cellular uptake and excretion of fexofenadine, *Drug Metab. Disp.* **1999**, *27*, 866–871.

20 Cui, Y., Konig, J., Keppler, D., Vectorial transport by double-transfected cells expressing the human uptake transporter SLC21A8 and the apical export pump ABCC2, *Mol. Pharmacol.* **2001**, *60*, 934–943.

21 Sasaki, M., Suzuki, H., Ito, K., Abe, T., Sugiyama, Y., Transcellular transport of organic anions across double-transfected Madin–Darby canine kidney II cell monolayers expressing both human organic anion-transporting polypeptide (OATP2/SLC21A6) and Multidrug resistance-associated protein 2 (MRP2/ABCC2), *J. Biol. Chem.* **2002**, *277*, 6497–6503.

22 Abel, S., Beaumont, K. C., Crespi, C. L., Eve, M. D., Fox, L., Hyland, R., Jones, B. C., Muirhead, G. J., Smith, D. A., Venn, R. F., Walker, D. K., Potential role of P-glycoprotein in the non-proportional pharmacokinetics of UK-343-664 in man, *Xenobiotica* **2001**, *31*, 665–676.

23 Ekins, S., Kim, R. B., Leake, B. F., Dantzig, A. H., Schuetz, E. G., Lan, L. B., Yasuda, K., Shepard, R. L., Winter, M. A., Schuetz, J. D., Wikel, J. H., Wrighton, S. A., Applications of three-dimensional quantitative structure–activity relationships of P-glycoprotein inhibitors and substrates, *Mol. Pharmacol.* **2002**, *61*, 974–981.

24 Ganapathy, M. E., Huang, W., Wang, H., Ganapathy, V., Leibach, F. H., Valacyclovir: a substrate for the intestinal and renal peptide transporters PEPT1 and PEPT2, *Biochem. Biophys. Res. Commun.* **1998**, *246*, 470–475.

25 Hsu, C. P., Walter, E., Merkle, H. P., Rothen-Rutishauser, B., Wunderli-Allenpach, H., Hilfinger, J. M., Amidon, G. L., Functional and immunolocalization of overexpressed human intestinal H+/peptide cotransporter in Adenovirus-transduced Caco-2 cells, *AAPS Pharm. Sci.* **1999**, *1*, E12.

26 Covitz, K. M., Amidon, G. L., Sadee, W., Human dipeptide transporter, hPEPT1, stably transfected into Chinese hamster ovary cells, *Pharm. Res.* **1996**, *13*, 1631–1634.

27 Daniel, H., Nutrient transporter function studied in heterologous expression systems, *Ann. N. Y. Acad. Sci.* **2000**, *915*, 184–192.

IV
Computational Approaches to Drug Absorption and Bioavailability

Drug Bioavailability: Estimation of Solubility, Permeability, Absorption and Bioavailability.
Edited by Han van de Waterbeemd, Hans Lennernäs and Per Artursson

ISBN: 3-527-30438-X

15
Intestinal Absorption: the Role of Polar Surface Area

Per Artursson and Christel A. S. Bergström

Abbreviations

ADME	Absorption, distribution, metabolism, elimination (excretion)
BBB	Blood-brain barrier
BCS	Biopharmaceutics classification system
Caco-2	Adenocarcinoma cell line derived from human colon
CNS	Central nervous system
FDA	Food and Drug Administration
HTS	High through-put screening
NPSA	Non-polar surface area
PLS	Partial least squares projection to latent structures
PSA	Polar surface area
PSA_d	Dynamic polar surface area
PTSA	Partitioned total surface area
QSAR	Quantitative structure-activity relationship
$RMSE_{te}$	Root mean square error for the test set
$RMSE_{tr}$	Root mean square error for the training set
SMILES	Simplified molecular input line entry specification

Symbols

log *P*	Partition coefficient octanol/water
R^2	Coefficient of determination
Q^2	Cross-validated R^2
2-D	Two-dimensional
3-D	Three-dimensional
Å	Ångstrom ($1 \cdot 10^{-10}$ m)

15.1
Introduction

The development of predictive computational methods is one of the fastest growing disciplines in pharmacokinetics and absorption, distribution, metabolism,

Drug Bioavailability: Estimation of Solubility, Permeability, Absorption and Bioavailability.
Edited by Han van de Waterbeemd, Hans Lennernäs and Per Artursson

ISBN: 3-527-30438-X

elimination (i.e. excretion) (ADME) evaluation [1]. The reason for this growth is the realisation that, given the vast size of the chemical space of drug-like compounds (10^{18}–10^{64}, depending on the applied algorithm), drug discovery cannot be simplified to a "synthesise and test" lottery [2–4]. It is clearly not possible to cover the drug-like space even with state-of-the art *in vitro* high through-put screening (HTS) methods, which makes virtual screening of functions such as drug ADME an attractive alternative [5]. Inferior ADME properties are still being cited as the most important reason for failure of drug candidates in the clinical phase of drug development [6], and it has therefore been suggested that in the future, screening of ADME properties may even precede biological receptor activity screening [7].

At the present time many software packages devoted to ADME prediction, especially those predicting drug metabolism [8–10], are not yet fully developed and undergo constant evolution [11–14]. Consequently many of the existing computational approaches give at best rough predictions of ADME properties, resulting in qualitative ranking rather than absolute numbers. However, some quantitative *in silico* predictions are possible, especially with regard to drug permeability across epithelial and endothelial tissue barriers such as the intestinal epithelium and the endothelium of the blood-brain barrier (BBB) [4, 15–20]. In fact, there is an emerging consensus that the computer predictions of passive membrane permeability are no worse than predictions made using *in vitro* tests, such as artificial membranes or Caco-2 cells used for HTS [1]. In this regard, it must be remembered that although passive transmembrane permeability is still considered as the dominating pathway across epithelial and endothelial tissue barriers for most drugs, other pathways, such as the passive paracellular pathway and active carrier-mediated pathways, also play a significant role in intestinal absorption of many drugs. These drug transport pathways are still better predicted *in vitro* than *in silico* (see Chapter 4 by Artursson and Tavelin in this book).

In predicting drug absorption even before the candidate drugs are synthesised, theoretical models for properties such as intestinal permeability are warranted. Both two-dimensional (2-D) and three-dimensional (3-D) descriptors have proved to be useful for these permeability predictions [18, 19, 21–26]. The generation of these descriptors is quite different. To calculate 2-D descriptors either the 2-D structure or the simplified molecular input line entry specification (SMILES) [27] can be used as input. These representations identify atoms and functional groups and can be used for rapid generation of physicochemical properties such as number of hydrogen bonds [28], number of rotatable bonds [29], lipophilicity [30, 31], molecular weight and charge. The 2-D input can also be used for generation of electrotopological indices [32]. However, 2-D representation may provide incomplete information and the 3-D structure may be needed to incorporate information enclosed in the displayed conformation of the molecule in a certain environment. The generation of 3-D conformations can for instance reveal intramolecular interactions and the influence of molecular flexibility. Descriptors generated by methods such as molecular mechanics calculations include molecular surface area [33, 34], number of intramolecular hydrogen bonds, volume [34] and conformationally dependent lipophilicity [35]. Moreover, generation of 3-D descriptors by quantum mechanics calculations results in massive information on the electron distribution

of the molecule, which allows virtually all known computational descriptors to be calculated. The drawback of the 3-D descriptors in comparison with the 2-D-generated descriptors is the time needed for the calculations. While a single 3-D conformation is generated in a fraction of a second, a full molecular mechanics calculation of the low-energy conformations of a molecule with high flexibility can take days. If quantum mechanics is applied, the calculation is very time-consuming, taking hours, even if only one conformation is calculated. Nevertheless, both 2-D and 3-D-generated descriptors have shown applicability in property-based design, resulting in candidate drugs screened not only for pharmacological effect, but also for intestinal permeability [36].

Here we will discuss in depth two principally different methodologies used to develop predictive models of drug permeability, namely computer-based models built from i) a few easily interpretable properties; and ii) multivariate data analysis of several calculated descriptors. For a more comprehensive review of computational approaches to the prediction of intestinal drug permeability, the reader is referred to several recent reviews [5, 29, 37, 38]. We will briefly discuss simple physicochemical properties of drug molecules, such as lipophilicity, number of hydrogen bond forming groups and molecular weight [23, 26, 39–42], and their influence on passive drug permeability. We will focus especially on more recently suggested predictive descriptors for permeability, namely molecular surface properties [43–47] and molecular flexibility [29, 38]. The advantage of basing computational predictions on these easily interpretable parameters is that they are understood by a broader range of scientists than the computational chemists. The models also allow the construction of structure-property relationships or rule-based systems that can be broadly applied in drug discovery [3, 48, 49]. However, the drawback of using only one or even a few easily interpreted molecular properties is that with an increase in the diversity and size of the training set used for model development, the predictions obtained are fairly rough. Therefore, in order to build more generally applicable models, a larger number of molecular properties and more complex multivariate data analysis methods and/or neural networks are applied [16–20, 22, 50–52]. Using this approach, better models that predict intestinal permeability in a more quantitative manner can be obtained. A further development is to combine several of these models, using so-called ''consensus modelling''. The improved predictability of such models often results from the correction of outliers obtained by the different analysis methodologies. The drawback of the more complex models is that they become less transparent, which is why they often require interpretation by the expert user, the computational chemist.

In this chapter, we will, after giving a brief background to passive transcellular transport, discuss the advantages and limitations of easily comprehended molecular surface areas as predictors of intestinal drug absorption. First we will discuss the use of the polar surface area (PSA) as a simple predictor of intestinal drug permeability and give examples of the application of PSA in drug discovery. Then we will discuss how the total molecular surface area can be fragmented into smaller units which in combination with multivariate analysis give more predictive models of drug permeability of more complex datasets. Moreover, we will briefly discuss the use of these molecular surface areas in predictions of another impor-

tant drug property, aqueous drug solubility, involved in absorption. Finally, some future perspectives will be given on theoretical biopharmaceutical classification based on theoretical models for solubility and permeability.

15.2 Drug Transport Across the Intestinal Epithelium

Epithelial cells form tissue barriers which a drug taken orally must pass in order to distribute to the systemic blood circulation. A single layer of epithelial cells covers the interior of the intestinal wall and forms the barrier in the intestine. Although there are many other factors that limit the bioavailability of a drug (Fig. 15.1), the intestinal epithelium has proved in many cases to be rate-limiting for the absorption of registered orally administered drug molecules. It is for this reason that it is possible to estimate human intestinal absorption of drug molecules *in vitro* by using cell models such as Caco-2 cell monolayers [53–55].

There are two pathways by which a drug molecule can cross the epithelial cell: the transcellular pathway, which requires the drug to permeate the cell membranes, and the paracellular pathway, in which diffusion occurs through water-filled pores of the tight junctions between the cells. Both the passive and the active transport processes may contribute to the permeability of drugs via the transcellular pathway. These transport pathways are distinctly different, and the molecular properties that influence drug transport by these routes are also different (Fig.

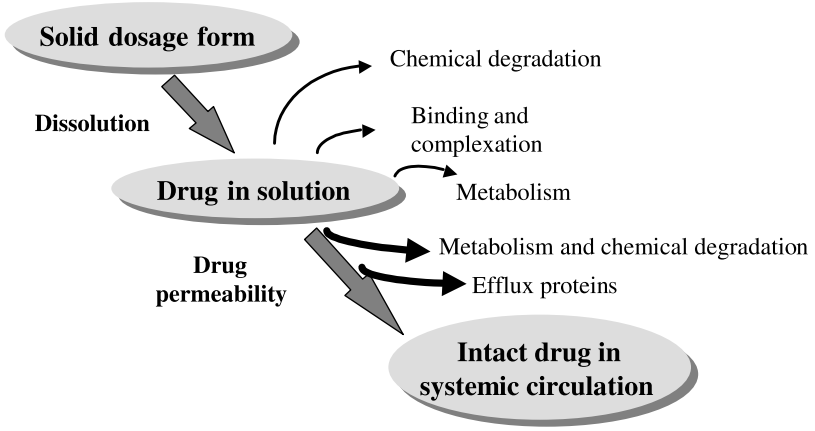

Fig. 15.1. Factors limiting oral drug absorption. Dissolution and the aqueous drug solubility in the gastrointestinal fluids are two of the properties influencing oral drug absorption. When the drug is in solution, it can be subjected to chemical degradation and complex binding with components of the gastrointestinal fluids and/or be metabolised by luminal enzymes. However, the dissolved state is a prerequisite for the compound to permeate the intestinal barrier. The permeability can be hindered by metabolism and chemical degradation in the gut wall and efflux systems located apically and/or baso-laterally in the enterocytes.

15.2). To develop computational models of drug permeability we therefore need to investigate which of these pathways and processes is the most important. One examination of the transport mechanisms for registered oral drugs has shown that the dominating (though not always the only) pathway remains the passive transmembrane pathway [56]. In certain cases there are other transport processes that contribute significantly to the transport; however, their contribution varies widely from region to region in the intestinal tract. Knowledge of passive transcellular permeability is therefore important also in these cases, especially since it is well known that drug molecules that are sufficiently lipophilic to distribute into the cell membrane and that can be desolvated with an acceptable energy cost will generally have a high passive transmembrane permeability [24, 55, 57, 58].

Let us conclude this section by proposing that provided that the drug is sufficiently soluble in the gastrointestinal fluids, the complex process of intestinal drug absorption can often be satisfactorily described by focusing on passive transport across the cell membrane, and that the development of models that predict passive transcellular permeability is particularly important. Such models are the focus of the remaining part of this chapter.

15.3
Passive Membrane Permeability and the Polar Surface Area

Passive transport across the cell membrane was initially believed to occur according to the solubility-diffusion model [59]. The cell membrane in this model is described as a homogeneous barrier, and the transport proceeds by distribution into and subsequent diffusion across the membrane. The pH-partitioning theory predicts that only the uncharged molecular species of protolytic drugs will partition into the membrane [60]. The transport process, according to the solubility-diffusion model and the pH-partitioning theory, is dependent on three properties: i) the partitioning between membrane and water; ii) the charge; and iii) the size of the solute (since the diffusion rate in the membrane is assumed to be dependent on the size of the solute).

The solubility-diffusion model assumes that membrane partitioning is a one-step process. This explains why drug partitioning in isotropic solvent systems such as the octanol/water system has been used frequently to predict passive membrane permeability [55, 61–64]. However, this assumption fails to take into account the anisotropic nature of the cell membrane [65]. Anisotropicity results in different diffusion rates of a drug substance in the various regions of the membrane [66] and in the forces governing the partitioning into the membrane being different in the different regions of the membrane [67]. In order to better understand the anisotropic nature of the membrane, membrane partitioning has been considered as a two-step process [68] and this model has been applied successfully to describe passive drug transport across the cell membrane [45].

The application of a two-step partitioning process can be motivated if we consider the insertion of a polar, but lipophilic, molecule into a phospholipid membrane. In the first step, lipophilicity is the major driving force for drug incorpora-

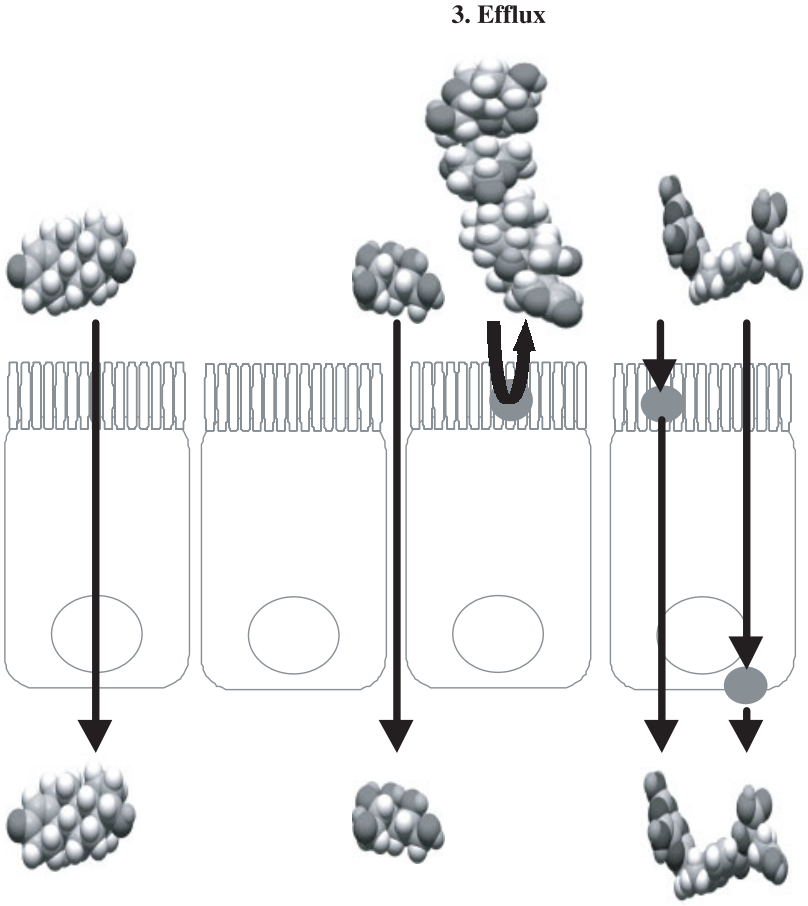

Fig. 15.2. Physicochemical molecular descriptors affect the transport route utilised across the intestinal epithelium. To passively diffuse through the membrane (1), the compound (here illustrated with testosterone) should preferably be small, with a molecular weight <500 Da, as well as uncharged and fairly lipophilic. However, compounds that are too lipophilic can stick to the membrane and will not pass through the cells. The paracellular route (2), here exemplified with mannitol, is mainly utilised by smaller (Mw < 200 Da) polar compounds that may also be charged. Compounds subjected to efflux (3), here shown using digoxin as example, may also be larger molecules with a molecular weight >500 Da, that display both large groups of polar atoms and non-polar atoms. The effluxed compound can either be charged or be a neutral species. Actively transported compounds (4) are generally medium-sized, hydrophilic molecules (illustrated with methotrexate). Both neutral and charged species can be transported.

tion into the phospholipid bilayer. By contrast, in the second step, in which the drug is transferred into the interior of the phospholipid bilayer, the interactions between the bilayer and the polar parts of the solute are more important than is the lipophilicity and can be largely accounted for by hydrogen bonding and polarity [67]. Support for this process is obtained from molecular dynamics simulations [65], which suggest that the partitioning of polar solutes into the dense apolar region of the membrane interior is a major barrier in the transport process [65, 67, 69]. Therefore, regardless of whether the solubility-diffusion model or a multiple-region membrane model is adopted to describe passive membrane permeability, the permeation rate is largely dependent on simple molecular descriptors such as hydrogen bond capacity, lipophilicity, size and charge of the molecule. This is why calculations of these descriptors have received particular attention in simple theoretical models of passive membrane permeability.

Since the calculations of hydrogen bond capacity are generally based on 2-D structures, we hypothesised that easily comprehended 3-D descriptors would be suitable for the construction of better computational models of drug absorption. A review of the literature showed that previously, molecular surface properties had been related to several physicochemical properties such as lipophilicity [70], solvation [71] and solubility [72]. With the two-step partitioning process, we speculated that the polar surface area (PSA), which is generally assumed to be related to hydrogen bonding capacity, would be a particularly good predictor of passive membrane permeability. Indeed, a search of the literature showed that this factor had already been introduced as a descriptor for blood-brain partitioning [73].

15.4
Generation of Molecular Surface Area Descriptors

We generate molecular surface properties, such as PSA and non-polar surface area (NPSA), from 3-D conformations obtained from Monte Carlo conformational analysis using molecular mechanics calculations. The analysis is performed to cover all low-energy conformations ($\Delta E_s < 2.5$ kcal mol^{-1}) of each compound, but in the screening mode any low-energy conformation may be used (see Section 15.5 below). The molecular surface areas of each conformation are calculated using the in-house program MAREA [34]. The generated 3-D conformation is imported into the program and a set of Van der Waals radii are used to calculate the free surface area and volume of each atom. The PSA is defined as the surface area occupied by oxygen and nitrogen, and hydrogen atoms bound to these heteroatoms, whereas NPSA is defined as the total surface area minus the PSA.

15.5
The Polar Surface Area and Its Application in Drug Discovery

Using small datasets we initially showed that the dynamic PSA (PSA_d), which is calculated from a Boltzman distribution of all low-energy conformations of the

molecule generated in molecular mechanics calculations, was strongly correlated ($R^2 = 0.99$) with the membrane permeability of a series of beta-blocking agents in Caco-2 cells [21]. The strong correlation between PSA_d and Caco-2 permeability of beta-blockers has thereafter been confirmed by others [44]. However, the finding that the PSA_d predicted the absorption (after oral administration to humans) of a set of 20 structurally diverse registered drugs, ranging in the absorbed fraction from 0.3% to 100%, was surprising [43]. For these compounds, a sigmoidal relationship was found between the PSA_d and the fraction absorbed ($R^2 = 0.94$).

From these results, it was concluded that drugs that are completely (>90%) absorbed should have a $PSA_d < 60\,Å^2$ and that a PSA_d of $>140\,Å^2$ results in unacceptably low (<10%) oral absorption. These findings were confirmed by Kelder *et al.* who calculated the PSA_d for more than 2000 oral drugs that had reached at least clinical Phase II efficacy studies [49]. Interestingly, these authors divided the drugs into oral non-central nervous system (non-CNS) drugs ($n = 1590$) and oral CNS drugs ($n = 776$). They concluded that orally active drugs that are transported passively by the transcellular route should not display a $PSA > 120\,Å^2$. Furthermore, since the oral CNS drugs were reported to be less polar than the non-CNS drugs, they also speculated that oral drugs can be tailored to brain penetration by decreasing the PSA to $<60–70\,Å^2$. The latter speculation was supported by the strong inverse relationship obtained between the measured brain penetration of 45 drugs and PSA, indicating that PSA can be used as a predictor of membrane permeability also in tissues other than the intestinal epithelium. A similar conclusion was reached by Clark, who derived a simple quantitative structure-activity relationship (QSAR) model for brain penetration from a combination of PSA and log *P* [47]. The finding that a smaller PSA is needed for the compound to permeate the BBB than for it to permeate the intestine makes sense, since the endothelial cell monolayer of the BBB forms a much tighter barrier than the intestinal epithelial cell barrier [55, 74].

Both Kelder with coworkers and Clark proposed that simpler approaches can be used for generating PSA, which would be more suitable for permeability screening [46, 47, 49]. Thus, Kelder and co-authors proposed that PSA is not very dependent on conformation and that a single, reasonably well-generated 3-D structure gives a "static" PSA, which is close to the value of the PSA_d [49]. Similarly, Clark proposed that the PSA of a single static conformer gives an excellent correlation with intestinal absorption data, and that the time-consuming conformational analysis required for calculation of the PSA_d can thus be saved [46, 47]. Although it was apparent from our initial work that the registered model drugs have a limited flexibility and, hence, limited variability in the conformations generated in the conformational analysis, we were initially reluctant to introduce this concept since our studies on more flexible drug molecules had indicated that conformational analysis was required to obtain good correlations [75]. Indeed, reduced flexibility, as measured by the number of rotable bonds, together with low PSA, has recently been reported as an important predictor of good oral bioavailability [29]. However, provided there is an awareness of the role of molecular flexibility, we support the proposal that single molecular conformers may be sufficient for calculating PSA of

molecular libraries in the high through-put mode [17]. Another issue concerns whether the conformers should be generated in vacuum or water. Surprisingly, also this parameter seems to be of limited importance, since strong correlations between vacuum and water generated conformations were observed in our laboratory, at least for compounds of limited flexibility ($R^2 = 0.99$) [17, 78]. However, we emphasize that the selection of medium will be more important when molecules with higher flexibility or molecules that may form intramolecular hydrogen bonds are to be studied.

The scatter in the correlations between PSA and transcellular membrane permeability will increase as the number of therapeutic classes studied increase and larger molecular libraries are investigated. The PSA has therefore been combined with other predictive molecular descriptors such as calculated log *P* [47, 51, 52] and the number of rotable bonds [29], or been included in rule-based systems [4] such as the rule of five [48], with good results. Likewise, in our earlier studies it became apparent that the simple calculation of PSA was not sufficient to describe the passive membrane permeability of some analogous series such as dipeptides and endothelin antagonists [45, 76]. However, rather than combining the PSA with a calculated lipophilicity measure, we continued to focus on the molecular surface area descriptors. Thus, the requirement of a hydrophobic component could be satisfied by using the NPSA and a linear combination of the PSA and NPSA was found to give satisfactory models [45, 76]. Collectively, these results suggested that a general model of membrane permeability would require consideration of several different structural properties of the drug rather than requiring a single descriptor such as PSA [26]. We therefore decided to deconvolute the PSA and establish whether the incorporation of other descriptors for molecular surface areas would result in more general, but still understandable, models of passive transmembrane permeability.

15.6 The Partitioned Total Surface Areas and Their Potential Application in the Drug Discovery Process

In order to find out what PSA actually represents, we deconvoluted it to various well-known, and presumably readily interpreted, physicochemical properties [17]. Various molecular properties related to lipophilicity, hydrogen bonding and charge were therefore calculated for a diverse training set of 128 drugs using quantum mechanics calculations. We utilised partial least squares projection to latent structures (PLS), a multivariate data analysis approach applying a linear regression methodology in the correlation between the response parameter and the descriptor space, to describe the PSA in terms of the calculated parameters. A second dataset of 69 compounds was used as a test set of the proposed model. The number rather than the strength of the hydrogen bonds was found to best describe PSA, while descriptors related to size and polarity were less important. The resulting PLS model showed that the number of hydrogen bond acceptors originating from oxy-

gen atoms, the number of hydrogen bond acceptors originating from nitrogen atoms, and the number of hydrogen bond donors accounted for 93% of the variance in PSA. Deconvolution of PSA therefore revealed a major role of the number of hydrogen bond moieties rather than the strength of the hydrogen bond interaction. Moreover, the limited role of molecular size and polarity in the description of the PSA gave further support to the notion that other molecular surface descriptors besides PSA are required in more general models of passive transmembrane permeability. This was supported by the finding that when the Caco-2 permeability to a very structurally diverse dataset (which apart from conventional drug molecules also included some peptide derivatives as well as some newer, more lipophilic drugs) was correlated to PSA, a fairly poor sigmoidal correlation ($R^2 = 0.63$) was obtained; and an even weaker correlation ($R^2 = 0.58$) was obtained when PSA, as predicted by the hydrogen bond count, was used [17].

We therefore investigated whether it was possible to further fragment the total molecular surface area [17], to result in permeability models based on so-called "partitioned total surface area (PTSA)". Each of the PTSA descriptors corresponds to the surface area of a certain type of atom. For example, the NPSA originating from carbon atoms can be partitioned into the surface areas of sp-, sp^2- and sp^3-hybridised carbon atoms and the hydrogen atoms bound to these carbon atoms. In a similar way, the PSA originating from oxygen atoms can be partitioned into the surface areas of single-bonded oxygen, double-bonded oxygen, and hydrogen atoms bound to single-bonded oxygen atoms (Fig. 15.3). Therefore, for the dataset used in

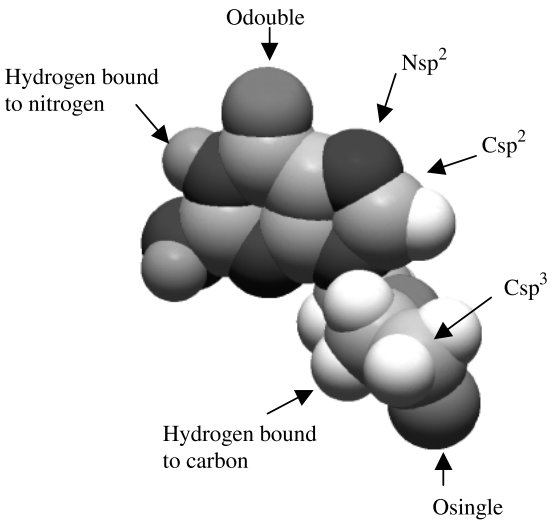

Fig. 15.3. Examples of partitioned total surface areas (PTSAs) included in the multivariate data analysis. The PTSAs represent the surface areas of each type of atom calculated with MAREA [34]. Polar surface area (PSA) is comprised of PTSAs of oxygen atoms, nitrogen atoms and hydrogen atoms bound to these heteroatoms. All other atom types are included in the non-polar surface area (NPSA).

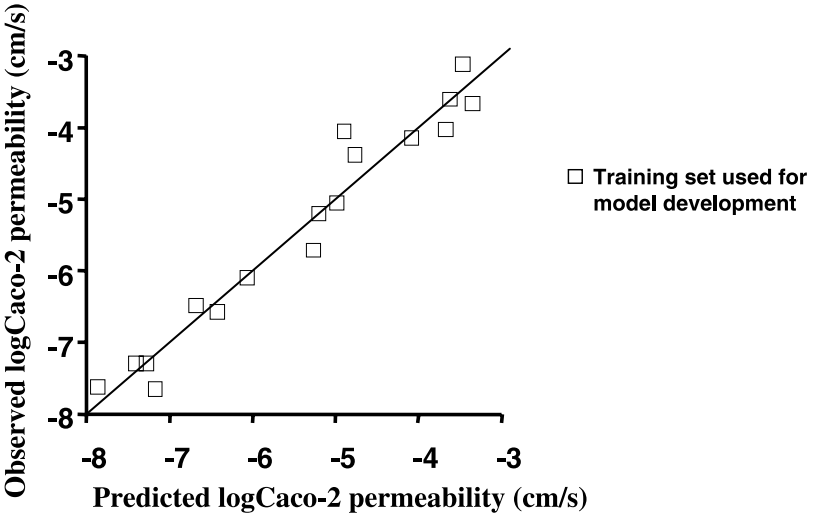

Fig. 15.4. Relationship between experimentally determined and PTSA-predicted Caco-2 permeability. PLS predicted permeability from PTSAs (predicted log Caco-2) is plotted versus experimentally obtained Caco-2 data (observed log Caco-2) [17]. The PTSAs used for the prediction were (in order of importance): PSA, fraction of total surface area that was polar (%PSA), the surface areas of double-bonded oxygen atoms, sp^3-hybridised nitrogen atoms, hydrogen atoms bound to oxygen atoms, sp^3-hybridised carbon atoms, single-bonded oxygen atoms and the NPSA and the saturated part of the NPSA. Therefore, six polar descriptors and three non-polar descriptors were used in the PLS model.

this study, 19 molecular surface properties were calculated from a single conformation. These were treated with PLS and variable selection, excluding the least important descriptors for permeability. In the model development the dataset was divided into a training set for model generation and a test set for model validation. The obtained model was also validated with the leave-one-out cross-validated R^2 (Q^2). Nine surface properties remained after the variable selection (Fig. 15.4). Despite the presence of oxygen, nitrogen and polar hydrogen surfaces in the model the most important descriptor for the prediction of the Caco-2 permeability to the drugs was PSA. The model also revealed that some non-polar descriptors contain information necessary for obtaining a permeability model of high accuracy. The explanatory power and internal predictivity of this PTSA model was excellent ($R^2 = 0.95$, $Q^2 = 0.86$, $RMSE_{tr} = 0.33$ log units $RMSE_{te} = 0.85$ log units) as compared with that of PSA alone ($R^2 = 0.63$) (Fig. 15.4) [17].

15.7 Future Perspectives and Conclusions

The promising results obtained with the PTSAs, together with the previously published relationships between molecular surface areas and other physicochemical

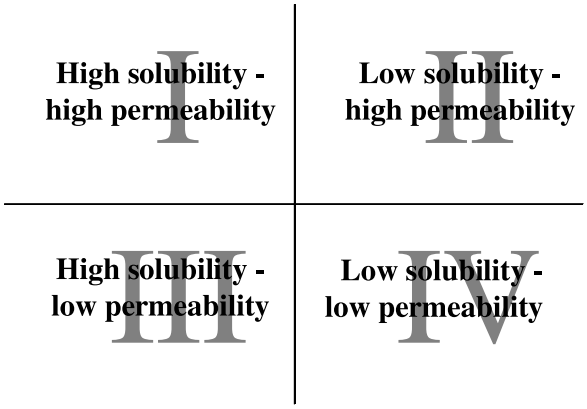

Fig. 15.5. The biopharmaceutics classification system (BCS). Drug-like molecules are grouped into four BCS classes based on their solubility and permeability. A drug is regarded as a highly soluble compound if the maximum dose given orally is soluble in 250 mL fluid in the pH interval 1–7.5. Permeability is defined as high if >90% of the given dose is absorbed in humans. Thus, compounds sorted as class I drugs get a ''green light'' for further development, whereas compounds sorted as class IV drugs receive a warning flag.

properties [70–72], prompted us to expand our work on these properties. Initially, we applied the PTSA concept in the prediction of drug solubility, with excellent results [77, 78]. So far only a limited number of compounds have been studied; however, preliminary results from larger datasets suggest that PTSA models with a predictive power comparable to other, more advanced theoretical solubility models can be constructed.

As can be seen in Fig. 15.1, both solubility and permeability are important factors that determine drug absorption. This fact has resulted in a biopharmaceutics classification system (BCS), which classifies the compounds into four classes depending on whether they have a high or low solubility and permeability (Fig. 15.5) [79] (see also Chapter 21 by Lennernäs in this book). The BCS has found wide application in the drug development and the US government's Food and Drug Administration (FDA) has recently published guidelines for bio-equivalence studies of generic drugs based on the BCS [80]. Although initially meant to be used in drug development, there is now an increasing interest in applying this classification system in drug discovery, since it is more informative than the currently used standards, such as the rule of five [48]. With the aim to adapt the BCS to a drug discovery setting format we studied a series of orally administered drugs ($n = 23$), and predicted the BCS class from calculated PTSAs only [78]. The PLS models generated for solubility and permeability resulted in correct biopharmaceutical classification for as many as 87% of the compounds, and an external test set comprised of FDA standard drugs for biopharmaceutical classification resulted in correct prediction of 77% [78].

In conclusion, descriptors of molecular surface area, such as PSA, NPSA and PTSAs, are important molecular descriptors influencing different properties such

as drug permeability and solubility. In developing models with a capacity to predict homologue series, we found that a few descriptors and multiple linear regression often result in high predictive accuracy of the dataset. However, to obtain more generally applicable models, with the capacity to predict permeability or solubility for structurally diverse datasets, we may need to perform multivariate data analysis of several descriptors. The preliminary results, namely that a combination of the theoretical PTSA models for solubility and permeability allows a computer-based biopharmaceutical classification, give further support to our hypothesis that molecular surface properties may, probably together with other molecular descriptors, find wider applications in computational pharmacokinetics and ADME evaluation than in prediction of passive membrane permeability. Whether such computational predictions will be used as a basis for the development of more advanced physiological models of such properties as oral drug bioavailability [81] remains to be seen.

Acknowledgement

This work was supported by grants from The Swedish National Board for Laboratory Animals (97-46), The Swedish Foundation for Research without Animal Experiments, The Swedish Research Council (9478), The Wallenberg Foundation, The Swedish Foundation for Strategic Research, AstraZeneca, Bristol-Myers Squibb and GlaxoSmithKline.

References

1 Boobis, A., Gundert-Remy, U., Kremers, P., Macheras, P., and Pelkonen, O., In silico prediction of ADME and pharmacokinetics: Report of an expert meeting organised by COST B15*, *Eur. J. Pharm. Sci.*, **2002**, *17*, 183–193 in press.

2 Lahana, R., How many leads from HTS? *Drug Discov. Today*, **1999**, *4*, 447–448.

3 Clark, D. E. and Pickett, S. D., Computational methods for the prediction of 'drug-likeness', *Drug Discov. Today*, **2000**, *5*, 49–58.

4 Pickett, S. D., McLay, I. M., and Clark, D. E., Enhancing the hit-to-lead properties of lead optimization libraries, *J. Chem. Inf. Comput. Sci.*, **2000**, *40*, 263–272.

5 Stenberg, P., Bergström, C. A. S., Luthman, K., and Artursson, P., Theoretical predictions of drug absorption in drug discovery and development, *Clin. Pharmacokin.*, **2002**, *41*, 877–899.

6 Kennedy, T., Managing the drug discovery/development interface, *Drug Discov. Today*, **1997**, *2*, 436–444.

7 Lipinski, C. A., Drug-like properties and the causes of poor solubility and poor permeability, *J. Pharmacol. Toxicol. Methods*, **2000**, *44*, 235–249.

8 de Groot, M. J. and Ekins, S., Pharmacophore modeling of cytochromes P450, *Adv. Drug Deliv. Rev.*, **2002**, *54*, 367–383.

9 Langowski, J. and Long, A., Computer systems for the prediction of xenobiotic metabolism, *Adv. Drug Deliv. Rev.*, **2002**, *54*, 407–415.

10 Keseruu, G. M. and Molnar, L., METAPRINT: a metabolic fingerprint. Application to cassette design for high-throughput ADME screening, *J. Chem. Inf. Comput. Sci.*, **2002**, *42*, 437–444.

11 Absolv solute property prediction version 1.2. For further information, visit http://www.sirius-analytical.com/absolv.htm.

12 QikProp. For further information, visit http://www.schrodinger.com/Products/qikprop.html.

13 GastroPlus. For further information visit http://www.simulations-plus.com.

14 iDEA™ Simulation System. For further information visit http://www.lionbioscience.com.

15 Ertl, P., Rohde, B., and Selzer, P., Fast calculation of molecular polar surface area as a sum of fragment-based contributions and its application to the prediction of drug transport properties, *J. Med. Chem.*, **2000**, *43*, 3714–3717.

16 Cruciani, G., Pastor, M., and Guba, W., VolSurf: a new tool for the pharmacokinetic optimization of lead compounds, *Eur. J. Pharm. Sci.*, **2000**, *11 Suppl 2*, S29–39.

17 Stenberg, P., Norinder, U., Luthman, K., and Artursson, P., Experimental and computational screening models for the prediction of intestinal drug absorption, *J. Med. Chem.*, **2001**, *44*, 1927–1937.

18 Österberg, T. and Norinder, U., Prediction of drug transport processes using simple parameters and PLS statistics. The use of ACD/log P and ACD/ChemSketch descriptors, *Eur. J. Pharm. Sci.*, **2001**, *12*, 327–337.

19 Norinder, U. and Österberg, T., Theoretical calculation and prediction of drug transport processes using simple parameters and partial least squares projections to latent structures (PLS) statistics. The use of electro-topological state indices., *J. Pharm. Sci.*, **2001**, *90*, 1076–1085.

20 Fujiwara, S., Yamashita, F., and Hashida, M., Prediction of Caco-2 cell permeability using a combination of MO-calculation and neural network, *Int. J. Pharm.*, **2002**, *237*, 95–105.

21 Palm, K., Luthman, K., Ungell, A.-L., Strandlund, G., and Artursson, P., Correlation of drug absorption with molecular surface properties, *J. Pharm. Sci.*, **1996**, *85*, 32–39.

22 Norinder, U., Österberg, T., and Artursson, P., Theoretical calculation and prediction of Caco-2 cell permeability using MolSurf parametrization and PLS statistics, *Pharm. Res.*, **1997**, *14*, 1786–1791.

23 Camenisch, G., Alsenz, J., van de Waterbeemd, H., and Folkers, G., Estimation of permeability by passive diffusion through Caco-2 cell monolayers using the drugs' lipophilicity and molecular weight, *Eur. J. Pharm. Sci.*, **1998**, *6*, 317–324.

24 Goodwin, J. T., Mao, B., Vidmar, T. J., Conradi, R. A., and Burton, P. S., Strategies toward predicting peptide cellular permeability from computed molecular descriptors, *J. Pept. Res.*, **1999**, *53*, 355–369.

25 Ekins, S., Waller, C. L., Swaan, P. W., Cruciani, G., Wrighton, S. A., and Wikel, J. H., Progress in predicting human ADME parameters in silico, *J. Pharmacol. Toxicol. Methods*, **2000**, *44*, 251–272.

26 Goodwin, J. T., Conradi, R. A., Ho, N. F., and Burton, P. S., Physicochemical determinants of passive membrane permeability: role of solute hydrogen-bonding potential and volume, *J. Med. Chem.*, **2001**, *44*, 3721–9.

27 Daylight Chemical Information Systems Inc. SMILES home page. http://www.daylight.com/dayhtml/smiles/index.html.

28 Raevsky, O., Hydrogen bond strength estimation by means of the HYBOT program package, in *Computer-assisted lead finding and optimization*, H. van de Waterbeemd, B. Testa and G. Folkers, eds, Verlag Helvetica Chimica Acta, Basel, **1997**, 367–378.

29 Veber, D. F., Johnson, S. R., Cheng, H.-Y., Smith, B. R., Ward, K. W., and Kopple, K. D., Molecular properties that influence the oral bioavailability of drug candidates, *J. Med. Chem.*, **2002**, *45*, 2615–2623.

30 Leo, A., Jow, P. Y. C., Silipo, C., and Hansch, C., Calculation of hydrophobic constant (log P) from Π and

f constants, *J. Med. Chem.*, **1975**, *18*, 865–868.

31 Rekker, R. F., *The hydrophobic fragmental constant.* Vol. 1., Elsevier Scientific Publishing Company, Amsterdam, **1977**.

32 Hall, L. H., Mohney, B., and Kier, L. B., The electrotopological state: structure information at the atomic level for molecular graphs, *J. Chem. Inf. Comput. Sci.*, **1991**, *31*, 76–82.

33 Lee, B. and Richards, F. M., The interpretation of protein structures: estimation of static accessibility, *J. Mol. Biol.*, **1971**, *55*, 379–400.

34 The program MAREA is available upon request from the authors. The program is provided free of charge for academic users. Contact Johan Gråsjö (e-mail johan.grasjo@farmaci.uu.se).

35 Testa, B., Carrupt, P.-A., Gaillard, P., Billois, F., and Weber, P., Lipophilicity in molecular modeling, *Pharm. Res.*, **1996**, *13*, 335–343.

36 van de Waterbeemd, H., Smith, D. A., Beaumont, K., and Walker, D. K., Property-based design: optimization of drug absorption and pharmacokinetics, *J. Med. Chem.*, **2001**, *44*, 1313–1333.

37 Egan, W. J. and Lauri, G., Prediction of intestinal permeability, *Adv. Drug Deliv. Rev.*, **2002**, *54*, 273–289.

38 Kulkarni, A., Han, Y., and Hopfinger, A. J., Predicting Caco-2 cell permeation coefficients of organic molecules using membrane-interaction QSAR analysis, *J. Chem. Inf. Comput. Sci.*, **2002**, *42*, 331–342.

39 Conradi, R. A., Hilgers, A. R., Ho, N. F., and Burton, P. S., The influence of peptide structure on transport across Caco-2 cells, *Pharm. Res.*, **1991**, *8*, 1453–1460.

40 van de Waterbeemd, H., The fundamental variables of the biopharmaceutics classification system (BCS): a commentary, *Eur. J. Pharm. Sci.*, **1998**, *7*, 1–3.

41 van de Waterbeemd, H., Camenisch, G., Folkers, G., Chrétien, J. R., and Raevsky, O. A., Estimation of blood-brain barrier crossing of drugs using molecular size and shape, and H-bonding descriptors, *J. Drug Target.*, **1998**, *6*, 151–165.

42 Ren, S. and Lien, E. J., Caco-2 cell permeability vs human gastrointestinal absorption: QSPR analysis, *Prog. Drug Res.*, **2000**, *54*, 1–23.

43 Palm, K., Stenberg, P., Luthman, K., and Artursson, P., Polar molecular surface properties predict the intestinal absorption of drugs in humans, *Pharm. Res.*, **1997**, *14*, 568–571.

44 Hjorth Krarup, L., Christensen, I. T., Hovgaard, L., and Frokjaer, S., Predicting drug absorption from molecular surface properties based on molecular dynamics simulations, *Pharm. Res.*, **1998**, *15*, 972–978.

45 Stenberg, P., Luthman, K., and Artursson, P., Prediction of membrane permeability to peptides from calculated dynamic molecular surface properties, *Pharm. Res.*, **1999**, *16*, 205–212.

46 Clark, D. E., Rapid calculation of polar molecular surface area and its application to the prediction of transport phenomena. 1. Prediction of intestinal absorption, *J. Pharm. Sci.*, **1999**, *88*, 807–814.

47 Clark, D. E., Rapid calculation of polar molecular surface area and its application to the prediction of transport phenomena. 2. Prediction of blood-brain barrier penetration, *J. Pharm. Sci.*, **1999**, *88*, 815–821.

48 Lipinski, C. A., Lombardo, F., Dominy, B. W., and Feeny, P. J., Experimental and computational approaches to estimate solubility and permeability in drug discovery and development settings., *Adv. Drug Deliv. Rev.*, **1997**, *23*, 3–25.

49 Kelder, J., Grootenhuis, P. D., Bayada, D. M., Delbressine, L. P., and Ploemen, J. P., Polar molecular surface as a dominating determinant for oral absorption and brain penetration of drugs, *Pharm. Res.*, **1999**, *16*, 1514–1519.

50 Wessel, M. D., Jurs, P. C., Tolan, J. W., and Muskal, S. M., Prediction of human intestinal absorption of drug compounds from molecular

structure, *J. Chem. Inf. Comput. Sci.*, **1998**, *38*, 726–735.

51 Egan, W. J., Merz, K. M., Jr., and Baldwin, J. J., Prediction of drug absorption using multivariate statistics, *J. Med. Chem.*, **2000**, *43*, 3867–3877.

52 Clark, D. E., Prediction of intestinal absorption and blood-brain barrier penetration by computational methods, *Comb. Chem. High Throughput Screen.*, **2001**, *4*, 477–496.

53 Hidalgo, I. J., Raub, T. J., and Borchardt, R. T., Characterization of the human colon carcinoma cell line (Caco-2) as a model system for intestinal epithelial permeability, *Gastroenterology*, **1989**, *96*, 736–749.

54 Artursson, P., Epithelial transport of drugs in cell culture. I: A model for studying the passive diffusion of drugs over intestinal absorptive (Caco-2) cells, *J. Pharm. Sci.*, **1990**, *79*, 476–482.

55 Artursson, P. and Karlsson, J., Correlation between oral drug absorption in humans and apparent drug permeability coefficients in human intestinal epithelial (Caco-2) cells, *Biochem. Biophys. Res. Commun.*, **1991**, *175*, 880–885.

56 Stenberg, P., Luthman, K., and Artursson, P., Virtual screening of intestinal drug permeability, *J. Contr. Rel.*, **2000**, *65*, 231–243.

57 Collander, R., The partition of organic compounds between higher alcohols and water, *Acta Chemica Scandinavica*, **1951**, *5*, 774–780.

58 Seiler, P., Interconversion of lipophilicities from hydrocarbon/water systems into octanol/water system, *Eur. J. Med. Chem.*, **1974**, *9*, 473–479.

59 Collander, R., The permeability of Nitella cells to non-electrolytes, *Physiol. Plant.*, **1954**, *7*, 420–445.

60 Shore, P. A., Brodie, B. B., and Hogben, C. A., The gastric secretion of drugs: a pH-partition hypothesis., *J. Pharmacol. Exp. Ther.*, **1957**, *119*, 361–369.

61 Martin, Y. C., A practioner's perspective of the role of quantitative structure-activity analysis in medicinal chemistry, *J. Med. Chem.*, **1981**, *24*, 229–237.

62 Schoenwald, R. D. and Huang, H.-S., Corneal penetration behavior of beta-blocking agents I: Physicochemical factors., *J. Pharm. Sci.*, **1983**, *72*, 1266–1271.

63 Anderson, B. D. and Raykar, P. V., Solute structure-permeability relationships in human stratum corneum, *J. Invest. Derm.*, **1989**, *93*, 280–286.

64 Potts, R. O. and Guy, R. H., Predicting skin permeability, *Pharm. Res.*, **1992**, *9*, 663–669.

65 Marrink, S. J. and Berendsen, H. J. C., Simulation of water transport through a lipid membrane, *J. Phys. Chem.*, **1994**, *98*, 4155–4168.

66 Bassolino, D., Alper, H., and Stouch, T. R., Drug-membrane interactions studied by molecular dynamics simulation: size dependence of diffusion, *Drug Des. Discov.*, **1996**, *13*, 135–141.

67 Jacobs, R. E. and White, S. E., The nature of the hydrophobic binding of small peptides at the bilayer interfaces: implications for the insertion of transbilayer helices, *Biochem.*, **1989**, *28*, 3421–3437.

68 Burton, P. S., Conradi, R. A., Hilgers, A. R., Ho, N. N. F., and Maggiora, L. L., The relationship between peptide structure and transport across epithelial cell monolayers, *J. Contr. Rel.*, **1992**, *19*, 87–98.

69 Tieleman, D. P., Marrink, S. J., and Berendsen, H. J. C., A computer perspective of membranes: molecular dynamics studies of lipid bilayer systems, *Biochim. Biophys. Acta.*, **1997**, *1331*, 235–270.

70 Dearden, J. C., Partitioning and lipophilicity in quantitative structure-activity relationships, *Environ. Health. Perspect.*, **1985**, *61*, 203–228.

71 von Freyberg, B., Richmond, T. J., and Braun, W., Surface area included in energy refinement of proteins. A comparative study on atomic solvation parameters, *J. Mol. Biol.*, **1993**, *233*, 275–292.

72 Yalkowsky, S. H., Valvani, S. C., and Amidon, G. L., Solubility of nonelectrolytes in polar solvents IV: nonpolar drugs in mixed solvents, *J. Pharm. Sci.*, **1976**, *65*, 1488–1494.

73 van de Waterbeemd, H. and Kansy, M., Hydrogen-bonding capacity and brain penetration, *Chimia*, **1992**, *46*, 299–303.

74 Pardridge, W. M., Brain drug delivery and blood-brain barrier transport, *Drug Deliv.*, **1996**, *3*, 99–115.

75 Palm, K., Luthman, K., Ungell, A.-L., Strandlund, G., Beigi, F., Lundahl, P., and Artursson, P., Evaluation of dynamic polar molecular surface area as predictor of drug absorption: comparison with other computational and experimental predictors, *J. Med. Chem.*, **1998**, *41*, 5382–5392.

76 Stenberg, P., Luthman, K., Ellens, H., Lee, C. P., Smith, P. L., Lago, A., Elliott, J. D., and Artursson, P., Prediction of the intestinal absorption of endothelin receptor antagonists using three theoretical methods of increasing complexity, *Pharm. Res.*, **1999**, *16*, 1520–1526.

77 Bergström, C. A. S., Norinder, U., Luthman, K., and Artursson, P., Experimental and computational screening models for the prediction of aqueous drug solubility, *Pharm. Res.*, **2002**, 182–188.

78 Bergström, C. A. S., Strafford, M., Lazorova, L., Avdeef, A., Luthman, K., and Artursson, P., Absorption classification of oral drugs based on molecular surface properties *J. Med. Chem.* **2003**, *46*, 558–570.

79 Amidon, G. L., Lennernäs, H., Shah, V. P., and Crison, J. R., A theoretical basis for a biopharmaceutic drug classification: the correlation of *in vitro* drug product dissolution an *in vivo* bioavailability, *Pharm. Res.*, **1995**, *12*, 413–420.

80 FDA, Guidance for Industry. Waiver of in vivo bioavailability and bioequivalence studies for immediate-release solid oral dosage forms based on a biopharmaceutics classification system. For further informatio, visit http://www.fda.gov/cder/guidance/index.htm.

81 Parrott, N. and Lavé, T., Prediction of intestinal absorption: comparative assessment of GASTROPLUS and IDEA, *Eur. J. Pharm. Sci.*, **2002**, *17*, 51–61.

16
Calculated Molecular Properties and Multivariate Statistical Analysis in Absorption Prediction

Ulf Norinder and Markus Haeberlein

Abbreviations

ADAPT	Automated data analysis and pattern recognition toolkit
AM1	Austin model 1
BCS	Biopharmaceutics classification system
CMC	Comprehensive medicinal chemistry
CoMFA	Comparative Molecular Field Analysis
E-state	Electrotopologcal state
MLR	Multiple linear regression
MRP	Multi-resistance protein
NN	Neural networks
P-gp	P-glycoprotein
PLS	Partial least squares
QSPR	Quantitative structure–property relationship
RMSE	Root mean squared error
RSD	Residual standard deviation
WDI	World Drug Index

Symbols

%FA	Percent fraction absorbed
A	Total area
ALOGP	Logarithm of the calculated octanol/water partition coefficient
c	Concentration
CLOGP	Logarithm of the calculated octanol/water partition coefficient
d	Density
J	Flux
log P	Logarithm of the measured octanol/water partition coefficient
m	Mass
MLOGP	Logarithm of the calculated octanol/water partition coefficient
MR	Molar refraction
MW	Molecular weight

Drug Bioavailability: Estimation of Solubility, Permeability, Absorption and Bioavailability.
Edited by Han van de Waterbeemd, Hans Lennernäs and Per Artursson

ISBN: 3-527-30438-X

n	Refractive index
P	Permeability
P_r	Parachor
PSA	Polar surface area, static PSA
PSA_d	Dynamic PSA
t	Time
TPSA	Topological PSA

16.1 Introduction

During the past five years, commencing with the publications of Lipinski and co-workers [1] and Palm and co-workers [2], a considerable amount of research has been performed in order to develop mathematical models for intestinal absorption in humans as well as other transport properties. The purpose of these investigations has been to develop computationally fast and accurate models for *in silico* electronic screening of large virtual compound libraries.

16.2 Descriptors Influencing Absorption

The intestinal wall is optimized to absorb fluids and nutrients while keeping away different xenobiotics. Which factors, from a theoretical point of view, are the most influential in intestinal absorption?

Let us start by applying Fick's first law to the flux through the intestinal wall. At each point i on the intestinal surface the flux J_i is:

$$J_i = c_i P_i \tag{1}$$

where c_i is the concentration of the drug at a point i. P_i is the permeability of the drug at the same point. Hence, the total mass m of absorbed drug at a time t can be written:

$$m(t) = \int_0^t \iint_A c_i P_i \, dA \, dt \tag{2}$$

where A is the total area of the intestinal tract. The fraction absorbed, %FA, is defined by the total mass absorbed divided by the given dose of the drug:

$$\%FA = \frac{m(\infty)}{Dose} \tag{3}$$

This brief simplified analysis shows that the absorption is mainly dependent on

the concentration at the intestinal wall, the permeability of the drug, and the given dose [3]. Let us analyze these three factors further.

16.2.1 Solubility

The concentration of the drug at a point *i* at the intestinal wall is dependent on the dissolution rate and the gastrointestinal transit. Optimally, the concentration of the drug is at its solubility. The dissolution rate of a drug molecule is affected by the energy difference between being surrounded by similar molecules (or molecules in the formulation) and being surrounded by solvent molecules. Hence, some influencing factors are formulation, particle size, particle aggregation, pH in different segments of the intestine, food content and the physico-chemical properties of the drug molecule itself. Considering these factors, one can expect a quite large variation for the same drug with different formulations in different subjects.

If we look at the physico-chemical factors governing solubility, among the first identified were log P [4] and melting point [5]. It can also theoretically be shown that these two factors describe solubility [6]. However, both these properties cannot be computed directly as molecular descriptors. It has been shown that solubility can be described more directly by molecular size, polarity and hydrogen bonding [7]. There are numerous studies on solubility predictions from directly computed descriptors (see Refs. [8–11]).

16.2.2 Membrane Permeability

The other mechanistically important component is the actual passage over the cell membrane. Before reaching the cell membrane, the drug molecule must diffuse through the unstirred water layer. However, theoretical considerations suggest that in most cases this diffusion is not the rate-limiting step for permeability. When at the cell wall, there are a number of different mechanisms for which a compound can be transported across the cell barrier, the most important being transcellular passive diffusion, paracellular diffusion, active transport with a transporter, and transcytosis. In addition, the drug can be metabolized at the cell wall by CYP3A4 and/or effluxed by P-gp or MRP.

For a theoretical model, each mechanism must be described in a very different way. If we restrict ourselves to discuss transcellular diffusion, there are numerous theoretical approaches, which differ depending on the underlying assumptions. In general, permeability is mainly dependent on lipophilicity, molecular weight and other factors [12]. If we use the findings from computational models on permeability measurements on cell lines, e.g., Caco-2 cells, the following factors are among the most important: polar surface area (PSA; hydrogen-bonding), polarity, molecular weight, size, shape, and degree of ionization (see e.g. Refs. [13–15]).

Amidon et al. devised a biopharmaceutics classification system (BCS) where they divided drugs into four different classes depending on their solubility and permeability:

- class 1 (high solubility, high permeability)
- class 2 (low solubility, high permeability)
- class 3 (high solubility, low permeability) and
- class 4 (low solubility, low permeability).

The rate-limiting step to drug absorption – and hence the factors affecting drug absorption – will differ depending on which class the drug belongs to. For example, for class 2 the rate-limiting step is dissolution and the permeability plays a minor role. On the other hand, for class 3 the permeability is rate-limiting and the dissolution has very little influence on the absorption.

Given the above-mentioned considerations, it is difficult to believe that it would be possible to fit drugs from all four classes into one single model. However, it is noteworthy that several molecular descriptors do highly influence both permeability and solubility. For example, it has been suggested that the four BCS classes can be divided solely by considering the molecular weight and PSA [16].

16.3 Datasets

The number of publicly available datasets with reasonable quality of data is quite limited. In this part of the chapter, we will list datasets related to intestinal absorption and oral availability, and of which we are aware at the present time.

16.3.1 The Palm Dataset

Palm and co-workers, as part of their research regarding the applicability of PSA, selected 20 compounds (Table 16.1) with quite reliable values for the percent fraction absorbed (%FA) in humans that were devoid of, or compensated for, problems such as active transport and efflux mechanisms [2]. The dataset consists of a variety of compounds: drugs, drug-like compounds, as well as sugar-like structures. A number of studies based on this dataset using various structural descriptions have been performed [2, 17–22].

16.3.2 The Wessel Dataset

Another set of compounds that have been collected and used for modeling human intestinal absorption is that of Wessel and co-workers [23]. This dataset consists

Tab. 16.1. Palm dataset.

#	*Compound*	*FA*	*logit(FA)*	*SMILES*
1	Alprenolol	96	2.024	c1(c(cccc1)CC=C)OCC(CNC(C)C)O
2	Atenolol	54	0.134	c1(ccc(cc1)CC(=O)N)OCC(CNC(C)C)O
3	Ciprofloxacin	69	0.656	c31c(cc(c(c1)N2CCNCC2)F)C(=O)C(=CN3C4CC4)C(=O)O
4	Diazepam	97	2.108	C1(=NCC(=O)N(c2c1cc(cc2)Cl)C)c3ccccc3
5	Foscarnet	17	−1.237	P(=O)(C(=O)O)(O)O
6	Lactulose	0.6	−2.334	C1(OC(C(C(=O)CO)O)C(CO)O)OC(C(C(C1O)O)O)CO
7	Mannitol	26	−0.847	C(C(C(CO)O)O)(C(CO)O)O
8	Metolazone	64	0.475	c21c(cc(c(c1)S(=O)(=O)N)Cl)NC(N(C2=O)c3c(cccc3)C)C
9	Metoprolol	102	2.639	c1(ccc(cc1)CCOC)OCC(CNC(C)C)O
10	Nordiazepam	99	2.293	c21c(ccc(c1)Cl)NC(=O)CN=C2c3ccccc3
11	Olsalazine	2.3	−2.17	c1(ccc(c(c1)C(=O)O)O)N=Nc2ccc(c(c2)C(=O)O)O
12	Oxazepam	97	2.108	c21c(ccc(c1)Cl)NC(=O)C(N=C2c3ccccc3)O
13	Oxprenolol	97	2.108	c1(c(cccc1)OCC=C)OCC(CNC(C)C)O
14	Phenazone	97	2.108	N2(c1ccccc1)N(C(=CC2=O)C)C
15	Pindolol	92	1.735	c21c([nH]cc1)cccc2OCC(CNC(C)C)O
16	Practolol	95	1.946	c1(ccc(cc1)NC(=O)C)OCC(CNC(C)C)O
17	Raffinose	0.3	−2.366	C3(OC2OC(COC1OC(C(C(C1O)O)O)O)CO)C(C(C2O)O)O)(OC(C(C3O)O)CO)CO
18	Sulpiride	36	−0.475	c1(c(ccc(c1)S(=O)(=O)N)OC)C(=O)NCC2N(CCC2)CC
19	Sulphasalazine	12	−1.494	c1(ccc(c(c1)C(=O)O)O)N=Nc2ccc(cc2)S(=O)(=O)Nc3ccccn3
20	Tranexamic acid	55	0.167	C1(CCC(CC1)CN)C(=O)O

of 86 drug and drug-like molecules (Table 16.2). A complication with this dataset is the fact that it contains some actively transported compounds, which should be removed before analysis (see Table 16.2). This dataset has also been used by various researchers [18, 24, 25].

16.3.3 The Egan Dataset

The Egan dataset is a literature compilation of 199 passively well-absorbed compounds (>90% intestinal absorption or >90% oral bioavailability) and 35 poorly absorbed compounds (<30% intestinal absorption). However, this compilation includes both the Palm dataset as well as the Wessel dataset, which means that Egan *et al.* added an additional 28 compounds from other literature sources. The original publication from Egan *et al.* [26] did not reveal the identity of those additional compounds; however, Table 16.3 represents a compilation of the compounds used (courtesy of the authors and Pharmacopeia [27]). Egan and co-workers have used this data set in a classification analysis of intestinal absorption [26].

16.3.4 Yoshida Dataset

Yoshida and Topliss compiled a dataset of 232 structurally diverse drugs (Table 16.4) and evaluated the possibility of constructing a predictive model for human oral bioavailability on categorical data [28]. The bioavailability data were classified into four categories:

- Class 1: <20% bioavailability
- Class 2: 20–49% bioavailability
- Class 3: 50–79% bioavailability
- Class 4: >80% bioavailability

16.4 Computational Models of Absorption

16.4.1 Rule-of-5

Probably the most widely adopted and well-known method for estimating the likelihood of a compound (drug) being well absorbed is the "rule-of-5" described by Lipinski and co-workers [1]. In analyzing 2245 compounds from the World Drug Index (WDI) database that were either considered for, or entered into, Phase II clinical trials, these authors developed the following rules:

Poor absorption is likely whenever two or more of the following rules are invoked

Tab. 16.2. Wessel dataset.

Name	*non-passive transport*	*%FA experimental*	*%FA calculated*	*SMILES*
gentamicin		0	0	C2(C(C(OC1OC(CCC1N)C(NC)C)C(CC2N)N)O)OC3C(C(C(CO3)(C)O)NC)O
cromolyn		0.5	0	C4(=O)c1c(cccc1OCC(COc2c3c(ccc2)OC(=CC3=O)C(=O)O)O)OC(=C4)C(=O)O
olsalazine		2.3	4.82	c1(c(ccc(c1)N=Nc2cc(c(cc2)O)C(=O)O)O)C(=O)O
ganciclovir		3.8	6.21	c21c(ncn1COC(CO)CO)C(=O)NC(=N2)N
cefuroxime		5	0	N21C(=O)C(C1SCC(=C2C(=O)O)COC(=O)N)NC(=O)C(=NOC)c3occc3
chlorothiazide		13	20.99	S2(=O)(=O)c1cc(c(cc1N=CN2)Cl)S(=O)(=O)N
mannitol		15	16.05	C(C(C(CO)O)O)(C(CO)O)O
nadolol		34.5	36	c21c(cccc1OCC(CNC(C)(C)C)O)CC(C(C2)O)O
norfloxacin		35	53.63	C3(=CN(c1c(cc(c(c1)N2CCNCC2)F)C3=O)CC)C(=O)O
phenoxymethylpenicillinic acid		45	43.89	N31C(C(C1=O)NC(=O)COc2ccccc2)SC(C3C(=O)O)(C)C
etoposide	×	50	51.65	C43C(c1c(cc2c(c1)OCO2)C(C3C(=O)OC4)c5cc(c(c(c5)OC)OP(=O)(O)O)OC)OC6C(C(C7C(O6)COC(O7)C)O)O
atenolol		50	79.62	C(=O)(Cc1ccc(cc1)OCC(CNC(C)C)O)N
ziprasidone		60	70.32	c1(nsc2c1cccc2)N5CCN(CCc3c(cc4c(c3)CC(=O)N4)Cl)CC5
sulfasalazine		65	65.9	S(=O)(=O)(Nc1ncccc1)c2ccc(cc2)N=Nc3cc(c(cc3)O)C(=O)O
hydrochlorothiazide		67	62.08	c21c(cc(c(c1)S(=O)(=O)N)Cl)NCNS2(=O)=O
sumatriptan		75	74.76	S(=O)(=O)(Cc2cc1c(c[nH]c1cc2)CCN(C)C)NC
guanabenz		75	85.03	c1(c(cccc1Cl)Cl)C=NNC(=N)N
propylthiouracil		75	100	N1C(=S)NC(=CC1=O)CCC
quinidine		80	95.07	c21c(ccnc1ccc(c2)OC)C(C3N4CC(C(C3)CC4)C=C)O
acetaminophen		80	100	c1(ccc(cc1)O)NC(=O)C
methylprednisolone		82	95.86	C42C1C(C(CC1)(C(=O)CO)O)(CC(C2C3(C(=CC(=O)C=C3)C(C4)C)C)O)C
sorivudine		82	99.56	N2(C1C(C(C(O1)CO)O)O)C(=O)NC(=O)C(=C2)C=CBr
bupropion		87	83.05	C(=O)(c1cc(ccc1)Cl)C(NC(C)(C)C)C

trovoflaxicin		88	95.12	c41c(cc(c(n1)N2CC3C(C2)C3N)F)C(=O)C(=CN4c5c(cc(cc5)F)F)C(=O)O
acrivastine		88	100	C(=CCN1CCCC1)(c2nc(ccc2)C=CC(=O)O)c3ccc(cc3)C
acebutolol		89.5	93.02	c1(c(ccc(c1)NC(=O)CCC)OCC(CNC(C)C)O)C(=O)C
timolol maleate		90	77.43	c1(c(nsn1)OCC(CNC(C)(C)C)O)N2CCOCC2
phenytoin		90	91.79	C1(=O)NC(=NC1(c2ccccc2)c3ccccc3)O
betaxolol		90	95.1	C1CC1COCCc2ccc(cc2)OCC(CNC(C)C)O
oxprenolol		90	95.35	O(c1c(cccc1)OCC=C)CC(CNC(C)C)O
scopolamine		90	95.58	C21C(O1)C3N(C2CC(C3)OC(=O)C(c4ccccc4)CO)C
propranolol		90	95.77	c21c(cccc1cccc2)OCC(CNC(C)C)O
tenidap		90	96.78	N2(C(=O)C(=C(c1sccc1)O)c3c2ccc(c3)Cl)C(=O)N
chloramphenicol		90	100	[N+](=O)(c1ccc(cc1)C(C(NC(=O)C(Cl)Cl)CO)O)[O−]
terazosin		91	93.87	c1(nc(c2c(n1)cc(c(c2)OC)OC)N)N4CCN(C(=O)C3OCCC3)CC4
hydrocortisone		91	96.3	C41(C(C(=O)CO)(CCC1C3C(C2(C(=CC(=O)CC2)CC3)C)C(C4)O)O)C
amoxicillin	×	93.5	88.82	N31C(C(C1=O)NC(=O)C(c2ccc(cc2)O)N)SC(C3C(=O)O)(C)C
fluconazole		95	89.66	C(c1c(cc(cc1)F)F)(Cn2ncnc2)(Cn3ncnc3)O
metoprolol		95	90.89	N(CC(COc1ccc(cc1)CCOC)O)C(C)C
sotalol		95	91.53	S(=O)(=O)(Nc1ccc(cc1)C(CNC(C)C)O)C
clonidine		95	96.02	C2(=Nc1c(cccc1Cl)Cl)NCCN2
imipramine		95	96.3	N2(c1c(cccc1)CCc3c2cccc3)CCCN(C)C
labetalol		95	100	c1(cc(ccc1O)C(CNC(CCc2ccccc2)C)O)C(=O)N
trimethoprim		97	93.34	n1c(c(cnc1N)Cc2cc(c(c(c2)OC)OC)OC)N
cephalexin		98	84.95	N21C(=O)C(C1SCC(=C2C(=O)O)C)NC(=O)C(c3ccccc3)N
warfarin		98	100	C2(=C(c1c(cccc1)OC2=O)O)C(CC(=O)C)c3ccccc3
prednisolone		98.8	96.5	C41(C(C(=O)CO)(CCC1C3C(C2(C(=CC(=O)C=C2)CC3)C)C(C4)O)O)C
naproxen		99	100	c2(cc1c(cc(cc1)OC)cc2)C(C(=O)O)C
practolol		100	74.79	c1(ccc(cc1)NC(=O)C)OCC(CNC(C)C)O
loracarbef		100	78.23	N31C(C(C1=O)NC(=O)C(c2ccccc2)N)CCC(=C3C(=O)O)Cl
fluvastatin		100	88.13	c1(n(c3c(c1-c2ccc(cc2)F)cccc3)C(C)C)C=CC(CC(CC(=O)O)O)O
antipyrine		100	91.79	N2(c1ccccc1)N(C(=CC2=O)C)C

Tab. 16.2. *(continued)*

Name	*non-passive transport*	*%FA experimental*	*%FA calculated*	*SMILES*
caffeine		100	92.02	c21c(n(cn1)C)C(=O)N(C(=O)N2C)C
lormetazepam		100	92.7	c21c(ccc(c1)Cl)N(C(=O)C(N=C2c3c(cccc3)Cl)O)C
bumetanide		100	93.89	c1(c(cc(cc1S(=O)(=O)N)C(=O)O)NCCCC)Oc2ccccc2
testosterone		100	93.97	C32C(C1(C(=CC(=O)CC1)CC2)C)CCC4(C3CCC4O)C
corticosterone		100	94.14	C31C(C2C(CC1O)(C(CC2)C(=O)CO)C)CCC4=CC(=O)CCC43C
felodipine		100	95.29	C1(=C(NC(=C(C1c2c(c(ccc2)Cl)Cl)C(=O)OC)C)C)C(=O)OCC
prazosin		100	95.37	c41c(nc(nc1N)N2CCN(CC2)C(=O)c3ccco3)cc(c(c4)OC)OC
ondansetron		100	95.65	c21c4c(n(c1CCC(C2=O)Cn3c(ncc3)C)C)cccc4
desipramine		100	96.24	N2(c1c(cccc1)CCc3c2cccc3)CCCNC
dexamethasone		100	96.35	C43(C(C2C(C1(C(=CC(=O)C=C1)CC2)C)(C(C3)O)F)CC(C4(C(=O)CO)O)C)C
ibuprofen		100	97.14	C(=O)(C(c1ccc(cc1)CC(C)C)C)O
valproic acid		100	98.6	C(CCC)(CCC)C(=O)O
acetylsalicylic acid		100	100	c1(c(cccc1)OC(=O)C)C(=O)O
ketoprofen		100	100	c1(cc(ccc1)C(C(=O)O)C)C(=O)c2ccccc2
zidovudine	×	100	100	C2(N1C(=O)NC(=O)C(=C1)C)CC(C(O2)CO)N=[N+]=[N−]
Cross-Validation Set				
enalaprilat		10	47.68	N2(C(=O)C(NC(C(=O)O)CCc1ccccc1)C)C(C(=O)O)CCC2
pravastatin		34	41.06	C21=CC(CC(C1C(CCC(CC(CC(=O)O)O)O)C(C=C2)C)OC(=O)C(CC)C)O
ranitidine		50	76.56	[N+](=O)(C=C(NC)NCCSCc1oc(cc1)CN(C)C)[O−]
furosemide		61	89.25	S(=O)(=O)(c1cc(c(cc1Cl)NCc2occc2)C(=O)O)N
lamotrigine		70	87.27	c1(c(nc(nn1)N)N)-c2c(c(ccc2)Cl)Cl
bromazepam		84	87.38	c21c(ccc(c1)Br)NC(=O)CN=C2c3ncccc3
pindolol		90	95.11	c21c([nH]cc1)cccc2OCC(CNC(C)C)O
diazepam		100	86.7	c21c(ccc(c1)Cl)N(C(=O)CN=C2c3ccccc3)C
methotrexate	×	100	100	c31c(ncc(n1)CN(c2ccc(cc2)C(=O)NC(CCC(=O)O)C(=O)O)C)nc(nc3N)N

External Prediction Set				
doxorubicin		5	0	c51c(c(c2c(c1O)CC(CC2OC3OC(C(C(C3)N)O)C)(C(=O)CO)O)O)C(=O)c4c(cccc4OC)C5=O
lisinopril	×	25	0	N2(C(=O)C(NC(C(=O)O)CCc1ccccc1)CCCCN)C(C(=O)O)CCC2
cefuroxime axetil	×	36	9.76	N21C(=O)C(C1SCC(=C2C(=O)OC(OC(=O)C)C)COC(=O)N)NC(=O)C(=NOC)c3occc3
gabapentin		50	51.36	C(=O)(CC1(CN)CCCCC1)O
captopril		67	100	N1(C(=O)C(CS)C)C(C(=O)O)CCC1
cefatrizine	×	76	73.98	N31C(C(C1=O)NC(=O)C(c2ccc(cc2)O)N)SCC(=C3C(=O)O)CSc4cnn[nH]4
cimetidine		85	76.53	N(=C(NC)NCCSCc1nc[nH]c1C)C#N
progesterone		91	93.99	C43(C(C2C(C1(C(=CC(=O)CC1)CC2)C)CC3)CCC4C(=O)C)C
alprenolol		93	95.95	C(=NO)(COc1c(cccc1)CC=C)CNC(C)C
salicylic acid		100	100	c1(c(cccc1)O)C(=O)O

Tab. 16.3. Egan dataset.

Structure Name	*CODE*	*% Absorbed*	*Absolute Oral Bioavailability*	*SMILES*
ACEBUTOLOL	0	89.5	37	c1(c(cc(cc1)NC(=O)CCC)C(=O)C)OCC(CNC(C)C)O
ACETYLPROCAINAMIDE	0		92	c1(ccc(cc1)NC(=O)C)C(=O)NCCN(CC)CC
ACETYLSALICYLIC-ACID	0	100	68	c1(c(cccc1)OC(=O)C)C(=O)O
ALPRENOLOL	0	93	9	c1(c(cccc1)CC=C)OCC(CNC(C)C)O
AMANTADINE	0	well	95	C21(CC3CC(C1)CC(C2)C3)N
AMINOCAPROIC-ACID	0	complete		C(CC(=O)O)CCCN
AMINOGLUTETHIMIDE	0	complete		C2(c1ccc(cc1)N)(C(=O)NC(=O)CC2)CC
AMOSULALOL	0		100	c1(cc(ccc1C)C(CNCCOc2c(cccc2)OC)O)S(=O)(=O)N
AMOXICILLIN	1	93.5	93	N31C(C(C1=O)NC(=O)C(c2ccc(cc2)O)N)SC(C3C(=O)O)(C)C
AMRINONE	0		93	C1(=CNC(=O)C(=C1)N)c2ccncc2
ANTIPYRINE	0	97		N2(c1ccccc1)N(C(=CC2=O)C)C
BEPRIDIL	0	complete	60	N(c1ccccc1)(CC(N2CCCC2)COCC(C)C)Cc3ccccc3
BETAXOLOL	0	95		c1(ccc(cc1)CCOCC2CC2)OCC(CNC(C)C)O
BISOPROLOL	0	well	91	c1(ccc(cc1)COCCOC(C)C)OCC(CNC(C)C)O
BUMETANIDE	0	100	66	c1(c(cc(cc1S(=O)(=O)N)C(=O)O)NCCCC)Oc2ccccc2
CAFFEINE	0	100	100	c21c(ncn1C)N(C(=O)N(C2=O)C)C
CAMAZEPAM	0	99		c21c(ccc(c1)Cl)N(C(=O)C(N=C2c3ccccc3)OC(=O)N(C)C)C
CANRENOATE-POTASSIUM	0		100	C43C2C(C1(C(=CC(=O)CC1)C=C2)C)CCC3(C(CC4)(CCC(=O)[O−])O)C
CARBAMAZEPINE	0	almost complete	75–85	N2(c1c(cccc1)C=Cc3c2cccc3)C(=O)N
CEFACLOR	1	well	90	N31C(C(C1=O)NC(=O)C(c2ccccc2)N)SCC(=C3C(=O)O)Cl
CEFADROXIL	1	100	78–90	N31C(C(C1=O)NC(=O)C(c2ccc(cc2)O)N)SCC(=C3C(=O)O)C
CEFAMANDOLE	1		96	N31C(C(C1=O)NC(=O)C(c2ccccc2)O)SCC(=C3C(=O)O)CSc4n(nnn4)C
CEFAZOLIN	1		>90	N31C(C(C1=O)NC(=O)Cn2cnnn2)SCC(=C3C(=O)O)CSc4sc(nn4)C
CEFPROZIL	1	95	90	N31C(C(C1=O)NC(=O)C(c2ccc(cc2)O)N)SCC(=C3C(=O)O)C=CC
CEPHALEXIN	1	98	90	N31C(C(C1=O)NC(=O)C(c2ccccc2)N)SCC(=C3C(=O)O)C
CEPHRADINE	1		94	N31C(C(C1=O)NC(=O)C(C2=CCC=CC2)N)SCC(=C3C(=O)O)C

CHLORAMBUCIL	0	complete	73–102	c1(ccc(cc1)CCCC(=O)O)N(CCCl)CCCl
CHLORAMPHENICOL	0	90	69	c1(ccc(cc1)[N+](=O)[O−])C(C(NC(=O)C(Cl)Cl)CO)O
CHLORDIAZEPOXIDE	0		100	c21c(ccc(c1)Cl)N=C(C[N+](=C2c3ccccc3)[O−])NC
CHLOROQUINE	0	almost complete	89–98	c21c(nccc1NC(CCCN(CC)CC)C)cc(cc2)Cl
CHLORPROPAMIDE	0	rapid	118	c1(ccc(cc1)Cl)S(=O)(=O)NC(=O)NCCC
CICLOPROLOL	0		100	c1(ccc(cc1)OCCOCC2CC2)OCC(CNC(C)C)O
CISAPRIDE	0	100	40–50	c1(c(cc(c(c1)Cl)N)OC)C(=O)NC2C(CN(CC2)CCCOc3ccc(cc3)F)OC
CLOFIBRATE	0	96	95	c1(ccc(cc1)Cl)OC(C(=O)OCC)(C)C
CLONAZEPAM	0	complete	98	c21c(ccc(c1)[N+](=O)[O−])NC(=O)CN=C2c3c(cccc3)Cl
CLONIDINE	0	95	95	c1(c(cccc1Cl)Cl)N=C2NCCN2
CLOPREDNOL	0		complete	C42C1C(C(CC1)(C(=O)CO)O)(CC(C2C3(C(=CC(=O)C=C3)C(=C4)Cl)C)O)C
CLOZAPINE	0	almost complete		C2(=Nc1c(ccc(c1)Cl)Nc3c2cccc3)N4CCN(CC4)C
CODEINE	0	95	55	C532c1c4c(ccc1CC(C2C=CC(C3O4)O)N(CC5)C)OC
CORTICOSTERONE	0	100		C31C(C2C(CC1O)(C(CC2)C(=O)CO)C)CCC4=CC(=O)CCC43C
COUMARIN	0	100		c21c(cccc1)C=CC(=O)O2
CYCLOPHOSPHAMIDE	0		90–96	P1(=O)(N(CCCl)CCCl)NCCCO1
DAPSONE	0	complete	93(8)	S(=O)(=O)(c1ccc(cc1)N)c2ccc(cc2)N
DESIPRAMINE	0	100	38	N2(c1c(cccc1)CCc3c2cccc3)CCCNC
DEXAMETHASONE	0	100	78	C31(C(C2C(CC1O)(C(C(C2)C)(C(=O)CO)O)C)CCC4=CC(=O)C=CC43C)F
DIAZEPAM	0	97	98	C1(=NCC(=O)N(c2c1cc(cc2)Cl)C)c3ccccc3
DIAZOXIDE	0		86–96	c21c(cc(cc1)Cl)S(=O)(=O)NC(=N2)C
DICLOFENAC	0	100	58	c1(c(cccc1)CC(=O)[O−])Nc2c(cccc2Cl)Cl
DIFLUNISAL	0	complete	100	c1(c(cc(cc1)F)F)-c2cc(c(cc2)O)C(=O)O
DIGITOXIN	1		>90	C76(C1C(C2(C(CC1)CC(CC2)OC3CC(C(C(O3)C)OC4CC(C(C(O4)C)OC5CC(C(C(O5)C)O)O)O)O)C)CCC6(C(CC7)C8=CC(=O)OC8)C)O
DIGOXIN	1	95	70	C31(C(C(CC1)C2=CC(=O)OC2)(C(CC4C3CCC5C4(CCC(C5)OC6CC(C(C(O6)C)OC7CC(C(C(O7)C)OC8CC(C(C(O8)C)O)O)O)O)C)O)C)O
DILTIAZEM	0	92	44	C2(C(C(=O)N(c1c(cccc1)S2)CCN(C)C)OC(=O)C)c3ccc(cc3)OC
DOFETILIDE	0	99		c1(ccc(cc1)CCN(CCOc2ccc(cc2)NS(=O)(=O)C)C)NS(=O)(=O)C
DONEPEZIL	0	complete		c21c(cc(c(c1)OC)OC)CC(C2=O)CC3CCN(CC3)Cc4ccccc4

Tab. 16.3. *(continued)*

Structure Name	*CODE*	*% Absorbed*	*Absolute Oral Bioavailability*	*SMILES*
DOXYCYCLINE	1	93		C41C(C(=C3C(C1O)C(c2c(c(ccc2)O)C3=O)C)O)(C(=O)C(=C(C4N(C)C)O)C(=O)N)O
DRONABINOL	0	90		C32c1c(cc(cc1O)CCCCC)OC(C2CCC(=C3)C)(C)C
ENOXACIN	0	well	87	c31c(cc(c(n1)N2CCNCC2)F)C(=O)C(=CN3CC)C(=O)O
ETHINYL-ESTRADIOL	0	100	43	C21C(C(CC1)(C#C)O)(CCC3C2CCc4c3ccc(c4)O)C
ETHIONAMIDE	0	complete		c1(cc(ncc1)CC)C(=S)N
ETHOSUXIMIDE	0		100	C1(C(=O)NC(=O)C1)(CC)C
FELODIPINE	0	100	16	C2(c1c(c(ccc1)Cl)Cl)C(=C(NC(=C2C(=O)OC)C)C)C(=O)OCC
FENCLOFENAC	0	100		c1(c(cccc1)CC(=O)O)Oc2c(cc(cc2)Cl)Cl
FENFLURAMINE	0		89	c1(cc(ccc1)C(F)(F)F)CC(NCC)C
FLAVOXATE	0		90	c31c(cccc1C(=O)OCCN2CCCCC2)C(=O)C(=C(O3)c4ccccc4)C
FLUCONAZOLE	0	95	>90	c1(c(cc(cc1)F)F)C(Cn2cncn2)(Cn3cncn3)O
FLUCYTOSINE	0	90	84	C1(=NC(=O)NC=C1F)N
FLUMAZENIL	0	95		n-21c(c(nc1)C(=O)OCC)CN(C(=O)c3c-2ccc(c3)F)C
FLUORESCEIN	0		99	C42(c1c(cccc1)C(=O)O2)c3c(cc(cc3)O)Oc5c4ccc(c5)O
FLURBIPROFEN	0		92	c1(c(cc(cc1)C(C(=O)O)C)F)-c2ccccc2
FLUTAMIDE	0	complete		c1(c(ccc(c1)NC(=O)C(C)C)[N+](=O)[O-])C(F)(F)F
FLUVASTATIN	0	100		c1(c2c(n(c1C=CC(CC(CC(=O)O)O)O)C(C)C)cccc2)-c3ccc(cc3)F
GEMFIBROZIL	0	well	98	c1(c(ccc(c1)C)C)OCCCC(C(=O)O)(C)C
GITOXIN	1		95	C76(C1C(C2(C(CC1)CC(CC2)OC3CC(C(C(O3)C)OC4CC(C(C(O4)C)OC5CC(C(C(O5)C)O)O)O)O)C)CCC6(C(C(C7)O)C8=CC(=O)OC8)C)O
GLIMEPIRIDE	0	100		N1(C(=O)C(=C(C1)C)CC)C(=O)NCCc2ccc(cc2)S(=O)(=O)NC(=O)NC3CCC(CC3)C
GLIPIZIDE	0	100	100	c1(ccc(cc1)CCNC(=O)c2cnc(cn2)C)S(=O)(=O)NC(=O)NC3CCCCC3
GLYBURIDE	0	well	64–90	c1(c(ccc(c1)Cl)OC)C(=O)NCCc2ccc(cc2)S(=O)(=O)NC(=O)NC3CCCCC3
GRANISETRON	0	100		c21c(nn(c1cccc2)C)C(=O)NC3CC4N(C(C3)CCC4)C

GRISEOFULVIN	0		95	C32(C(=O)c1c(c(c(cc1OC)OC)Cl)O2)C(=CC(=O)CC3C)OC
HEXOBARBITAL	0		>90	C2(C1=CCCCC1)(C(=O)N(C(=O)NC2=O)C)C
HYDROCORTISONE	0	91		C43C2C(C1(C(=CC(=O)CC1)CC2)C)C(CC3(C(CC4)(C(=O)CO)O)C)O
HYDROXYCHLOROQUINE	0	complete		c21c(nccc1NC(CCCN(CCO)CC)C)cc(cc2)Cl
HYOSCYAMINE	0	complete		C1(CC2N(C(C1)CC2)C)OC(=O)C(c3ccccc3)CO
IBUPROFEN	0	100		c1(ccc(cc1)CC(C)C)C(C(=O)O)C
IMIPRAMINE	0	95		N2(c1c(cccc1)CCc3c2cccc3)CCCN(C)C
INDOMETHACIN	0	90	98	c31c(c(c(n1C(=O)c2ccc(cc2)Cl)C)CC(=O)O)cc(cc3)OC
IRBESARTAN	0	complete		C51(C(=O)N(C(=N1)CCCC)Cc2ccc(cc2)-c3c(cccc3)-c4[nH]nnn4)CCCC5
ISONIAZID	0	almost complete		c1(ccncc1)C(=O)NN
ISOSORBIDE-MONONITRATE	0	almost complete	100	C21C(C(CO1)O)OCC2O[N+](=O)[O−]
ISRADIPINE	0	90		C3(c1c2c(ccc1)non2)C(=C(NC(=C3C(=O)OC)C)C)C(=O)OC(C)C
KETOPROFEN	0	100	85	c1(cc(ccc1)C(C(=O)O)C)C(=O)c2ccccc2
KETOROLAC	0	100		n31c(ccc1C(=O)c2ccccc2)C(CC3)C(=O)O
LABETALOL	0	95	18	c1(cc(c(cc1)O)C(=O)N)C(CNC(CCc2ccccc2)C)O
LAMOTRIGINE	0	98		c1(c(nc(nn1)N)N)-c2c(c(ccc2)Cl)Cl
LETROZOLE	0	complete		C(c1ccc(cc1)C#N)(c2ccc(cc2)C#N)n3cncn3
LEVODOPA	1	100	41	c1(c(ccc(c1)CC(C(=O)O)N)O)O
LEVOFLOXACIN	0	95		c21c3c(c(cc1C(=O)C(=CN2C(CO3)C)C(=O)O)F)N4CCN(CC4)C
LEVOLEUCOVORIN-CALCIUM	1		97	C31=C(NCC(N1C=O)CNc2ccc(cc2)C(=O)NC(CCC(=O)[O−])C(=O)[O−])NC(=NC3=O)N
LEVONORGESTREL	0	99.7	94	C41(C(C3C(CC1)C2C(=CC(=O)CC2)CC3)CCC4(C#C)O)CC
LOMEFLOXACIN	0	95	97	c31c(cc(c(c1F)N2CC(NCC2)C)F)C(=O)C(=CN3CC)C(=O)O
LORACARBEF	0	90	94	N31C(C(C1=O)NC(=O)C(c2ccccc2)N)CCC(=C3C(=O)O)Cl
LORAZEPAM	0		93	C1(=NC(C(=O)Nc2c1cc(cc2)Cl)O)c3c(cccc3)Cl
LORMETAZEPAM	0	100		c21c(ccc(c1)Cl)N(C(=O)C(N=C2c3c(cccc3)Cl)O)C
MECAMYLAMINE	0	almost complete		C1(C2CC(C1(C)C)CC2)(NC)C
METHADONE	0		92	C(c1ccccc1)(c2ccccc2)(CC(N(C)C)C)C(=O)CC
METHIMAZOLE	0		93	C1(=S)N(C=CN1)C
METHOTREXATE	1	100	70	c31c(ncc(n1)CN(c2ccc(cc2)C(=O)NC(CCC(=O)O)C(=O)O)C)nc(nc3N)N

Tab. 16.3. *(continued)*

Structure Name	*CODE*	*% Absorbed*	*Absolute Oral Bioavailability*	*SMILES*
METOPROLOL	0	95	50	c1(ccc(cc1)CCOC)OCC(CNC(C)C)O
METRONIDAZOLE	0		99	n1(c(cnc1C)[N+](=O)[O−])CCO
MEXILETINE	0	90		c1(c(cccc1C)C)OCC(C)N
MIDODRINE	0		93	c1(c(ccc(c1)OC)OC)C(CNC(=O)CN)O
MILRINONE	0		92	C1(=C(NC(=O)C(=C1)C#N)C)c2ccncc2
MINOCYCLINE	1	100	100	C41C(C(=C3C(C1)Cc2c(c(ccc2N(C)C)O)C3=O)O)(C(=O)C(=C(C4N(C)C)O)C(=O)N)O
MIRTAZAPINE	0	complete		N42C(c1c(cccc1)Cc3c2nccc3)CN(CC4)C
MYCOPHENOLATE-MOFETIL	0		94	c31c(c(c(c(c1C)OC)CC=C(CCC(=O)OCCN2CCOCC2)C)O)C(=O)OC3
NAPROXEN	0	99		c21c(cc(cc1)OC)ccc(c2)C(C(=O)O)C
NEFAZODONE	0	complete		N1(C(=NN(C1=O)CCCN2CCN(CC2)c3cc(ccc3)Cl)CC)CCOc4ccccc4
NEVIRAPINE	0	90		N2(c1c(c(ccn1)C)NC(=O)c3c2nccc3)C4CC4
NIACIN	0	almost complete		c1(cccnc1)C(=O)O
NIFEDIPINE	0	complete	50	C2(c1c(cccc1)[N+](=O)[O−])C(=C(NC(=C2C(=O)OC)C)C)C(=O)OC
NILUTAMIDE	0	complete		N2(c1cc(c(cc1)[N+](=O)[O−])C(F)(F)F)C(=O)C(NC2=O)(C)C
NITROFURANTOIN	0		100	N1(CC(=O)NC1=O)N=Cc2oc(cc2)[N+](=O)[O−]
NIZATIDINE	0	100		c1(nc(cs1)CSCCNC(=C[N+](=O)[O−])NC)CN(C)C
NORDAZEPAM	0	99		C1(=NCC(=O)Nc2c1cc(cc2)Cl)c3ccccc3
OFLOXACIN	0	complete	100	c21c3c(c(cc1C(=O)C(=CN2C(CO3)C)C(=O)O)F)N4CCN(CC4)C
ONDANSETRON	0	100	62	c21c4c(n(c1CCC(C2=O)Cn3c(ncc3)C)C)cccc4
OXAPROZIN	0		95–100	c1(c(oc(n1)CCC(=O)O)-c2ccccc2)-c3ccccc3
OXATOMIDE	0	99		C(N1CCN(CC1)CCCN3c2c(cccc2)NC3=O)(c4ccccc4)c5ccccc5
OXAZEPAM	0	97	97	c21c(ccc(c1)Cl)NC(=O)C(N=C2c3ccccc3)O
OXPRENOLOL	0	97	24–60	c1(c(cccc1)OCC=C)OCC(CNC(C)C)O
PAROXETINE	0	complete		C3(C(COc1cc2c(cc1)OCO2)CNCC3)c4ccc(cc4)F
PEFLOXACIN	0		80–110	c31c(cc(c(c1)N2CCN(CC2)C)F)C(=O)C(=CN3CC)C(=O)O

PENBUTOLOL	0	complete		c1(c(cccc1)OCC(CNC(C)(C)C)O)C2CCCC2
PENTOBARBITAL	0		94	C1(C(=O)NC(=O)NC1=O)(C(CCC)C)CC
PENTOXIFYLLINE	0	almost complete	19–31	c21c(ncn1C)N(C(=O)N(C2=O)CCCCC(=O)C)C
PHENIRAMINE	0		120	C(c1ccccc1)(c2ccccn2)CCN(C)C
PHENOBARBITAL	0		100	C2(c1ccccc1)(C(=O)NC(=O)NC2=O)CC
PHENYLBUTAZONE	0		80–100	N2(N(c1ccccc1)C(=O)C(C2=O)CCCC)c3ccccc3
PHENYLETHYLMALONAMIDE	0		91	C(c1ccccc1)(C(=O)N)(C(=O)N)CC
PHENYTOIN	0	90	90	C3(c1ccccc1)(c2ccccc2)NC(=O)NC3=O
PINDOLOL	0	90	75	c21c([nH]cc1)cccc2OCC(CNC(C)C)O
PIRAZOLAC	0		88–99	c1(c(nn(c1)-c2ccc(cc2)F)CC(=O)O)-c3ccc(cc3)Cl
PIROXICAM	0		100	c21c(cccc1)S(=O)(=O)N(C(=C2O)C(=O)Nc3ccccn3)C
PRACTOLOL	0	95	100	c1(ccc(cc1)NC(=O)C)OCC(CNC(C)C)O
PRAMIPEXOLE	0		>90	c21c(sc(n1)N)CC(CC2)NCCC
PRAZEPAM	0	complete	>90	c21c(cc(cc1)Cl)C(=NCC(=O)N2CC3CC3)c4ccccc4
PRAZOSIN	0	100	68	c41c(nc(nc1N)N2CCN(CC2)C(=O)c3ccco3)cc(c(c4)OC)OC
PREDNISOLONE	0	98.8	82	C43C2C(C1(C(=CC(=O)C=C1)CC2)C)C(CC3(C(CC4)(C(=O)CO)O)C)O
PRIMAQUINE	0		96	c1(c2c(cc(c1)OC)cccn2)NC(CCCN)C
PRIMIDONE	0		92	C2(c1ccccc1)(C(=O)NCNC2=O)CC
PROBENECID	0	complete	100	c1(ccc(cc1)C(=O)O)S(=O)(=O)N(CCC)CCC
PROGESTERONE	0	91		C31C(C2C(CC1)(C(CC2)C(=O)C)C)CCC4=CC(=O)CCC43C
PROPAFENONE	0	almost complete	5–12	c1(c(cccc1)C(=O)CCc2ccccc2)OCC(CNCCC)O
PROPRANOLOL	0	90	26	c21c(cccc1cccc2)OCC(CNC(C)C)O
PROXYPHYLLINE	0		100	c21c(ncn1CC(C)O)N(C(=O)N(C2=O)C)C
PSEUDOEPHEDRINE	0	almost complete		c1(ccccc1)C(C(NC)C)O
QUININE	0		109	c21c(ccnc1ccc(c2)OC)C(C3N4CC(C(C3)CC4)C=C)O
REPAGLINIDE	0	complete		c1(c(cccc1)C(NC(=O)Cc2cc(c(cc2)C(=O)O)OCC)CC(C)C)N3CCCCC3
RIFAMPIN	1	100		c21c4c5c(c(c1c(c(c(c2O)C=NN3CCN(CC3)C)NC(=O)C(=CC=CC(C(C(C(C(C(C(C(=COC(C4=O)(O5)C)OC)C)OC(=O)C)C)O)C)O)C)C)O)O)C
RILUZOLE	0	90		C(Oc1cc2c(cc1)nc(s2)N)(F)(F)F
RIZATRIPTAN	0	complete		c21c([nH]cc1CCN(C)C)ccc(c2)Cn3cncn3

Tab. 16.3. *(continued)*

Structure Name	*CODE*	*% Absorbed*	*Absolute Oral Bioavailability*	*SMILES*
SACCHARIN	0	97		c21c(cccc1)C(=O)NS2(=O)=O
SALICYLIC-ACID	0	100	100	c1(c(cccc1)O)C(=O)O
SCOPOLAMINE	0	90		C21C(O1)C3N(C2CC(C3)OC(=O)C(c4ccccc4)CO)C
SELEGILINE	0	readily		c1(ccccc1)CC(N(CC#C)C)C
SOTALOL	0	95	90–100	c1(ccc(cc1)NS(=O)(=O)C)C(CNC(C)C)O
SPARFLOXACIN	0		92	c31c(c(c(c(c1F)N2CC(NC(C2)C)C)F)N)C(=O)C(=CN3C4CC4)C(=O)O
SULFADIAZINE	0		100	c1(ccc(cc1)N)S(=O)(=O)Nc2ncccn2
SULFAMETHOXAZOLE	0	95	100	c1(ccc(cc1)N)S(=O)(=O)Nc2cc(on2)C
SULFINPYRAZONE	0	complete	100	N2(N(c1ccccc1)C(=O)C(C2=O)CCS(=O)c3ccccc3)c4ccccc4
SULFISOXAZOLE	0		96	c1(ccc(cc1)N)S(=O)(=O)Nc2c(c(no2)C)C
SULINDAC	0	90		c21c(cc(cc1)F)C(=C(C2=Cc3ccc(cc3)S(=O)C)C)CC(=O)O
SUPROFEN	0		92	c1(ccc(cc1)C(C(=O)O)C)C(=O)c2cccs2
TAMSULOSIN	0	90		c1(c(ccc(c1)CC(NCCOc2c(cccc2)OCC)C)OC)S(=O)(=O)N
TEMAZEPAM	0		91	c21c(ccc(c1)Cl)N(C(=O)C(N=C2c3ccccc3)O)C
TENIDAP	0	90		C3(=C(c1cccs1)O)c2c(ccc(c2)Cl)N(C3=O)C(=O)N
TERAZOSIN	0	91	90	c41c(nc(nc1N)N2CCN(CC2)C(=O)C3CCCO3)cc(c(c4)OC)OC
TESTOSTERONE	0	100		C32C(C1(C(=CC(=O)CC1)CC2)C)CCC4(C3CCC4O)C
THEOPHYLLINE	0	98	96	c21c(nc[nH]1)N(C(=O)N(C2=O)C)C
TIACRILAST	0	99		c21c(ccc(c1)SC)N=CN(C2=O)C=CC(=O)O
TIAGABINE	0	95		C(=CCCN1CC(CCC1)C(=O)O)(c2c(ccs2)C)c3c(ccs3)C
TIMOLOL	0	90	50	c1(c(nsn1)OCC(CNC(C)(C)C)O)N2CCOCC2
TINIDAZOLE	0		108	S(=O)(=O)(CCn1c(cnc1C)[N+](=O)[O−])CC
TIZANIDINE	0	complete		c21c(c(ccc1nsn2)Cl)NC3=NCCN3
TOCAINIDE	0		100	c1(c(cccc1C)C)NC(=O)C(C)N
TOLBUTAMIDE	0		93	c1(ccc(cc1)C)S(=O)(=O)NC(=O)NCCCC
TOLIPROLOL	0		90	c1(cc(ccc1)C)OCC(CNC(C)C)O

TOLMESOXIDE	0	100		c1(c(cc(c(c1)OC)OC)C)S(=O)C
TOLMETIN	0	almost complete		c1(n(c(cc1)CC(=O)O)C)C(=O)c2ccc(cc2)C
TORASEMIDE	0		91	c1(c(ccnc1)Nc2cc(ccc2)C)S(=O)(=O)NC(=O)NC(C)C
TRAMADOL	0	almost complete		C2(c1cc(ccc1)OC)(C(CCCC2)CN(C)C)O
TRIMETHOPRIM	0	97	100	c1(cc(c(c(c1)OC)OC)OC)Cc2c(nc(nc2)N)N
URSODEOXYCHOLIC-ACID	0	90		C43C1C(C2(C(CC1O)CC(CC2)O)C)CCC3(C(CC4)C(CCC(=O)O)C)C
VALPROIC-ACID	0	100	100	C(CCC)(CCC)C(=O)O
VENLAFAXINE	0	92		C2(C(c1ccc(cc1)OC)CN(C)C)(CCCCC2)O
VERAPAMIL	0	90	22	C(c1cc(c(cc1)OC)OC)(CCCN(CCc2cc(c(cc2)OC)OC)C)(C(C)C)C#N
VILOXAZINE	0	100	85	c1(c(cccc1)OCC)OCC2CNCCO2
WARFARIN	0	98	93	C2(=C(c1c(cccc1)OC2=O)O)C(c3ccccc3)CC(=O)C
XIMOPROFEN	0	100	98	c1(ccc(cc1)C(C(=O)O)C)C2CC(=NO)CCC2
ZIDOVUDINE	0	100	63	C2(N1C(=O)NC(=O)C(=C1)C)CC(C(O2)CO)N=[N+]=[N−]
ACARBOSE	2	2		C1(C(OC(C(C1O)O)OC2C(OC(C(C2O)O)O)CO)CO)OC3C(C(C(C(O3)C)NC4C=C(C(C(C4O)O)O)CO)O)O
ACYCLOVIR	2	20	10–20	c21c(ncn1COCCO)C(=O)NC(=N2)N
ADEFOVIR	2	12		c21c(ncn1CCOCP(=O)(O)O)c(ncn2)N
AMIKACIN	2	1		C1(C(CC(C(C1O)OC2OC(C(C(C2O)O)O)CN)N)NC(=O)C(CCN)O)OC3OC(C(C(C3O)N)O)CO
AMILORIDE	2	20		c1(c(nc(c(n1)Cl)N)N)C(=O)NC(=N)N
AMPHOTERICIN B	2	5	<10	C21C(C(CC(O1)(CC(CC(C(CCC(CC(CC(=O)OC(C(C(C(C=CC=CC=CC=CC=CC=CC(C2)OC3C(C(C(C(O3)C)O)N)O)C)O)C)C)O)O)O)O)O)O)O)C(=O)O
BLEOMYCIN A2	2	0	0	C(C(NC(=O)c1nc(nc(c1C)N)C(NCC(C(=O)N)N)CC(=O)N)C(=O)NC(C(C(C(=O)NC(C(=O)NCCc2nc(cs2)-c3sc(cn3)C(=O)NCCC[S+](C)C)C(C)O)C)O)C)(OC5C(OC4C(C(C(C(O4)CO)O)OC(=O)N)O)C(C(C(O5)CO)O)O)c6c[nH]cn6
BROMOCRIPTINE	2	28		N31C(C2N(C(=O)C1CC(C)C)CCC2)(OC(C3=O)(NC(=O)C7C=C6c5c4c(c([nH]c4ccc5)Br)CC6N(C7)C)C(C)C)O

Tab. 16.3. *(continued)*

Structure Name	*CODE*	*% Absorbed*	*Absolute Oral Bioavailability*	*SMILES*
CAPREOMYCIN 1B	2	0		C2(C1NC(=N)NCC1)NC(=O)C(=CNC(=O)N)NC(=O)C(NC(=O)C(NC(=O)C(CNC2=O)N)C)CNC(=O)CC(CCCN)N
CEFTRIAXONE	2	1	0	N31C(C(C1=O)NC(=O)C(=NOC)c2csc(n2)N)SCC(=C3C(=O)O)CSC4=NC(=O)C(=O)NN4C
CHLOROTHIAZIDE	2	13		c21c(cc(c(c1)S(=O)(=O)N)Cl)N=CNS2(=O)=O
CHLORTETRACYCLINE	2	30		C41C(C(=C3C(C1)C(c2c(c(ccc2Cl)O)C3=O)(C)O)O)(C(=O)C(=C(C4N(C)C)O)C(=O)N)O
CROMOLYN	2	0.5		c41c(cccc1OCC(COc2c3c(ccc2)OC(=CC3=O)C(=O)O)O)OC(=CC4=O)C(=O)O
CYTARABINE	2	20		C2(N1C(=O)N=C(C=C1)N)OC(C(C2O)O)CO
DOXORUBICIN	2	5		c41c(c(c3c(c1O)C(=O)c2c(c(ccc2)OC)C3=O)O)C(CC(C4)(C(=O)CO)O)OC5CC(C(C(O5)C)O)N
ETIDRONIC ACID	2	3		C(P(=O)(O)O)(P(=O)(O)O)(C)O
FOSCARNET	2	17		P(=O)(C(=O)O)(O)O
GANCICLOVIR	2	3.8		c21c(ncn1COC(CO)CO)c(nc(n2)N)O
GENTAMICIN C1	2	0	0	C2(C(C(OC1OC(CCC1N)C(NC)C)C(CC2N)N)O)OC3C(C(C(CO3)(C)O)NC)O
IMIPENEM	2	0		N21C(C(C1=O)C(C)O)CC(=C2C(=O)O)SCCNC=N
KANAMYCIN	2	1		C2(C(C(OC1OC(C(C(C1O)O)O)O)CN)C(CC2N)N)O)OC3OC(C(C(C3O)N)O)CO
LACTULOSE	2	0.6		C1(OC(C(C(=O)CO)O)C(CO)O)OC(C(C(C1O)O)O)CO
LISINOPRIL	2	30	25	N1(C(CCC1)C(=O)O)C(=O)C(NC(CCc2ccccc2)C(=O)O)CCCCN
MANNITOL	2	15		C(C(C(CO)O)O)(C(CO)O)O
MEZLOCILLIN	2	0		C21N(C(C(S1)(C)C)C(=O)O)C(=O)C2NC(=O)C(c3ccccc3)NC(=O)N4C(=O)N(CC4)S(=O)(=O)C

NEOMYCIN	2	3		C3(C(OC1C(C(C(O1)CO)OC2OC(C(C(C2N)O)O)CN)O)C(C(CC3N)N)O)OC4OC(C(C(C4N)O)O)CN
NYSTATIN A1	2	0		C1(C2OC(CC1O)(CC(C(CCC(CC(CC(CC(=O)OC(C(C(C(C=CC=CCCC=CC=CC=CC=CC(C2)OC3C(C(C(C(O3)C)O)N)O)C)O)C)C)O)O)O)O)O)O)C(=O)O
OLSALAZINE	2	2.3		c1(cc(c(cc1)O)C(=O)O)N=Nc2cc(c(cc2)O)C(=O)O
PENTOSAN	2	3		C1(C(C(OCC1O)C)OS(=O)(=O)O)OS(=O)(=O)O
PIPERACILLIN	2	0		C21N(C(C(S1)(C)C)C(=O)O)C(=O)C2NC(=O)C(c3ccccc3)NC(=O)N4C(=O)C(=O)N(CC4)CC
RAFFINOSE	2	0.3		C3(OC2OC(COC1OC(C(C(C1O)O)O)CO)C(C(C2O)O)O)(OC(C(C3O)O)CO)CO
STREPTOMYCIN	2	1		C2(C(OC1C(C(C(C(C1O)O)NC(=N)N)O)NC(=N)N)OC(C2(C=O)O)C)OC3C(C(C(C(O3)CO)O)O)NC
TICARCILLIN	2	0	0	C21N(C(C(S1)(C)C)C(=O)O)C(=O)C2NC(=O)C(c3ccsc3)C(=O)O
TOBRAMYCIN	2	1		C2(C(C(OC1OC(C(CC1N)O)CN)C(CC2N)N)O)OC3OC(C(C(C3O)N)O)CO
				c1(c7cc3cc1Oc2c(cc(cc2)C(C(C(=O)NC(CC(=O)NC3C(=O)NC8c4cc(c(cc4)O)-c5c(cc(cc5O)O)C(NC(=O)C(C(c6cc(c(cc6)O7)Cl)O)NC8=O)C(=O)O)CC(=O)N)NC(=O)C(CC(C)C)NC)O)Cl)O
VANCOMYCIN	2	1	0	C%10C(OC9CC(C(C(O9)C)O)(C)N)C(C(C(O%10)CO)O)O

Code:
0 = Well-absorbed dataset.
1 = Actively transported compounds in Well-absorbed dataset.
2 = Poorly absorbed dataset.

Tab. 16.4. Yoshida dataset.

drug	*set*	*obsd*	*SMILES*
adrenaline	trset	1	c1(cc(c(cc1)O)O)C(CNC)O
alprenolol	trset	1	c1(c(cccc1)OCC(CNC(C)C)O)CCC.Cl
clomethiazole	trset	1	c1(c(ncs1)C)CCCl
coumarin	trset	1	c21c(cccc1)C=CC(=O)O2
dobutamine	trset	1	C(c1ccccc1)(c2ccccn2)(CCN(C(C)C)C(C)C)C(=O)N
domperidone	trset	1	c1(ccc(cc1)CCN(CCOc2ccc(cc2)NS(=O)(=O)C)C)NS(=O)(=O)C
dopamine	trset	1	N2(c1c(cc(cc1)Cl)NC2=O)C3CCN(CC3)CCCN5c4c(cccc4)NC5=O
epanolol	trset	1	c1(c(cccc1)C#N)OCC(CNCCNC(=O)Cc2ccc(cc2)O)O
estradiol	trset	1	C43C2C(c1c(cc(cc1)O)CC2)CCC3(C(CC4)O)C
felodipine	trset	1	C2(c1c(c(ccc1)Cl)Cl)C(=C(NC(=C2C(=O)OC)C)C)C(=O)OCC
hydralazine	trset	1	c21c(cnnc1NN)cccc2
isradipine	trset	1	C3(c1c2c(ccc1)non2)C(=C(NC(=C3C(=O)OC)C)C)C(=O)OC(C)C
ketamine	trset	1	C2(c1ccc(cc1)Cl)(C(=O)CCCC2)NC
lofepramine	trset	1	N2(c1c(cccc1)CCc3c2cccc3)CCCN(CC(=O)c4ccc(cc4)Cl)C
lovastatin	trset	1	C21C(OC(=O)C(CC)C)CC(C=C1C=CC(C2CCC3CC(CC(=O)O3)O)C)C
mebendazole	trset	1	c21c([nH]c(n1)NC(=O)OC)ccc(c2)C(=O)c3ccccc3
meptazinol	trset	1	C2(c1cc(ccc1)O)(CN(CCCC2)C)CC
mercaptopurine	trset	1	c21c(ncnc1S)nc[nH]2
nabumetone	trset	1	c21c(cc(cc1)OC)ccc(c2)CCC(=O)C
nalbuphine	trset	1	C532c1c4c(ccc1CC(C2(CCC(C3O4)O)O)N(CC5)CC6CCC6)O
naloxone	trset	1	C532c1c4c(ccc1CC(C2(CCC(=O)C3O4)O)N(CC5)CC=C)O
nimodipine	trset	1	C2(c1cc(ccc1)[N+](=O)[O−])C(=C(NC(=C2C(=O)OC(C)C)C)C)C(=O)OCCOC
nisoldipine	trset	1	C2(c1c(cccc1)[N+](=O)[O−])C(=C(NC(=C2C(=O)OC)C)C)C(=O)OCC(C)C
nitrendipine	trset	1	C1(C(=C(NC(=C1C(=O)OC)C)C)C(=O)OCC)c2cc(ccc2)[N+](=O)[O−]
phenolphthalein	trset	1	C2(c1c(cccc1)C(=O)O2)(c3ccc(cc3)O)c4ccc(cc4)O
probucol	trset	1	C(c1c(c(cc(c1)SC(Sc2cc(c(c(c2)C(C)(C)C)O)C(C)(C)C)(C)C)C(C)(C)C)O)(C)(C)C
prochlorperazine	trset	1	N2(c1c(ccc(c1)Cl)Sc3c2cccc3)CCCN4CCN(CC4)C

progesterone	trset	1	C31C(C2C(CC1)(C(CC2)C(=O)C)C)CCC4=CC(=O)CCC43C
selegiline	trset	1	c1(ccccc1)CC(N(CC#C)C)C
simvastatin	trset	1	C21C(OC(=O)C(CC)(C)C)CC(C=C1C=CC(C2CCC3CC(CC(=O)O3)O)C)C
sumatriptan	trset	1	c21c([nH]cc1CCN(C)C)ccc(c2)CS(=O)(=O)NC
tacrine	trset	1	c31c(c(c2c(n1)CCCC2)N)cccc3
terbutaline	trset	1	c1(cc(cc(c1)C(CNC(C)(C)C)O)O)O
testosterone	trset	1	C32C(C1(C(=CC(=O)CC1)CC2)C)CCC4(C3CCC4O)C
tetrahydrocannabinol	trset	1	c21c(cc(cc1O)CCCCC)OC(C3C2C=C(CC3)C)(C)C
venlafaxine	trset	1	C2(C(c1ccc(cc1)OC)CN(C)C)(CCCCC2)O
xamoterol	trset	1	N2(C(=O)NCCNCC(COc1ccc(cc1)O)O)CCOCC2
acebutolol	trset	2	c1(c(cc(cc1)NC(=O)CCC)C(=O)C)OCC(CNC(C)C)O
alprazolam	trset	2	c-21c(cc(cc1)Cl)C(=NCc3n-2c(nn3)C)c4ccccc4
amitriptyline	trset	2	C2(=CCCN(C)C)c1c(cccc1)CCc3c2cccc3
chlorpromazine	trset	2	N2(c1c(ccc(c1)Cl)Sc3c2cccc3)CCCN(C)C
cisapride	trset	2	c1(c(cc(c(c1)Cl)N)OC)C(=O)NC2C(CN(CC2)CCCOc3ccc(cc3)F)OC
clemastin	trset	2	C(c1ccc(cc1)Cl)(c2ccccc2)(OCCC3N(CCC3)C)C
chlorothiazide	trset	2	c21c(cc(c(c1)S(=O)(=O)N)Cl)N=CNS2(=O)=O
desipramine	trset	2	c31c(c(c(c(c1[3H])[3H])[3H])[3H])C(C(c2c(c(c(c(c2[3H])[3H])[3H])[3H])N3CCCNC)([3H])[3H])([3H])[3H]
dextropropoxyphene	trset	2	C(C(CN(C)C)C)(OC(=O)CC)(Cc1ccccc1)c2ccccc2
diltiazem	trset	2	c1(c(cc(cc1)F)F)-c2cc(c(cc2)O)C(=O)O
diprafenone	trset	2	C(c1ccccc1)(c2ccccc2)OCCN(C)C
doxepin	trset	2	c31c(cccc1)Cc2c(cccc2)OC3=CCCN(C)C
encainide	trset	2	c1(c(cccc1)NC(=O)c2ccc(cc2)OC)CCC3N(CCCC3)C
ethinyl_estradiol	trset	2	C21C(C(CC1)(C#C)O)(CCC3C2CCc4c3ccc(c4)O)C
etilefrine	trset	2	c1(cc(ccc1)O)C(CNCC)O
famotidine	trset	2	c1(nc(cs1)CSCCC(=N)NS(=O)(=O)N)N=C(N)N
fluorouracil	trset	2	C1(=O)C(=CNC(=O)N1)F
imipramine	trset	2	N2(c1c(cccc1)CCc3c2cccc3)CCCN(C)C
indoramine	trset	2	C(=O)(NC3CCN(CCc1c[nH]c2c1cccc2)CC3)c4ccccc4

Tab. 16.4. *(continued)*

drug	*set*	*obsd*	*SMILES*
isoprenaline	trset	2	c1c(c(ccc1C(CNC(C)C)O)O)O
isotretinoin	trset	2	C1(=C(CCCC1(C)C)C)C=CC(=CC=CC(=CC(=O)O)C)C
labetalol	trset	2	c1(cc(c(cc1)O)C(=O)N)C(CNC(CCc2ccccc2)C)O
lidocaine	trset	2	c1(c(cccc1C)C)NC(=O)CN(CC)CC
lorcainide	trset	2	N(C1CCN(CC1)C(C)C)(c2cc(ccc2)Cl)C(=O)Cc3ccccc3
medifoxamine	trset	2	C(Oc1ccccc1)(Oc2ccccc2)CN(C)C
metoprolol	trset	2	c1(ccc(cc1)CCOC)OCC(CNC(C)C)O
mianserin	trset	2	N42C(c1c(cccc1)Cc3c2cccc3)CN(CC4)C
midazolam	trset	2	c-21c(cc(cc1)Cl)C(=NCc3n-2c(nc3)C)c4c(cccc4)F
moricizine	trset	2	c31c(ccc(c1)NC(=O)OCC)Sc2c(cccc2)N3C(=O)CCN4CCOCC4
morphine	trset	2	C532c1c4c(ccc1CC(C2C=CC(C3O4)O)N(CC5)C)O
nadolol	trset	2	c21c(cccc1OCC(CNC(C)(C)C)O)CC(C(C2)O)O
nafcillin	trset	2	N41C(C(C1=O)NC(=O)c2c3c(ccc2OCC)cccc3)SC(C4C(=O)O)(C)C
naltrexone	trset	2	C532c1c4c(ccc1CC(C2(CCC(=O)C3O4)O)N(CC5)CC6CC6)O
nicardipine	trset	2	C2(c1cc(ccc1)[N+](=O)[O-])C(=C(NC(=C2C(=O)OC)C)C)C(=O)OCCN(Cc3ccccc3)C
nicotine	trset	2	C2(c1cccnc1)N(CCC2)C
oxacillin	trset	2	N41C(C(C1=O)NC(=O)c2c(noc2C)-c3ccccc3)SC(C4C(=O)O)(C)C
oxprenolol	trset	2	c1(c(cccc1)OCC=C)OCC(CNC(C)C)O
pentazocine	trset	2	C32(c1c(ccc(c1)O)CC(C2C)N(CC3)CC=C(C)C)C
pentoxifylline	trset	2	c21c(ncn1C)N(C(=O)N(C2=O)CCCCC(=O)C)C
phenylephrine	trset	2	c1(cc(ccc1)O)C(CNC)O
pimozide	trset	2	N2(c1c(cccc1)NC2=O)C3CCN(CC3)CCCC(c4ccc(cc4)F)c5ccc(cc5)F
pirenzepine	trset	2	N2(c1c(cccn1)NC(=O)c3c2cccc3)C(=O)CN4CCN(CC4)C
prenalterol	trset	2	c1(ccc(cc1)O)OCC(CNC(C)C)O
promethazine	trset	2	N2(c1c(cccc1)Sc3c2cccc3)CC(N(C)C)C
propafenone	trset	2	c1(c(cccc1)C(=O)CCc2ccccc2)OCC(CNCCC)O
propanolol	trset	2	c21c(cccc1OCC(CNC(C)C)O)cccc2

ritodrine	trset	2	c1(ccc(cc1)O)C(C(NCCc2ccc(cc2)O)C)O
salbutamol	trset	2	c1(cc(c(cc1)O)CO)C(CNC(C)(C)C)O
scopolamine	trset	2	C21C(O1)C3N(C2CC(C3)OC(=O)C(c4ccccc4)CO)C
spironolactone	trset	2	C51(C2(C(CC1)C4C(CC2)C3(C(=CC(=O)CC3)CC4SC(=O)C)C)C)OC(=O)CC5
sulpiride	trset	2	c1(c(ccc(c1)S(=O)(=O)N)OC)C(=O)NCC2N(CCC2)CC
thioridazine	trset	2	N2(c1c(ccc(c1)SC)Sc3c2cccc3)CCC4N(CCCC4)C
triazolam	trset	2	c-21c(cc(cc1)Cl)C(=NCc3n-2c(nn3)C)c4c(cccc4)Cl
verapamil	trset	2	C(c1cc(c(cc1)OC)OC)(CCCN(CCc2cc(c(cc2)OC)OC)C)(C(C)C)C#N
acetaminophen	trset	3	c1(ccc(cc1)O)NC(=O)C
acetylsalicylic_acid	trset	3	c1(c(cccc1)OC(=O)C)C(=O)O
amantadine	trset	3	C21(CC3CC(C1)CC(C2)C3)N
amiodarone	trset	3	c1(c2c(oc1CCCC)cccc2)C(=O)c3cc(c(c(c3)I)OCCN(CC)CC)I
amlodipine	trset	3	C1(C(=C(NC(=C1C(=O)OC)C)COCCN)C(=O)OCC)c2c(cccc2)Cl
atenolol	trset	3	C2(=C(C(=O)c1c(cccc1)C2=O)O)C3CCC(CC3)c4ccc(cc4)Cl
atropine	trset	3	N42C(c1c(cccc1)Cc3c2nccc3)CN(CC4)C
bepridil	trset	3	N(c1ccccc1)(CC(N2CCCC2)COCC(C)C)Cc3ccccc3
betamethasone	trset	3	C31(C(C2C(CC1O)(C(C(C2)C)(C(=O)CO)O)C)CCC4=CC(=O)C=CC43C)F
bevantolol	trset	3	c1(c(cc(cc1)CCNCC(COc2cc(ccc2)C)O)OC)OC
brotizolam	trset	3	c31c(sc(c1)Br)-n2c(nnc2C)CN=C3c4c(cccc4)Cl
bufuralol	trset	3	c21c(cc(o1)C(CNC(C)(C)C)O)cccc2CC
captopril	trset	3	N1(C(CCC1)C(=O)O)C(=O)C(CS)C
chloramphenicol	trset	3	c1(ccc(cc1)[N+](=O)[O-])C(C(NC(=O)C(Cl)Cl)CO)O
chlorpheniramine	trset	3	C(c1ccc(cc1)Cl)(c2ccccn2)CCN(C)C
chlorphthalidone	trset	3	C1(NC(=O)c2c1cccc2)(c3cc(c(cc3)Cl)S(=O)(=O)N)O
cimetidine	trset	3	c1(c([nH]cn1)C)CSCCN=C(NC#N)NC
clomipramine	trset	3	N2(c1c(ccc(c1)Cl)CCc3c2cccc3)CCCN(C)C
clopenthixol	trset	3	C3(=CCCN1CCN(CC1)CCO)c2c(ccc(c2)Cl)Sc4c3cccc4
clozapine	trset	3	C2(=Nc1c(ccc(c1)Cl)Nc3c2cccc3)N4CCN(CC4)C
codeine	trset	3	C532c1c4c(ccc1CC(C2C=CC(C3O4)O)N(CC5)C)OC
dexamethasone	trset	3	C31(C(C2C(CC1O)(C(C(C2)C)(C(=O)CO)O)C)CCC4=CC(=O)C=CC43C)F

Tab. 16.4. *(continued)*

drug	*set*	*obsd*	*SMILES*
diclofenac	trset	3	c1(c(cccc1)CC(=O)[O−])Nc2c(cccc2Cl)Cl
dicloxacillin	trset	3	c1(c(cccc1)CC(=O)[O−])Nc2c(cccc2Cl)Cl
diphenhydramine	trset	3	c1(c(cccc1)OCC(CNC(C)C)O)C(C(C([3H])([3H])[3H])([3H])[3H])([3H])[3H]
doxazosin	trset	3	c21c(cc(c(c1)OC)OC)c(nc(n2)N3CCN(CC3)C(=O)C5Oc4c(cccc4)OC5)N
enoximone	trset	3	C1(=C(NC(=O)N1)C)C(=O)c2ccc(cc2)SC
ethambutol	trset	3	C(NCCNC(CC)CO)(CC)CO
finasteride	trset	3	C43C1C(C2(C(CC1)NC(=O)C=C2)C)CCC3(C(CC4)C(=O)NC(C)(C)C)C
fluoxetine	trset	3	C(c1ccccc1)(Oc2ccc(cc2)C(F)(F)F)CCNC
flupenthixol	trset	3	C3(=CCCN1CCN(CC1)CCO)c2c(ccc(c2)C(F)(F)F)Sc4c3cccc4
fluvoxamine	trset	3	c1(ccc(cc1)C(F)(F)F)C(=NOCCN)CCCCOC
furosemide	trset	3	c1(c(cc(c(c1)S(=O)(=O)N)Cl)NCc2ccco2)C(=O)O
haloperidol	trset	3	c1(ccc(cc1)Cl)C2(CCN(CC2)CCCC(=O)c3ccc(cc3)F)O
hydrochlorothiazide	trset	3	c21c(cc(c(c1)S(=O)(=O)N)Cl)NCNS2(=O)=O
levobunolol	trset	3	c21c(cccc1OCC(CNC(C)(C)C)O)C(=O)CCC2
levomepromazine	trset	3	N2(c1c(ccc(c1)OC)Sc3c2cccc3)CC(CN(C)C)C
maprotiline	trset	3	C42(c1c(cccc1)C(c3c2cccc3)CC4)CCCNC
meperidine	trset	3	C2(c1ccccc1)(C(=O)OCC)CCN(CC2)C
metoclopramide	trset	3	c1(c(cc(c(c1)Cl)N)OC)C(=O)NCCN(CC)CC
moclobemide	trset	3	c1(ccc(cc1)Cl)C(=O)NCCN2CCOCC2
nifedipine	trset	3	C2(c1c(cccc1)[N+](=O)[O−])C(=C(NC(=C2C(=O)OC)C)C)C(=O)OC
nifurtimox	trset	3	S1(=O)(=O)CC(N(CC1)N=Cc2oc(cc2)[N+](=O)[O−])C
nitrazepam	trset	3	c21c(ccc(c1)[N+](=O)[O−])NC(=O)CN=C2c3ccccc3
norethisterone	trset	3	C21C(C(CC1)(C#C)O)(CCC3C2CCC4=CC(=O)CCC43)C
nortriptyline	trset	3	C2(=CCCNC)c1c(cccc1)CCc3c2cccc3
omeprazole	trset	3	c31c([nH]c(n1)S(=O)Cc2c(c(c(cn2)C)OC)C)ccc(c3)OC
ondansetron	trset	3	c21c4c(n(c1CCC(C2=O)Cn3c(ncc3)C)C)cccc4
paroxetine	trset	3	C3(C(COc1cc2c(cc1)OCO2)CNCC3)c4ccc(cc4)F

penbutolol	trset	3	c1(c(cccc1)OCC(CNC(C)(C)C)O)C2CCCC2
perphenazine	trset	3	N2(c1c(ccc(c1)Cl)Sc3c2cccc3)CCCN4CCN(CC4)CCO
pindolol	trset	3	c21c([nH]cc1)cccc2OCC(CNC(C)C)O
prazosin	trset	3	c41c(nc(nc1N)N2CCN(CC2)C(=O)c3ccco3)cc(c(c4)OC)OC
primaquine	trset	3	c1(c2c(cc(c1)OC)cccn2)NC(CCCN)C
procainamide	trset	3	c1(ccc(cc1)N)C(=O)NCCN(CC)CC
procyclidine	trset	3	C(c1ccccc1)(C2CCCCC2)(CCN3CCCC3)O
quinidine	trset	3	c21c(ccnc1ccc(c2)OC)C(C3N4CC(C(C3)CC4)C=C)O
raclopride	trset	3	c1(c(c(cc(c1O)Cl)Cl)OC)C(=O)NCC2N(CCC2)CC
ranitidine	trset	3	c1(oc(cc1)CSCCNC(=C[N+](=O)[O-])NC)CN(C)C
timolol	trset	3	c1(c(nsn1)OCC(CNC(C)(C)C)O)N2CCOCC2
triamterene	trset	3	c31c(nc(c(n1)N)-c2ccccc2)c(nc(n3)N)N
urapidil	trset	3	c1(c(cccc1)OC)N2CCN(CC2)CCCNC3=CC(=O)N(C(=O)N3C)C
zofenoprilat	trset	3	N1(C(CC(C1)Sc2ccccc2)C(=O)O)C(=O)C(CS)C
allopurinol	trset	4	c21c(ncnc1O)[nH]nc2
amobarbital	trset	4	C1(C(=O)NC(=O)NC1=O)(CCC(C)C)CC
amrinone	trset	4	C1(=CNC(=O)C(=C1)N)c2ccncc2
betaxolol	trset	4	c1(ccc(cc1)CCOCC2CC2)OCC(CNC(C)C)O
bisoprolol	trset	4	c1(ccc(cc1)COCCOC(C)C)OCC(CNC(C)C)O
bumetanide	trset	4	c1(c(cc(cc1S(=O)(=O)N)C(=O)O)NCCCC)Oc2ccccc2
caffeine	trset	4	c21c(ncn1C)N(C(=O)N(C2=O)C)C
carbamazepine	trset	4	N2(c1c(cccc1)C=Cc3c2cccc3)C(=O)N
carteolol	trset	4	c21c(cccc1OCC(CNC(C)(C)C)O)NC(=O)CC2
chlorambucil	trset	4	c1(ccc(cc1)CCCC(=O)O)N(CCCl)CCCl
chlordiazepoxide	trset	4	c21c(ccc(c1)Cl)N=C(C[N+](=C2c3ccccc3)[O-])NC
chloroquine	trset	4	c21c(nccc1NC(CCCN(CC)CC)C)cc(cc2)Cl
chlorpropamide	trset	4	c1(ccc(cc1)Cl)S(=O)(=O)NC(=O)NCCC
cibenzoline	trset	4	C1(C(C1)C2=NCCN2)(c3ccccc3)c4ccccc4
clobazam	trset	4	c21c(ccc(c1)Cl)N(C(=O)CC(=O)N2c3ccccc3)C
clonazepam	trset	4	c21c(ccc(c1)[N+](=O)[O-])NC(=O)CN=C2c3c(cccc3)Cl

Tab. 16.4. *(continued)*

drug	*set*	*obsd*	*SMILES*
clonidine	trset	4	c1(c(cccc1Cl)Cl)NC2=NCCN2
cyclophosphamide	trset	4	P1(=O)(N(CCCl)CCCl)NCCCO1
desmethyldiazepam	trset	4	C1(=NCC(=O)Nc2c1cc(cc2)Cl)c3ccccc3
diazepam	trset	4	C1(=NCC(=O)N(c2c1cc(cc2)Cl)C)c3ccccc3
diazoxide	trset	4	c21c(cc(cc1)Cl)S(=O)(=O)NC(=N2)C
diflunisal	trset	4	N41C(C(C1=O)NC(=O)c2c(noc2C)-c3c(cccc3Cl)Cl)SC(C4C(=O)O)(C)C
disopyramide	trset	4	c1(c(cccc1)OCC(CNC(CC)(C)C)O)C(=O)CCc2ccccc2
ethanol	trset	4	C(C)O
ethosuximide	trset	4	C1(C(=O)NC(=O)C1)(CC)C
flecaninide	trset	4	c1(c(ccc(c1)OCC(F)(F)F)OCC(F)(F)F)C(=O)NCC2NCCCC2
flurbiprofen	trset	4	c1(c(cc(cc1)C(C(=O)O)C)F)-c2ccccc2
fluconazole	trset	4	c1(c(cc(cc1)F)F)C(Cn2cncn2)(Cn3cncn3)O
flucytosine	trset	4	C1(=NC(=O)NC=C1F)N
flunitrazepam	trset	4	c21c(ccc(c1)[N+](=O)[O-])N(C(=O)CN=C2c3c(cccc3)F)C
gemfibrozil	trset	4	c1(c(ccc(c1)C)C)OCCCC(C(=O)O)(C)C
glipizide	trset	4	c1(c(ccc(c1)Cl)OC)C(=O)NCCc2ccc(cc2)S(=O)(=O)NC(=O)NC3CCCCC3
glyburide	trset	4	c1(ccc(cc1)CCNC(=O)c2cnc(cn2)C)S(=O)(=O)NC(=O)NC3CCCCC3
hexobarbital	trset	4	C2(C1=CCCCC1)(C(=O)N(C(=O)NC2=O)C)C
ibuprofen	trset	4	c1(ccc(cc1)CC(C)C)C(C(=O)O)C
indomethacin	trset	4	c31c(c(c(n1C(=O)c2ccc(cc2)Cl)C)CC(=O)O)cc(cc3)OC
isoniazide	trset	4	c1(ccncc1)C(=O)NN
isosorbide_2-nitrate	trset	4	C21C(C(CO1)O[N+](=O)[O-])OCC2O[N+](=O)[O-]
isosorbide_5-nitrate	trset	4	C21C(C(CO1)O)OCC2O[N+](=O)[O-]
ketoprofen	trset	4	c1(cc(ccc1)C(C(=O)O)C)C(=O)c2ccccc2
ketolorac	trset	4	
lorazepam	trset	4	C1(=NC(C(=O)Nc2c1cc(cc2)Cl)O)c3c(cccc3)Cl
mabuterol	trset	4	c1(cc(cc(c1N)Cl)C(CNC(C)(C)C)O)C(F)(F)F

methadone	trset	4	C(c1ccccc1)(c2ccccc2)(CC(N(C)C)C)C(=O)CC
methylprednisolone	trset	4	C42C1C(C(CC1)(C(=O)CO)O)(CC(C2C3(C(=CC(=O)C=C3)C(C4)C)C)O)C
metronidazole	trset	4	n1(c(cnc1C)[N+](=O)[O-])CCO
mexiletine	trset	4	c1(c(cccc1C)C)OCC(C)N
naproxen	trset	4	c21c(cc(cc1)OC)ccc(c2)C(C(=O)O)C
nitrofurantoin	trset	4	N1(CC(=O)NC1=O)N=Cc2oc(cc2)[N+](=O)[O-]
nizatidine	trset	4	[N+](=O)(C=C(NC)NCCSCc1nc(sc1)CN(C)C)[O-]
oxaprozin	trset	4	c1(c(oc(n1)CCC(=O)O)-c2ccccc2)-c3ccccc3
oxazepam	trset	4	c21c(ccc(c1)Cl)NC(=O)C(N=C2c3ccccc3)O
phenobarbital	trset	4	C2(c1ccccc1)(C(=O)NC(=O)NC2=O)CC
phenylbutazone	trset	4	N2(N(c1ccccc1)C(=O)C(C2=O)CCCC)c3ccccc3
phenylethylmalonamide	trset	4	C(C(=O)N)(C(=O)N)Cc1ccccc1
phenytoin	trset	4	C3(c1ccccc1)(c2ccccc2)NC(=O)NC3=O
prednisolone	trset	4	C43C2C(C1(C(=CC(=O)C=C1)CC2)C)C(CC3(C(CC4)(C(=O)CO)O)C)O
prednisone	trset	4	C43C2C(C1(C(=CC(=O)C=C1)CC2)C)C(=O)CC3(C(CC4)(C(=O)CO)O)C
primidone	trset	4	C2(c1ccccc1)(C(=O)NCNC2=O)CC
probenecid	trset	4	c1(ccc(cc1)C(=O)O)S(=O)(=O)N(CCC)CCC
protriptyline	trset	4	C2(c1c(cccc1)C=Cc3c2cccc3)CCCNC
quinine	trset	4	c21c(ccnc1ccc(c2)OC)C(C3N4CC(C(C3)CC4)C=C)O
salicylic_acid	trset	4	c1(c(cccc1)O)C(=O)O
sulfadiazine	trset	4	c1(ccc(cc1)N)S(=O)(=O)Nc2ncccn2
sulfamethoxazole	trset	4	c1(ccc(cc1)N)S(=O)(=O)Nc2cc(on2)C
sulfinpyrazone	trset	4	N2(N(c1ccccc1)C(=O)C(C2=O)CCS(=O)c3ccccc3)c4ccccc4
sulfisoxazole	trset	4	c1(ccc(cc1)N)S(=O)(=O)Nc2c(c(no2)C)C
temazepam	trset	4	c21c(ccc(c1)Cl)N(C(=O)C(N=C2c3ccccc3)O)C
tenoxicam	trset	4	c21c(ccs1)S(=O)(=O)N(C(=C2O)C(=O)Nc3ccccn3)C
theophylline	trset	4	c21c([nH]cn1)N(C(=O)N(C2=O)C)C
tocainide	trset	4	c1(c(cccc1C)C)NC(=O)C(C)N
tolbutamide	trset	4	c1(ccc(cc1)C)S(=O)(=O)NC(=O)NCCCC
tolmetin	trset	4	c1(n(c(cc1)CC(=O)O)C)C(=O)c2ccc(cc2)C

Tab. 16.4. *(continued)*

drug	*set*	*obsd*	*SMILES*
trazodone	trset	4	N41C(=NN(C1=O)CCCN2CCN(CC2)c3cc(ccc3)Cl)C=CC=C4
trimethoprim	trset	4	c1(cc(c(c(c1)OC)OC)OC)Cc2c(nc(nc2)N)N
valproic_acid	trset	4	C(CCC)(CCC)C(=O)O
warfarin	trset	4	C2(=C(c1c(cccc1)OC2=O)O)C(c3ccccc3)CC(=O)C
zalcitabine	trset	4	C2(N1C(=O)N=C(C=C1)N)OC(CC2)CO
budenoside	test	1	C43(C(C2C(C1(C(=CC(=O)C=C1)CC2)C)C(C3)O)CC5C4(C(=O)CO)OC(O5)CCC)C
fenoterol	test	1	c1(cc(cc(c1)O)O)C(CNC(Cc2ccc(cc2)O)C)O
flumazenil	test	1	n-21c(c(nc1)C(=O)OCC)CN(C(=O)c3c-2ccc(c3)F)C
nivadipine	test	1	C1(C(CN(C)C)CCCC1)(c2cc(ccc2)OC)O
metaproterenol	test	1	c1(cc(cc(c1)O)O)C(CNC(C)C)O
rimiterol	test	1	c1(cc(c(cc1)O)O)C(C2CCCCN2)O
terguride	test	1	c21c3cccc1[nH]cc2CC4C3CC(CN4C)NC(=O)N(CC)CC
raloxifene	test	1	c1(c(sc2c1ccc(c2)O)-c3ccc(cc3)O)C(=O)c4ccc(cc4)OCCN5CCCCC5
ajmaline	test	2	C521C(C3N4C(C1)C(C2O)C(C3)C(C4O)CC)N(c6c5cccc6)C
atovaquone	test	2	C1(CC2N(C(C1)CC2)C)OC(=O)C(c3ccccc3)CO
carvedilol	test	2	c21c4c([nH]c1cccc2OCC(CNCCOc3c(cccc3)OC)O)cccc4
tizanidine	test	2	c21c(c(ccc1nsn2)Cl)NC3=NCCN3
rizatriptan	test	2	c21c([nH]cc1CCN(C)C)ccc(c2)Cn3cncn3
fluvastatin	test	2	c1(c2c(n(c1C=CC(CC(CC(=O)O)O)O)C(C)C)cccc2)-c3ccc(cc3)F
terbinafin	test	2	c21c(cccc1cccc2)CN(CC=CC#CC(C)(C)C)C
amiloride	test	3	c1(c(nc(c(n1)Cl)N)N)C(=O)NC(=N)N
bromfenac	test	3	c1(c(c(ccc1)CC(=O)[O−])N)C(=O)c2ccc(cc2)Br
cerevastatin	test	3	
dexfenfluramine	test	3	c1(cc(ccc1)C(F)(F)F)CC(NCC)C
methotrexate	test	3	c31c(ncc(n1)CN(c2ccc(cc2)C(=O)NC(CCC(=O)O)C(=O)O)C)nc(nc3N)N
mibefradil	test	3	C2(C(c1c(cc(cc1)F)CC2)C(C)C)(CCN(CCCc3[nH]c4c(n3)cccc4)C)OC(=O)COC
mirtazapine	test	3	N42C(c1c(cccc1)Cc3c2nccc3)CN(CC4)C

olanzapine	test	3	C2(=Nc1c(cccc1)Nc3c2cc(s3)C)N4CCN(CC4)C
riluzole	test	3	C(Oc1cc2c(cc1)nc(s2)N)(F)(F)F
risperidone	test	3	c1(c2c(on1)cc(cc2)F)C3CCN(CC3)CCC4=C(N=C5N(C4=O)CCCC5)C
tramodol	test	3	C1(C(CN(C)C)CCCC1)(c2cc(ccc2)OC)O
zidovudine	test	3	C2(N1C(=O)NC(=O)C(=C1)C)CC(C(O2)CO)N=[N+]=[N−]
citalopram	test	4	C2(c1c(cc(cc1)C#N)CO2)(c3ccc(cc3)F)CCCN(C)C
dofetilide	test	4	c1(cc(c(cc1)O)O)CCNC(CCc2ccc(cc2)O)C
etodolac	test	4	C3(c1c(c2c([nH]1)c(ccc2)CC)CCO3)(CC(=O)O)CC
guanafacine	test	4	N(C(=N)N)C(=O)Cc1c(cccc1Cl)Cl
lamotrigine	test	4	c1(c(nc(nn1)N)N)-c2c(c(ccc2)Cl)Cl
lansoprazole	test	4	c31c(nc([nH]1)S(=O)Cc2c(c(ccn2)OCC(F)(F)F)C)cccc3
levonorgestrel	test	4	C41(C(C3C(CC1)C2C(=CC(=O)CC2)CC3)CCC4(C#C)O)CC
milrinone	test	4	C1(=C(NC(=O)C(=C1)C#N)C)c2ccncc2
nevirapine	test	4	N2(c1c(c(ccn1)C)NC(=O)c3c2nccc3)C4CC4
pirmenol	test	4	C(c1ccccc1)(c2ccccn2)(CCCN3C(CCCC3C)C)O
pramipexole	test	4	c21c(sc(n1)N)CC(CC2)NCCC
rilmenidine	test	4	C(C1CC1)(C2CC2)NC3=NCCO3
terazosin	test	4	c41c(nc(nc1N)N2CCN(CC2)C(=O)C3CCCO3)cc(c(c4)OC)OC

1. Hydrogen-bonding donors (NH or OH groups) > 5
2. Hydrogen-bonding acceptors (N or O atoms) > 10
3. Molecular weight > 500
4. C log P > 5.0 (or M log P > 4.15)

16.4.2 Polar Surface Area (PSA)

The PSA represents a very useful property for predicting absorption. It is usually defined as those parts of the van der Waals or solvent-accessible surface of a molecule that are associated with hydrogen bond-accepting capability (e.g., N or O atoms) and hydrogen bond-donating capability (e.g., NH or OH groups). Three types of PSA have been used in studying absorption:

1. Dynamic PSA (PSA_d) [2]
2. Static PSA (PSA) [18]
3. Two-dimensional (or topological) PSA (TPSA) [20]

The first of the PSAs to be developed was dynamic PSA, PSA_d, by Palm *et al.* [2]. PSA_d is calculated by a Monte Carlo conformational search with subsequent energy minimization. This generates a set of low-energy conformers where the van der Waals surface-based PSAs for all conformers are within 2.5 kcal mol^{-1} of the "global" minimum, i.e., the lowest energy conformer found, are computed. The Boltzmann-weighted average of the calculated PSAs are then used as the PSA_d. Palm and co-workers found a good sigmoidal correlation ($r^2 = 0.94$) between PSA_d and human fraction absorbed (%FA) for 20 well-characterized drugs [2]. Using this computational protocol, Palm *et al.* proposed the following:

- Poor absorption (<10%) if $PSA_d > 140\,Å^2$
- Good absorption (>90%) if $PSA_d < 60\,Å^2$

A major drawback of the PSA_d is, however, the rather time-consuming calculation, particularly, the Monte Carlo conformational search, which makes PSA_d inappropriate for computational screening (e-screening) of large virtual libraries.

This prompted the development of the static PSA based on only one conformer. This simplification would save considerable computational time, but it is not without complications as it raises the question: Which conformation should be used?

Most probably, a low-energy conformation could be considered as a good estimation of the bioactive conformation. However, some type of conformational search, although short, must then be employed, and most of the advantage of using PSA instead of PSA_d would be lost. Fortunately, the use of a single conformer generated directly from the 2D molecular structure by the CONCORD (or CORINA) programs without minimization can be used. This approximation did

not compromise the excellent correlation with absorption [29, 30]. This approach reduces the computational time to such a level (~10 compounds per second on a SGI R10k machine) to make PSA useful for *in silico* screening of virtual libraries. However, a persistent (albeit slight) drawback of PSA is the generation of the 3D conformation. The problem is not the computational time, but occurs from a conformational viewpoint in that no matter how well the 2D to 3D conversion programs (e.g., CONCORD or CORINA) perform on an overall basis, the generation may in some cases result in unreasonable 3D structures. Thus, it would be even more favorable if this step could be circumvented or eliminated in some manner.

Ertl and co-workers [20] have developed such a method for generating a topological PSA (TPSA) based on 3D PSA values for 43 fragments resulting from an analysis of 34,810 compounds taken from the WDI database. The correlation between PSA and TPSA is very high ($r^2 = 0.982$).

A further simplification, avoiding even the use of 3D fragments, has been developed by Sherbukhin [31]. This method used a 2D projection technique whereby the TPSA (TSA-2D) is computed. Furthermore, since the definition of PSA is related to hydrogen-bonding groups, it is not surprising that a good correlation can also be obtained by simply counting the number of hydrogen bonding donors and acceptors. Using this method, excellent correlations ($r^2 > 0.9$ and $q^2 > 0.9$) have been reported by several authors (see Ref. [32]). One thing to bear in mind here is of course that conformational dependencies may bury parts of the PSA, thus resulting in an overestimation of the computed TPSA which, in turn, may lead to an underestimation of the predicted intestinal absorption for a particular compound.

The overall trend described in this section in going from a more complex and time-consuming computational protocol, such as PSA_d, to simpler and faster techniques, such as TPSA or hydrogen-bonding counts, while still capturing the same information content is a general one that will be an overall theme in this chapter: ''The simpler, the better but do not fumble the ball''.

16.4.3
PSA and A log P

PSA can of course be combined with other descriptors to develop further improved models compared with using PSA alone. Egan and co-workers have developed a method for predicting intestinal absorption, which uses PSA in conjunction with A log P [26]. Using these two easily interpretable parameters, these authors were able successfully to differentiate well-absorbed (%FA > 90%) compounds from less well-absorbed ones (%FA 74–92%), depending upon the dataset. It is important to note is that both parameters are of composite nature. PSA consists of both hydrogen-bond donating and accepting terms, while the underlying factors for log P-variables are size, polarizability and, again, hydrogen-bonding. Might it be possible to use the noncomposite factors instead with equally well – or perhaps even better – results when developing statistical models for intestinal absorption? We will return to this question in Section 16.4.11.

16.4.4 MolSurf Descriptors

MolSurf parameters [33] are descriptors derived from quantum mechanical calculations. These descriptors are computed at a surface of constant electron density, with which a very fine description of the properties of a molecule at the Van der Waals surface can be obtained. They describe various electrostatic properties such as hydrogen-bonding strengths and polarizability, as well as Lewis base and acid strengths. MolSurf parameters are computed using the following protocol.

The structures of the investigated compounds were built in Macromodel and modeled in their neutral forms. The three-dimensional structures were determined by Monte-Carlo based conformational analysis performed with the Macromodel program package using the Merck Molecular Force Field (MMFF). A total of 100 starting conformations was generated for each structure. The energy minimizations were performed in vacuum. Unique minimized conformations within 5 kJ mol^{-1} of the lowest energy conformation were saved for further analysis.

The conformation with the lowest found energy from the previous conformational analysis was subjected to a geometry optimization (energy minimization) using the semi-empirical quantum chemistry-based AM1 method available in the Spartan program.

A quantum mechanical *ab initio* calculation using a 3-21G* basis set without further geometry optimization (single point calculation) was subsequently performed on all AM1 optimized (minimized) conformations using the Spartan program.

The wave-function from each *ab initio* calculation was used by MolSurf to compute various properties related to the molecular valence region. The chemical behavior, and thus the calculated properties, depend on the distribution of electrons and energy in the valence region. This region is represented by a surface of constant electron density (0.001 electrons/$Bohr^3$) encompassing the molecule. The electrostatic potential, V(**r**), and the local ionization energy, I(**r**), are calculated at points evenly distributed (0.28 Bohr apart) on this surface. The former property, V(**r**), is related to the potential registered by a probe with positive unit charge positioned at each of the points on the surface. Similarly, the latter property, I(**r**), is the energy required to remove an electron from the molecule at each of the points on the surface. The computed descriptors describe properties such as base strength, hydrophobicity, hydrogen bonding and polarity as well as polarizability. MolSurf parameters were calculated for the entire compound as well as for individual atoms contributing to hydrogen bonding. The number of possible hydrogen-bond acceptors and donors, respectively, were also used as descriptors. The former were partitioned into two categories of the oxygen and nitrogen type. This division of hydrogen bond acceptor types also applies to the corresponding variables using the actual computed hydrogen bond acceptor strengths. Additionally, the sum of the hydrogen bond acceptor and donor strengths was used as a descriptor.

It is possible to derive a statistically good and predictive model for intestinal absorption using the MolSurf parameters ($r^2 = 0.916$, $q^2 = 0.798$).

In view of latter developments (see Sections 16.4.9–16.4.11 for further details) the procedure, even with simplifications such as using a single CONCORD/CORINA-derived 3D geometry instead of performing a Monte Carlo conformational search, is too computationally expensive to be applied to e-screening of virtual libraries. However, it may still be a useful alternative/complement for computing more detailed information about a compound, or to provide a more easily interpretable model to complement other models based on more rapidly computable parameters but which are difficult to interpret in terms of how to modify compounds in order for them to have better intestinal absorption characteristics.

Another possible advantage with MolSurf descriptors (and also other multi parameter descriptors) is the fact that they describe the investigated compounds not only with a single value, as in the case of PSA and log P descriptors, but in a multivariate way. This approach provides a more balanced description of the requirements that a structure must have in order to be well absorbed and may, in turn, provide additional insight on how to develop compounds having favorable absorption properties. However, as will be described in Section 16.4.10, simpler – i.e., less computationally demanding – parameters carrying similar information content with equal interpretability may be used to derive models for intestinal absorption at the same level of statistical quality.

16.4.5
Molecular Hash Key Descriptors

Sage and co-workers have constructed a numerical molecular representation, which they called a molecular hash key [21]. A hash key represents surface properties of a molecule and is represented as pair-wise similarities against a basis-set of common reference molecules (20 diverse selected compounds from the CMC database). The properties are computed at the surface of a 2 Å sphere surrounding each molecule. Each surface point is characterized by six values referring to the inverse field strength and directionality of steric, positive polar and negative polar features, respectively, A stochastic conformational sampling is employed starting from a CONCORD-generated 3D structure with a maximum use of 20 conformations. Each of the 20 hash keys (one with respect to each of the 20 basis-set compounds) is the corresponding maximum similarity obtained from the generated conformations. The generation of a complete hash key set for a compound takes about 30–45 minutes on a SGI R10k machine.

The authors used the hash keys to predict intestinal absorption on the 20 compounds originally used by Palm *et al.* [2]. The results (Table 16.5) were less impressive, although it might be suspected that they would have been slightly better had the authors used a logit transformation of the dependent variable (%FA) instead of %FA itself, keeping in mind that the percent fraction absorbed represents a closed scale (0–100%FA). Again, the computational time involved in hash key generation makes them less well suited for e-screening of virtual libraries.

Tab. 16.5. Molecular hash key descriptor model for the Palm dataset.

#	*Compound*	% *FA*	% *FA calc*
1	Alprenolol	96	100
2	Atenolol	54	74.7
3	Ciprofloxacin	69	62.5
4	Diazepam	97	99
5	Foscarnet	17	26.3
6	Lactulose	0.6	20.7
7	Mannitol	26	37.7
8	Metolazone	64	45.6
9	Metoprolol	102	59.4
10	Nordiazepam	99	83.9
11	Olsalazine	2.3	62.2
12	Oxazepam	97	78.5
13	Oxprenolol	97	98.1
14	Phenazone	97	97
15	Pindolol	92	86.9
16	Practolol	95	70.6
17	Raffinose	0.3	3.3
18	Sulpiride	36	37.9
19	Sulphasalazine	12	54.5
20	Tranexamic acid	55	74.4

16.4.6
GRID-related Descriptors

Another set of useful 3D-based descriptors for predicting intestinal absorption is through the use of the GRID program. Applications of these descriptors are discussed in Chapter 4.

16.4.7
ADAPT Descriptors

Jurs and co-workers have used parameters generated by the ADAPT system [34]. The descriptors fall into three categories: topological, electronic, and geometric.

The first category of parameters (topological) is derived from 2D structures, while the latter two categories of variables (electronic and geometric) are based on 3D geometries generated by CORINA. In addition, 566 2D molecular fragments, derived from over 7000 compounds in the CMC database, were added to the ADAPT descriptors for the analysis of intestinal absorption [23]. The authors used a variable selection routine, discarding variables having similar information content and keeping one variable from each such family for further analysis. This procedure reduced the original descriptor pool to 127 variables: 25 topological descriptors; 21 electronic descriptors; 20 geometric descriptors; and 61 fragment descriptors. Jurs *et al.* developed a good model for human intestinal absorption

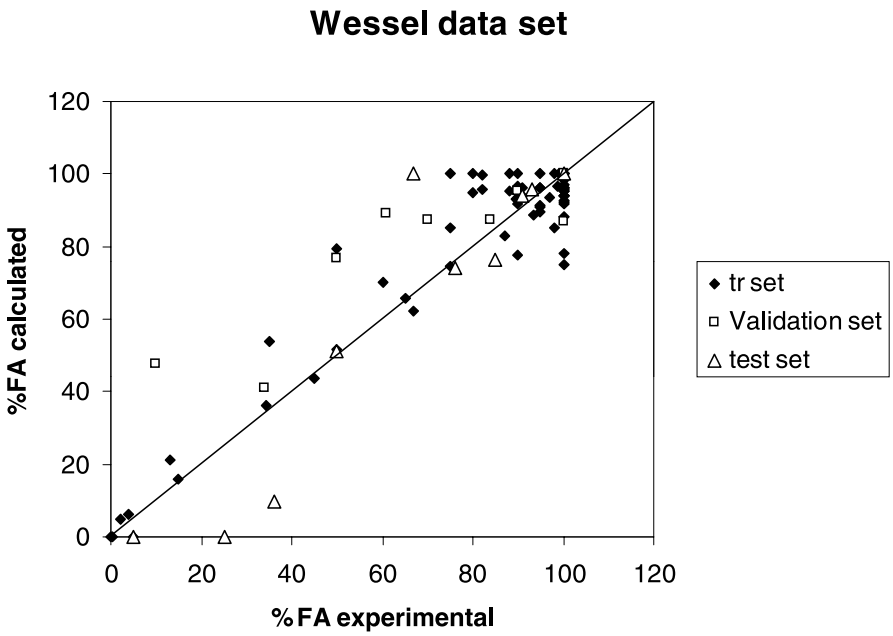

Fig. 16.1. Experimental versus calculated %FA for the Wessel data set using ADAPT descriptors and neural network statistics.

with RMSE values of 9.4%FA units, 19.7%FA units and 16.0%FA units for the training set, (cross-) validation set and test set, respectively (Fig. 16.1).

More interestingly is the range of parameters, both within the ADAPT system and the fragment descriptors, used by the authors in their analysis. This pool of descriptors contains both rapidly computed 2D descriptors as well as more time-consuming 3D descriptors based on the semi-empirical AM1 method. Thus, this approach somewhat bridges the gap between the 3D-based approaches, which we have discussed previously, and the 2D-based approaches which are described in Sections 16.4.9–16.4.11. From a computational e-screening point of view, this approach has similar difficulties as other 3D-based methods in being too time-consuming to allow rapid enough calculation of virtual compound libraries. During the variable reduction process of going from 728 to 127 descriptors, it might have been possible to preferentially keep 2D-based descriptors from each family, or perhaps base the analysis on only the 650 computed 2D-based descriptors without too much of a loss in statistical quality of the derived model if computational speed was the primary concern.

16.4.8
HYBOT Descriptors

Raevsky and co-workers have collected a large database of thermodynamic data related to hydrogen bonding with which they have developed the HYBOT program

[17]. HYBOT will compute hydrogen bond donor (ΣC_d) and acceptor (ΣC_a) factors that describe the donor and acceptor strengths, respectively, of a compound. Using these two parameters, the authors developed models with significant statistical quality ($r^2 = 0.91$, $q^2 = 0.87$) of intestinal absorption.

The HYBOT parameters represent another interesting aspect of computational descriptors containing relevant information for studying intestinal absorption, namely the use of a 2D fragment approach related to experimental data. In this case, 3D-based experimental thermodynamic data is organized into various rapidly computable 2D-based parameters related to hydrogen bonding that allows investigations of large virtual libraries of compounds.

16.4.9
2D Topological Descriptors

There are a large number of topological descriptors available (Table 16.6) that can be calculated from the 2D structure (graph) of a compound. The advantage with these descriptors is that they can be rapidly computed (several compounds per CPU second), and that they only require a 2D representation of the structure, thereby eliminating potential problems with conformer generation as discussed earlier. The disadvantage with these descriptors is that, in many cases, they are difficult to interpret in terms of how the current structures should be modified to obtain a compound with better properties (in this case intestinal absorption). However, the topological descriptors are quite useful for computational screening of large virtual libraries (''brute force approach'') when a good statistical model has been developed for a particular property. This aspect of developing a gray box (i.e., difficult to understand/interpret) or a black box (i.e., impossible to understand/interpret) model purely for e-screening purposes to rank proposed structures for synthesis and/or further pharmaceutical work is a quite pragmatic and useful one. Such models gain even further in usefulness if they can be combined with other models of good statistical quality that may require more computational efforts in terms of CPU time to develop but which may be easier to interpret, thus answering the question ''Which are the next molecules to make?'' in a better way. In this way, the researcher may construct a number reasonably sized focused libraries for e-screening based on insight from the latter type of models to be evaluated by the former gray/black box models instead of generating very large virtual libraries with limited insight into the problem at hand.

Norinder and Haeberlein (unpublished results) have developed a model based on the Palm dataset [2] using rapidly computable 2D-based descriptors, among them a number of topological indices, using an in-house AstraZeneca software package called SaSA [35], and with the good quality (Table 16.7).

16.4.10
2D Electrotopological Descriptors

Another set of particularly useful 2D-based topological descriptors are the so-called electrotopological state index (E-state) descriptors developed by Kier and Hall [36].

Tab. 16.6. List of examples of topological descriptors.

Topological descriptor
information index on molecular size
total information index of atomic composition
mean information index on atomic composition
first Zagreb index M1
first Zagreb index by valence vertex degrees
second Zagreb index M2
second Zagreb index by valence vertex degrees
Quadratic index
Narumi simple topological index (log)
Narumi harmonic topological index
Narumi geometric topological index
Total structure connectivity index
Pogliani index
ramification index
polarity number
log of product row sums (PRS)
average vertex distance degree
mean square distance index (Balaban)
Schultz Molecular Topological Index (MTI)
Schultz MTI by valence vertex degrees
Gutman Molecular Topological Index
Gutman MTI by valence vertex degrees
Xu index
superpendentic index
Wiener W index
mean Wiener index
reciprocal distance Wiener-type index
Harary H index
quasi-Wiener index (Kirchhoff number)
first Mohar index TI1
second Mohar index TI2
hyper-distance-path index
reciprocal hyper-distance-path index
detour index
hyper-detour index
reciprocal hyper-detour index
distance/detour index
all-path Wiener index
Wiener-type index from Z weighted distance matrix (Barysz matrix)
Wiener-type index from mass weighted distance matrix
Wiener-type index from van der Waals weighted distance matrix
Wiener-type index from electronegativity weighted distance matrix
Wiener-type index from polarizability weighted distance matrix
Balaban J index
Balaban-type index from Z weighted distance matrix (Barysz matrix)
Balaban-type index from mass weighted distance matrix
Balaban-type index from van der Waals weighted distance matrix
Balaban-type index from electronegativity weighted distance matrix

Tab. 16.6 *(continued)*

Topological descriptor
Balaban-type index from polarizability weighted distance matrix
connectivity index chi-0
connectivity index chi-1 (Randic connectivity index)
connectivity index chi-2
connectivity index chi-3
connectivity index chi-4
connectivity index chi-5
average connectivity index chi-0
average connectivity index chi-1
average connectivity index chi-2
average connectivity index chi-3

As was the case for the ''regular'' topological descriptors, the E-state descriptors are also rapidly computed without the need for 3D structure generation. However, unlike the former type of parameters, the E-state parameters are easy to understand. Today, a number of program packages have included the E-state descriptors among the list of parameters, which these programs are capable of calculating. In Molconn-Z, the software emanating from Kier and Hall and co-workers [37], a number of E-state descriptors related to a variety of atoms including hydrogen atoms having different bond types to their respective neighbors are calculated. Since the E-state parameters are easy to interpret, they are capable of answering the question ''Which are the next molecules to make?'' in a relatively straightforward manner. These two aspects (computational speed and interpretability) make these descriptors quite attractive both for e-screening purposes, as well as for having an interpretable model with which to focus the virtual library generation and for other pharmaceutical work.

The sum of hydrogen bonding donor and acceptor related E-state descriptors are well correlated with the corresponding HYBOT parameters, with r^2-values of 0.8–0.95 [38]. This gives the E-state descriptors a link to experimental values, which is positive but not necessary for the purpose of generating useful models with good statistical quality for, in this case, intestinal absorption.

Models have been developed based on the Palm data set [2] using E-state descriptors ($r^2 = 0.93$, $q^2 = 0.89$; Fig. 16.2) [22].

Tab. 16.7. Statistics for the E-state model of the Palm dataset.

set	*# compounds*	*r2*	*q2*	*rmse*
training set	13	0.94	0.75	0.41
test set	7	0.95		0.38

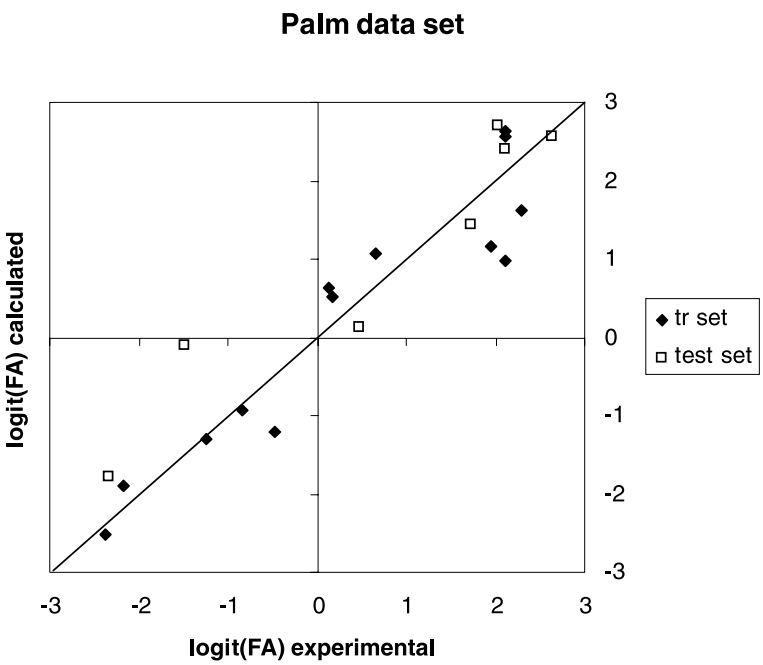

Fig. 16.2. Experimental versus calculated logit (%FA) for the Palm data set using E-state descriptors and PLS statistics.

16.4.11
1D Descriptors

In most cases, the various 2D- and 3D-based descriptors previously described in Sections 16.4.3–16.4.11 are augmented with several descriptors of 1D physicochemical type, e.g., log P, log D, molecular weight, molar refractivity, parachor; or of 1D fragment type, i.e., the presence or absence of a particular substructure/fragment, to construct a more comprehensive description of the compounds under investigation. In many (if not most) cases, the resulting model is a combination of 1D- and 2D- and/or 3D-based parameters. 1D descriptors are, for the most part, rather intuitive, easy to interpret and fast to compute – which makes them attractive to use in statistical modeling. However, some of these descriptors, such as the log P- and log D-descriptors as well as parachor (P_r) and molar refractivity (MR), are composite in nature, i.e., they are composed of other underlying factors. For example, MR is composed of the refractive index, density and molecular weight:

$$MR = [(n^2 - 1)/(n^2 + 2)] \times (MW/d)$$

While log P has hydrogen bonding, size and polarizability as underlying factors, it has been pointed out that for intestinal absorption [22] the use of composite vari-

ables (at best) marginally improved the model. However, this was not always the case as it depended on which algorithm was used. Not accounting for the underlying factors – especially hydrogen bonding – in an adequate manner was quite detrimental to the statistical quality of the derived model. The reason for these observations is probably the fact that partitioning of the underlying factors as expressed through (for instance) the log P (log D) variable is not an optimum approach when attempting to develop a model for intestinal absorption.

The limitation with 1D fragment-based descriptors is their lack of extrapolative character to even their closest neighborhood. For example, if a particular substituent position in a compound series had included substituents/fragments such as methyl-, ethyl- and *n*-propyl-groups, a continuous description – such as the number of carbon atoms – would allow the possibility of estimating the sought-after property of compounds with *n*-butyl and *n*-pentyl substituents. The corresponding fragment-based approach does not allow for that, since it ''knows'' only of the fragments contained in the compounds used to derive the model (training set). Fragment-based approaches may not work very well, but for them to do so it is crucial that the training set compounds span a large number of fragments; this permits the derived model to be useful in its combinatorial nature and limitation, i.e., putting the right fragments in the right places.

16.5 Statistical Methods

16.5.1 Multiple Linear Regression

Multiple linear regression (MLR) is a classic mathematical multivariate regression analysis technique [39] that has been applied to quantitative structure–property relationship (QSPR) modeling. However, when using MLR there are some aspects, with respect to statistical issues, that the researcher must be aware of:

1. A general comment that affects all statistical multivariate data analysis techniques, namely that each of the variables should be given equal chance to influence the outcome of the analysis. This can be achieved by scaling the variables in appropriative way. One popular method for scaling variables is autoscaling, whereby the variance of each variable is adjusted to 1.
2. MLR assumes each variable to be exact and relevant.
3. Strong co-linear variables must be eliminated by removing all but one of the strongly correlated variables. Otherwise, spurious chance correlation may result.
4. Some sort of estimation of the statistical ''distance'' to the overall model (see Section 16.5.4) should be reported for each compound to provide an estimate of how much an intra- or extrapolation in multivariate descriptor space the prediction actually is.

16.5.2 Partial Least Squares

Partial least squares (PLS) projections to latent structures [40] is a multivariate data analysis tool that has gained much attention during past decade, especially after introduction of the 3D-QSAR method CoMFA [41]. PLS is a projection technique that uses latent variables (linear combinations of the original variables) to construct multidimensional projections while focusing on explaining as much as possible of the information in the dependent variable (in this case intestinal absorption) and not among the descriptors used to describe the compounds under investigation (the independent variables). PLS differs from MLR in a number of ways (apart from point 1 in Section 16.5.1):

1. The descriptors are not treated as exact and relevant but as consisting of two parts: one part related to the dependent variable and the other part not related (noise).
2. Strong correlations between relevant variables is not a problem in PLS, and all such variables can be retained in the analysis. In fact, the models derived using PLS become more stable with the inclusion of strongly correlated and relevant parameters.
3. The number of original descriptors may vastly exceed the number of compounds in the analysis (as opposed to MLR), since PLS is using only a few (usually less than 5–10) latent variables for the actual statistical analysis.
4. In PLS analysis a ''distance'' to the overall model (distance-to-model), defined as the variance in the descriptors remaining after the analysis (residual standard deviation RSD), is given for each predicted compound. This is a very important piece of information that is presented to the researcher (see Section 16.5.4).

There are of course also difficulties when using the PLS technique:

1. The number of latent variables (PLS components) must be determined by some sort of validation technique, e.g., cross-validation [42]. The PLS solution will coincide with the corresponding MLR solution when the number of latent variables becomes equal to the number of descriptors used in the analysis. The validation technique, at the same time, also serves the purpose to avoid overfitting of the model.
2. The possibility of using a very large number of descriptors, where many of them may not be particularly correlated with the dependent variable and thus represent large amounts of noise, must be considered with great care. Otherwise, the signal-to-noise ratio becomes too low for PLS to be able to create useful projections (latent variables).

PLS has been used to develop models for intestinal absorption using a number of different parameterizations (see Refs. [19, 22]).

16.5.3 Neural Networks

Neural networks (NN) represent, as opposed to PLS and MLR, a nonlinear statistical analysis technique [43]. As is the case for both PLS and MLR, several aspects of NN should be considered when using this type of analysis technique:

1. The number of middle layers (hidden nodes) in a NN must be identified either through a particular choice or through an optimization procedure with careful monitoring of the predictive behavior of the derived model (see point 2).
2. NN are well-known to overtrain, i.e., to be able to explain a large portion of the variance of the dependent variable for the training set but to fail grossly in predicting a correct answer for the compounds that are not part of the model (external test set). Overtraining of NN can be avoided by setting aside a fixed number of compounds to validate the predictive ability of the NN model (validation set) as part of the NN training, and to stop when the predictive ability begins to deteriorate.
3. The interpretability of the derived NN model may be difficult to understand, even though the influences of the descriptors on the derived model can be simulated.

NN methods have been used by Wessel and co-workers [23], Agatonovic-Kustrin *et al.* [25] and Ghuloum *et al.* [21] to model intestinal absorption.

16.5.4 Distance-to-model Considerations

In all statistical modeling, including multivariate data analysis, it is crucially important to determine the applicability of the derived model, and for several reasons:

1. To make users of the model aware of its applicability and limitations.
2. To avoid misuse of a model for predicting (in this case) the intestinal absorption of compounds outside the model's present statistical limits, thus rendering the model (and/or statistical technique as well as the parameterization) a false ''bad reputation''.
3. To be able to use extrapolations from the present model in a constructive manner to expand it to cover a larger descriptor space.

However, many statistical modeling techniques do not, in a simple and straightforward way, enable by default the estimation of whether a prediction is an interpolation to the model (thus rendering the prediction more credible), or is an extrapolation to the model (in which case the prediction must be evaluated with greater care).

Furthermore, there are two other aspects to the extrapolation problem: one structural and one statistical. An illustrative example of these various cases can be found in a dataset of benzamides (S16.1). that one of the present authors (U.N.) published some time ago [44]. If one develops a PLS model based on the same descriptors and the same, experimental design-based, training set (compounds 1–16) augmented by compound 17 (Table 16.8) in order to prove the points raised above [the prediction limit (1.502) set to two times the overall RSD of the model (0.751) which roughly gives 95% confidence interval], one can observe the following with respect to predictions on the remaining test set compounds:

- A compound can be an extrapolation from a structural point of view, such as compound 24 that has a *n*-butyl substituent in the 3-position while the training set (compounds 1–17) only contain methyl-, ethyl- and *n*-propyl-substituents (among other non-alkyl substituents). Still, compound 24 is not considered to be an outlier from a statistical point of view. At the same time, compounds 18 and 19 which also contains substituents – in this case in the 5-position – that are not part of the training set are statistical outliers as well as structural outliers.
- A compound can also be an extrapolation from a statistical point of view, which is especially common in statistical modeling using multivariate descriptions of the investigated compounds, even though the compound to be predicted is within the structural space, e.g., substituent space, covered by the training set compounds. Thus, compound 20 – which is identified as being just outside the limit of prediction of the model – has a hydrogen ''substituent'' in both the 3- and 5-positions, respectively (a ''substituent'' found among the training set compounds) is still identified as a statistical outlier. Furthermore, among compounds 21–35, all of which are within the statistical prediction limit of the model but with larger RSD-values than the largest RSD-value found among the training set compounds, there are several examples of substituents found among the compounds of the training set.

We hope that this example will serve as an illustrative case of the importance of computing the distance-to-model parameter in statistical modeling. However,

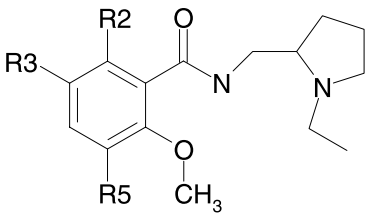

Scheme 16.1.

Tab. 16.8. Benzamide model.

number	*3-position*	*5-position*	*2-position*	*experimental plC50*	*calculated plC50*	*rsd*
1	CL	CL	OH	7.49	7.69	0.35
2	BR	OH	H	8	7.94	0.94
3	OME	CL	OH	7.15	7.18	0.92
4	PR	CL	OH	8.49	8.58	0.82
5	NO2	BR	OH	5.2	5.12	0.42
6	BR	BR	H	8.1	7.94	0.33
7	ME	BR	OH	8.26	8.12	0.45
8	ET	BR	H	7.96	8.28	0.72
9	BR	OME	H	6.84	6.70	0.55
10	I	OME	H	9.17	8.90	0.84
11	ME	OME	H	8.28	8.40	0.64
12	PR	ME	OH	8.3	8.47	0.38
13	CL	PR	OH	6.96	7.14	0.36
14	BR	ET	OH	7.77	7.79	0.30
15	H	ET	OH	6.91	7.12	0.48
16	ET	ET	OH	8.75	8.13	0.38
17	I	H	OH	8.52	8.64	0.71
18	BR	NO2	OH	6.73	7.83	2.96
19	BR	NH2	OH	7.48	7.29	2.24
20	H	H	H	5.96	6.54	1.54
21	F	H	OH	6.44	6.85	1.34
22	H	H	OH	6.5	7.25	1.29
23	OME	BR	OH	5.21	5.63	1.20
24	BU	OME	H	8.57	8.96	1.18
25	OME	H	OH	6.69	7.14	1.15
26	BR	H	OH	6.34	6.44	1.15
27	CL	H	H	6.59	7.67	1.10
28	BR	H	H	7.37	7.21	1.08
29	NO2	H	OH	5.52	5.88	1.07
30	OME	BR	OH	7.17	7.12	1.01
31	CL	H	OH	7.41	7.64	1.00
32	BR	H	H	7.34	7.96	0.99
33	BR	H	OH	7.57	7.18	0.99
34	ME	H	OH	7.72	8.14	0.96
35	H	BR	OH	6.91	6.49	0.95

as mentioned in point 3 before, a constructive way of using the distance-to-model parameter for the benzamide example would be to synthesize and test not only the highest predicted compounds of the test set but also some (all) of the statistical outliers and some of the compounds with the largest RSD-values of the test set.

References

1 Lipinski, C. A., Lombardo, F., Dominy, B. W., Feeney, P. J., Experimental and computational approaches to estimate solubility and permeability in drug discovery and development settings, *Adv. Drug Deliv. Rev.* **1997**, *23*, 3–25.

2 Palm, K., Stenberg, P., Luthman, K., Artursson, P., Polar molecular surface properties predict the intestinal absorption of drugs in humans, *Pharm. Res.* **1997**, *14*, 568–571.

3 Amidon, G. L., Lennernas, H., Shah, V. P., Crison, J. R., A theoretical basis for a biopharmaceutic drug classification: the correlation of in vitro drug product dissolution and in vivo bioavailability, *Pharm. Res.* **1995**, *12*, 413–420.

4 Hansch, C., Quinlan, J. E., Lawrence, G. L., Linear free energy relationship between partition coefficients and the aqueous solubility of organic liquids, *J. Org. Chem.* **1968**, *33*, 347–350.

5 Yalkowsky, S. H., Valvani, S. C., Solubility and partitioning I: Solubility of nonelectrolytes in water, *J. Pharm. Sci.* **1980**, *69*, 912–922.

6 Jain, N., Yalkowsky, S. H., Estimation of the aqueous solubility I: application to organic nonelectrolytes, *J. Pharm. Sci.* **2001**, *90*, 234–252.

7 Kamlet, M. J., Doherty, R. M., Abboud, J. L., Abraham, M. H., Taft, R. W., Linear solvation energy relationships: 36. Molecular properties governing solubilities of organic nonelectrolytes in water, *J. Pharm. Sci.* **1986**, *75*, 338–349.

8 Huuskonen, J., Salo, M., Taskinen, J., Neural network modeling for estimation of the aqueous solubility of structurally related drugs, *J. Pharm. Sci.* **1997**, *86*, 450–454.

9 Bruneau, P., Search for predictive generic model of aqueous solubility using Bayesian neural nets, *J. Chem. Inf. Comp. Sci.* **2001**, *41*, 1605–1616.

10 Liu, R. F., So, S. S., Development of quantitative structure–property relationship models for early ADME evaluation in drug discovery. 1. Aqueous solubility, *J. Chem. Inf. Comp. Sci.* **2001**, *41*, 1633–1639.

11 Livingstone, D. J., Ford, M. G., Huuskonen, J. J., Salt, D. W., Simultaneous prediction of aqueous solubility and octanol/water partition coefficient based on descriptors derived from molecular structure, *J. Comput.-Aid. Mol. Des.* **2001**, *15*, 741–752.

12 Camenisch, G., Folkers, G., Van de Waterbeemd, H., Review of theoretical passive drug absorption models: historical background, recent developments and limitations, *Pharm. Acta Helv.* **1996**, *71*, 309–327.

13 Abraham, M. H., Chadha, H. S., Mitchell, R. C., The factors that influence skin penetration of solutes, *J. Pharm. Pharmacol.* **1995**, *47*, 8–16.

14 Palm, K., Luthman, K., Ungell, A. L., Strandlund, G., Artursson, P., Correlation of drug absorption with molecular surface properties, *J. Pharm. Sci.* **1996**, *85*, 32–39.

15 Norinder, U., Osterberg, T., Artursson, P., Theoretical calculation and prediction of Caco-2 cell permeability using MolSurf parametrization and PLS statistics, *Pharm. Res.* **1997**, *14*, 1786–1791.

16 Van de Waterbeemd, H., The fundamental variables of the biopharmaceutics classification system (BCS): a commentary. *Eur. J. Pharm. Sci.* **1998**, *7*, 1–3.

17 Raevsky, O. A., Hydrogen bond estimation by means of HYBOT, in: *Computer-Assisted Lead Finding and Optimisation*. Waterbeemd, H. van de, Testa, B., Folkers, G. (eds), Wiley-VCH, Basel, **1997**, pp. 367–378.

18 Clark, D. E., Rapid calculation of polar surface area and its application to the prediction of transport phenomena. 1. Prediction of intestinal absorption, *J. Pharm. Sci.* **1999**, 807–814.

19 Norinder, U., Österberg, T., Artursson, P., Theoretical calculation

and prediction of intestinal absorption of drugs using Molsurf parametrization and PLS statistics, *Eur. J. Pharm. Sci.* **1999**, *8*, 49–56.

20 Ertl, P., Rohde, B., Selzer, P., Fast calculation of molecular polar surface area as a sum of fragment-based contributions and its application to the prediction of drug transport properties, *J. Med. Chem.* **2000**, *43*, 3714–3717.

21 Ghuloum, A. M., Sage, C. R., Jain, A. N., Molecular hashkeys: a novel method for molecular characterisation and its application for predicting important pharmaceutical properties of molecules, *J. Med. Chem.* **2000**, *42*, 1739–1748.

22 Norinder, U., Österberg, T., Theoretical calculation and prediction of drug transport processes using simple parameters and partial least squares projections to latent structures (PLS) statistics. The use of electrotopological state indices, *J. Pharm. Sci.* **2001**, *90*, 1076–1084.

23 Wessel, M. D., Jurs, P. C., Tolan, J. W., Muskal, S. M., Prediction of human intestinal absorption of drug compounds from molecular structure, *J. Chem. Inf. Comput. Sci.* **1998**, *38*, 726–735.

24 Oprea, T. I., Gottfries, J., Toward minimalistic modelling of oral drug absorption, *J. Mol. Graph. Model.* **1999**, *17*, 261–274.

25 Agatonovic-Kustrin, S., Beresford, R., Yusof, A. P. M., Theoretically-derived molecular descriptors important in human intestinal absorption, *J. Pharm. Biomed. Anal.* **2001**, *25*, 227–237.

26 Egan, W. J., Merz, K. M., Baldwin, J. J., Prediction of drug absorption using multivariate methods, *J. Med. Chem.* **2000**, *43*, 3867–3877.

27 Egan, W. J., personal communication 2002.

28 Yoshida, F., Topliss, J. G., QSAR model for drug human oral bioavailability, *J. Med. Chem.* **2000**, *43*, 2575–2585.

29 Clark, D. E., Pickett, S. D., Computational methods for the prediction of 'drug-likeness', *Drug. Discov. Today* **2000**, *5*, 49–58.

30 Clark, D. E., Prediction of intestinal absorption and blood-brain barrier penetration by computational methods, *Comb. Chem. High Throughput Screening* **2001**, *4*, 477–496.

31 Sherbukhin, V. V., personal communication 2002.

32 Österberg, T., Norinder, U., Prediction of polar surface area and drug transport processes using simple parameters and PLS statistics, *J. Chem. Inf. Comput. Sci.* **2000**, *40*, 1408–1411.

33 MolSurf version 3.10, Q. A., Hertig Carls Allé 29, SE-691 41, Karlskoga, Sweden, (e-mail: qemist@swipnet.se).

34 Stuper, A. J., Brugger, W. E., Jurs. P. C., Computer-Assisted Studies of Chemical Structure and Biological Function, New York, 1979, http://research.chem.psu.edu/pcjgroup/ADAPT.html.

35 Sherbukhin, V. V., Olsson, T., SaSA (Synthesis and Structure Administra-tion), personal communication 2001.

36 Kier, L. B., Hall, L. H., *Molecular Structure Description: The Electrotopological State*. Academic Press, New York, **1999**.

37 Molconn-Z, version 3.50, http://www.eslc.vabiotech.com/molconn/manuals/350/chapone.html.

38 Stenberg, P., Norinder, U., Luthman, K., Artursson, P., Experimental and computational screening models for the prediction of intestinal drug absorption, *J. Med. Chem.* **2001**, *44*, 1927–1937.

39 Livingstone, D., *Data Analysis for Chemists. Applications to QSAR and Chemical Product Design*. Oxford University Press, Oxford, **1995**.

40 Wold, S., Johansson, E., Cocchi, M., PLS – Partial least-squares projections to latent structures, in: *3D QSAR in Drug Design*. Kubinyi, H. (ed.). ESCOM, Leiden, **1993**, pp. 523–550.

41 Cramer, R. D., Patterson, D. E., Bunce, J. D., Comparative Molecular

Field Analysis (CoMFA). 1. Effect of shape on binding of steroids to carrier proteins, *J. Am. Chem. Soc.* **1988**, *110*, 5959–5967.

42 Wold, S., Cross-validatory estimation of the number of components in factor and principal components models, *Technometrics* **1979**, *20*, 379–405.

43 Rojas, R., *Neural Networks – A Systematic Introduction*. Springer Verlag, Berlin, **1996**.

44 Norinder, U., Högberg, T., A quantitative structure–activity relationship for some dopamine D_2 antagonists of benzamide type, *Acta Pharm. Nord.* **1992**, *4*, 73–78.

17
VOLSURF: A Tool for Drug ADME-properties Prediction

Gabriele Cruciani, Mirco Meniconi, Emanuele Carosati, Ismael Zamora, and Raimund Mannhold

Abbreviations

ADME	absorption/distribution/metabolism/elimination (excretion)
Caco-2	Cell line used to predict human oral absorption
cDNA	Complementary DNA
CYP3A4	Cytochrome 3A4
DA	Discriminant analysis
DMPK	Drug metabolism and pharmacokinetics
MIF	Molecular interaction field
LC/MS	Liquid chromatography/mass spectrometry
P450	Cytochrome P-450
PCA	Principal component analysis
PCs	Principal components
PepT1	Peptide transporter 1
P-gp	P-glycoprotein
PLS	Partial least squares
QSPR	Quantitative structure–property relationships (more restricted also quantitative structure–pharmacokinetic relationships)

Symbols

$E_{entropy}$	Entropic energy
E_{HB}	Hydrogen bonding energy
E_{LJ}	Lennard-Jones energy
P_{app}	Apparent permeability (in Caco-2 cells)

17.1 Introduction

It is only during the past few years that the importance of the metabolic and pharmacokinetic behavior of drug molecules in the drug discovery process has been recognized. One of the causes for failure in drug development is the lack of suitable pharmacokinetic properties of drug candidates. At the same time, the development

Drug Bioavailability: Estimation of Solubility, Permeability, Absorption and Bioavailability.
Edited by Han van de Waterbeemd, Hans Lennernäs and Per Artursson

ISBN: 3-527-30438-X

of new analytical techniques and *in vitro* assays has allowed the measurement of these properties to be made much more rapidly than before. Therefore, within the pharmaceutical companies the studies of drug metabolism and pharmacokinetics have been moved to a much earlier position in the drug discovery process.

During the early stages of drug discovery, a suitable candidate must be selected from a limited number of structurally related compounds that may have a similar pharmacological profile. At that point, information from *in vitro* systems would provide important and particularly useful selection criteria. However, results from *in vitro* models are often not yet available at the early phases of development, or they exist only for a limited number of compounds. Accordingly, there is an urgent need for *in silico* methods that would allow prediction of the pharmacological properties in humans from the experimental model systems.

This is the framework where computational chemistry could play an important role in the prediction of these properties in order to achieve more efficient and faster drug discovery cycles.

One of the major goals of computational chemistry in the field of drug metabolism and pharmacokinetics (DMPK) is the prediction of oral availability. Several computational approaches have been published to predict this important parameter, starting from the molecular structure [1–3]. However, when applied to real case studies, none of these provided totally convincing results and, correspondingly, there is a lack of any general strategy to address this problem.

Oral availability is a complex parameter that involves several chemical and physiological processes such as solubility, chemical stability, permeability and first-pass metabolism, to mention a few. All of these subprocesses depend on two different types of factor: (i) interaction of the drug compound with certain macromolecules, such as the metabolism mediated by the cytochromes P450 family; and (ii) interaction of the drug molecule with a certain chemical or biological environment, that will determine the solubility or the passive permeability.

Each subprocess can be the cause of a poor oral availability or, vice versa, a poor oral availability can be due to several different reasons. Therefore, we are truly convinced that the *ab initio* prediction of oral availability as such, without considering the impact of the other physico-chemical processes, is still impossible.

To date, however, present several computational approaches have been reported to predict the important subprocesses for oral availability. This chapter will present some examples for the prediction of such pharmacokinetic properties, starting from the three-dimensional (3D) structure of the drug candidates. In our experience it is much better to develop and use a number of different simple local models, than to use a unique complex model that depends on a multitude of poorly understood subfactors.

17.2
The Molecular Descriptors

There are some very simple heuristic rules concerning cut-offs on molecular weight, number of hydrogen bond donors and acceptors as well as lipophilicity,

which are routinely applied in medicinal chemistry nowadays. However, these rules only represent crude guidelines which work best at the lead finding stage, and are less suitable for establishing structure–property relationships in lead optimization. Other frequently used descriptor schemes are topological indices, but the interpretation of the results in terms of molecular structure is not straightforward. The dynamical averaging of polar and hydrophobic surface areas works well in congeneric series, but the applicability in heterogeneous sets remains to be proven. Furthermore, the conformers for a given molecule are generated either in an implicit or explicit solvent environment which does not represent the true conformational equilibrium at a biological membrane. Several recent publications (e.g., Ref. [4]) have dealt with the calculation of physico-chemically relevant descriptors from an electronic wavefunction, but the computational requirements are prohibitive for even medium-sized datasets. Thus, there is ongoing quest for new descriptors encoding physico-chemically relevant properties, which can be linked with molecular structure and calculated with reasonable speed.

The interaction of drug molecules with biological membranes is a three-dimensional (3D) recognition that is mediated by surface properties such as shape, Van der Waals forces, electrostatics, hydrogen bonding, and hydrophobicity. Therefore, the GRID force field [5–7], which is able to calculate energetically favorable interaction sites around a molecule, was selected to produce 3D molecular interaction fields.

A molecular field involves mapping the chemical forces between an interacting partner and a target (macro)molecule. As the information contained in 3D molecular fields is related to the interacting molecular partners, the amount of information in molecular interaction fields (MIFs) is in general superior to other mono-dimensionally or bi-dimensionally computed molecular descriptors.

The GRID force field uses a potential based on the total energy of interaction (the sum of Lennard-Jones, H-bonding and electrostatic terms) between a target molecule and a probe, and can be used to characterize putative polar and hydrophobic interaction sites around target molecules. The water probe was used to simulate solvation–desolvation processes, whereas the hydrophobic probe (called DRY in the GRID program) and the carbonyl probe (called O) were used to simulate drug–membrane interactions. The DRY probe is a specific probe to compute the hydrophobic energy [7]; the overall energy of the hydrophobic probe is computed at each grid point as $E_{\text{entropy}} + E_{\text{LJ}} - E_{\text{HB}}$, where E_{entropy} is the ideal entropic component of the hydrophobic effect in an aqueous environment, E_{LJ} measures the induction and dispersion interactions occurring between any pair of molecules, and E_{HB} measures the H-bonding interactions between water molecules and polar groups on the target surface.

Thus, a molecule can be characterized in terms of its potential hydrogen bonding, polar, hydrophobic and ionic interactions in 3D space. The size and the spatial distribution of these molecular interaction contours is translated into a quantitative scheme, the VolSurf descriptors, without the need to align the molecules in 3D space [8, 9] (Fig. 17.1).

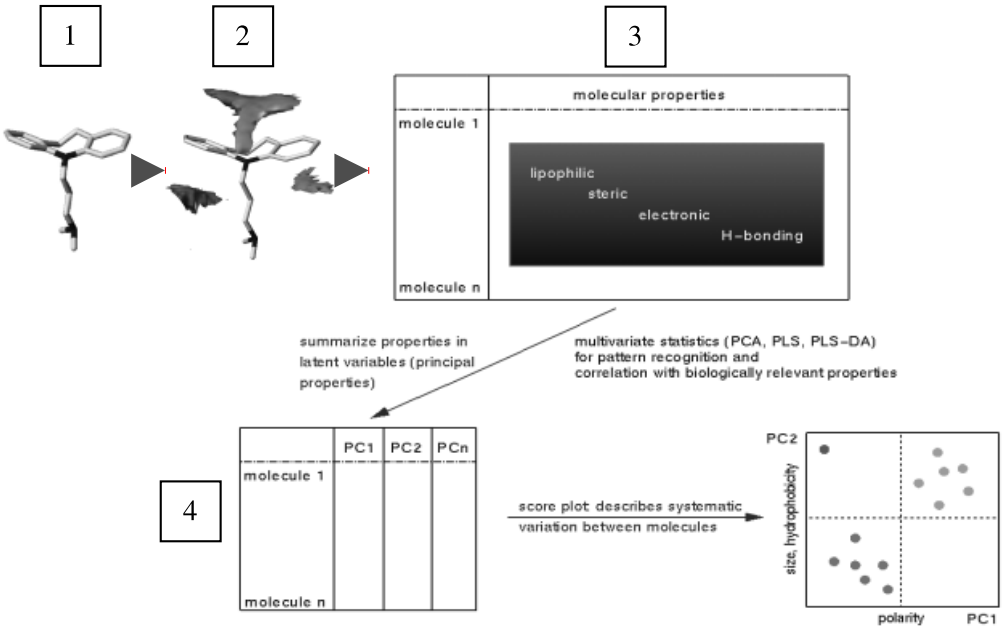

Fig. 17.1. Multivariate characterization with VolSurf descriptors. Molecular Interaction Fields (MIF; shaded areas) are computed from the 3D-molecular structure. MIFs are transformed in a table of descriptors, and statistical multivariate analysis is performed.

The molecular descriptors refer to the molecular size and shape, to the size and shape of hydrophilic and hydrophobic regions, and to the balance between them. Hydrogen bonding, amphiphilic moments, critical packing parameters are other useful descriptors. The VolSurf descriptors have been presented and explained in detail elsewhere [8]. The VolSurf descriptors encode physico-chemical properties and, therefore, allow both for a design in the physico-chemical property space in order to rationally modulate pharmacokinetic properties, and for establishing quantitative structure–property relationships (QSPR).

In the following section, the calculation of the VolSurf parameters from GRID interaction energies will be explained and the physico-chemical relevance of these novel descriptors demonstrated by correlation with measured absorption/distribution/metabolism/elimination (ADME) properties. The applications will be shown by correlating 3D molecular structures with Caco-2 cell permeabilities, thermodynamic solubilities and metabolic stabilities. Special emphasis will be placed on interpretation of the models by multivariate statistics, because a rational design to improve molecular properties is critically dependent on an understanding of how molecular features influence physico-chemical and ADME properties.

17.3
Practical Examples: Structure–Disposition Relationships

17.3.1
Predicting Membrane Partitioning

The use of Caco-2 cell monolayers has gained in popularity as an *in vivo* human absorption surrogate; moreover, the monolayers are generally accepted as a primary absorption screening tool by several pharmaceutical companies [10]. However, Caco-2 cell permeability measurements exhibit certain limitations due to the mechanisms involved. Both passive and active pathways exist: active transport tends to increase the absorption across the cells and, since Caco-2 cells overexpress the P-glycoprotein (P-gp) efflux pump, the absorption of some compounds across these cells may be underestimated.

The applicability range of any model should be limited to molecules having a similar mechanism of transport. Therefore, we have selected from the literature only those compounds with well-characterized Caco-2 cell permeability and excluded compounds with a high efflux ratio. Known P-gp substrates and actively transported compounds were also excluded from the list.

When comparing different experimental sources of Caco-2 permeability data, quantitative comparison is almost impossible, due to intervariations of experimental procedures between laboratories, although standard protocols and reference molecules are often used.

In order to avoid a lack of consistent literature-based data, the Caco-2 permeability values of our selected compounds were transformed according to the following scheme: the majority of compounds with $P_{app} < 4 \times 10^{-6}$ cm s^{-1} were classified as poorly absorbed and assigned a score of -1; compounds with $P_{app} > 8 \times 10^{-6}$ cm s^{-1} were classified as well-absorbed and assigned a score of $+1$. Different assumptions were made in special cases, when the experimental protocols were different or no internal standard compounds were used.

Summing up, the selected Caco-2 data contain qualitative permeability measurements for 450 related (but chemically diverse) compounds that had been either collected from the literature or measured experimentally in laboratories connected with our group. Penetrating compounds were indicated by a score of $+1$, whereas a score of -1 was attributed to compounds having little (if any) ability to penetrate the epithelial cells. Passive permeation was used as a basic assumption of the model.

The VolSurf method was used to produce molecular descriptors, and PLS discriminant analysis (DA) was applied. The statistical model showed two significant latent variables after cross-validation. The 2D PLS score model offers a discrimination between the permeable and less permeable compounds. When the spectrum color is active (Fig. 17.2), red points refer to high permeability, whereas blue points indicate low permeability. There is a region in the central part of the plot with both red and blue compounds. In this region, and in between the two continuous lines, the permeability prediction is less reliable. The permeability model

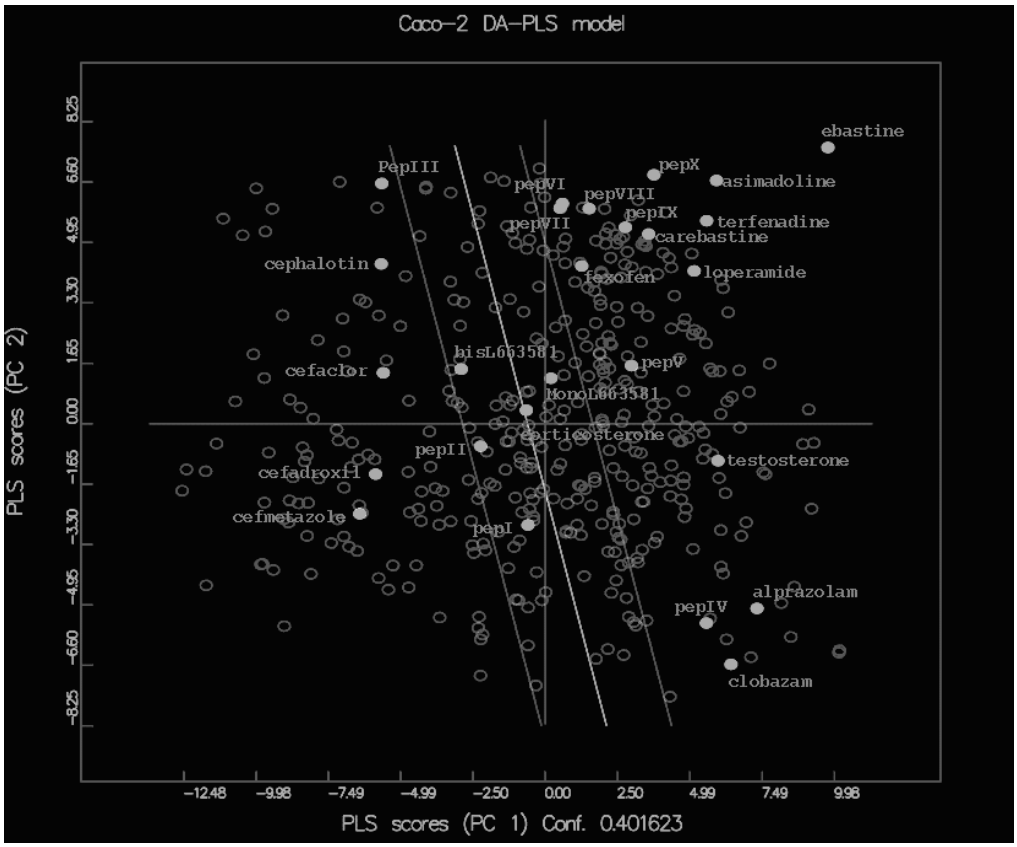

Fig. 17.2. PLS score plot for the VolSurf Caco-2 model. Light open circles represent penetrating compounds; dark open circles represent nonpenetrating compounds. Filled circles represent the projection (prediction) of compounds in Table 17.1 in the Caco-2 model.

obtained can be used to project external compounds in the chemical space represented by the model in order to rank the Caco-2 permeability behavior of new, untested compounds.

The structures of the drugs used as a small test set for the model are listed in Table 17.1. Loperamide and asimadoline are P-gp substrates; terfenadine and ebastine are compounds that are rapidly metabolized; alprazolam, clobazam, di- and mono-hydroxy-L66858 [11] are benzodiazepines; testosterone and corticosterone are hormones; and cefadroxyl, cefaclor, cephalotin and cefmetazole are cephalosporins [12]. Finally, peptides 1 to 10 are peptidomimetic drugs [13].

An examination of the results of the external predictions shows interesting findings. The compounds of Table 17.1 that are projected in the Discriminant Analysis-PLS model made with the training set compounds are shown in Fig. 17.2 (the

Tab. 17.1. Smiles codes and names of the test set compounds used in Caco-2 external permeability prediction example.

c1ccccc1C(c1ccccc1)(CCN1CCC(O)(CC1)c1ccc(cc1)Cl)C(=O)N(C)C	loperamide
c1ccccc1[C@H](N(C(C(c1ccccc1)c1ccccc1)=O)C)CN1CC[C@@H](C1)O	asimadoline
c1cc(ccc1)C(c1ccccc1)(O)C1CCN(CC1)CCC[C@H](c1ccc(cc1)C(C)(C)C)O	terfenadine
c1c(ccc(c1)C(C)(C)C)C(CCC[NH]1CCC(CC1)OC(c1ccccc1)c1ccccc1)=O	ebastine
c1cc(ccc1)C(c1ccccc1)(O)C1CCN(CC1)CCC[C@H](c1ccc(cc1)C(C)(C(O)=O)C)O	fexofenadine
c1c(ccc(c1)C(C)(C)C(=O)O)C(CCCN1CCC(CC1)OC(c1ccccc1)c1ccccc1)=O	carebastine
c1(cc2c(cc1)n1c(CN=C2c2ccccc2)nnc1C)Cl	alprazolam
c1(cc2c(cc1)N(C(CC(N2c1ccccc1)=O)=O)C)Cl	clobazam
c1ccc2c(c1Cl)C(N(Cc1n2cnc1c1noc(n1)C(C)(C)O)C)=O	monoOH-L663581
c1ccc2c(c1Cl)C(N(Cc1n2cnc1c1noc(n1)[C@@](C)(CO)O)C)=O	bisOH-L663581
C1(C=C2CCC3[C@@H]([C@]2(CC1)C)CC[C@]1([C@H]3CC[C@@H]1O)C)=O	testosterone
C1CC(C=C2[C@]1([C@H]1[C@@H](CC2)[C@@H]2[C@](C[C@@H]1O)([C@H](CC2)C(CO)=O)C)C)=O	corticosterone
C1(=O)N2[C@@H]([C@@H]1NC(=O)[C@@H](N)c1ccccc1)CCC(=C2C(=O)O)Cl	cefaclor
C1(=O)N2[C@@H]([C@@H]1NC(=O)[C@@H](N)c1ccc(cc1)O)CCC(=C2C(=O)O)C	cefadroxil
C1(=O)N2[C@@H]([C@@H]1NC(=O)CSCC#N)CCC(=C2C(=O)O)CSc1n(C)nnn1	cefmetazole
C1(=O)N2[C@@H]([C@@]1(NC(=O)CC=1SC=CC1)OC)SCC(=C2C(=O)O)COC(OC)=O	cephalotin
[NH3][C@@H](Cc1ccccc1)C(=O)NCC(=O)O	pepI
[NH3][C@@H](Cc1ccccc1)C(=O)N[C@@H](Cc1ccccc1)C(=O)NCC(=O)O	pepII
[NH3][C@@H](Cc1ccccc1)C(=O)N[C@@H](Cc1ccccc1)C(=O)N[C@@H](Cc1ccccc1)C(=O)NCC(=O)O	pepIII
CC(=O)N[C@H](Cc1ccccc1)C(=O)N	pepIV
N([C@@H](Cc1ccccc1)C(=O)N[C@@H](Cc1ccccc1)C(=O)N)C(=O)C	pepV
N([C@@H](Cc1ccccc1)C(=O)N[C@@H](Cc1ccccc1)C(=O)N[C@@H](Cc1ccccc1)C(=O)N)C(=O)C	pepVI
N([C@@H](Cc1ccccc1)C(=O)N[C@@H](Cc1ccccc1)C(=O)N([C@@H](Cc1ccccc1)C(=O)N)C)C(=O)C	pepVII
N([C@@H](Cc1ccccc1)C(=O)N([C@@H](Cc1ccccc1)C(=O)N([C@@H](Cc1ccccc1)C(=O)N)C)C)C(=O)C	pepVIII
N([C@@H](Cc1ccccc1)C(=O)N([C@@H](Cc1ccccc1)C(=O)N([C@@H](Cc1ccccc1)C(=O)N)C)C)(C(=O)C)C	pepIX
N([C@@H](Cc1ccccc1)C(=O)N([C@@H](Cc1ccccc1)C(=O)N([C@@H](Cc1ccccc1)C(=O)NC)C)C)(C(=O)C)C	pepX

projected compounds are those shown as filled circles). Although loperamide and asimadoline are predicted as well-penetrating compounds, they are often reported as poorly absorbed compounds, most likely because of the P-gp efflux. This model, which is exclusively based on the diffusion mechanism, is not able to predict this important component of absorption in humans. Terfenadine and ebastine are predicted to be Caco-2-penetrating compounds, though contradictory results are often reported for these two molecules. It is well known that terfenadine and ebastine are rapidly metabolized to fexofenadine and carebastine respectively, and this may be the reason for the variation in experimental findings. In fact, the model predicts that fexofenadine and carebastine are less prone to cross the Caco-2 cells than their parent compounds. The four benzodiazepines and two

hormones are correctly predicted. It is interesting to note that although alprazolam and clobazam have a similar lipophilicity to mono- and di-hydroxy-L668581, they are both able to penetrate Caco-2 cells – unlike the latter two compounds. Moreover, penetration was correctly predicted in both cases. Thus, it is clear that factors other than lipophilicity play a role in permeability across the Caco-2 monolayer.

Cefadroxyl and cefaclor are beta-lactam antibiotics which show high affinity for the PepT1 carrier system, whereas the other two beta-lactams, cephalotin and cefmetazole, are not recognized by PepT1 protein and are not actively transported in the intestine. However, as the VolSurf Caco-2 model predicts that all the beta-lactams are nonpenetrating compounds, it is very probable that, as they rely only the diffusion mechanism, cefadroxyl and cefaclor will not cross the cell monolayer.

Ten peptides were selected to study the influence of charge, lipophilicity and chain length on transport across the helium. Some of these were zwitterionic and some were neutral at physiological pH. Although peptides are very flexible, only one conformation was used in the analysis, as it has been shown that most VolSurf descriptors are only marginally influenced by conformational sampling. The sequence of experimental Caco-2 permeation was pepX > pepIX > pepVIII, pepIV, pepVI, pepVII > pepI, pepII, pepIII. The model correctly predicted the experimental permeation trend, although the peptides were built without conformational search and sampling. Moreover, it should be pointed out that no correlation of peptide permeability with experimental partition coefficient was found, thus reinforcing the previous finding that VolSurf descriptors are well suited to describe molecular permeability (at least passive diffusion), and that they are often better than lipophilicity measurements.

The coefficients plot (not reported here) of the obtained model suggests that descriptors of polarity such as hydrophilic regions, capacity factors, and H-bonding are inversely correlated with permeability. This means that besides the H-bonding potential, additional factors such as charge distribution and electron lone pairs influence permeation. While diffuse polar regions are tolerable for permeation, dense and localized polar regions are markedly detrimental. An increase in H-bonding capacity is known to be detrimental for permeation. In addition, the contribution of the integy moment descriptors demonstrates that besides the number of H-bonds, their 3D distribution also influences permeation. Hydrophobic interactions are directly correlated with permeation, but their role appears less important than the polar descriptors one. The molecular size and shape have no marked impact on permeation. In contrast, critical packing and the hydrophilic–lipophilic balance are important descriptors.

The model interpretation is in good agreement with the known molecular factors influencing Caco-2 permeability. In addition – and this outlines the originality of the method – VolSurf allows the relevant 3D molecular properties to be quantified. Once the model is developed, as reported above, simple projection of the compound descriptors into it allows predictions to be made for new compounds.

As such, VolSurf affords much structural information of use in designing compounds with optimal permeability profile, and in defining an ideal property space in similarity searches.

17.3.2 Predicting Thermodynamic Water Solubility

The thermodynamic solubility of a drug is the concentration of the compound that is dissolved in aqueous solution in equilibrium with the undissolved amount, when measured at 25°C after an appropriate time period. Aqueous solubility has long been recognized as a key molecular property in pharmaceutical science. Drug delivery, transport and distribution phenomena depend on solubility; thus, it is of considerable value to possess information of the solubility value of a drug candidate, to be able to predict the solubility for unknown compounds and, finally, to be able to modify the structure of a compound in order to modulate its solubility value in an appropriate manner.

Many groups have discussed the correlation between solubility and molecular properties [14–19], and the octanol/water partition coefficient, the molecular volume and surface area, the boiling point and charge distribution in the molecules are well-documented molecular descriptors that correlate strongly with experimental solubility.

However, from our point of view, there remains a lack of sufficiently precise and reliable methods to compute thermodynamic water solubility. The majority of methods work only for congeneric series of compounds, and many have not been developed to function in areas of pharmaceutical research using drug-like molecules. Most of the methods do not use the three-dimensional structure of the compounds, while some depend on previous knowledge of certain experimental properties of the compounds of interest. Moreover, all of the methods are dependent upon the quality of solubility values in the training set used to develop the model; indeed, this latter point is a critical limitation that has a major influence on solubility estimations.

It is well known that many compounds are able to change their physical form whilst suspended in solution. For example, a compound of interest may change from one polymorphic form to another, while different crystalline aggregations of the same compound can have different solubility profiles. Impurities can mask the true solubility, and aggregation in solution can also change the thermodynamic equilibrium. Finally, errors which have been published in the literature data may in fact magnify from publication to publication.

For all these reasons, and despite what is reported in many publications, an acceptable error of 0.5 log unit in predicted solubility value remains an acceptable target.

The VolSurf approach was used to correlate the 3D molecular descriptors by utilizing the water solubilities for as many compounds as could be found. Although over 2000 solubility values were identified, many showed contradictory results (both low and high values published). Moreover, some of the estimations had not been made by the authors and the original reference was not reported, while others were simply wrong, having not been measured under the standard conditions required. From the 2000 compounds, about 850 were carefully selected; in addi-

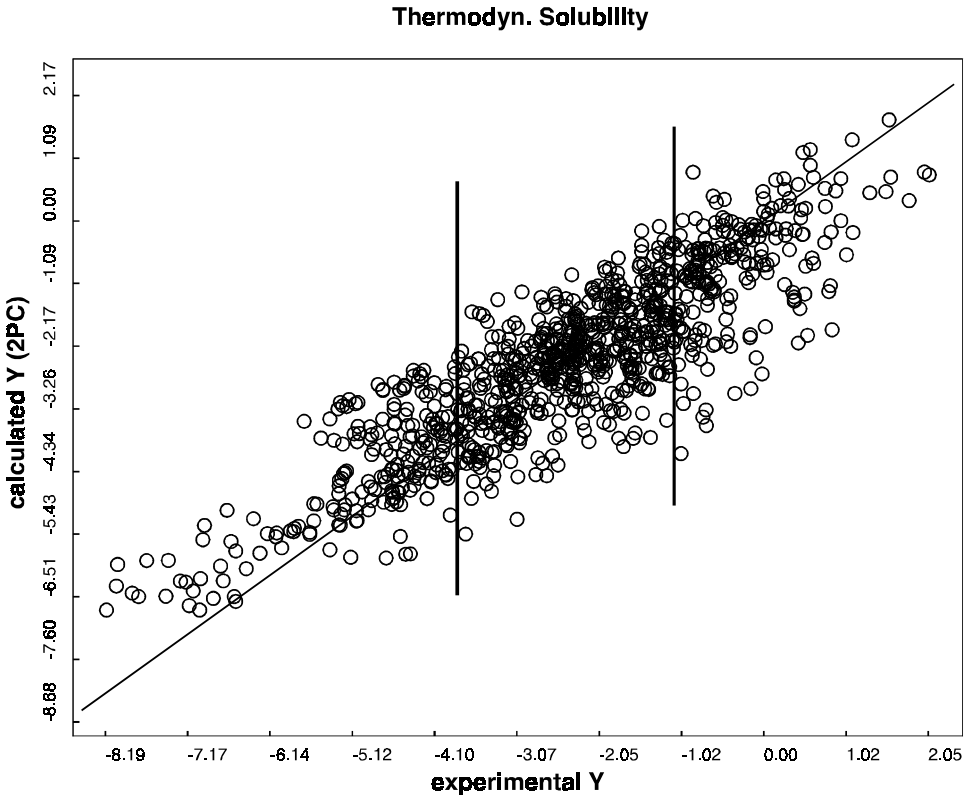

Fig. 17.3. Experimental versus calculated solubility from VolSurf model. Lower left part, poor solubility; central part, medium solubility; upper right part, high-solubility compounds.

tion, we carried out solubility measurements for almost 200 compounds such that the final total number of compounds for which data were available was 970.

The correlation was made using PLS analysis within the VolSurf software. The solubility was quantified via the $-\log[\text{Soly}]$-values, where Soly was expressed in mol L^{-1} at 25°C. The quantitative PLS analysis resulted in a two-component model. The recalculated versus experimental PLS plot (Fig. 17.3) shows the correlation obtained. From the objects pattern, a differentiation between very poorly/poorly/medium/highly/very highly soluble compounds was seen to be possible, though fine quantitative predictions were difficult to achieve.

The average error in the external prediction was about ± 0.8 log unit. Although this range was still not suitable to predict the precise solubility values of external compounds, it was sufficient to rank compounds in different solubility categories and to use it for the filtering of compounds in virtual databases.

Overall, it seemed unlikely that this model could be improved upon, and any

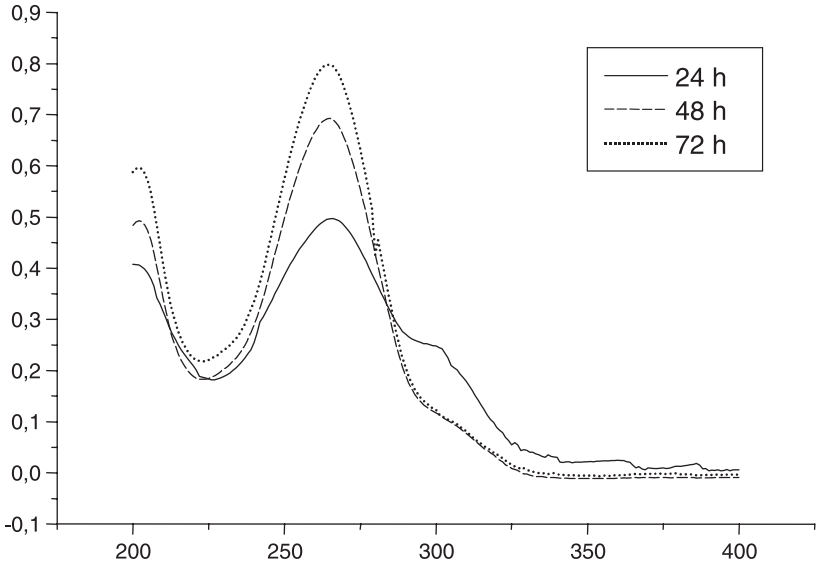

Fig. 17.4. Absorbance versus wavelength (nM) spectroscopic measurement for acetazolamide compound. The solubility equilibrium is obtained at 72 hours after dissolution.

attempt made to do so resulted in dangerous overfitting and overpredicting. As stated previously, a great many factors can play a role in solubility, and most of these are virtually impossible to control.

The solubility profile for acetazolamide, after 24, 48 and 72 hours from dissolution in water at 25°C is shown in Fig. 17.4. Equilibrium is reached only after 72 hours from dissolution, and any solubility measurements made before that time may lead to major errors in solubility determination. Hence, it is unclear whether all the solubility data reported in the literature has been obtained with careful checking of such phenomena.

We must accept that some solubility measurements are not precise, and for those obtained from the literature it is virtually impossible to check errors that, most likely, have been caused by limitations of experimental data in the training set.

17.3.3 Predicting Metabolic Stability

Metabolic stability in human liver preparations may represent a suitable experimental tool to obtain relevant pharmacokinetic information in an early phase of drug discovery. Compounds which are metabolized principally by the liver can be identified and studied in more detail to determine the principal sites of biotransformation.

The aim of the present example was to investigate whether the assessment of an *in silico* model of metabolic stability from a training set of several hundred drugs or drug-like compounds in human CYP3A4 cDNA-expressed microsomal preparations, would offer a suitable approach to predict the metabolic stability of external compounds.

The training set consisted of about 500 compounds from Pharmacia Corporation. Each compound was incubated at a fixed concentration for 60 min with a fixed concentration of protein at 37°C. The reaction was stopped by adding acetonitrile to the solution and, after centrifugation to remove the protein, the supernatant was analyzed using LC/MS and MS. Compounds with a final concentration $\geq$90% of the corresponding control sample were defined as stable, whereas compounds with final concentrations below 20% of the corresponding control were defined as unstable [20].

A simple protocol was used to build the compounds: compounds were modeled with the corresponding net charges, after which 2D-3D structure conversion was carried out using the program Concord [21]. The 3D dataset obtained was submitted to the VolSurf program, and principal component analysis (PCA) was applied for chemometric interpretation. No metabolic stability information was applied to the model.

Two significant principal components were extracted. The score plot of the two principal components is shown in Fig. 17.5, where the compounds are color-coded according to their metabolic stability (filled points represent unstable compounds,

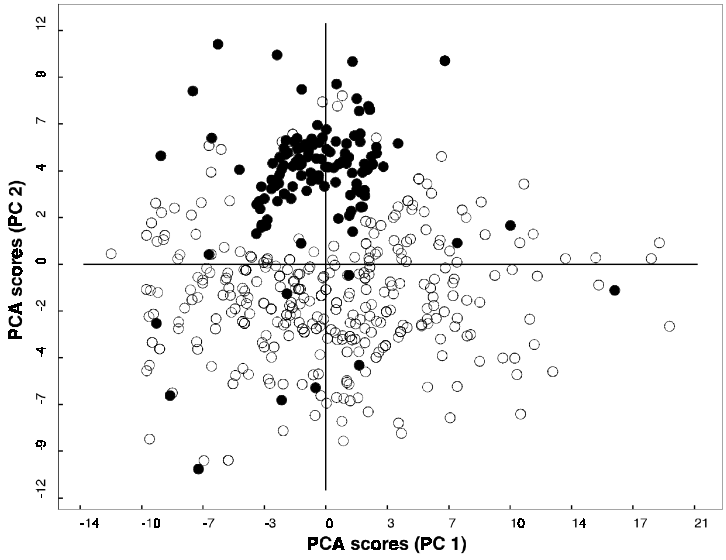

Fig. 17.5. PCA score plot for the example on metabolic stability. Filled points represent compounds with metabolic stability $\leq$20%; open points refer to compounds with metabolic stability $\geq$90%. (See text for explanation.)

open points indicate stable compounds). It should be noted that the majority of unstable compounds are clustered in a restricted region in the principal component space.

Such a result appears to be of major interest given that neither any classification of compounds, nor any training information was applied to the PCA model. A more detailed inspection of the score plot in Fig. 17.5 indicates that some compounds are misclassified, although experimental evaluation of these compounds revealed problems with their chemical stability or solubility. Thus, it appears that this model can be used to evaluate the false-positive (or false-negative) experiments. Moreover, it can also be used to evaluate the metabolic stability from the 3D structure of drug candidate prior to experimental measurements.

17.4 Conclusions

Calculated molecular properties from 3D molecular fields of interaction energies are a novel approach to correlate 3D molecular structures with pharmacodynamic, pharmacokinetic and physico-chemical properties. The novel VolSurf descriptors quantitatively characterize size, shape, polarity, hydrophobicity and the balance between them.

By quantifying the favorable and unfavorable contributions of physico-chemical and structural properties, VolSurf also offers valuable insights for drug design, pharmacological profiling, and screening. The computational procedure is fully automated, relatively rapid to use, and therefore seems to be a valuable new tool in virtual screening where selection or prioritization of candidates is required from large collections of compounds.

It is also important to remember that, in contrast to other methods, VolSurf can calculate descriptors for small, medium and large molecules, as well as for biopolymers such as DNA fragments, peptides and proteins.

Software

GRID and VolSurf are free programs available from the Internet at the site http://moldiscovery.com. The Almond program is a available from the Internet at: www.moldiscovery.com.

Acknowledgements

The authors are grateful to MD (Molecular Discovery, London, UK www.moldiscovery.com) for the use of the software, and to P. Grossi, B. Speed and P. Crivori (Pharmacia Corporation, Nerviano, Italy), for making available the dataset regarding metabolic stability.

References

1 Oprea, T. I., Gottfries, J., *J. Mol. Graphics Mod.* **1999**, *17*, 261–274.
2 Norris, D. A., Leesman, G. D., Sinko, P. J., Grass, G. M., *J. Controlled Release* **2000**, *65*, 55–62.
3 Yoshida, F., Topliss, J., *J. Med. Chem.* **2000**, *43*, 2575–2585.
4 Sjoberg, P., in: *Computer-Assisted Lead Finding and Optimization*. van de Waterbeemd, H., Testa, B., Folkers, G. (eds), Verlag Helvetica Chimica Acta, Basel, **1997**, pp. 83–92.
5 Goodford, P. J., *J. Med. Chem.* **1985**, *28*, 849.
6 Bobbyer, D. N. A., Goodford, P. J., McWhinnie, P. M., *J. Med. Chem.* **1989**, *32*, 1083.
7 GRID version 20, Molecular Discovery Ltd., London, GB, **2002**.
8 Cruciani, G., Crivori, P., Carrupt, P. A., Testa, B., *Theochem.* **2000**, *503*, 17–30.
9 Crivori, P., Cruciani, G., Carrupt, P. A., Testa, B., *J. Med. Chem.* **2000**, *43*, 2204–2216.
10 Yee, S., *Pharm. Res.* **1997**, *14*, 763–768.
11 Lin, H. J., Wu Chen, I., Lin, T. H., *Pharm. Exp. Ther.* **1994**, *271*, 1197–1202.
12 Bretschneider, B., Brandsch, M., Neubert, R., *Pharm. Res.* **1999**, *16*, 55–61.
13 Burton, S., Conradi, R. A., Hilgers, A. R., *Adv. Drug. Del. Rev.* **1991**, *7*, 370–376.
14 Hansch, C., Quinlan, J. E., Lawrence, G. L., *J. Org. Chem.* **1968**, *33*, 347.
15 Mackay, D., Bobra, A., Shiu, W. Y., Yalkowsky, S. H., *Chemosphere* **1980**, *9*, 701.
16 Tewari, Y. B., Miller, M. M., Wasik, S. P., Martire, D. E., *J. Chem. Eng. Data* **1982**, *27*, 451.
17 Pearlman, R. S., Yalkowsky, S. H., Banerjee, S., *J. Phys. Chem. Ref. Data* **1980**, *13*, 555.
18 Huuskonen, J., Salo, M., Taskinen, J., *J. Chem. Inf. Comput. Sci.* **1998**, *38*, 450–456.
19 Abraham, M., Le, J., *J. Pharm. Sci.* **1999**, *88*, 9, 868–880.
20 Personal communications.
21 Pearlman, R. S., in: *3D-QSAR in Drug Design*. Kubini, H. (ed.), ESCOM, Leiden **1993**, pp. 41–79.

18
Simulation of Absorption, Metabolism, and Bioavailability

Michael B. Bolger, Balaji Agoram, Robert Fraczkiewicz, and Boyd Steere

Abbreviations

AUC	Area under the time–concentration curve
Caco-2	Adenocarcinoma cell line derived from human colon
%HIA	Percent human intestinal absorption
LADMER	Liberation, absorption, distribution, metabolism, elimination (excretion), response
PK	Pharmacokinetics
QMPR	Quantitative molecular–property relationship
SFM	Segregated-flow model
RFCP	Reduced folate carrier protein

Symbols

CLOGP	Logarithm of the calculated octanol/water partition coefficient (for neutral species)
Δ log P	Difference between log P in octanol/water and log D at a given pH
log D	Logarithm of the distribution coefficient, usually in octanol/water at a specified pH
log P	Logarithm of the partition coefficient, usually in octanol/water (for neutral species)
MW	Molecular weight
pK_a	Ionization constant in water
Sw	Solubility
SITT	Small intestinal transit time (3.3 h = 199 min)
V	Volume

18.1
Introduction: Simulation Studies Relevant to Oral Absorption

Physiologically based mechanistic gastrointestinal simulation can be used for identification and ranking of drug discovery candidates with regard to their lib-

Drug Bioavailability: Estimation of Solubility, Permeability, Absorption and Bioavailability.
Edited by Han van de Waterbeemd, Hans Lennernäs and Per Artursson

ISBN: 3-527-30438-X

eration, absorption, distribution, metabolism, excretion, or response (LADMER) properties. Formulation of development candidates can be enhanced by using this same type of simulation. Finally, clinical trial prediction and individualized dosage optimization may benefit from simulation technology in the future [1, 2].

The observed oral bioavailability and biological activity of a particular therapeutic agent can be broken down into components that reflect delivery to the intestine, Liberation from formulated product (gastric emptying, intestinal transit, pH, food), Absorption from the lumen (dissolution, lipophilicity, particle size, active transport), intestinal and hepatic first-pass Metabolism, Distribution into tissues, and subsequent Excretion, and Response (LADMER) [3]. Experimental *in vitro* and estimated *in silico* biopharmaceutical properties can be used to predict drug LADMER characteristics. This chapter will focus on *in silico* approaches that have the potential to save valuable resources in the drug discovery and development process. We will review some of the more successful recent theoretical methods employed to simulate gastrointestinal absorption and we will discuss our results in simulating gastrointestinal absorption using the Advanced Compartmental Absorption and Transit (ACAT) model.

18.2 Background

For the purposes of gastrointestinal simulation, it is important to distinguish absorption (transfer of drug from the lumen of the intestine across the apical membrane into the enterocyte) from bioavailability (the fraction of administered dose that is available in the systemic circulation for interaction with the target tissue). Simulation of absorption and bioavailability must account for many factors that fall into three classes [4]. The first class represents physico-chemical factors including pK_a, solubility, stability, diffusivity, lipophilicity, and salt forms. The second class comprises physiological factors including gastrointestinal pH, gastric emptying, small and large bowel transit times, active transport and efflux, and gut wall and liver metabolism. The third class comprises formulation factors such as surface area, drug particle size and crystal form, and dosage forms such as solution, tablet, capsule, suspension, and modified release.

An early concept governing oral absorption of organic molecules was called the ''pH-partition'' hypothesis. Under this hypothesis, only the unionized form of ionizable molecules was thought to partition into the membranes of epithelial cells lining the gastrointestinal tract [5, 6]. The contribution of pH to permeability and dissolution of solid dosage forms has been proven to be a critical factor, but ionized molecules have now been shown to be absorbed by a variety of mechanisms. Ho and colleagues developed one of the most sophisticated early theoretical approaches to simulating drug absorption based on the diffusional transport of drugs across a compartmental membrane [7–9]. Their physical model consisted of a well-stirred bulk aqueous phase, an aqueous diffusion layer, and a heterogeneous lipid barrier composed of several compartments ending in a perfect sink. Their model represented the first example of the rigorous application of a physical model

to the quantitative and mechanistic interpretation of *in vivo* absorption [10]. The simultaneous chemical equilibria and mass transfer of basic and acidic drugs were modeled and compared favorably to in-situ measurements of intestinal, gastric, and rectal absorption in animals. The pH-partition theory was shown to be a limiting case of the more general model they developed, but because of its complexity the diffusional mass transit model has not been widely utilized. During the 1980s, a simple and intuitive alternative approach based on a series of mixing tank compartments was developed [11]. Pharmacokinetic models incorporating discontinuous gastrointestinal absorption from at least two absorption sites separated by N non-absorbing sites have been used to explain the occurrence of double peaks in plasma concentration versus time (C_p-time) profiles for ranitidine and cimetidine [12]. A similar discontinuous oral absorption model based on two absorption compartments and two transit compartments was developed to explain the bioavailability of nucleoside analogs [13]. Using a poorly described gastrointestinal simulation model, Norris *et al.* were able to estimate C_p-time profiles for ganciclovir [14]. A physiologically based, segregated-flow model (SFM) was developed to examine the influence of intestinal transport (absorption and exsorption), metabolism, flow, tissue-partitioning characteristics, and elimination in other organs on intestinal clearance, intestinal availability, and systemic bioavailability [15]. Using a completely different approach, a stochastic simulation of drug molecules moving through a cylinder of fixed radius with random geometric placement of dendritic-type virtual ''villi'', it was possible to account accurately for the observed human small intestine transit time distribution [16, 17]. Ito *et al.* have developed a pharmacokinetic model for drug absorption that includes metabolism by CYP3A4 inside the epithelial cells, P-glycoprotein (P-gp)-mediated efflux into the lumen, intracellular diffusion from the luminal side to the basal side, and subsequent permeation through the basal membrane [18]. As expected, these authors demonstrated that the fraction absorbed was synergistically elevated by simultaneous inhibition of both CYP3A4 and P-gp. Finally, we have recently demonstrated the utility of gastrointestinal absorption simulation based on the advanced compartmental absorption and transit (ACAT) model in predicting impact of physiological and biochemical processes on oral drug bioavailability [19, 20].

The ACAT model is loosely based on the work of Amidon and Yu who found that seven equal transit time compartments are required to represent the observed cumulative frequency distribution for small intestine transit times [4]. Their original compartmental absorption and transit (CAT) model was able to explain the oral plasma concentration profiles of atenolol [21].

18.3
Use of Rule-Based Computational Alerts in Early Discovery

In silico ADME profiling of compound libraries in early discovery has become a valuable addition to the research toolbox of computational and medicinal chemists. A computational alert was developed by Lipinski based on the physico-chemical

characteristics of approximately 90% of 2245 drugs with USAN names that have had clinical exposure found in the World Drug Index [22]. Most of these drugs have entered Phase II clinical trials. The ''Rule of 5'' has had a significant impact on early drug discovery and has stimulated development of similar computational alerts [23–27]. Application of a computational alert to compound libraries prior to synthesis helps limit the requirements for *in vitro* testing to those compounds that are most likely to have ''drug-like'' characteristics.

We have developed a new set of rules, called ''J-Alert'', that contains cut-offs for human jejunal permeability, water solubility, the number of oxygen-based H-bond acceptors, partial charge sums on the oxygen-based H-bond donors and acceptors, and a low level cut-off for the Moriguchi log P [28]. The J-Alert rules and a two-letter abbreviation are listed as follows:

LP	$MlogP < -0.619$		
Pr	$S + P_{eff} < 1.36$		
2P	$S + P_{eff} < 0.1$		
Sw	$S + Sw - MP < 0.004$	OR	$S + Sw - NoMP < 0.004$
Hd	$HBDoch > 1.0$		
Ha	$HBAoch < -2.23$	OR	$HBAo > 5$

where:

MlogP = Moriguchi log P
S + Peff = Simulations Plus predicted human jejunal effective permeability
S + Sw − MP = Simulations Plus predicted water solubility (known melting point)
S + Sw NoMP = Simulations Plus predicted water solubility (unknown melting point)
HBDoch = charge on hydrogen bond donors on oxygen atoms
HBAoch = charge on hydrogen bond acceptors on oxygen atoms
HBAo = number of hydrogen bond acceptors on oxygen atoms

All the descriptors and properties necessary to calculate J-Alert are generated by the software program QMPRPlus™ (Simulations Plus, Inc.). The current set of QMPRPlus™ computational models for biopharmaceutical properties is listed below:

Log P ($\log_{10}$ of octanol/water partition coefficient for un-ionized molecules)
Effective permeability (human jejunum) at pH 6.5 (P_{eff}, cm $s^{-1} \times 10^4$)
MDCK cell monolayer permeability (P_{app}, nm s^{-1})
Blood–Brain Barrier permeation (High, Low, Undecided)
Saturated aqueous solubility (mg mL^{-1})
Diffusivity (diffusion coefficient, cm^2 s^{-1})
Percent unbound to plasma proteins (%)
Pharmacokinetic volume of distribution (L kg^{-1})

These models are based on calculation of approximately 180 molecular descriptors obtained by parsing the 2D or 3D molecular structures of drug molecules as represented either in SMILES string format or as ISIS-.RDF, .SDF, or .MOL file format (MDL Information Systems, Inc., http://www.mdli.com/). Molecular descriptor values are used as inputs to independent mathematical models in order to generate estimates for each of the biopharmaceutical properties listed above. Using these property estimates or experimentally determined properties as inputs to the ACAT model, drug molecules may be classified according to their absorption, distribution, metabolism, and excretion (ADME) qualities. While no computer program is able to estimate exact experimental values for these properties, we have demonstrated that the estimated values generated by our method are sufficiently accurate to allow rank ordering of a large number of compounds for ''overall ADME quality''. In fact, *in vitro* methods also fail to predict *in vivo* ADME properties under certain conditions. We have found that the *in silico* methods are comparable with *in vitro* methods for predictive capability.

We tested the usefulness of these *in silico* biopharmaceutical properties in predicting the rank order of human intestinal absorption (%HIA). The percent absorbed for 138 drug molecules was collected from various literature sources [29, 30]. These drugs are known to be absorbed by a number of mechanisms including: passive transcellular, passive paracellular, active transport, and some were actively effluxed. Starting from 3D structures calculated by CORINA (http://www2.ccc.uni-erlangen.de/software/corina/), we used QMPRPlus to generate molecular descriptors, to estimate the biopharmaceutical properties, and to calculate the J-Alert values as described above.

Results from QMPRPlus using a rule-based method were first ranked by the value of J-Alert and within a J-Alert category (0–5), were ranked by increasing permeability (*in silico* estimate of human effective permeability). Table 18.1 lists the experimental %HIA and compares their rank order to the rank order predicted using the rule-based method for the 138 drugs. We found a significant Spearman rank correlation coefficient of 0.58 ($p < 0.001$) when the rule-based method of predicting the rank order of oral faction absorbed was applied to all 138 compounds. Figure 18.1 shows a plot of the experimental rank order compared with the J-Alert based rank order method for 108 compounds that are know to be absorbed by a passive transcellular or paracellular route. It can be seen that there is a good correlation for the passively absorbed compounds. By contrast, Fig. 18.2 shows a similar plot for the 30 compounds that are known to be absorbed by an active route or are known to be actively effluxed. For these compounds, the correlation is non-existent.

In a comparison between Lipinski's rules and the J-Alert, we have found that the ''Rule of 5'' accurately identifies some of the compounds that have unfavorable ADME properties, but also allows many of the poor compounds to go undetected. By contrast, the J-Alert identifies a much higher fraction of the unfavorable compounds but additionally identifies many ADME positives.

QMPRPlus^{TM} was used to generate *in silico* estimates of log P, aqueous solubility, and human jejunal permeability from 3D molecular structures. The predictive

Tab. 18.1. Comparison of rule-based ranking to mechanistic simulation-based ranking of 138 common drugs.

Name	*Fa%*	*Fa-Rank*	*J-Alert Rank*	*Active transport*
Acebutolol	89.5	65	50	n/a
Acetaminophen	100	107	72	n/a
Acrivastine	88	63	126	n/a
Acyclovir	20	11	15	n/a
Adriamycin	5	6	1	P-gp?
Allopurinol	90	66	21	Hypoxanthine
Alprenolol	93	80	103	n/a
Amantadine	95	84	122	n/a
Amiloride	50	29	95	P-gp
Amoxicillin	93	81	31	PepT1 Conc Dep
Ampicillin	35	20	35	n/a
Antipyrine	100	108	134	n/a
Aspirin	90	67	120	n/a
Atenolol	56	35	47	n/a
Benazepril	37	25	25	n/a
Benserazide	90	68	26	n/a
Betaxolol	90	69	80	n/a
Bromazepam	84	60	102	n/a
Bumetanide	100	109	23	Bile acid?
Bupropion	87	62	127	n/a
Caffeine	100	110	101	n/a
Captopril	67	44	75	n/a
Carbamazepine	97	95	125	n/a
Cefadroxil	100	111	48	PepT1
Cefatrizine	76	52	41	PepT1
Cefuroxime	5	7	17	n/a
Cefuroxime axetil	36	23	12	n/a
Cephalexin	98	99	59	PepT1
Chloramphenicol	85	61	52	n/a
Chlorothiazide	56	36	14	n/a
Cimetidine	60	39	32	n/a
Cisapride	100	112	82	n/a
Clonazepam	98	100	107	n/a
Clonidine	95	85	104	n/a
Corticosterone	100	113	116	n/a
Cromolyn	1	2	2	n/a
Desipramine	100	114	128	n/a
Dexamethasone	100	115	100	n/a
Diazepam	97	96	135	n/a
Diclofenac	99	103	121	n/a
Diflunisal	100	116	136	n/a
Digoxin	68	46	7	n/a
Diltiazem	100	117	110	n/a
Enalapril	59	38	38	n/a
Enalaprilat	10	8	6	n/a
Etoposide	50	30	19	P-gp

Tab. 18.1. *(continued)*

Name	*Fa%*	*Fa-Rank*	*J-Alert Rank*	*Active transport*
Famotidine	45	27	53	n/a
Felodipine	100	118	85	n/a
Fluconazole	95	86	111	n/a
Fluoxetine	80	53	133	n/a
Fluvastatin	98	101	112	n/a
Foscarnet	17	12	16	n/a
Fosinopril	30	17	27	n/a
Furosemide	61	42	30	n/a
Gabapentin	50	31	74	n/a
Ganciclovir	3.8	5	13	n/a
Gentamicin	0	1	10	n/a
Glipizide	100	119	51	n/a
Guanabenz	75	49	87	n/a
Hydrochlorothiazide	67	45	29	n/a
Hydrocortisone	95	87	96	n/a
Ibuprofen	95	88	132	n/a
Imipramine	95	89	138	n/a
Indapamide	97	97	69	n/a
Ketoprofen	100	120	130	n/a
Labetalol	95	90	109	n/a
Lamotrigine	70	47	76	n/a
Leucine	100	121	89	n/a
Levodopa	100	122	90	n/a
Lisinopril	25	14	5	PepT1
Loracarbef	100	123	60	PepT1
Lormetazepam	100	124	131	n/a
Mannitol	15	10	3	n/a
Methotrexate	100	125	28	RFCP
Methyldopa	43	26	22	n/a
Methylprednisolone	82	58	97	n/a
Metoprolol	95	91	77	n/a
Miconazole	25	15	91	P-gp
Moxonidine	99	104	65	n/a
Nadolol	35	21	57	P-gp
Naloxone	91	77	123	n/a
Naproxen	94	82	124	n/a
Nitrofurantoin	100	126	42	Secretory ActTrans?
Nizatidine	99	105	58	Organic cation
Norfloxacin	35	22	66	P-gp
Olanzapine	75	50	108	n/a
Olsalazine	2	3	4	n/a
Ondansetron	100	127	129	n/a
Oxprenolol	90	70	79	n/a
Paromomycin	3	4	11	n/a
Pefloxacin	95	92	99	n/a
Penicillin V	30	18	45	n/a
Phenoxymethylpenicillin	45	28	46	PepT1

Tab. 18.1. *(continued)*

Name	*Fa%*	*Fa-Rank*	*J-Alert Rank*	*Active transport*
Phenytoin	90	71	78	n/a
Pindolol	90	72	54	n/a
Pirenzepine	27	16	61	P-gp
Piroxicam	100	128	84	n/a
Practolol	100	129	49	n/a
Pravastatin	34	19	9	ActiveTrans?
Prazosin	50	32	36	n/a
Prednisolone	99	106	94	n/a
Probenecid	100	130	98	n/a
Progesterone	91	78	92	P-gp
Propranolol	94	83	105	n/a
Propylthiouracil	75	51	62	n/a
Quinidine	80	54	115	P-gp
Ranitidine	58	37	63	P-gp
Remikiren	10	9	18	n/a
Rifabutine	53	33	8	n/a
Salicylic Acid	100	131	113	n/a
Saquinavir	80	55	70	n/a
Scopolamine	90	73	86	n/a
Sorivudine	82	59	20	Nucleoside??
Sotalol	95	93	43	n/a
Sulfamethoxazole	100	132	39	Organic anion
Sulfasalazine	20	13	24	n/a
Sulpiride	36	24	55	n/a
Sumatriptan	62	43	44	n/a
Tenidap	90	74	114	n/a
Terazosin	91	79	40	n/a
Terbinafine	80	56	93	n/a
Terbutaline	60	40	68	n/a
Testosterone	100	133	137	n/a
Theophylline	96	94	56	Low S + Peff ??
Timolol	90	75	33	n/a
Tinidazole	100	134	73	n/a
Tranexamic acid	55	34	64	n/a
Trimethoprim	97	98	37	RFCP?
Trovafloxacin	88	64	81	MDR1 in bacteria
Valproic acid	100	135	117	n/a
Verapamil	100	136	88	P-gp
Viloxazine	100	137	67	n/a
Warfarin	98	102	119	n/a
Ximoprofen	100	138	118	n/a
Xipamide	70	48	83	n/a
Zidovudine	90	76	34	Nucleoside
Ziprasidone	60	41	106	n/a
Zopiclone	80	57	71	n/a

n/a = not available.

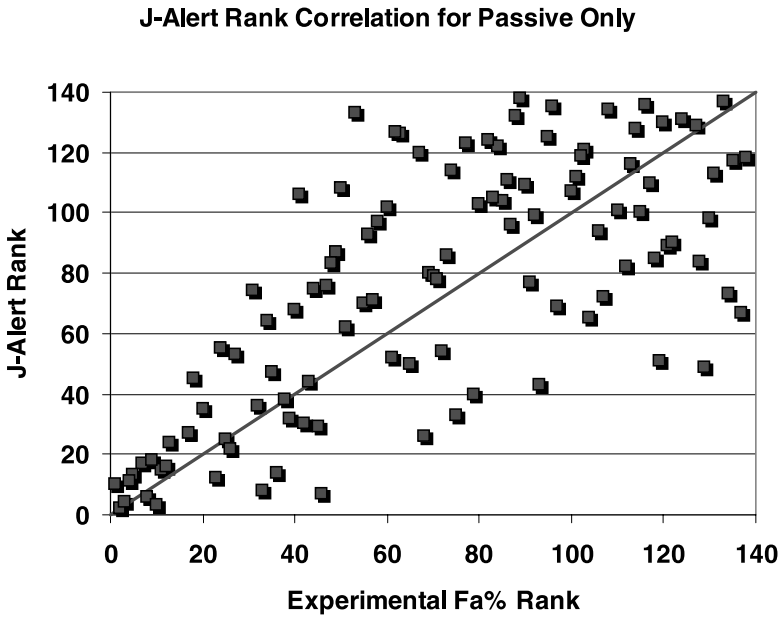

Fig. 18.1. J-Alert rank correlation for passively absorbed drugs only. The ranking of drug molecules on the Y-axis was obtained by first sorting the drugs on the basis of increasing J-Alert value, and then within a J-Alert value on the basis of the estimated human effective permeability (calculated from a 3D structure by QMPRPlus). The ranking on the X-axis was directly by increasing fraction absorbed value.

performance of Lipinski's original Rule of Five ([22]) was compared with the predictive performance of the J-Alert. A positive was defined as %HIA $>$ 50%, and a negative was defined as %HIA $\leq$ 50%.

Both sets of rules correctly identified 100%, or close to 100%, of the true positives. However, because of the liberal criteria found in Lipinski's Rule of Five, only 22% true negatives were predicted correctly and 78% were predicted as false positives. The default QMPRPlus J-Alert rules predicted 72% of the true negatives and lowered the false positives to only 28%. Unlike the original Rule of Five, however, J-Alert marked 3% as false negatives – a result of more conservative rules. Both cases of false negatives could be explained in terms of active transport and dose dependence. Thus, application of ultra-high throughput *in silico* estimation of biopharmaceutical properties to generation of computational alerts has the potential to improve compound selection to those drug candidates that are likely to have less trouble in development.

18.4 Mechanistic Simulation (ACAT models) in Early Discovery

We have developed a two-step procedure for *in silico* screening of compound libraries based on biopharmaceutical property estimation linked to a mechanistic

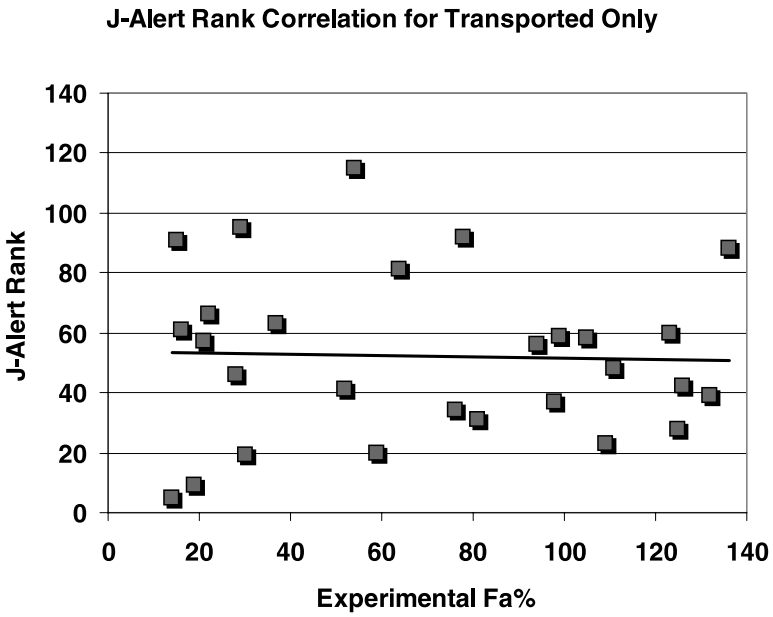

Fig. 18.2. J-Alert rank correlation for drugs affected by active processes during absorption. The ranking of drug molecules on the Y-axis was obtained by first sorting the drugs on the basis of increasing J-Alert value, and then within a J-Alert value on the basis of the estimated human effective permeability (calculated from a 3D structure by QMPRPlus). The ranking on the X-axis was directly by increasing fraction absorbed value.

simulation of gastrointestinal absorption. The first step involves biopharmaceutical property estimation by application of partial least squares (PLS) and artificial neural network (ANN) procedures to a set of molecular descriptors derived from 2D and 3D molecular structures. *In silico* methods were used to estimate such biopharmaceutical properties as effective human jejunal permeability, cell culture permeability, aqueous solubility, and molecular diffusivity. In the second step, differential equations for the ACAT model were numerically integrated in order to determine the rate, extent, and approximate gastrointestinal location of drug liberation (for controlled release), dissolution, and absorption. Figure 18.3 shows the schematic diagram of the ACAT model in which each of the arrows represents an ordinary differential equation.

The form of the ACAT model implemented in GastroPlus™ describes the release, dissolution, luminal degradation (if any), metabolism, and absorption/exsorption of a drug as it transits through successive compartments. The kinetics associated with these processes is modeled by a system of coupled linear and nonlinear rate equations. The equations include the consideration of six states (unreleased, undissolved, dissolved, degraded, metabolized, and absorbed), 18 compartments [nine gastrointestinal (stomach, seven small intestine, and colon) and nine enterocyte], three states of excreted material (unreleased, undissolved,

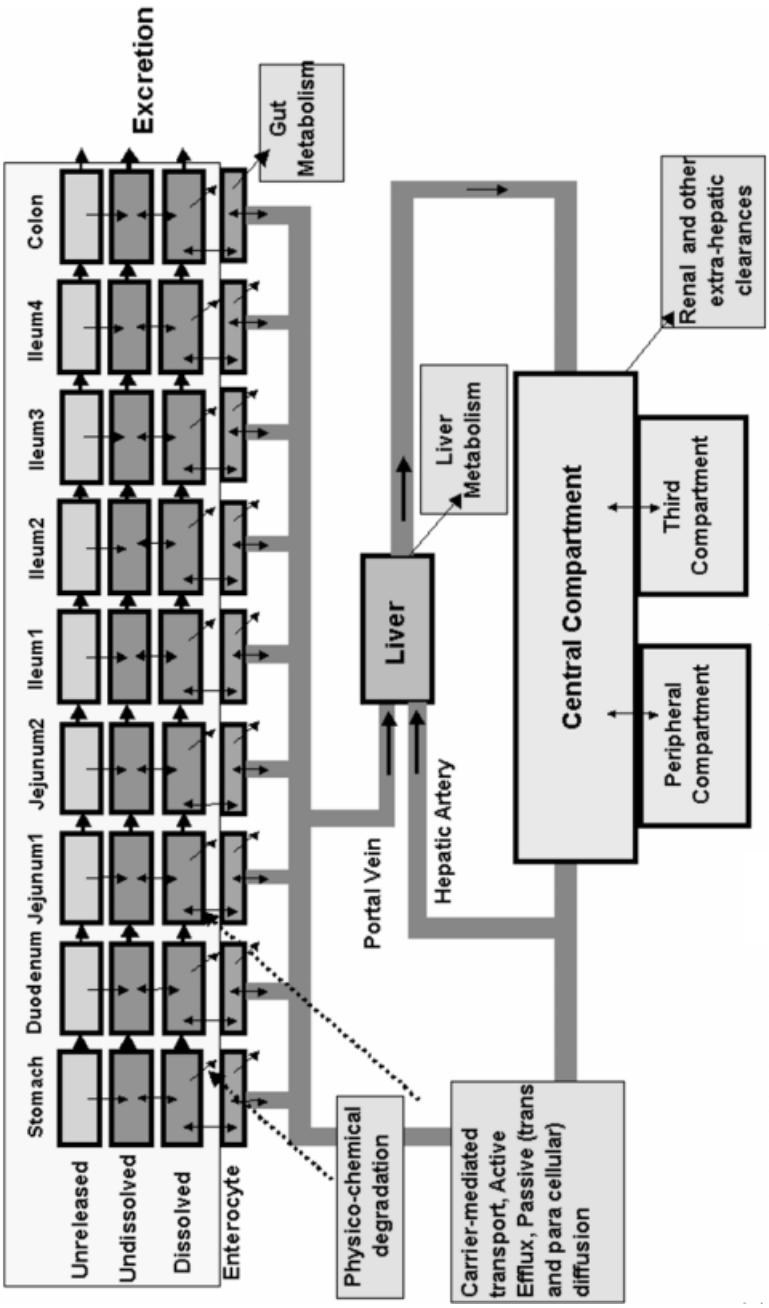

Fig. 18.3. ACAT model schematic. The diagram includes the consideration of six states (unreleased, undissolved, dissolved, degraded, metabolized, and absorbed), 18 compartments [nine gastrointestinal (stomach, seven small intestine, and colon) and nine enterocyte], three states of excreted material (unreleased, undissolved, and dissolved), and the amount of drug in up to three pharmacokinetic compartments (when pharmacokinetic parameters are available).

and dissolved), and the amount of drug in up to three pharmacokinetic compartments (when pharmacokinetic parameters are available). The total amount of absorbed material is summed over the integrated amounts being absorbed/exsorbed from each absorption/transit compartment.

For example, the rate of change of dissolved drug concentration in a luminal gastrointestinal compartment depends on six different processes:

1. Transit of drug into a compartment.
2. Transit of drug out of a compartment.
3. Release of drug from the formulation in the compartment.
4. Dissolution/precipitation of drug particles.
5. Luminal degradation of the drug.
6. Absorption/exsorption of the drug.

The time scale associated with luminal transit through a compartment is determined by a transfer rate constant, k_t, that is calculated as the reciprocal of the mean transit time within the compartment. The time scale of the dissolution process is set by a rate constant, k_d, that is computed from a drug's solubility (as a function of pH), its effective particle size, its particle density, its lumen concentration, its diffusion coefficient, and the diffusion layer thickness (Eq. (1)). The time scale associated with the absorption process is set by a rate constant, k_a, that depends on the effective permeability of the drug (Peff, units of cm s^{-1}) multiplied by an absorption scale factor (ASF, units of cm^{-1}) for each compartment (Eq. (2)). The nominal value of the ASF is the surface-to-volume ratio of the compartment, which reduces to 2/radius. ASF values are adjusted from these nominal values to correct for changes in permeability due to changing physiology along the gastrointestinal tract; e.g., absorption surface area, pH, tight junction gap width, and transport protein (influx or efflux) densities. The rates of absorption and exsorption depend on the concentration gradients across the apical and basolateral enterocyte membranes (Eqs. (3) and (4)). The time scale for luminal degradation is set by a rate constant, k_{Degrad} that is determined by interpolation from an input table of degradation rate (or half-life) versus pH, and the pH in the compartment.

The system of differential equations is integrated using a 4th/5th-order Runge-Kutta numerical integration package with adaptive step size [31]. The fraction of dose absorbed is calculated as the sum of all drug amounts crossing the apical membrane as a function of time, divided by the dose, or by the sum of all doses if multiple dosing is used.

$$k_{(i)d} = 3\gamma \frac{C_{S(i)} - C_{(i)L}}{\rho r_0 T} \tag{1}$$

$$k'_{(i)a} = \alpha_{(i)} Peff_{(i)} \tag{2}$$

$$Absorption/Exsorption_{(i)} = k'_{(i)a} V_{(i)} (C_{(i)L} - C_{(i)E}) \tag{3}$$

$$BasolateralTransfer_{(i)} = k'_{(i)b} V_{(i)} (C_{(i)E} - C_P) \tag{4}$$

where:

$k_{(i)d}$ = dissolution rate constant for the i-th compartment
$k'_{(i)a}$ = absorption rate coefficient for the i-th compartment
$k'_{(i)b}$ = absorption rate coefficient specific for the basolateral membrane of the i-th compartment
C_S = aqueous solubility at local pH
$C_{(i)L}$ = lumen concentration for the i-th compartment
$C_{(i)E}$ = intracellular enterocyte concentration for the i-th compartment
C_P = plasma central compartment concentration
$V_{(i)}$ = lumen volume of i-th compartment
γ = molecular diffusion coefficient
ρ = drug particle density
r_0 = effective initial drug particle radius
T = diffusion layer thickness
$\alpha_{(i)}$ = compartmental absorption scale factor for i-th compartment
$Peff_{(i)}$ = human effective permeability for i-th compartment

Starting from 3D structures, QMPRPlus™ was used to generate the molecular descriptors and estimates of log P, solubility, permeability, and diffusivity that were used in the gastrointestinal simulations. The extent of gastrointestinal absorption for each drug was determined *in silico* using the ACAT model after making the following simplifying assumptions: (default dose, particle radius, human fasted physiology, etc.) in GastroPlus™ and was compared to literature values. The simplest assumption for the regional dependence of the rate of absorption (Eq. (2)) is that the compartmental absorption scale factor is equal to two divided by the radius of the small intestine (1.2 cm), and that this value of α(i) (1.667) is applied to all compounds equally. The rank order of %HIA from GastroPlus was directly compared to rank order experimental %HIA. A significant Spearman rank correlation coefficient for the mechanistic simulation-based method of 0.53 ($p < 0.001$) was found. This mechanistic simulation produced 71% of %HIA predictions within 25% of the experimental values.

18.4.1
Automatic Scaling of k'_a as a Function of Peff, pH, and log D

The size and shape of a drug molecule, its acid and base dissociation constants, and the pH of the gastrointestinal tract all influence the absorption rate constant for specific regions of the gastrointestinal. Pade and co-workers measured the Caco-2 cellular permeability for a diverse set of acidic and basic drug molecules at two pH values [32]. They concluded that the permeability coefficients of the acidic drugs was greater at pH 5.4, whereas that of the basic drugs was greater at pH 7.2 and the transcellular pathway was the favored pathway for most drugs, probably due to its larger accessible surface area. The paracellular permeability of the drugs was size- and charge-dependent. The permeability of the drugs through the tight

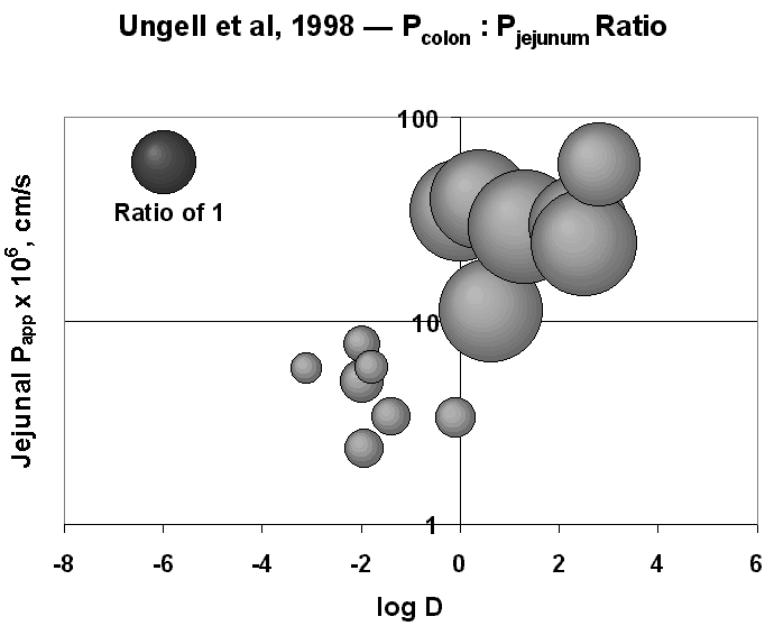

Fig. 18.4. Regional permeability from isolated rat gastrointestinal epithelial tissue as a function of log D for a small database of drug molecules. This figure is a replot of data from Ungell *et al.* [33] who reported that the colonic permeability for lipophilic drugs was found to be higher than the jejunal permeability, but the reverse was true for hydrophilic drugs.

junctions decreased with increasing molecular size. Further, the pathway also appeared to be cation-selective, with the positively charged cations of weak bases permeating the aqueous pores of the paracellular pathway at a faster rate than the negatively charged anions of weak acids. Thus, the extent to which the paracellular and transcellular routes are utilized in drug transport is influenced by the fraction of ionized and unionized species (which in turn depends upon the pK_a of the drug and the pH of the solution), the intrinsic partition coefficient of the drug, the size of the molecule and its charge.

Figure 18.4 is a representation of regional permeability coefficients of 19 drugs with different physico-chemical properties determined by Ungell *et al.* using excised segments from three regions of rat intestine: jejunum, ileum, and colon [33]. These authors observed a significant decrease in permeability to hydrophilic drugs, and a significant increase in permeability for hydrophobic drugs aborally to the small intestine ($p < 0.0001$). Figure 18.4 illustrates that for hydrophilic drugs (low permeability and low log D) the ratio of colon:jejunal permeability was <1, while for hydrophobic drugs (higher permeability and higher log D) the ratio of colon:jejunal permeability was observed to be >1. At certain pH values the permeability of small hydrophilic drugs may have a large paracellular component [34], and it is well known that the transepithelial electrical resistance (TEER) of the colon is much higher than that of the small intestine. TEER increases as the width

of tight junctions decreases, and the tight junction width has been determined to be 0.75–0.8 nm in jejunum, 0.3–0.35 nm in ileum, and 0.2–0.25 nm in colon [35–38]. The narrower tight junctions in colon suggest that paracellular transport will be much less significant in the colon, which helps to explain the lower ratio of colon:jejunal permeability for hydrophilic drugs. To our knowledge, a conclusive explanation for the increased colon permeability of drugs with high small intestine permeability is not yet available. We have used the ACAT model with experimental biopharmaceutical properties for a series of hydrophilic and hydrophobic drug molecules to calibrate a "log D model" that explains the observed rate and extent of absorption.

The mechanistic simulation ACAT model was modified to account automatically for the change in small intestinal and colon k_a' as a function of the local (pH-dependent) log D of the drug molecule. The rank order of %HIA from GastroPlus was directly compared with rank order experimental %HIA with this correction for the log D of each molecule in each of the pH environments of the small intestine. A significant Spearman rank correlation coefficient for the mechanistic simulation-based method of 0.58 ($p < 0.001$) was found. The mechanistic simulation produced 71% of %HIA predictions within 25% of the experimental values.

18.4.2
Mechanistic Correction for Active Transport and Efflux

Table 18.2 lists 30 of the molecules used in this study that are known to be substrates for active transport or active efflux. The mechanistic ACAT model was modified to accommodate saturable uptake and saturable efflux using standard Michaelis–Menten equations. It was assumed that enzymes responsible for active uptake of drug molecules from the lumen and active efflux from the enterocytes to the lumen were homogeneously dispersed within each luminal compartment and each corresponding enterocyte compartment, respectively. Equation (5) is the overall mass balance for drug in the enterocyte compartment lining the intestinal wall.

$$\frac{dM_{ent(i)}}{dt} = ADR_{(i)} + ATR_{(i)} - BDR_{(i)} - GMR_{(i)} \tag{5}$$

$$ATR = DF_{\inf\ lux(i)} \frac{V_{\max(\inf\ lux)} C_{(i)}}{(K_{m(\inf\ lux)} + C_{(i)}} - DF_{efflux(i)} \frac{V_{\max(efflux)} C_{ent(i)}}{(K_{m(efflux)} + C_{ent(i)}} \tag{6}$$

where:

$M_{ent(i)}$ = mass of drug in the enterocyte compartment *i*.
$ADR_{(i)}$ = Apical Diffusion Rate for i-th compartment
$ATR_{(i)}$ = Apical Transport Rate for i-th compartment
$BDR_{(i)}$ = Basolateral Diffusion Rate for i-th compartment
$GMR_{(i)}$ = Gut Metabolism Rate for i-th compartment
$DF_{influx(i)}$ = Distribution factor for influx transporter in compartment *i*.

Tab. 18.2. Drugs with some evidence of active uptake or efflux.

Name/ID	*Transport/Efflux*	*Reference*
Adriamycin	P-gp	44
Allopurinol	Hypoxanthine	46
Amiloride	P-gp	48
Amoxicillin	PepT1 Conc Dep	49
Bumetanide	Bile acid	51
Cefadroxil	PepT1	49
Cefatrizine	PepT1	49
Cephalexin	PepT1	49
Etoposide	P-gp	54
Lisinopril	PepT1	49
Loracarbef	PepT1	49
Methotrexate	RFCP	58
Miconazole	P-gp	60
Nadolol	P-gp	62
Nitrofurantoin	Secretory ActTrans	64
Nizatidine	Organic cation transport	45
Norfloxacin	P-gp	47
Phenoxymethylpenicillin	PepT1	49
Pirenzepine	P-gp	50
Pravastatin	H-coupled ActiveTrans	52
Progesterone	P-gp	53
Quinidine	P-gp	54
Ranitidine	P-gp	55
Sorivudine	Nucleoside?	Structural analogy to zidovudine
Sulfamethoxazole	Organic anion transport	56
Theophylline	Active uptake?	57
Trimethoprim	RFCP?	59
Trovafloxacin	MDR1 in bacteria	61
Verapamil	P-gp	63
Zidovudine	Nucleoside	65

$DF_{efflux(i)}$ = Distribution factor for efflux transporter in compartment i.
$V_{max(influx\ or\ efflux)}$ = Maximal velocity of the saturable transporter
$K_{m(influx\ or\ efflux)}$ = Michaelis constant for the saturable transporter
C_i = Concentration of drug inside the lumen of the intestine
$C_{ent(i)}$ = Concentration of drug inside the enterocyte in compartment i

Because the amounts and density of these transporters vary along the gastrointestinal tract, it is necessary to introduce a correction factor for the varying transport rates in the different luminal and enterocyte compartments. Due to the lack of experimental data for the regional distribution, and Michaelis–Menten constants for each drug in Table 18.2, we fitted an intrinsic (concentration-independent) transport rate for each drug to closely approximate the experimental %HIA. This

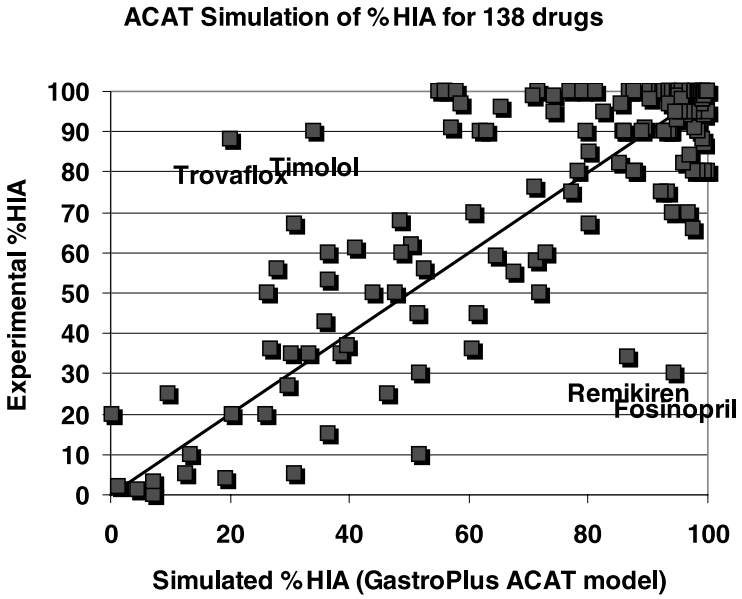

Fig. 18.5. Correlation of simulated %HIA and experimental %HIA. The fraction absorbed was simulated using GastroPlus with input values of permeability, solubility, diffusivity, and pKa values calculated purely *in silico*.

correction of the mechanism-based method for recognition of substrates that are transported or effluxed, and selection of 5 μm particle size for compounds with estimated solubility <0.008 mg mL^{-1}, improved the Spearman rank correlation to 0.69 ($p < 0.001$) and 86% of the predicted %HIA were within 25% of the experimental. Figure 18.5 shows a correlation between the simulated %HIA and the experimental %HIA for all 138 compounds when the corrections described above are implemented.

18.5 Mechanistic Simulation of Bioavailability (Drug Development)

In addition to the mechanistic simulation of absorptive and secretive saturable carrier-mediated transport, we have developed a model of saturable metabolism for the gut and liver that simulates nonlinear responses in drug bioavailability and pharmacokinetics [19]. Hepatic extraction is modeled using a modified venous equilibrium model that is applicable under transient and nonlinear conditions. For drugs undergoing gut metabolism by the same enzymes responsible for liver metabolism (e.g., CYPs 3A4 and 2D6), gut metabolism kinetic parameters are scaled from liver metabolism parameters by scaling V_{max} by the ratios of the amounts of metabolizing enzymes in each of the intestinal enterocyte compart-

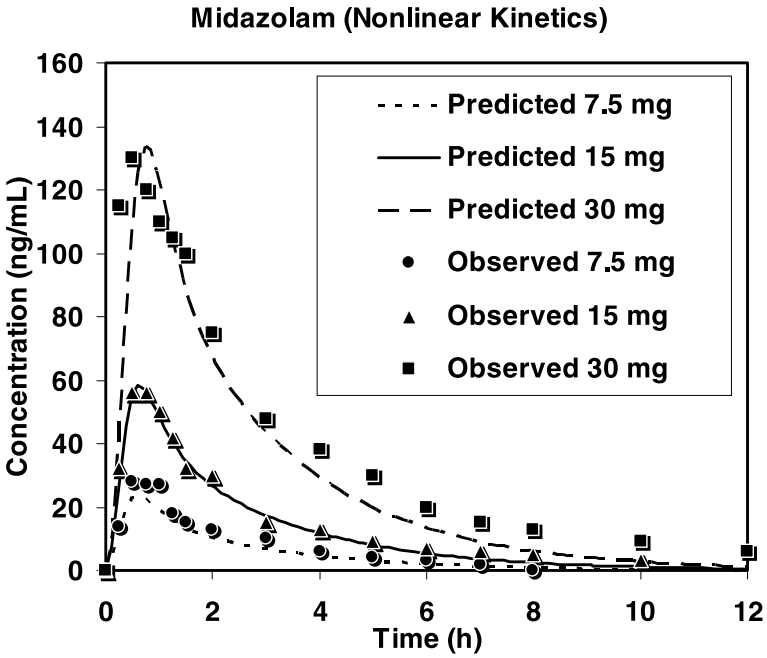

Fig. 18.6. Midazolam administration with and without grapefruit juice (GFJ) treatment [41]. Midazolam (15 mg tablet) was administered to eight male subjects (average body weight 82 kg) before and after consumption of two glasses (200 mL each) of GFJ, 1 h before drug administration. QMPRPlus was used to estimate human effective permeability (12×10^{-4} cm s^{-1}), pure aqueous water solubility (8.76 μg mL^{-1}), and log P (3.86). The metabolic enzyme kinetic constants were obtained from *in vitro* experiments on liver and intestinal microsomes ($V_{max} = 0.44$ mg s^{-1}; $K_m = 1.21$ mg L^{-1}) [39]. After GFJ treatment, the oral bioavailability was observed to increase by 33% relative to dose administered without GFJ. (Figure reproduced with permis-sion from Agoram *et al.* [19].)

ments relative to the liver. Significant work in identifying the distribution of CYP3A4 and CYP2D6 isozymes in the gut has been done by Paine *et al.* and Madani *et al.* respectively [39, 40], and their data were used in our simulations. We have validated the model against experimental data for drugs that undergo liver metabolism alone (propranolol, metoprolol), gut metabolism and liver metabolism (midazolam), and efflux, gut metabolism and liver metabolism (saquinavir).

In vitro kinetic constants obtained from homogenate or whole-cell experiments under controlled conditions were used, and the constants were scaled to the *in vivo* scenario using appropriate physiological scale factors. Figure 18.6 shows our simulated results for absorption and metabolism of midazolam when dosed with and without grapefruit juice. Midazolam is metabolized by the gut and liver by cytochrome 3A4. Saquinavir is also metabolized in the gut and liver by 3A4, and it is also a substrate for efflux by P-gp. Figure 18.7 shows our simulated results for absorption and metabolism of saquinavir when dosed with and without grapefruit juice. In both cases, it can be seen that the simulation correctly predicts the

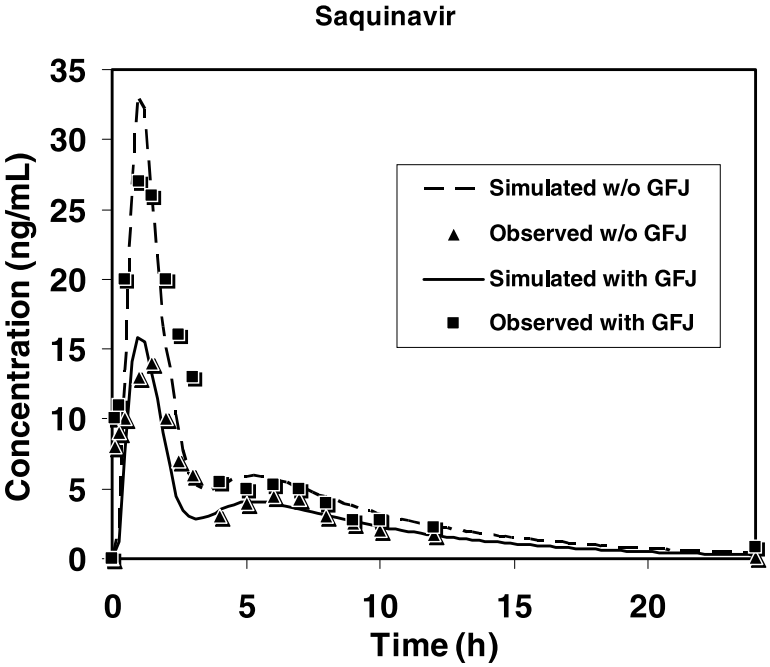

Fig. 18.7. Oral bioavailability of saquinavir with and without GFJ [42]. Saquinavir (600 mg; three capsules of Invirase, 200 mg each tablet) was administered to eight healthy male subjects (average body weight 76 kg) before and after consumption of two glasses (200 mL each) of GFJ at 15 and 45 min before drug administration. QMPRPlus was used to estimate human effective permeability (0.93×10^{-4} cm s^{-1}), pure aqueous water solubility (57.1 μg mL^{-1}), and log P (3.7). The metabolic enzyme kinetic constants were obtained from *in vitro* experiments on liver and intestinal microsomes ($V_{max} = 4.24$ mg s^{-1}; $K_m = 0.27$ mg L^{-1}) [43]. The kinetic constants, V_{max} and K_m, for P-gp efflux were optimized to fit the data and found to be 0.009 mg s^{-1} and 10 mg L^{-1}, respectively. After GFJ treatment, the oral bioavailability was observed to increase two-fold.

increase in oral area under the time–concentration curve (AUC) and bioavailability when the drugs are dosed after the patient ingested grapefruit juice. It is well known that grapefruit juice is able to inhibit CYP3A4 metabolism in the gut by ~60%, but not in the liver. Our results show that *in vitro* kinetic constants can be used to predict drug behavior *in vivo*, provided that adequate data on enzyme distribution and activity are available, and that the *in vitro* method adequately measures the metabolic processes for the compound. The use of *in vitro* data from human liver microsomes, as was used for midazolam and saquinavir above, is adequate when the metabolism of the compound is well described by only Phase I processes that take place in the microsomes. For compounds with significant Phase II metabolism (e.g., propranolol), microsomal measurements will not reflect all of the metabolism, and clearance will be underpredicted. Data from hepatocytes can provide both Phase I and Phase II metabolism, and so the use of hepatocytes would be preferred when Phase II metabolism is involved. Even with the best of

experimental data, factors such as inter-individual variability in enzyme content and activity strongly limit extension of predictions across different demographics.

More experimental information is needed regarding the distribution and densities of metabolizing enzymes and efflux proteins in the gastrointestinal tract. This information is crucial, since dissolution and absorption are site-dependent all along the gastrointestinal tract. A knowledge of the variation in enzyme and efflux transporter amounts in the intestine and colon can also be utilized to design formulations with increased bioavailabilities by avoiding sites of high intestinal first-pass and efflux. For example, the bioavailability of a CYP3A4 substrate can be increased by modifying the formulation to release most of the drug in the distal gastrointestinal region, provided that absorption is not a limiting factor. Similarly, the bioavailability of a P-gp substrate might be increased by using a gastric-retentive formulation to release the drug in the proximal gastrointestine where the P-gp density is relatively low. The influence of inhibitors and inducers of enzymes can be modeled using appropriate scale factors to mimic changes in enzyme amounts, activity, and competitive inhibition. Similarly, drug–drug interactions can be modeled using the same techniques. For drugs that are substrates of both efflux proteins and metabolic enzymes in the small intestine, these proteins work in tandem in reducing the oral bioavailability of drugs.

In spite of its limitations, the ACAT model combined with modeling of saturable processes has become a powerful tool in the study of oral absorption and pharmacokinetics. To our knowledge, it is the only tool that can translate *in vitro* data from early drug discovery experiments all the way to plasma concentration profiles and nonlinear dose–relationship predictions. As more experimental data become available, we believe that the model will become more comprehensive and its predictive capabilities will be further enhanced.

18.6 Conclusions

Application of ultra-high-throughput *in silico* estimation of biopharmaceutical properties to the generation of rule-based computational alerts has the potential to improve compound selection to those drug candidates that are likely to prove less troublesome in their development. The extension of purely *in silico* methods to the realm of mechanistic simulation further enhances our ability to predict the impact of physiological and biochemical process on drug absorption and bioavailability.

References

1 Selick, H. E., Beresford, A. P., Tarbit, M. H., The emerging importance of predictive ADME simulation in drug discovery, *Drug Discov. Today* **2002**, *7*, 109–116.

2 Gobburu, J. V., Marroum, P. J., Utilisation of pharmacokinetic–pharmacodynamic modelling and simulation in regulatory decision-making, *Clin. Pharmacokinet.* **2001**, *40*, 883–892.

3 Hall, S. D., Thummel, K. E., Watkins, P. B., Lown, K. S., Benet, L. Z., Paine, M. F., Mayo, R. R., Turgeon, D. K., Bailey, D. G., Fontana, R. J., Wrighton, S. A., Molecular and physical mechanisms of first-pass extraction, *Drug. Metab. Dispos.* **1999**, *27*, 161–166.

4 Yu, L. X., Lipka, E., Crison, J. R., Amidon, G. L., Transport approaches to the biopharmaceutical design of oral drug delivery system: prediction of intestinal absorption, *Adv. Drug Deliv. Rev.* **1996**, *19*, 359–376.

5 Jacobs, M. H., Some aspects of cell permeability to weak electrolytes, *Cold Spring Harbor Symp. Quant. Biol.* **1940**, *8*, 30–39.

6 Hogben, C. A. M., Tocco, D. J., Brodie, B. B., Schanker, L. S., On the mechanism of intestinal absorption of drugs, *J. Pharmacol. Exp. Ther.* **1959**, *125*, 275–282.

7 Suzuki, A., Higuchi, W. I., Ho, N. F., Theoretical model studies of drug absorption and transport in the gastrointestinal tract. II., *J. Pharm. Sci.* **1970**, *59*, 651–659.

8 Suzuki, A., Higuchi, W. I., Ho, N. F., Theoretical model studies of drug absorption and transport in the gastrointestinal tract. I., *J. Pharm. Sci.* **1970**, *59*, 644–651.

9 Ho, N. F., Higuchi, W. I., Turi, J., Theoretical model studies of drug absorption and transport in the gastrointestinal tract. III., *J. Pharm. Sci.* **1972**, *61*, 192–197.

10 Ho, N. F., Higuchi, W. I., Quantitative interpretation of in vivo buccal absorption of n-alkanoic acids by the physical model approach, *J. Pharm. Sci.* **1971**, *60*, 537–541.

11 Dressman, J. B., Fleisher, D., Amidon, G. L., Physicochemical model for dose-dependent drug absorption, *J. Pharm. Sci.* **1984**, *73*, 1274–1279.

12 Suttle, A. B., Pollack, G. M., Brouwer, K. L., Use of a pharmacokinetic model incorporating discontinuous gastrointestinal absorption to examine the occurrence of double peaks in oral concentration–time profiles, *Pharm. Res.* **1992**, *9*, 350–356.

13 Wright, J. D., Ma, T., Chu, C. K., Boudinot, F. D., Discontinuous oral absorption pharmacokinetic model and bioavailability of 1-(2-fluoro-5-methyl-beta-L-arabinofuranosyl)uracil (L-FMAU) in rats, *Biopharm. Drug Dispos.* **1996**, *17*, 197–207.

14 Norris, D. A., Leesman, G. D., Sinko, P. J., Grass, G. M., Development of predictive pharmacokinetic simulation models for drug discovery, *J. Controlled Release* **2000**, *65*, 55–62.

15 Cong, D., Doherty, M., Pang, K. S., A new physiologically based, segregated-flow model to explain route-dependent intestinal metabolism, *Drug. Metab. Dispos.* **2000**, *28*, 224–235.

16 Kalampokis, A., Argyrakis, P., Macheras, P., A heterogeneous tube model of intestinal drug absorption based on probabilistic concepts, *Pharm. Res.* **1999**, *16*, 1764–1769.

17 Kalampokis, A., Argyrakis, P., Macheras, P., Heterogeneous tube model for the study of small intestinal transit flow, *Pharm. Res.* **1999**, *16*, 87–91.

18 Ito, K., Kusuhara, H., Sugiyama, Y., Effects of intestinal CYP3A4 and P-glycoprotein on oral drug absorption-theoretical approach, *Pharm. Res.* **1999**, *16*, 225–231.

19 Agoram, B., Woltosz, W. S., Bolger, M. B., Predicting the impact of physiological and biochemical processes on oral drug bioavailability, *Adv. Drug Deliv. Rev.* **2001**, *50* (Suppl. 1), S41–S67.

20 Aarons, L., Karlsson, M. O., Mentre, F., Rombout, F., Steimer, J. L., van Peer, A., Role of modelling and simulation in Phase I drug development, Eur. *J. Pharm. Sci.* **2001**, *13*, 115–122.

21 Yu, L. X., Amidon, G. L., A compartmental absorption and transit model for estimating oral drug absorption, *Int. J. Pharm.* **1999**, *186*, 119–125.

22 Lipinski, C. A., Lombardo, F., Dominy, B. W., Feeney, P. J., Experimental and computational

approaches to estimate solubility and permeability in drug discovery and development settings, *Adv. Drug Deliv. Rev.* **1997**, *23*, 3–25.

23 Andrews, C. W., Bennett, L., Yu, L. X., Predicting human oral bioavailability of a compound: development of a novel quantitative structure–bioavailability relationship, *Pharm. Res.* **2000**, *17*, 639–644.

24 Oprea, T. I., Gottfries, J., Toward minimalistic modeling of oral drug absorption, *J. Mol. Graph. Model* **1999**, *17*, 261–274, 329.

25 Stenberg, P., Luthman, K., Ellens, H., Lee, C. P., Smith, P. L., Lago, A., Elliott, J. D., Artursson, P., Prediction of the intestinal absorption of endothelin receptor antagonists using three theoretical methods of increasing complexity, *Pharm. Res.* **1999**, *16*, 1520–1526.

26 Matter, H., Baringhaus, K. H., Naumann, T., Klabunde, T., Pirard, B., Computational approaches towards the rational design of drug-like compound libraries, *Comb. Chem. High Throughput Screen.* **2001**, *4*, 453–475.

27 Osterberg, T., Norinder, U., Prediction of polar surface area and drug transport processes using simple parameters and PLS statistics, *J. Chem. Inf. Comput. Sci.* **2000**, *40*, 1408–1411.

28 Moriguchi, I., Hirono, S., Liu, Q., Nakagome, I., Matsushita, Y., Simple method of calculating octanol/water partition coefficient, *Chem. Pharm. Bull. (Tokyo)* **1992**, *40*, 127–130.

29 Chiou, W. L., Barve, A., Linear correlation of the fraction of oral dose absorbed of 64 drugs between humans and rats, *Pharm. Res.* **1998**, *15*, 1792–1795.

30 Zhao, Y. H., Le, J., Abraham, M. H., Hersey, A., Eddershaw, P. J., Luscombe, C. N., Butina, D., Beck, G., Sherborne, B., Cooper, I., Platts, J. A., Boutina, D., Evaluation of human intestinal absorption data and subsequent derivation of a quantitative structure–activity relationship (QSAR) with the Abraham descriptors, *J. Pharm. Sci.* **2001**, *90*, 749–784.

31 Press, W. H., Numerical recipes, in: *C: The Art of Scientific Computing.* Cambridge University Press, Cambridge, New York, **1992.**

32 Pade, V., Stavchansky, S., Estimation of the relative contribution of the transcellular and paracellular pathway to the transport of passively absorbed drugs in the Caco-2 cell culture model, *Pharm. Res.* **1997**, *14*, 1210–1215.

33 Ungell, A. L., Nylander, S., Bergstrand, S., Sjoberg, A., Lennernas, H., Membrane transport of drugs in different regions of the intestinal tract of the rat, *J. Pharm. Sci.* **1998**, *87*, 360–366.

34 Adson, A., Burton, P. S., Raub, T. J., Barsuhn, C. L., Audus, K. L., Ho, N. F., Passive diffusion of weak organic electrolytes across Caco-2 cell monolayers: uncoupling the contributions of hydrodynamic, transcellular, and paracellular barriers, *J. Pharm. Sci.* **1995**, *84*, 1197–1204.

35 Fordtran, J. S., Rector, F. C., Jr., Ewton, M. F., Soter, N., Kinney, J., Permeability characteristics of the human small intestine, *J. Clin. Invest.* **1965**, *44*, 1935–1944.

36 Soergel, K. H., Whalen, G. E., Harris, J. A., Passive movement of water and sodium across the human small intestinal mucosa, *J. Appl. Physiol.* **1968**, *24*, 40–48.

37 Artursson, P., Karlsson, J., Correlation between oral drug absorption in humans and apparent drug permeability coefficients in human intestinal epithelial (Caco-2) cells, *Biochem. Biophys. Res. Commun.* **1991**, *175*, 880–885.

38 Billich, C. O., Levitan, R., Effects of sodium concentration and osmolality on water and electrolyte absorption form the intact human colon, *J. Clin. Invest.* **1969**, *48*, 1336–1347.

39 Paine, M. F., Khalighi, M., Fisher, J. M., Shen, D. D., Kunze, K. L., Marsh, C. L., Perkins, J. D., Thummel, K. E., Characterization of interintestinal and intraintestinal variations in human CYP3A-dependent metabolism, *J. Pharmacol. Exp. Ther.* **1997**, *283*, 1552–1562.

40 Madani, S., Paine, M. F., Lewis, L., Thummel, K. E., Shen, D. D., Comparison of CYP2D6 content and metoprolol oxidation between microsomes isolated from human livers and small intestines, *Pharm. Res.* **1999**, *16*, 1199–1205.

41 Kupferschmidt, H. H., Ha, H. R., Ziegler, W. H., Meier, P. J., Krahenbuhl, S., Interaction between grapefruit juice and midazolam in humans, *Clin. Pharmacol. Ther.* **1995**, *58*, 20–28.

42 Kupferschmidt, H. H., Fattinger, K. E., Ha, H. R., Follath, F., Krahenbuhl, S., Grapefruit juice enhances the bioavailability of the HIV protease inhibitor saquinavir in man, *Br. J. Clin. Pharmacol.* **1998**, *45*, 355–359.

43 Fitzsimmons, M. E., Collins, J. M., Selective biotransformation of the human immunodeficiency virus protease inhibitor saquinavir by human small-intestinal cytochrome P4503A4: potential contribution to high first-pass metabolism, *Drug. Metab. Dispos.* **1997**, *25*, 256–266.

44 Leonce, S., Pierre, A., Anstett, M., Perez, V., Genton, A., Bizzari, J. P., Atassi, G., Effects of a new triazinoaminopiperidine derivative on adriamycin accumulation and retention in cells displaying P-glycoprotein-mediated multidrug resistance, *Biochem. Pharmacol.* **1992**, *44*, 1707–1715.

45 Nakamura, H., Sano, H., Yamazaki, M., Sugiyama, Y., Carrier-mediated active transport of histamine H2 receptor antagonists, cimetidine and nizatidine, into isolated rat hepatocytes: contribution of type I system, *J. Pharmacol. Exp. Ther.* **1994**, *269*, 1220–1227.

46 de Koning, H. P., Jarvis, S. M., Hypoxanthine uptake through a purine-selective nucleobase transporter in *Trypanosoma brucei* procyclic cells is driven by protonmotive force, *Eur. J. Biochem.* **1997**, *247*, 1102–1110.

47 de Lange, E. C., Marchand, S., van den Berg, D., van der Sandt, I. C., de Boer, A. G., Delon, A., Bouquet, S., Couet, W., In vitro and in vivo investigations on fluoroquinolones; effects of the P-glycoprotein efflux transporter on brain distribution of sparfloxacin, *Eur. J. Pharm. Sci.* **2000**, *12*, 85–93.

48 Martel, F., Martins, M. J., Hipolito-Reis, C., Azevedo, I., Inward transport of [3H]-1-methyl-4-phenylpyridinium in rat isolated hepatocytes: putative involvement of a P-glycoprotein transporter, *Br. J. Pharmacol.* **1996**, *119*, 1519–1524.

49 Swaan, P. W., Tukker, J. J., Molecular determinants of recognition for the intestinal peptide carrier, *J. Pharm. Sci.* **1997**, *86*, 596–602.

50 Lauterbach, F., Intestinal permeation of nonquaternary amines: a study with telenzepine and pirenzepine in the isolated mucosa of guinea pig jejunum and colon, *J. Pharmacol. Exp. Ther.* **1987**, *243*, 1121–1130.

51 Honscha, W., Schulz, K., Muller, D., Petzinger, E., Two different mRNAs from rat liver code for the transport of bumetanide and taurocholate in *Xenopus laevis* oocytes, *Eur. J. Pharmacol.* **1993**, *246*, 227–232.

52 Hatanaka, T., Clinical pharmacokinetics of pravastatin: mechanisms of pharmacokinetic events, *Clin. Pharmacokinet.* **2000**, *39*, 397–412.

53 van Kalken, C. K., Broxterman, H. J., Pinedo, H. M., Feller, N., Dekker, H., Lankelma, J., Giaccone, G., Cortisol is transported by the multidrug resistance gene product P- glycoprotein, *Br. J. Cancer* **1993**, *67*, 284–289.

54 Makhey, V. D., Guo, A., Norris, D. A., Hu, P., Yan, J., Sinko, P. J., Characterization of the regional intestinal kinetics of drug efflux in rat and human intestine and in Caco-2 cells, *Pharm. Res.* **1998**, *15*, 1160–1167.

55 Collett, A., Higgs, N. B., Sims, E., Rowland, M., Warhurst, G., Modulation of the permeability of H2 receptor antagonists cimetidine and ranitidine by P-glycoprotein in rat intestine and the human colonic cell line Caco-2, *J. Pharmacol. Exp. Ther.* **1999**, *288*, 171–178.

56 Lee, J., Hollyer, R., Rodelas, R., Preuss, H. G., The influence of trimethoprim, sulfamethoxazole, and creatinine on renal organic anion and cation transport in rat kidney tissue, *Toxicol. Appl. Pharmacol.* **1981**, *58*, 184–193.

57 Johansson, O., Lindberg, T., Melander, A., Wahlin-Boll, E., Different effects of different nutrients on theophylline absorption in man, *Drug Nutr. Interact.* **1985**, *3*, 205–211.

58 Nagakubo, J., Tomimatsu, T., Kitajima, M., Takayama, H., Aimi, N., Horie, T., Characteristics of transport of fluoresceinated methotrexate in rat small intestine, *Life Sci.* **2001**, *69*, 739–747.

59 Lambie, D. G., Johnson, R. H., Drugs and folate metabolism, Drugs **1985**, *30*, 145–155.

60 Katiyar, S. K., Edlind, T. D., Identification and expression of multidrug resistance-related ABC transporter genes in *Candida krusei*, *Med. Mycol.* **2001**, *39*, 109–116.

61 Zhang, L., Li, X. Z., Poole, K., Fluoroquinolone susceptibilities of efflux-mediated multidrug-resistant *Pseudomonas aeruginosa*, *Stenotrophomonas maltophilia* and *Burkholderia cepacia*, *J. Antimicrob. Chemother.* **2001**, *48*, 549–552.

62 Terao, T., Hisanaga, E., Sai, Y., Tamai, I., Tsuji, A., Active secretion of drugs from the small intestinal epithelium in rats by P-glycoprotein functioning as an absorption barrier, *J. Pharm. Pharmacol.* **1996**, *48*, 1083–1089.

63 Saitoh, H., Aungst, B. J., Possible involvement of multiple P-glycoprotein-mediated efflux systems in the transport of verapamil and other organic cations across rat intestine, *Pharm. Res.* **1995**, *12*, 1304–1310.

64 Gerk, P. M., Oo, C. Y., Paxton, E. W., Moscow, J. A., McNamara, P. J., Interactions between cimetidine, nitrofurantoin, and probenecid active transport into rat milk, *J. Pharmacol. Exp. Ther.* **2001**, *296*, 175–180.

65 Ngo, L. Y., Patil, S. D., Unadkat, J. D., Ontogenic and longitudinal activity of Na(+)-nucleoside transporters in the human intestine, *Am. J. Physiol. Gastrointest. Liver Physiol.* **2001**, *280*, G475–G481.

19
Prediction of Bioavailability

Arun K. Mandagere and Barry Jones

Abbreviations

ADME	Absorption, distribution, metabolism, elimination (excretion)
BA	Oral bioavailability
Caco-2	Adenocarcinoma cell line derived from human colon
FDA	Food and Drug Administration
HTS	High-throughput screening
PK	Pharmacokinetics
SAR	Structure–activity relationship
QSAR	Quantitative structure–activity relationship
QSBR	Quantitative structure–bioavailability relationship

Symbols

CLOGP	Logarithm of the calculated octanol/water partition coefficient (for neutral species)
Δlog D	log $D_{6.5}$ − log $D_{7.4}$
%F	Absolute oral bioavailability
log D	Logarithm of the distribution coefficient, usually in octanol/water at pH 7.4
log P	Logarithm of the partition coefficient, usually in octanol/water (for neutral species)
MW	Molecular weight
pK_a	Ionization constant in water
R_S	Correlation coefficient
S	Solubility

19.1
Introduction

A model for predicting oral bioavailability is an important tool, both in the early phases of drug discovery to select the most promising leads for further optimization, and in the later stages to select candidates for clinical development. The

Drug Bioavailability: Estimation of Solubility, Permeability, Absorption and Bioavailability.
Edited by Han van de Waterbeemd, Hans Lennernäs and Per Artursson

ISBN: 3-527-30438-X

objective of this model is to aid in the rapid identification of compounds that will exhibit good efficacy, systemic exposure and safety profiles. Application of the predictive model can provide a rational and efficient means of utilizing the limited *in vivo* resources for evaluating potential lead compounds that have a higher probability of success in development. Another benefit of such a model is to assist in the organization of structure–absorption/metabolism/physical property data to enhance solubility, absorption, and metabolic properties via the application of rational drug design. These models must have reasonably good probability of success in selecting candidates with good oral bioavailability while rejecting those with low probability. In addition, these models need not predict the precise oral bioavailability, but rather, rapidly forecast with a high degree of confidence whether the compound will have satisfactory or unsatisfactory oral bioavailability in humans and in animals. Predicting bioavailability is more challenging because of multiple variables that are involved. However, in recent years very promising progress has been made using a combination of several *in vitro* measures, as well as the development of *in silico* tools. This chapter will review the *in vitro* and *in silico* approaches to estimating oral bioavailability.

19.2 Oral Bioavailability Definition

The FDA defines oral bioavailability as ''the rate and extent to which the active ingredient or active moiety is absorbed from a drug product and becomes available at the site of action'' [1]. However, it is not always feasible to measure the drug at the site of action. Therefore, oral bioavailability is assessed based on drug concentrations in the general circulation. Absolute oral bioavailability (%F) is a measure of systemic exposure of an orally dosed drug relative to an intravenous dose. %F is determined by measuring the blood concentration of the active drug at numerous time intervals following an intravenous and an oral dose. The area under the concentration–time curve (AUC) is determined from the blood or plasma concentrations and the absolute oral bioavailability is calculated using the following equation:

$$\%\mathrm{F} = \frac{\mathrm{AUC}_{\mathrm{oral}} \times \text{iv dose}}{\mathrm{AUC}_{\mathrm{iv}} \times \text{oral dose}} \times 100$$

Thus, %F is defined as the area under the curve normalized for administered dose. Blood drug concentration is affected by the dynamics of dissolution, solubility, absorption, metabolism, distribution, and elimination. In addition to %F, other pharmacokinetic parameters are derived from the drug concentration versus time plots. These include the terms to describe the compound's absorption, distribution, metabolism and excretion, but they are dependent to some degree on the route of administration of the drug. For instance, if the drug is administered by the intravenous route it will undergo rapid distribution into the tissues, including those tissues that are responsible for its elimination.

When a drug is given orally it may be subject to additional factors not seen with intravenous administration. These include gastrointestinal transit, transporter-mediated secretion, chemical instability in the gastrointestinal tract and first-pass metabolism in the gut and/or the liver. Any or all of these processes can serve to attenuate the amount of drug reaching the systemic circulation for a given oral dose. High bioavailability assures that the lowest efficacious dose can be used, and also limits inter-patient variability.

It is important to make a distinction between oral bioavailability and absorption, as the terms are often used incorrectly and interchangeably [2]. Sinko [3] has defined absorption as "the amount of drug that passes through the intestinal tissue and enters the portal vein". On the other hand, for a drug to be orally bioavailable, it must reach the general circulation by not only passing through the intestine, but also through the liver where it is subject to first-pass metabolism (hepatic clearance).

Physiologically, the blood supply from the gastrointestinal tract passes through the liver via the hepatic portal vein on its way to the heart and lungs. Hence, for any compound that is orally administered, the entire dose will be presented to the liver. Thus, the entire dose is subject to liver extraction and, depending on the magnitude of the extraction, this can substantially affect the post-hepatic concentrations of the drug, and hence its bioavailability. Therefore, for compounds that have high hepatic extractions due to rapid metabolism, the first-pass effect will also be high, resulting in a low bioavailability. If the compound is slowly metabolized, then the first-pass effect will likely be low and the exposure seen after an oral dose will be similar to that seen after an intravenous dose; that is, it will have high bioavailability. Therefore absolute oral bioavailability is a function of *both* absorption and clearance.

19.2.1 Cassette Dosing

The application of high-throughput synthesis and biological screening methodologies within the pharmaceutical industry has resulted in the production of very large numbers of pharmacologically active molecules that require pharmacokinetic assessment. There have been concomitant developments in the areas of *in silico* and *in vitro* drug metabolism assessments, but this still results in large numbers of molecules requiring pharmacokinetic assessment. One solution to this is to use cassette or "n-in-one" dosing [4]. Pharmacokinetic studies are normally carried out by administering a single compound and following its time course in the body. However, in cassette dosing a number of different compounds are administered in the same dosing solution and the time courses for all of the compounds are followed. This allows for the initial pharmacokinetic parameters for all the compounds to be assessed in one experiment, and those that appear of interest are then repeated using the traditional single-compound approach.

There are a number of issues with using cassette dosing, not only in terms of

interpretation of the data, but also in terms of experimental design and analytical methodology [4, 5]. However, with sufficient planning these issues can be overcome such that it is possible to obtain meaningful data from cassettes of over 80 compounds. More pertinent to the current discussion is the utility of this technique to determine bioavailability, and cassette dosing via the oral route has been found to be problematic [4]. The reason for this may be because the very high concentrations of compounds reaching the liver from the hepatic portal vein causes inhibition of drug-metabolizing enzymes, transporters, etc., and this results in an over-estimation of oral bioavailability. This is less of a concern with intravenous dosing, where the hepatic concentrations will be lower. Whilst this technique increases the rate at which pharmacokinetic data can be produced, it does not circumvent the issue of species differences in absorption and metabolism.

19.2.2
Across-species Prediction of Bioavailability

As previously noted, the bioavailability of a compound is a complex function that includes contributions from absorption and clearance. Since the molecule must undergo these biological processes in all species, there is a temptation to assume a relationship between the bioavailability between species, and hence that human bioavailability can be predicted by such relationships. Although a linear correlation has been demonstrated for the rate/extent of absorption (% oral dose absorbed) between species for various drugs [6–8], there is clearly a lack of correlation for bioavailability between species [2, 8]. Figure 19.1 shows the excellent correlation in

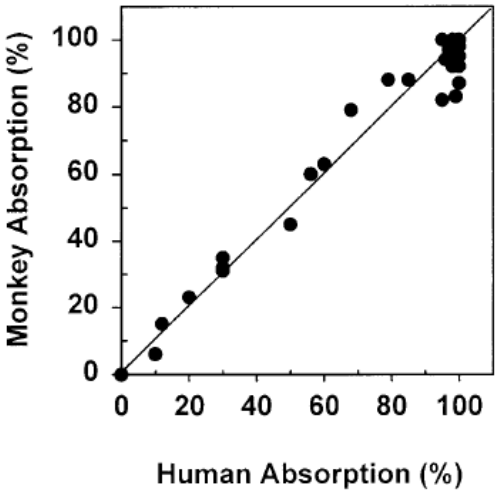

Fig. 19.1. Correlation of percentage oral dose absorbed between humans and monkeys for 43 drugs [8].

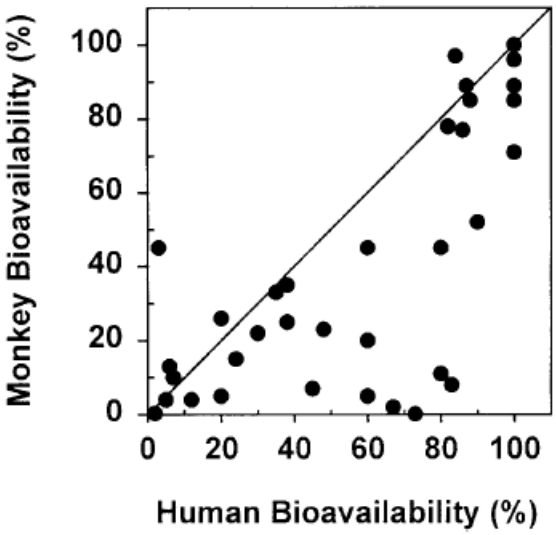

Fig. 19.2. Comparison of absolute oral bioavailability between humans and monkeys [8].

percent dose absorbed between humans and monkeys [8]. Similar correlation was observed between rats and humans for a diverse group of drugs [6], despite wide differences in physico-chemical properties of the drugs and the physiological differences among the species. The exact mechanism behind the near-perfect correlation in the rate of absorption between rat versus human and monkey versus human is not clear, though it is suggested that factors such as a similarity in first-order absorption rate constants might be responsible [8].

In contrast to absorption, oral bioavailability shows a clear lack of correlation between species, as seen in Figs 19.2, 19.3, and 19.4 for a diverse group of drug molecules in monkey versus human, rat versus human, and dog versus human, respectively [2, 8]. It is fair to say that these plots suggest a trend in the bioavailability, but not a predictive correlation. The assumption that bioavailability is the same between species ignores any species differences in absorption and/or metabolism. In fact, differences in absorption and metabolism between rat, dog, monkey and human have been well documented [9–12]. The dog has been shown to have larger aqueous pores than other species, and so allows a greater degree of paracellular absorption. In addition, the dog is not compatible with human in terms of one of the cytochrome P450 enzymes, CYP2C9. This enzyme is responsible for most of the metabolism of acidic compounds, such as the nonsteriodal anti-inflammatory drugs diclofenac and ibuprofen. Similarly, monkey has been shown to have greater level of cytochrome P450 activity than humans and thus exhibits a greater first-pass metabolism of drugs [9]. Hence it is not surprising that there is little correlation between rat, dog, monkey and human bioavailability values.

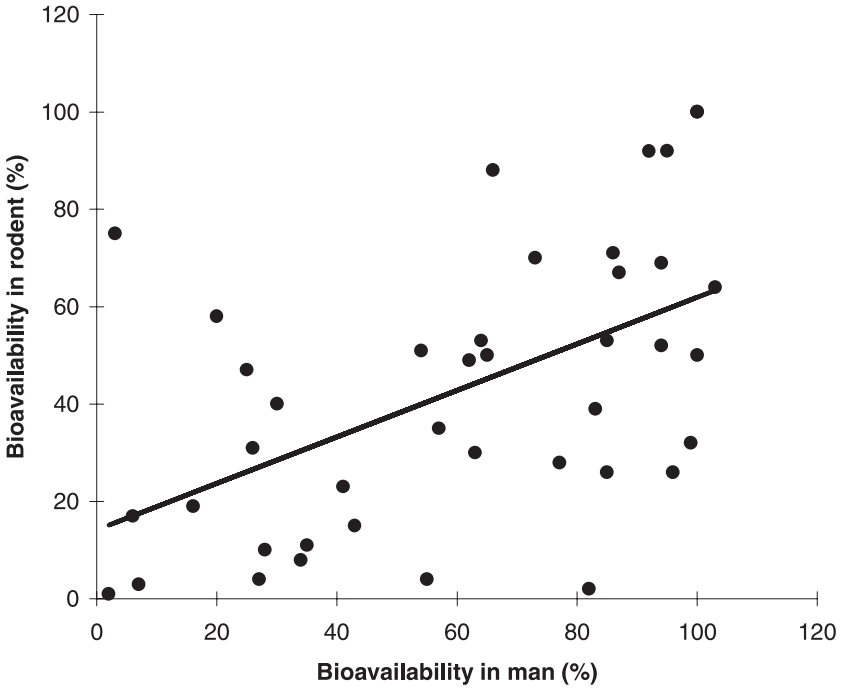

Fig. 19.3. Comparison of bioavailability in rodents and human [2, 25].

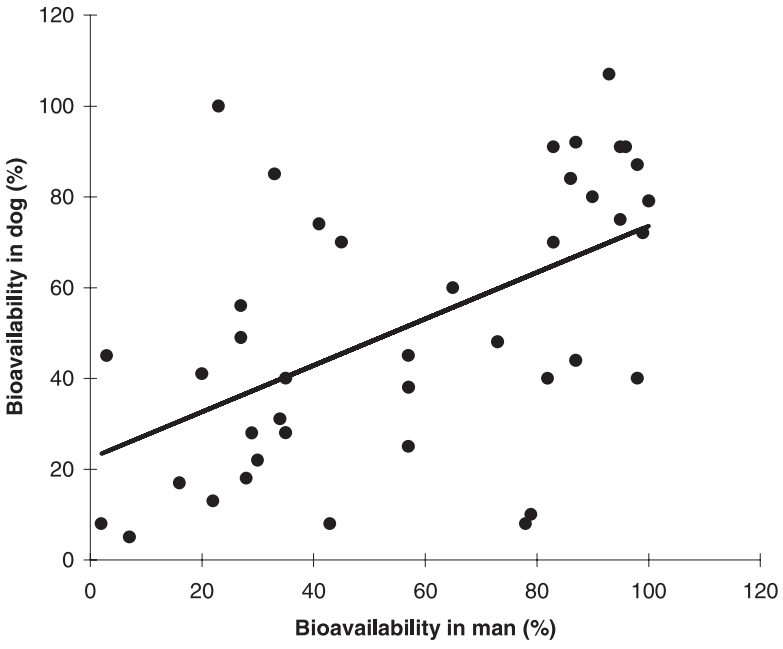

Fig. 19.4. Comparison of bioavailability in dog and human [2, 25].

19.3
In silico Models for Estimating Human Oral Bioavailability

The genesis of *in silico* oral bioavailability predictions can be traced back to Lipinski's Rule of Five and others' qualitative attempts to describe drug-like molecules [13–15]. These processes are useful primarily as a qualitative tool in the early stage library design and in the candidate selection. Despite its large number of false-positive results, Lipinski's Rule of Five has come into wide use as a qualitative tool to help the chemist design bioavailable compounds. It was concluded that compounds are most likely to have poor absorption when the molecular weight is >500, the calculated octan-1-ol/water partition coefficient (c log P) is >5, the number of H-bond donors is >5, and the number of H-bond acceptors is >10. Computation of these properties is now available as an ADME (absorption, distribution, metabolism, excretion) screen in commercial software such as Tsar (from Accelrys). The ''rule-of-5'' should be seen as a qualitative, rather than quantitative, predictor of absorption and permeability [16, 17].

19.3.1
Quantitative Structure–Activity Relationship (QSAR) Approaches

Predictive methods for oral absorption are a first step towards the prediction of human oral bioavailability. One of the earlier attempts to produce a QSAR model of human bioavailability used the method of fuzzy adaptive least squares and a combination of continuous, discrete and indicator variables [18]. The molecules used in the study were assessed in terms of the value of bioavailability and chemical nature. Thus, molecules were given a bioavailability rating (1: <50%, 2: 50–89% and 3: >90%) and were assessed as either being nonaromatic (having no aromatic rings), aromatic (having aromatic rings but no heteroaromatic rings), or heteroaromatic (having heteroaromatic rings). The total number of molecules used in the study was 188, with 28 in the nonaromatic group, 100 in the aromatic group, and 60 in the heteroaromatic group. Initially, models were produced for each of the chemical classes using log P, $(\log P)^2$ and molecular weight. However, as the statistical reliability of these models was poor, discrete and indicator variables were added for the various structural fragments present in the molecules.

Further analysis yielded new models for each of the chemical classes with improved statistical significance. The final model for nonaromatics contained six descriptors and had an R_S of 0.932 (leave-one-out 0.878), the final model for the aromatics contained 21 descriptors and had an R_S of 0.942 (leave-one-out 0.823), and the final model for the heteroaromatics contained 13 descriptors and had an R_S value of 0.863 (leave-one-out 0.758). These statistical results were considered reliable enough for the models to be regarded as predictive. The analysis did yield some interesting insights into the impact of various structural fragments on human oral bioavailability. However, these observations were based on the sign of the coefficient and so must be treated with some caution.

This model highlights the need for inclusion of variables that relate to the presence of particular structural fragments and the resultant impact on bioavailability. It suggests that whilst the fundamental chemical mechanism for this may remain unclear, the impact can still be accounted for.

Yoshida and Topliss [19] describe a quantitative *in silico* model (QSAR) for predicting human oral bioavailability. This model assigns oral bioavailability determinations into one of four rating and analyze them in relation to physico-chemical and structural factors by the ordered multi-categorical classification method using a simplex technique (ORMUCS), which is an adaptive least squares (ALS) related approach. Though not commonly used – and therefore not readily reproducible – the published equation can be applied to new compounds. It has been claimed that similar results can be obtained on the same dataset using SIMCA [20, 21]. Oral bioavailability predictions were derived by analyzing a systematic examination of physico-chemical parameters relating to absorption and structural elements that could influence metabolism. Further, based on the observations of acidic, neutral and basic drugs, a new parameter, $\Delta\log D(\log D_{6.5} - \log D_{7.4})$ was formulated, which proved to be important in improving the classification results. The results show that highly bioavailable compounds have log $D_{6.5}$ values in the range of -2.0 to 3.0. Three physico-chemical descriptors, log P and log D and Δlog D, along with 15 structural descriptors for primary metabolic pathways, yielded a QSAR equation with a correct classification rate of 71%. The relationships formulated for each compound identified the significant factors influencing oral bioavailability and assigned them quantitative values expressing relative contribution. One of the main advantages of this model is that it indicates which factors may affect bioavailability and the extent of the effect. Further, perspective oral bioavailability estimates can be obtained for compounds yet to be synthesized, and consequently it is useful in designing compounds, which are more bioavailable.

In another approach using oral bioavailability data of 591 compounds, a regression model was built employing 85 structural descriptors [22]. The final regression model had an $r^2 = 0.71$. In Fig. 19.5, the plot of predicted versus experimental oral bioavailability (%F) shows the considerable scatter. Comparing this model with the predictive ability of the Lipinski rule-of-5, in general, it was found that the structure-based model performed better than the rule-of-5 in terms of reducing the number of false positives. However, it should be borne in mind that the rule-of-5 is not a method for predicting bioavailability; rather it is a method of defining good absorption properties. With this in mind, it is perhaps not surprising that it did not perform as well as the structure-based model since there is no consideration of the chemical properties that govern clearance in the rule-of-5.

One advantage of the structure-based model is that it was able to identify the impact of certain functional groups on bioavailability. Thus, groups such as tetrazole and 4-aminopyridine are highlighted as having a significant negative effect on bioavailability, whilst 1-methylcyclopentyl alcohol is a group which has a significant positive effect on bioavailability. Whilst the model does not provide any mechanistic explanation for these observations in terms of affecting absorption or clearance, this model can still be used to estimate the bioavailability of new compounds.

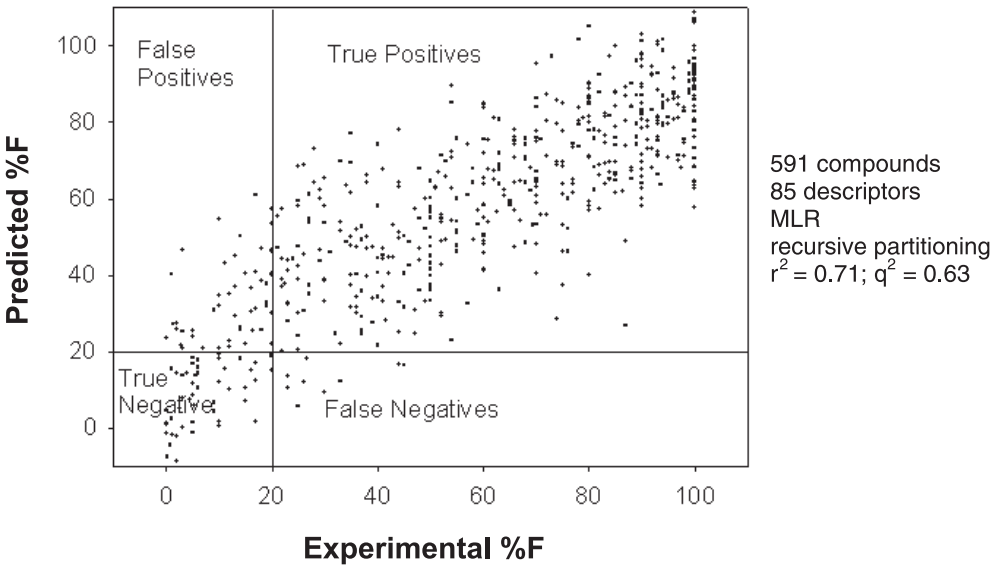

Fig. 19.5. *In silico* model for estimating oral bioavailability. Plot of predicted versus observed bioavailability in humans for 591 drugs [22].

Genetic programming, a specific form of evolutionary computing, has recently been used for predicting oral bioavailability [23]. The results show a slight improvement compared with the ORMUCS Yoshida–Topliss approach. This supervised learning method and other described methods demonstrate that at least qualitative (binned) predictions of oral bioavailability seem tractable directly from the structure.

19.3.2 Molecular Properties Influencing Bioavailability

Oral bioavailability measurements in rats for over 1100 drug candidates have allowed an analysis of the relative importance of molecular properties considered to influence bioavailability to be performed [24]. It was suggested that reduced molecular flexibility, as measured by the number of rotatable bonds, and low polar surface area (PSA) or total hydrogen bond count are important predictors of good oral bioavailability, independent of molecular weight. This latter observation is controversial, since often it is assumed that low molecular weight (e.g., <500 as in Lipinski's rule-of-5) is a prerequisite. Various aspects of this study need further clarification. Since oral bioavailability is a combination of oral absorption and clearance, the rat data may not fully translate to man. In particular, differences in drug-metabolizing enzymes and transporters may be important. The interrelationship between various properties is another point to consider carefully. Larger molecules of course tend to have more H-bonds and potentially are more flexible. In addition to flexibility it may be important to consider overall shape of the molecule.

Finally, one of the main limitations of this model is the large false-positive rate and large experimental errors. Indeed, the primary limitation of the QSAR and *in silico* models is the high false-positive rates in oral bioavailability predictions.

19.3.3 Estimation of Bioavailability from Calculated Absorption

For compounds not metabolized by the gut wall, liver, or affected by transporters, a direct relationship between oral absorption and bioavailability should be observed. The calculated oral absorption, using PSA as a measure for passive membrane permeability reflecting the absorption step, relates to the *in vivo* observed bioavailability for three classes of compounds – angiotensin-converting enzymes (ACE) inhibitors, β-blockers, and calcium antagonists – is shown below [25].

19.3.3.1 ACE Inhibitors

In the first example, the predicted oral absorption for a series of ACE inhibitors has been compared with published values of human bioavailability. For the generation of calculated absorption, a sigmoidal curve between observed human absorption and PSA for a series of reference compounds was used [25]. The predicted oral absorption for ACE inhibitors is plotted against the calculated PSA values is shown in Fig. 19.6; however, as expected, only a partial correlation existed between predicted absorption and observed *in vivo* bioavailability.

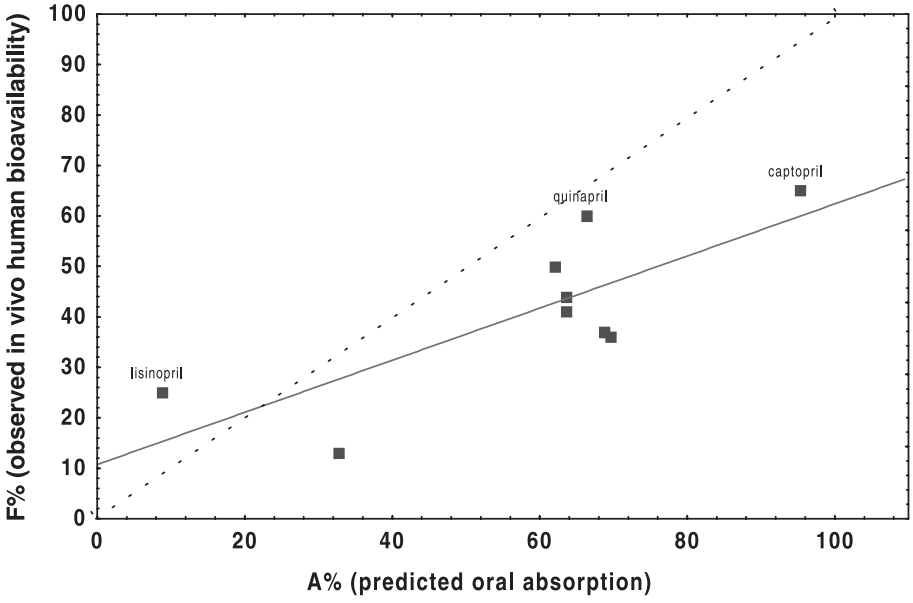

Fig. 19.6. Relationship between *in vivo* bioavailability and predicted oral absorption using polar surface area for a series of ACE inhibitors [25].

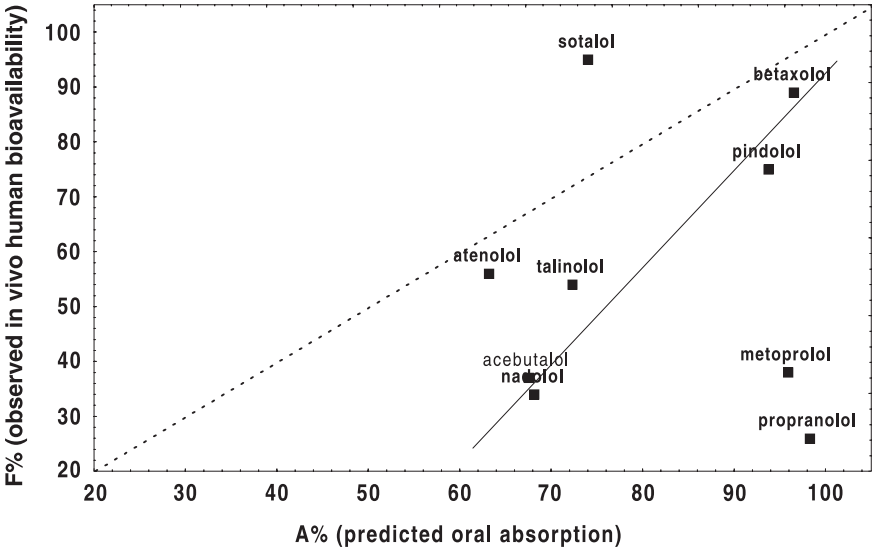

Fig. 19.7. Correlation between predicted oral absorption based on polar surface area (PSA) and *in vivo* oral bioavailability for a series of beta-blockers. The nonlinearity is related to the different levels of P-gp efflux and differences in CYP3A4 metabolism of these compounds [25].

19.3.3.2 β-Blockers

A similar plot was prepared using the PSA and reference curve oral absorption data for a series of β-blockers (Fig. 19.7), with predicted oral absorption data plotted against observed bioavailability. The differences in metabolic behavior were clearly apparent, as were the largely unquantified effects of P-glycoprotein (P-gp) and other possible transporters [25].

19.3.3.3 Calcium Antagonists

An additional example of a bioavailability–predicted absorption plot is shown for a series of calcium antagonists (Fig. 19.8). Again there is considerable scatter in the data, and the four compounds – felodipine, nisoldipine, diltiazem, and verapamil – are predicted to be much better absorbed than was actually observed. Some of these compounds are known to undergo rapid first-pass metabolic clearance, and are also P-gp inhibitors or substrates (diltiazem and felodipine are P-gp substrates; nicardipine and nitrendipine are P-gp inhibitors [25]; verapamil is a P-gp inhibitor), and this might contribute to the scatter obtained in the graph.

It is important to remember that absolute oral bioavailability is a function of *both* absorption and first-pass metabolism. Therefore, a linear approach to predicting absolute oral bioavailability based on a single parameter, such as rate or extent of absorption (fraction of dose absorbed or estimated dose absorbed) or the rate of metabolism (microsomal or hepatic intrinsic clearance), may result in an inaccu-

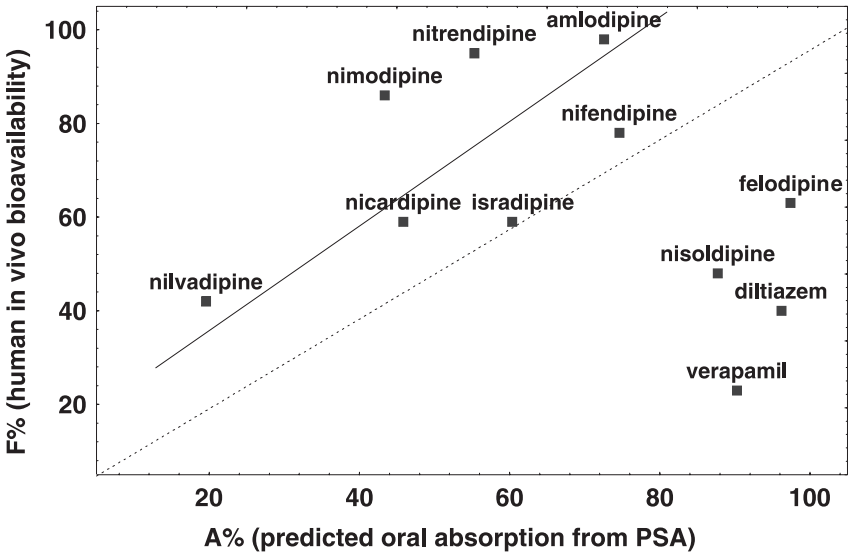

Fig. 19.8. Prediction of human bioavailability from calculated human absorption using polar surface area (PSA) for a series of calcium antagonists [25].

rate prediction due to these effects. The linear approach will not reconcile the %F for highly absorbed and highly metabolized drugs, or for poorly absorbed and slowly metabolized drugs. Therefore, if either permeability or metabolism data are considered in isolation, the estimate of oral bioavailability may be inaccurate. However, such plots may be a first indication on the influence of transporters and metabolism on the bioavailability of the compounds studied.

19.4 *In vitro* Model for Predicting Oral Bioavailability in Human and other Species

Absorption and clearance are two of the fundamental parameters that determine oral bioavailability. There are many *in vitro* methods to assess the absorption and metabolic potential of a given molecule, and it can be argued that a combination of these data should produce a model capable of predicting oral bioavailability. Such a model, based on a graphical approach has recently been published [26].

This model integrates existing *in vitro* data, such as Caco-2 permeability (P_{app}) and metabolic stability in liver S9 or microsomes, to estimate bioavailability as being either low, medium, or high. Oral bioavailability predictions for not only humans but also other species can be made by using the metabolic stability values of drugs in liver microsomal enzyme preparations from that species. A premise of this model is that metabolic clearance is more important than renal or biliary clearance in determining bioavailability. However, despite the lack of *in vitro* renal

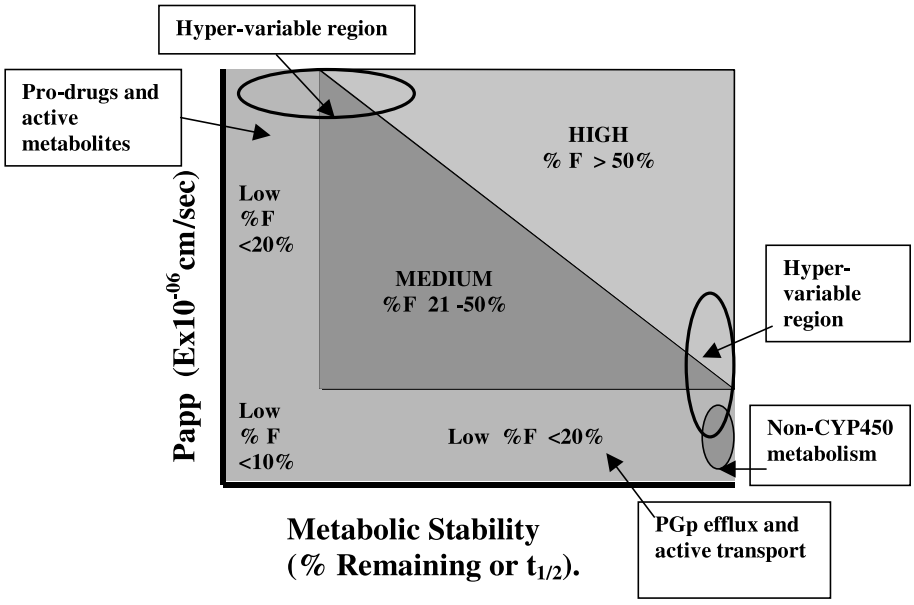

Fig. 19.9. Graphical oral bioavailability estimation map. (Reproduced with permission from Ref. [26]; © 2002 American Chemical Society.)

or biliary clearance data, good estimates of bioavailability are obtained with this model. In addition, the model's predictability is best applied to passively diffused compounds, which accounts for ~80% of all compounds. The model – the basis of which is illustrated in Fig. 19.9 – may underestimate the bioavailability of actively transported compounds.

The plot is divided into three sections representing low (<20%), medium (20–50%) and high (50–100%) bioavailability. The low bioavailability region is defined by $P_{app} < 10 \times 10^{-6}$ cm s^{-1} and 0–100% drug remaining, and by P_{app} 0–70 $\times 10^{-6}$ cm s^{-1} and <15% parent drug remaining. The *in vitro* properties of four reference compounds were used to define the low, medium and high regions of the bioavailability map. Verapamil and mannitol defined the boundaries for the low region, metoprolol the medium region, and carbamazepine the high region.

Model variability occurs when compounds fall into the two hyper-variable regions in the bioavailability map, or where all three bioavailability regions converge (Fig. 19.9). In these cases, bioavailability could easily be under- or over-estimated if there is even a small degree of variance in the *in vitro* determinations. For example, compounds that are found in the lower right hyper-variable region which might exhibit this kind of variability include small polar compounds, larger compounds with a carboxylic acid group, or charged functional groups. Similarly, when ester pro-drugs and highly lipophilic compounds are present in the upper left hyper-variable region, there may also be a higher degree of variability.

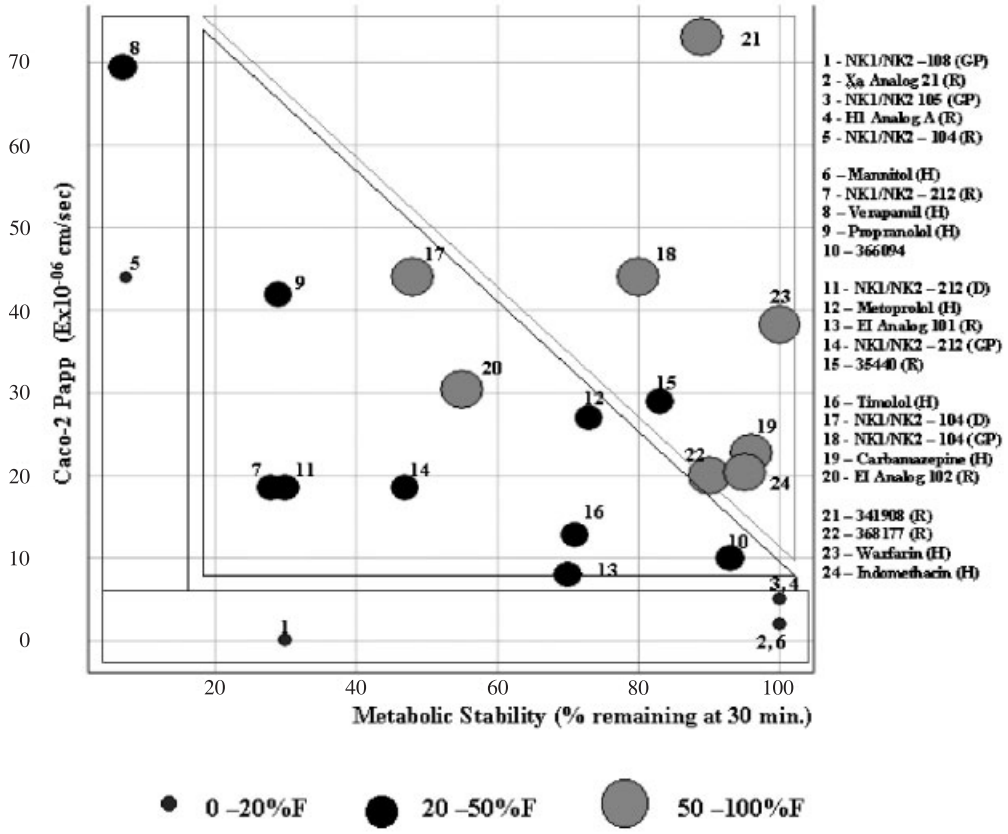

Fig. 19.10. Oral bioavailability estimates of drugs in rat, guinea pig, dog and human from their respective Caco-2 Papp and metabolic stability in liver microsomes or S9. (Reproduced with permission from Ref. [26]. © 2002 American Chemical Society.)

To test the predictive accuracy of the model, 21 drugs and drug candidates from a number of different structural classes, and with a wide range of oral bioavailability values in human, rat, dog and guinea pig were used (Fig. 19.10). *In vitro* data from model compounds were used to define the boundaries of the low, medium and high regions of the bioavailability estimation plot. On the basis of these *in vitro* data, warfarin (93%), indomethacin (98%), timolol (50%) and carbamazepine (70%) were assigned to the high bioavailability region; propranolol (26%) and metoprolol (38%) to the medium bioavailability region; and verapamil (22%) and mannitol (18%) to the low bioavailability region. Similarly, the bioavailabilities of 11 drug candidates from different structural classes were correctly estimated in rat, guinea pig and dog.

This model uses *in vitro* data to estimate the oral bioavailability ranges of chemically diverse compounds in a range of species, and represents a potentially powerful tool when combined with high-throughput *in vitro* screening.

19.5
In vivo Method for Estimating Human Oral Bioavailability from Animal Pharmacokinetic Studies

Obach et al. [27] proposed a model to predict human bioavailability from a retrospective study of *in vitro* metabolism and *in vivo* animal pharmacokinetic (PK) data. While their model yielded acceptable predictions (within a factor of 2) for an expansive group of compounds, it relied extensively on *in vivo* animal PK data for interspecies scaling in order to estimate human PK parameters. Animal data are more time-consuming and costly to obtain than are permeability and metabolic clearance data; hence, this approach may be limited to the later stages of discovery support when the numbers of compounds being evaluated are fewer.

19.6
Factors to Consider in Optimizing Oral Bioavailability

Oral bioavailability of a drug is primarily dependent upon its rate and extent of drug absorption and systemic clearance. Systemic clearance is primarily composed of hepatic, renal and biliary clearance. The PK properties are in turn directly impacted by the drug's physical properties, such as, log P, log D and pK_a. The physical properties are in turn a function of the compound's structure, molecular weight, number of hydrogen bond donors and acceptors, and number of rotatable bonds. Oral bioavailability is the outcome from the dynamic interplay of these factors in the biological system.

When predicting oral bioavailability from *in vitro* data it is important to remember that such data are dependent on both permeability *and* first-pass metabolism. Further, permeability and metabolism often have opposing structural properties. For example, highly lipophilic compounds tend to be more permeable and also serve as good substrates for cytochrome P450 enzymes; this may result in rapid metabolism [12] and consequently highly lipophilic compounds tend to have low bioavailability. In contrast, polar or ionizable (anionic and cationic) compounds exhibit low permeability and high stability in microsomal or S9 incubations. However, these compounds tend to be metabolized by phase II conjugative or cytosolic enzymes or excreted unchanged *in vivo*. It has been reported by Lien [28] that absorption from the intestinal tract of rats shows a parabolic relationship with log P, with the optimal absorption being at a log P value of ~2.0. However, first-pass metabolism tends to increase with an increase in log P. Yoshida and Toplis reported an optimal log D6.5 value of 0.7 for good oral bioavailability.

A linear approach to predicting absolute oral bioavailability based on a single parameter, such as rate or extent of absorption (fraction of dose absorbed or estimated dose absorbed) or the rate of metabolism (microsomal or hepatic intrinsic clearance), may result in an inaccurate prediction. The linear approach will not reconcile the bioavailability for highly absorbed and highly metabolized drugs or for poorly absorbed and slowly metabolized drugs. Therefore, if either permeability

or metabolism data are considered in isolation, the estimate of oral bioavailability may be grossly inaccurate. An additional factor that complicates this issue is the large inter-species variation in the bioavailability of drugs. The lack of correlation between human and animal bioavailability for many drugs is most likely due to differences in rate, extent and pathway of metabolism among species [2, 9–12].

Bioavailability optimization through structure modifications can be daunting, given the opposing requirements for solubility, permeability and metabolic stability. For example, solving metabolic stability problems in one area of the molecule may result in the increase in the rate of metabolism at another area – a phenomenon known as ''metabolic switching''. Further, an apparent improvement of an *in vitro* metabolism property may not result in improved *in vivo* performance, as the compound may exhibit saturable metabolism or nonlinear pharmacokinetics. In addition, the reduction in metabolic (hepatic) clearance may lead to increased renal or biliary clearance of the parent drug or inhibition of one or more drug-metabolizing enzymes. Thus, structure modifications to solve a metabolic stability problem may not necessarily lead to a compound with an overall improvement in bioavailability.

References

1 Chen, M. L., Shah, V., Patniak, R., Adams, W., Hussain, A., Conner, D., Mehta, M., Malinowski, H., Lazor, J., Huang, S. M., Hare, D., Lesko, L., Sporn, D., Williams, R., Bioavailability and bioequivalence: an FDA regulatory overview, *Pharm. Res.* **2001**, *18*, 1645–1648.

2 Sietsema, W. K., The absolute oral bioavailability of selected drugs, *Int. J. Clin. Pharmacol. Ther. Toxicol.* **1989**, *27*, 179–211.

3 Sinko, P. J., Drug selection in early drug development: screening for acceptable pharmacokinetic properties using combined in vitro and computational approaches, *Curr. Opin. Drug Disc. Dev.* **1999**, *2*, 42–48.

4 Bayliss, M. K., Frick, L. W., High-throughput pharmacokinetics: cassette dosing, *Curr. Opin. Drug Disc. Dev.* **1999**, *2*, 20–25.

5 White, R. E., Manitpisitkul, P., Pharmacokinetic theory of cassette dosing in drug discovery screening, *Drug Metab. Dispos.* **2001**, *29*, 957–966.

6 Chiou, W. L., Ma, C., Chung, S. M., Jeong, Y. H., Wu, T. C., Similarities in the linear and non-linear oral absorption of drugs between human and rat, *Int. J. Clin. Pharmacol. Ther.* **2000**, *38*, 532–539.

7 Chiou, W. L., Jeong, Y. H., Chung, S. M., Wu, T. C., Evaluation of dog as an animal model to study the fraction of oral dose absorbed for 43 drugs in humans, *Pharm. Res.* **2000**, *17*, 135–140.

8 Chiou, W. L., Buehler, P. W., Comparison of oral absorption and bioavailability of drugs between monkey and human, *Pharm. Res.* **2002**, *17*, 868–874.

9 Van de Waterbeemd, H., Smith, D. A., Beaumont, K., Walker, D. A., Property-based Design: Optimization of drug absorption and pharmacokinetics, *J. Med. Chem.* **2001**, *44*, 1313–1333.

10 Smith, D. A., Design of drugs through a consideration of drug metabolism and pharmacokinetics, *Eur. J. Drug Metab. Pharmacokinet.* **1994**, *3*, 193–199.

11 Sharer, J. C., Shipley, L. A., Vandenbraden, M. R., Binley, S. N., Wrighton, S. A., Comparison of

Phase I and Phase II in vitro hepatic enzyme activities of human, dog, rhesus monkey and cynomolgus monkey, *Drug Metab. Dispos.* **1995**, *23*, 1231–1241.

12 Shimada, T., Mimura, M., Inoue, K., Nakamura, S., Oda, H., Ohimori, S., Yamazaki, H., Cytochrome P450-dependent drug oxidation activities in liver microsomes of various animal species including rats, guinea pigs, dogs, monkeys and humans, *Arch. Toxicol.* **1977**, *71*, 401–408.

13 Lipinski, C. A., Lombardo, F., Dominy, B. W., Feeney, P. J., Experimental and computational approaches to estimate solubility and permeability in drug discovery and development settings, *Adv. Drug Del. Rev.* **1997**, *23*, 3–25.

14 Ajay, Walters, W. P., Murcko, M. A., Can we learn to distinguish between "drug-like" and "non-drug-like" molecules?, *J. Med. Chem.* **1998**, *41*, 3314–3324.

15 Sadowski, J., Kubinyi, H., A scoring scheme for discriminating between drugs and non-drugs, *J. Med. Chem.* **1998**, *41*, 3325–3329.

16 Pagliara, A., Resist, M., Geinoz, S., Carrupt, P.-A., Testa, B., Evaluation and prediction of drug permeation, *J. Pharm. Pharmacol.* **1999**, *51*, 1339–1357.

17 Stenberg, P., Luthman, K., Ellens, H., Lee, C. P., Smith, Ph. L., Lago, A., Elliott, J. D., Artursson, P., Prediction of the intestinal absorption of endothelin receptor antagonists using three methods of increasing complexity, *Pharm. Res.* **1999**, *16*, 1520–1526.

18 Hirono, S., Nakagome, I., Hirano, H. Matsuhita, Y., Yoshi, F., Moriguchi, I., Non-congeneric structure–pharmacokinetic property correlation studies using fuzzy adaptive least squared: oral bioavailability, *Biol. Pharm. Bull.* **1994**, *17*, 306–309.

19 Yoshida, F., Topliss, J. G., QSAR model for drug human oral bioavailability, *J. Med. Chem.* **2000**, *43*, 2575–2585.

20 Podlogar, B. L., Muegge, I., Brice, L. J., Computational methods to estimate drug development parameters, *Curr. Opin. Drug Disc. Dev.* **2001**, *4*, 102–109.

21 Podlogar, B. L., Muegge, I., "Holistic" in silico methods to estimate the systemic and CNS bioavailabilities of potential chemotherapeutic agents, *Curr. Top. Med. Chem.* **2001**, *1*, 257–275.

22 Andrews, C. W., Bennett, L., Yu, L. X., Predicting human oral bioavailability of a compound: Development of a novel quantitative structure–bioavailability relationship, *Pharm. Res.* **2000**, *17*, 639–644.

23 Bains, W., Gilbert, R., Sviridenko, L., Gascon, J.-M., Scoffin, R., Birchall, K., Harvey, I., Caldwell, J., Evolutionary computational methods to predict oral bioavailability QSPRs, *Curr. Opin. Drug Disc. Dev.* **2002**, *5*, 44–51.

24 Veber, D. F., Johnson, S. R., Cheng, H.-Y., Smith, B. R., Ward, K. W., Kopple, K. D., Molecular properties that influence the oral bioavailability of drug candidates, *J. Med. Chem.* **2002**, *45*, 2615–2623.

25 Van de Waterbeemd, H., Jones, B. C., Predicting oral absorption and bioavailability, *Prog. Med. Chem.* **2003** (in press).

26 Mandagere, A. K., Thompson, T. N., Hwang, K. K., Graphical model for estimating oral bioavailability of drugs in humans and other species from their Caco-2 permeability and in vitro liver enzyme metabolic stability rates, *J. Med. Chem.* **2002**, *45*, 304–311.

27 Obach, R. S., Baxter, J. G., Liston, T. E., Silber, M. R., Jones, B. C., MacIntyre, F., Rance, D. J., Wastall, P., The prediction of human pharmacokinetic parameters from preclinical and *in vitro* metabolism data, *J. Pharmacol. Exp. Ther.* **1997**, *283*, 46–58.

28 Lien, E. J., Structure–activity relationships and drug disposition, *Annu. Rev. Pharmacol. Toxicol.* **1981**, *21*, 32–61.

20
Towards P-Glycoprotein Structure–Activity Relationships

Anna Seelig, Ewa Landwojtowicz, Holger Fischer, and Xiaochun Li Blatter

Abbreviations

ABC	ATP-binding cassette (transport protein)
EU_H	Units of H-bond energy (arbitrary units)
MDR	Multidrug resistance
P-gp	P-glycoprotein (MDR1)
(Q)SAR	(Quantitative) structure–activity relationship
TM	Transmembrane (domain)
H-bonding	Hydrogen bonding

Symbols

A	Strong H-bond acceptor (or strong electron donor)
a	Weak H-bond acceptor (or weak electron donor)
ΔG_{aw}	Free energy of partitioning into the air/water interface
ΔG_{lw}	Free energy of partitioning into the lipid phase from water
ΔG_{tw}	Free energy of binding to transporter from water
ΔG_{tl}	Free energy of binding to transporter from lipid phase
ΔG_{app}	Apparent free energy of binding to transporter from water

20.1
Introduction

20.1.1
P-glycoprotein

P-glycoprotein (P-gp) extrudes a wide variety of chemically unrelated endogenous and exogenous compounds out of cell membranes (for a review, see Refs. [1–4]).

Drug Bioavailability: Estimation of Solubility, Permeability, Absorption and Bioavailability.
Edited by Han van de Waterbeemd, Hans Lennernäs and Per Artursson

ISBN: 3-527-30438-X

P-gp is a member of the phylogenetically highly conserved superfamily of ATP-binding cassette (ABC) transport proteins [5, 6]. In simple organisms, these proteins are assumed to consist of a transmembrane domain, formed by six transmembrane α-helices, and a cytosolic nucleotide-binding domain. The functional unit seems to consist of a homodimer. The six-transmembrane α-helices have recently been confirmed by X-ray crystallography for the bacterial transporter, MsbA [7]. In higher organisms, two homologous parts, each consisting of a transmembrane and a nucleotide-binding domain, are coupled by a cytosolic linker region; P-gp, with a molecular weight of 170 kDa belongs to the latter type. So far, only a low-resolution structure determined by electron microscopy is available, and this suggests the presence of a large central pore [8].

The catalytic cycle of P-gp has been investigated extensively (for a review, see Ref. [24]). The two nucleotide-binding domains were shown to act in a synchronized manner for catalytic activity [25] such that only one nucleotide site, recruited at random, is utilized at a given time, while the binding affinity to the other is drastically reduced [26]. The drug extrusion cycle of P-gp most probably includes two ATP hydrolysis steps, the first required to induce the drug-releasing conformation, and the second to reset the transporter to the drug-binding conformation [26]. P-gp displays constitutive ATPase activity in the absence of exogenous substrates in inside-out cellular vesicles [27–29] and when reconstituted in proteoliposomes [30]. Whether basal activity is due to uncoupled ATPase activity [31] or to the transport of endogenous substrates is not yet fully clarified. If basal activity is indeed due to the transport of endogenous substrates, the most likely candidates – at least in reconstituted systems – are lipids ([32]; for reviews, see Refs. [33, 34]). The addition of exogenous substrates (e.g., toxins or drugs) causes either an increase or a decrease of the basal rate of ATP hydrolysis, depending on the nature and the concentration of the substrate applied.

In humans, P-gp is encoded by the *MDR1* gene. High levels of P-gp expression have been observed in cells with protective functions [9], as found in the blood–brain barrier [10, 11], the placental barrier [12], the blood–testis barrier [13], the adrenal gland, liver, pancreas, kidney, colon, jejunum [14], and the digestive tract [15]. High expression levels of P-gp are also observed in many cancer cells [10]. Cells which express the MDR phenotype can over-express P-gp after exposure to a single agent (e.g., cytotoxic anticancer drugs, certain antibiotics or certain food components) [16] or after exposure to physical stress, such as X-rays [17], UV light irradiation [18] and heat shock [19]. Over-expression of P-gp leads to multidrug resistance, i.e., a resistance to all drugs, which are substrates of P-gp. The same stimuli, which induce multidrug resistance in humans, can also induce multidrug resistance in bacteria, parasites, and fungi. Multidrug resistance is detrimental for chemotherapy of cancer (for a review, see Ref. [20]), and also hampers chemotherapy of bacterial [21], parasitic [22], and fungal [23] diseases.

A rational approach to problems such as drug targeting to regions protected by P-gp, inhibition or even prevention of multidrug resistance in different organisms, and prediction of drug–drug interactions due to P-gp should become possible with reliable structure–activity relationship (SAR) studies.

20.1.2
Conventional SAR Studies

Structure–activity relationship studies attempt to identify complementary spatial features in a ligand–receptor or ligand–transporter interaction. The critical three-dimensional arrangement of functional groups in the ligand that is responsible for creating biological response is defined as the pharmacophore (cf. Refs. [35, 36]). A wealth of information on substrate–P-gp interactions has been accumulated since the discovery of P-gp in the late 1970s [37], and this has been summarized in a number of excellent reviews [6, 36, 38–40]. SAR approaches are usually based on multiple linear regression using a variable number of descriptors. Descriptors proposed for P-gp substrates are lipophilicity [63] (for reviews, see Refs. [4, 41]), H-bonding ability [42–45, 63], molecular weight, size, and surface area [28, 46, 47], as well as structural elements such as a basic amine and/or unsaturated rings [48].

20.1.3
Why Conventional SAR Studies may not be Adequate to Understand P-gp

So far, SAR studies for P-gp have been performed on the basis of classical QSAR principles which were designed for transporters or receptors, which naturally bind *one* specific substrate from an *aqueous environment*. The assumptions made are that: (i) the modeled conformation is the bioactive one; (ii) the binding site and/or mode is the same for all modeled compounds; (iii) interactions between the drug and the binding site are mainly due to enthalpic processes (e.g., van der Waals interactions); and (iv) solvent or membrane effects are negligible (cf. Ref. [35]).

A closer inspection of the action mechanism of P-gp will reveal that the classical QSAR assumptions are not adequate. First, P-gp differs from conventional transporters in that it transports not one specific compound but many chemically unrelated substrates. It may thus recognize not one but several ''bioactive'' structures. Moreover, not one but several binding sites have been identified in P-gp [49, 50]. The sites defined as specific binding sites may even not be single stationary binding sites but belong to an ensemble of binding sites transiently encountered by one substrate during transport [51].

Second, P-gp differs from other transporters in that it recognizes its substrates when dissolved in the lipid membrane [52], and not when dissolved in aqueous solution. The site of recognition and binding has been shown to be located in the membrane leaflet facing the cytosol [53, 54]. This implies that the *membrane* concentration of the substrate, C_{sm}, determines activation [57]. Since the nature of a molecular interaction is strongly influenced by the solvent, the lipid membrane must be taken into account as the ''solvent'' for the SAR analysis of P-gp. Under certain conditions, the effect of additional solvents or excipients (used to apply hydrophobic substrates or inhibitors) on the lipid membrane and/or on the transporter must also be considered. Lipophilicity of substrates has long been known to play an important role in P-gp–substrate interactions; nevertheless, the correlation of the octanol/water partition coefficients with the concentration of half-maximum

activation, K_m, of P-gp [28, 42, 55] remains a matter of debate. So far, lipid/water partition coefficients have not been implemented in SAR studies.

To be successful, SAR studies must be adapted to P-gp by implementing membrane partitioning of substrates, modifiers or inhibitors as suggested previously [36]. The aim of the present chapter is to evaluate the contribution of: (i) membrane partitioning; and (ii) receptor binding proper to the apparent binding of a compound to P-gp.

20.2
The Role of Lipid Binding for SAR

20.2.1
Membrane Partitioning Determines Drug Concentration at Half-Maximum P-gp-ATPase Activation, K_m

Most known transporters, T, move their substrates from the periplasm to the cytoplasm or vice versa. Under these conditions, a substrate dissolved in aqueous solution, S_{aq}, generally binds to a hydrophobic transporter site according to the scheme shown on Eq. (1):

$$S_{aq} + T + ATP \underset{k_{-1}}{\overset{k_1}{\rightleftharpoons}} T(ATP)S \overset{k'}{\rightarrow} T(ADP) + S_{rel} + P_i + H^+, \quad (1)$$

where k_1 and k_{-1} are the rate constants for the formation and dissociation of the T(ATP)S complex, respectively, and k' is the catalytic rate constant. Assuming steady-state conditions, the reciprocal of the concentration of half-maximum activation, K_m, $(1/K_m)$, is directly proportional to the binding affinity of the substrate (dissolved in water) to the transporter, K_{tw}, and $\log(1/K_m)$ is proportional to the free energy of interaction between the substrate and the transporter, ΔG_{tw}:

$$\Delta G_{tw} = -RT \ln(55.5 \times K_{tw}), \quad (2)$$

where RT is the thermal energy. This simple approach has so far also been applied in SAR studies of P-gp [35, 44, 56].

However, if substrate binding takes place in the lipid it is preceded by a membrane-partitioning step as shown in Eq. (3):

$$S_{aq} \underset{k_{-0}}{\overset{k_0}{\rightleftharpoons}} S_M + T + ATP \underset{k_{-1}}{\overset{k_1}{\rightleftharpoons}} T(ATP)S \overset{k'}{\rightarrow} T(ADP) + S_{rel} + P_i + H^+, \quad (3)$$

where S_{aq} is the substrate concentration in the aqueous phase and S_M the substrate concentration in the membrane phase, k_0 and k_{-0} are the rate constants for lipid partitioning, and $(k_0/k_{-0}) = K_{lw}$ is the lipid/water partition coefficient [57]. After stimulation of P-gp by a drug, a steady state develops in a short period of time ($\sim$2 min) [58]. Under steady-state conditions, the apparent binding affinity of the substrate to the receptor, $K_{app} \sim (1/K_m)$ is the product of the lipid/water partition

coefficient, K_{lw}, and the binding affinity to the receptor in the lipid phase, K_{tl}

$$K_{app} \sim (1/K_m) = K_{lw} \times K_{tl} \tag{4}$$

and $\log(1/K_m)$ is then proportional to the apparent free energy of binding, ΔG_{app}, which is the sum of the free energy of partitioning into the lipid membrane, ΔG_{lw}, and the free energy of receptor binding, ΔG_{tl}

$$\Delta G_{app} = \Delta G_{lw} + \Delta G_{tl}. \tag{5}$$

As will be shown below, ΔG_{app} and ΔG_{lw} can be determined independently, which allows an estimation of ΔG_{tl}.

The simplest way to predict the lipid/water partition coefficient, K_{lw}, of a drug is based on measurements of the surface pressure, π_D, of the drug as a function of its concentration in the aqueous subphase (Gibbs adsorption isotherm). The Gibbs adsorption isotherm provides the air/water partition coefficient, K_{aw}, and the cross-sectional area, A_D of the drug and allows calculation of the lipid/water partition coefficient, K_{lw}, according to Eq. (6) [59]:

$$K_{lw} = K_{aw} \times e^{-\pi_M A_D/kT}, \tag{6}$$

where π_M is the packing density of the lipid bilayer [60] and kT the thermal energy. To evaluate the contribution of the lipid/water partition coefficient, K_{lw}, to the overall binding constant, K_{app}, according to Eq. (4), the air/water partition coefficient, K_{aw}, was compared with the concentration of half-maximum activation, K_m for a number of P-gp substrates (Fig. 20.1).

As seen in Fig. 20.1, a linear correlation was observed between the logarithm of the air/water partition coefficient, $\log K_{aw}$, and the $\log(1/K_m)$ [57, 58]. This strong correlation implies that the membrane concentration of substrates is indeed essential for activation of P-gp and leads to the following empirical correlation:

$$(K_m)^{-1} \approx K_{aw} \approx \rho K_{lw}. \tag{7}$$

With $A_D = 50\text{–}100\,\text{Å}^2$ for typical drug molecules [59] and $\pi_M \sim 30$ mN m^{-1} [60], the proportionality factor $\rho = e^{\pi A_D/kT}$ [61] is of the order:

$$100 < \rho < 1000. \tag{8}$$

For average drugs (cf. Fig. 20.1), the apparent free energy of binding to P-gp is of the order of $\Delta G_{app} \sim -27$ to -56 kJ mole^{-1}, the free energy of membrane partitioning $\Delta G_{lw} \sim -16$ to -39 kJ mole^{-1}, and the free energy of binding to the transporter $\Delta G_{tl} \sim -11$ to -17 kJ mole^{-1}. Since the free energy of membrane partitioning, ΔG_{lw}, is generally more negative than the free energy of binding to the transporter, ΔG_{tl}, the former dominates the apparent free energy of binding, ΔG_{app}. Only for very hydrophilic but efficient substrates are the two free energies

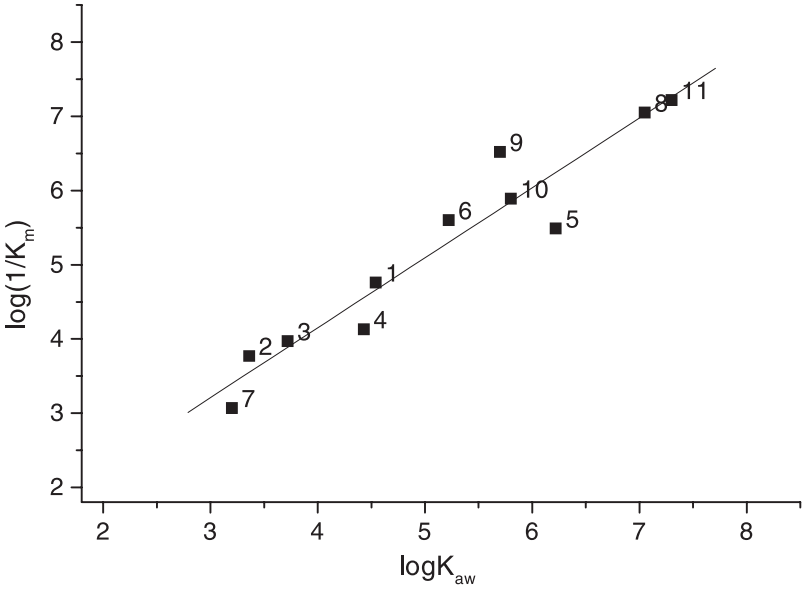

Fig. 20.1. Correlation between the air/water partition coefficient, K_{aw}, determined from measurements of the surface pressure as a function of drug concentration (Gibbs adsorption isotherm) in buffer solution (50 mM Tris/HCl, containing 114 mM NaCl) at pH 8.0 and the inverse of the Michaelis Menten constant, K_m obtained from phosphate release measurements in inside-out membrane vesicles from MDR1-transfected cells [28]. Compounds measured: progesterone (1); propranolol (2); amitriptyline (3); diltiazem (4); amiodarone (5); racemic verapamil (6); colchicine (7); gramicidin S (8); daunorubicin (9); vinblastine (10); cyclosporin A (11). (Adapted from Ref. [57].)

in a similar range ($\Delta G_{lw} \sim \Delta G_{tl}$). If either ΔG_{lw} or ΔG_{tl} approach zero, a compound will not interact with P-gp.

As seen in Eq. (6), ΔG_{lw} depends on the packing density, π_M, of the lipid membrane which in turn depends on the lipid composition. According to the above results, K_m is expected to increase with increasing packing density of the membrane, and this has indeed been demonstrated by functionally reconstituting P-gp in different lipid bilayers [62].

20.2.2
The Membrane Concentration of Substrates Relevant for P-gp Activation

The empirical correlation (Eq. (7)) allows an estimation of the membrane concentration of substrates required for half-maximum activation of P-gp. For hydrophobic substrates, the membrane concentration C_{Sm}, is usually much higher than the concentration in aqueous solution, C_{Saq}, and is given by $C_{Sm} = K_{lw} \times C_{Saq}$, where C_{Sm} is given in [moles drug/mole lipid] ≈ [moles drug/liter lipid]. Replacing the aqueous substrate concentration C_{Saq}, in the Michaelis–Menten equation (Eq. (9)) by the membrane concentration, C_{Sm} allows comparison of the activation

parameter, K_m, with the lipid binding affinity K_{lw}

$$V = V_{max}\frac{C_{Saq}}{C_{Saq} + K_m} = V_{max}\frac{C_{Sm}/K_{lw}}{C_{Sm}/K_{lw} + K_m} = V_{max}\frac{C_{Sm}}{C_{Sm} + K_m \times K_{lw}}. \quad (9)$$

Half-maximum rate is observed if

$$C_{Sm} = K_m \times K_{lw}, \quad (10)$$

where C_{Sm} is given in [moles drug/mole lipid] $\approx$ [moles drug/liter lipid]. With Eqs. (7) and (8), the product of $K_m \times K_{lw}$ can be estimated as

$$K_m \times K_{lw} \approx 0.001 - 0.01. \quad (11)$$

It thus follows that the membrane concentration of typical P-gp substrates for half-maximum activation of P-gp falls in the range of 1 to 10 mmole drug per mole lipid. This is a much narrower concentration range than that required for the same substances in the aqueous phase $\sim 10^{-8}$ to 10^{-3} M. A similar phenomenon has been observed in anesthesia. The membrane concentration of anesthetics required for anesthesia has been found to be $\sim$33 mM, independent of the anesthetic applied (Meyer–Overton rule).

20.2.3
Molecular Size: Is it Relevant for P-gp Activation?

Molecular size has previously been suggested to play a role for substrate recognition by P-gp [28]. Surface activity measurements provide the cross-sectional area, A_D, of substrates and thus allow one to investigate the role of A_D in interaction with P-gp. Combining Eqs. (2) and (6) yields

$$\Delta G_{aw} = \Delta G_{lw} - \pi_M N A_D, \quad (12)$$

where N is the number of molecules per mole. The free energy of partitioning into the air/water interface, ΔG_{aw}, can thus be considered as the sum of the free energy of partitioning into the lipid/water interface, ΔG_{lw}, and a term comprising the cross-sectional area, A_D of the drug molecule. Combining Eq. (12) with the information inferred from Fig. 20.1 ($\Delta G_{aw} \approx \Delta G_{app}$) leads to the following approximation:

$$\Delta G_{app} \approx \Delta G_{aw} = \Delta G_{lw} - \pi_M N A_D \quad \text{or} \quad \Delta G_{tl} \approx -\pi_M N A_D. \quad (13)$$

Equation (13) indeed suggests a correlation between the cross-sectional area, A_D, of the compound and the free energy of binding to the transporter, ΔG_{tl}. Although this rough approximation is valid for many compounds, it holds true only if the cross-sectional area, A_D, correlates with the number of H-bond acceptor units per

substrate which most likely constitute the pharmacophore for P-gp (cf. Section 20.3.4). Compounds which lack the relevant H-bond acceptor units (cf. Section 20.3) will not interact with P-gp, independent of their size.

20.3 In Search of a Pharmacophore

The above analysis has shown, that, on the one hand, the lipid/water partition coefficient, K_{lw}, essentially determines the concentration of half-maximum activation of P-gp, K_m, and, on the other hand, even hydrophilic compounds can interact with P-gp as long as their membrane concentration is high enough (1–10 mmole per liter lipid). This means that a lack of hydrophobicity can be compensated, at least to a certain extent, by increasing the drug concentration. Hydrophobic elements are therefore not considered as essential recognition elements for the substrate–P-gp interaction proper. This is in contrast to most previous SAR studies, which include hydrophobic elements as key factors in a pharmacophore (e.g. Ref. [63]). To simplify the discussion of possible recognition elements constituting a pharmacophore for P-gp, first, the type of interactions dominating in a hydrophobic membrane environment (see Section 20.3.1) will be discussed; second, the results from an analysis of possible interaction sites within the putative transmembrane sequences of P-gp [51] will be summarized (Section 20.3.2).

20.3.1 The Local Environment Determines the Nature of Substrate–Transporter Interactions

The nature of the interaction between a ligand and its receptor or a substrate and its transporter is strongly determined by the local environment (or solvent) in which the molecular encounter takes place. If the encounter takes place in an aqueous environment (with a dielectric constant, $\varepsilon \cong 80$), then hydrophobic, van der Waals, or stacking interactions are predominant. Electrostatic interactions are also possible.

The recent crystallization of the small water-soluble transcriptional regulator of *Bacillus subtilis* multidrug transporter Bmr, BmrR, which binds hydrophobic cations from the cytosol [64, 65] provides a good example for an interaction determined primarily by van der Waals interactions. Interestingly, the same drugs, which bind to the water-soluble BmrR are also substrates for the transmembrane multidrug transporter Bmr. As will be discussed below, the latter interactions could well be of different nature.

In a lipid environment, van der Waals interactions become less specific. Electrostatic effects are enhanced up to 40-fold (according to Coulomb's law) due to the low dielectric constant, $\varepsilon \cong 2$, of the hydrophobic core of membranes. As a result, weak electrostatic interactions, e.g., between the π-electrons of an aromatic ring and a cation [51], may come into play. In addition, H-bond interactions, which can be considered as dipole–dipole interactions can also become relevant.

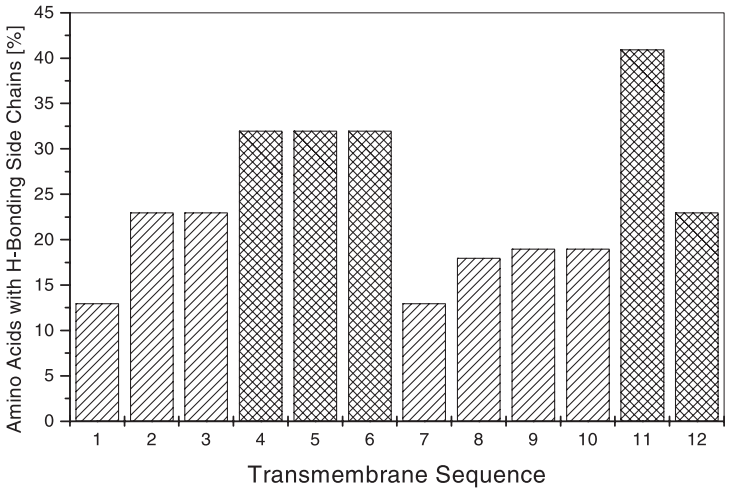

Fig. 20.2. Percentage of amino acids with H-bond donor side chains in the 12 putative transmembrane sequences of P-glycoprotein (P-gp). The transmembrane sequences were determined by means of a hydropathy plot according to Kyte and Doolitttle [100] and chosen to be 22 amino acids long. The first amino acid of each transmembrane sequence is given in brackets: TM1 (50), TM2 (115), TM3 (185), TM4 (209), TM5 (297), TM6 (322), TM7 (707), TM8 (751), TM9 (828), TM10 (850), TM11 (932), TM12 (971). The transmembrane sequences shown experimentally to be involved in substrate transport are cross-hatched. (This is an updated version of Fig. 3 in Ref. [43].)

20.3.2
H-bond Donors in Putative Transmembrane α-Helices of P-gp

The amino acid sequences of the proposed TM helices of P-gp were analyzed for possible interaction sites with drug molecules; such interaction sites are H-bond donor groups, aromatic side chains, and charged residues [43, 51]. Figure 20.2 illustrates the percentage of amino acids with H-bond donor side chains in the putative TM helices of P-gp determined by hydropathy plots. The TM helices TM 4 [67], TM 5–6 and TM 11–12 (reviewed in Ref. [6]) that are known to be relevant for drug binding and transport display a specifically high percentage (30–40%) of amino acids with H-bond donor side chains.

A helical wheel-representation of the TM sequences [51] furthermore reveals a distinct amphipathic arrangement, with the H-bonding amino acids predominantly on one side and the non-H-bonding amino acids on the other side for most of the 12 α-helices. The H-bonding side of the TM helices was speculated to face the transport route of substrates and the non-H-bonding side the lipid environment. The helices exhibiting two H-bonding sides might act as recognition sites, and could allow for substrate entry to the transport route. Furthermore, these putative α-helices of P-gp show clusters of phenyl residues as well as several cationic residues. However, no negatively charged amino acid residues were found within these sequences. This is in contrast to related transporters for which a negative charge in the TM region has been assumed to be essential [64].

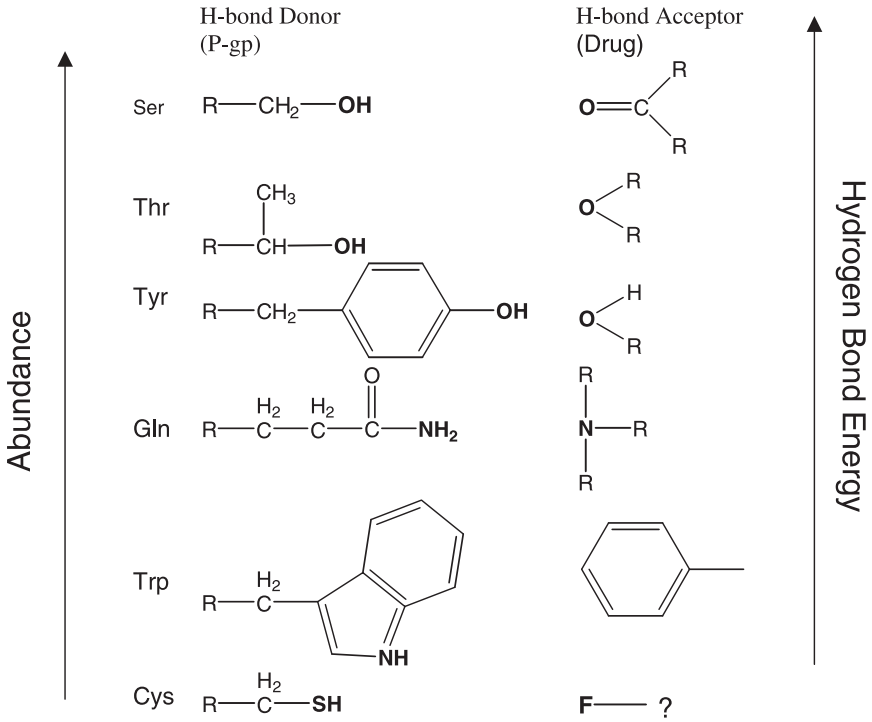

Fig. 20.3. H-bond donor groups found in the transmenbrane sequences of P-gp shown in order of abundance, and H-bond acceptor groups shown in order of H-bond donor strength.

As seen in Fig. 20.3, the most abundant amino acids with H-bond donor properties seem to be serine > threonine > tyrosine. Substrates exhibit a correspondingly high density of H-bond acceptor groups [43, 51], as will be discussed below (Section 20.3.3). Together, these findings suggested a role for H-bonding interactions in substrate recognition (in the membrane), transport, and release (into the aqueous phase). Other interactions, such as stacking between substrates and aromatic amino acid side chains of P-gp [66], weak electrostatic attraction between cationic groups of substrates and phenyl residues of P-gp [51], and strong repulsive electrostatic interactions between cationic drugs and cationic amino acid residues of P-gp (suggested to be relevant for the flippase activity of related transporters [3]) may also play a role.

20.3.3
H-Bond Acceptor Patterns in Compounds Interacting with P-gp

Clusters of H-bond acceptor (electron donor) groups were observed in compounds, which are known to be substrates or modulators of P-gp. Electron donors are electronegative atoms (O, N, S, or X = F, Cl) with an unshared electron pair, or unsat-

urated systems with a π-electron orbital (e.g., phenyl ring) [68]. Oxygen occurs in carbonyl groups (>C=O) of aldehydes, ketones, acids, esters, and amides and also in alkoxy (–OR) or hydroxy (–OH) groups. Nitrogen occurs in imines (–N=), pyrroles and pyridines, and in amines ($-NR_2$) or amides. However, only tertiary and quaternary amines and N-methyl amides seem to be involved in an interaction with P-gp (cf. below). Groups assumed to be involved in pharmacophores of P-gp are shown in Fig. 20.3.

Our approach to search for pharmacophores [43] differs from general SAR analyses, and is therefore described briefly:

(i) On the basis of the above considerations, H-bond acceptors (and H-bond donors) were tested as components of a pharmacophore. Their average abundance per compound was determined (for details, see Ref. [43], Fig. 1). The H-bond acceptor groups with the highest abundance are the carbonyl and alkoxy groups (average abundance per compound ~1.5). Groups which can act as H-bond acceptors as well as H-bond donors (–OH, –NRH) are present to a lesser extent (average abundance per compound ~0.7).

(ii) Three-dimensional structures of drugs were modeled (using e.g., the program HyperChem Release 2 for Windows; Autodesk, Inc.) and the spatial correlations between the different acceptors as well as between acceptors and donors were analyzed. The analysis was started with low molecular-weight substrates (transported) and "borderline substrates" (bound but not transported) to find the minimal requirements for an interaction with P-gp. This yielded a number of possible recognition patterns with well-defined spatial correlations.

(iii) A test set of 100 molecules was then screened for the presence of these potential recognition patterns. Only patterns, which were found either in *all* substrates or in *all* inducers of P-gp overexpression were considered as relevant. The others (e.g., those containing H-bond donor groups) were eliminated. This is in contrast to a recent SAR study using the same test set of compounds [63]. Finally two types of patterns, called type I (present in all substrates) and type II units (present in all inducers and many substrates) were retained and are shown in Fig. 20.4. Type I units are formed by two H-bond acceptor groups with a spatial separation of 2.5 ± 0.3 Å. Type II units are formed either by three H-bond acceptor groups separated from each other by 2.5 ± 0.3 Å, with a spatial separation of the outer two acceptor groups of 4.6 ± 0.6 Å, or by only two H-bond acceptor groups with a spatial separation of 4.6 ± 0.6 Å.

(iv) The average abundance of recognition elements per compound involved in these patterns was determined and differed from average abundance of recognition elements present per compound (i) due to the elimination of primary and secondary amines or amides (cf. Ref. [43], Fig. 1). Hydroxyl groups were assumed to interact occasionally with P-gp as H-bond acceptors in combination with a carbonyl group, or in a few cases in combination with a tertiary amino group, but never with a second potential H-bond donor. Type I and type II units were considered as pharmacophores for P-gp.

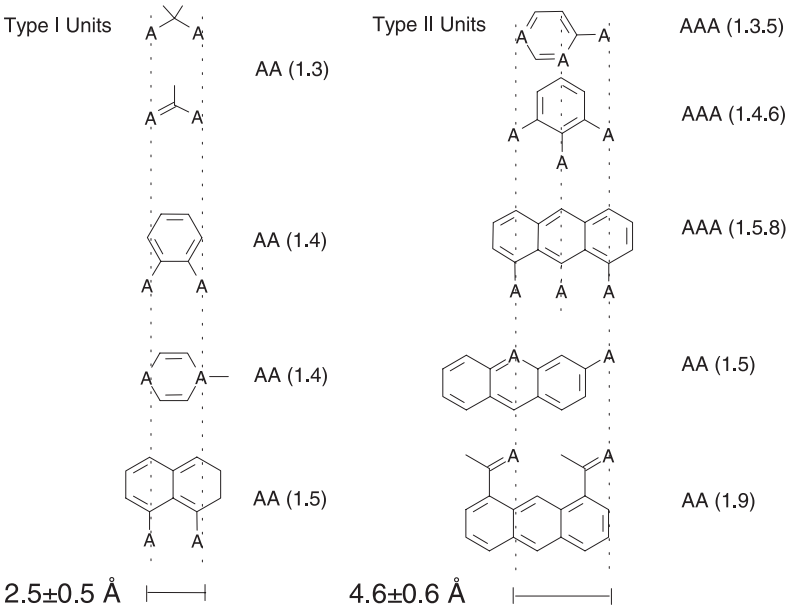

Fig. 20.4. H-bond acceptor patterns observed in P-gp substrates. Type I units: patterns formed by electron donor pairs with a spatial separation of 2.5 ± 0.3 Å. Type II units: patterns formed either by three electron donor groups with a spatial separation of the outer two electron donor groups of 4.6 ± 0.6 Å, or by two electron donor groups with a spatial separation of 4.6 ± 0.6 Å. A denotes a H-bonding acceptor group (electron donor group); numbers in brackets indicate the first and the *n*th atom with a free electron pair. (Adapted from Ref. [43].)

20.3.4
The Number and Strength of H-Bonds Determines the Drug-Transporter Affinity

Figure 20.5 shows a small but representative selection of compounds that interact with P-gp. In order to interact with P-gp, minimally one type I or one type II unit and for transport minimally two type I units seems to be required (cf. also Fig. 20.11). Noninteracting compounds contain neither type I nor type II units (Fig. 20.6). As a rough estimate, the oxygen-containing H-bond acceptor groups (>C=O, –OR) were assumed to contribute one H-bonding energy unit ($EU_H = 1$) (30–60 kJ mole^{-1}). Nitrogen has a similar H-bonding strength to oxygen; however, nitrogen often appears in close proximity to oxygen (e.g., cyclosporin A), and this reduces its electron donor strength. Therefore, half of the H-bonding energy value ($EU_H = 0.5$) was attributed to nitrogen. The same value was also attributed to sulfur- and fluorine-containing groups (-SR, –C≤F) as well as to the phenyl group (-C_6H_5) [43]. The electron donor strength of -C_6H_5 and especially of -RF may be somewhat overestimated. Whether fluorine indeed acts as H-bond acceptor or whether it merely enhances the lipid/water partition coefficient has yet to be tested for P-gp substrates. The strength of H-bond interactions is presently reinvestigated

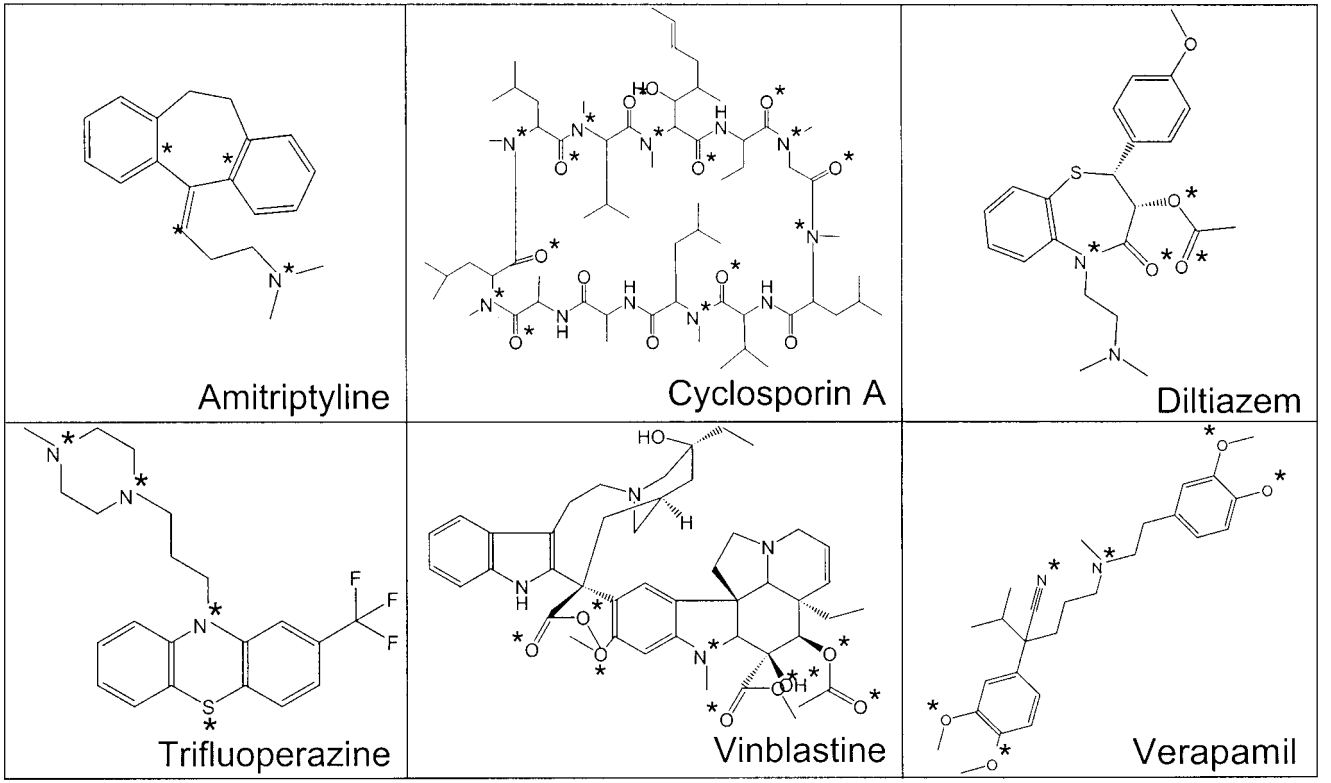

Fig. 20.5. A selection of compounds (corresponding to compounds in Figs. 20.8 and 20.9) interacting with P-gp. * = H-bond acceptor groups forming recognition patterns for P-gp.

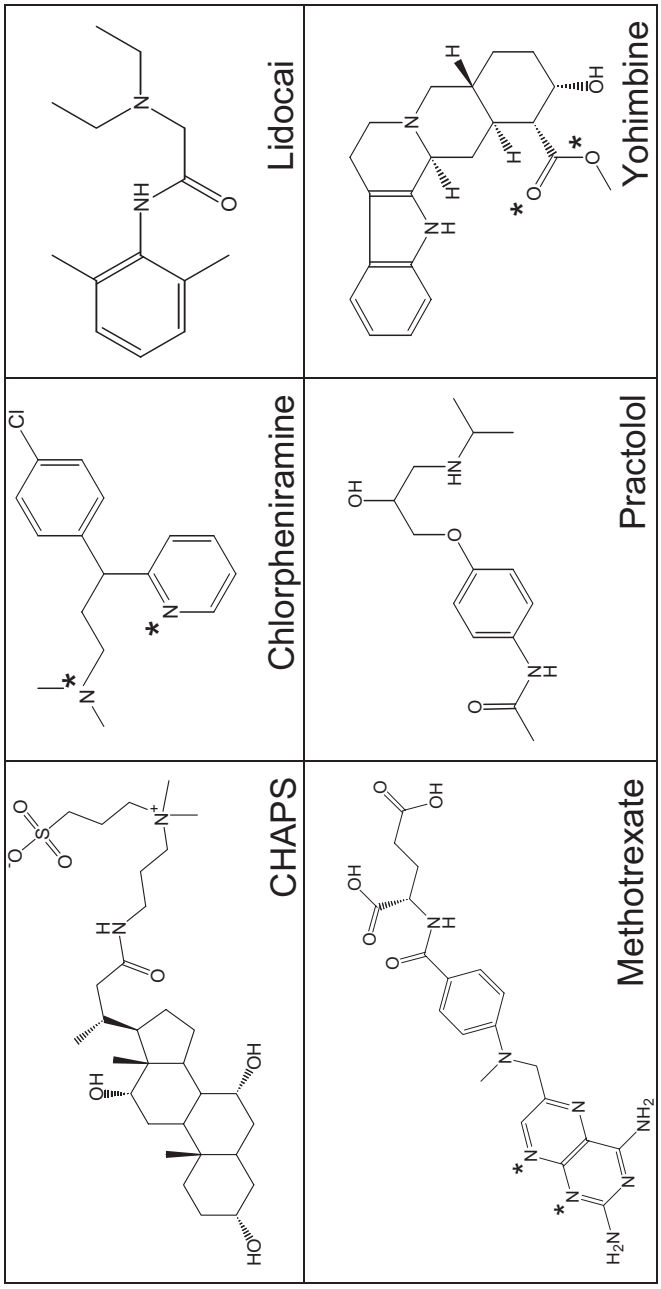

Fig. 20.6. Examples of nonsubstrates of P-gp. CHAPS and Methotrexate carry negatively changed groups.

on the basis of a modified version of HYBOT [69] (E. Landwojtowicz, unpublished results). Possible adjustments will not, however, affect the basic principles described above. The binding strength of patterns seems to depend not only on the type of H-bond acceptors but also on the rigidity of structures. Rigid patterns are distinctly more efficient than flexible ones.

Many substrates show several type I units. Since type I and type II units are rather small entities, it is possible that their arrangement relative to each other must also play a role. The free energy of substrate binding to P-gp was suggested to be proportional to the number and strength of H-bonds [43]. It thus corresponds to the sum of the free energies of binding of the individual H-bond acceptor elements $\sum \Delta G_{Ai} \approx \Delta G_{tl}$.

20.3.5
The Effect of Charge for Interaction with P-gp

P-gp substrates are in general either neutral or cationic at physiological pH (weak bases). Weak bases can cross the lipid membrane in the uncharged form and reprotonate in the negatively charged cytosolic leaflet of the membrane. With a few exceptions (e.g., the tetraphenyl phosphonium ion, which can reach the cytosolic membrane leaflet due to charge delocalization [70]), permanently charged cations do not cross the cell membrane and therefore cannot interact with P-gp in intact cells. They can, however, insert into the ''cytosolic'' leaflet in inside-out cellular vesicles and are then transported by P-gp [42, 71].

Type I units with a negative charge (e.g., carboxylic acid residue, sulfonate group, mesomeric nitro group) are unfavorable for an interaction with P-gp in intact cells as well as in inside-out vesicles [43]. Compounds that carry a negatively charged group are substrates for P-gp only if several favorable H-bond acceptor patterns over-compensate this unfavorable effect [43], or if the pK_a is high enough to allow for protonation. Anionic type I units are, however, substrates for the multidrug resistance-associated protein, MRP1 [51].

20.3.6
H-bond Acceptor Patterns in P-gp Inducers

Figure 20.7 illustrates compounds that are substrates and, in addition, are inducers of P-gp over-expression. MDR inducers appear to carry at least one type II electron donor unit. Compounds commonly cited as P-gp inducers [72] have a molecular mass of ~400–1200 Da and carry on average four type I/type II units. Recently, P-gp up-regulation was also demonstrated for a series of low molecular-mass compounds (~200–400 Da) such as phenobarbital, clotrimazole, isosafrole, and midazolam [73]. Interestingly, the one and only electron donor unit found in these compounds was of type II, which suggests that this motif is essential for P-gp up-regulation.

A different pharmacophore [74], containing only one H-bond acceptor was suggested for the interaction of drugs with the transcriptional regulator PXR (pregnane X receptor) [75].

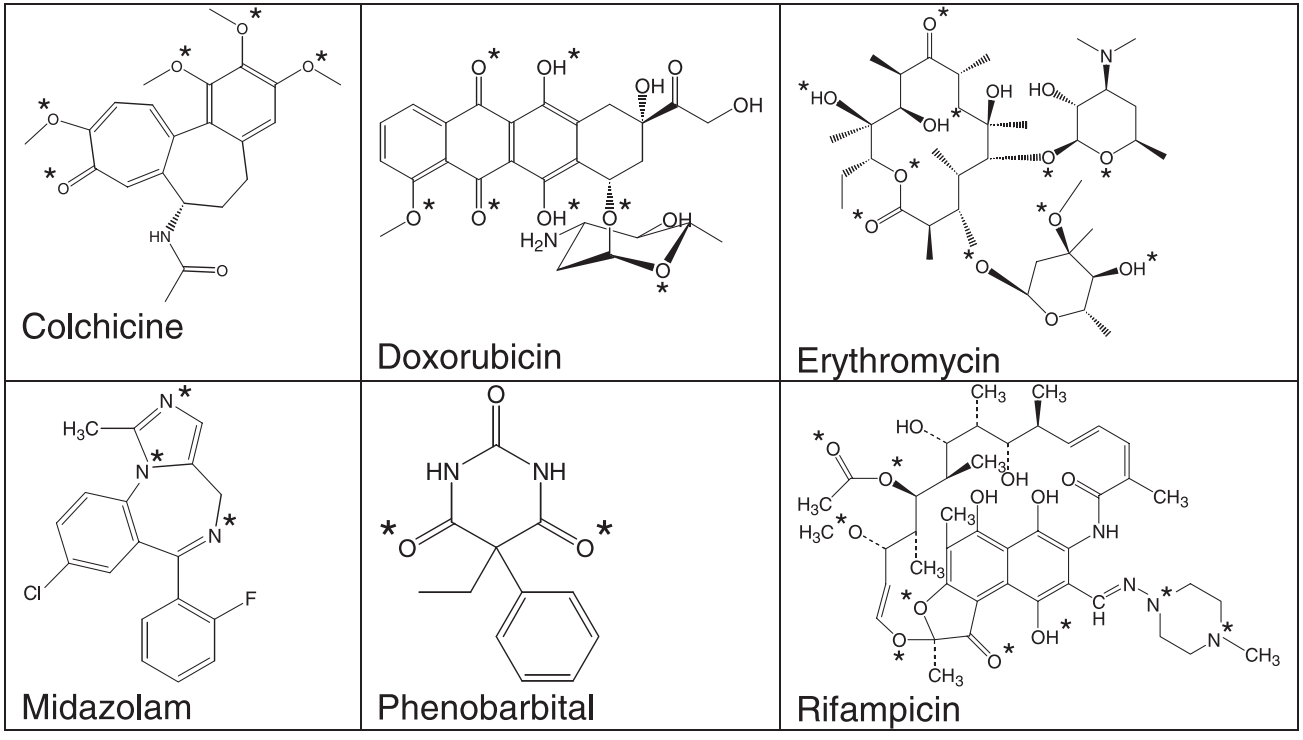

Fig. 20.7. Inducers of P-gp overexpression. * = H-bond acceptor groups forming recognition patterns relevant to P-gp induction.

20.4
SAR Applied to Experimental Results

A comparison of experimental data related to P-gp–drug interactions is complicated by the fact that the different assays used report on different aspects of this interaction [36]. Processes monitored most frequently are: (i) the rate of drug-induced ATP hydrolysis; (ii) competition between two drugs for P-gp binding sites; and (iii) drug transport through polarized cell monolayers. The different assays tend to require different experimental conditions. Factors that influence experimental results are, for example the expression level of P-gp, the lipid composition and packing density of cell membranes, the composition of the medium, the type of excipients used to improve drug dissolution or absorption, and last – but not least – the drug concentration used for P-gp stimulation. (cf. Fig. 20.8). Depending on the concept of investigation, either equimolar (e.g. Ref. [76]) or equitoxic (e.g. Refs. [77, 78]) concentrations have been used for the comparison of substrates and modulators, though this can lead to differences in classification with respect to the modifying activity of compounds (cf. Section 20.4.1). The different assays will be described briefly in the following section, and representative datasets will be analyzed in terms of the above concepts for SARs of P-gp.

20.4.1
P-gp-ATPase Activation Assays: H-Bonding Determines Activation Rate

P-gp-ATPase activation has been measured in inside-out cellular vesicles of MDR1-transfected cells either by monitoring the rate of inorganic phosphate release [28, 79, 80] or by means of a coupled enzyme assay [81]. In MDR1-transfected cells, ATP hydrolysis has also been measured by monitoring the rate of extracellular proton release (extracellular acidification rate, ECAR) [58]. The rate of drug-induced phosphate release or proton release shows a bell-shaped dependence on the drug concentration (log scale), with an increase above basal values at low and a decrease at high concentrations (Fig. 20.8). The fact that the same drugs can either activate or inhibit P-gp depending on the concentration applied explains the numerous inconsistencies in classification with respect to a modifying action.

The kinetic data from phosphate [28] and proton [58] release experiments were analyzed quantitatively by means of a modified Michaelis–Menten equation assuming activation when only one substrate molecule, S, is bound and inhibition when two substrate molecules are bound to P-gp as described by the following scheme:

$$\begin{array}{l} T + ATP + S \underset{k_{-1}}{\overset{k_1}{\rightleftharpoons}} T(ATP)S + S \xrightarrow{k_2} T(ATP)S_2 \xrightarrow{k''} T(ADP) + 2S_{rel} + P_i + H^+ \\ \qquad\qquad\qquad\qquad \downarrow k' \\ \qquad\qquad\qquad\qquad T(ADP) + P_i + H^+ + S_{rel} \end{array} \qquad (14)$$

T(ATP)S and T(ATP)S_2 are transporter–ATP complexes with one and two substrate

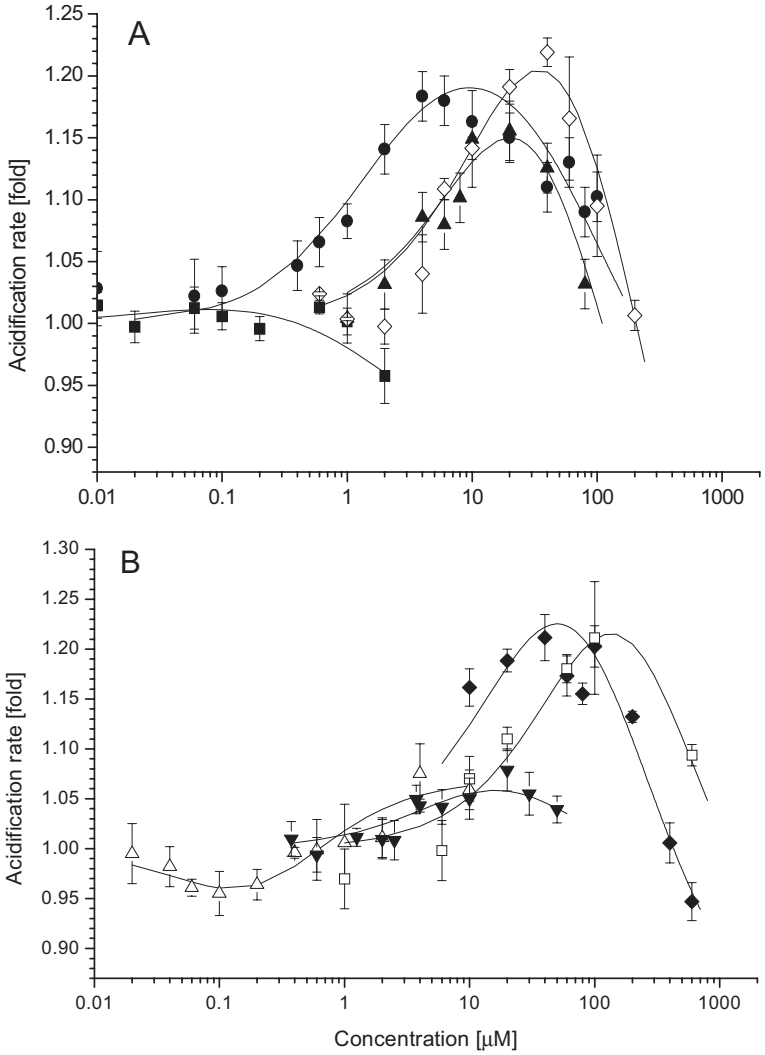

Fig. 20.8. P-gp-ATPase activation profiles obtained by measurements of extracellular acidification rates in living cells by means of a cytosensor physiometer. (A) Cyclosporin A (■), progesterone (◇), trifluoperazine (▲) and verapamil (●) in LLC-MDR1 cells; (B) amitriptyline (□), calcein-AM (△), diltiazem (◆) and vinblastine (▼) in LLC-MDR1 cells. The solid or dashed lines correspond to modified Michaelis–Menten kinetics assuming activation with one and inhibition with two molecules bound according to Eq. (15). Solid symbols represent average value of $n = 3–5$ parallel measurements made with one single cell preparation. (Adapted from Ref. [58].)

molecules bound, respectively, T(ADP) is the transporter–ADP complex, P_i the inorganic phosphate released intracellularly, S_{rel} the substrate molecule and H^+ the proton, both released extracellularly, k_1, k_{-1}, and k_2 are the rate constants of the first and the second substrate binding step and k' and k'' the rate constants of the catalytic steps. The corresponding rate equation for the hydrolysis of ATP upon P-gp can be written as:

$$V_{(Saq)} = \frac{K_1K_2V_0 + K_2V_1C_{Saq} + V_2C_{Saq}^2}{K_1K_2 + K_2C_{Saq} + C_{Saq}^2}, \tag{15}$$

where V_{Saq} is rate of P_i or H^+ release as a function of the substrate concentration in solution (C_{Saq}), V_0 is the basal activity in the absence of substrate, V_1 is the maximum transporter activity (if only activation occurred) and V_2 is the minimum activity at infinite substrate concentration, K_1 is the drug concentration at half-maximum activation and K_2 at half-minimum activation. Under steady-state conditions $1/K_1$ and $1/K_2$ are apparent affinities to the transporter. At low drug concentrations, Eq. (15) simplifies to a normal Michaelis–Menten equation.

Figure 20.9 shows the maximum, V_1, and the minimum, V_2, rate of P-gp-ATPase activation [58] as a function of the potential H-bond energy of the different drugs. The maximum activity, V_1, is high for compounds with a low H-bond energy and assumed to have a low affinity to the transporter, and slows down exponentially

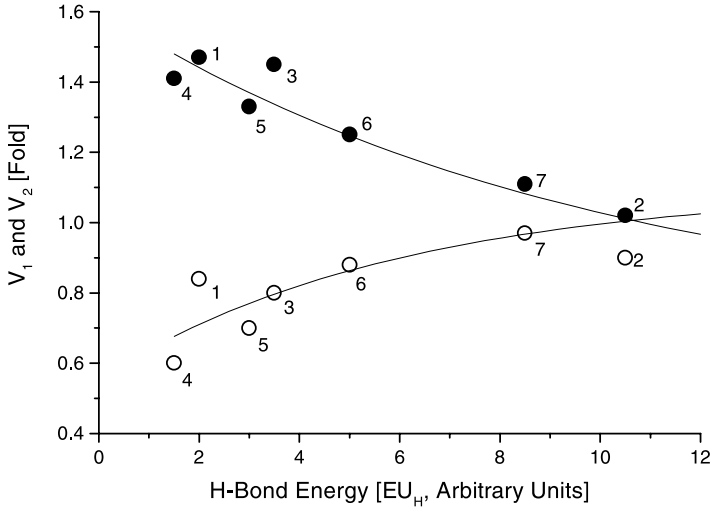

Fig. 20.9. Influence of the H-bonding energy per substrate on the rate of ATPase activation as determined by measurement of the extracellular acidification rate of intact MDR1-transfected pig kidney cells [58]. The maximum (V_1), (solid symbols) and minimum (V_2), (open symbols) rates of extracellular acidification given as fold of the basal extracellular acidification rate is plotted as a function of the H-bonding energy for amitriptyline (1), cyclosporin A (2), diltiazem (3), progesterone (4), trifluoperazine (5), verapamil (6), and vinblastine (7). The solid lines are exponential decay curves to guide the eye.

with increasing substrate affinity to the transporter. In contrast the minimum activity, V_2, is very low for compounds with a low affinity and increases with increasing potential to form H-bonds. It will be shown below that compounds with a low potential to form H-bonds are not transported efficiently and compounds with $EU_H < 2$ are not transported at all (cf. Fig. 20.11). As shown previously [58], these effects are independent of K_I values.

Combining results from P-gp-ATPase activation as a function of drug concentration with the concept of H-bonding directly shows that compounds with low EU_H at high concentrations, or with high EU_H at low concentrations, have a potential to act as modulators or inhibitors.

20.4.2
Competition Assays: The Compound with the Higher Potential to Form H-Bonds Inhibits the Compound with the Lower Potential

The calcein-AM assay [82–84] and cytotoxicity assays (e.g., performed with doxorubicin) [77, 78] are both basically competition assays. The accumulation of a primary substrate (e.g., calcein-AM or doxorubicin) in the cytosol of living cells is measured after addition of a second substrate (also called modifier or reverser) that reduces the efflux of the primary substrate. In the case of the calcein-AM assay, the primary substrate, calcein-AM, is hydrolyzed as soon as it reaches the cytosol, and the highly fluorescent hydrolysis product (calcein) can be determined using fluorescence spectroscopy. The more effective the reversal agent, the stronger is the increase in calcein fluorescence. Data can be quantified in terms of inhibitory constants, K_I, of the reversal agent.

In cytotoxicity assays the concentration of the cytotoxic compound reaching the cytosol is estimated via its apparent toxicity. Cytotoxicity is expressed as the concentration that inhibits the growth of the MDR-expressing cells by 50% or 20% (known as IC_{50} or IC_{20} values, respectively), and indicates whether the secondary, co-administered compound is a substrate or a modulator of P-gp. The activity of the reversal agent is generally expressed as a fold reversion called the MDR ratio [36]:

$$\text{MDR ratio} = IC_{50}(\text{cytotoxic drug alone})/IC_{50}(\text{cytotoxic drug} + \text{modulator}) \quad (16)$$

When examining cytotoxicity data it is important to bear in mind that they are based on a general assessment of cytotoxicity, and thus may account for more than one acting mechanism in the resistant cells used [36].

Figure 20.10 illustrates a cytotoxicity experiment performed with doxorubicin as primary substrate and a series of verapamil analogues as modifiers or reversing agents [77]. It demonstrates that the compound with the higher potential to form H-bonds with the transporter also has the higher reversing potential. A good estimate of the reversing potential of compounds on the basis of the total H-bond acceptor strength alone is possible if the lipid binding properties of the compounds are comparable [57].

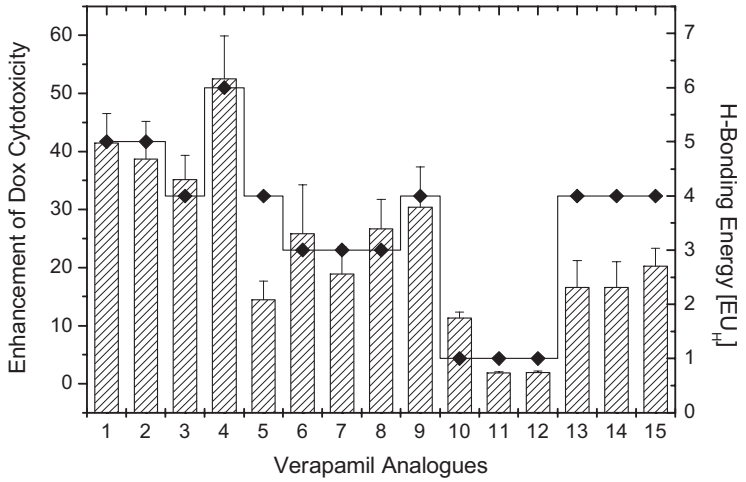

Fig. 20.10. Enhancement of doxorubicin cytotoxicity in LoVo-resistant cells by verapamil and analogues. (Adapted from Ref. [77]). The results are expressed as fold increase in cytotoxicity represented by the ratio of doxorubicin IC_{50} in the absence and presence of verapamil and analogues (solid bars). The verapamil concentrations used were the minimal cytotoxic concentrations (IC_{20}). The compounds used were: verapamil (1); *R*-verapamil (2); nor-verapamil (3); gallopamil (4); LU46605 (5); devapamil (6); LU46324 (7); LU43918 (8); LU49667 (9); emopamil (10); *S*-anipamil (11); *R*-anipamil (12); LU49940 (13); LU48895 (14); and LU51903 (15). The inhibitory potency of verapamil and analogues (diamonds) as predicted on the basis of the potential H-bonding energy given in arbitrary energy units, EU [57].

20.4.3
Transport Assays: Two Type I Units are Required for Transport

The presence of a transporter can be assessed by comparing basolateral-to-apical with apical-to-basolateral transport of substrates in polarized cell monolayers. If P-gp is present, then basolateral-to-apical transport is enhanced and apical-to basolateral transport is reduced. Transport experiments are in general performed with radioactively labeled compounds. Several studies have been performed with Caco-2 cell lines (e.g. Ref. [85]). Since Caco-2 cells express a number of different transporters, the effects measured are most probably specific for the ensemble of transporters rather than for P-gp alone. P-gp-specific transport has been assayed across confluent cell layers formed by polarized kidney epithelial cells transfected with the MDR1 gene [86]. Figure 20.11 shows experimental data obtained with these cell lines. A rank order for transport called ''substrate quality'' was determined for a number of compounds [86]. The ''substrate quality'' is a qualitative estimate, but nevertheless allows an investigation of the role of the air/water (or lipid/water) partition coefficient, log K_{aw}, for transport as seen in Fig. 20.11(A). For most of the compounds, a linear correlation is observed between ''substrate quality'' and log K_{aw}. However, four compounds are not transported at all despite their distinct lipophilicity. A plot of the ''substrate quality'' as a function of the potential of a

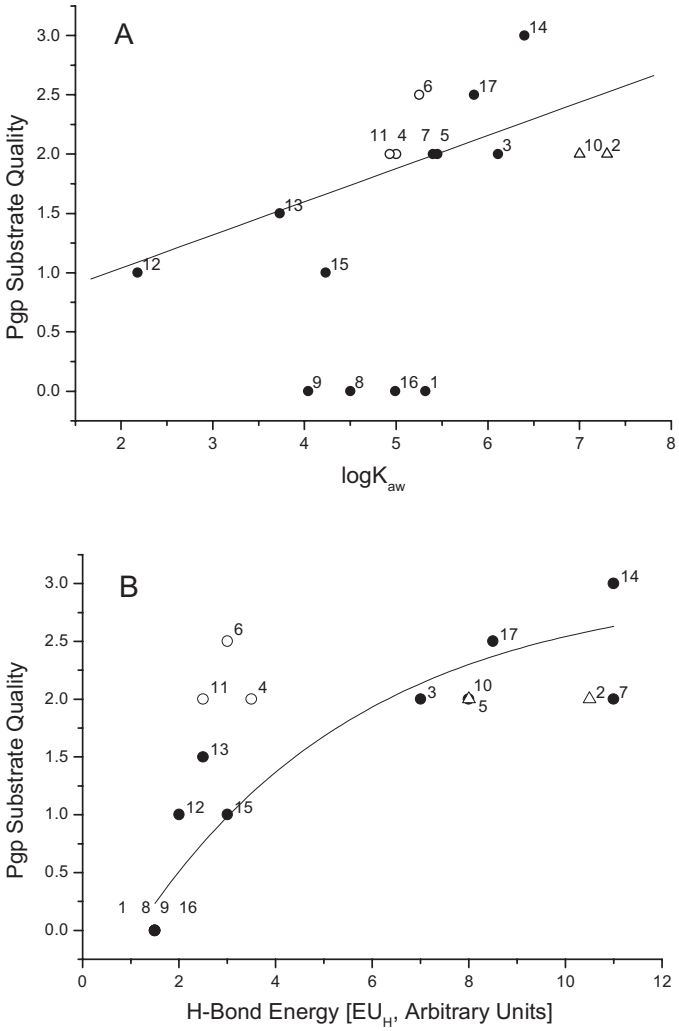

Fig. 20.11. "Substrate quality" obtained by comparing basolateral-to-apical with apical-to-basolateral transport of substrates in polarized cell monolayers of MDR1-transfected cell lines [86] plotted versus (A) the log of the air/water partition coefficient, or (B) H-bond energy (arbitrary units, EU_H cf. text). Units of the air/water partition coefficient were [M^{-1}]. Compound (concentrations in Ref. [86] in brackets) were: clozapine (50 nM) (1); cyclosporin A (2 μM) (2); daunorubicin (3); dexamethasone (2 μM) (4); digoxin (2 μM) (5); domperidone (2 μM) (6); etoposide (7); flunitrazepam (500 nM) (8); haloperidol (50 nM) (9); ivermectin (50 nM) (10); loperamide (2 μM) (11); morphine (2 μM) (12); ondansetron (2 μM) (13); paclitaxel (14); phenytoin (2 μM) (15); progesterone added from Ref. [88] (16); and vinblastine (17). Compounds applied at concentrations below K_m (estimated from surface activity measurements; cf. Fig. 20.1) including those for which concentrations are not given (solid circles), compounds applied at inhibitory concentrations (open triangles) are expected to be comparatively low, compounds applied at concentrations close to the concentration of half-maximum activation, K_m (open circles) are expected to be comparatively high. The linear and the exponential fits to the data in (A) and (B), respectively, were added to guide the eye.

compound to form H-bonds (Fig. 20.11(B)) shows that those compounds which are not transported have only a low potential to form H-bonds ($EU_H \leq 2$) and exhibit less than two H-bond acceptor patterns.

A comparison of the ''transport quality'' (Fig. 20.11(B)) with the rate of P-gp-ATPase activation (see Fig. 20.9) as a function of the H-bond energy (EU_H) shows that compounds inducing a high rate of ATP hydrolysis (e.g., progesterone) can have a low ''substrate quality'', and vice versa (e.g., cyclosporin).

20.5 P-gp Modulation or Inhibition

P-gp modulation or inhibition can be achieved by: (i) inhibition of ATP binding or ATP hydrolysis; or (ii) direct interaction with one or more binding sites on P-gp, thus blocking transport by acting as competitive or noncompetitive inhibitors [6]. The use of inhibitors of ATP binding or ATP hydrolysis is generally not feasible for drug therapy as they tend to cross intact cell membranes sparsely and also affect other ATPases. The pharmacologically used modulators or inhibitors generally act as either competitive or noncompetitive inhibitors. Many excipients formerly believed to act mainly via modification of the membrane packing density [6] have recently been shown to be modifiers of P-gp [P. Nervi, unpublished results].

A comprehensive list of P-gp modulators or inhibitors, classified according to their chemical structures, has been published recently [87]. This shows that the structures of inhibitors are almost as heterogeneous as those of the substrates. A small but representative selection of inhibitors is shown in Fig. 20.12 and Table 20.1. In an attempt to clarify the different mechanisms of P-gp modulation or inhibition, the H-bonding concept discussed above is applied. To this end, the modulators or inhibitors in Table 20.1 were ordered according to their H-bond acceptor potential and divided in three groups comprising compounds with: (i) a low EU_H ($\leq$2; i.e., not transported); (ii) an intermediate EU_H ($\sim$3–6); and (iii) a high H-bond acceptor potential ($\sim EU_H \geq 10$; i.e., transported slowly).

As a general rule, when two drugs are co-administered the compound with the higher potential to form H-bonds with the transporter inhibits or reverses the transport of the compound with the lower potential to form H-bonds, provided that the membrane concentration of compounds are comparable (e.g., $\sim K_m$). This phenomenon tends also to dominate drug–drug interactions related to P-gp, and is demonstrated in Figs. 20.11 and 20.13.

The process of inhibition becomes somewhat more complex if no restriction is made with respect to the concentration of modulators. As seen in Fig. 20.13, compounds with a low affinity to the transporter ($EU_H \leq 2$) are able to activate if applied at low concentrations. However, if these compounds are applied at high concentration, ATP hydrolysis slows down (low V_2 values) and they act as inhibitors (cf. Fig. 20.9). Compounds with $EU_H \leq 2$ seem not to be transported (see Fig. 20.11). This may lead to an obstruction of the transport route and thus to a slow down of the activation cycle. Examples of this type of inhibitor include pro-

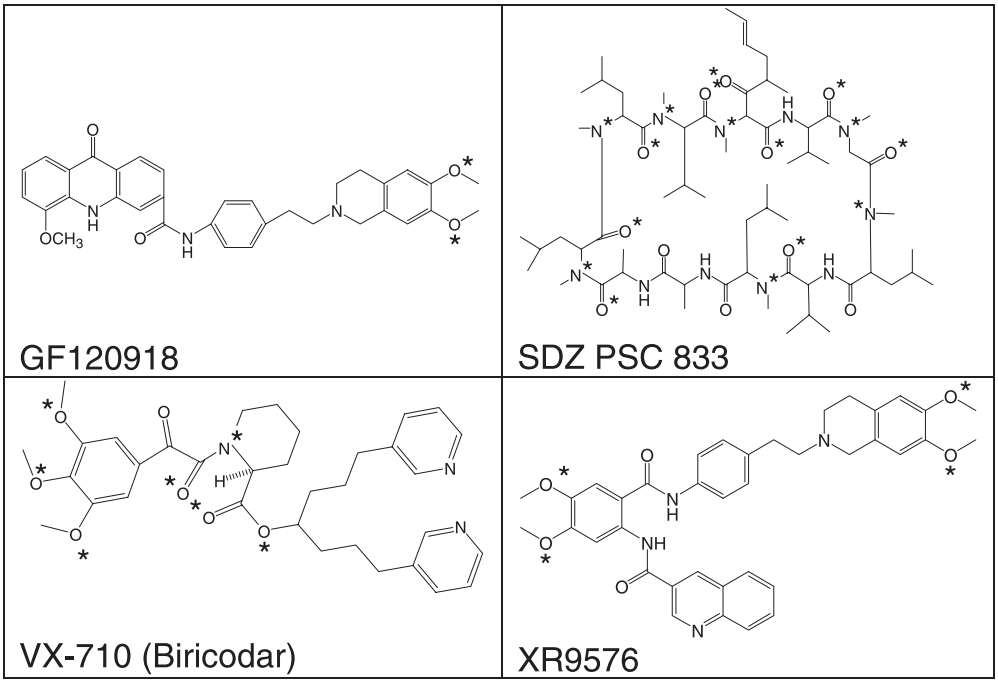

Fig. 20.12. Inhibitors of P-glycoprotein.

gesterone [88], dexamethasone, hydrocortisone, quinidine, and terfenadine (cf. Supplementary Table 2 in Ref. [63] and references therein).

Second- and third-generation inhibitors with a low H-bond acceptor potential have been synthesized (e.g., GF120918 and S9788). These molecules have higher molecular weights (>500 Da) than the corresponding first-generation inhibitors

Tab. 20.1. Inhibitors.

H-bond acceptor strength	*Drug*	*MW*	*Formula*	*EU*	*Reference*
EU $\leq$ 2	OC-144-093	494.67	$C_{32}H_{38}N_4O$	1	89
	GF120918	563.64	$C_{34}H_{33}N_3O_5$	2	90
	S9788	505.61	$C_{28}H_{33}N_7F_2$	2	91
EU $\sim$ 2–6	XR9051	642.74	$C_{39}H_{38}N_4O_5$	3.5	92
	R101933	586.72	$C_{37}H_{38}N_4O_3$	3	93
	LY335979	527.60	$C_{32}H_{31}N_3O_2F_2$	4.5	94
	MS-209	509.64	$C_{32}H_{35}N_3O_3$	4.5	95
	XR9576	646.73	$C_{38}H_{38}N_4O_6$	5.5	96
	VX-710	603.71	$C_{34}H_{41}N_3O_7$	6.5	97
EU 8	PervilleineA	587.61	$C_{30}H_{37}NO_{11}$	11	98
	PSC833	1214.63	$C_{62}H_{109}N_{11}O_{12}$	10.5	99

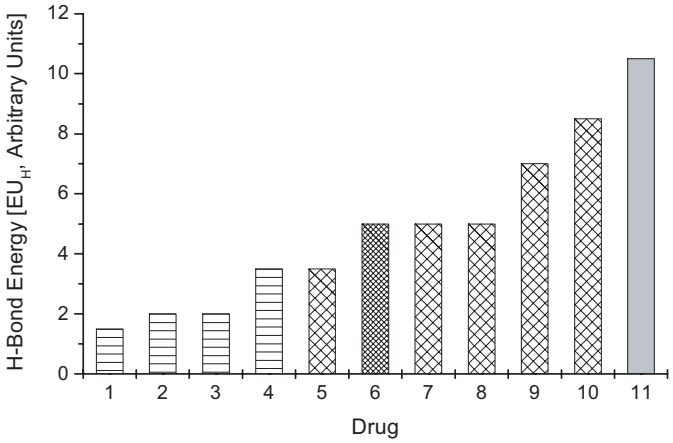

Fig. 20.13. Potential H-bonding energy, released upon interaction with the transmembrane domains of P-gp (in arbitrary energy units, EU) for progesterone (1), propranolol (2), amitriptyline (3), diltiazem (4), amiodarone (5), colchicine (7), gramicidin S (8), daunorubicin (9), vinblastine (10), cyclosporin A, in comparison with verapamil (6). The type of interaction of verapamil (solid bar) in the presence of one of the other compounds is indicated: Cooperative stimulation (hatched bars); allosteric noncompetitive inhibition (cross-hatched bars); and competitive inhibition (gray bars). (Adapted from Ref. [57].)

and exhibit elongated structures, presumably with small cross-sectional areas, A_D. They can thus be expected to have higher lipid/water partition coefficients, K_{lw}, and consequently lower concentrations of half-maximum activation/inhibition, K_I, than the corresponding first-generation modifiers.

First-generation modifiers with an intermediate H-bond acceptor potential ($EU_H = 2–5$) include aldosterone, *cis*-flupenthixol, diltiazem, nicardipine, trifluoperazine or verapamil [78]. They again act as inhibitors at relatively high concentrations ($C > 10$ μM), but in contrast to compounds with $EU_H \leq 2$ they are transported by P-gp. More potent and less toxic second- and third-generation inhibitors that have been developed include R101933, LY335979, and MS-205, all of which exhibit molecular weights > 500 Da. Their structures and charge distribution suggest again rather small cross-sectional areas, A_D, and a considerable length which might be larger than that of an average lipid molecule. They might thus occupy more than half of the TM space of the transporter and might inhibit transport. For some of these compounds the distance between the individual patterns is especially large, and this may further hamper transport.

Compounds with a high H-bond acceptor potential ($EU_H \geq 8$) (e.g., cyclosporine A, SDZ PSC-833) act as competitive inhibitors, presumably because they occupy all H-bond donor sites of the transporter. Due to the strong interaction of these compounds with P-gp they are transported slowly, and this is reflected in a low rate of ATP hydrolysis. Many of these compounds exhibit high lipid/water partition coefficients and thus also low K_i values.

20.5.1 How to Design an Inhibitor

Cytostatic drugs for which inhibitors are primarily needed are often not only substrates of P-gp but also inducers of P-gp overexpression with one or even several type II units. An important point to clarify would be whether or not type II units are required to achieve a cytostatic effect. If they were not required, it might be possible to eliminate the P-gp-inducing effect that causes multidrug resistance by eliminating type II units. So far, the only other possibility of overcoming multidrug resistance is to inhibit the transporters involved. Inhibition can be achieved essentially by two different concepts:

1. By synthesis of compounds with a very large number and a strength of type I units (whereby the type I units must be more numerous and stronger than those of the cytostatic compound to be inhibited).
2. By synthesis of compounds with a low number of type I units.

The latter type of compounds should preferably carry either one type I unit or at most two units (positioned as far apart as possible), and have an elongated structure (which does not fold as verapamil, for example) with a small cross-sectional area, A_D. The first type of compounds is expected to be transported slowly, whereas the second type may not be transported. Table 20.2 summarizes the drug properties relevant for transporter binding and lipid partitioning of a substrate (modulator or inhibitor) of P-gp. Inspection of the information contained in Table 20.2 shows that the synthesis and membrane incorporation of inhibitors with a low number of H-bond acceptor patterns should be simpler and more efficient than that of inhibitors with a large number of patterns.

In conclusion, this analysis shows that QSAR studies have to be adapted to the special situation of P-gp, and that lipid partitioning and receptor binding must be addressed separately in order to reach a high predictive value.

Tab. 20.2. Drug properties which influence the lipid/water partition coefficient, K_{lw} and the transporter binding constant, K_t.

Drug properties	*Relevance for increase in K_{lw} and decrease in K_m*	*Relevance for increase in K_t, change in $V_{1/2}$, increase in "substrate quality"*
Number of H-bond donors	Low	Irrelevant?
Number of H-bond acceptors	Low	High
Cationic charge	Low	High
Anionic charge	Low	Low
Cross-sectional area, A_D	Small	Probably no correlation, but drugs with many type I units often have large A_D
Lipophilicity	High	Irrelevant

References

1 Gottesman, M. M., Pastan, I., Biochemistry of multidrug resistance mediated by the multidrug transporter, *Annu. Rev. Biochem.* **1993**, *62*, 385–427.

2 Borst, P., Schinkel, A. H., Genetic dissection of the function of mammalian P-glycoproteins, *Trends Genet.* **1997**, *13*, 217–222.

3 Ambudkar, S. V., Dey, S., Hrycyna, C. A., Ramachandra, M., Pastan, I., Gottesman, M. M., Biochemical, cellular, and pharmacological aspects of the multidrug transporter, *Annu. Rev. Pharmacol. Toxicol.* **1999**, *39*, 361–398.

4 Litman, T., Druley, T. E., Stein, W. D., Bates, S. E., From MDR to MXR: new understanding of multidrug resistance systems, their properties and clinical significance, *Cell Mol. Life Sci.* **2001**, *58*, 931–959.

5 Doige, C. A., Ames, G. F., ATP-dependent transport systems in bacteria and humans: relevance to cystic fibrosis and multidrug resistance, *Annu. Rev. Microbiol.* **1993**, *47*, 291–319.

6 Higgins, C. F., ABC transporters: from microorganisms to man, *Annu. Rev. Cell Biol.* **1992**, *8*, 67–113.

7 Chang, G., Roth, C. B., Structure of MsbA from *E. coli*: a homolog of the multidrug resistance ATP binding cassette (ABC) transporters, *Science* **2001**, *293*, 1793–1800.

8 Rosenberg, M. F., Callaghan, R., Ford, R. C., Higgins, C. F., Structure of the multidrug resistance P-glycoprotein to 2.5 nm resolution determined by electron microscopy and image analysis, *J. Biol. Chem.* **1997**, *272*, 10685–10694.

9 Sarkadi, B., Muller, M., Hollo, Z., The multidrug transporters – proteins of an ancient immune system, *Immunol. Lett.* **1996**, *54*, 215–219.

10 Cordon-Cardo, C., O'Brien, J. P., Boccia, J., Casals, D., Bertino, J. R., Melamed, M. R., Expression of the multidrug resistance gene product (P-glycoprotein) in human normal and tumor tissues, *J. Histochem. Cytochem.* **1990**, *38*, 1277–1287.

11 Thiebaut, F., Tsuruo, T., Hamada, H., Gottesman, M. M., Pastan, I., Willingham, M. C., Immunohistochemical localization in normal tissues of different epitopes in the multidrug transport protein P170: evidence for localization in brain capillaries and crossreactivity of one antibody with a muscle protein, *J. Histochem. Cytochem.* **1989**, *37*, 159–164.

12 Smit, J. W., Huisman, M. T., van Tellingen, O., Wiltshire, H. R., Schinkel, A. H., Absence or pharmacological blocking of placental P-glycoprotein profoundly increases fetal drug exposure, *J. Clin. Invest.* **1999**, *104*, 1441–1447.

13 Holash, J. A., Harik, S. I., Perry, G., Stewart, P. A., Barrier properties of testis microvessels, *Proc. Natl. Acad. Sci. USA* **1993**, *90*, 11069–11073.

14 Thiebaut, F., Tsuruo, T., Hamada, H., Gottesman, M. M., Pastan, I., Willingham, M. C., Cellular localization of the multidrug-resistance gene product P-glycoprotein in normal human tissues, *Proc. Natl. Acad. Sci. USA* **1987**, *84*, 7735–7738.

15 Mukhopadhyay, T., Batsakis, J. G., Kuo, M. T., Expression of the mdr (P-glycoprotein) gene in Chinese hamster digestive tracts, *J. Natl. Cancer Inst.* **1988**, *80*, 269–275.

16 Endicott, J. A., Ling, V., The biochemistry of P-glycoprotein-mediated multidrug resistance, *Annu. Rev. Biochem.* **1989**, *58*, 137–171.

17 McClean, S., Whelan, R. D., Hosking, L. K., Hodges, G. M., Thompson, F. H., Meyers, M. B., Schuurhuis, G. J., Hill, B. T., Characterization of the P-glycoprotein over-expressing drug resistance phenotype exhibited by Chinese hamster ovary cells following their in-vitro exposure to fractionated X-irradiation, *Biochim. Biophys. Acta* **1993**, *1177*, 117–126.

18 Uchiumi, T., Kohno, K., Tanimura, H., Matsuo, K., Sato, S., Uchida, Y., Kuwano, M., Enhanced expression of the human multidrug resistance 1 gene in response to UV light irradiation, *Cell Growth Differ.* **1993**, *4*, 147–157.

19 Chin, K. V., Tanaka, S., Darlington, G., Pastan, I., Gottesman, M. M., Heat shock and arsenite increase expression of the multidrug resistance (MDR1) gene in human renal carcinoma cells, *J. Biol. Chem.* **1990**, *265*, 221–226.

20 Gottesman, M. M., Fojo, T., Bates, S. E., Multidrug resistance in cancer: role of ATP-dependent transporters, *Nature Rev. Cancer* **2002**, *2*, 48–58.

21 Van Bambeke, F., Balzi, E., Tulkens, P. M., Antibiotic efflux pumps, *Biochem. Pharmacol.* **2000**, *60*, 457–470.

22 Borst, P., Ouellette, M., New mechanisms of drug resistance in parasitic protozoa, *Annu. Rev. Microbiol.* **1995**, *49*, 427–460.

23 Wolfger, H., Mamnun, Y. M., Kuchler, K., Fungal ABC proteins: pleiotropic drug resistance, stress response and cellular detoxification, *Res. Microbiol.* **2001**, *152*, 375–389.

24 Sauna, Z. E., Smith, M. M., Muller, M., Kerr, K. M., Ambudkar, S. V., The mechanism of action of multidrug-resistance-linked P-glycoprotein, *J. Bioenerg. Biomembr.* **2001**, *33*, 481–491.

25 Urbatsch, I. L., Sankaran, B., Bhagat, S., Senior, A. E., Both P-glycoprotein nucleotide-binding sites are catalytically active, *J. Biol. Chem.* **1995**, *270*, 26956–26961.

26 Sauna, Z. E., Ambudkar, S. V., Characterization of the catalytic cycle of ATP hydrolysis by human p-glycoprotein. The two ATP hydrolysis events in a single catalytic cycle are kinetically similar but affect different functional outcomes, *J. Biol. Chem.* **2001**, *276*, 11653–11661.

27 Sharom, F. J., Yu, X., Chu, J. W., Doige, C. A., Characterization of the ATPase activity of P-glycoprotein from multidrug-resistant Chinese hamster ovary cells, *Biochem. J.* **1995**, *308*, 381–390.

28 Litman, T., Zeuthen, T., Skovsgaard, T., Stein, W. D., Structure–activity relationships of P-glycoprotein interacting drugs: kinetic characterization of their effects on ATPase activity, *Biochim. Biophys. Acta* **1997**, *1361*, 159–168.

29 Kerr, K. M., Sauna, Z. E., Ambudkar, S. V., Correlation between steady-state ATP hydrolysis and vanadate-induced ADP trapping in human P-glycoprotein. Evidence for ADP release as the rate-limiting step in the catalytic cycle and its modulation by substrates, *J. Biol. Chem.* **2001**, *276*, 8657–8664.

30 Ramachandra, M., Ambudkar, S. V., Chen, D., Hrycyna, C. A., Dey, S., Gottesman, M. M., Pastan, I., Human P-glycoprotein exhibits reduced affinity for substrates during a catalytic transition state, *Biochemistry* **1998**, *37*, 5010–5019.

31 Krupka, R. M., Uncoupled active transport mechanisms accounting for low selectivity in multidrug carriers: P-glycoprotein and SMR antiporters, *J. Membr. Biol.* **1999**, *172*, 129–143.

32 Romsicki, Y., Sharom, F. J., Phospholipid flippase activity of the reconstituted P-glycoprotein multidrug transporter, *Biochemistry* **2001**, *40*, 6937–6947.

33 Borst, P., Zelcer, N., van Helvoort, A., ABC transporters in lipid transport, *Biochim. Biophys. Acta* **2000**, *1486*, 128–144.

34 Raggers, R. J., Pomorski, T., Holthuis, J. C., Kalin, N., van Meer, G., Lipid traffic: the ABC of transbilayer movement, *Traffic* **2000**, *1*, 226–234.

35 Ekins, S., Waller, C. L., Swaan, P. W., Cruciani, G., Wrighton, S. A., Wikel, J. H., Progress in predicting human ADME parameters in silico, *J. Pharmacol. Toxicol. Methods* **2000**, *44*, 251–272.

36 Stouch, T. R., Gudmundsson, O., Progress in understanding the structure–activity relationships of P-glycoprotein, *Adv. Drug Deliv. Rev.* **2002**, *54*, 315–328.

37 Juliano, R. L., Ling, V., A surface glycoprotein modulating drug permeability in Chinese hamster ovary cell mutants, *Biochim. Biophys. Acta* **1976**, *455*, 152–162.

38 Stein, W. D., Kinetics of the P-glycoprotein, the multidrug transporter, *Exp. Physiol.* **1998**, *83*, 221–232.

39 Wiese, M., Pajeva, I. K., Structure–activity relationships of multidrug resistance reversers, *Curr. Med. Chem.* **2001**, *8*, 685–713.

40 Ekins, S., Kim, R. B., Leake, B. F., Dantzig, A. H., Schuetz, E. G., Lan, L. B., Yasuda, K., Shepard, R. L., Winter, M. A., Schuetz, J. D., Wikel, J. H., Wrighton, S. A., Application of three-dimensional quantitative structure–activity relationships of P-glycoprotein inhibitors and substrates, *Mol. Pharmacol.* **2002**, *61*, 974–981.

41 Ferte, J., Analysis of the tangled relationships between P-glycoprotein-mediated multidrug resistance and the lipid phase of the cell membrane, *Eur. J. Biochem.* **2000**, *267*, 277–294.

42 Schmid, D., Ecker, G., Kopp, S., Hitzler, M., Chiba, P., Structure–activity relationship studies of propafenone analogs based on P-glycoprotein ATPase activity measurements, *Biochem. Pharmacol.* **1999**, *58*, 1447–1456.

43 Seelig, A., A general pattern for substrate recognition by P-glycoprotein, *Eur. J. Biochem.* **1998**, *251*, 252–261.

44 Klopman, G., Shi, L. M., Ramu, A., Quantitative structure–activity relationship of multidrug resistance reversal agents, *Mol. Pharmacol.* **1997**, *52*, 323–334.

45 Ecker, G., Huber, M., Schmid, D., Chiba, P., The importance of a nitrogen atom in modulators of multidrug resistance, *Mol. Pharmacol.* **1999**, *56*, 791–796.

46 Eytan, G. D., Kuchel, P. W., Mechanism of action of P-glycoprotein in relation to passive membrane permeation, *Int. Rev. Cytol.* **1999**, *190*, 175–250.

47 Lentz, K. A., Polli, J. W., Wring, S. A., Humphreys, J. E., Polli, J. E., Influence of passive permeability on apparent P-glycoprotein kinetics, *Pharm. Res.* **2000**, *17*, 1456–1460.

48 Zamora, J. M., Pearce, H. L., Beck, W. T., Physical-chemical properties shared by compounds that modulate multidrug resistance in human leukemic cells, *Mol. Pharmacol.* **1988**, *33*, 454–462.

49 Dey, S., Ramachandra, M., Pastan, I., Gottesman, M. M., Ambudkar, S. V., Evidence for two nonidentical drug-interaction sites in the human P-glycoprotein, *Proc. Natl. Acad. Sci. USA* **1997**, *94*, 10594–10599.

50 Martin, C., Berridge, G., Higgins, C. F., Mistry, P., Charlton, P., Callaghan, R., Communication between multiple drug binding sites on P-glycoprotein, *Mol. Pharmacol.* **2000**, *58*, 624–632.

51 Seelig, A., Blatter, X. L., Wohnsland, F., Substrate recognition by P-glycoprotein and the multidrug resistance-associated protein MRP1: a comparison, *Int. J. Clin. Pharmacol. Ther.* **2000**, *38*, 111–121.

52 Raviv, Y., Pollard, H. B., Bruggemann, E. P., Pastan, I., Gottesman, M. M., Photosensitized labeling of a functional multidrug transporter in living drug-resistant tumor cells, *J. Biol. Chem.* **1990**, *265*, 3975–3980.

53 Chen, Y., Simon, S. M., In situ biochemical demonstration that P-glycoprotein is a drug efflux pump with broad specificity, *J. Cell Biol.* **2000**, *148*, 863–870.

54 Shapiro, A. B., Ling, V., Extraction of Hoechst 33342 from the cytoplasmic leaflet of the plasma membrane by P-glycoprotein, *Eur. J. Biochem.* **1997**, *250*, 122–129.

55 Khan, E. U., Reichel, A., Begley, D. J., Roffey, S. J., Jezequel, S. G., Abbott, N. J., The effect of drug lipophilicity on P-glycoprotein-mediated colchicine efflux at the blood-brain barrier, *Int. J. Clin. Pharmacol. Ther.* **1998**, *36*, 84–86.

56 Norinder, U., Haeberlein, M., Computational approaches to the prediction of the blood-brain distribution, *Adv. Drug Deliv. Rev.* **2002**, *54*, 291–313.

57 Seelig, A., Landwojtowicz, E., Structure–activity relationship of P-glycoprotein substrates and modifiers, *Eur. J. Pharm. Sci.* **2000**, *12*, 31–40.

58 Landwojtowicz, E., Nervi, P., Seelig, A., Real-time monitoring of P-glycoprotein activation in living cells, *Biochemistry* **2002**, *41*, 8050–8057.

59 Fischer, H., Gottschlich, R., Seelig, A., Blood-brain barrier permeation: molecular parameters governing passive diffusion, *J. Membr. Biol.* **1998**, *165*, 201–211.

60 Seelig, A., Local anesthetics and pressure: a comparison of dibucaine binding to lipid monolayers and bilayers, *Biochim. Biophys. Acta* **1987**, *899*, 196–204.

61 Boguslavsky, V., Rebecchi, M., Morris, A. J., Jhon, D. Y., Rhee, S. G., McLaughlin, S., Effect of monolayer surface pressure on the activities of phosphoinositide-specific phospholipase C-beta 1, -gamma 1, and -delta 1, *Biochemistry* **1994**, *33*, 3032–3037.

62 Romsicki, Y., Sharom, F. J., The membrane lipid environment modulates drug interactions with the P-glycoprotein multidrug transporter, *Biochemistry* **1999**, *38*, 6887–6896.

63 Penzotti, J. E., Lamb, M. L., Evensen, E., Grootenhuis, P. D., A computational ensemble pharmacophore model for identifying substrates of P-glycoprotein, *J. Med. Chem.* **2002**, *45*, 1737–1740.

64 Zheleznova, E. E., Markham, P., Edgar, R., Bibi, E., Neyfakh, A. A., Brennan, R. G., A structure-based mechanism for drug binding by multidrug transporters, *Trends Biochem. Sci.* **2000**, *25*, 39–43.

65 Vazquez-Laslop, N., Zheleznova, E. E., Markham, P. N., Brennan, R. G., Neyfakh, A. A., Recognition of multiple drugs by a single protein: a trivial solution of an old paradox, *Biochem. Soc. Trans.* **2000**, *28*, 517–520.

66 Pawagi, A. B., Wang, J., Silverman, M., Reithmeier, R. A., Deber, C. M., Transmembrane aromatic amino acid distribution in P-glycoprotein. A functional role in broad substrate specificity, *J. Mol. Biol.* **1994**, *235*, 554–564.

67 Loo, T. W., Clarke, D. M., Vanadate trapping of nucleotide at the ATP-binding sites of human multidrug resistance P-glycoprotein exposes different residues to the drug-binding site, *Proc. Natl. Acad. Sci. USA* **2002**, *99*, 3511–3516.

68 Vinogradov, S., Linell, R., *Hydrogen Bonding*. Van Nostrand Reinhold, New York, **1971.**

69 Raevsky, O., Quantification of non-covalent interactions on the basis of the thermodynamic hydrogen bond parameters, *J. Phys. Org. Chem.* **1997**, *10*, 405–413.

70 Flewelling, R. F., Hubbell, W. L., Hydrophobic ion interactions with membranes. Thermodynamic analysis of tetraphenylphosphonium binding to vesicles, *Biophys. J.* **1986**, *49*, 531–540.

71 Muller, M., Mayer, R., Hero, U., Keppler, D., ATP-dependent transport of amphiphilic cations across the hepatocyte canalicular membrane mediated by mdr1 P-glycoprotein, *FEBS Lett.* **1994**, *343*, 168–172.

72 Safa, A. R., Roberts, S., Agresti, M., Fine, R. L., Tamoxifen aziridine, a novel affinity probe for P-glycoprotein in multidrug resistant cells, *Biochem. Biophys. Res. Commun.* **1994**, *202*, 606–612.

73 Schuetz, E. G., Beck, W. T., Schuetz, J. D., Modulators and substrates of P-glycoprotein and cytochrome P4503A coordinately up-regulate these proteins in human colon carcinoma cells, *Mol. Pharmacol.* **1996**, *49*, 311–318.

74 Ekins, S., Erickson, J. A., A pharmacophore for human pregnane X receptor ligands, *Drug Metab. Dispos.* **2002**, *30*, 96–99.

75 Schuetz, E., Strom, S., Promiscuous regulator of xenobiotic removal, *Nature Med.* **2001**, *7*, 536–537.

76 Polli, J. W., Wring, S. A., Humphreys, J. E., Huang, L., Morgan, J. B., Webster, L. O., Serabjit-Singh, C. S., Rational use of in vitro P-glycoprotein assays in drug discovery, *J. Pharmacol. Exp. Ther.* **2001**, *299*, 620–628.

77 Toffoli, G., Simone, F., Corona, G., Raschack, M., Cappelletto, B., Gigante, M., Boiocchi, M., Structure–activity relationship of verapamil analogs and reversal of multidrug resistance, *Biochem. Pharmacol.* **1995**, *50*, 1245–1255.

78 Ford, J. M., Prozialeck, W. C., Hait, W. N., Structural features determining activity of phenothiazines and related drugs for inhibition of cell growth and reversal of multidrug resistance, *Mol. Pharmacol.* **1989**, *35*, 105–115.

79 Litman, T., Zeuthen, T., Skovsgaard, T., Stein, W. D., Competitive, non-competitive and cooperative interactions between substrates of P-glycoprotein as measured by its ATPase activity, *Biochim. Biophys. Acta* **1997**, *1361*, 169–176.

80 Litman, T., Nielsen, D., Skovsgaard, T., Zeuthen, T., Stein, W. D., ATPase activity of P-glycoprotein related to emergence of drug resistance in Ehrlich ascites tumor cell lines, *Biochim. Biophys. Acta* **1997**, *1361*, 147–158.

81 Orlowski, S., Mir, L. M., Belehradek, J., Jr., Garrigos, M., Effects of steroids and verapamil on P-glycoprotein ATPase activity: progesterone, desoxycorticosterone, corticosterone and verapamil are mutually non-exclusive modulators, *Biochem. J.* **1996**, *317*, 515–522.

82 Hollo, Z., Homolya, L., Davis, C. W., Sarkadi, B., Calcein accumulation as a fluorometric functional assay of the multidrug transporter, *Biochim. Biophys. Acta* **1994**, *1191*, 384–388.

83 Essodaigui, M., Broxterman, H. J., Garnier-Suillerot, A., Kinetic analysis of calcein and calcein-acetoxymethylester efflux mediated by the multidrug resistance protein and P-glycoprotein, *Biochemistry* **1998**, *37*, 2243–2250.

84 Fricker, G., Drug transport across the blood-brain barrier, in: *Pharmacokinetic Challenges in Drug Discovery.* Eds. Pelkonen, O., Baumann, A., Reichel, A., Springer-Verlag Berlin Heidelberg, Germany, **2002**, Pelkonen, O., Baumann, A., Reichel, A. (eds), Springer, **2002**, pp. 139–154.

85 Anderle, P., Niederer, E., Rubas, W., Hilgendorf, C., Spahn-Langguth, H., Wunderli-Allenspach, H., Merkle, H. P., Langguth, P., P-Glycoprotein (P-gp) mediated efflux in Caco-2 cell monolayers: the influence of culturing conditions and drug exposure on P-gp expression levels, *J. Pharm. Sci.* **1998**, *87*, 757–762.

86 Schinkel, A. H., Wagenaar, E., van Deemter, L., Mol, C. A., Borst, P., Absence of the mdr1a P-Glycoprotein in mice affects tissue distribution and pharmacokinetics of dexamethasone, digoxin, and cyclosporin A, *J. Clin. Invest.* **1995**, *96*, 1698–1705.

87 Avendano, C., Menendez, J. C., Inhibitors of multidrug resistance to antitumor agents (MDR), *Curr. Med. Chem.* **2002**, *9*, 159–193.

88 Barnes, K. M., Dickstein, B., Cutler, G. B., Fojo, T., Bates, S. E., Steroid treatment, accumulation, and antagonism of P-glycoprotein in multidrug-resistant cells, *Biochemistry* **1996**, *35*, 4820–4827.

89 Newman, M. J., Rodarte, J. C., Benbatoul, K. D., Romano, S. J., Zhang, C., Krane, S., Moran, E. J., Uyeda, R. T., Dixon, R., Guns, E. S., Mayer, L. D., Discovery and characterization of OC144-093, a novel inhibitor of P-glycoprotein-mediated multidrug resistance, *Cancer Res.* **2000**, *60*, 2964–2972.

90 Hyafil, F., Vergely, C., Du Vignaud, P., Grand-Perret, T., In vitro and in vivo reversal of multidrug resistance by GF120918, an acridonecarboxamide derivative, *Cancer Res.* **1993**, *53*, 4595–4602.

91 Huet, S., Chapey, C., Robert, J., Reversal of multidrug resistance by a new lipophilic cationic molecule, S9788. Comparison with 11 other MDR-modulating agents in a model of doxorubicin-resistant rat glioblastoma cells, *Eur. J. Cancer* **1993**, *10*, 1377–1383.

92 Dale, I. L., Tuffley, W., Callaghan, R., Holmes, J. A., Martin, K., Luscombe, M., Mistry, P., Ryder, H., Stewart, A. J., Charlton, P., Twentyman, P. R., Bevan, P., Reversal of P-glycoprotein-mediated multidrug resistance by XR9051, a novel diketopiperazine derivative, *Br. J. Cancer* **1998**, *78*, 885–892.

93 van Zuylen, L., Sparreboom, A., van der Gaast, A., van der Burg, M. E., van Beurden, V., Bol, C. J., Woestenborghs, R., Palmer, P. A., Verweij, J., The orally administered P-glycoprotein inhibitor R101933 does not alter the plasma pharmacokinetics of docetaxel, *Clin. Cancer Res.* **2000**, *6*, 1365–1371.

94 Dantzig, A. H., Shepard, R. L., Cao, J., Law, K. L., Ehlhardt, W. J., Baughman, T. M., Bumol, T. F., Starling, J. J., Reversal of P-glycoprotein-mediated multidrug resistance by a potent cyclopropyldibenzosuberane modulator, LY335979, *Cancer Res.* **1996**, *56*, 4171–4179.

95 Sato, W., Fukazawa, N., Nakanishi, O., Baba, M., Suzuki, T., Yano, O., Naito, M., Tsuruo, T., Reversal of multidrug resistance by a novel quinoline derivative, MS-209, *Cancer Chemother. Pharmacol.* **1995**, *35*, 271–277.

96 Roe, M., Folkes, A., Ashworth, P., Brumwell, J., Chima, L., Hunjan, S., Pretswell, I., Dangerfield, W., Ryder, H., Charlton, P., Reversal of P-glycoprotein mediated multidrug resistance by novel anthranilamide derivatives, *Bioorg. Med. Chem. Lett.* **1999**, *9*, 595–600.

97 Germann, U. A., Shlyakhter, D., Mason, V. S., Zelle, R. E., Duffy, J. P., Galullo, V., Armistead, D. M., Saunders, J. O., Boger, J., Harding, M. W., Cellular and biochemical characterization of VX-710 as a chemosensitizer: reversal of P-glycoprotein-mediated multidrug resistance in vitro, *Anticancer Drugs* **1997**, *8*, 125–140.

98 Mi, Q., Cui, B., Silva, G. L., Lantvit, D., Lim, E., Chai, H., You, M., Hollingshead, M. G., Mayo, J. G., Kinghorn, A. D., Pezzuto, J. M., Pervilleine A, a novel tropane alkaloid that reverses the multidrug-resistance phenotype, *Cancer Res.* **2001**, *61*, 4030–4037.

99 Twentyman, P. R., Bleehen, N. M., Resistance modification by PSC-833, a novel non-immunosuppressive cyclosporin [corrected], *Eur. J. Cancer* **1991**, *27*, 1639–1642.

100 Kyte, J., Doolittle, R. F., A simple method for displaying the hydropathic character of a protein. *J. Mol. Biol.* **1982**, *157*, 105.

V
Drug Development Issues

Drug Bioavailability: Estimation of Solubility, Permeability, Absorption and Bioavailability.
Edited by Han van de Waterbeemd, Hans Lennernäs and Per Artursson

ISBN: 3-527-30438-X

21
Application of the Biopharmaceutic Classification System Now and in the Future

Bertil Abrahamsson and Hans Lennernäs

Abbreviations

ANDA	Abbreviated New Drug Application
BCRP	Breast cancer-resistant protein
BCS	Biopharmaceutic classification system
CYP 3A4	Cytrochrome P450 3A4
EMEA	European Medical Evaluation Agency
ER	Extended release
FDA	Food and Drug Administration
HBD	Number of hydrogen bond donors
hPepT1	Oligo peptide carrier for di- and tripeptides
ICH	International Committee for Harmonisation
IR	Immediate release
IVIVC	*In vitro*/*in vivo* correlation
MCT	Monocarboxylic acid cotransporter
NDA	New drug application
P-gp	P-glycoprotein
MRP	Multidrug resistant-related protein family
PSA	Polar molecular surface area
SR	Solubilization ratio
SUPAC	Scale-up and post-approval changes

Symbols

Clint	Intrinsic clearance
CLOGP	Logarithm of the calculated octanol/water partition coefficient (for neutral species)
E_G	Gut wall extraction
E_H	Hepatic extraction
F	Bioavailability
fa	fraction dose absorbed
fu	Fraction drug unbound in plasma

Drug Bioavailability: Estimation of Solubility, Permeability, Absorption and Bioavailability.
Edited by Han van de Waterbeemd, Hans Lennernäs and Per Artursson

ISBN: 3-527-30438-X

$\log D_{6.5}$	Logarithm of the distribution coefficient in octanol/water at pH 6.5
MW	Molecular weight
P_{eff}	Effective intestinal permeability
Q_h	Hepatic blood flow

21.1 Introduction

The dominant part of the 50 most-sold drug products in the United States and European markets are administered orally (Fig. 21.1). Significant drug absorption and appropriate drug delivery are prerequisites for successful oral treatment of diseases. Through retrospective analysis, the reasons behind failures in the development of oral drugs for the market have been poor pharmacokinetic properties, lack of efficacy, safety issues and marketing, as shown in Fig. 21.2 [1–3]. Among the pharmacokinetic aspects, a low and highly variable bioavailability – i.e., the amount of drug that reaches the plasma compartment – is indeed considered to be the main reason for stopping further development of the pharmaceutical product [3]. It is not surprising that pharmacokinetics is crucial for a successful drug development, since the plasma drug levels are related in various ways to the effects at the sites of pharmacological and toxicological actions (pharmacodynamics) (Fig. 21.3).

It is also well recognized that the design and composition of the pharmaceutical dosage form may have an important impact on the bioavailability and hence therapeutic outcome of a drug product. This includes both intentional effects such as altered drug absorption rates by modified-release formulations or increased bioavailability for dosage forms including absorption-enhancing principles, as well as undesirable effects such as reductions in the amount of drug reaching the systemic circulation due to poor product design. Consequently, bioavailability also reflects the pharmaceutical product quality and *in vivo* performance for oral dosage forms. This has to be considered in the development of generic products, which should be

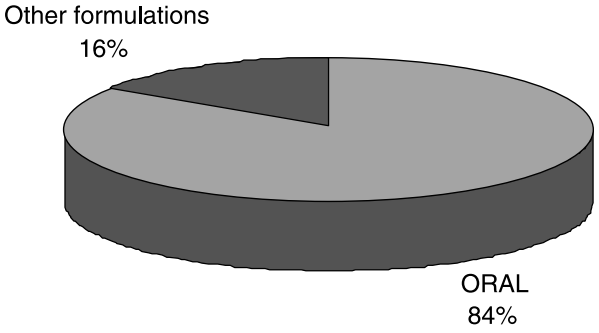

Fig. 21.1. Percent sales of orally administered drugs for the 50 most sold products in US and Europe (from IMS Health 2001).

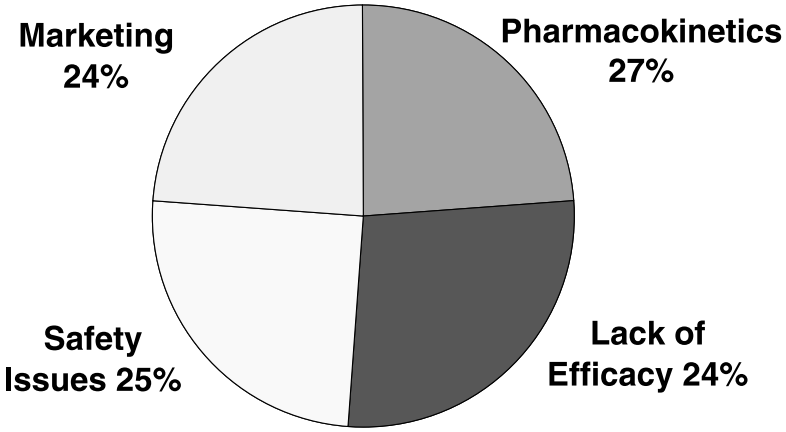

Fig. 21.2. Reasons why the clinical development of drugs is sometimes terminated and the drug does not reach the market include safety issues, marketing reasons, lack of efficacy and/or pharmacokinetics/bioavailability. (Reproduced courtesy of Dr. Lawrence Lesko, FDA regulatory standards: BA/BE & PK/PD; in Strategies for oral Drug Delivery, Lake Tahoe, USA March 6–10, 2000).

interchangeable with the original product and provide the same clinical outcome, or when formulations and manufacturing processes are changed during clinical development or for a marketed product. *In vivo* investigations comparing the bioavailability of two formulations of the same drug with the aim to verify sufficient

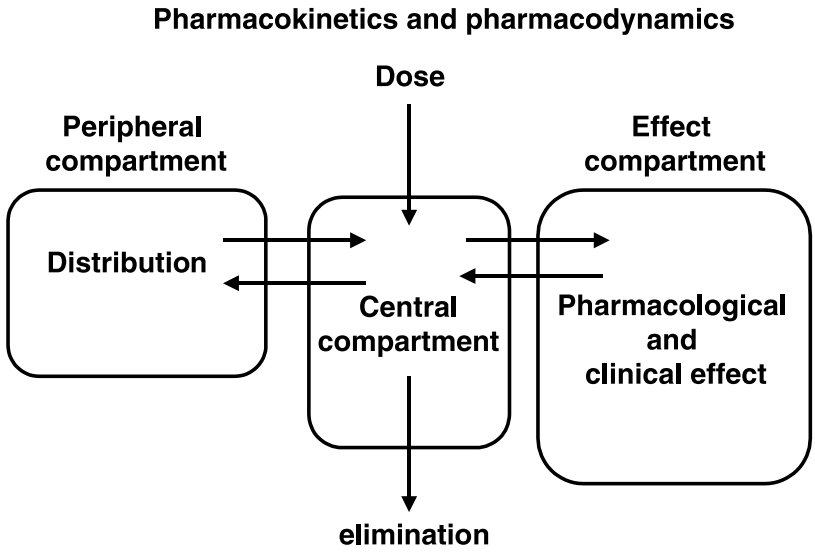

Fig. 21.3. Schematic diagram of the relationship between pharmacokinetics and pharmacodynamics in order to better understand the action of drugs.

similarity from a clinical perspective for a "new" versus an "old" formulation are called bioequivalence studies.

The successful development of pharmaceutical products for oral use requires identification of the rate-limiting step(s) of the intestinal absorption process of the drug. This will aid in the selection of suitable candidate molecules for drug development, as well as in the design of a dosage form. Biopharmaceutical investigations are needed to obtain the necessary understanding of the intestinal absorption process. The rate and extent of drug absorption (fa) from a solid dosage form during its transit through the small and large intestine includes several steps: drug release and dissolution; potential stability and binding issues in the lumen; transit time; and effective intestinal permeability (P_{eff}) [4, 5]. The transport of a drug across the intestinal barrier (P_{eff}) may be complex and involve multiple transport mechanisms as illustrated in Fig. 21.4. For instance, the transport measured is a consequence of parallel processes in the absorptive directions such as passive diffusion and carrier-mediated uptake through proteins such as oligopeptide (PepT1), monocarboxylic cotransporter (MCT-H^+) amino acid transporters and others [6–9]. Today, there is also evidence that transport in the secretory directions through various efflux proteins may restrict both the rate and extent of intestinal absorption. The following efflux proteins are located in the human intestine: P-glycoprotein (P-gp); multidrug-resistant protein family (MRP-family 1–6); and breast cancer-resistant protein (BCRP) [10]. However, many efflux transport substrates show complete intestinal absorption and the pharmacokinetic are superimposable with increasing dose [11–13].

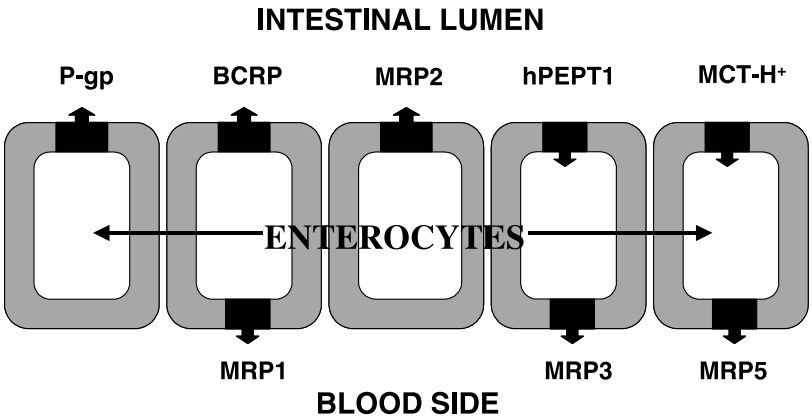

Fig. 21.4. Intestinal permeability of drugs *in vivo* is the total transport parameter that may be affected by several parallel transport mechanisms in both absorptive and secretory directions. Some of the most important transport proteins involved in the intestinal transport of drugs and their metabolites across intestinal epithelial membrane barriers in humans are shown. P-gp, P-glycoprotein; BCRP, breast cancer-resistant protein; MRP1–5, multidrug-resistant protein family; hPepT1, oligopeptide carrier for di- and tripeptides; MCT-$H^{(+)}$, monocarboxylic acid cotransporter.

In many cases, the intestinal P_{eff} is considered to be the rate-limiting step in the overall absorption process, and this poor intestinal permeability of drugs constitutes a major bottleneck in the successful development of candidate drugs [2, 5, 14–16]. However, in drug discovery today several new pharmacological targets – for instance, intracellular receptors and the use of high-throughput techniques, including permeability screens – have brought more lipophilic compounds into drug development [2, 14]. Novel candidate drugs will therefore often be poorly soluble in water [2, 14], and while this could limit the bioavailability to an extent that endangers successful product development, poor permeability could be expected to be less of an issue for these molecules. However, several formulation principles are available that could be applied to increase dissolution and solubility. Hence, drug molecules with a favorable pharmacological profile but poor biopharmaceutical properties could occasionally be saved from development failure and turned into useful pharmaceutical products. Such a reliance on formulations that reduce the shortcomings of the pure active drug is more controversial for poor permeability drugs, for which the use of permeation enhancers to increase P_{eff} has been described, though this is still more of an explorative research area than an established tool in product development.

The Biopharmaceutics Classification System (BCS) provides a scientific basis for predicting intestinal drug absorption and for identifying the rate-limiting step based on primary biopharmaceutical properties such as solubility and effective intestinal permeability (P_{eff}) [4, 17, 18]. Within the BCS, drugs are divided into four different classes based on their solubility and intestinal permeability (Fig. 21.5). Drug regulation aspects related to *in vivo* performance of pharmaceutical dosage forms have been the driving force in the development of BCS. Guidance for industry based on BCS mainly clarifies when bioavailability/bioequivalence (BA/BE) studies can be replaced by *in vitro* bioequivalence testing [17, 19].

The aim of the present chapter is to describe the BCS, the science behind it, and to discuss its use in the development of oral pharmaceutical products both from regulatory and non-regulatory aspects.

21.2 Definition of Absorption and Bioavailability of Drugs following Oral Administration

The general definition of the bioavailability (F) of a drug following oral administration is the rate at, and extent to which, a pharmacologically active drug reaches the systemic circulation. The bioavailability (F) of a compound is a consequence of several processes shown in Eq. (1):

$$F = fa \times (1 - E_G) \times (1 - E_H) \quad (1)$$

where the extent of absorption (fa) is defined as all processes from dissolution of the solid dosage form, to the intestinal transport of the drug into the intestinal tis-

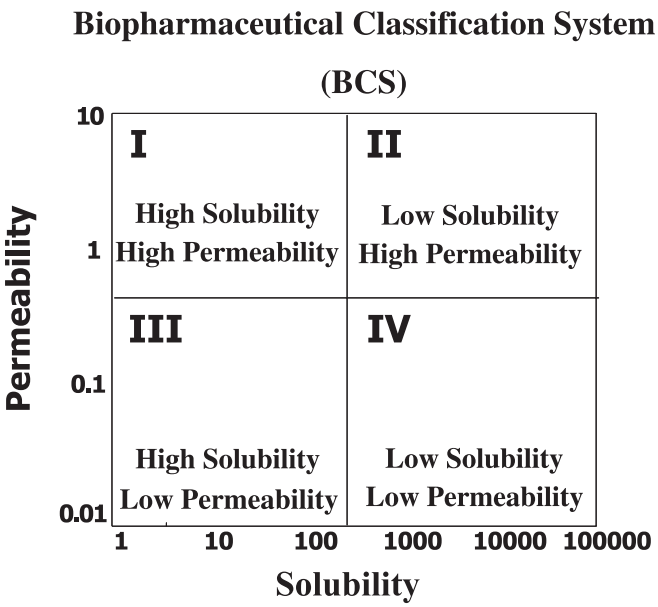

Fig. 21.5. The Biopharmaceutics Classification System (BCS) provides a scientific basis for predicting intestinal drug absorption and for identifying the rate-limiting step based on primary biopharmaceutical properties such as solubility and effective intestinal permeability (P_{eff}). The BCS divides drugs into four different classes based on their solubility and intestinal permeability. Drug regulation aspects related to *in vivo* performance of pharmaceutical dosage forms have been the driving force in the development of BCS. Guidance for industry based on BCS mainly clarifies when bioavailability/bioequivalence (BA/BE) studies can be replaced by *in vitro* bioequivalence testing (www.fda.gov/cder/guidance/3618fnl.htm).

sue, i.e., across the apical membrane of the enterocyte. This is the general definition of extent of absorption, and does not include metabolic first-pass effect in the gut (E_G) and/or metabolism/biliary excretion in the liver (E_H) [4, 5].

The rate (mass/time) and fractional extent of drug absorption (mass/dose = fa) from the intestinal lumen *in vivo* at any time t is shown schematically in Eq. (2) [4]:

$$\frac{M(t)}{dose} = \int_0^t \int_A P_{eff} \cdot C_{lumen}\, dA\, dt \qquad (2)$$

where A is the available intestinal surface area, P_{eff} is the average value of the effective intestinal permeability along the intestinal region where absorption occurs, and C_{lumen} is the free concentration of the drug in the lumen from the corresponding intestinal part [4, 20]. Several processes such as dissolution rate, degradation, metabolism and binding in the gastrointestinal tract affect the free drug concentration in the lumen.

21.3 Dissolution and Solubility

Dissolution of a drug molecule into the gastrointestinal fluids is a prerequisite for drug absorption, as the permeability of particulate material over the gastrointestinal mucosa is negligible in the context of oral drug bioavailability. The dissolution process could thereby affect both the rate and extent of oral drug absorption. The use of high-throughput techniques in the modern drug discovery process brings more lipophilic compounds into drug development [2, 14]. This means that drug dissolution in the gastrointestinal fluids has become increasingly important to consider in the design, development and optimization of a solid oral drug product.

Drug dissolution is the dynamic process by which solid material is dissolved in a solvent and characterized by a rate (amount/time), whereas solubility describes an equilibrium state, where the maximal amount of drug per volume unit is dissolved. The solubility, as well as the dissolution, in a water solution depends on factors such as pH, content of salts and surfactants.

The solubility is most often experimentally determined from the drug concentration in the liquid phase after adding excessive amounts of a solid drug substance to the test medium. This apparent solubility is affected by the solid-state properties of the drug, for example, polymorphs, solvates, impurities and amorphous content. An equilibrium with the thermodynamically most stable solid-state form, being the least soluble, should eventually be reached. This could however be a very slow process requiring several days. More short-term super-saturation phenomena may also occur, i.e., the measured solubility is much higher than the true saturation solubility during an initial phase before precipitation occurs from the supersaturated solution and an equilibrium can be reached. Thus, although solubility is a simple concept, it is far from unproblematic to obtain robust data due to the indicated time dependence and effects of differences in solid-state properties as well as other sources of experimental variability.

The dissolution of drugs has been described by the Noyes–Whitney equation as later modified by Nernst and Brunner [21, 22]:

$$dX/dt = AD/h(Cs - Xd/V) \quad (3)$$

where dX/dt is the dissolution rate in terms of mass X per unit time t, A is the available surface area of the solid drug, D is the drug diffusion coefficient, h is the effective diffusion boundary layer thickness, Cs is the saturation solubility of the drug in the test medium, Xd is the amount of drug already in solution, and V is the volume of fluid in the lumen available for dissolution. The dissolution rate is not an inherent property for a drug substance but will vary with the solid-state properties such as particles size, degree of crystallinity and crystal form.

The drug dissolution rate could be determined by dispersing the powder in a test medium under suitable agitation or by studying the dissolution for a constant surface area by using the rotating-disc method (Fig. 21.6). The latter method should be the technique of choice, except when studies of the effect of particle size are of

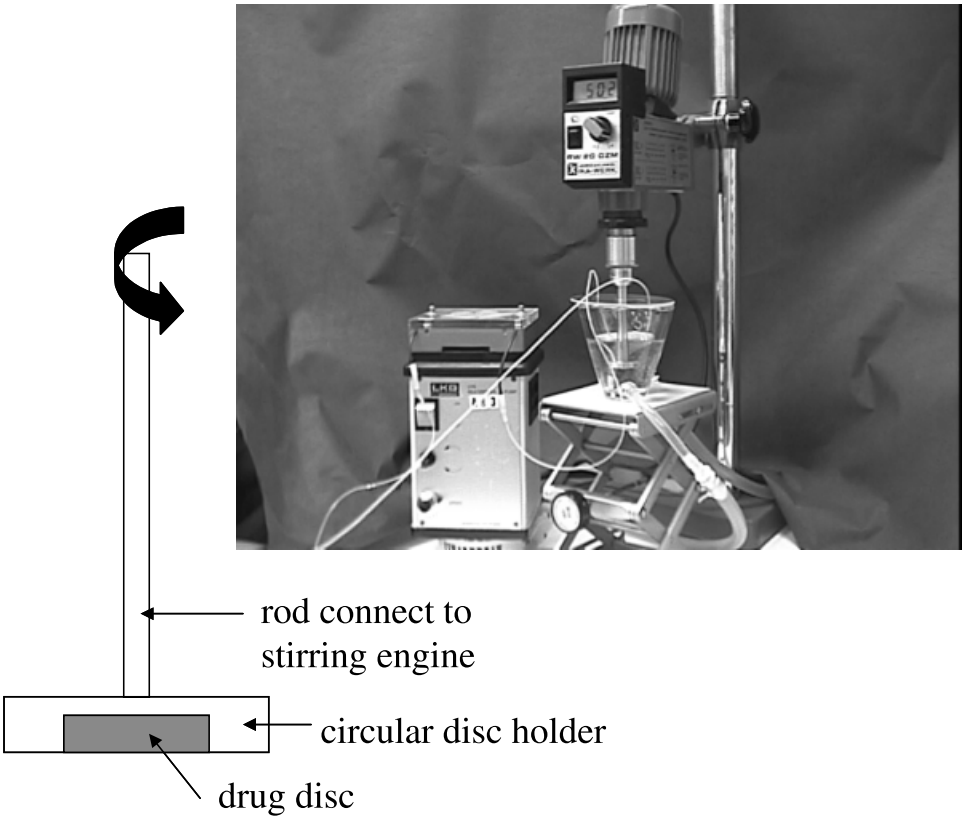

Fig. 21.6. Schematic diagram and photograph of the rotating-disc method.

special relevance. The rotating disc method, which is described in USPXXV, has the advantage of providing very well-defined hydrodynamic test conditions, which reduces the risk for artifacts and allows for accurate comparisons of data obtained for different drugs and/or different laboratories. In addition, the test conditions in the rotating-disc method also allow for more mechanistic evaluations of the dissolution process such as determination of the drug diffusion coefficient and estimation of an intrinsic dissolution rate, being independent of hydrodynamic conditions [23].

The solubility as well as the dissolution rate in the gastrointestinal tract is affected by several physiological factors, which must be taken into account when predicting the influence of drug dissolution on oral bioavailability. This includes physico-chemical properties of the gastrointestinal fluids, agitation provided by the gastrointestinal motility, and available volumes of gastrointestinal fluids. The *in vivo* situation is highly complex and depends, for example, on the nutritional status. The conditions also differ in different regions within the gastrointestinal tract. Human gastrointestinal juices have been characterized both after fasting

Tab. 21.1. Summary of physiological gastrointestinal characteristics in fasted and fed state of importance for drug dissolution and solubility.

	Fasted	*Fed*
Stomach		
Fluid volume (mL)	50–100	Up to 1000 mL
pH	1–2	2–5
Ionic strength	0.10	Varying
Motility pattern/intensity	Cyclic/low–high	Continuous/high
Surface tension (mN m^{-1})	40	Often lower than fasted
Osmolarity (mOsm)	200	Up to 600
Upper small intestine		
Flow rate (mL min^{-1})	0.6–1.2	2.0–4.2
pH	5.5–6.5	5.5–6.5
Bile acids (mM)	4–6	10–40
Ionic strength	0.16	0.16

and fed conditions by measuring aspiration through tubes [24, 25]. A summary of the most important variables for the fasting and fed state is given in Table 21.1. In addition to these main effects, the gastrointestinal conditions of relevance for drug dissolution may also be affected by other cyclic variations, diurnal effects, diseases, age, and concomitant medications [22].

A summary of how physiological factors affect the dissolution rate is given in Table 21.2. The effective surface area will be affected by the wetting properties of the bile acids and other surface-active agents in the gastrointestinal tract. The diffusivity of a drug molecule in the intestinal juice will be altered by changes in viscosity that are induced, for instance, by meal components. An increased dissolution rate could be obtained at more intense intestinal motility patterns or increased

Tab. 21.2. Physico-chemical and physiological parameters important to drug dissolution in the gastrointestinal tract [22].

Factor	*Physico-chemical parameter*	*Physiological parameter*
Surface area of drug (A)	Particle size, wettability	Surfactants in gastric juice and bile
Diffusivity of drug (D)	Molecular size	Viscosity of lumenal contents
Boundary layer thickness (h)		Motility patterns and flow rate
Solubility (Cs)	Hydrophilicity, crystal structure, solubilization	pH, buffer capacity, bile, food components
Amount of drug already dissolved (Xd)		Permeability
Volume of solvent available (V)		Secretions, coadministered fluids

Reproduced with kind permission from Kluwer Academic Publishers.

flow rates [22]. The effect on the dissolution of a poorly soluble compound of different hydrodynamic conditions, being relevant for the fasting and fed state, was recently investigated in an *in vivo* study [26]. It was found that the hydrodynamic conditions significantly affected both rate and extent of bioavailability for slowly dissolving unmilled drug particles, whereas for more rapidly dissolving micronized drug substances no effect was detected. The saturation solubility in the gastrointestinal fluids could be affected by several factors such as pH, solubilization by bile acids or dissolution in lipid food components [27]. The pH, which varies according to region as well as food intake, is a key factor for protolytic drugs with pK_a values within or close to the physiological pH interval. The bile concentrations increase after food intake, and mixed micelles with nutritional lipids are formed; however, significantly enhanced solubility due to solubilization can be achieved already under fasting conditions. An example of the dramatic increase in solubility due to solubilization by bile components is given in Fig. 21.7. The solubilization by bile acids increases by increased drug lipophilicity, and an empirical algorithm for the solubilization ratio (SR) of drugs in bile acids has been developed (Eq. (4)) which indicates that, for drugs with a log P < 2, no solubility improvement should be expected [28]. In a pharmacokinetic database of a total of 472 drugs, it was found that 235 drugs (50%) had a log P value > 2, which means that this process applies to a large part of the clinically used drugs [29].

$$\log SR = 2.09 + 0.64 \log P \tag{4}$$

The amount of drug in solution, that will affect the drug dissolution rate at ''non-sink conditions'', is dependent on the available volume that is controlled by oral intake, secretions and water flux over the gastrointestinal wall. For instance, it has

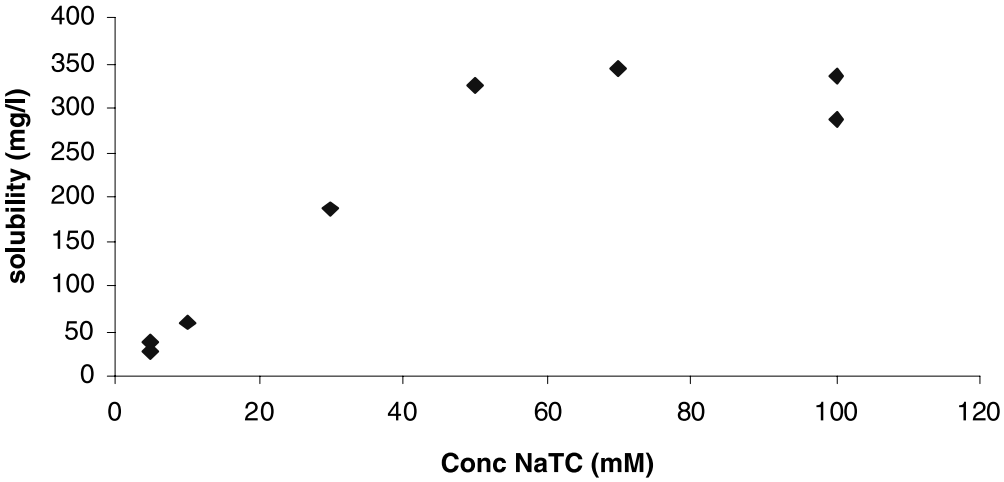

Fig. 21.7. Solubility of a very poorly soluble drug, candersartan cilexitil, at different concentrations of bile acid/lecithin (2.5:1).

been estimated that the physiological volume of the small intestine varies from approximately 50 to 1100 mL, with an average of 500 mL in the fasted state [4, 18]. The drug concentration in the intestinal lumen is also dependent on the drug permeability, which will be of importance when the drug levels in the intestine approach the saturation level.

It should be noted however that it is almost impossible to predict fully the *in vivo* dissolution rate due to the many factors involved, of which several have not yet been completely characterized. The introduction of new study techniques to directly follow drug dissolution *in vivo* in the human intestine should therefore be of importance [30, 31]. For example, *in vivo* dissolution studies discriminated between the dissolution rates of the two different particle sizes of spironolactone, based on the intestinal perfusate samples. In addition, dissolution rates of carbamazepine obtained *in vitro* were significantly slower than the direct *in vivo* measurements obtained using the perfusion method. The higher *in vivo* dissolution rate was probably due to the efficient sink conditions provided by the high permeability of carbamazepine [30, 31].

It is highly desirable in drug discovery and early drug development to predict the influence of drug dissolution on oral absorption, based on rather simple measurements of dissolution or solubility [2, 14]. The primary variable for judgments of *in vivo* absorption is the dissolution rate rather than the solubility. Drug dissolution can be the rate-limiting step in the absorption process and thereby affect the rate of bioavailability and, often more importantly, it can also limit the extent of bioavailability when the dissolution rate is too slow to provide complete dissolution within the absorptive region(s) of the gastrointestinal tract. However, most often solubility data are more readily available than dissolution rates for a drug candidate, especially in early phases when only minute amounts of drug are available, preventing accurate dissolution rate determinations. Consequently, predictions of *in vivo* effects on absorption caused by poor dissolution must often be made on the basis of solubility data rather than on dissolution rate. This can, in theory, be justified by the direct proportionality between dissolution rate and solubility under ''sink conditions'' according to Eq. (3). A list of proposed criteria to be used to avoid absorption problems caused by poor dissolution is given in Table 21.3 [4, 32, 33], and is further discussed below. A solubility in water of $\geq$10 mg mL^{-1} in pH range 1 to 7 has been proposed as an acceptance limit to avoid absorption problems,

Tab. 21.3. Proposed limits of drug dissolution on solubility to avoid absorption problems.

Factor	*Limit*	*Reference*
Solubility in pH 1–7	$>$10 mg mL^{-1} at all pH	33
Solubility in pH 1–8 and dose	Complete dose dissolved in 250 mL at all pH	4
Water solubility	$>$0.1 mg mL^{-1}	32
Dissolution rate in pH 1–7	$>$1 mg min^{-1} cm^{-2} (0.1–1 mg min^{-1} cm^{-2} borderline) at all pH	33

while another suggestion is that drugs with water solubilities <0.1 mg mL^{-1} often lead to dissolution limitations of absorption. It should be noted that these arbitrary limits may be conservative, i.e., the bioavailability of drugs with even lower solubility may not always be limited by drug dissolution. For example, a drug with much lower solubility, such as felodipine (0.001 mg mL^{-1}), provides complete absorption when administered in an appropriate solid dosage form [34]. This may be explained both by successful application of dissolution-enhancing formulation principles and more favorable drug solubility *in vivo* owing to the presence of solubilizing agents such as bile acids.

The BCS provides another model for biopharmaceutical interpretation of solubility data. Two different classes of drugs have been identified based on the drug solubility as outlined in Fig. 21.5, i.e., high and low solubility. If the administered dose is completely dissolved in the fluids in the stomach, the volume of which is assumed to be 250 mL (50 mL basal level in stomach plus administration of the solid dose with 200 mL of water), the drug is classified as a ''high-solubility drug'' [4, 17]. Such a good solubility should be obtained within a range of pH 1 to 8 to cover all possible conditions in a patient, and also to exclude the risk of precipitation in the small intestine due to the generally higher pH there than in the stomach. Drug absorption is expected to be independent of drug dissolution for drugs that fulfill this requirement, as the total amount of the drug will be in solution before entering the major absorptive area in the small intestine, and the rate of absorption will then be determined by the gastric emptying of fluids. Such ''highly soluble drugs'' are advantageous in pharmaceutical development since no dissolution-enhancing principles are needed and process parameters that could affect drug particle form and size are generally not critical formulation factors. However, many low-solubility drugs according to BCS have been developed into clinically useful products; in other words, this classification is barely useful as a screen criterion in drug discovery.

A special case in dissolution-limited bioavailability occurs when the assumption of ''sink condition'' *in vivo* fails; that is, the drug concentration in the intestine is close to the saturation solubility. Class IV compounds, according to BCS, are most prone to this situation due to the combination of low solubility and low permeability, although the same could also happen for class II compounds, depending primarily on the ratio between dose and solubility. ''Non-sink conditions'' *in vivo* lead to less than proportional increases of bioavailability for increased doses. This is illustrated in Fig. 21.8, where the fraction of drug absorbed has been simulated by use of an compartmental absorption and intestinal transit model [35] for different doses and for different permeabilities of a low-solubility, aprotic compound.

21.4 The Effective Intestinal Permeability (P_{eff})

The intestinal permeability (P_{eff}) is a major determinant of fraction drug absorbed, and quantitatively represents the principal membrane transport coefficient of the

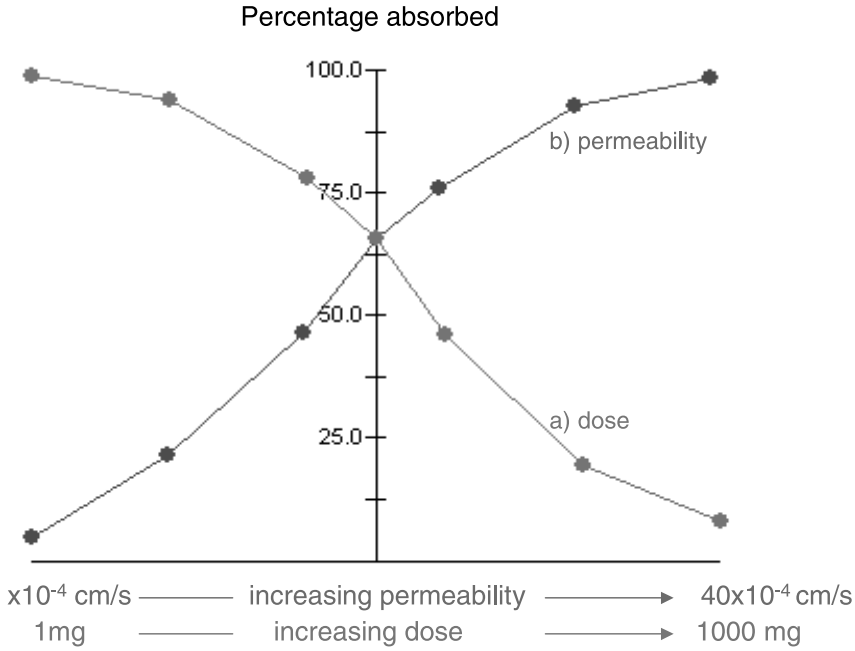

Fig. 21.8. Fraction of drug absorbed predicted by Gastroplus™ (SimulationPlus, Lancaster, CA, USA) for oral administration of a poorly soluble (1 μg mL^{-1}), aprotic drug at: (a) different doses with a constant, high permeability (4×10^{-4} cm s^{-1}); and (b) different permeabilities with a constant dose (100 mg).

intestinal mucosa of a drug, which is possible to use regardless of the transport mechanism across the mucosa [4, 5, 36]. The different transport mechanisms by which a drug may be transported across the intestinal barrier are displayed in Fig. 21.4. There are different approaches to predicting and measuring intestinal permeability, as summarized in Fig. 21.9. Most *in vitro* models, such as cell monolayers (Caco-2 model) and excised tissue segment in a diffusion chamber (Ussing model) are based on appearance of the drug on the serosal (basolateral) side. The measured *in vitro* P_{app} includes drug transport across the apical cell membrane, cytosol, basolateral membrane for cell monolayers, as well as the interstitial fluid and connective tissue for the Ussing chamber model [20]. Consequently, such a definition also includes gut first-pass metabolism that may occur in the cytosol of the enterocyte (for instance by CYP P450 isoenzymes and cytosolic localized peptidases). The activity of these intracellular enzymes will particularly influence the appearance rate of the drug on the basolateral side (i.e., in the portal vein *in vivo*). Thus, it may be useful to switch on and off genes coding for intestinal CYP3A4 in the Caco-2 model [37]. Another (and probably more accurate) definition suggests that the intestinal epithelial P_{eff} for most drugs reflects the transport across the apical membrane of the enterocyte [4, 5, 36]. This view is valid for most drugs that

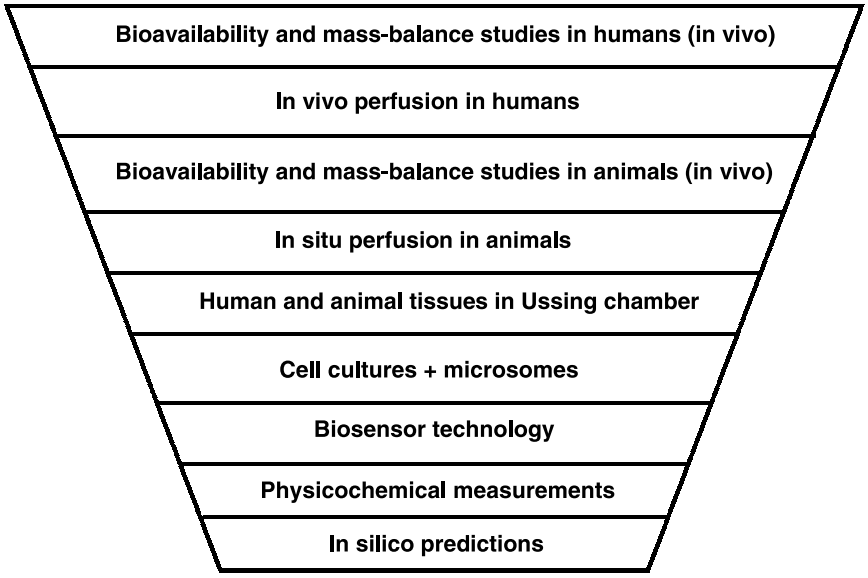

Fig. 21.9. A short overview, from *in silico* to *in vivo* in humans, of methods available to investigate and predict fraction dose absorbed and bioavailability following oral dosing.

are absorbed by passive diffusion and/or carrier-mediated transport. Recently, it has also been reported that passive transcellular permeability across epithelial cells is determined by the largest resistance, which is the apical epithelial membrane [38, 39]. Accordingly, intestinal permeability represents the transport of compounds into the enterocyte cytosol [4, 5, 36], and this view is certainly the case for passive transcellular diffusion across the apical membrane, which is considered to be rate-limiting. Intestinal perfusion models of the animal and human intestine are often based on disappearance of the drug from the perfused gut lumen. Interestingly, both results from single-pass perfusion of rat and human small intestine have been shown to predict fraction dose absorbed in humans with high accuracy [5, 20, 40].

The BCS is based on a human *in vivo* permeability (P_{eff}) database of about 20 different drugs. This database was established by using the Loc-I-Gut technique, an *in vivo* single-pass perfusion technique, in the human proximal jejunum [41]. This region of the proximal small intestine is where the major absorption of most drugs takes place when they are given in immediate-release (IR) dosage form. These *in vivo* values of P_{eff} have been used to establish a correlation between measured *in vivo* permeability and fraction dose absorbed in humans for soluble drugs, as shown in Fig. 21.10. This fundamental *in vivo* correlation between permeability and fraction of dose absorbed has established *in vitro–in vivo* correlations between human *in vivo* jejunal P_{eff} and permeabilities from animal and tissue cell culture [5, 20, 41–43]. Model correlations based on *in vivo* permeability data will be

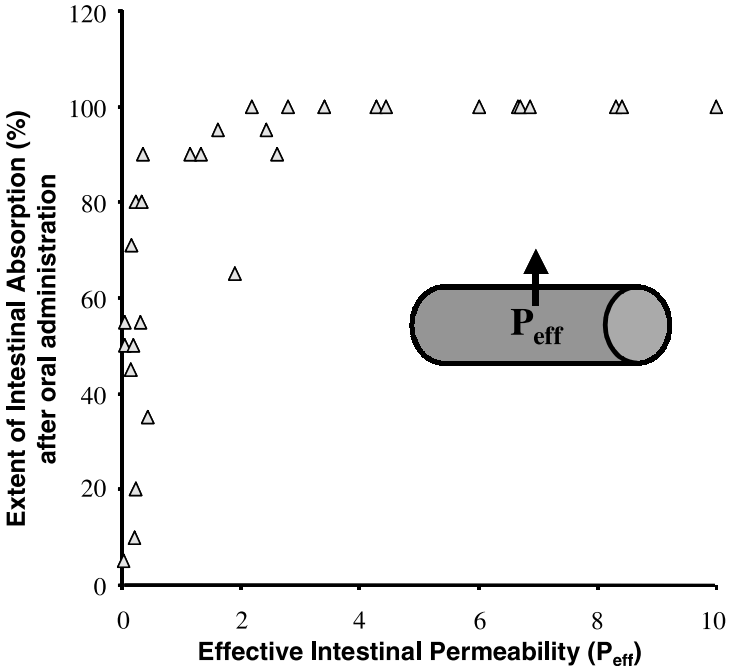

Fig. 21.10. Human *in vivo* permeability values (P_{eff}) can be determined using a single-pass perfusion technique (Loc-I-Gut®) in humans. The human P_{eff}-values correlate excellently to fraction dose absorbed (fa) of oral doses for many drugs of different pharmacological classes, which consequently represents structural diversity.

very useful when preclinical models are developed and validated regarding predictions of human intestinal absorption. They are also important for the development of theoretical models (*in silico*) where intestinal drug absorption is predicted from molecular structure [2, 16, 44]. Taken together, these models provide tools that might be very helpful in classifying drugs according to the BCS, and consequently contribute to the regulatory evaluation of both bioavailability and bioequivalence [4, 18, 45].

According to the FDA BCS guideline, measurements of the permeability and fraction dose absorbed of a drug can be made by mass balance, absolute bioavailability or intestinal perfusion methods. The intestinal permeability of a drug can be determined by:

- *in vivo* intestinal perfusion in man [41];
- *in vivo* or in-situ perfusion of a suitable animal model [40];
- *in vitro* transport across excised human or animal tissues [43, 46]; and
- *in vitro* transport across epithelial cell monolayers [47] (www.fda.gov/cder/guidance/3618fnl.htm).

When applying any of these models it is crucial to understand the main transport mechanisms as well as the metabolic route and characterization of the activity of the transporter/enzyme involved. It is well recognized that the activities of carrier-mediated processes in Caco-2 cells are considerably lower than *in vivo* [20, 42, 48]; therefore, it is crucial to extrapolate *in vitro* cell culture data to the *in vivo* situation with great care [18, 20, 42, 48]. This is especially important when carrier-mediated processes are involved, as evidenced by a recent report which showed significant differences in gene expression levels for transporters, channels and metabolizing enzymes in Caco-2 cells than in human duodenum [48]. If an animal model is used, then potential species differences must also be considered [18, 20, 45].

The human *in vivo* permeability for various drugs is one of the cornerstones in the BCS, and the correlation of fraction dose absorbed and permeability values with other permeability models mentioned above would make it feasible to classify drugs according to the BCS, and also to define bioequivalence regulations for pharmaceutical product approval. These human *in vivo* P_{eff} values were determined with a regional double-balloon perfusion approach (Loc-I-Gut®), which is described briefly in the following text (Fig. 21.11). The tube was introduced through the mouth after application of a local anesthetic (lidocaine) to the throat. The position of the tube was checked using fluoroscopy, and the perfused segment was located in the proximal part of the jejunum. Once the perfusion tube was in place, the two balloons were inflated with ~26–30 mL of air, thereby creating a 10 cm-long segment. The jejunal segment was then rinsed with isotonic saline (37°C) for at least 20 min and a flow rate of 2.0 mL min^{-1} was most often applied. A more extensive description of this intestinal perfusion technique is published elsewhere [41, 49].

Jejunal P_{eff} and other variables were calculated from the steady-state level in the perfusate leaving the intestinal segment. It has been reported previously that a well-mixed model best describes the hydrodynamics within the perfused jejunal segment, and P_{eff} is calculated according to Eq. (5):

$$P_{eff} = \frac{Qin \cdot (Cin - Cout)}{Cout \cdot 2\pi rL} \tag{5}$$

where Q_{in} is the inlet perfusate rate, C_{in} and C_{out} are the inlet and outlet perfusate concentrations of the drug, respectively, r is the radius (r = 1.75 cm), and L is the length of the jejunal segment (10 cm) [41, 50].

The jejunal perfusion approach generates data which may be used to predict absorption/bioavailability and to establish *in vivo–in vitro* correlation (IVIVC) even for extended release (ER) products. If a drug is transported mainly by passive diffusion and has a jejunal P_{eff} higher than metoprolol (1.5×10^{-4} cm s^{-1} = high-permeability compound), it can be expected to be completely absorbed throughout the small and large intestine [5, 46].

Predictions of human *in vivo* permeability can be made with a particularly high degree of accuracy in all preclinical models for drugs with passive diffusion as their main mechanism. It is only the dog model that seems to absorb low-permeability

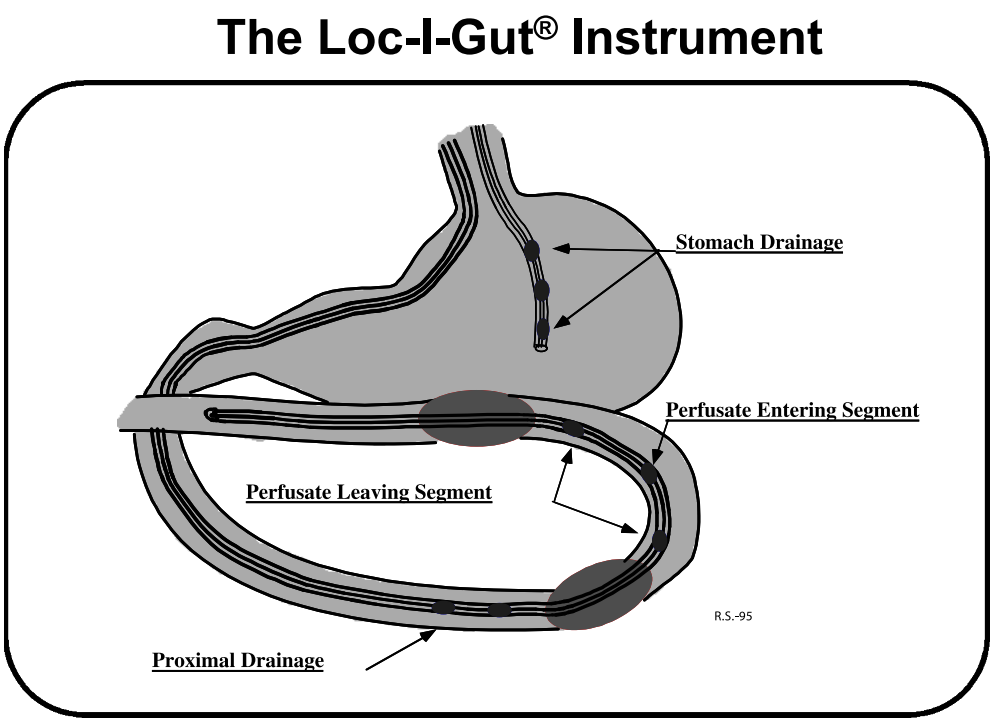

Fig. 21.11. The Loc-I-Gut® perfusion technique for the proximal human jejunum. The multichannel tube is made from polyvinyl chloride, and is 175 cm long with an external diameter of 5.3 mm. It contains six channels and is provided distally with two 40 mm-long, elongated latex balloons, placed 10 cm apart, with each separately connected to one of the smaller channels. The two wider channels in the center of the tube are for infusion and aspiration of perfusate. The two remaining peripheral smaller channels are used for administration of marker substances and/or drainage. A tungsten weight is attached to the distal end of the tube; this facilitates passage of the tube into the jejunum. The balloons are filled with air when the proximal balloon has passed the ligament of Treitz; gastric suction is obtained via a separate tube. ^{14}C-PEG 4000 is used as a volume marker to detect water flux across the intestinal barrier.

(passively) drugs more efficiently than both humans and rats [5, 20]. Special care must be taken for drugs that are absorbed by a carrier-mediated transport mechanism as the main mechanism. It has been shown that absorptive carriers, such as the oligopeptide and amino acids carriers, have a low functional activity due to low protein expression in the Caco-2 model [7, 18, 42, 51, 52]. For these drugs, a scaling factor must be developed and introduced; otherwise the *in vivo* permeability will be underestimated. This low expression is not surprising, as preliminary gene chip assays have reported that the Caco-2 cells have ~40% of the genes turned on compared with normal gene expression in the human small intestine. Carrier-mediated absorption by the oligopeptide carrier and the amino acid transport family in rats has not shown a significant species difference [7, 20, 40, 48, 51, 53–56].

It is important to recognize that the *in vitro* permeability obtained in cell monolayers (such as Caco-2 models) should be considered as a qualitative rather than quantitative value. Especially poor are predictions of fraction dose absorbed for carrier-mediated drugs with low Caco-2 permeability and predictions of high fraction dose absorbed in humans [7, 20, 42, 48, 51]. However, it is possible to establish a reasonably good IVIVC correlation when passive diffusion is the dominating absorption mechanism.

21.5 Luminal Degradation and Binding

The degradation and formation of nonabsorbable drug complexes in the intestinal lumen is the third factor, in addition to dissolution and permeability, which could affect fraction absorption. Limitations of bioavailability due to these factors seem to be less frequent compared with the two other main factors. Regulatory guidelines for BCS-based biowaivers still ask for *in vitro* studies of luminal degradation in relevant test media, whereas specific binding studies are not required [17].

The acidic environment in the stomach could degrade some substances. For example, the proton pump inhibitor omeprazole has a half-life of <5 min at pH 1, whereas it is practically stable in the intestinal pH range. Such limitations can be handled by use of properly designed modified-release formulations with enteric-coating, which protects the drug from the acid, which is the case for omeprazole [57]. Reverse forms of pH-dependent drug degradation could also occur, i.e., the drug is stable at lower pH but has significant degradation at close to neutral pH.

Drugs may also undergo hydrolysis by intestinal esterases (hydrolases), more specifically carboxylesterases (EC 3.1.1.1) in the intestinal lumen and at the brush border membrane [58, 59]. It has been shown that intestinal hydrolase activity in humans was closer to that of the rat than the dog or Caco-2 cells [60]. In these studies, six propranolol ester prodrugs and *p*-nitrophenylacetate were used as substrates, and the hydrolase activity found was ranked in the order: human $>$ rat $\gg$ Caco-2 cells $>$ dog for intestinal microsomes. The rank order in hydrolase activity for the intestinal cytosolic fraction was rat $>$ Caco-2 cells $=$ human $>$ dog. The hydrolase activity towards *p*-nitrophenylacetate and tenofovir disoproxil has also been reported in various intestinal segments from rats, pigs and humans. The enzyme activity in intestinal homogenates was found to be both site-specific (duodenum $\geq$ jejunum $>$ ileum $>$ colon) and species-dependent (rat $>$ man $>$ pig).

The bacteria in the intestinal tract serve as another well-known source of luminal drug degradation [61], though this is only important for the colon region as the luminal concentration of bacteria is 10^4 to 10^9-fold higher in the colon compared with the small intestine. Thus, this aspect is only relevant for drugs that reach this region, for example, due to poor permeability, slow dissolution or delivery by modified-release formulations. Hydrolytic and other reductive reactions are predominantly mediated by bacterial enzymes, and a list of the most prominent types

Tab. 21.4. Drug degradation reactions by intestinal bacteria.

Enzyme	*Reaction*	*Representative substrate*
Hydrolysis:		
Amidase	Cleavage of amides of carboxylic acids	Methotrexate
Decarboxylase	Decarboxylation of amino acids and simple phenolic acids, primarily p-hydroxylated	L-dopa, tyrosine
Dehydroxylase	Dehydroxylation of C- and N-hydroxy groups	Bile acids, N-hydroxyfluorenyl-acetamide
Esterase	Cleavage of esters of carboxylic acids	Acetyldigoxin
Glucuronidase	Cleavage of β-glucoronides of alcohols and phenols	Estradiol-3-glucoronides, morphine glucoronide
Glucosidase	Cleavage of β-glucosides of alcohols and phenols	Cycasin, rutin
Nitrases	Cleavage of nitrate	Pentaerythritol-trinitrate
Sulfatase	Cleavage of O-sulfates and sulfamates	Cyclamate, amygdalin, estrone sulfate
Reduction:		
Alcohol dehydrogenase	Reduction of aldehydes	Benzylaldehydes
Azoreductase	Reductive cleavage of azo compounds	Food dyes, sulfasalazine
Hydrogenase	Reduction of carbonyl groups, aliphatic double bonds	Unsaturated fatty acids, estrone
Nitroreductase	Reduction of aromatic and heterocyclic nitro compounds, nitrosamine formation	*p*-nitrobenzoic acids, chloramphenicol metronidazole, nitrazepam
N-oxide reductase	Removal of oxygen from N-oxides	4-Nitroquinolone-1-oxide, nicotine-N-oxide
Sulfoxide reductase	Removal of oxygen from sulfoxide	Sulfinpyrazone
Other reactions:		
	Aromatization	quinic acid
	D-demethylation	biochanin A
	Dealkylation	3,4,5-trimethoxy cinnamic acid
	Deamination	amino acids
	Dehalogenation	DDT
	Esterification	histamine

of enzymes, reactions and examples of substrates is provided in Table 21.4 [62, 63]. The effectiveness of this process has been exemplified by use of *in vitro* incubation studies showing rapid drug degradation [64].

Reduced absorption due to complex formation or other interactions between drugs and intestinal components leading to poor absorption has been described in a few cases. One example is the precipitation of cationic drugs as very poorly-soluble salts with bile acids, which has been reported for several compounds [62]. Another well-known example is the complex formation between tetracycline together with calcium due to chelation after administration of the drug together

with milk. It has also been shown that proteases inhibitor drugs can bind very strongly to enzymes secreted by the pancreas [65].

The interaction between drugs in the lumen and intestinal components is generally a poorly studied area, and it is difficult based on *in vivo* data to discriminate such effects from other factors affecting absorption. In addition, evidence for the *in vivo* relevance of available *in vitro* methods is sparse.

21.6 The Biopharmaceutical Classification System

21.6.1 Regulatory Aspects

21.6.1.1 Present Situation

The BCS has been developed primarily for regulatory applications, although its use has been extended beyond this area (as discussed in more detail below). The aim of the BCS in a regulatory context is to provide a basis for replacing certain bioequivalence studies by equally or more accurate *in vitro* dissolution tests. This could reduce costs and time in the development process as well as reducing unnecessary drug exposure in healthy volunteers, which is normally the study population in bioequivalence studies.

Numerous bioequivalence studies are presently being conducted for new drug applications (NDAs) of new compounds, in supplementary NDAs for new indications and line-extensions, in abbreviated new drug applications (ANDAs) of generic products and in applications for scale-up and post-approval changes (SUPAC). For example, NDA bioequivalence studies may be required comparing different clinical formulations in pivotal clinical trials and products aimed for market. The complexity and number of studies required is often boosted by the fact that several dose strengths might be included in the development process. In addition, bioequivalence documentation may also be needed comparing blinded and original comparator products in clinical trials. Thus, an NDA typically contains a multitude of bioequivalence studies.

The BCS was first applied in a regulatory context in the US FDA guideline for SUPAC's of oral immediate-release formulations [66]. More recently, guidelines for applying BCS in NDAs and ANDAs have been finalized both by the FDA and the European agency, EMEA [17, 19]. In addition, the BCS principles are also included in ICH guidelines for requirements of *in vitro* dissolution testing as a quality control in manufacturing [67].

The BCS classes are defined as:

- Class I: high solubility (S) – high P_{eff}
- Class II: low solubility – high P_{eff}
- Class III: high solubility – low P_{eff}
- Class IV: low solubility – low P_{eff}.

A drug is considered as highly permeable when the extent of absorption is complete in humans – defined by the US FDA as being more than 90% – whereas EMEA requires "complete" absorption [17, 19]. This could be determined by any of the following study methods:

- absolute bioavailability in humans (in case of no first-pass metabolism);
- mass balance studies in humans using radiolabeled drug;
- determination of P_{eff} in humans by the "Loc-I-Gut method" and applying the correlation between P_{eff} and fraction absorbed presented in Fig. 21.10;
- determination of P_{eff} in any animal *in vivo* perfusion or *in vitro* permeation method that provides a solid correlation to the fraction dose absorbed in humans for a predefined set of drug substances. Special consideration must be given to indications of carrier-mediated transport across the intestinal membrane, in both the secretory and absorptive direction.

A compound can be classified as a high-solubility drug if the highest strength can be dissolved in 250 mL buffer at all pH values within the range of 1 to 8. This criterion is applied both by the European and US guidelines [17, 19].

The BCS is primarily used in this context to identify which substances are suitable for *in vitro* bioequivalence testing, which in the US is preceded by a request to the authority to gain a biowaiver, i.e., an acceptance for replacing an *in vivo* study with *in vitro* dissolution testing. It is presently only oral IR formulations of class I compounds, i.e., highly soluble/highly permeable drugs, for which such an option is available. Additional criteria for allowance of *in vitro* bioequivalence testing are that the drug stability in the gastrointestinal fluids must be verified, and it should also be a non-narrow therapeutic index drug. If these criteria are fulfilled, then the test and reference products can be compared by *in vitro* dissolution testing and deemed bioequivalent if sufficiently similar results are obtained. The *in vitro* dissolution testing should be carried out at three different pH values within the physiological range, typically pH 1, 4, and 6.8. The product dissolution must be complete (>85%) within 30 min in order to utilize the *in vitro* bioequivalence route. The underlying rationale for this demand on product performance is to ascertain that drug dissolution is fast enough so as not to become the rate-limiting step. It is assumed that gastric emptying will control the absorption rate for class I substances in products with such a rapid dissolution, and no effect on bioavailability will be obtained for different dissolution profiles, within acceptance limits. This has also been verified *in vivo* by studying metoprolol tablets with different *in vitro* release profiles [68].

The difference between a test (T) and a reference (R) product should be evaluated by use of the f_2-test (see Eq. (5)), where $f_2 > 50$ is the required limit for equivalence. This limit corresponds to an average difference in amount dissolved at different times (t) of less than 10%. If the dissolution is very rapid, i.e., complete dissolution within 15 min, the f_2-testing is not necessary.

$$f_2 = 50 \log \left[\left(1 + (1/n) \sum_{t=1}^{n} (R_t - T_t)^2 \right)^{-0.5} \times 100 \right] \tag{5}$$

In addition to the *in vitro* testing, the test and reference products must not contain excipients that could modify drug absorption in any way except for dissolution effects. For example, the potential for permeability-enhancing effects by surface active agents (which are sometimes included in solid formulations) has been identified as one potential concern. Furthermore, the effect on gastrointestinal transit by large amounts of sugars has been highlighted as another issue [18, 69].

21.6.1.2 **Potential Future Extensions**

One important limitation of the present application of BCS is that class I substances are quite rare in pharmaceutical development. For instance, the proportion of class I compounds in active development for oral IR formulations at AstraZeneca, a major research-based pharmaceutical company, was less than 10% in the year 2001. Thus, the usefulness of BCS for documentation of new chemical entities is limited. It has also been recognized that the present application represents a deliberately conservative approach, and proposals for extensions have been discussed since the original publication of the BCS. For example, in a recent report it was suggested that the requirement of highest pH for the solubility measurements could be changed from 7.5 to 6.8, as the latter value is more relevant for the pH in the stomach and upper small intestine [18]. This revision would thus somewhat relax the requirements for basic drugs. Another proposal in this report by Yu was to reduce the high-permeability definition from 90% to 85% fraction absorbed, based on observations that many drugs which are considered completely absorbed provide experimental values below 90%; that is, 90% seems to be too rigid a criterion considering the precision of the experimental methods. Other more radical relaxations of criteria, such as the inclusion of class II drugs, using simulated intestinal media with bile acids or increasing volumes and further reducing the pH interval in solubility measurements, would most likely require further research and analysis of past experiences.

Extensions of BCS beyond the oral IR area has also been suggested, for example to apply BCS in the extended-release area. However, this will provide a major challenge since the release from different formulations will interact in different ways with *in vitro* test conditions and the physiological milieu in the gastrointestinal tract. For example, the plasma concentration–time profile differed for two felodipine ER tablets for which very similar *in vitro* profiles had been obtained, despite the fact that both tablets were of the hydrophilic matrix type based on cellulose derivates [70]. This misleading result *in vitro* was due to interactions between the gel strength of the matrix and components in the dissolution test medium of no *in vivo* relevance. The situation for ER formulations would be further complicated by the need to predict potential food effects on the drug release *in vivo*.

Although the present use of BCS is limited, extensions of applications should clearly be made without jeopardizing the quality of products on the market. This would more likely be achieved within the area of oral IR than for ER formulations.

21.6.2 Drug Development Aspects

Although the BCS has primarily been developed for regulatory applications, it also has several other implications in the drug development process, and has gained wide recognition within the research-based industry. The importance of drug dissolution in the gastrointestinal tract and permeability over the gut wall in the oral absorption process has been well known since the 1960s, but more recent research which has been conducted to constitute the BCS has provided new quantitative data of importance for drug development, especially within the area of drug permeability. Another merit of the BCS in a development context is that it provides very clear and easily applied rules to determine rate-limiting factors in the drug absorption process. Thereby, BCS has implications in the selection of candidate drugs for full development, predictions and elucidations of food interactions, choice of formulation principle including suitability for oral ER administration, and the possibility for IVIVCs in the dissolution testing of solid formulations. Most of these aspects will be discussed and exemplified in further detail below.

21.6.2.1 Selection of Candidate Drugs

Permeability and solubility is of key importance in the selection of candidate drugs for development [2]. Molecules with too-low permeability and/or solubility will provide low and variable bioavailability, which increases the risk that a clinically useful product might not be developed. Experimental methods and relevant acceptance criteria regarding permeability and solubility are needed during the early drug discovery process. Such procedures have also been introduced into the industry, including solubility screens using turbidimetric measurements and automatic permeability screens based on the Caco-2 cell model. Computational approaches have also been developed for permeability and solubility determinations [66, 71, 72]. If further refinement can be achieved for such methods – leading to improved predictions – it might be possible in the future to displace cell-based permeability screens and early solubility estimates. It has even been suggested that BCS can be further developed towards consideration of true fundamental molecular properties for membrane permeability, as well as for drug solubility [82].

The selection of candidates that fulfill the BCS requirement of high permeability/high solubility (class I) almost guarantees the absence of failures due to poor absorption by the oral route. However, these limits are generally too conservative to use as acceptance criteria as many useful drugs can be found in classes II and III, and even class IV. First of all, whilst a class I drug is expected to provide complete absorption, a certain reduction in bioavailability due to permeability or solubility, as well as other reasons (e.g., first-pass metabolism), is generally acceptable. A summary of the different factors that must be taken into account when defining more relevant acceptance criteria include:

- acceptability of a low and highly variable bioavailability depending on:
  - medical need

  - width of the therapeutic window
  - potency
  - substance manufacturing costs
- potential for poor *in vivo* predictability of early permeability and solubility characterizations, due for example to:
  - active transport across the gut wall
  - high paracellular transport through gut wall
  - *in vivo* solubilization by bile salt micelles
- possibilities to use formulation approaches that improve bioavailability, e.g.:
  - dissolution and solubility enhancement
  - permeation enhancers

Thus, the BCS identifies some important variables in the screening of drug candidates, whereas the proposed limits are less useful as acceptance criteria in a drug discovery context.

21.6.2.2 **Choice of Formulation Principle**

Oral dosage forms are often developed under time constraints, and preferably by an efficient use of available resources. One way to reduce time and increase efficiency could be to minimize the number of different formulations included in the different stages of clinical development. The BCS could be used, as a framework to decide which types of formulation should be suitable for a certain compound.

If a drug is classified as having low solubility, it is clear that its bioavailability properties could be improved by the use of formulation principles that increase the dissolution rate and/or drug solubility. Several different principles of varying complexity exist to achieve such improvements, ranging from selecting a suitable solid-state form or salt to the use of technologically more advanced formulation principles. Although their application could be limited by several practical factors such as poor drug stability, excessive size due to the need for large amounts of excipients in relation to the dose, technical manufacturing problems and the high cost of goods, it is believed that many poorly soluble compounds with good pharmacological properties could be "saved" by such approaches. A list of different formulation principles for oral solid formulations including modifications of the drug substance form is given below:

- Substance form:
  - Salt: choose the most water-soluble form.
  - Crystal form: select the most soluble polymorph/anhydrate, if possible, from stability and technical points of view.
  - Amorphous form: provide the most rapid dissolution and the most often increased solubility by supersaturation; however, practical usefulness is limited by stability issues, including transformation of the solid state form.
  - Size reduction by milling/micronization: increase the surface area in contact with the dissolution medium.

- Formulation approaches for solids:
  - Addition of wetting agents
  - Solid solutions/eutectic mixtures
  - Cyclodextrin complexes
  - Lipid systems such as oils/emulsions/microemulsions/self-emulsifying systems in capsules
  - Nanoparticles

This list illustrates the numerous pharmaceutical possibilities available to handle bioavailability problems caused by low solubility. This is a continuously developing area exemplified by more recent developments, such as self-emulsifying lipid systems and nanoparticles.

The optimal formulation should provide such a good dissolution and/or solubility that this step is no longer the rate-limiting step in the absorption process, i.e., a situation comparable with the one for class I drugs. The most obvious approach to achieve this goal is to formulate the drug as a solution which is maintained even after mixing and diluting with gastric fluids. However, such formulations are generally not feasible to use as drug products, where solid formulations such as tablets and capsules are strongly preferred. Absorption properties similar to a solution may, however, be obtained for a solid formulation of poorly soluble drugs in case of successful application of dissolution-enhancing principles.

Another important decision in oral formulation development where the BCS could provide guidance is the start of an oral ER development. ER formulations could significantly improve the clinical usefulness of a drug substance by reducing the peak-to-trough ratio of drug levels in the body, and in turn the need for less frequent dosing. However, not all drugs that would benefit from ER delivery are suitable candidates due to unfavorable absorption properties. Solubility and permeability are crucial factors to consider before deciding to embark on an ER development program. The realization of desirable clinical advantages most often requires a duration of drug release of 12–24 h. Thus, since the typical transit time of formulations through the small intestine is 3–4 h, a significant part of the dose will be delivered to the colon and absorption of the drug over almost the entire gastrointestinal tract is a prerequisite. Class I drugs, which have both good solubility and good permeability, should therefore be the best candidates for ER development. Several well-documented ER formulations are also based on class I compounds (e.g., metoprolol), but class II drugs are also frequently used. For example, felodipine ER tablets provide an example where a low-solubility compound is included in a useful ER product. Felodipine, which has a water solubility in the physiological pH range of $\sim$1 μg mL^{-1}, has been administered as a once-daily product in doses up to at least 10 mg, without any reduced bioavailability compared with an oral solution [34]. Such a successful performance is indeed dependent on the use of a dissolution-enhancing formulation principle where the drug is given in a solubilized form.

A special consideration can be made regarding classification of low-solubility compounds in ER forms. The standard classification is based on the idea that the

drug should be completely dissolved in the gastric fluids, the volume of which has been estimated as 250 mL. However, this way of classifying drugs may be less relevant for ER formulations as only a very small part of the dose is made available for dissolution in the stomach. The dose is generally spread over the entire gastrointestinal tract, thereby making the effective water volume available as a dissolution medium for the drug probably greater than the 250 mL used in the original BCS. Furthermore, the drug permeability of these compounds is often much faster than the drug release, further preventing solubility limitations for class II drugs in ER formulations. Thus, this provides a further explanation of the relative frequent abundance of class II drugs developed as ER products; moreover, if the BCS is to be applied to ER formulations in future a different classification criterion regarding solubility might be needed. The permeability classification of a drug according to BCS, based on theoretical considerations, should be very useful as a criterion for selecting a drug as an ER formulation. Classification of a drug as a low-permeability compound means that the drug is not completely absorbed after oral administration of either a solution or an IR tablet. A certain amount of drug for such compounds is clearly delivered to the colon, and permeability in the colon is so poor that a significant part of the dose passes through the entire colon without being absorbed. This implies that permeability in the colon is very slow, thereby preventing any significant drug absorption. Using rat intestinal and colonic tissue in an Ussing chamber, it has also been shown *in vitro* that the permeability of class III–IV drugs is even slower in the colon than the small intestine, whereas class I–II drugs show a slightly higher permeability in the colon when passive diffusion is the dominating mechanism [46]. This permeability pattern has also been shown to be relevant for small and large intestinal specimens from humans when the Ussing chamber model [73] is applied. Consequently, it will not be possible to control the rate of absorption by an ER formulation for low-permeability drugs. In addition, a large part of the dose will not be absorbed, leading to a low and uneven variability. This is exemplified in ER tablets of amoxicillin; this high-solubility drug is classified as a low P_{eff}, even if it is transported across the intestinal barrier via the oligopeptide carrier (PepT1) [56]. Essentially no absorption occurred from an ER tablet when it entered the colon, as determined by gamma scintigraphy [74].

21.6.2.3 **IVIVC**

In vitro dissolution testing is an important tool in the development of solid drug products, as well as in batch quality controls. The aim of the test is to see that the drug is appropriately dissolved in the gastrointestinal tract and made available for absorption. It is therefore highly desirable that the *in vitro* tests provide data that correlate to the *in vivo* situation. However, attainment of IVIVC has often failed- and the concept of IVIVC has been challenged.

The BCS could be used as a framework for predictions when IVIVC could be expected for solid IR products, as summarized in Table 21.5. It is important to realize that the *in vitro* dissolution test only models the release and dissolution of the active drug substance from the formulation, and it is only when these processes are rate-limiting in the absorption process that IVIVC can be expected. In

Tab. 21.5. Expectations for *in vitro–in vivo* correlations (IVIVC) for immediate release (IR) products based on BCS.

Class	*IVIVC expectations*
I High solubility/High P_{eff}	No IVIVC until product dissolution becomes slower than gastric emptying
II Low solubility/High P_{eff}	IVIVC should be possible to establish provided that *in vitro* relevant dissolution test method are used and drug absorption is limited by dissolution rate rather than saturation solubility
III High solubility/Low P_{eff}	No IVIVC until product dissolution becomes slower than intestinal permeability
IV Low solubility/Low P_{eff}	Low chance for IVIVC

the case of class I drugs, the complete dose will be dissolved already in the stomach and, provided that the absorption over the gut wall is negligible, the gastric emptying of the dissolved drug will be the rate-limiting step. This is clearly not a factor that is included in the *in vitro* dissolution test. Thus, no IVIVC should be expected for class I drugs as long as the release of drug is faster than gastric emptying. The half-life of gastric emptying of fluids in the fasting state is normally ~10 min, although this could vary due to several factors such as the timing of drug administration in relation to gastric motility phase, and also fluid volume [75]. The relationship between *in vitro* dissolution, described as the time to dissolve half of the dose ($t_{50\%}$), and the peak plasma concentration (C_{max}) for a fictive class I drug is exemplified in Fig. 21.12. This type of *in vitro/in vivo* relationship should only be expected for variables that are influenced by the absorption rate, whereas variables reflecting the extent of bioavailability, e.g., AUC, should be independent of dissolution rate.

Class II drugs, i.e., low-solubility/high-permeability compounds, are expected to have a dissolution-limited absorption. Thus, for these types of drugs an IVIVC

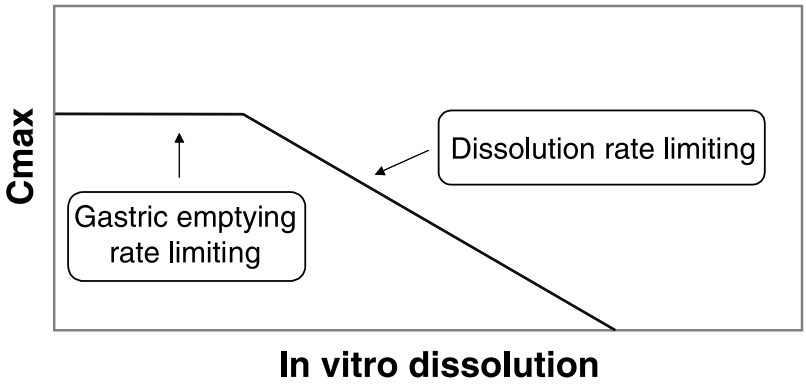

Fig. 21.12. Principal level C *in vitro/in vivo* correlation for immediate-release (IR) formulation of class I substance.

should be possible to establish by use of a well-designed *in vitro* dissolution test. One way to investigate and establish such a correlation is to study formulations containing drug particles with different surface areas. An example of such a study is given in Fig. 21.13, where profiles of *in vitro* dissolution (Fig. 21.13(a)) and

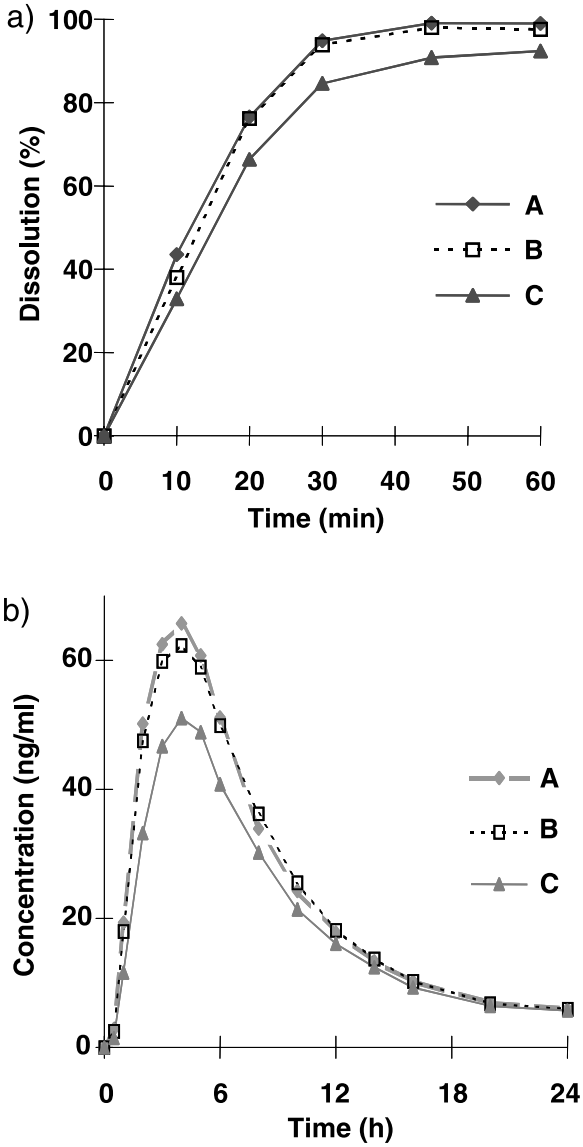

Fig. 21.13. (a) Mean *in vitro* dissolution and (b) human plasma concentrations of candersartan cilexitil tablets containing drug particles with three different mean particle diameters (A, 3.9 μm; B, 5.7 μm; C, 9.1 μm).

plasma concentration–time (Fig. 21.13(b)) are given for administration of tablets containing drug substance with two different mean particle sizes. The mean reduction of about 30% in C_{max} for the larger particles was predicted in this case by a somewhat slower dissolution *in vitro*.

Two cases could be identified for class II drugs when the establishment of simple IVIVCs were not feasible. First, there are a number of formulation principles that could enhance the dissolution rate and solubility of low-solubility compounds, as discussed above. It might be possible to achieve such a rapid and complete dissolution of a class II drug that the gastric emptying becomes the rate-limiting step, i.e., the bioavailability of the solid dosage forms equals that of an oral solution. Thus, in such a case the prerequisites for IVIVC would be identical to the situation for class I drugs, i.e., no correlation would be obtained as long as the dissolution rate was significantly faster than the gastric emptying.

The second situation when IVIVC is not likely for class II drugs is where the absorption is limited by the saturation solubility in the gastrointestinal tract rather than the dissolution rate, as discussed in more detail above. In this situation, the drug concentration in the gastrointestinal tract will be close to the saturation solubility, and changes of the dissolution rate will not affect the plasma concentration–time profile and *in vivo* bioavailability. Standard *in vitro* dissolution tests are carried out under "sink conditions", i.e., at concentrations well below the saturation solubility. Thus, only effects related to dissolution rate can be predicted *in vitro*. If more physiologically relevant dissolution media are used, which do not necessarily provide "sink conditions", the possibility for IVIVC could be improved, as has been indicated by the results of recent studies using simulated intestinal medium [76].

The absorption of class III drugs is limited by their permeability over the intestinal wall. Thus, as this process is not at all modeled by the classical *in vitro* dissolution test, no IVIVC should be expected. When drug dissolution becomes slower than gastric emptying, a reduction in the extent of bioavailability will be found in slower dissolution rates as the time when the drug is available for permeation over the gut wall in the small intestine will then be reduced. Thus, the same type of relationship can be expected between bioavailability and *in vitro* dissolution, as shown in Fig. 21.12 for a class I drug.

21.6.2.4 **Food–Drug Interactions**

Alterations of bioavailability due to concomitant food intake can have serious implications for the clinical usefulness of a drug, and it is therefore beneficial to predict such effects at an early stage. However, this is not easily done due to the multitude of factors involved in food–drug interactions, including: physicochemical effects such as increased solubility; binding to secretory or food components; physiological effects in the gastrointestinal tract such as altered flow rates and gastric emptying; mechanical effects on formulations due to different motility patterns; permeability effects due to interactions with active transporters or effects on the membrane; and altered first-pass metabolism. A more extensive review of different mechanisms for food–drug interactions in the absorption step (including formulation factors) can be found elsewhere [77].

Tab. 21.6. Potential food effects on drug absorption for BCS class I–III drugs.

BCS Class	*Absorption effect by food*	*Mechanism*
I	Reduced rate but same extent	Slower gastric emptying
II (bases)	Reduced rate and possibly extent	Decreased solubility due to increased pH in the stomach
II (acids)	Increased rate and possibly extent	Increased solubility due to increased pH in the stomach
II	Increased extent and possibly rate	Large fluid volume in stomach. Solubilization in mixed micelles and dietary lipids
III	Generally no effect	–

The BCS can be used as a framework for predictions and to set up hypotheses for mechanisms of food effects related to permeability, solubility and gastric emptying as outlined in Table 21.6. The most severe cases of food interactions due to factors considered in BCS are generally found in the group of poorly soluble compounds given in high doses, i.e., those that approach the saturation solubility in the gastrointestinal tract. For such compounds (e.g., griseofulvin), bioavailability has been reported to be increased up to five-fold by the presence food, and dosing recommendations requiring concomitant intake of the drug with a meal are often used in these cases [27]. The saturation solubility will be significantly improved by food due to solubilization in mixed micelles, including bile acids, lecithin and monoglycerides obtained from the dietary fat intake, and dissolution into emulsified nutritional lipids. In this way, the amount of drug available for absorption will be significantly increased. A further contributing effect to an increased bioavailability might be the increased fluid volume in the stomach after a meal, i.e., allowing an increased amount of drug that could be dissolved compared with the fasting situation. Protolytic drugs with a pK_a within the physiological pH range will also be affected by food-mediated pH changes in the stomach. A protein-rich meal could increase the pH from the fasting level of pH 1–2 to close to neutral (pH 7). Basic drugs, which are often freely dissolved in the acidic stomach, could thereby experience a reduced bioavailability with food, whereas the reverse situation might apply for low-solubility acids.

For highly permeable, poorly soluble drugs given in lower doses, the dissolution rate rather than the saturation solubility is the limiting factor. An increase in dissolution rate due to *in vivo* solubilization mediated by food intake could theoretically be obtained, but this situation is not always found *in vivo*. For example, food does not affect the rate and extent of bioavailability for candesartan cilexitil, a very poorly soluble compound [78]. An *in vitro* dissolution and solubility study of this compound in simulated intestinal media provided a potential explanation; it was revealed that the solubility was increased as a function of bile concentration as expected, whereas the dissolution rate was not increased by the higher bile concentrations being representative for the fed state (see Fig. 21.14). Thus, although

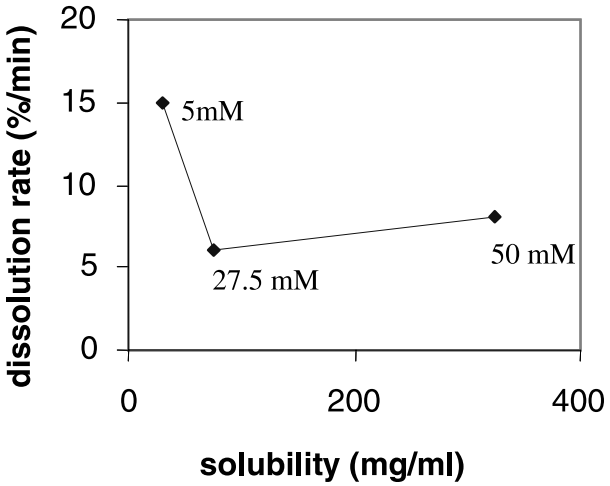

Fig. 21.14. *In vitro* dissolution rate versus saturation solubility for candersartan cilexitil in different concentrations of sodium taurocholate:lecithin ratio 2.5:1.

intestinal solubility most often will be increased in the fed state for class II drugs, this will not always lead to a more rapid dissolution.

For class I drugs, a slower rate of absorption could be expected after concomitant intake with food due to the decreased gastric emptying rate induced by a meal. Gastric emptying in the fed state varies significantly depending on the meal composition, including factors such as energy content, osmolality, and pH. A gastric emptying half-life of ~45 min has been reported for fluids when measured under nonfasting conditions [79]. In addition to the meal composition, the extent of reduction and delay in peak plasma concentration induced by food for a class I drug will also be influenced by the plasma concentration half-life, i.e., food effects will be more pronounced for drugs with a shorter half-life.

Class III drugs will generally be less susceptible to both gastric-emptying effects as a result of the slow permeability as well as solubility effects due to the high solubility already under fasting conditions. This type of drug is perhaps the one least sensitive to food intake; this was shown in a recent study where the bioavailability of a class III compound was almost identical after either fasting or nonfasting administration [80].

A potential source of interactions between food components and low-permeability drugs might occur in the case of drugs that are actively transported in the intestine, especially if nutritional carriers are involved. The two most important nutrient absorption carriers for drugs are the oligopeptide carrier (hPepT1) and the amino acid transport family. These carrier proteins have a high transport capacity in the human small intestine, and they seem less likely to be involved in direct food–drug interactions, unless high doses are given together with a protein-rich meal. The nutritional status could also cause transcriptional activation of the

PepT1 gene by selective amino acids and dipeptides in the diet [81]. It has also been reported that the integrated response to certain stimuli may increase PepT1 activity by translocation from a preformed cytoplasm pool [52].

21.7 Conclusion

In this chapter we have discussed and emphasized the importance of the fundamental factors in BCS, solubility and intestinal permeability for oral drug absorption. The main regulatory impact today is the use of BCS as a framework for identifying drugs for which *in vitro* dissolution testing could replace *in vivo* studies to determine bioequivalence. Extensions of this approach to cases other than IR formulations of the rather rare class I drugs would significantly enhance the impact of BCS [18]. However, product quality assurance must not be jeopardized, and a brief discussion illustrated the possible difficulties involved if BCS were extended, for example, to oral ER products. Finally, we emphasize the wide use of BCS as a simple tool in early drug development to determine the rate-limiting step in the oral absorption process.

Disclaimer

The information contained in this chapter represents the personal opinions of the authors, and does not necessarily represent the views or politics of AstraZeneca.

References

1 Venkatesh, S., Lipper, R. A., Role of the development scientist in compound lead selection and optimization, *J. Pharm. Sci.* **2000**, *89*, 145–154.

2 Van de Waterbeemd, H., Smith, D. A., Beaumont, K., Walker, D. K., Property-based design: optimization of drug absorption and pharmacokinetics, *J. Med. Chem.* **2001**, *44*, 1313–1333.

3 Prentis, R. A., Lis, Y., Walker, S. R., Pharmaceutical innovation by the seven UK-owned pharmaceutical companies (1964–1985), *Br. J. Clin. Pharmacol.* **1988**, *25*, 387–396.

4 Amidon, G. L., Lennernas, H., Shah, V. P., Crison, J. R., A theoretical basis for a biopharmaceutic drug classification: the correlation of in vitro drug product dissolution and in vivo bioavailability, *Pharm. Res.* **1995**, *12*, 413–420.

5 Lennernas, H., Human intestinal permeability, *J. Pharm. Sci.* **1998**, *87*, 403–410.

6 Benet, L. Z., Wu, C. Y., Hebert, M. F., Wacher, V. J., Intestinal drug metabolism and antitransport processes: potential paradigm shift in oral drug delivery, *J. Controlled Release* **1996**, *39*, 139–143.

7 Chu, X. Y., Sanchez-Castano, G. P., Higaki, K., Oh, D. M., Hsu, C. P. *et al.*, Correlation between epithelial cell permeability of cephalexin and expression of intestinal oligopeptide transporter, *J. Pharmacol. Exp. Ther.* **2001**, *299*, 575–582.

8 Jonker, J. W., Smit, J. W., Brinkhuis, R. F., Maliepaard, M.,

Beijnen, J. H. *et al.*, Role of breast cancer resistance protein in the bioavailability and fetal penetration of topotecan, *J. Natl. Cancer Inst.* **2000**, *92*, 1651–1656.

9 Greiner, B., Eichelbaum, M., Fritz, P., Kreichgauer, H. P., von Richter, O. *et al.*, The role of intestinal P-glycoprotein in the interaction of digoxin and rifampin, *J. Clin. Invest.* **1999**, *104*, 147–153.

10 Fricker, G., Miller, D. S., Relevance of multidrug resistance proteins for intestinal drug absorption in vitro and in vivo, *Pharmacol. Toxicol.* **2002**, *90*, 5–13.

11 Sandstrom, R., Karlsson, A., Knutson, L., Lennernas, H., Jejunal absorption and metabolism of R/S-verapamil in humans, *Pharm. Res.* **1998**, *15*, 856–862.

12 Lindahl, A., Sandstrom, R., Ungell, A. L., Abrahamsson, B., Knutson, T. W. *et al.*, Jejunal permeability and hepatic extraction of fluvastatin in humans, *Clin. Pharmacol. Ther.* **1996**, *60*, 493–503.

13 Chiou, W. L., Chung, S. M., Wu, T. C., Ma, C., A comprehensive account on the role of efflux transporters in the gastrointestinal absorption of 13 commonly used substrate drugs in humans, *Int. J. Clin. Pharmacol. Ther.* **2001**, *39*, 93–101.

14 Lipinski, C. A., Lombardo, F., Dominy, B. W., Feeney, P. J., Experimental and computational approaches to estimate solubility and permeability in drug discovery and development settings, *Adv. Drug Deliv. Rev.* **2001**, *46*, 3–26.

15 Mandagere, A. K., Thompson, T. N., Hwang, K. K., Graphical model for estimating oral bioavailability of drugs in humans and other species from their Caco-2 permeability and in vitro liver enzyme metabolic stability rates, *J. Med. Chem.* **2002**, *45*, 304–311.

16 Winiwarter, S., Bonham, N. M., Ax, F., Hallberg, A., Lennernas, H. *et al.*, Correlation of human jejunal permeability (in vivo) of drugs with experimentally and theoretically derived parameters. A multivariate data analysis approach, *J. Med. Chem.* **1998**, *41*, 4939–4949.

17 CDER Waiver of in vivo bioavailability and bioequivalence studies for immediate-release solid oral dosage forms based on a biopharmaceutics classification system; Food and Drug Administration, **2000**.

18 Yu, L. X., Amidon, G. L., Polli, J. E., Zhao, H., Mehta, M. U. *et al.*, Biopharmaceutics classification system: the scientific basis for biowaiver extensions, *Pharm. Res.* **2002**, *19*, 921–925.

19 CPMP Note for Guidance on the Investigation of Bioavailability and bioequivalence (CPMP/EWP/QWP/1401/98); The European Agency for the Evaluation of Medicinal Products, **2001**.

20 Lennernas, H., Human jejunal effective permeability and its correlation with preclinical drug absorption models, *J. Pharm. Pharmacol.* **1997**, *49*, 627–638.

21 Nernst, W., Brunner, E., Theorie der Reaktionsgeschwindigkeit in heterogenen Systemen, *Z. Phys. Chem.* **1904**, *47*, 52–110.

22 Dressman, J. B., Amidon, G. L., Reppas, C., Shah, V. P., Dissolution testing as a prognostic tool for oral drug absorption: immediate release dosage forms, *Pharm. Res.* **1998**, *15*, 11–22.

23 Nicklasson, M., Brodin, A., Sundelof, L.-O., Studies of some characteristics of molecular dissolution kinetics from rotating discs, *Int. J. Pharm.* **1985**, *23*, 97–108.

24 Hernell, O., Staggers, J. E., Carey, M. C., Physical-chemical behavior of dietary and biliary lipids during intestinal digestion and absorption. 2. Phase analysis and aggregation states of luminal lipids during duodenal fat digestion in healthy adult human beings, *Biochemistry* **1990**, *29*, 2041–2056.

25 Lindahl, A., Ungell, A. L., Knutson, L., Lennernas, H., Characterization of fluids from the stomach and proximal jejunum in men and women, *Pharm. Res.* **1997**, *14*, 497–502.

26 Scholz, A., Abrahamsson, B., Diebold, S. M., Kostewicz, E., Polentarutti, B. I. *et al.*, Influence of hydrodynamics and particle size on the absorption of felodipine in labradors, *Pharm. Res.* **2002**, *19*, 42–46.

27 Charman, W. N., Porter, C. J., Mithani, S., Dressman, J. B., Physiochemical and physiological mechanisms for the effects of food on drug absorption: the role of lipids and pH, *J. Pharm. Sci.* **1997**, *86*, 269–282.

28 Mithani, S. D., Bakatselou, V., TenHoor, C. N., Dressman, J. B., Estimation of the increase in solubility of drugs as a function of bile salt concentration, *Pharm. Res.* **1996**, *13*, 163–167.

29 Jack, D. B., *Handbook of Clinical Pharmacokinetic Data*. Macmillan Publishers Ltd, Basingstoke, **1992**.

30 Bonlokke, L., Christensen, F. N., Knutson, L., Kristensen, H. G., Lennernas, H. A., A new approach for direct in vivo dissolution studies of poorly soluble drugs, *Pharm. Res.* **1997**, *14*, 1490–1492.

31 Bonlokke, L., Hovgaard, L., Kristensen, H. G., Knutson, L., Lennernas, H., Direct estimation of the in vivo dissolution of spironolactone, in two particle size ranges, using the single-pass perfusion technique (Loc-I-Gut) in humans, *Eur. J. Pharm. Sci.* **2001**, *12*, 239–250.

32 Horter, D., Dressman, J. B., Influence of physicochemical properties on dissolution of drugs in the gastrointestinal tract, *Adv. Drug Deliv. Rev.* **1997**, *25*, 3–14.

33 Kaplan, S. A., Biopharmaceutical considerations in drug formulation and design and evaluation, *Drug Metab. Rev.* **1972**, *1*, 15–34.

34 Wingstrand, K., Abrahamsson, B., Edgar, B., Bioavailability from felodipine extended-release tablets with different dissolution properties, *Int. J. Pharm.* **1990**, *60*, 151–156.

35 Agoram, B., Woltosz, W. S., Bolger, M. B., Predicting the impact of physiological and biochemical processes on oral drug bioavailability, *Adv. Drug Deliv. Rev.* **2001**, *50 (Suppl. 1)*, S41–S67.

36 Csáky, T. Z., Methods for investigation of intestinal permeability, in: *Pharmacology of Intestinal Permeability I*. Springer-Verlag, Berlin, **1984**, pp. 91–112.

37 Engman, H. A., Lennernas, H., Taipalensuu, J., Otter, C., Leidvik, B. *et al.*, CYP3A4, CYP3A5, and MDR1 in human small and large intestinal cell lines suitable for drug transport studies, *J. Pharm. Sci.* **2001**, *90*, 1736–1751.

38 Lande, M. B., Priver, N. A., Zeidel, M. L., Determinants of apical membrane permeabilities of barrier epithelia, *Am. J. Physiol.* **1994**, *267*, C367–C374.

39 Lande, M. B., Donovan, J. M., Zeidel, M. L., The relationship between membrane fluidity and permeabilities to water, solutes, ammonia, and protons, *J. Gen. Physiol.* **1995**, *106*, 67–84.

40 Fagerholm, U., Johansson, M., Lennernas, H., Comparison between permeability coefficients in rat and human jejunum, *Pharm. Res.* **1996**, *13*, 1336–1342.

41 Lennernas, H., Ahrenstedt, O., Hallgren, R., Knutson, L., Ryde, M. *et al.*, Regional jejunal perfusion, a new in vivo approach to study oral drug absorption in man, *Pharm. Res.* **1992**, *9*, 1243–1251.

42 Lennernas, H., Palm, K., Fagerholm, U., Artursson, P., Comparison between active and passive drug transport in human intestinal epithelial (Caco-2) cells in vitro and human jejunum in vivo, *Int. J. Pharm.* **1996**, *127*, 103–107.

43 Lennernas, H., Nylander, S., Ungell, A. L., Jejunal permeability: a comparison between the Ussing chamber technique and the single-pass perfusion in humans, *Pharm. Res.* **1997**, *14*, 667–671.

44 Palm, K., Stenberg, P., Luthman, K., Artursson, P., Polar molecular surface properties predict the intestinal absorption of drugs in humans, *Pharm. Res.* **1997**, *14*, 568–571.

45 CDER Guidance for Industry. SUPAC-IR: Immediate-Release Solid Oral Dosage Forms: Scale-Up and Post-Approval Changes: Chemistry, Manufacturing and Controls, In Vitro Dissolution Testing, and In Vivo Bioequivalence Documentation; US Food and Drug Administration, **1995**.

46 Ungell, A. L., Nylander, S., Bergstrand, S., Sjoberg, A., Lennernas, H., Membrane transport of drugs in different regions of the intestinal tract of the rat, *J. Pharm. Sci.* **1998**, *87*, 360–366.

47 Artursson, P., Epithelial transport of drugs in cell culture. I: A model for studying the passive diffusion of drugs over intestinal absorptive (Caco-2) cells, *J. Pharm. Sci.* **1990**, *79*, 476–482.

48 Sun, D., Lennernas, H., Welage, L. S., Barnett, J., Landowaki, C. P. *et al.*, A comparison of human and Caco 2 gene expression profiles for 12,000 genes and the permeabilities of 26 drugs in the human intestine and Caco 2 cells, *Pharm. Res.* **2002**, *19*, 1398–1413.

49 Knutson, L., Odlind, B., Hallgren, R., A new technique for segmental jejunal perfusion in man, *Am. J. Gastroenterol.* **1989**, *84*, 1278–1284.

50 Lennernas, H., Lee, I. D., Fagerholm, U., Amidon, G. L., A residence-time distribution analysis of the hydrodynamics within the intestine in man during a regional single-pass perfusion with Loc-I-Gut: in-vivo permeability estimation, *J. Pharm. Pharmacol.* **1997**, *49*, 682–686.

51 Steffansen, B., Lepist, E. I., Taub, M. E., Larsen, B. D., Frokjaer, S. *et al.*, Stability, metabolism and transport of D-Asp(OBzl)-Ala – a model prodrug with affinity for the oligopeptide transporter, *Eur. J. Pharm. Sci.* **1999**, *8*, 67–73.

52 Thamotharan, M., Bawani, S. Z., Zhou, X., Adibi, S. A., Hormonal regulation of oligopeptide transporter pept-1 in a human intestinal cell line, *Am. J. Physiol.* **1999**, *276*, C821–C826.

53 Amidon, G. L., Sinko, P. J., Fleisher, D., Estimating human oral fraction dose absorbed: a correlation using rat intestinal membrane permeability for passive and carrier-mediated compounds, *Pharm. Res.* **1988**, *5*, 651–654.

54 Sinko, P. J., Leesman, G. D., Amidon, G. L., Predicting fraction dose absorbed in humans using a macroscopic mass balance approach, *Pharm. Res.* **1991**, *8*, 979–988.

55 Oh, D. M., Sinko, P. J., Amidon, G. L., Characterization of the oral absorption of some beta-lactams: effect of the alpha-amino side chain group, *J. Pharm. Sci.* **1993**, *82*, 897–900.

56 Lennernas, H., Knutson, L., Knutson, T., Hussain, A., Lesko, L. *et al.*, The effect of amiloride on the in vivo effective permeability of amoxicillin in human jejunum: experience from a regional perfusion technique, *Eur. J. Pharm. Sci.* **2002**, *15*, 271–277.

57 Pilbrant, A., Cederberg, C., Development of an oral formulation of omeprazole, *Scand. J. Gastroenterol. Suppl.* **1985**, *108*, 113–120.

58 Inoue, M., Morikawa, M., Tsuboi, M., Sugiura, M., Species difference and characterization of intestinal esterase on the hydrolyzing activity of ester-type drugs, *Jpn. J. Pharmacol.* **1979**, *29*, 9–16.

59 Inoue, M., Morikawa, M., Tsuboi, M., Ito, Y., Sugiura, M., Comparative study of human intestinal and hepatic esterases as related to enzymatic properties and hydrolyzing activity for ester-type drugs, *Jpn. J. Pharmacol.* **1980**, *30*, 529–535.

60 Yoshigae, Y., Imai, T., Horita, A., Matsukane, H., Otagiri, M., Species differences in stereoselective hydrolase activity in intestinal mucosa, *Pharm. Res.* **1998**, *15*, 626–631.

61 Faigle, J. W., Drug metabolism in the colon wall and lumen, in: *Colonic Drug Absorption and Metabolism.* Marcel Dekker Inc., Tübingen, **1993**, pp. 29–54.

62 Goldin, B. R., Intestinal microflora: metabolism of drugs and carcinogens, *Ann. Med.* **1990**, *22*, 43–48.

63 Scheline, R. R., Metabolism of foreign compounds by gastrointestinal

microorganisms, *Pharmacol. Rev.* **1973**, *25*, 451–532.

64 Basit, A. W., Lacey, L. F., Colonic metabolism of ranitidine: implications for its delivery and absorption, *Int. J. Pharm.* **2001**, *227*, 157–165.

65 Sjostrom, M., Lindfors, L., Ungell, A. L., Inhibition of binding of an enzymatically stable thrombin inhibitor to lumenal proteases as an additional mechanism of intestinal absorption enhancement, *Pharm. Res.* **1999**, *16*, 74–79.

66 Bergstrom, C. A., Norinder, U., Luthman, K., Artursson, P., Experimental and computational screening models for prediction of aqueous drug solubility, *Pharm. Res.* **2002**, *19*, 182–188.

67 ICH Topic Q6A, Step 4 Note for Guidance Specifications: Test procedures and Acceptance Criteria for New Drug Substances and New Drug Products: Chemical Substances (CPMP/ICH/367/96 – Adopted Nov. 99); The European Agency for the Evaluation of Medicinal Products, **1999**.

68 Rekhi, G. S., Eddington, N. D., Fossler, M. J., Schwartz, P., Lesko, L. J. *et al.*, Evaluation of in vitro release rate and in vivo absorption characteristics of four metoprolol tartrate immediate-release tablet formulations, *Pharm. Dev. Technol.* **1997**, *2*, 11–24.

69 Adkin, D. A., Davis, S. S., Sparrow, R. A., Huckle, P. D., Phillips, A. J. *et al.*, The effects of pharmaceutical excipients on small intestinal transit, *Br. J. Clin. Pharmacol.* **1995**, *39*, 381–387.

70 Abrahamsson, B., Johansson, D., Torstensson, A., Wingstrand, K., Evaluation of solubilizers in the drug release testing of hydrophilic matrix extended-release tablets of felodipine, *Pharm. Res.* **1994**, *11*, 1093–1097.

71 Stenberg, P., Norinder, U., Luthman, K., Artursson, P., Experimental and computational screening models for the prediction of intestinal drug absorption, *J. Med. Chem.* **2001**, *44*, 1927–1937.

72 Yang, G., Ran, Y., Yalkowsky, S. H., Prediction of the aqueous solubility: comparison of the general solubility equation and the method using an amended solvation energy relationship, *J. Pharm. Sci.* **2002**, *91*, 517–533.

73 Berggren, S., Lennernas, P., Ekelund, M., Westrom, B., Hoogstraate, J. *et al.*, Regional difference in permeability and metabolism of ropivacaine and its CYP 3A4 metabolite PPX in human intestine, *Drug Metab. Dispos.* **2002** (in press).

74 Gottfries, J., Svenheden, A., Alpsten, M., Bake, B., Larsson, A. *et al.*, Gastrointestinal transit of amoxicillin modified-release tablets and a placebo tablet including pharmacokinetic assessments of amoxicillin, *Scand. J. Gastroenterol.* **1996**, *31*, 49–53.

75 Oberle, R. L., Chen, T. S., Lloyd, C., Barnett, J. L., Owyang, C. *et al.*, The influence of the interdigestive migrating myoelectric complex on the gastric emptying of liquids, *Gastroenterology* **1990**, *99*, 1275–1282.

76 Kostewicz, E. S., Brauns, U., Becker, R., Dressman, J. B., Forecasting the oral absorption behavior of poorly soluble weak bases using solubility and dissolution studies in biorelevant media, *Pharm. Res.* **2002**, *19*, 345–349.

77 Fleisher, D., Li, C., Zhou, Y., Pao, L. H., Karim, A., Drug, meal and formulation interactions influencing drug absorption after oral administration. Clinical implications, *Clin. Pharmacokinet.* **1999**, *36*, 233–254.

78 Gleiter, C. H., Morike, K. E., Clinical pharmacokinetics of candesartan, *Clin. Pharmacokinet.* **2002**, *41*, 7–17.

79 Ziessman, H. A., Fahey, F. H., Collen, M. J., Biphasic solid and liquid gastric emptying in normal controls and diabetics using continuous acquisition in LAO view, *Dig. Dis. Sci.* **1992**, *37*, 744–750.

80 Eriksson, B. I., Arfwidsson, A. C., Frison, L., Eriksson, U. G., Bylock, A. *et al.*, A dose-ranging study of the oral direct thrombin inhibitor,

ximelagatran, and its subcutaneous form, melagatran, compared with dalteparin in the prophylaxis of thromboembolism after hip or knee replacement: METHRO I. MElagatran for THRombin inhibition in Orthopaedic surgery, *Thromb. Haemost.* **2002**, *87*, 231–237.

81 Shiraga, T., Miyamoto, K., Tanaka, H., Yamamoto, H., Taketani, Y. *et al.*, Cellular and molecular mechanisms of dietary regulation on rat intestinal H+/Peptide transporter PepT1, *Gastroenterology* **1999**, *116*, 354–362.

82 Waterbeemd, H. van de, The fundamental variables of the biopharmaceutic classification system (BCS): a commentary, *Eur. J. Pharm. Sci.* **1998**, *7*, 1–3.

22
Prodrugs

Bente Steffansen, Anne Engelbrecht Thomsen, and Sven Frokjaer

Abbreviations

TRH	Thyrotropin-releasing hormone
DADLE	H-Tyr-D-Ala-Gly-Phe-D-Leu-OH
[Leu^5]-enkephalin	H-Tyr-Gly-Gly-Phe-Leu-OH
hPepT1	Human peptide transporter 1
PepT1	Peptide transporter 1
ACE-inhibitor	Angiotensin-converting enzyme inhibitor
Valaciclovir	L-Valyl-aciclovir
Valganciclovir	L-Valyl-ganciclovir
Caco-2	Colon adenocarcinoma epithelial cell line
SKPT	Rat renal proximal tubular epithelial cell line
THF	Tetrahydrofuranyl
VACVase	Valacyclovir hydrolase

22.1
Introduction

Prodrugs are compounds that undergo chemical transformation within the body prior to eliciting their therapeutic action [1]. The prodrug approach may be applied for various reasons, but in this chapter the focus is on the use of prodrugs to increase drug bioavailability and drug targeting after oral administration. Consequently, the prodrug strategy is chemically to attach pro-moieties to pharmacophores, to form prodrugs that ideally should overcome the biochemical and physical barriers against drug transport that are located in the small intestine (Fig. 22.1). Following administration, and either during or after transport across the intestinal membrane, the prodrugs should release the parent compounds either into the blood circulation or/and at their site of action [2, 3]. Clearly, the prodrug approach is a multidisciplinary drug delivery strategy that includes advanced chemical, physiological, biochemical, and biopharmaceutical insight, and so it is likely that many different areas of research should be involved. At present, several success-

Drug Bioavailability: Estimation of Solubility, Permeability, Absorption and Bioavailability.
Edited by Han van de Waterbeemd, Hans Lennernäs and Per Artursson

ISBN: 3-527-30438-X

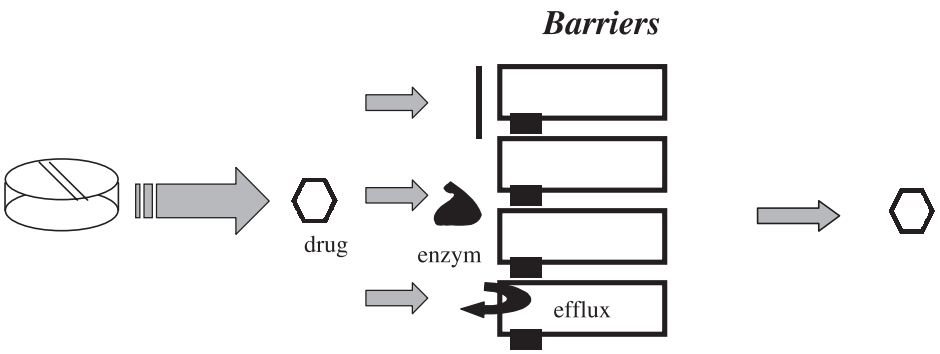

Fig. 22.1. Barriers to drug absorption.

ful marketed drugs are based on prodrug formulations, and the approach may indeed be considered as a well-established strategy to improve the bioavailability and targeting of pharmacophores with poor drug-delivery properties. Examples of prodrugs that are currently available on the European market are shown in Table 22.1.

22.2 Prodrug Design

In order to produce a successful drug, it is of major importance that the basic delivery properties of a selected pharmacophore are investigated at an early stage of its development. Indeed, it is at this point that a decision must be made as to whether any drug delivery strategy, including the prodrug approach, should be employed during the development phase of any lead compounds. The pioneering studies of Bundgaard *et al.* [4] were fundamental in the applied prodrug chemistry, these authors having designed prodrugs based on registered drug molecules, pharmacophores, or model drugs by chemical attachment to the parent molecules of a variety of pro-moieties to functional groups such as carboxyl, hydroxyl, amine, imine, NH-acidic, phosphate, and CH-acidic. The compounds were characterized by investigating drug release in aqueous and various biological media by profound stability studies [4]. For the interested reader, this topic has been excellently reviewed (see Refs. [2, 5, 6]).

Limited oral drug bioavailability may be explained by poor membrane permeability, low aqueous solubility in gastrointestinal fluids, or extensive first-pass metabolism in the gastrointestinal tract or liver. Successful lipophilic prodrugs

Tab. 22.1. Various prodrugs on the European market.

Prodrug	*Drug*
Amifostine	The corresponding dephosphorylated compound
Azathioprine	6-Mecaptopurine
Balsalazide	Mesalazine
Bambuterol	Terbutaline
Benazepril	Benazeprilat
Bisacodyl	Bis-(*p*-hydroxyphenyl)-pyridyl-2-methane (BHPH)
Candesartan cilexetil	Candesartan
Carbimazole	Metiamazole
Cefuroxime axetil	Cefuroxime
Cis(Z)-flupenthixol decanoate	Cis(Z)-flupenthixol
Clopidogrel	The corresponding thiol derivative
Colistin	Polymyxin E
Dipivefrine	Epinephrine
Disulfiram	Diethylthiocarbaminsyre-methylester
Erythromycinethyl succinate	Erythromycin
Enalapril	Enalaprilat
Esomeprazole	The corresponding sulfenamide
Famciclovir	Penciclovir
Fluphenazine decanoate	Fluphenazine
Fosinopril	Fosinoprilat
Fosphenytoin	Phenytoin
Haloperidol decanoate	Haloperidol
Lansoprazole	The corresponding sulfenamide
Latanoprost	The corresponding acid
Lovastatin (lactone)	Corresponding β-hydroxycarboxylic acid
Lymecycline	Tetracycline
Metronidazole benzoate	Metronidazole
Mycophenolate mofetil	Mycophenolatic acid (MPA)
Nabumetone	6-Methoxy-2-naphthylacetic acid
Olsalazine	Mesalazine
Omeprazole	The corresponding sulfenamide
Oxcarbazepine	10-Hydroxy-carbazepine (MHD)
Pantoprazole	The corresponding sulfenamide
Parecoxib	Valdecoxib
Perindopril	Perindoprilat
Perphenazine decanoate	Perphenazine
Pivampicillin	Ampicillin
Pivmecillinam	Mecillinam
Proguanil	Cycloguanil
Propacetamol	Paracetamol
Quinapril	Quinaprilat
Rabeprazole	The corresponding sulfenamide
Ramipril	Ramiprilat
Simvastatin (lactone)	Corresponding β-hydroxycarboxylic acid
Temozolomide	Monomethyl-triazenoimidazole-carboxamide (MTIC)
Trandolapril	Trandolaprilat
Travoprost	The corresponding acid
Valaciclovir	Aciclovir
Valganciclovir	Ganciclovir
Zuclopenthixol decanoate	Zuclopenthixol

with increased transcellular diffusion across the intestinal epithelia have traditionally been designed to increase oral bioavailability of the parent compounds. For example, the free carboxylic acid function in ampicillin has been used to produce its lipophilic pivaloylester prodrug, which has oral bioavailability superior to that of the parent compound [7, 8]. Furthermore, as the pivaloylester is hydrolyzed primarily inside the mucosal cells, the remaining pivampicillin which is present in the gut lumen as the inactive ester is less likely to cause diarrhea than is ampicillin [9]. The prodrug approach may also be used to increase the bioavailability of poorly soluble drugs where solubility in the gastrointestinal fluids is the rate-limiting factor with regard to absorption.

22.3 Peptide-Prodrugs and the Cyclic Peptide-Prodrug Concept

During the past two decades, many investigations have been conducted into prodrug approaches aimed at increasing the oral bioavailability of peptide pharmacophores. Although several prodrugs have shown reduced *in vitro* metabolism of the parent peptide and increased *in vitro* membrane permeability (e.g., prodrugs of desmopressin and thyrotropin-releasing hormone, TRH), the overall peptide-prodrug approach in which derivatives are prepared on single functional groups in the parent peptide molecule, has proved to be a disappointment [6, 10–13]. Nonetheless, by utilizing the cyclic peptide-prodrug approach (e.g., as for 4-imidazolidinones of enkephalins), the terminal primary amine of the parent peptide is transformed into a secondary amine and the vulnerable N-terminal peptide bond is alkylated. The 4-imidazolidinones are much weaker bases (typical pK_as of 3–3.5) than the parent peptides, and this results in increased lipophilicity of the entire N-terminal amino acid at physiological pH, as confirmed in partition experiments [14, 15]. The cyclic peptide-prodrug approach has been further developed by Borchardt and colleagues [16–20], who have produced acyloxyalkoxy, phenylpropionic acid, or coumarinic acid-based prodrugs of [Leu^5]-enkephalin (H-Tyr-Gly-Gly-Phe-Leu-OH) and its metabolically stable analogues DADLE (H-Tyr-D-Ala-Gly-Phe-D-Leu-OH) [16–20]. The acyloxyalkoxy-based [Leu^5]-enkephalin and DADLE prodrugs showed very low *in vitro* permeation through Caco-2 cell monolayers, but this was attributed to their substrate activity for Caco-2 cell efflux systems [16, 21]. Initially, these prodrugs of [Leu^5]-enkephalin and DADLE were believed to permeate significantly better than the parent opioid peptides in Caco-2 cell monolayers, although it has been shown recently that they are also substrates for efflux mechanism(s) in Caco-2 cells [23–25]. Despite these findings, a cyclic peptide-prodrug strategy combined with a metabolic stabilizing approach, and targeted at peptides with membrane permeability and metabolism-limiting oral absorption, has been introduced in the development phase and show promise for increasing oral bioavailability in small peptidomimetics. However, future studies clearly need to be conducted on cyclic-peptide prodrugs in order to confirm the value of this concept.

22.4
Prodrug Designed for PepT1-Mediated Absorption

Previously, limited drug transport across biological membranes was generally ascribed to the limited lipophilicity of a pharmacophore, thereby reducing its passive transcellular diffusion, and so strategies to develop prodrugs were naturally based on that paradigm. Consequently, carriers which played any significant role in oral drug bioavailability were seldom considered. Nonetheless, during the past 10–15 years several prodrug strategies intended to use carriers to improve oral pharmacophore bioavailability have been introduced. Given its broad substrate specificity, the human peptide transporter 1 (PepT1), which is located in the apical enterocytic membrane of the upper small intestine, has been the most intensively studied carrier to improve oral bioavailability using the prodrug approach, and this strategy will be detailed in this chapter. PepT1 was first cloned from rabbit small intestine in 1994 by Fei *et al.* and Boll *et al.* [26, 27], and this was followed in 1995 by cloning of the human peptide transporter, hPepT1 [28]. Several reviews on peptide transporters have been produced, and these cover the history of di/tripeptide transport [29], its physiological significance [30], its molecular biology [31, 32], its influence on oral drug availability [33, 34] and substrate structure and affinity relationships [35].

Over the past few decades, Amidon and colleagues have investigated the transport mechanism of ACE-inhibitor prodrugs (e.g., enalapril, fosinopril) using an in-situ rat single-pass perfused intestine technique. These authors have suggested that enalapril, but not fosinopril, binds to PepT1 and that the increased oral bioavailability of enalapril compared with the parent enalaprilat might be due to hPepT1-mediated absorption [36]. In contrast, Shu *et al.* have shown increased apical-to-basolateral transepithelial transport of fosinopril compared with basolateral-to-apical transepithelial transport in both Caco-2 and SKPT cell monolayers, indicating that hPepT1 (respectively hPepT2) are involved in the transport process [37]; moreover, transepithelial transport studies on enalapril have shown primarily passive nonsaturable transport [38, 39]. Future transepithelial transport studies may prove whether or not enalapril binds only to PepT1, or whether it is also transported transepithelially by PepT.

In a study investigating the intestinal transport of various β-lactam antibiotics, a correlation between *in vitro* cellular transport parameters and oral bioavailability of these drugs suggested that oral bioavailability (notably of the prodrug cefuroxime axetil) was determined mainly by its affinity to PepT1 [40]. The influence of PepT1-mediated transport on oral absorption of β-lactams has been reviewed by Danzig [41]. Although the orally bioavailable ACE-inhibitors and β-lactams (as well as some of their prodrugs) were not designed for hPepT1-mediated absorption, some have been shown retrospectively to have an affinity for hPepT1. However, whether this has any major influence on their oral bioavailability remains a subject of controversy.

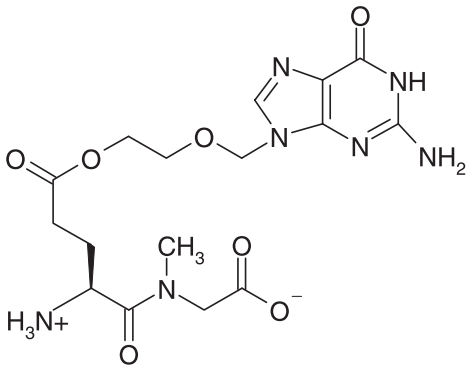

Fig. 22.2. Structure of L-Glu[aciclovir]-Sar.

22.4.1
Stabilized Dipeptide Promoieties

The results of initial studies on hPepT1-mediated uptake of registered ACE-inhibitor- and β-lactam-prodrugs led to a surge in the design of prodrugs utilizing hPepT1-mediated absorption. One hPepT1-mediated prodrug approach is to use stabilized dipeptides such as D-Asp-Ala, D-Glu-Ala, Asp-Sar and Glu-Sar as promoieties for various benzyl alcohol-based model compounds, as well as for the purine and pyrimidine analog, aciclovir and 1-(2-hydroxyethyl)thymine. In these (model) prodrugs, the carboxylic acid function, which is located in the side chain of the first amino acid, has been used for ester- or amide-based (model) drug attachment (Fig. 22.2) [42–52]. The *in vitro* release of model drug from the ester-linked dipeptidyl prodrugs, which has been investigated in various aqueous and biological media, was controlled primarily by a nonenzymic (but specific) base-catalyzed hydrolysis in the pH region between ~5 and 10. This indicates that the model prodrugs would be relatively stable in the lumen of the upper small intestine (pH ~ 6), yet release the parent drug at intracellular and blood pH of ~7.4 [46–49]. The rate of the specific base-catalyzed hydrolysis was thought to be influenced by the electronegativity of the model drug, and this was investigated with various D-Glu-Ala and D-Asp-Ala benzyl alcohol ester-linked model drugs; results showed hydrolysis to be increased with rising drug electronegativity [49]. Whereas the D-Glu-Ala and D-Asp-Ala-based prodrugs release the parent compounds quantitatively over the pH range from 1 to 10, the Glu-Sar- and Asp-Sar-based prodrugs are believed to degrade via two parallel pathways in acidic solution, with a cyclization product being formed as well as the parent compound [45, 47].

The affinity of the various stabilized dipeptidyl prodrugs to hPepT1 in Caco-2 cells was also investigated [42, 43, 50]. In the case of the D-Glu-Ala ester-linked benzyl alcohols, an improved hPepT1 affinity with increasing drug lipophilicity was observed [50]. Furthermore, these model prodrugs are transported transepithelially across Caco-2 cells by virtue of a hPepT1-mediated process [50]. Preliminary hPepT1 affinity studies made on Asp-Sar- and Glu-Sar-based (model)-

prodrugs indicated high affinity for hPepT1 in Caco-2 cells [43, 52], and future *in vivo* studies may prove the value of this concept.

In other studies, bisphosphonate-pamidronate or alendronate were linked to the terminal carboxylic acid of the stabilized dipeptide Pro-Phe to improve the bioavailability of bisphosphonates by hPepT1-mediated absorption. In-situ single-pass perfused rat intestine studies revealed competitive inhibition of transport by Pro-Phe, suggesting carrier-mediated transport. Oral administration of the dipeptidyl prodrugs resulted in a 3-fold increase in drug absorption following oral administration to rats. The authors suggested that oral bioavailability of bisphosphonates may be improved by PepT1-mediated absorption when administered as peptidyl prodrugs [53]. Future mechanistic studies may prove if hPepT1 is involved in the absorption process.

22.4.2 Amino Acid Prodrugs

Various dipeptidyl derivatives of α-methyl-dopa display a significant increase in their permeability compared with α-methyl-dopa, though when studied using a rat in-situ intestinal perfusion method this increased permeability was reduced when α-methyl-dopa was co-administered with 20 mM Gly-Gly [54]. Using the same in-situ perfusion technique, Bai has shown that the di-amino acid prodrug, p-Glu-L-dopa-Pro, shows increased permeability compared with L-dopa, and that the permeability is inhibited when co-administered with 5 mM Gly-Pro or 20 mM Gly-Gly [55]. In both studies, the authors suggested that the increased permeability may be explained by a PepT1-mediated absorption. In another study, the amino acid prodrug, L-dopa-Phe was examined in Caco-2 cells and in *Xenopus* oocytes. Uptake of L-dopa-Phe was increased by expression of hPepT1 in *Xenopus* oocytes. Secondly, the appearance of L-dopa and its metabolite dopamine on the basolateral site of Caco-2 cells was significantly increased after addition of L-dopa-Phe than after that of L-dopa, and was reduced in the presence of Gly-Sar on the apical side [56]. Taken together, these results indicate that di- or mono amino acid-linked L-dopa may be taken up by PepT1, demonstrating the possibility of targeting hPepT1 as a means of improving the oral bioavailability of amino acid-linked L-dopa [54–57].

In order to improve the efficacy of orally administered aminomethyl tetrahydrofuranyl (THF-methylcarbapenem), various amino acids have been linked to the methyl-THF side chain of the carbapenem molecule. When administered orally to mice with acute lethal infection (3.8 mg kg^{-1} body weight against *Escherichia coli* and 0.9 mg kg^{-1} against *Staphylococcus aureus*), the L-amino acid prodrugs showed an improved efficacy, but the D-amino acid prodrugs were less active than the parent THF-methylcarbapenem. It was suggested that this increased efficacy might be due to PepT1-mediated absorption [58, 59], though further studies must be conducted to verify whether PepT-mediated processes are involved in this situation.

Aciclovir is used extensively in prophylaxis and treatment of infections caused by herpesviruses. The L-valyl ester prodrug of aciclovir, valaciclovir, has been developed during the past decade and enhances the 20% oral bioavailability of aciclovir

by some 3- to 5-fold [60–63]. In fact, orally administered valaciclovir produces plasma aciclovir levels similar to those achieved with intravenous aciclovir (Fig. 22.3) [62]. In retrospect, it has been shown that this increase might be due to hPepT1-mediated uptake of valaciclovir, whereas aciclovir itself has no affinity for hPepT1 [64–66]. In addition, valaciclovir undergoes extensive presystemic conversion to aciclovir by an enzyme-catalyzed hydrolysis. In clinical trials only minor amounts of unmetabolized valaciclovir have been detected in plasma, indicating the presence of intestinal and/or hepatic first-pass metabolism [62, 63]. *In vitro* studies similarly indicate that valaciclovir was hydrolyzed intracellularly during cellular transport across Caco-2 monolayers [64, 65]. The enzyme valaciclovir hydrolase (VACVase), which has been purified and characterized in rat liver, and also found in other tissues (including intestinal homogenate), may play a significant role in the presystemic metabolism [69]. It has been suggested that aciclovir may have affinity for an efflux mechanism [70]. The suggested transport mechanism of valaciclovir is outlined in Fig. 22.4. A similar mechanism may explain the enhanced oral bioavailability of the purine analogue, ganciclovir, the oral bioavailability of which increases from ~5% to 60% when administered as the L-valyl ester prodrug valganciclovir [71, 72]. This enhanced bioavailability has also been suggested to result from a hPepT1 carrier-mediated process and rapid hydrolysis to the parent compound ganciclovir [72, 73].

22.5 Site Activation

When administered as valaciclovir, aciclovir is released during absorption, and ~60% of the drug reaches the bloodstream, as described above. Site activation also occurs in herpesvirus-infected cells where aciclovir is biochemically transformed to the phosphorylated active drug by virus-specific thymidine kinase [74].

The anti-ulcer agents omeprazole, lanzoprazole, and pantoprazole have been introduced during the past decade for the treatment of peptic ulcers. Gastric acid secretion is efficiently reduced by prazole inhibition of H^+K^+-ATPase in the parietal cells of the gastrointestinal mucosa [75]. The prazoles themselves are not active inhibitors of the enzyme, but are transformed to cyclic sulfenamides in the intracellular acidic compartment of parietal cells [76]. The active inhibitors are permanent cations at $pH < 4$, with limited possibilities of leaving the parietal cells, and thus are retained and activated at the site of action. In the neutral body compartments the prazoles are stable, and only trace amounts are converted to the active drugs. (For a review on omeprazole, see Ref. [77].)

22.6 Conclusions

Since the introduction of the prodrug concept during the late 1950s, many such compounds which increase the oral bioavailability of small pharmacophores have

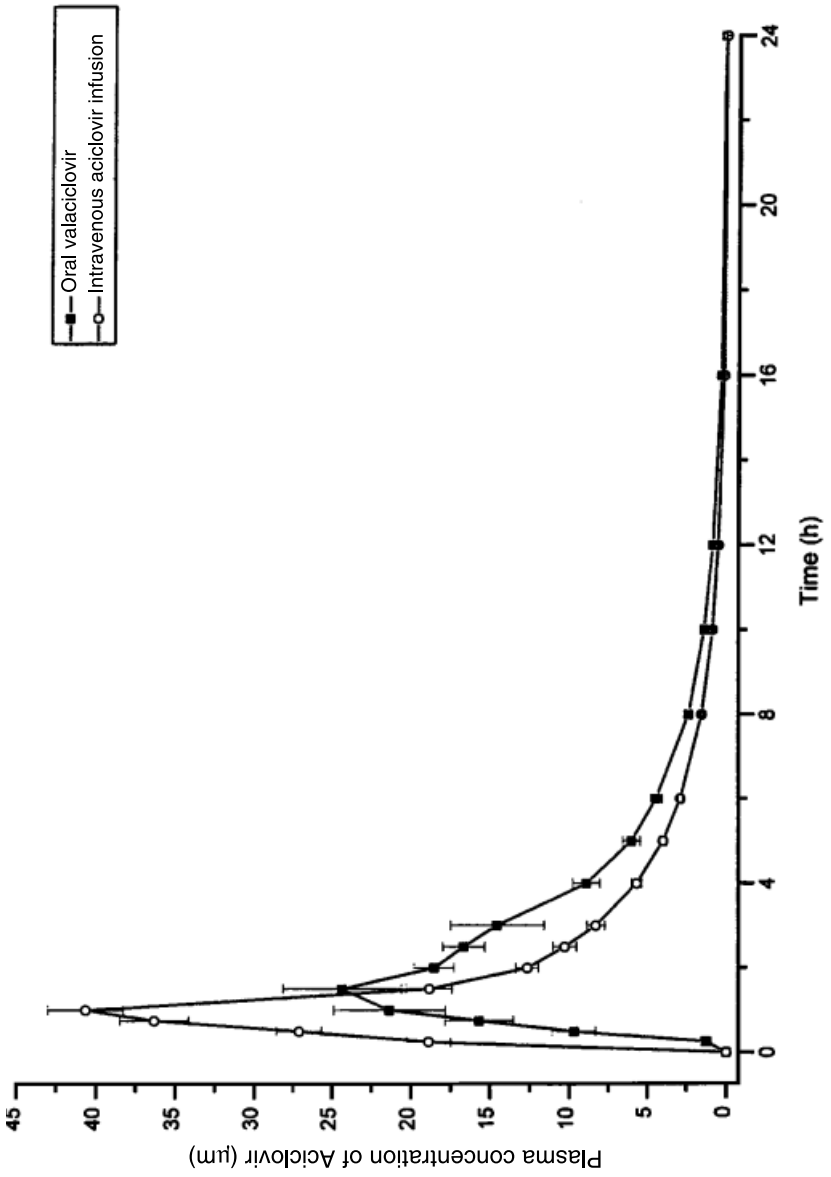

Fig. 22.3. Mean plasma concentration–time profiles of aciclovir following administration of 1000 mg oral valaciclovir or a 350-mg intravenous infusion of aciclovir over a 1-h period. (Adapted from Soul-Lawton *et al.* [62].)

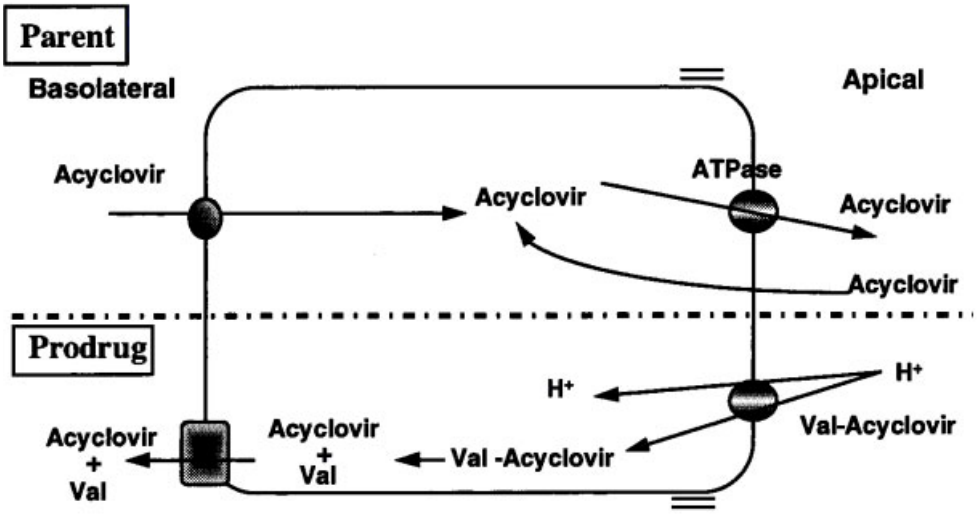

Fig. 22.4. Model of aciclovir and Val-aciclovir transport. The prodrug Val-aciclovir is taken up at the apical cell membrane via the di/tri-peptide transporter, hydrolyzed intracellularly in the enterocyte, with basal exit of valine and aciclovir. (Adapted from Smith *et al*. [78].)

been developed and commercialized. In the future, the prodrug concept might also prove valuable in the development of more complex molecules such as peptides, peptidomimetics and macromolecules, and future studies on cyclic peptide prodrugs will prove whether this concept is valuable, or not.

Carrier-mediated prodrug absorption has especially focused upon the use of PepT1, and a variety of strategies using stabilized dipeptides and amino acid-based prodrugs with affinity to hPepT1 appear promising. In retrospect, it has been shown that the commercially available prodrugs valaciclovir and valganciclovir are both absorbed via hPepT1, which provides evidence for the value of the carrier-mediated concept.

Overall, the prodrug approach is a well-established strategy to improve the bioavailability and targeting of pharmacophores, and is a vital component in the development of therapeutics and drug-delivery strategies.

References

1 Albert, A., Chemical aspects of selective toxicity, *Nature*, **1958**, *182*, 421–423.

2 Bundgaard, H., Design of prodrugs: bioreversible derivatives for various functional groups and chemical entities, in: *Design of Prodrugs*. Bundgaard, H. (ed.), Elsevier, Amsterdam, **1985**, pp. 1–92.

3 Christrup, L. L., Moss, J., Steffansen, B., Prodrugs, in: *Encyclopedia of Pharmaceutical Technology*, volume 13. Swarbrick, J., Boyland,

J. C. (eds), Marcel Dekker Inc., New York, **1996**, pp. 39–70.

4 Buur, A., Bundgaard, H., Prodrugs of 5-fluorouracil V. 1-alkoxycarbonyl derivatives as potential prodrug forms for improved rectal and oral delivery of 5-fluorouracil, *J. Pharm. Sci.* **1986**, *75*, 522–527.

5 Bundgaard, H., Trends in design of prodrugs for improved drug delivery, in: *Medicinal Chemistry for the 21st Century.* Wermuth, C. G., Koga, N., Konig, H., Metcalf, B. W. (eds), Blackwell Scientific Publications, **1992**, pp. 321–347.

6 Bundgaard, H., Means to enhance penetration. Prodrugs as means to improve the delivery of peptide drugs, *Adv. Drug Deliv. Rev.* **1992**, *8*, 1–38.

7 Daehne, W. V., Frederiksen, E., Gundersen, E., Lund, F., Mørch, P., Petersen, H. J., Roholt, K., Tybring, L., Godfredsen, W. O., Acycloxymethyl esters of ampicillin, *J. Med. Chem.* **1970**, *13*, 607–612.

8 Bodin, N. O., Ekström, B., Forsgren, U., Jalar, L. P., Magni, L., Ramsey, C. H., Sjöberg, B., *Antimicrob. Agents Chemother.* **1975**, *9*, 518–525.

9 Bolme, P., Dahlstrøm, B., Diding, N. A., Flink, O., Paalzow, L., Ampicillin: comparison of bioavailability and pharmacokinetics after oral and intravenous administration of three brands, *Eur. J. Clin. Pharmacol.* **1976**, *10*, 237–243.

10 Møss, J., Bundgaard, H., Kinetic pattern of degradation of thyrotropin-releasing hormone (TRH) in human plasma, *Pharm. Res.* **1990**, *7*, 751–755.

11 Møss, J., Bundgaard, H., Prodrugs of peptides 8. In vitro study of intestinal metabolism and penetration of thyrotropin-releasing hormone (TRH) and its prodrugs, *Int. J. Pharm.* **1990**, *66*, 39–45.

12 Kahns, A., Bundgaard, H., Prodrugs of peptides 18. Synthesis and evaluation of various esters of desmopressin (dDAVP), *Pharm. Res.* **1991**, *10*, 6874.

13 Kahns, A. H., Moss, J., Bundgaard, H., Human skin permeability studies of desmopressin and some prodrug derivatives, *Acta Pharm. Nord.* **1992**, *4*, 187–188.

14 Rasmussen, G. J., Bundgaard, H., Prodrugs of peptides. 10. Protection of di- and tripeptides against aminopeptidase by formation of bioreversible 4-imidazolidinone derivatives, *Int. J. Pharm.* **1991**, *31*, 45–53.

15 Rasmussen, G. J., Bundgaard, H., Prodrugs of peptides 15. 4-Imidazolidinone prodrug derivatives of enkephalines to prevent aminopeptidase-catalyzed metabolism in plasma and absorptive mucosae, *Int. J. Pharm.* **1991**, *76*, 113–122.

16 Bak, A., Gudmundsson, O. S., Friis, G. J., Siahaan, T. J., Borchardt, R. T., Acyloxyalkoxy-based cyclic prodrugs of opioid peptides: evaluation of their chemical and enzymatic stability as well as their transport properties across Caco-2 cell monolayers, *Pharm. Res.*, **1999**, *16*, 24–29.

17 Borchardt, R. T., Optimizing oral absorption of peptides using prodrug strategies, *J. Controlled Release* **1999**, *62*, 231–238.

18 Pauletti, G. M., Gangwar, S., Siahaan, T. J., Aube, J., Borchardt, R. T., Improvement of oral peptide bioavailability: peptidomimetics and prodrug strategies, *Adv. Drug Del. Rev.* **1997**, *27*, 235–256.

19 Gudmundsson, O. S., Pauletti, G. M., Wang, W., Shan, D., Zhang, H., Wang, B., Borchardt, R. T., Coumarinic acid based cyclic prodrugs of opioid peptides that exhibit metabolic stability to peptidases and excellent cellular permeability, *Pharm. Res.* **1999**, *16*, 7–15.

20 Gudmundsson, O. S., Jois, S. D., Vander Velde, D. G., Siahaan, T. J., Wang, B., Borchardt, R. T., The effect of conformation on the membrane permeation of coumarinic acid- and phenylpropionic acid-based cyclic prodrugs of opioid peptides. *J. Peptide Res.* **1999**, *53*, 383–392.

21 Gudmundsson, O. S., Vander Velde, D. G., Jois, S. D., Bak, A., Siahaan, T. J., Borchardt, R. T., The effect of conformation of the acyloxyalkoxy-

based cyclic prodrugs of opioid peptides on their membrane permeability, *J. Peptide Res.* **1999**, *53*, 383–392.

22 Ouyang, H., Vander Velde, D. G., Borchardt, R. T., Synthesis and conformational analysis of a coumarinic acid-based cyclic prodrug of an opioid peptide with modified sensitivity to esterase-catalyzed bioconversion. *J. Peptide Res.* **2002**, *59*, 183–195.

23 Ouyang, H., Tang, F., Siahaan, T. J., Borchardt, R. T., A modified coumarinic acid-based cyclic prodrug of an opioid peptide: its enzymatic and chemical stability and cell permeation characteristics, *Pharm. Res.* **2002**, *19*, 794–801.

24 Tang, F., Borchardt, R. T., Characterization of the efflux transport(s) responsible for restricting intestinal mucosa permeation of acyloxy-alkoxy-based cyclic prodrug of the opioid peptide DADLE, *Pharm Res.* **2002**, *19*, 780–786.

25 Tang, F., Borchardt, R. T., Characterization of the efflux transporter(s) responsible for restricting intestinal mucosa permeation of the coumarinic acid-based cyclic prodrug of the opioid peptide DADLE, *Pharm. Res.* **2002**, *19*, 787–793.

26 Fei, Y. J., Kanai, Y., Nussberger, V., Ganapathy, F. H., Leibach, F. H., Romero, M. F., Singh, S. K., Boron, W. F., Hediger, M. A., Expression cloning of a mammalian proton-coupled oligopeptide transporter, *Nature* **1994**, *368*, 563–566.

27 Boll, M., Markovich, D., Weber, W. M., Korte, H., Daniel, H., Murer, H., Expression cloning of cDNA from rabbit small intestine related to proton-coupled transport of peptides, β-lactam antibiotics and ACE inhibitors, *Pflügers Arch.* **1994**, *429*, 146–149.

28 Liang, R., Fei, Y. J., Prasad, P. D., Ramamoorthy, S., Han, H., Yang-Feng, T. L., Hediger, M. A., Ganapathy, V., Leibach, F. H., Human intestinal H+/peptide cotransporter. Cloning, functional expression, and chromosomal localization, *J. Biol. Chem.* **1995**, *270*, 6456–6463.

29 Matthews, D. M., Mechanisms of peptide transport, *Beitr. Infusionsther. Klin. Ernahr.* **1987**, *17*, 6–53.

30 Adibi, S. A., The oligopeptide transporter (Pept-1) in human intestine: biology and function, *Gastroenterology* **1997**, *113*, 332–340.

31 Daniel, H., Function and molecular structure of brush border membrane peptide/H+ symporters, *J. Membr. Biol.* **1996**, *154*, 197–203.

32 Meridith, D., Boyd, C. A., Structure and function of eucaryotic peptide transporters, *Cell Mol. Life Sci.* **2000**, *57*, 754–778.

33 Yang, C. Y., Danzig, A. H., Pidgeon, C., Intestinal peptide transport systems and oral drug availability, *Pharm. Res.* **1999**, *16*, 1331–1343.

34 Smith, P. L., Eddy, E. P., Lee, C.-P., Wilson, G., Exploitation of the intestinal oligopeptide transporter to enhance drug absorption, *Drug Delivery* **1996**, *3*, 117–123.

35 Brodin, B., Nielsen, C. U., Steffansen, B., Frokjaer, F., Transport of peptidomimetic drugs by the intestinal di/tri-peptide transporter, PepT1, *Pharmacol. Toxicol.* **2002**, *90*, 285–296.

36 Friedman, D. I., Amidon, G. L., Passive and carrier mediated intestinal absorption components of two angiotensin-converting enzyme (ACE) inhibitor prodrugs in rats: enalapril and fosinopril, *Pharm. Res.* **1989**, *6*, 1043–1047.

37 Shu, C., Shen, H., Hopfer, U., Smith, D. E., Mechanism of intestinal absorption and renal reabsorption of an orally active ACE inhibitor: uptake and transport of fosinopril in cell cultures, *Drug Metab. Dispos.* **2001**, *29*, 1307–1314.

38 Swaan, P. W., Stenhouwer, M. C., Tukker, J., Molecular mechanism for the relative binding affinity to the intestinal peptide carrier. Comparison of three ACE-inhibitors: enalapril, enalaprilat, and lisinopril, *Biochim. Biophys. Acta* **1995**, *1236*, 31–38.

39 Morisson, R. A., Chong, S., Marino, A. M., Wasserman, M. A., Timmins, P., Moore, V. A., Irwin, W. J., Suitability of enalapril as a probe of the dipeptide transporter system: in vitro and in vivo studies, *Pharm. Res.*, **1996**, *13*, 1078–1082.

40 Bretschneider, B., Brandsch, M., Neubert, R., Intestinal transport of β-lactam antibiotics: analysis of the affinity at the H+/peptide symporter (PEPT1), the uptake into Caco-2 cell monolayers and transepithelial flux, *Pharm. Res.* **1999**, *16*, 55–61.

41 Danzig, A. H., Oral absorption of β-lactams by intestinal peptide transport proteins, *Adv. Drug Deliv. Rev.* **1997**, *23*, 63–76.

42 Taub, M. E., Larsen, B. D., Steffansen, B., Frokjaer, S., β-carboxylic acid esterified D-Asp-Ala retains a high affinity for the oligopeptide transporter in Caco-2 monolayers, *Int. J. Pharm.* **1997**, *146*, 205–212.

43 Taub, M. E., Moss, B. A., Steffansen, B., Frokjaer, S., Influence of oligopeptide transporter binding affinity upon uptake and transport of D-Asp(OBzl)-Ala and Asp(OBzl)-Sar in filter grown Caco-2 monolayers, *Int. J. Pharm.* **1997**, *156*, 219–228.

44 Friedrichsen, G. M., Nielsen, C. U., Steffansen, B., Begtrup, M., Model prodrugs designed for the intestinal peptide transporter. A synthetic approach for coupling of hydroxy-containing compounds to dipeptides, *Eur. J. Pharm. Sci.* **2001**, *14*, 13–19.

45 Friedrichsen, G. M., Jacobsen, P., Taub, M. E., Begtrup, M., Application of enzymatically stable dipeptides for enhancement of intestinal permeability. Synthesis and in vitro evaluation of dipeptide-coupled compounds, *Bioorg. Med. Chem.* **2001**, *9*, 2625–2632.

46 Thomsen, A. E., Friedrichsen, G., Sørensen, A. H., Andersen, R., Nielsen, C. U., Brodin, B., Begtrup, M., Frokjaer, S., Steffansen, B., Prodrugs of purine and pyrimidine analogues for the intestinal di/tripeptide transporter PepT1: affinity for hPepT1 in Caco-2 cells, drug release in aqueous media and *in vitro* metabolism. *Controlled Release* **2003**, *86*, 279–292.

47 Steffansen, B., Lepist, E.-I., Taub, M. E., Larsen, B. D., Frokjaer, S., Lennernas, H., Stability, metabolism and transport of D-Asp(OBzl)-Ala: a model prodrug with affinity for the oligopeptide transporter, *Eur. J. Pharm.* **1999**, *8*, 67–73.

48 Lepist, E.-I., Kusk, T., Larsen, D. H., Andersen, D., Frokjaer, S., Taub, M. E., Veski, P., Lennernas, H., Friedrichsen, G., Steffansen, B., Stability and in vitro metabolism of dipeptide model prodrugs with affinity for the oligopeptide transporter, *Eur. J. Pharm. Sci.* **2000**, *11*, 43–50.

49 Nielsen, C. U., Andersen, R., Brodin, B., Frokjaer, S., Steffansen, B., Model prodrugs for the intestinal oligopeptide transporter: model drug release in aqueous solution and in various biological media, *J. Controlled Release*, **2001**, *73*, 21–30.

50 Nielsen, C. U., Andersen, R., Brodin, B., Frokjaer, S., Taub, M. E., Dipeptide model prodrugs for the intestinal oligopeptide transporter. Affinity for and transport via hPepT1 in the human intestinal Caco-2 cell line, *J. Controlled Release* **2001**, *76*, 129–138.

51 Taub, M. E., Moss, B. A., Steffansen, B., Frokjaer, S., Oligopeptide transporter mediated uptake and transport of D-Asp(OBzl)-Ala, D-Glu(OBzl)-Ala, and D-Ser(Bzl)-Ala in filter grown Caco-2 monolayers, *Int. J. Pharm.* **1998**, *174*, 223–232.

52 Thomsen, A. E., Andersen, R., Nielsen, C. U., Friedrichsen, G. M., Brodin, B., Taub, M. E., Frokjaer, S., Steffansen, B., Prodrugs of purine and pyrimidine analogues for oligopeptide transporter, *AAPS Pharm. Sci.* **2001**, *3* suppl.

53 Ezra, A., Hoffman, A., Breuer, E., Alferiev, I. S., Mönkkönen, J., Hannany-Rozen, N. E., Weiss, G., Stephensky, D., Gati, I., Cohen, H., Törmälehto, S., Amidon, G. L.,

Golomb, G., A peptide prodrug approach for improving bisphosphonate oral absorption, *J. Med. Chem.* **2000**, *43*, 3641–3652.

54 Hu, M., Subramanian, P., Mosberg, H. I., Amidon, G. L., Use of dipeptide carrier system to improve the intestinal absorption of L-α-methyldopa: carrier kinetics, intestinal permeabilities and in vitro hydrolysis of dipeptidyl derivatives of L-α-methyldopa, *Pharm. Res.* **1989**, *6*, 66–70.

55 Bai, J. P. F., pGlu-L-Dopa-Pro: a tripeptider prodrug targeting the intestinal peptide transporter for absorption and tissue enzymes for conversation, *Pharm. Res.* **1995**, *12*, 1101–1104.

56 Tamai, I., Nakanishi, T., Nakahara, H., Sai, Y., Ganapathy, V., Leibach, F. H., Tsuji, A., Improvement of L-dopa absorption by dipeptidyl derivation utilizing peptide transporter PepT1, *J. Pharm. Sci.* **1998**, *87*, 1542–1546.

57 Wang, H. P., Lu, H. H., Lee, J. S., Chen, C. Y., Mah, J. R., Ku, C. Y., Hsu, W., Yen, C. F., Lin, C. J., Kuo, H. S., Intestinal absorption studies on peptide mimetic alpha-methyldopa prodrugs, *J. Pharm. Pharmacol.* **1996**, *48*, 270–276.

58 Tanaka, M., Hohmura, T., Nishi, K., Sato, K., Hayakawa, I., Antimicrobial activity of DU-6681a, a parent compound of novel oral carbapenem DZ2640, *Antimicrob. Agents Chemother.* **1997**, *41*, 1260–1268.

59 Weiss, W. J., Mikels, S. M., Petersen, P. J., Jacobus, N. V., Bitha, P., Lin, Y. I., Testa, T., In vivo activities of peptide prodrugs of novel aminomethyl tetrahydrofuranyl-1 beta-methylcarbapenems, *Antimicrob. Agents Chemother.* **1999**, *43*, 460–464.

60 de Miranda, P., Blum, M. R., Pharmacokinetics of acyclovir after intravenous and oral administration, *J. Antimicrob. Chemother.* **1983**, *12*, B29–B37.

61 Beauchamp, L. M., Orr, G. F., de Miranda, P., Burnette, T., Krenitsky, T. A., Amino acid ester prodrugs of acyclovir, *Antivir. Chem. Chemother.* **1992**, *3*, 157–164.

62 Soul-Lawton, J., Seaber, E., On, N., Wootton, R., Rolan, P., Posner, J., Absolute bioavailability and metabolic disposition of valaciclovir, the L-valyl ester of acyclovir, following oral administration to humans, *Antimicrob. Agents Chemother.* **1995**, *39*, 2759–2764.

63 Weller, S., Blum, M. R., Doucette, M., Burnette, T., Cederberg, D. M., de Miranda, P., Smiley, M. L., Pharmacokinetics of the acyclovir prodrug valaciclovir after escalating single- and multiple-dose administration to normal volunteers, *Clin. Pharmacol. Ther.* **1993**, *54*, 595–605.

64 de Vrueh, R. L. A., Smith, P. L., Lee, C.-P., Transport of L-valine-acyclovir via the oligopeptide transporter in the human intestinal cell line, Caco-2, *J. Pharmacol. Exp. Ther.* **1998**, *286*, 1166–1170.

65 Han, H.-K., de Vrueh, R. L. A., Rhie, J. K., Covitz, K.-M. Y., Smith, P. L., Lee, C.-P., Oh, D.-M., Sadee, W., Amidon, G. L., 5′-Amino acid esters of antiviral nucleosides, acyclovir and ATZ are absorbed by the intestinal PepT1 peptide transporter, *Pharm. Res.* **1998**, *15*, 1154–1159.

66 Ganapathy, M. E., Huang, W., Wang, H., Ganapathy, V., Valaciclovir: a substrate for the intestinal and renal peptide transporters PepT1 and PepT2, *Biochem. Biophys. Res. Commun.* **1998**, *246*, 470–475.

67 Burnette, T. C., de Miranda, P., Metabolic disposition of the acyclovir prodrug valaciclovir in the rat, *Drug Metab. Dispos.* **1994**, *22*, 60–64.

68 Han, H.-K., Oh, D.-M., Amidon, G. L., Cellular uptake mechanism of amino acid ester prodrugs in Caco-2/hPepT1 cells overexpressing a human peptide transporter, *Pharm. Res.* **1998**, *15*, 1382–1386.

69 Burnette, T. C., Harrington, J. A., Reardon, J. E., Merrill, B. M., de Miranda, P., Purification and characterization of a rat liver enzyme that hydrolyzes valaciclovir

the L-valyl ester prodrug of acyclovir, *J. Biol. Chem.* **1995**, *270*, 15827–15831.

70 Lee, C.-P., de Vrueh, R. L. A., Smith, P. L., Selection of development candidates based on in vitro permeability measurements, *Adv. Drug Deliv. Rev.* **1997**, *23*, 47–62.

71 Jacobsen, M. A., de Miranda, P., Cederberg, D. M., Burnette, T., Cobb, E., Brodie, H. R., Mills, J., Human pharmacokinetics and tolerance of oral ganciclovir, *Antimicrob. Agents Chemother.* **1987**, *31*, 1251–1254.

72 Jung, D., Dorr, A., Single-dose pharmacokinetics of valganciclovir in HIV- and CMV-seropositive subjects, *J. Clin. Pharmacol.* **1999**, *39*, 800–804.

73 Sugawara, M., Huang, W., Fei, Y.-J., Leibach, F. H., Ganapathy, V., Transport of valganciclovir, a ganciclovir prodrug, via peptide transporters PepT1 and PepT2, *J. Pharm. Sci.* **2000**, *89*, 781–789.

74 Fyfe, J. A., Keller, P. M., Furman, P. A., Miller, R. L., Elion, G. B., Thymine kinase from herpes simplex virus phosphorylates the new antiviral compound 9-(2-hydroxyethoxymethyl)guanine, *J. Biol. Chem.* **1978**, *253*, 8721–8727.

75 Sach, G., Pump blockers and ulcer disease, *N. Engl. J. Med.* **1984**, *310*, 785–786.

76 Howden, C. W., Reid, J. L., Omeprazole, a gastric proton pump inhibitor: lack of effect on renal handling of electrolyte and urinary acidification, *Eur. J. Clin. Pharmacol.* **1984**, *26*, 639–640.

77 Clissold, S. P., Campoli-Richards, D. M., Omeprazole. A preliminary review of its pharmacodynamic and pharmacokinetic properties and therapeutic potential in peptic ulcer disease and Zollinger–Ellison syndrome, *Drugs* **1986**, *32*, 15–47.

78 Smith, P. L., Ellens, H., de Vrueh, R. L. A., Yeh, P.-Y., Lee, C.-P., Enhancement of dosage form design through timely integration of biological studies, in: *Peptide and Protein Drug Delivery*. Froekjaer, S., Christrup, L. L., Krogsgaard-Larsen, P. (eds), Munksgaard, Copenhagen, **1997**, pp. 345–355.

23
Modern Delivery Strategies: Physiological Considerations for Orally Administered Medications

Clive G. Wilson

Abbreviations and Symbols

AUC	Area under the plasma concentration–time profile
[^{51}Cr] EDTA	Chromium-51-labeled ethylenediamine-tetraacetic acid
CYP3A4	Cytochrome P450, 3A4 isozyme
C_{max}	Maximum concentration reached in the concentration profile
[^{111}In]	Indium-111
IMC	Inter-digestive migrating contraction
T_{50}	Time for 50% emptying of the stomach
[^{99m}Tc]	Technetium-99m

23.1
Introduction

The control of physiological processes to achieve reliable plasma concentration–time profiles following oral drug administration is a key goal in therapy. At the investigational level, it would allow the scientist to utilize manageable numbers of volunteers in appropriately powered tests to proceed with formulation development; alternatively, as a medicine, it might allow more consistent outcomes. The weasel word ''might'' is important here, since disease and/or concomitant medication may alter transit, pH, disposition, metabolism and clearance in a manner unforeseen in the original clinical trials. The opposite scenario can also occasionally happen, with patients showing consistent blood level–time curves and studies in (normal) volunteers yielding huge differences in AUC and C_{max}. More generally, the issue relates to erratic blood levels with patients or volunteers grouped into ''poor'' and ''good'' absorbers, or those with troughs in the plasma profile. At this stage, there is usually a frantic appeal to the formulator to come up with a strategy to solve the problem. This will result in futile endeavors if the phenomenon relates to a physiological process, which was not controlled in the trial that provided the anomalous results. This state of affairs occurs because the impact of some elements of physiological processes – and particularly those relevant to drug

Drug Bioavailability: Estimation of Solubility, Permeability, Absorption and Bioavailability.
Edited by Han van de Waterbeemd, Hans Lennernäs and Per Artursson

ISBN: 3-527-30438-X

absorption – are poorly appreciated and physicians and pharmaceutical scientists have failed to reach a common perspective.

My view is that physiological and pathophysiological factors have to be considered hand-in-hand with pharmaceutical/physico-chemical issues in the exploitation of modern drug delivery strategies. In this chapter, an attempt is made to illustrate this point from a biopharmaceutics perspective, drawing largely on examples from imaging, patient, and volunteer studies. In order to make the task manageable, only the oral route will be considered, although similar considerations could certainly be applied to other routes of delivery.

23.2 The Targets

For most drugs, the limitations to delivery are defined in terms of solubility and permeability. The solubility issues are addressed by various means including selection of an amorphous form where appropriate, reduction in particle size, and the use of co-solvents. For permeability problems, a mechanism to increase flux by alteration of membrane/microenvironment conditions or even a simple increase in concentration gradient might achieve the goal. Examples of design strategies include the use of absorption enhancers and the use of formulations designed to keep the drug in the upper gastrointestinal tract which may achieve reduction of first-pass effect (buccal), increased solubility in acid (stomach) or avoidance of degradation in the colon (e.g., nitrofurantoin) by slowed upper gastrointestinal transit. When the compound selected is problematic in terms of both solubility and permeability, the number of permutations becomes almost infinite, especially when juggling with the added dimensions of dose and plasma half-life. In general, the desired outcomes could be listed as in Table 23.1.

The gastrointestinal tract is conveniently divided into a number of areas, primarily on the basis of morphology and function. For most pharmaceutical purposes, we can group the target tissues into three regions: the upper, mid- and lower gastrointestinal tract.

23.3 Upper Gastrointestinal Tract: Mouth and Esophagus

The primary role of the mouth is to chew the material into an appropriate size and use saliva to moisten food into a bolus, which can be swallowed via the esophagus. The surface tissue is squamous epithelium, and the cells lining the cheek are dead and enucleated. Clearance of drugs from the buccal mucosa is generally slow, which may reflect high nonspecific binding in the tissue: plasma morphine concentrations for example decline more slowly than from an intramuscular site and may be used with advantage to extend the period of analgesia [1, 2]. Diffusion through the tissue can therefore be improved by manipulation of lipophilicity

Tab. 23.1. Desired outcomes of targeted treatments to various regions of the gut.

Region	*Objective*	*Strategy*	*Issues*
Buccal	Avoid first pass	Adhere to buccal mucosa (prophylaxis) OR Sublingual (immediate)	Taste Saliva (some drugs cause dry mouth) Potency (has to be high) Talking, eating, drinking
	Increase flux	Open tight junctions	Irritancy
	Increase convenience	Use fast-dissolving system	Will not be equivalent to simple IR systems
Esophagus	Ensure transit Avoid sticking	Adjust tablet shape Take with water	Surface area/weight ratio (How much? When?) Age, previous Rx, Posture
Stomach	Promote rapid absorption	Control intrinsic dissolution Control emptying	In vitro/in vivo correlation Fed/Fasted effects
	Prevent degradation	Enteric coat	Achlorhydria in elderly (especially Japanese)
	Extend absorption (in intestine)	Float Swell Adhere	Posture Rate of degradation post delivery, bezoars Food effects, gastric Inhomogeneity, disease effects
Intestine	Extend exposure	Adhere to villus tip Promote Peyer's patch uptake	Access? Wall-lumen mixing
	Increase absorption	Decrease P-glycoprotein efflux Block cytochrome P450 3A Open tight junctions	Timing Concomitant administration Unselective
	Utilize lymphatic system	Increase absorption of lipophiles	Food effects persist for longer than 24 h
Colon	Increase exposure	Target with coated preparation Utilize bacterial fermentation Increase surface area of preparation	Variability in transit and pH Variability, disease effects? Stirring, dispersion, available water, gas, time of dosing

(prodrug or pH control) to increase partitioning into the tissue. A simple application of this concept is in the development of nicotine formulations, where raising buccal pH increases the flux significantly. Recent trials of a 2-mg submucosal nicotine lozenge showed encouraging results [3], and other pharmaceutical companies are examining similar systems. In spite of the presence of a damaged super-

ficial layer, access to deeper vital layers must occur since the buccal tissue shows stereoselectivity with regard to the absorption of D-glucose and L-arabinose [4]; studies during the same year by Kurosaki *et al.* showed that buccal absorption of a cephalosporin antibiotic, cephadroxil was inhibited by cephalexin [5].

Utilizing absorption enhancers in this area is probably more benign than elsewhere in the gastrointestinal tract. The maximum size of a buccal patch that would be acceptable to a patient has been defined as >15 cm^2 (or more usually between 0.5 and 3 cm^2), and Hoogstraate and colleagues have commented that an absorption enhancer would therefore probably be necessary [6]. In addition, the small area for delivery dictates that the drug must be potent. As a final design consideration for peptide delivery, although the buccal mucosa is less hostile with regard to peptidase and other enzymatic activity, it may be necessary to incorporate enzyme inhibitors as excipients in the formulation.

Although gels can be used to increase contact and promote absorption [7], the requirement for uni-directional delivery cannot be met by simple systems and release of actives from erodible matrices are influenced by physiological abrasion from the cheek surfaces by talking [8]. Novel systems for oral delivery have been extensively investigated by 3M and Hoogstraate, and others have reviewed recent developments in the field including melatonin delivery and low molecular-weight heparin in the Cydot system [6]. Theratech have used a related system for the delivery of glucagon-like insulinotropic peptide (GLP-1), a peptide comprising 30 amino acids which has application in the management of type II diabetes.

Fast-dissolving formulations (flash-dispersing) are not primarily intended to be for buccal delivery; the issue here is that they may be taken without water. This causes an important difference in performance relative to ordinary immediate-release products, especially if the drug is in suspension. If the material is swallowed dry, it may adhere to the fundus area, where the amount of shear is low. This causes a significant fraction of the material to be retained resulting in tailing of the absorption phase and an apparently decreased AUC as the material is released over several hours.

23.3.1 Swallowing the Bitter Pill ...

It is commonly assumed that swallowed dosage forms pass without hindrance into the stomach unless an underlying esophageal condition is present. Radiological studies of an asymptomatic group of 56 patients (mean age 83 years) showed that a normal pattern of deglutition was present in only 16% of patients [9]. In 63% of this population, patients experienced difficulty in swallowing. To assist swallowing of a tablet, patients are instructed to take a dosage form in an upright position with plenty of water. It might be expected that simple encouragement and education could encourage compliance. In practice, when patients are presented with a 240-mL glass of water and instructed to swallow a tablet "according to normal practice", they imbibe only two to three mouthfuls (between 50 and 100 mL). Radiological studies conducted during the mid-1980s concluded that the effect of taking

diazepam with either 10 or 50 mL water made little difference to absorption, except in the case of about 20% of the study group who showed delayed absorption irrespective of the volume imbibed [10]. In our studies, the effect of small volumes of water (30 or 50 mL) on the esophageal clearance of either a small uncoated circular tablet or film-coated oval tablet were compared [11]. Clearance of the oval tablet was significantly faster, and stasis occurred in five instances with the uncoated tablet against zero in the same 28 patients taking the film-coated oval tablet.

Deliberate attempts to cause formulations to adhere to the esophagus have been attempted, in order to treat ulcer sites in esophagus and stomach [12]. These data suggested that acid-activated sucralfate showed high retention, and encouraging data were obtained in the dog. These data proved misleading however, and a later study [13] failed to confirm the results of Hardy and co-workers. The explanation for visible coating in the dog is probably related to the angle of the esophagus in this species. In veterinary medicine it has been observed that esophageal clearance in the cat is remarkably slow, and cats have problems with regard to esophageal injury which may not be seen in other species.

The development of an esophageal bandage based on graft polymers which possess mucoadhesive and thermosetting properties was investigated in our laboratory, and some limited success achieved [14]. However, the issue of inconsistent starting temperatures and slow heat transfer during mouth-hold and deglutition proved to be problematic.

23.4 Mid-gastrointestinal Tract: Stomach and Intestine

The stomach provides a reservoir which allows food to be made available to the small intestine at a rate appropriate for efficient assimilation. In order to do this, the food contents are churned with acid and enzymes which begin the digestive process. The early stage of digestion allows the duodenum to sample the contents and adjust the gastroduodenal pressure difference to regulate the supply of calories. This function explains some of the characteristics of the first part of the intestine, namely that: (i) absorption will be extremely efficient; and (ii) transit through this region will be very rapid to allow modulation of emptying following continued food intake.

23.4.1 Gastric Inhomogeneity

For the most part, the resting pH of the stomach is nearer to 2 than 1; however, during feeding the meal causes a transient rise in pH to 4–5 depending on the volume and nature of the meal consumed. The fundus undergoes receptive relaxation to allow the proximal stomach to accommodate the food mass: in the distal stomach, the food is triturated to form chyme, which is ejected into the duodenum in spurts of 2–5 mL. The division of function causes significant inhomogeneity in

the conditions of the stomach, as the proximal stomach is more stagnant and the number of parietal cells are much less in the fundal area. If a raft-forming drug formulation is taken after a meal, with the subject upright or seated, the formulation will be retained in the upper stomach by a mixture of flotation and stratification (assuming that there is enough acid to liberate gas and to cause precipitation of the matrix-forming agent). The timing of formulation relative to the meal is therefore quite critical. By labeling an antacid or an anti-reflux formulation with indium, flotation assisted by stratification can be demonstrated after a meal. For example, an almagate-based preparation Flot-Coat was demonstrated to reside in the stomach on top of the meal and empty from the stomach more slowly than the food. The time for 50% of the Flot-Coat granulate to empty (T_{50}) was more than 4.5 h compared with 2.3 h for the meal. The standard granulate mixed and emptied with the digestible solid phase of the meal, with 50% emptying at 1.7 h [15].

At the bottom of the stomach, swallowed food will be squeezed together to form a mass. For a high-carbohydrate snack such as a sandwich or a baguette, the material will not be fully hydrated during travel through the esophagus. On arrival in the body of the stomach, this meal – which is cohesive and plastic – will be kneaded together to form a solid ball which over a period of an hour or so will become hydrated and form a uniform phase. A typical magnetic resonance imaging (MRI) scan in which the stomach and food mass is seen in horizontal section is shown in Fig. 23.1.

In response to food, the parietal cells secrete acid which will be moved upwards by contractions of the pylorus. In an individual with an incompetent cardiac sphincter, this can result in a reflux of acid into the esophagus. In order to assess food and acid reflux, patients were provided with a refluxogenic meal, after which the reflux of food (which was labeled with technetium-99m) and acid appearance in the esophagus was monitored [16]. Using ambulatory telemetry, the reflux of acid and food was seen to be quite separate and consistent with a mechanism by which acid can move around the food mass. In a recent collaboration, the reformulation of paracetamol (acetaminophen) into both fast-acting and sustained-acting preparations was examined. In particular, gamma scintigraphy was utilized to examine the emptying of a novel paracetamol formulation in the fed and fasted state. In the fasted state, we expected to be able to show faster dissolution of the formulation and a consequent increased rate of gastric emptying. This we were able to do; however, we also found that the novel formulation showed faster gastric emptying in the fed state. The scintiscans in Fig. 23.2 indicate that the phenomenon is probably due to rapid dissolution and movement of the formulation around the food mass in the stomach [17]. It is known that liquid and solids empty the stomach at different rates, although the significance of the discrete boundary phase has been ignored. In the elderly, the rate of liquid emptying is slower than in young subjects, although solid rates of emptying are similar [18]. This might be due to a decrease in the rate of secretion associated with age.

It is well established that a meal containing sufficient fat will stratify. By using MRI, several investigators have been able to show the appearance of a fat layer on

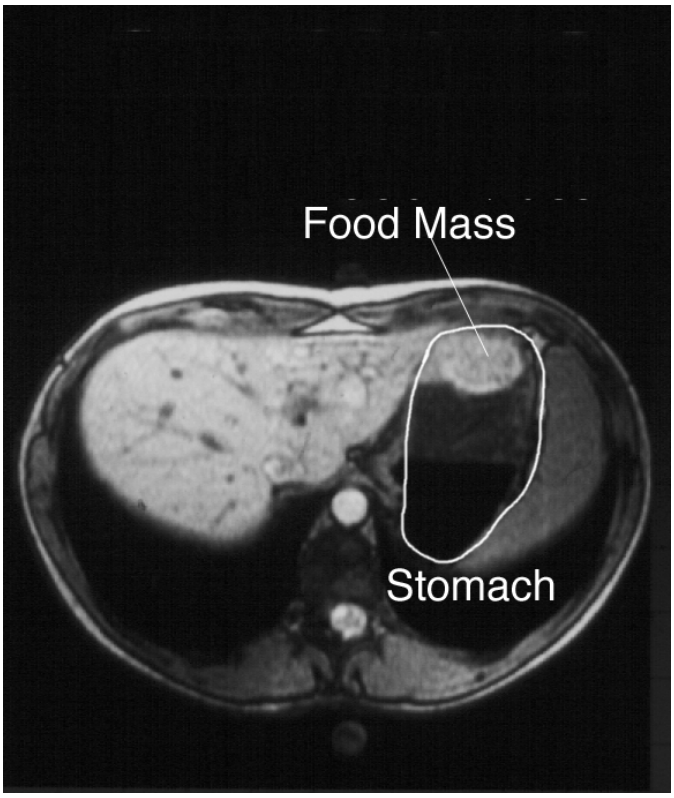

Fig. 23.1. Transverse T_1-weighted image of a consolidated food ball in the base of the stomach.

the fundal gastric contents after a fatty meal. In this situation, the inhibitory effects of fats are reduced, since the fat must be homogenized, emulsified and presented to the duodenal receptors before an action is initiated. If a suitable substrate for dispersion of fat is provided (i.e., minced beef) the inhibitory effects of fats on the rate of gastric emptying is increased [20]. This indicates that significant differences in intragastric distribution of fat occur after eating. (For a review on the imaging of oils utilizing scintigraphy and MRI, see Ref. [21].)

The issue of the shape and size of formulations on gastric emptying has been debated at length, and some investigators have seen size–shape effects where others have not. In part, this is probably due to postural effects. In our experiments, it has been found that sitting semi-recumbent is likely to produce a faster rate of emptying of oval tablets than when standing. This is important, as gamma camera investigations are usually performed with the subject standing, whereas for a pharmacokinetic study the subject will be seated with the back inclined at an angle and the arms supported to facilitate blood-taking. When these conditions are mimicked using an appropriately angled imaging couch, scintigraphic trials of food effects show closer correlation than when the subject stands.

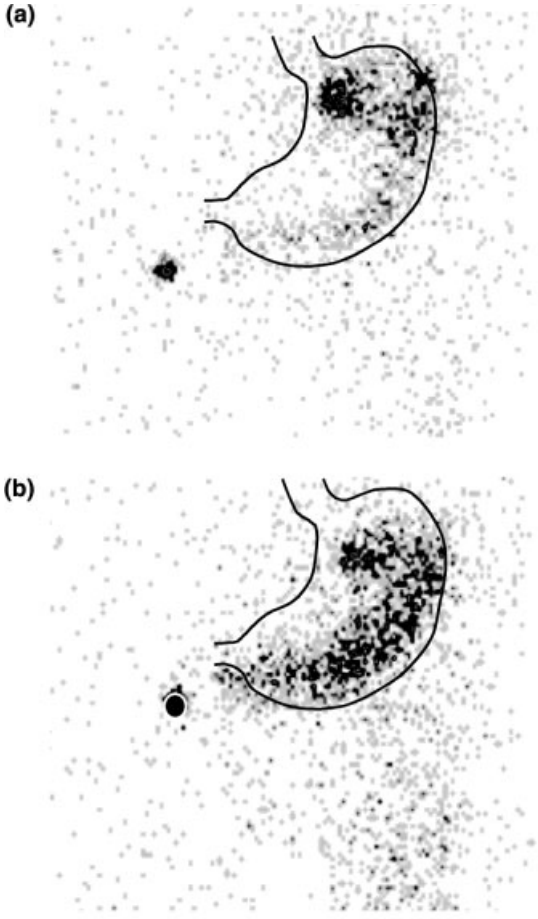

Fig. 23. 2. The start of sequential static views of orally administered, radiolabeled paracetamol tablet. Top: the tablet has started to dissolved, and the released drug and radioactivity moves along the greater curvature of the stomach. Bottom: antral mixing has started to move the radiolabel and the drug into the food mass in the pyloric antrum.

Several investigators have attempted to show that ageing is associated with a slowed gastrointestinal transit, although the effect must be small in comparison to inter-subject variability, as many workers have failed to demonstrate clear effects. Gender – or more particularly the menstrual cycle – has also been mentioned as a significant influence on whole-gut transit. Madsen and colleagues carried out a study to elucidate the influences of gender, age, and body mass index on gastrointestinal transit times using a meal containing [^{99m}Tc]-labeled cellulose as a fiber and 2- to 3-mm [^{111}In]-labeled plastic particles. Seventeen healthy young subjects (nine men, eight women; age 21–27 years; body mass index (BMI) 18.4–25.1 kg m^{-2}) and 16 healthy older subjects (eight men, eight women; age 55–74 years;

BMI 19.8–36.0 kg m^{-2}) were studied. All transit variables were unaffected by gender. The older subjects had a slower mean colonic transit time of radiolabeled plastic particles than the young subjects ($p < 0.05$), while BMI affected the gastric emptying of fiber but not other gastrointestinal variables [22]. In a more recent study, comparison was made between cohorts of young and elderly males, but no age-related effect could be determined [23].

During pregnancy, there appears to be a reduction in the rate of small-bowel and colonic transit according to a survey of the literature between 1963 and 1992 conducted by Baron and colleagues [24]. Gastrointestinal symptoms were reported predominantly as abdominal bloating and constipation. These effects are mediated by progesterone, with estrogen probably acting as a primer.

23.4.2
Modulation of Transit to Prolong the Absorption Phase

Adhesion or slowing intestinal transit are two mechanisms which have been proposed to extend the absorption phase of drugs, particularly if colonic permeability is poor. Weitsches and colleagues have utilized formulations doped with iron to conduct real-time magnetic measurements of the transit of formulations along the gastrointestinal tract [25, 26]. These data elegantly demonstrate that, during the initial phases of transit through the duodenum and jejunum, the formulation is swept forward in a series of pulsatile movements which would leave little opportunity for adhesion in the upper gut in the fasted state. Gamma scintigraphy shows that similar movements occur whether the formulation is multiparticulate, matrix or liquid. A static acquisition of measuring the transit of a tablet in the proximal intestine illustrates periods of stasis and pulsatile movement though the duodenum and jejunum (Fig. 23.3). These data suggest that utilizing bioadhesion to prolong drug delivery in the proximal intestine is unlikely to work; however, it is known that the strong propulsive wave gradually becomes quiescent at the ileocecal junction. It would be at this point that weak interactive forces would probably be most effective; hence, this would be a better area to target if formulation–cell interactions were to be exploited.

23.4.3
Ileocecal Movement

Many years ago, Marvola *et al.* showed that the residence time at the ileocecal junction was quite variable and could be prolonged in some individuals [27]. Our scintigraphic studies showed that pellet formulations bunch at the ileocecal junction as the propulsion waves become weaker. Eventually, feeding causes short-range propulsive forces that move the formulation into the cecum. Philips and others have shown, using scintigraphy, that the pattern of cecal filling varies considerably between individuals, with fast and slow patterns of transit across the ileocecal valve being observed [28].

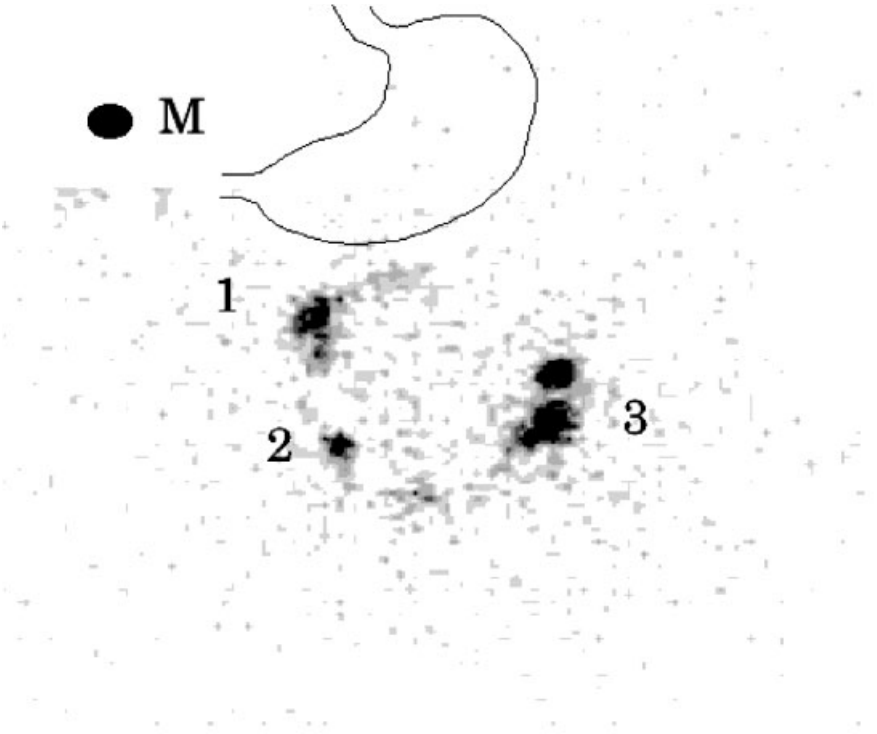

Fig. 23.3. Tablet movement during a static view (30-s duration). Note the movement from position 1 to position 3 during successive peristaltic waves. M, external marker.

23.4.4
Fat and the Small Intestine

It is well appreciated that dietary fat retards proximal gastrointestinal transit. For hydrophobic drugs with low aqueous solubility, dissolution becomes the rate-limiting process; the appreciation that fat might increase bioavailability by increasing time available for dissolution and that mixed triglycerides often provide a better solvent than aqueous media has not been lost on formulation scientists.

The role of lipids on absorption has been extensively reviewed by Porter and Charman [29, 30]. The influences are diverse and include effects on luminal drug solubility, altering the metabolic and barrier function of the intestinal wall, stimulating lymphatic transport and a reduction in gastric transit, thereby increasing the time available for dissolution.

23.4.5
Absorption Enhancement

Treatments which transiently open up intercellular gaps increase absorption significantly. In the villus, the loss of apical cells may cause large gaps at the tip,

allowing drug to enter through the lymphatic spaces. Prolonged insult leads to an alteration of the goblet cell/enterocyte ratio and a phenomenon known as goblet cell "capping". This effect can be seen after quite short exposures with low molecular-weight polyethylene glycol [31].

As pointed out by Baloum and colleagues [32], absorption enhancers are efficient in small body cavities such as the nasal cavity and the rectum. In the fed state, the issues of dilution during gastric mixing would probably obviate the possibility of interaction between the dispersed phase and the small intestine. Using a perfused rat model, these authors showed that synchronized administration of an absorption enhancer (sodium decanoate) is required for optimal absorption of a poorly absorbed drug (cefazoline), and that levels of the enhancer need to be sustained rather than high.

23.4.6
Alteration of Flux across the Small Intestine

The finding that grapefruit juice can increase the bioavailability of certain drugs, by reducing presystemic intestinal metabolism, led to interest in a new area of food–drug interactions. It has been suggested that this observation could be exploited to increase bioavailability, especially for poorly soluble compounds. Particular interest focused on the effects of the grapefruit flavonoid, naringin, and the furanocoumarin, 6′,7′-dihydroxybergamottin, on the activity of intestinal CYP3A4. Given that P-glycoprotein (P-gp) and canalicular multispecific organic anion transporters are involved in the intestinal absorption and biliary excretion of a wide range of drugs and metabolites, it is reasonable to suspect that isoflavones may alter drug disposition in humans [33]. Wagner and colleagues, in a review of food effects on intestinal drug efflux, have suggested that the effect of grapefruit juice is likely to be due to inhibition of intestinal P-gp rather than to metabolism [34].

Animal data suggest that dietary salt modulates the expression of renal CYPs, and Darbar *et al.* extended this observation to suggest that intestinal CYP3A4 may be similarly modulated by dietary salt. These authors studied the effects of dietary salt on the kinetics of quinidine on normal volunteers given high-salt (400 mEq per day) and low-salt (10 mEq per day) diets for 7–10 days each. Plasma concentrations of quinidine after oral administration were significantly lower during the high-salt phase, with the difference between the two treatments attributable to changes within the first 1–4 h [35].

The possibility of exploiting excipient effects, and particularly of nonionic detergents such as Tween 80 or Pluronic, has been of interest to several laboratories. The data suggest that a strategy based on bioavailability enhancement for drugs undergoing intestinal secretion might be valid with the caveats general to absorption enhancers (see above). The effects are evident with model peptides and with cyclosporin, the bioavailability of which is increased in normal subjects when it was co-administered with D-α-tocophenylpolyethylene glycol 1000 succinate [36].

23.5
Lower Gastrointestinal Tract: The Colon

By the end of the small intestine, deposition is almost complete and there is no need for intestinal secretions to aid assimilation. The principal role of the colon is to resorb water and reclaim sodium, which it does very efficiently. In fact, for every 2 L of water entering the colon, the residual water in the stools will be <200 mL. The environment becomes problematic for delivery past the hepatic flexure as the lack of water will restrict dispersion and dissolution. The flow of chyme from the ileum to the colon in healthy human beings is 1–2 L h^{-1}.

The material arriving in the colon will contain cellulosic materials from vegetables in the diet which cannot be broken down by intestinal secretions. In the cecum, a bacterial ecosystem digests the soluble, fermentable carbohydrates to yield short-chain fatty acids, which are assimilated into the systemic circulation by the colon, together with vitamin K released from the plant material. Carbon dioxide release is also a fermentation product, and if the redox potential is sufficiently low, the colonic bacteria can produce methane and hydrogen that can be detected in the breath, particularly after the ingestion of pulses. In the upright position, the gas will rise to the transverse colon: an adult produces approximately 2–3 L of gas per day, the majority of which is exchanged through the lungs.

23.5.1
Colonic Transit

Until gamma scintigraphy became a routine tool in pharmaceutical research, the available data relating to movement through the gut was confined to measurements of whole-gut transit time. Both the stomach and colon can be identified unambiguously in planar images, allowing the contribution of colonic absorption in the plasma–concentration time profile to be assessed in each individual. The colonic transit of single unit dosage forms when dosed at different times of the day are listed in Table 23.2.

There is a large variability among the data, but in general the units administered prior to retiring for the night have a slower colonic transit than those dosed in the morning. This is in agreement with the measured pattern of electrical and contractile activity measured by several groups [38–41]. Only a proportion of the colon

Tab. 23.2. Colonic transit times (h) of single unit dosage forms [37].

Colon region	*Time of dosing*			
	Morning Fasted	*Morning Light breakfast*	*Morning Heavy breakfast*	*Evening*
Ascending	3.6 ± 1.2	2.5 ± 1.5	4.8 ± 3.9	8.9 ± 4.3
Transverse	5.8 ± 2.9	–	–	11.25 ± 3.2

will be usable for drug delivery (unless prepared by irrigation), and the useful sites will generally include the cecum and the ascending and transverse colon. The length of time available for drug release in these regions of the gut, and the influence of formulation variables (size, shape, and density) on transit in "normal" and pathophysiological conditions is therefore of great interest to pharmaceutical scientists. There are conflicting values in the literature regarding transit from cecum to splenic flexure: indeed, in one study it was reported to be as long as 14 h [42].

In two studies conducted by our group, gamma scintigraphy was used to compare the colonic transit rate of different sizes of nondisintegrating radiolabeled model dosage forms in healthy subjects. In the first study, capsules of volume 0.3–1.8 cm^3 and density 0.7–1.5 g cm^{-3} were administered to 18 healthy subjects after an overnight fast. The capsules were seen to enter the colon (on average) at 5 h after dosing, and transit rates through the proximal colon were seen to be independent of capsule density. Any effect due to capsule volume was small when compared with intersubject variations in transit rates. Within 10 h of entering the colon, 80% of the units had reached the splenic flexure [43].

By administering both sizes of formulation simultaneously, a better discrimination of relative transit of the two phases can be made. In a cohort of 22 healthy young volunteers, an enteric-coated capsule was administered which contained tablets (^{99m}Tc-labeled 5 mm or 8.4 mm diameter) together with pellets (^{111}In-labeled 0.2 mm ion-exchange resin particles). The unit delivered the radiopharmaceuticals simultaneously to the ileocecal junction [44]. Under control conditions, no difference was observed between the rate of transit through the ascending colon of 0.2-mm particles versus 5-mm tablets, or 0.2-mm particles versus 8.4-mm tablets. The mean period of residence of 50% of the administered 0.2-mm particles in the ascending colon was 11.0 ± 4.0 h.

In contrast, Adkin *et al.* compared the transit of 3-, 6- and 12-mm nondisintegrating ^{111}In-labeled tablets in eight healthy male volunteers. The transit of tablets through the ileocecal junction was unaffected by tablet size, and all tablets entered the colon as a bolus. The 3-mm and 6-mm tablets were retained in the ascending colon for the longest period of time [45].

23.5.2 Time of Dosing

Time of dosing is an important parameter with regard to the whole-gut transit of nondisintegrating formulations. Sathyan and colleagues have noted that an analysis of 1163 administrations of OROS devices showed a bimodal distribution clustered at 12 and 36 h following night-time dosing, and 24 and 48 h after morning dosing [46]. After night-time dosing, a monolithic device will be propulsed forward during the strong contractile activity on waking and rising, but may not move far enough to be excreted. Our own data show that, subsequent to the mass movement in the first hour of rising, propulsive movements are weak until sometime after the lunchtime meal has been ingested [47].

23.5.3 Colonic Water

In our early attempts at producing models of diarrheal predominant disease, it was found that administration of the laxative lactulose provided a useful and reversible simulation of altered colonic hydrodynamics such as might be seen in colitis. Lactulose is used therapeutically to manage a number of conditions including hepatic encephalopathy, constipation, and salmonellosis. This semisynthetic disaccharide is neither metabolized nor absorbed in the normal small intestine, but may undergo bacterial fermentation in the colon to short-chain fatty acids and gases. Major consequences are a fall in pH and a change in composition and metabolic activity of the colonic flora [48]. The changes provoked by lactulose are sensitive to fiber supplementation [49] and can be reversed by codeine [50].

In the experiments with enteric-coated tablet plus pellet preparations [44], a second leg was conducted in which a preparation containing 5-mm tablets and 0.2-mm resin was administered after laxative treatment. Following lactulose dosing there was a significant acceleration in colonic transit. Under these conditions, the ascending colon residence time of the 0.2-mm resin was significantly shorter than for the 5-mm tablets, though the magnitude of the effect was small.

In later experiments in which stool water content was modulated using lactulose and codeine, an investigation was initiated to determine the influence of luminal water content on the absorption from the distal gut of either quinine (a transcellular probe) or [^{51}Cr]-EDTA (a paracellular probe). Absorption of these probe markers from a timed-release delivery system was determined following treatment with lactulose 20 mL t.d.s. (increasing water content), or codeine 30 g q.d.s. (decreasing water content), and compared with control untreated values. Stool water content was assessed by freeze-drying stool samples, and the site of release was determined using gamma scintigraphy. Plasma quinine concentrations and urinary recovery of quinine and [^{51}Cr]-EDTA was used to measure absorption under the different conditions. Lactulose accelerated ascending colon transit, increased stool water, caused greater dispersion of released material, and enhanced absorption of the quinine compared with control. Conversely, codeine slowed ascending colon, reduced stool water content, and also tended to diminish absorption. More distal release resulted in less absorption in the control arm, whereas lactulose enhanced drug absorption from the distal gut [51].

Other workers have shown that the increased fluid load produced by an osmotic laxative results in redistribution of colonic contents. Since the distal colon is considered to be mainly a conduit without extensive storage function, Hammer *et al.* considered whether the capacity of the colon to retain fluid might be relevant in compensating for increased fluid loads and preventing diarrhea. Changes in distribution following cecal infusion of an iso-osmotic solution labeled with [^{99m}Tc]-DTPA containing polyethylene glycol (PEG; 500 mL) was compared with changes following infusion of an equal amount of readily absorbable electrolyte solution. After the osmotic load, fecal output was increased significantly ($p < 0.05$), but whole-colonic transit after PEG infusion was not different from transit after the

electrolyte solution ($p > 0.05$), indicating that the distal colon retains non-absorbable fluid volumes to a large extent [52].

23.6 Pathophysiological Effects on Transit

Active left-sided colitis is often resistant to topical therapy, and resolution may only be achieved by administration of systemic therapy. This might be a reflection of the relative roles of the proximal (right) colon which has a reservoir function, whilst the distal colon acts a conduit, resulting in reduced contact time of lumenal contents with the administered dose. In studies comparing the exposure of various regions of the colon in healthy and patient populations, it was suggested that less material would reside in the left side of the colon compared with the right side, and that this difference might be altered in patients with active colitis [53]. Twenty-two volunteers and 10 patients were recruited into a clinical trial in which they received morning doses of a Eudragit-coated capsules containing ^{111}In-labeled resin pellets. Since ^{111}In has a half-life of 2.8 days, a gradual accumulation of the material (corrected for decay) represents the mean residence time in the region under investigation at steady state. At 4 days into the regime, the relative distribution of the marker was measured in the ascending, transverse, descending and rectosigmoid colon (Fig. 23.4).

The results showed there to be an asymmetry in colonic distribution among healthy subjects, with two-thirds of the administered dose in the proximal colon and one-third in the distal colon. In the patients, this difference was even more pronounced, with only one-tenth of the administered dose in the distal segment.

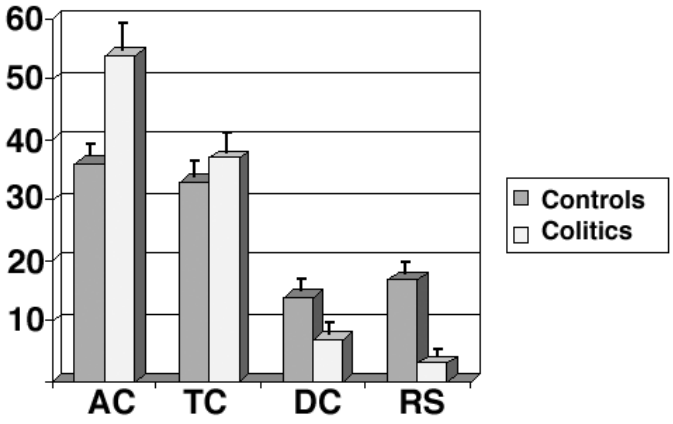

Fig. 23.4. Distribution of resin labeled with ^{111}In after four successive daily (morning) administrations among a cohort of normal volunteers and patients with active colitis. AC, ascending colon; DC, distal colon; RS, rectosigmoid colon; TC, transverse colon.

Rapid transit through this region suggests that the area is empty of colonic contents most of the time, and so the opportunity for topical treatment is consequently limited. If the exposure to a drug such as mesalazine is calculated on the basis of these data, the results show that treatment is probably inadequate. For example, the dose per day is approximately 3 g (800–1200 mg, t.d.s.), and so in active disease the effective dose would be about 300 mg on the basis of this regimen. Doses of 500–1000 mg are often given as a enema, but these doses are more effectively delivered and not sequestered within a viscous, partially dehydrated stool, as would be the case following oral administration.

Although discrete effects of diseases are often noted by studying a single parameter such as gastric emptying, the effects of pathophysiological conditions once established are usually evident throughout the gut. Mollen *et al.* attempted to describe the motor activity of the upper gastrointestinal tract in patients with slow-transit constipation by using perfusion manometry. Orocecal transit time was found to be similar between patients and controls, but esophageal motility was abnormal in five of 18 patients and gastric emptying was abnormal in eight of 15 patients. These data support the case that disorders of upper gut motility occur frequently in patients with slow-transit constipation [54].

Gattuso *et al.* studied 10 young patients with idiopathic megarectum using radiographic and scintigraphic methods. All patients had a dilated large bowel, with no radiographic evidence of upper gut dilation. Gastric emptying was normal in four patients and abnormally slow in six, which suggested that this bowel condition might be reflected in a disturbance of upper gut function. Both the radioisotope scans and radio-opaque marker studies showed abnormal colonic transit, and regions of delay corresponded with the region of dilated bowel [60].

Studies in dogs have shown that postoperative ileus following surgery resolves in the following order. First, weak irregular contractions of the gastrointestinal tract are recorded, after which transmission of the contractions from the upper gut to the lower gastrointestinal tract were observed. Using combined X-ray radiography and Fourier transformation, Tsukamoto *et al.* found that recovery from postoperative ileus was aided by a change in the pattern of gastrointestinal motility in which contractions were transmitted from the stomach to the lower gastrointestinal tract, like an inter-digestive migrating contraction (IMC) [61].

Bouchoucha *et al.* characterized colonic transit time in 30 healthy subjects and in 43 patients with inflammatory bowel disease using X-ray opaque markers. The response to food was different in the two populations: in controls, the cecum and ascending colon emptied and filled the distal bowel, whereas in the patients only the splenic flexure and left transverse colon emptied. Movement through both the right and left colon in patients was observed to be much slower than in controls, both before and after a meal [55].

Patients with anxiety and depression often have bowel symptoms. Gorad *et al.* compared 21 psychiatric outpatients with generalized anxiety disorders and depression with an equal number of healthy controls. Whole-gut transit time (WGTT) was measured using abdominal radiography after ingestion of radio-opaque markers, and found to be shorter in patients with anxiety (mean 14 h;

range 6–29 h) than in either those with depression (mean 49 h; range 35–71 h; $p < 0.001$) or controls (mean 42 h; range 10 to 68 h; $p < 0.001$). In patients with anxiety, orocecal transit time (measured using the lactulose hydrogen breath test) was shorter than in patients with depression and also shorter than in controls. The authors concluded that objective measurements of intestinal transit were consistent with the clinical impression that anxiety is associated with increased bowel frequency, while depressed patients tend to be constipated; taken together, these data strongly suggested that mood has an effect on intestinal motor function [56]. Bennett *et al.*, after using a scintigraphic method to examine gender and psychophysiological effects on colonic transit, concluded that male hypochondriacs had normal intestinal transit, whereas elderly females with depressive illness were more likely to have both colonic and gastric stasis [57].

Among several disease conditions which affect gastric emptying, diabetes is probably the most extensively studied. Folwaczny *et al.* utilized a metal-detector test to determine large bowel transit, as well as scintigraphy to assess esophageal motility and gastric emptying in patients with type I and type II diabetes. These authors concluded that both gastric emptying and large bowel transit were affected by both conditions [58].

The alteration of transit by disease, or a change produced by hydrodynamic factors such as diarrhea, will be highly significant for sophisticated zero-order release formulations such as osmotic pumps. For the pumps, inadequate retention may occur in some patients, perhaps leading to less optimal clinical outcome. Even in normal subjects, the range of intestinal transit time can be extreme: for example, the median gastrointestinal transit time for both the oxprenolol and metoprolol OROS drug delivery systems has been reported as 27.4 h, with individual times ranging from 5.1 to 58.3 h [59]. The possibility of inadequate gastrointestinal retention of osmotic pump-based systems is more likely in patients who have preexisting gastrointestinal motility disorders or who are taking other medications that enhance gastrointestinal motility.

Finally, Hammer *et al.* conducted an experiment in which volunteers received either autologous blood or egg white by duodenal intubation to simulate the condition of upper gastrointestinal bleeding [62]. [^{99m}Tc]-DTPA was added to each infusion and arrival at, and clearance from, the colon were recorded. At 4 h after the start of blood infusion, a median of 30% of counts was observed in the transverse colon compared with 0% after egg white administration; small intestinal transit was unaffected, however. Although it had been established that bleeding alters gastric motility, this was the first demonstration that heme-containing proteins have a significant effect on proximal bowel motility.

23.7
Pathophysiological Effects on Permeability

The situation with regard to the flux of materials in disease is quite different, since inflammation leads to changes in permeability for large and polar molecules. This

forms the basis of diagnostic tests such as urinary recovery of [^{51}Cr]-EDTA after oral administration. It would be suspected that, in the destruction of the epithelial barrier by severe inflammation, the permeability to very large molecules and perhaps even small particles would be increased, although evidence in humans is limited. In an experimental model of colitis in the rat, Lamprecht *et al.* demonstrated significant uptake of 100 nm-sized particles compared with controls [63].

23.8 pH

The pH changes of the gut are important triggers for the delivery of drug from enteric-coated preparations, in particular tablets used for the delivery of topical agents in the treatment of bowel disease. Sasaki and co-workers attempted to measure pH profiles in the gut in patients with Crohn's disease by using a radiotelemetry method coupled with a computer-assisted radiodirectional probe to localize a pH-sensitive radiotelemetry capsule as it traveled from the stomach to the cecum. Gastrointestinal pH profiles in four patients with Crohn's disease that involved the left side were measured and compared with those in four gender- and age-matched control subjects. In this small study, gastric and small intestinal luminal pH profiles in Crohn's disease were similar to those in the controls. In contrast, colonic luminal pH profiles in both right and left colon in active or quiescent Crohn's disease showed more coarse fluctuations, with significantly lower values than were seen in controls [64].

Many patients with Crohn's disease undergo an ileocecal resection, which might be expected to influence small intestinal pH and transit time. A ''radiopill'' technique (similar to that of Sasaki *et al.*) was used by Fallingborg *et al.* [65] to examine intraluminal pH and transit time in ileocecal-resected Crohn's disease patients. These data were compared with those obtained from 13 healthy volunteers. The mean small intestinal transit time (SITT) was significantly shorter in patients than in controls (5.2 h and 8.0 h, respectively). However, although the pH levels of the small intestine were identical in patients and controls, cecal pH was 0.9 pH units higher in resected Crohn's disease patients, and the period when the pH was elevated above 5.5 was significantly shorter in patients than in controls. The authors suggested that the reduced SITT was mainly a consequence of resection of the ileocecal valve and independent of the length of ileum resected. An ileocecal resection might therefore affect the delivery of active drug from tablets which use a pH-dependent delivery mechanism [65].

23.9 Conclusions

In summary, it is emphasized that disease conditions may result in changed physiological parameters that could strongly influence the effectiveness of orally

administered medications. Changes in patterns of motility, pH and amount of water available for dispersion and dissolution may be significant for patients as compared with the ''normal'' population. On this basis, it seems appropriate to investigate fully the impact of a target disease – whether it be diabetes, inflammatory bowel disease, or irritable bowel syndrome – on the deposition of drug from the candidate delivery system. Neglect of these issues might lead to suboptimal therapy and a waste of healthcare resources.

References

1 Bell, M. D. D., Murray, G. R., Mishra, P., Calvey, T. N., Weldon, B. D., Williams, N. E., Buccal morphine – a new route for analgesia, *Lancet* **1985**, *1*, 71–73.

2 McElnay, J. C., Hughes, C. M., Drug delivery: buccal route, in: *Encyclopaedia of Pharmaceutical Technology*. Swarbrick, J. (ed.), Marcel Dekker, **2002**, pp. 800–810.

3 Wallstrom, M., Sand, L., Nilsson, F., Hirsch, J. M., The long term effect of nicotine on the oral mucosa, *Addiction* **1999**, *94*, 417–423.

4 Harris, D., Robinson, J. R., Drug delivery via the mucous membranes of the oral cavity, *J. Pharm. Sci*. **1992**, *81*, 1–10.

5 Kurosaki, Y., Nishimura, H., Terao, K., Nakayama, T., Kimura, T., Existence of a specialised absorption mechanism for cefadroxil, an aminocephalosprorin antibiotic, in the human oral cavity, *Int. J. Pharm*. **1992**, *82*, 165–169.

6 Hoogstraate, J., Benes, J., Burgaud, S., Horriere, F., Seyler, I., Oral trans-mucosal drug delivery, in: *Drug Delivery and Targeting*. Hillery, A. M., Lloyd, A. W., Swarbrick, J. (eds), Taylor & Francis, London, **2001**, pp. 186–206.

7 Uzunoglu, B., Senel, S., Hincal, A. A., Ozalp, M., Wilson, C. G., Formulation of a bioadhesive bilayered buccal tablet of natamycin for oral candidiasis, *Proc. Intl. Symp. Control. Rel. Bioact. Mater.* **2000**, *27*, 8205.

8 Davis, S. S., Kennerley, J. W., Taylor, M. J., Hardy, J. G., Wilson, C. G., Scintigraphic studies on the in vivo dissolution of a buccal tablet, in: *Modern Concepts in Nitrate Delivery Systems*. Goldberg, A. A. J., Parsons, D. G. (eds), Royal College of Medicine, London, **1983**, pp. 29–37.

9 Ekeberg, O., Feinberg, M. J., Altered swallowing function in elderly patients without dysphagia: radiologic findings in 56 cases, *Am. J. Roentgenol.* **1991**, *156*, 1181–1184.

10 Richards, D. G., McPherson, J. J., Evans, K. T., Rosen, M., Effects of volume of water taken with diazepam tablets on absorption, *Br. J. Anaesth*. **1986**, *58*, 41–44.

11 Perkins, A. C., Wilson, C. G., Frier, M. *et al*., The use of scintigraphy to demonstrate the rapid esophageal transit of the oval film-coated placebo risedronate tablet compared to a round uncoated placebo tablet when administered with minimal volumes of water, *Int. J. Pharm.* **2001**, *222*, 295–303.

12 Hardy, J. G., Hooper, G., Ravelli, G., Steed, K. P., Wilding, I. R., A comparison of the gastric retention of a sucralfate gel and a sucralfate suspension, *Eur. J. Pharm. Biopharm.* **1993**, *39*, 70–74.

13 Dansereau, R. J., Dansereau, R. N., McRorie, J. W., Scintigraphic study of oesophageal transit and retention, in: *Nuclear Medicine in Pharmaceutical Research*. Perkins, A. C., Frier, M. (eds), Taylor & Francis, London, **1999**, pp. 57–69.

14 Potts, A. M., Wilson, C. G., Stevens, H. N. E., Dobrozsi, D. J., Washington, N., Frier, M., Perkins, A. C., Oesophageal bandaging: a new opportunity for thermosetting polymers, *S. T. P. Pharma Sciences* **2000**, *10*, 293–301.

15 Washington, N., Steed, K. P., Wilson, C. G., Evaluation of a sustained release formulation of the antacid almagate, *Eur. J. Gastroenterol. Hepatol.* **1992**, *4*, 495–500.

16 Washington, N., Moss, H. A., Washington, C., Wilson, C. G., Non-invasive detection of gastro-oesophageal reflux using an ambulatory system, *Gut* **1993**, *34*, 1482–1486.

17 Kelly, K., O'Mahony, B., Lindsay, B., Jones, T., Grattan, T. J., Stevens, H. N. E., Wilson, C. G., Comparison of the rates of dissolution, gastric emptying and serum concentrations following administration of paracetamol formulations (Panadol and Panadol Actifast) using gamma scintigraphy. *Pharm. Res.* (in press)

18 Cheskin, L. J., Schuster, M. M., Motility and ageing, *Motility* **1989**, 4–6.

19 Moore, J. G., Datz, F. L., Christian, P. E., Greenberg, E., Alazraki, N., Effect of body posture on radionuclide measurements of gastric emptying, *Dig. Dis. Sci.* **1988**, *33*, 1592–1595.

20 Edelbroek, M., Horowitz, M., Maddox, A., Bellen, J., Gastric emptying and intragastric distribution of oil in the presence of a liquid or a solid meal, *J. Nucl. Med.* **1992**, *33*, 1283–1290.

21 Wilson, C. G., McJury, M., O'Mahony, B., Frier, M., Perkins, A. C., Imaging of oily formulations in the gastrointestinal tract, *Adv. Drug Deliv. Rev.* **1997**, *25*, 91–101.

22 Madsen, J. L., Effects of gender, age, and body mass index on gastrointestinal transit times, *Dig. Dis. Sci.* **1992**, *37*, 1548–1553.

23 Brogna, A., Ferrara, R., Bucceri, A. M., Lanteri, E., Catalano, F., Influence of aging on gastrointestinal transit time – An ultrasonographic and radiologic study, *Invest. Radiol.* **1999**, *34*, 357–359.

24 Baron, T. H., Ramirez, B., Richter, J. E., Gastrointestinal motility disorders during pregnancy, *Ann. Intern. Med.* **1993**, *118*, 366–375.

25 Weitschies, W., Kotitz, R., Cordini, D., Trahms, L., High-resolution monitoring of the gastrointestinal transit of a magnetically marked capsule, *J. Pharm. Sci.* **1997**, *86*, S1218–S1222.

26 Weitschies, W., Cardini, D., Karaus, M., Trahms, L., Semmler, W., Magnetic marker monitoring of esophageal, gastric and duodenal transit of non-disintegrating capsules, *Pharmazie* **1999**, *54*, 426–430.

27 Marvola, M., Aito, H., Pohto, P., Kannikoski, A., Nykanen, S., Kokkonen, P., Gastrointestinal transit and concomitant absorption of verapamil from a single-unit sustained-release tablet, *Drug Dev. Ind. Pharm.* **1987**, *13*, 1593–1609.

28 Philips, S., The ileocolonic junction: its role in mediating transit, *Motility* **1991**, *Issue 13*, 8–12.

29 Charman, W. N., Porter, C. J. H., Mithani, S., Dressman, J. B., Physicochemical and physiological mechanisms for the effects of food on drug absorption: the role of lipids and pH, *J. Pharm. Sci.* **1997**, *86*, 269–282.

30 Porter, C., Charman, W., In vitro assessment of oral lipid based formulations, *Adv. Drug Deliv. Rev.* **2001**, *50*, S127–S147.

31 Bryan, A. J., Kaur, R., Robinson, G., Thomas, N. W., Wilson, C. G., Histological and physiological studies on the intestine of the rat exposed to solutions of Myrj 52 and PEG 2000, *Int. J. Pharmaceut.* **1980**, *7*, 145–156.

32 Baluom, M., Friedman, M., Rubinstein, A., The importance of intestinal residence time of absorption enhancer on drug absorption and implication on formulative considerations, *Int. J. Pharmaceut.* **1998**, *176*, 21–30.

33 Evans, A. M., Influence of dietary components on the gastrointestinal metabolism and transport of drugs, *Therap. Drug Monitor.* **2000**, *22*, 131–136.

34 Wagner, D., Spahn-Langguth, H., Hanafy, A., Koggel, A., Langguth, P., Intestinal drug efflux: formulation and food effects, *Adv. Drug Deliv. Rev.* **2001**, *50*, S13–S31.

35 Darbar, D., DellOrto, S., Morike, K., Wilkinson, G. R., Roden, D. M., Dietary salt increases first-pass elimination of oral quinidine, *Clin. Pharm. Ther.* **1997**, *61*, 292–300.

36 Chang, T., Benet, L. Z., Herbert, M. F., The effect of water-soluble vitamin E on cyclosporine kinetics in healthy volunteers, *Clin. Pharm. Ther.* **1996**, *59*, 297–303.

37 Washington, N., Washington, C., Wilson, C. G., *Physiological Pharmaceutics: Barriers to Drug Absorption*. 2nd edition. London, Taylor & Francis, **2001.**

38 Frexinos, J., Bueno, L., Fioramonti, J., Diurnal changes in myoelectrical spiking activity of the human colon, *Gastroenterology* **1985**, *88*, 1104–1110.

39 Narducci, F., Bassoti, G., Baburri, M., Morelli, A., Twenty four hour manometric recording of colonic motor activity in healthy man, *Gut* **1987**, *28*, 17–25.

40 Bassotti, G., Crowell, M. D., Whitehead, W. E., Contractile activity of the human colon: lessons from 24 hour studies, *Gut* **1993**, *34*, 129–133.

41 Bassotti, G., Iantorno, G., Fiorella, S., BustosFernandez, L., Bilder, C. R., Colonic motility in man: features in normal subjects and in patients with chronic idiopathic constipation, *Am. J. Gastroenterol.* **1999**, *94*, 1760–1770.

42 Metcalf, J. A., Roberts, S. J., Sutton, J. D., Variations in blood flow to and from the bovine mammary gland measured using transit time ultrasound and dye dilution, *Res. Vet. Sci.* **1992**, *53*, 59–63.

43 Parker, G., Wilson, C. G., Hardy, J. G., The effect of capsule size and density on transit through the proximal colon, *J. Pharm. Pharmacol.* **1988**, *40*, 376–377.

44 Watts, P. J., Barrow, L., Steed, K. P., Wilson, C. G., Spiller, R. C., Melia, C. D., Davies, M. C., The transit rate of different-sized model dosage forms through the human colon and the effects of a lactulose-induced catharsis, *Int. J. Pharmaceut.* **1992**, *87*, 215–221.

45 Adkin, D. A., Davis, S. S., Sparrow, R. A., Wilding, I. R., Colonic transit of different sized tablets in healthy subjects, *J. Controlled Release* **1993**, *23*, 147–156.

46 Sathyan, G., Hwang, S., Gupta, S. K., Effect of dosing time on the total intestinal transit time of non-disintegrating systems, *Int. J. Pharm.* **2000**, *204*, 47–51.

47 Hebden, J. M., Gilchrist, P. J., Blackshaw, E., Perkins, A. C., Wilson, C. G., Spiller, R. C., Night-time quiescence and morning activation in the human colon: effect on transit of dispersed versus large single unit formulations, *Eur. J. Gastroenterol. Hepatol.* **1999**, *11*, 1379–1385.

48 Huchzermeyer, H., Schumann, C., Lactulose – a multifaceted substance, *Zeitschr. Gastroenterol.* **1997**, *35*, 945–955.

49 Barrow, L., Steed, K. P., Spiller, R. C., Watts, P. J., Melia, C. D., Davies, M. C., Wilson, C. G., Scintigraphic demonstration of accelerated proximal colon transit by lactulose and its modification by gelling agents, *Gastroenterology* **1992**, *103*, 1167–1173.

50 Barrow, L., Steed, K. P., Spiller, R. C., *et al*., Quantitative, non-invasive assessment of antidiarrheal actions of codeine using an experi-mental model of diarrhea in man, *Dig. Dis. Sci.* **1993**, *38*, 996–1003.

51 Hebden, J. M., Gilchrist, P. J., Perkins, A. C., Wilson, C. G., Spiller, R. C., Stool water content and colonic drug absorption: contrasting effects of lactulose and codeine, *Pharm. Res.* **1999**, *16*, 1254–1259.

52 Hammer, J., Pruckmayer, M., Bergmann, H., Kletter, K., Gangl, A., The distal colon provides reserve storage capacity during colonic fluid overload, *Gut*, **1997**, *41*, 658–663.

53 Hebden, J. M., Blackshaw, E., Perkins, A. C., Wilson, C. G., Spiller, R. C., Limited exposure of the healthy distal colon to orally dosed

formulation is further exaggerated in active left-sided ulcerative colitis, *Aliment. Pharmacol. Ther.* **2000**, *14*, 155–161.

54 Mollen, R., Hopman, W. P. M., Kuijpers, H. H. C., Jansen, J. M. B. H., Abnormalities of upper gut motility in patients with slow-transit constipation, *Eur. J. Gastroenterol. Hepatol.* **1999**, *11*, 701–708.

55 Bouchahcha, M. L., Dorval, E., Arhan, P., Devroede, G., Arsac, M., Patterns of normal colorectal transit time in healthy subjects and in patients with an irritable bowel syndrome (IBS), *Gastroenterology* **1999**, *116*, G4192.

56 Gorard, D. A., Gomborone, J. E., Libby, G. W., Farthing, M. J. G., Intestinal transit in anxiety and depression, *Gut* **1996**, *39*, 551–555.

57 Bennett, E. J., Evans, P., Scott, A. M., *et al.*, Psychological and sex features of delayed gut transit in functional gastrointestinal disorders, *Gut* **2000**, *46*, 83–87.

58 Folwaczny, C., *et al.*, Measurement of transit disorders in different gastrointestinal segments of patients with diabetes mellitus in relation to duration and severity of the disease by use of the metal-detector test, *Zeitschr. Gastroenterol.* **1995**, *33*, 517–526.

59 Grundy, J. S., Foster, R. T., The nifedipine gastrointestinal therapeutic system (GITS) – Evaluation of pharmaceutical, pharmacokinetic and pharmacological properties, *Clin. Pharmacokinet.* **1996**, *30*, 28–51.

60 Gattuso, J. M., Kamm, M. A., Morris, G., Britton, K. E., Gastrointestinal transit in patients with idiopathic megarectum, *Dis. Colon Rectum* **1996**, *39*, 1044–1050.

61 Tsukamoto, K., Mizutani, M., Yamano, M., Suzuki, T., The relationship between gastrointestinal transit and motility in dogs with postoperative ileus, *Biol. Pharm. Bull.* **1999**, *22*, 1366–1371.

62 Hammer, J., Lang, K., Kletter, K., Accelerated right colonic emptying after simulated upper gut hemorrhage, *Am. J. Gastroenterol.* **1998**, *93*, 628–631.

63 Lamprecht, A., Schafer, U., Lehr, C. M., Size dependency of nanoparticle deposition in the inflamed colon in inflammatory bowel disease: in vivo results from the rat, *J. Controlled Release* **2001**, *72*, 235–237.

64 Sasaki, Y., Hada, R., Nakajima, H., Fukuda, S., Munakata, A., Improved localizing method of radiopill in measurement of entire gastrointestinal pH profiles: colonic luminal pH in normal subjects and patients with Crohn's disease, *Am. J. Gastroenterol.* **1997**, *92*, 114–118.

65 Fallingborg, J., Pedersen, F., Jacobsen, B. A., Small intestinal transit time and intraluminal pH in ileocecal resected patients with Crohn's disease, *Dig. Dis. Sci.* **1998**, *43*, 702–705.

Index

Drug Bioavailability: Estimation of Solubility, Permeability, Absorption and Bioavailability.
Edited by Han van de Waterbeemd, Hans Lennernäs and Per Artursson

ISBN: 3-527-30438-X